Acta Chimica Hungarica

VOLUME 116, NUMBER 1, MAY 1984

EDITOR-IN-CHIEF
F. MÁRTA

MANAGING EDITOR
GY. DEÁK

ASSISTANT EDITOR
L. HAZAI

EDITORIAL BOARD
M. T. BECK, R. BOGNÁR, GY. HARDY, K. LEMPERT, B. LENGYEL, K. POLINSZKY, E. PUNGOR, G. SCHAY, Z. G. SZABÓ, P. TÉTÉNYI

Akadémiai Kiadó, Budapest

ACTA CHIM. HUNG. ACASA2 116 (1) 1—109 (1984) HU ISSN 0231-3146

ACTA CHIMICA HUNGARICA

A JOURNAL OF THE HUNGARIAN ACADEMY OF SCIENCES

Acta Chimica publishes original reports on all aspects of chemistry in English.

Acta Chimica is published in three volumes per year, each volume consisting of four issues, by

AKADÉMIAI KIADÓ

Publishing House of the Hungarian Academy of Sciences
H-1054 Budapest, Alkotmány u. 21.

Manuscripts and editorial correspondence should be addressed to

Acta Chimica
H-1450 Budapest P.O. Box 67

Subscription information

Orders should be addressed to

KULTURA Foreign Trading Company
H-1389 Budapest P.O. Box 149

or to its representatives abroad

Acta Chimica is indexed in Current Contents

NOTICE TO AUTHORS

Acta Chimica publishes original papers on all aspects of chemistry in English. Before preparing a manuscript for submission to this journal authors are advised to consult recent issues.

Form of manuscript

Manuscripts, tables and illustrations should be submitted in triplicate. Manuscripts should be typewritten double spaced (25 lines, 50 characters per line including spaces). The *title page* should include (1) the title of the paper, (2) the full names of the author(s) in the sequence to be published; apply an asterisk to designate the name of the author to whom correspondence should be addressed, (3) name and address of the institution where the work was done. If the paper is part of a series, reference to the previous communication must be given as a footnote.

Abstract

A summary is printed at the head of each paper. This should not exceed 200 words and should state briefly the principal results and major conclusions of the work. It should be suitable for use by abstracting services.

ACTA CHIMICA HUNGARICA

EDITORIAL BOARD

M. T. BECK, R. BOGNÁR, GY. HARDY,
K. LEMPERT, B. LENGYEL, K. POLINSZKY,
E. PUNGOR, G. SCHAY,
Z. G. SZABÓ, P. TÉTÉNYI

EDITOR-IN-CHIEF

F. MÁRTA

MANAGING EDITOR

GY. DEÁK

ASSISTANT EDITOR

L. HAZAI

VOLUME 116

AKADÉMIAI KIADÓ, BUDAPEST

1984

Abd El-Rahman, A. N. s. **Nour, E. M.**
Aggarwal, R. C. s. **Singh, B.**
Agrawal, S. s. **Varshney, K. G.**
Aly, M. M. s. **Mahgoub, S. A.**
Ángyán, J., Náray-Szabó, G.: Comparison of some quantum chemical methods estimating hydration effects on the hydrogen fluoride-ammonia proton transfer reaction.... 141

Badr, M. Z. A. s. **Mahgoub, S. A.**
Bajaj, R. K., Sodhi, G. S., Kaushik, N. K., Johri, K. N.: Xanthate anions as salts of oxinato bis(η^5-idenyl)titanium(IV)zirconium(IV) chelates 261
Bakó, P., Fenichel, L., Tőke, L.: Synthesis of a novel diaza crown and a novel cryptand incorporating a methyl-4,6-*O*-benzylidene-α-D glucopyranoside unit (Preliminary communication) 323
Bánki, J., Billes, F., Grofcsik, A.: A complete CNDO force field of furan..... 283
Bányai, I. s. **Brücher, E.**
Baranyai, M., Radics, L., Kajtár, M., Kajtár, J., Bujtás, Gy., Szabolcs, J.: The structure of deoxyluteins 153
Barcza, L. s. **Lehoczky. B.**
Baskaran, S., Kapoor, R. N.: Synthesis and characterization of indium(III) compounds with Schiff bases 13
Bertalan, E. s. **Szabó, Z. L.**
Billes, F. s. **Bánki, J.**
Brlik, J. s. **Korányi, G.**
Brücher, E., Bányai, I., Krusper, L.: Aminopolycarboxylates of rare earths, XI. Kinetics of metal ion-exchange and ligand-exchange reactions of the ethyleneglycol-bis-(2-aminoethylether)-tetraacetate complex of cerium(III) 39
Bujtás, Gy. s. **Baranyai, M.**
Buzás, I., Szotyory, L., Ujhidy, A.: Selective production of *p*-dichlorobenzene from chlorobenzene 353

Chojnacka, I., Orszagh, A.: Viscosity of binary systems of the type: cresol-pyridine base 81
Costisella, B. s. **Gross, H.**
Coy, D. H. s. **Mező, I.**

Deák, Gy. s. **Hazai, L.**
Deák, Gy. s. **Zára-Kaczián, E.**
Delijska, A., Pravčeva, Chr., Donchev, I.: Application of organic compounds as thermochemical agents in spectral analysis 235
Donchev, I. s. **Delijska, A.**
Dubey, K. P., Qazi, M. A.: Chelometric determination of Mg^{2+} in presence of II-B group elements by the use of thioglycolic acid as a masking agent and potassium bisthioglycolato mercurate(II) as a precipitating agent 3

El-Ansary, A. L. s. **Issa, Y. M.**
El-Barbary, A. A. s. **Hammouda, H. A.**
Érchegyi, J. s. **Mező, I.**

Fahmy, A. M. s. **Mahgoub, S. A.**
Fenichel, L. s. **Bakó, P.**

Filo, O.: The application of addition methods in spectrographic analysis, II 245
Flerkó, B. s. **Mező, I.**

Gaber, M. s. **Issa, Y. M.**
Glavaty, E. V. s. **Glavaty, O. L.**
Glavaty, O. L., Marchenko, A. L., Kravchook, G. G., Glavaty, E. V.: New ideas about the mechanism of action of detergent-dispersant (DD) oil additives 367
Grofcsik, A. s. **Bánki, J.**
Gross, H., Keitel, I., Costisella. B.: Synthesis and reactions of 2,2-diphosphono-1,3-benzodioxoles 229
Gupta, A. s. **Saxena, R. S.**

Hammouda, H. A., El-Barbary, A. A.: 1-Benzoyl-1-phenylhydrazine as a pyrazole precursor 21
Haskó-Breuer, J. s. **Hazai, L.**
Hazai, L., Deák, Gy., Schnitta, A., Haskó-Breuer, J., Horváth, E.: Diels-Alder reaction of 3(2*H*)-isoquinolinones, II. Studies on the lactam-lactim tautomerism of 3(2*H*)-isoquinolinones 303
Horváth, A. s. **Mező, I.**
Horváth, E. s. **Hazai, L.**

Issa, R. M. s. **Issa, Y. M.**
Issa, Y. M., El-Ansary, A. L., Gaber, M., Issa, R. M.: Spectroscopic study of the donor behaviour of benzidine derivatives towards aromatic nitro compounds 273

Johri, K. N. s. **Bajaj, R. K.**

Kaetsu, I. s. **Kumakura, M.**
Kajtár, J. s. **Baranyai, M.**
Kajtár, M. s. **Baranyai, M.**
Kapoor, R. N. s. **Baskaran, S.**
Kasprzycka-Guttman, T., Wilczura, H.: Thermodynamic properties of binary mixtures pyridine base and *iso*-aliphatic alcohols 77
Kaushik, N. K. s. **Bajaj. R. K.**
Kaushik, N. K. s. **Sharma, A. K.**
Keitel, I. s. **Gross, H.**
Korányi, G., Szebényi-Győri, E., Vélin-Prikidánovics, A., Brlik, J.: Electrochemical behaviour of the benzimidazoles 131
Kovács, M. s. **Mező, I.**
Kőszegi, E. s. **Mánok, F.**
Kravchook, G. G. s. **Glavaty, O. L.**
Krusper, K. s. **Brücher, E.**
Kumakura, M., Kaetsu, I.: Immobilization of cells by radiation copolymerization of hydrophilic and hydrophobic monomers 345
Kürti, J. s. **Menczel, Gy.**

Lakatos, I., Lakatos, J.: Direct determination of trace elements in polyacrylamide solutions by flame atomic absorption spectrophotometry, II. The effect of polymers on nebulization phenomena 389
Lakatos, J. s. **Lakatos, I.**
Lehoczky, B., Barcza, L.: Influence of the liquid junction potential on hydroxide activity measurements 383
Lehőcz, R. s. **Menczel, Gy.**

Mahgoub, S. A., Fahmy, A. M., Aly, M. M., Badr, M. Z. A.: Condensation and ring closure reactions of phthalazinone derivatives 267
Mánok, F., Kőszegi, E., Várhelyi, Cs.: Polarographic study on the kinetics and mechanism of the hydrolysis of 1,2-cycloheptane dione dioxime 51
Marchenko, A. I. s. **Glavaty, O. L.**
Mazurkiewicz, R.: Structure of the self-condensation products of lactams 95
Menczel, Gy., Kürti, J., Lehőcz, R.: Crystal and molecular structure determination and ESR-study of [*N*-(*n*-butyl)quinolinium]$^+$ (7,7,8,8-tetracyanoquinodimethane)$_2^-$ .. 337

Mező, I., Seprődi, I., Érchegyi, J., Horváth, A., Nikolics, K., Teplán, I., Vigh, S., Kovács, M., Flerkó, B., Coy, D. H., Pedroza, E., Nekola, M. V., Schally, A. V.: Design and synthesis of inhibitory analogues of LH-RH with increased antiovulatory potency..... 173
Mishra, V. N.: Influence of surfactants on the fluorescence and absorption spectra of Eosin in aqueous solution 5

Náray-Szabó, G. s. **Ángyán, J.**
Nekola, M. V. s. **Mező, I.**
Nikolics, K. s. **Mező, I.**
Nour, E. M., Abd El-Rahman, A. N.: Vibrational analysis of the $(UO_2Cl_4)^{2-}$ and $(UO_2Br_4)^{2-}$ ions 377

Orszagh, A. s. **Chojnacka, I.**

Pandey, O. P., Sengupta, S. K., Tripathi, S. C.: Carboxylato derivatives of mono(cyclopentadienyl)titanium(IV)..... 29
Pandey, S. s. **Patel, P. N.**
Patel, P. N., Pandey, S.: Preparation, infrared absorption spectra and X-ray powder diffraction patterns of mixed (Ca + Ba + Pb) hydroxylapatites 63
Pedroza, E. s. **Mező, I.**
Pethő, G.: Application of a new potentiometric evaluation method for the determination of the concentration of monovalent weak bases..... 293
Pomonis, P. J.: Influence of the chemical potential of transition metals on their adsorptive and catalytic properties 163
Pravčeva, Chr. s. **Delijska, A.**

Qazi, M. A. s. **Dubey, K. P.**

Radics, L. s. **Baranyai, M.**

Saxena, R. S., Gupta, A.: Dissociation constants of L-pyrrolidine-2-carboxylic acid at different temperatures, ionic strengths and in different aquoorganic solvents..... 327
Schally, A. V. s. **Mező, L.**
Schnitta, A. s. **Hazai L.**
Sengupta, S. K. s. **Pandey, O. P.**
Seprődi, I. s. **Mező, I.**
Sharma, A. K., Kaushik, N. K.: Synthesis of (π-fluorenyl) and (π-pyrrolyl)thallium(I) and their group transfer reactions with $(\pi\text{-}C_5H_5)TiCl_3/(\pi\text{-}C_5H_5)ZrCl_3$ 361
Sharma, U. s. **Varshney, K. G.**
Singh, B., Yadava, B. P., Aggarwal, R. C.: Synthesis and characterization of 1-phenyl-3--formamidino thiocarbamide complexes with some bivalent metal ions..... 251
Sodhi, G. S. s. **Bajaj, R. K.**
Sólyom, S. s. **Szilágyi, K.**
Sólyom, S., Szilágyi, K., Toldy, L.: New 17-spirosteroids, V. Preparation and investigation of steroid-17-spiro-1',3',2'-oxazaphospholidines and -1',3',2'-dioxaphospholanes... 125
Szabolcs, J. s. **Baranyai, M.**
Szabó, Z. L., Bertalan, É., Tatár, E.: Behaviour of metal carbonates in spectroscopic arc, I. Preliminaries. Role of instability of carbonates..... 189
Szabó, Z. L., Bertalan, É., Tatár, E.: Behaviour of metal carbonates in spectroscopic arc, II. Investigation of $CaCO_3$. The effect of carbon powder mixed to the sample on the chemical behaviour of the main component 205
Szebényi-Győri, E. s. **Korányi, G.**
Szilágyi, K., Sólyom, S., Toldy, L.: New 17-spirosteroids, IV. Synthesis and examination of steroid 17S-spirodioxolanes 111
Szilágyi, K. s. **Sólyom, S.**
Szotyory, L. s. **Buzás, I.**

Tatár, E. s. **Szabó, Z. L.**
Teplán, I. s. **Mező, I.**
Toldy, L. s. **Sólyom, S.**
Toldy, L. s. **Szilágyi, K.**
Tőke, L. s. **Bakó, P.**
Tripathi, S. C. s. **Pandey, O. P.**

Ujhidy, A. s. **Buzás, I.**

Várhelyi, Cs. s. **Mánok, F.**
Varshney, K. G., Agrawal, S., Varshney, K.: Ion exchange kinetics of alkaline earths on Zr(IV) arsenosilicate cation exchanger. Activation energy as a linear function of the ionic mobilities and radii 69
Varshney, K. G., Sharma, U.: Kinetics of exchange of transition metals on zirconium(IV) and thorium(IV) phosphosilicate cation exchangers 103
Varshney, K. s. **Varshney, K. G.**
Vélin-Prikidanovics, A. s. **Korányi, G.**
Vigh, S. s. **Mező, I.**

Wilczura, H. s. **Kasprzycka-Guttman, T.**

Yadava, B. P. s. **Singh, B.**

Zára-Kaczián, E., Deák, Gy.: Synthesis of 1-aryl-2-carbamoyl-1,4-dihydro-3(2*H*)-isoquinolinones from 2-tritylcarbamoyl derivatives (Short communication) 89

CONTENTS

PHYSICAL AND INORGANIC CHEMISTRY

Influence of surfactants on the fluorescence and absorption spectra of Eosin in aqueous solution, **V. N. Mishra** 5

Aminopolycarboxylates of rare earths, XI. Kinetics of metal ion-exchange and ligand exchange reactions of the ethyleneglycol-bis-(2-aminoethylether)-tetraacetate complex of cerium(III), **E. Brücher, I. Bányai, L. Krusper** 39

Polarographic study on the kinetics and mechanism of the hydrolysis of 1,2-cycloheptane dione dioxime, **F. Mánok, E. Kőszegi, Cs. Várhelyi** 51

Preparation, infrared absorption spectra and X-ray powder diffraction patterns of mixed (Ca + Ba + Pb) hydroxylapatites, **P. N. Patel, S. Pandey** 63

Ion exchange kinetics of alkaline earths on Zr(IV) arsenosilicate cation exchanger. Activation energy as a linear function of the ionic mobilities and radii, **K. G. Varshney, S. Agrawal, K. Varshney** 69

Thermodynamic properties of binary mixtures pyridine base and *iso*-aliphatic alcohols, **T. Kasprzycka-Guttman, H. Wilczura** 77

Viscosity of binary systems of the type: cresol-pyridine base, **I. Chojnacka, A. Orszagh** 81

Kinetics of exchange of transition metals on zirconium(IV) and thorium(IV) phosphosilicate cation exchangers, **K. G. Varshney, U. Sharma** 103

ORGANIC CHEMISTRY

Synthesis and characterization of indium(III) compounds with Schiff bases, **S. Baskaran, R. N. Kapoor** 13

1-Benzoyl-1-phenylhydrazine as a pyrazole precursor, **H. A. Hammouda, A. A. El-Barbary** 21

Carboxylato derivatives of mono(cyclopentadienyl)titanium(IV), **O. P. Pandey, S. K. Sengupta, S. C. Tripathi** 29

Synthesis of 1-aryl-2-carbamoyl-1,4-dihydro-3(2*H*)-isoquinolinones from 2-tritylcarbamoyl derivatives (Short communication), **E. Zára-Kaczián, Gy. Deák** 89

Structure of the self-condensation products of lactams, **R. Mazurkiewicz** 95

ANALYTICAL CHEMISTRY

Chelometric determination of Mg^{2+} in presence of II-B group elements by the use of thioglycolic acid as masking agent and potassium bisthioglycolato mercurate(II) as precipitating agent, **K. P. Dubey, M. A. Quazi** 3

PRINTED IN HUNGARY

Akadémiai Kiadó és Nyomda, Budapest

Acta Chimica Hungarica 116 (1), pp. 3—4 (1984)

CHELOMETRIC DETERMINATION OF Mg^{2+} IN PRESENCE OF II-B GROUP ELEMENTS BY THE USE OF THIOGLYCOLIC ACID AS MASKING AGENT AND POTASSIUM BISTHIOGLYCOLATO MERCURATE(II) AS PRECIPITATING AGENT*

K. P. DUBEY** and M. A. QAZI

(Department of Chemistry, Kashmir University, University Campus, Hazratbal, Srinagar-190006, India)

Received March 24, 1982

In revised form September 8, 1983

Accepted for publication September 16, 1983

On the basis of greater stability complexes of II-B group elements, as compared to the stability of the similar complexes of Mg^{2+}, a method for the chelometric determination of Mg^{2+} in presence of II-B group elements using thioglycolic acid as masking agent and use of potassium bisthioglycolato mercurate(II) as precipitating agent for some metal ions have been described.

Here we use thioglycolic acid as a masking agent in the chelometric determination of Mg^{2+} in presence of II-B group elements using Eriochrome Black T as an indicator and gravimetric estimation of heavy metal ions by precipitation as bisthioglycolato mercurates(II).

Experimental

Thioglycolic acid was obtained from Evans Chemetics, New York. All other chemicals used are of (B.D.H.) A.R. quality.

Determination of Mg^{2+} in presence of II-B group elements

To the solutions of the metal ions 20.0 mL of NH_3—NH_4Cl buffer solution, and one drop of Eriochrome Black T indicator solution in alcohol were added, the metal ions were titrated with a standard (0.05 *M*) EDTA solution, till the colour of the solution changed from light pink to light blue [1]. The results obtained are given in Table I.

Similar titration was performed for the determination of Mg^{2+} in presence of Cd^{2+} and Hg^{2+} using same concentrations. The minimum and standard deviations observed are 0.00013 and 0.00016 respectively. At higher concentrations the end point is sluggish and the estimation is not possible.

* The paper is a contribution the our former paper [Koul, M. K., Dubey, K. P.: Acta Chim. (Budapest), **82**, 21 (1974)]

** To whom correspondence should be addressed

Table I

Determination of Mg^{2+} *in presence of* Zn^{2+} *and* Hg^{2+}

1. 20.0 mL 0.5 *M* H_2 TGA solution, 2. 10.0 mL of 0.1 *M* magnesium sulphate solution, 3. 0.1 *M/L* mercuric chloride solution, 4. 0.1 *M* zinc sulphate solution
Total volume = 100.0 mL

Amount of Mg^{2+} taken, g	Amount of II-B group elements taken				Amount of Mg^{2+}
	Hg^{2+}		Zn^{2+}		
	mL	g	mL	g	
0.0240	5.0	0.1	5.0	0.0325	0.0239
	4.0	0.08	6.0	0.0390	0.0241
	6.0	0.12	4.0	0.0260	0.0237

Mean deviation = 0.00013
Standard deviation = 0.00016

Table II

Quantitative estimation of some metal ions, as bisthioglycolato mercurate(II)

Cation	Compound	pH	Colour	Wt. of pp.t in grams		Deviation	
				F	*T*	Mean	Standard
La^{3+}	K_2L	4.6	White	0.574 0.572 0.570	0.573	0.0016	0.0020
Ce^{3+}	K_2L	5.2	White	0.570 0.572 0.574	0.5724	0.0015	0.0020
UO_2^{2+}	K_2L	4.4	Yellow	0.379 0.378 0.379	0.3887	0.0100	0.0010
Th^{4+}	K_2L	3.8	White	0.588 0.589 0.588	0.6757	0.0876	0.0016

$L = [Hg(TGA)_2]^{2-}$

Gravimetric estimation of heavy metal ions by precipitation as bisthioglycolato mercurates (II): metal ions (La^{3+}, Ce^{3+}, UO_2^{2+} and Th^{4+}) of 0.01 *M* concentration were treated with an excess of potassium bisthioglycolato mercurate, the precipitates formed digested on a water bath, filtered, dried at 40—50 °C and weighed. The results are given in Table II.

REFERENCES

[1] Welcher, F. J.: The Analytical Uses of EDTA, D. Van Nostrand Co. Inc. 149—164., 1961.

Acta Chimica Hungarica 116 (1), pp. 5—12 (1984)

INFLUENCE OF SURFACTANTS ON THE FLUORESCENCE AND ABSORPTION SPECTRA OF EOSIN IN AQUEOUS SOLUTION

V. N. MISHRA

(Department of Chemistry, Kumaon University Campus, Almora, India)

Received March 18, 1983

Accepted for publication June 7, 1983

The effect of certain nonionic, anionic and cationic surfactants on the fluorescence and absorption spectra of Eosin has been studied. Shift towards longer wave lengths in absorption and fluorescence peak wave lengths has been observed with a shoulder at lower wave length. Also there appears a marked enhancement in the fluorescence intensity of Eosin on adding small amount of surfactant. The shift in the absorption peak wave length appears to be due to interaction of surfactant with dye molecules. The enhancement in the fluorescence intensity is attributed to the desaggregation of Eosin dye dimer and multimer forms into monomeric form and non-radiative transition from higher energy level of the first singlet level. Enhancement in the fluorescence intensity on addition of ethanol has also been observed.

Introduction

Changes in absorption spectra due to the interaction of ionic dyes with ionic surfactant of opposite charges has been studied by many workers [1—10]. Change in absorption behaviour of dyes has been used to determine the critical micelle concentration (cmc) of surfactants [1, 9, 10]. The spectral changes in the dyes brought about by the action of surfactant of opposite charges below cmc have been attributed to other reasons such as formation of dye surfactant salt suspension(7), dye *n*-mer formation [1, 7], dye surfactant aggregation [1] or merely to formation of complexes of indefinite composition [10]. Reeves and coworkers [8] have studied the interaction of azo dyes with cationic surfactant.

Changes in fluorescence spectra of dyes due to the interaction with surfactant have been reported [11—13]. Homa and Tokawa [11] have studied interaction between dye and nonionic surfactant with the help of absorption and fluorescence spectroscopy. They have also observed enhancement in the fluorescence intensity on the addition of nonionic surfactant above cmc. Alfano and coworkers [14] have studied the change in quantum yield and fluorescence life-time of Rhodamine = 6G on the addition of nonionic surfactant Amnonyl LO. Kapoor and Mishra [15—18] have studied the effect of some nonionic, cationic and anionic surfactants on the fluorescence and absorption spectra of 9—10 DPA, Rhodamine-B, Erythrosin and Rose Bengal.

Influence of nonionic, cationic and anionic surfactants on the fluorescence and absorption spectra of Eosin is being reported in this communication.

Experimental

The fluorescence studies were made on Amico-Bowman spectrofluorophotometer with a cell of 1 cm path length. The absorption studies were made "Carl Zeiss Spectrophotometer" SPEKOL. All the reagents employed were of analytical grade. The experiments were carried out at room temperature (23—25 °C).

The following surfactants were used:

Anionic: (i) Dodecyl benzene sodium sulphonate (DBSS), (ii) Dioctyl sodium sulphosuccinate (DSSS).

Cationic: (i) Cetyl trimethyl ammonium bromide (CTAB), (ii) Cetyl pyridinium bromide (CPB).

Nonionic surfactant: (i) Polyoxyethylene *ter.*octyl phenol (Eq-10) (Tx-100), (ii) Polyoxyethylene (23) Laurylether (Brij-35), (iii) Polyoxyethylene sorbitain monolaurate (Tween-20), (iv) Polyoxyethylene sorbitain monopalmitate (Tween-40), (v) Polyoxyethylene sorbitain monoleate (Tween-80).

The purity of surfactants was checked by measuring their cmc values by drop-weight methods which were found similar to the reported literature values. All the surfactants were from Sigma (U.S.A.) Product, and used as such.

Absorption spectra

Nonionic surfactants

Pure Eosin (10^{-5} *M*) has an absorption peak at 515 nm. A shift of 18—20 nm towards longer wave length was observed on the addition of all nonionic surfactants. During initial addition of the surfactant a decrease was noticeable in the height of the absorption peak at 515 nm. The shift in the peak appeared only after addition of a particular concentration of the surfactant. Figure 1 shows spectral changes occurring during the addition of Tx-100 to Eosin solutions. The behaviour of all the other nonionic surfactants was almost similar to that shown in Fig. 1.

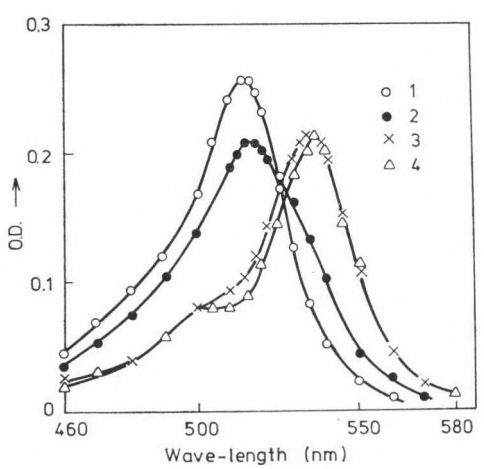


Fig. 1. Changes in absorption spectra of Eosin (10^{-5} *M*) on changing the concentration of Tx-100. (1) Eosin (10^{-5} *M*), (2) Eosin + 0.05% Tx-100, (3) Eosin + 0.20% Tx-100, (4) Eosin + 0.50% Tx-100

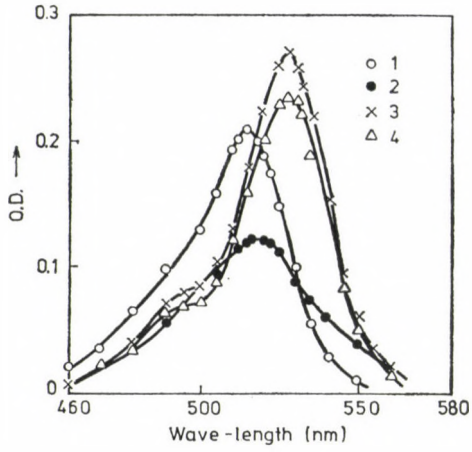


Fig. 2. Changes in absorption spectra of Eosin (10^{-5} *M*) on changing the concentration of CPB. (1) Eosin (10^{-5} *M*), (2) Eosin + 0.004% CPB, (3) Eosin + 0.100% CPB, (4) Eosin + 0.160% CPB

Concurrently with the shift in λ_{max} a shoulder appeared in the absorption spectrum at lower wave length on adding Tx-100, Brij-35 and Tween-20 to the dye solution. The shoulder became prominent at higher concentrations of surfactants.

Cationic surfactants

On the addition of cationic surfacants to the aqueous solution of Eosin, a decrease in absorbance occurred initially which was followed by shift in λ_{max} towards longer wave length. However, the shift was only of the order of 10 nm and was accompanied by an enhancement in the absorbance at the shifted λ_{max} which reached a maximum value at higher concentrations of the surfactants. Concurrently with the shift in λ_{max} a shoulder at lower wave length also appeared in the absorption spectrum. The changes in absorption spectra of Eosin occurring at different concentrations of CPB are shown in Fig. 2.

Anionic surfactants

The employed anionic surfactants had no effect on the absorption spectrum of aqueous solution of Eosin.

Fluorescence emission spectra

The aqueous solution of Eosin showed maximum excitation wave length at 510 nm and maximum emission wave length at 538 nm. Studies on excitation and emission spectra in presence of various concentrations of surfactants indicated that cationic and nonionic surfactants had similar influence on the fluorescence spectrum of Eosin.

Nonionic surfactants

A shift (of nearly 18 nm) towards longer wave length occurred both in the excitation and emission spectra on the addition of every surfactant. Initially a decrease in fluorescence intensity occurred at lower concentration of surfactant, which was followed by a shift in the λ_{max} of the spectrum. The shift was accompanied with enhancement in the fluorescence intensity which reached its limiting value at higher surfactant concentration. The Table II observations with different surfactants are given.

The minimum concentration of each surfactant needed for the shift in λ_{max} of fluorescence spectrum was found to be much lower than the concentration of surfactants needed for the shift in λ_{max} of its absorption spectrum. The concentration of surfactant needed for

Table I

Minimum concentration of surfactant needed for a shift in fluorescence spectra, and cmc value of each surfactant

Name of surfactant	Reported values of cmc	Conc. of surfactants needed for a shift in λ_{max}
Tx-100	2.8×10^{-4} *M*	2×10^{-2} gm/L (3.2×10^{-2} *M*)
Brij-35	1.2×10^{-4} *M*	1×10^{-2} g/mL (1.0×10^{-4} *M*)
Tween-20	5.0×10^{-2} gm/L	4.0×10^{-2} gm/L
Tween-40	—	5.0×10^{-2} gm/L
Tween-80	3.0×10^{-2} gm/L	2.5×10^{-2} gm/L
TAB	8.0×10^{-4} *M*	2×10^{-2} gm/L (6.0×10^{-4} *M*)
CPB	1.23×10^{-3} *M*	5×10^{-2} gm/L (1.33×10^{-3} *M*)

The results obtained with different classes of surfactants are given below.

Table II

Changes in fluorescence intensity (F.I.) *of Eosin* (10^{-5} *M*) *on changing the concentration of nonionic surfactants*

λ_{ex} = 510 nm λ_{em} = 538 nm (Serial number 1—4) and λ_{ex} = 530 nm λ_{em} = 554 nm (Serial number 5—13)

S. No.	% of Tx-100	F.I.	% of Brij-35	F.I.	% of Tween-20	F.I.	% of Tween-40	F.I.	% of Tween-80	F.I.
1.	0.000	72	0.000	70	0.000	72	0.0000	72	0.000	72
2.	0.001	70	0.003	64	0.0025	67	0.0001	62	0.0005	67
3.	0.005	68	0.005	55	0.004	65	0.0050	58	0.004	62
4.	0.010	67	0.008	45	0.025	57	0.0100	57	0.005	57
5.	0.050	87	0.010	43	0.040	68	0.0250	69	0.010	62
6.	0.080	100	0.020	67	0.050	74	0.0500	82	0.025	73
7.	0.100	102	0.050	89	0.100	90	0.0800	89	0.050	90
8.	0.200	102	0.080	89	0.150	98	0.1500	100	1.100	105
9.	0.300	102	0.100	89	0.200	105	0.2000	102	0.150	108
10.	0.500	102	0.150	87	0.300	105	0.3000	102	0.250	108
11.	0.800	102	0.200	79	0.450	108	0.4500	102	0.300	108
12.	—	—	0.500	68	—	—	—	—	—	—
13.	—	—	0.800	61	—	—	—	—	—	—

the shift in λ_{max} of fluorescence spectrum was in the vicinity of its critical micelle concentration. A comparison of the reported cmc values of the surfactants and their minimum concentration needed for the shift in λ_{max} is given in Table I.

The fluorescence spectra at various concentrations of Tween-20 are given in Fig. 3. The influence of other nonionic surfactants on the fluorescence emission spectrum was similar to that of Tween-20. No shoulder appeared in the emission spectrum of Eosin.

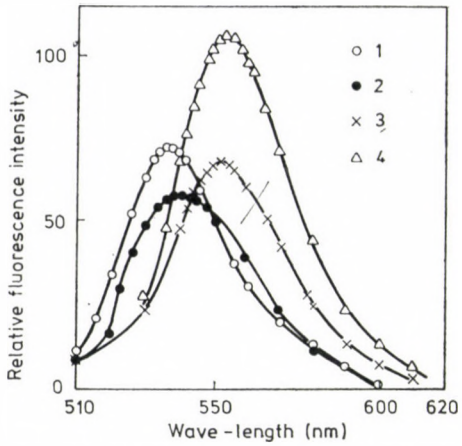


Fig. 3. Changes in fluorescence spectra of Eosin (10^{-5} *M*) on changing the concentration of Tween-20. (1) Eosin (10^{-5} *M*), (2) Eosin + 0.025% Tween-20, (3) Eosin + 0.040% Tween-20, (4) Eosin + 0.300% Tween-20

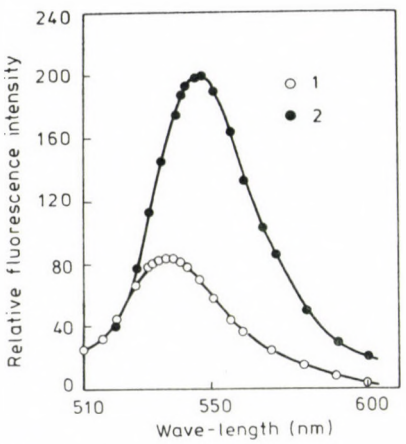


Fig. 4. Changes in fluorescence spectra of Eosin (10^{-5} *M*) on changing the concentration of CTAB. (1) Eosin (10^{-5}, *M*), (2) Eosin + 0.09% CTAB

Cationic surfactants

Cationic surfactants exerted peculiar influence on the fluorescence characteristics of Eosin solution. During initial addition the fluoreascence intensity dropped almost of to zero level. However, the colour of the solution did not undergo any perceptable change. Subsequently on increasing the concentration of the surfactant a shift in the λ_{max} (about 7—8 nm) occurred towards longer wave length. The shift in the λ_{max} was followed by a large enhancement in the fluorescence intensity which reached a value nearly three times that of the original value observed in the absence of the surfactant. The changes taking place during the addition of CTAB are shown in Fig. 4. The variation in the fluorescence intensity on changing the concentrations of surfactants are given in Table III. The minimum amounts of surfactant needed for a shift in fluorescence spectrum are given in Table I. The reported cmc values of surfactants are also given concurrently. Due to the low solubility of the surfactants, observations at higher concentrations could not be recorded.

Table III

Changes in fluorescence intensity (F.I.) *of Eosin* (10^{-5} *M*) *on changing the concentration of cationic surfactants*

S. No.	% of CTAB	F.I.	% of CPB	F.I.	λ_{ex} in nm	λ_{em} in nm
1.	0.000	84	0.000	84	510	538
2.	0.002	62	0.002	56	510	538
3.	0.005	2	0.005	12	510	538
4.	0.010	1	0.010	3	510	538
5.	0.020	65	0.050	16	520	544
6.	0.050	168	0.060	62	520	544
7.	0.070	184	0.080	89	520	544
8.	0.090	201	0.090	129	520	544

Table IV

Changes in fluorescence intensity (F.I.) *of Eosin* (10^{-5} *M*) *on changing the concentration of ethanol (v/v)*

$\lambda_{ex} = 510$ nm $\lambda_{em} = 538$ nm (Serial No. 1—9) and $\lambda_{ex} = 520$ nm $\lambda_{em} = 542$ nm (Serial No. 10—12)

S. No.	% of ethanol	F.I.	S. No.	% of ethanol	F.I.
1.	0	72	7.	40	111
2.	1	71	8.	50	118
3.	5	74	9.	60	121
4.	16	80	10.	70	123
5.	20	90	11.	80	126
6.	30	98	12.	94	126

Anionic surfactants

No change in fluorescence spectrum was observed on adding anionic surfactant.

Effect of ethanol

Enhancement in the fluorescence intensity was observed on addition of ethanol to the aqueous solution of Eosin. The limiting value was attained in 75 $v/v\%$ ethanol. Changes in fluorescence intensity at various concentrations of ethanol are given in Table IV. However, the shape of the fluorescence spectrum remained unchanged during the addition of ethanol.

Discussion

The significant findings of this study can be summarized as follows;

(a) There occurs a shift in the absorption and fluorescence emission spectral peaks of the dye on the addition of surfactants.

(b) Initially there occurs a decrease in the absorbance of the dye which is followed by a shift in λ_{max} and a small enhancement in the absorbance peak. A shoulder towards lower wave length also appears on adding Tx-100, Brij-35 and Tween-20.

(c) The fluorescence intensity is enhanced at the shifted λ_{max} on further addition of the surfactant.

The above observations can be explained on the following lines.

Nonionic surfactants

Interaction between dye molecules and the surfactants appears to cause shift in fluorescence peak wave length. During this process the hydrophilic part of the surfactant interacts with the dye dimer and multimer forms [13]. The shift occurs in the cmc region of the surfactant where the interaction of dye with surfactant is most likely to occur.

Enhancement in fluorescence will then be due to the subsequent interaction of dye molecule with a surfactant micelle. At higher surfactant concentrations the dye dimer and multimer present in the solution, disaggregate into monomeric or simpler forms [14]. This results in an increase in the number of dye units causing enhancement in the fluorescence intensity. The shoulder appearing in the absorption spectrum at higher energy may indicate non-radiative transition from higher energy level to the first singlet energy level resulting in enhancement in the fluorescence intensity. This view is supported from the fact that no shoulder appears in the fluorescence emission spectrum, whereas the excitation spectrum displays a shoulder at higher concentrations of the surfactant.

Cation surfactants

With cationic surfactant interaction would occur with the anionic dye due to mutual electrostatic attraction. The initial decrease in both the fluorescence intensity as well as absorption peak indicates change occurring in the geometry of the dye molecule causing inactivation of the fluorescence sites.

It is interesting to note that fluorescence intensity almost drops to zero at a particular concentration range of cationic surfactants. At this stage the interaction causes a shift in λ_{max}. The shoulder observed in the absorption spectrum can be due to trapping of some dye molecules inside the surfactant micelle.

Subsequent enhancement in the fluorescence intensity would be due to disaggregation of the dye multimer into monomeric or simpler forms in presence of higher concentration of cationic surfactant. The dye molecule in its new conformation appears more susceptible to disaggregation on further addition of the cationic surfactants.

Anionic surfactants

Anionic surfactants cause no effect on absorption and fluorescence emission spectra of the dye. Since the surfactant as well as the dye are anionic in nature one would not expect any significant mutual interaction. Further, the anionic surfactants have no available hydroxyl groups which could interact with the dye molecules.

Effect of ethanol

Addition of ethanol to dye solution causes enhancement in the absorption peak as well as in the fluorescence emission peak.

The hypothesis of interaction between hydroxyl group and the dye molecules is confirmed by these observations.

*

Author is thankful to Prof. M. R. Paohye, Chemical Technology Department, Bombay, or permitting to use their fluorescence spectrometer.

REFERENCES

[1] Corrin, M. L., Horkins, W. D.: J. Am. Chem. Soc., **59,** 679 (1947)
[2] Shinoda, K.: J. Phys. Chem., **58,** 541 (1954)
[3] Hartley, G. S.: Trans. Faraday Soc., **30,** 44 (1934)
[4] Harrap, B. S., Shylman, J. H.: Disc. Faraday Soc., **13,** 71 (1953)
[5] Sailo, S.: J. Coll. Sci., **15,** 283 (1960)
[6] Mukerjee, P., Mysels, K. J.: J. Am. Chem. Soc., **77,** 2937 (1955)
[7] Hayashi, M.: Bull. Chem. Soc. Japan, **34,** 119 (1961)
[8] Reeves, R. I., Kaiser, R. S., Mark, H. W.: J. Coll. Interface Sci., **45,** 396 (1973)
[9] Malik, W. U., Verma, S. P.: J. Phys. Chem., **70,** 26 (1966)
[10] Malik, W. U., Jamb, O. P.: J. Electroanal. Chem., **27,** 151 (1970)
[11] Homa, I., Tokawa, F.: Chem. Abst., **83,** 65912g (1975)
[12] Harada, H., Toya, T.: Chem. Abstr., **62,** 5363b (1965)
[13] Ghosh, A. K.: Ind. J. Chem., **12,** 313 (1974)
[14] Alfano, R. R., Shapira, S. L., Yu, W.: Optics Commun., **7,** 191 (1973)
[15] Kapoor, R. C., Mishra, V. N.: Indian J. Chem., **14A,** 123 (1976)
[16] Kapoor, R. C., Mishra, V. N.: J. Indian Chem. Soc., **53,** 965 (1976)
[17] Kapoor, R. C., Mishra, V. N.: J. Lum., **17,** 175 (1978)
[18] Kapoor, R. C., Mishra, V. N., Jain, M. K.: J. Lum., **22,** 429 (1981)

Acta Chimica Hungarica 116 (1), pp. 13—20 (1984)

SYNTHESES AND CHARACTERIZATION OF INDIUM(III) COMPOUNDS WITH SCHIFF BASES

S. BASKARAN and R. N. KAPOOR*

(Department of Chemistry, University of Delhi, Delhi-110007, India)

Received March 25, 1983

Accepted for publication June 7, 1983

The reactions of indium(III) isopropoxide with bidentate and tridentate Schiff bases, such as, salicylidene-aniline (SB_1H), salicylidene-*o*-toluidine (SB_2H), salicylidene-*m*-toluidine (SB_3H), salicylidene-*p*-toluidine (SB_4H), 2-hydroxyacetophenone-aniline (SB'_4H) 2-hydroxy-1-naphthylidene-aniline (SB'_8H), acetylacetone-*o*-aminophenol ($SB'H_2$) and benzoylacetone-*o*-aminophenol (SB'_8H_2), have been carried out in 1 : 1, 1 : 2 or 2 : 3 molar ratios in dry benzene under anhydrous conditions. The compounds of the type: $In(OPr^i)_2L$, $In(OPr^i)L_2$, $In(OPr^i)L'$ and $In_2L'_3$, where L = bidentate Schiff base and L^1 = tridentate Schiff base, have been synthesized and characterized by elemental analysis, molecular weight and spectral (infrared, ^{1}H-NMR and electronic) studies.

Introduction

Unlike to the transition metals, reports on the compounds of non-transition metals with Schiff bases are rather vague. In one of our earlier communications [1] on the reactions of indium(III) isopropoxide with sulphur containing Schiff bases, we have reported on some interesting results. Thus, it was considered worthwhile to perform systematic investigations on indium-(III) complexes with a number of other Schiff bases.

The structures of the Schiff bases used in the present studied are shown below.

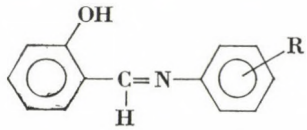
Results and discussion

The reactions of indium(III) isopropoxide with monobasic bidentate Schiff bases in 1 : 1 and 1 : 2 molar ratios can be represented by the following equations;

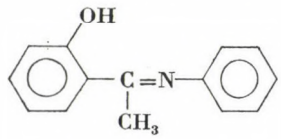
$$In(OPr^i)_3 + SBH \xrightarrow[\text{reflux}]{\text{benzene}} In(OPr^i)_2(SB) + Pr^iOH\uparrow$$

$$In(OPr^i)_3 + 2SBH \xrightarrow[\text{reflux}]{\text{benzene}} In(OPr^i)(SB)_2 + 2Pr^iOH\uparrow$$

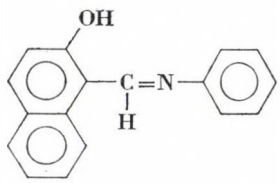
* To whom correspondence should be addressed



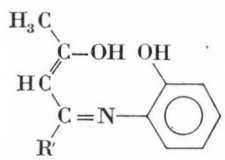
where R = H (SB_1H)
R = *o*-CH_3 (SB_2H)
R = *m*-CH_3 (SB_3H)
R = *p*-CH_3 (SB_4H)



(SB_5H)



(SB_6H)



where R′ = CH_3 ($SB_7'H_2$)
R′ = C_6H_5 ($SB_8'H_2$)

With dibasic tridentate Schiff bases in 1:1 and 2 : 3 molar ratios the following types of compounds are formed.

$$In(OPr^i)_3 + SB'H_2 \xrightarrow[\text{reflux}]{\text{benzene}} In(OPr^i)\,(SB') + 2Pr^iOH\uparrow$$

$$2In(OPr^i)_3 + 3SB'H_2 \xrightarrow[\text{reflux}]{\text{benzene}} In_2(SB')_3 + 6Pr^iOH\uparrow$$

All these newly synthesized metal complexes are yellow to orange-yellow solids (Table I) which are soluble in benzene, chloroform, acetone and tetrahydrofuran. The mono- and di-isopropoxy complexes are highly susceptible to hydrolysis. Their molecular weights have been determined and correspond to dimers. In 1 : 1 complexes of bidentate and tridentate Schiff bases the isopropoxy group acts as a bridge between the two indium atoms in which the indium atoms are penta-coordinated [2, 3] (**I** and **III** in Fig. 1), and in the 1 : 2 complexes, the indium atoms are hexa-coordinated (**II** in Fig. 1).

However, the 2 : 3 reaction products are quite stable towards hydrolysis and their molecular weights correspond to monomers. Keeping in view the monomeric nature of these complexes, the metal atom is tetra-coordinated [4] (**IV** in Fig. 1).

On hydrolysis of the complexes with aqueous benzene, the ligands could be separated and identified by TLC and IR.

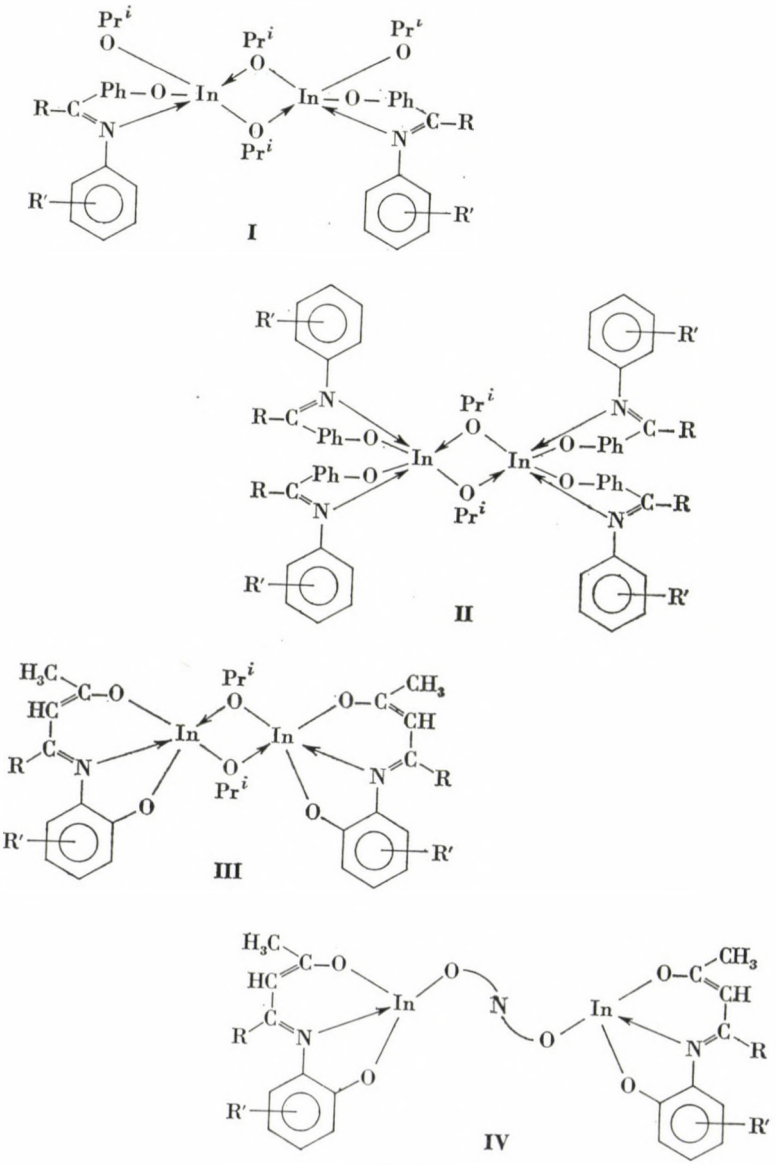


Fig. 1

Table I

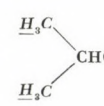
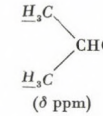
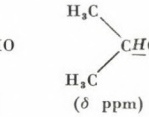
Reactions of indium(III) isopropoxide with Schiff bases in benzene

Reactants g (m-moles)	Molar ratio	Refluxing time (hrs)	Product and colour (yield %)	Melting point °C	Amount of isopropanol in the azeotrope (g) Found (Calcd)	Analysis % Found (Calcd)			
						In	C	H	N
$In(OPr^i)_3$ + SB_1H 0.47 0.32 (1.6) (1.6)	1 : 1	3	$In(OPr^i)_2(SB_1)$ Yellow (85)	148	0.09 (0.09)	26.1 (26.7)	52.6 (53.1)	5.5 (5.6)	3.0 (3.2)
$In(OPr^i)_3$ + SB_1H 0.54 0.73 (1.8) (3.7)	1 : 2	6	$In(OPr^i)(SB_1)_2$ Yellow (85)	69	0.21 (0.22)	20.0 (20.2)	61.1 (61.5)	4.8 (4.8)	4.5 (4.9)
$In(OPr^i)_3$ + SB_2H 0.54 0.37 (1.8) (1.8)	1 : 1	3	$In(OPr^i)_2(SB_2)$ Yellow (85)	172	0.10 (0.10)	25.3 (25.9)	53.8 (54.2)	5.8 (5.9)	3.0 (3.2)
$In(OPr^i)_3$ + SB_2H 0.38 0.56 (1.3) (2.5)	1 : 2	6	$In(OPr^i)(SB_2)_2$ Yellow (80)	73	0.15 (0.15)	18.8 (19.2)	62.0 (62.6)	5.1 (5.2)	4.4 (4.7)
$In(OPr^i)_3$ + SB_3H 0.47 0.34 (1.6) (1.6)	1 : 1	3	$In(OPr^i)_2(SB_3)$ Yellow (84)	146	0.09 (0.09)	25.3 (25.9)	53.8 (54.2)	5.8 (5.9)	2.9 (3.2)
$In(OPr^i)_3$ + SB_3H 0.50 0.73 (1.7) (3.4)	1 : 2	6	$In(OPr^i)(SB_3)_2$ Yellow (85)	70	0.19 (0.20)	18.9 (19.2)	62.1 (62.6)	5.2 (5.2)	4.3 (4.7)
$In(OPr^i)_3$ + SB_4H 0.48 0.35 (1.6) (1.6)	1 : 1	3	$In(OPr^i)_2(SB_4)$ Yellow (80)	166	0.10 (0.10)	25.4 (25.9)	53.8 (54.2)	5.8 (5.9)	3.0 (3.2)
$In(OPr^i)_3$ + SB_4H 0.39 0.57 (1.3) (2.7)	1 : 2	6	$In(OPr^i)(SB_4)_2$ Yellow (84)	71	0.16 (0.16)	18.8 (19.2)	62.1 (62.6)	5.2 (5.2)	4.4 (4.7)
$In(OPr^i)_3$ + SB_5H 0.46 0.33 (1.5) (1.5)	1 : 1	3	$In(OPr^i)_2(SB_5)$ Yellow (85)	179	0.09 (0.09)	25.2 (25.9)	53.8 (54.2)	5.7 (5.9)	3.0 (3.2)

$In(OPr)_3 + SB_5H$ 0.33 0.48 (1.1) (2.2)	1 : 2	6	$In(OPr^i)(SB_5)_2$ Yellow (80)	77	0.14 (0.14)	18.8 (19.2)	62.0 (62.6)	5.0 (5.2)	4.3 (4.7)
$In(OPr^i)_3 + SB_6H$ 0.56 0.48 (1.9) (1.9)	1 : 1	3	$In(OPr^i)_2(SB_6)$ Yellow (82)	171	0.11 (0.11)	23.3 (23.9)	57.1 (57.6)	5.3 (5.4)	2.5 (2.9)
$In(OPr^i)_3 + SB_6H$ 0.44 0.73 (1.5) (3.0)	1 : 2	6	$In(OPr^i)(SB_6)_2$ Yellow (80)	72	0.17 (0.18)	16.8 (17.2)	66.1 (66.7)	4.7 (4.7)	4.0 (4.2)
$In(OPr^i)_3 + SB'_7H_2$ 0.50 0.33 (1.7) (1.7)	1 : 1	8	$In(OPr^i)(SB'_7)$ Yellow (80)	253	0.19 (0.20)	31.3 (31.6)	45.9 (46.3)	5.0 (5.0)	3.4 (3.8)
$In(OPr^i)_3 + SB'_7H_2$ 0.44 0.48 (1.5) (2.3)	2 : 3	20	$In_2(SB'_7)_3$ Yellow (75)	270	0.26 (0.27)	28.6 (28.8)	49.2 (49.7)	4.0 (4.1)	5.0 (5.3)
$In(OPr^i)_3 + SB'_8H_2$ 0.42 0.36 (1.4) (1.4)	1 : 1	8	$In(OPr^i)(SB'_8)$ Orange yellow (82)	260	0.16 (0.17)	26.2 (27.0)	53.1 (53.8)	4.6 (4.7)	3.0 (3.3)
$In(OPr^i)_3 + SB'_8H_2$ 0.46 0.59 (1.6) (2.4)	2 : 3	20	$In_2(SB'_8)_3$ Orange yellow (80)	282	0.26 (0.28)	23.0 (23.3)	58.2 (58.7)	4.0 (4.0)	4.1 (4.3)

Table II

Spectral data (IR and ^1H NMR) of metal complexes

Compound	ν(C=N)	ν(C—O)	ν(M—O)	ν(M—N)		 (δ ppm)	 (δ ppm)
(1)	(2)	(3)	(4)	(5)	(6)	(7)	(8)
$In(OPr^i)_2(SB_1)$	1590s	1285s	600m	450w	1375m	1.3	4.1
$In(OPr^i)(SB_1)_2$	1590s	1285s	600m	440w	1375m	1.3	4.1
$In(OPr^i)_2(SB_2)$	1590s	1280s	580m	440w	1365m	1.2	4.1
$In(OPr^i)(SB_2)_2$	1590s	1280s	575m	450m	1365m	1.2	4.1
$In(OPr^i)_2(SB_3)$	1595s	1280s	600m	460m	1370s	1.3	4.1
$In(OPr^i)(SB_3)_2$	1590s	1285s	600m	460w	1385m	1.3	4.2
$In(OPr^i)_2(SB_4)$	1600s	1285m	590m	420w	1370m	1.4	4.2
$In(OPr^i)(SB_4)_2$	1600s	1280s	580m	430w	1370m	1.4	4.2
$In(OPr^i)_2(SB_5)$	1600s	1260m	530m	440w	1360m	1.4	4.2
$In(OPr^i)(SB_5)_2$	1600s	1265m	530m	440m	1360m	1.4	4.2
$In(OPr^i)_2(SB_6)$	1605s	1265s	560m	440w	1380s	1.2	4.2
$In(OPr^i)(SB_6)_2$	1605s	1265s	560m	440m	1380m	1.2	4.1
$In(OPr^i)(SB'_7)$	1585s	1260s	565m	450m	1360m	1.3	4.1
$In_2(SB'_7)_3$	1585s	1270s	560m	450m	—	—	—
$In(OPr^i)(SB'_8)$	1585s	1280s	550m	450m	1365m	1.3	4.1
$In_2(SB'_8)_3$	1590s	1280m	550m	460m	—	—	—

IR spectra (Table II of the Schiff bases show a band at ~3300—3100 cm^{-1} which is assigned to ν(OH) vibration. In complexes the ν(OH) band disappears completely indicating the deprotonation of the ligands on chelation with the metal atom. IR spectra of the ligands show an intense band in the region 1620—1610 cm^{-1} which is assigned to the ν(C=N) vibration of the azomethine linkage. This band is lowered by ~10—15 cm^{-1} in the spectra of the complexes. The downward shift of this band is consistent with the coordination of the azomethine nitrogen to the metal atom [5, 6]. In the Schiff bases, a strong band occurring at ~1270—1240 cm^{-1} can be assigned to phenolic ν(C—O) vibrations. In the complexes, this band is shifted ~10—20 cm^{-1} towards higher frequencies indicating bond formation with the phenolic oxygen atom. The bands observed in the region 610—370 cm^{-1} may be attributed to the different vibrational modes of (M—O) and (M—N) bonds [7]. In addition to this, the IR spectra of the complexes containing isopropoxy groups show new bands in the region 1380—1360 cm^{-1} 1160—1140 cm^{-1} and 1130—1120 cm^{-1}. The first band is characteristic of a gem-dimethyl group and the latter of isobranching vibrations of the isopropoxy group [8].

Thus the infrared spectra reflect that these Schiff bases behave as bidentate (ON) or tridentate (ONO) ligands and form rings through the azomethine nitrogen and the phenolic oxygen.

The ^{1}H NMR spectra of the ligands show the OH proton signal at δ 12.8—13.4 ppm. The disappearance of this signal in the complexes thereby shows the deprotonation of the ligand. The complexes further show a septet centered at δ 4.1—4.2 ppm and a doublet centered at δ 1.2—1.3 ppm due to $>$CH and CH_3 protons, of the isopropoxy group, respectively.

The electronic spectra of the complexes recorded in benzene show a single band in the region 25,640—24,096 cm^{-1} (390—415 nm) which may be assigned to a charge transfer transition. This may also be assigned to either n-π^* or π—π^* transitions of the azomethine group ($>$C=N).

Thus on the basis of analytical data, molecular weight and spectral (infrared, ^{1}H NMR and electronic) studies, the following structures can be suggested for the complexes.

Experimental

All glass apparatus fitted with interchangeable joints was used and special precaution was taken to exclude moisture. Hydrated indium(III) chloride ($InCl_3 \cdot 3H_2O$, B.D.H.) was made anhydrous by refluxing with dry thionylchloride for about 6 hours and finally dried under vacuum before use. Indium(III) isopropoxide was prepared by the sodium method [9]. The ligands were synthesized by the condensation of an aldehyde/ketone with aryl amine in dry ethanol [10, 11].

The metal content was determined gravimetrically as oxide. Isopropanol was estimated by oxidation with potassium dichromate (1 *M*) in 12.5% sulphuric acid [12]. Molecular weights were determined ebullioscopically in refluxing benzene using a Gallenkamp instrument using thermistor sensing. IR spectra were recorded on a grating spectrophotometer, Perkin-Elmer-621, as KBr pellets. The electronic spectra were recorded on a Perkin-Elmer-554 (UV-VIS) spectrophotometer and ^{1}H-NMR spectra on a Parkin-Elmer R-32 spectrometer in $CDCl_3$.

Reaction of indium(III) isopropoxide with salicylideneaniline (SB_1H) (1 : 1 molar ratio)

A clear solution of indium(III) isopropoxide (0.47 g, 1.6 mm) and salicylidene-aniline (0.32 g, 1.6 mm) in dry benzene (60 mL) was refluxed in an oil bath at 110° for three hours. The benzene : isopropanol azeotrope was distilled slowly between 74 and 80° followed by benzene, leaving a yellow solution in the reaction flask. The remaining benzene was distilled under reduced pressure to give a yellow solid in quantitative yield. The yellow solid was recrystallized from a 1 : 1 *n*-hexane-benzene mixture.

As the synthetic procedure used in all the reactions was the same, details are given for the 1 : 1 molar ratio only. The other reactions are summarized in Table I.

The labile nature of the isopropoxy group of the complexes was shown by their exchange reactions with *t*-butanol, and the resulting *t*-butoxy products have been isolated and analyzed.

*

One of us (S.B.) thanks the University Grants Commission, Delhi, and the Government of Tamil Nadu for the award of a Teacher-Fellowship under the Faculty Improvement Programme.

REFERENCES

[1] Baskaran, S., Kapoor, R. N.: Synth. React. Inorg. Met. Org. Chem., **13,** 305 (1983)
[2] Beattie, L. R., Tilson, T., Ozin, G. A.: J. Chem. Soc. (London) A, **1968,** 1092
[3] Agrawal, M., Tandon, J. P., Mehrotra, R. C.: Ind. J. Chem., **18A,** 151 (1979)
[4] Agrawal, M., Tandon, J. P., Mehrotra, R. C.: Current Sci., **50,** 174 (1981)
[5] Kovacic, J. E.: Spectrochim. Acta, **23A,** 183 (1967)
[6] Patton, R. D., Taylor, L. T.: Inorg. Chim. Acta, **8,** 191 (1974)
[7] Biradar, N. S., Locker, A. L.: J. Inorg. Nucl. Chem., **36,** 1915 (1974)
[8] Lynch, C. T., Masdiyaani, K. S., Smith. J. S., Grawford, W. J.: Anal. Chem., **36,** 2332 (1964)
[9] Mehrotra, R. C., Bindal, S. R., Chatterjee, S.: J. Indian Chem. Soc., **53,** 867 (1976)
[10] Osipov, O. A., Minkin, V. I., Dsh. Verknovodova Knyazhanskii, M. L.: Zh. Org. Khim., **12,** 1549 (1967)
[11] Mayadeo, M. S.: J. Ind. Chem. Soc., **11,** 502 (1975)
[12] Mehrotra, R. C.: J. Ind. Chem. Soc., **31,** 904 (1954)

Acta Chimica Hungarica 116 (1), pp. 21—27 (1984)

1-BENZOYL-1-PHENYLHYDRAZINE AS A PYRAZOLE PRECURSOR

H. A. HAMMOUDA[1]* and A. A. EL-BARBARY[2]

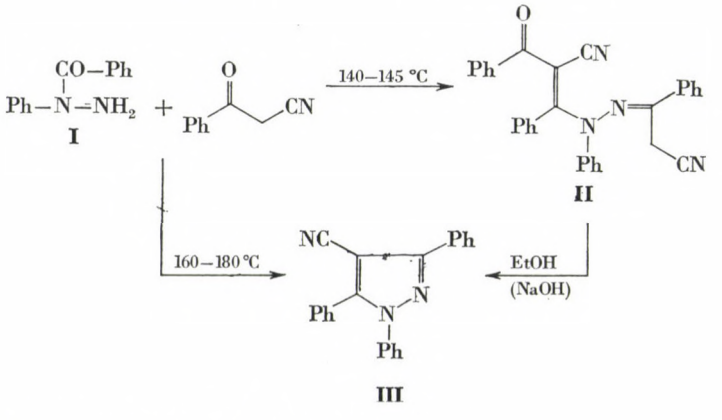
([1]Chemistry Department, Faculty of Science, Cairo University, Giza and [2]Tanta University, Tanta, A. R. Egypt)

Received March 28, 1983
Accepted for publication June 7, 1983

1-Benzoyl-1-phenylhydrazine (**I**) reacted with benzoylacetonitrile and ethyl cyanoacetate to afford pyrazole derivatives, **III** and **V**, respectively. The reactions of **I** with fluorinated β-diketones were also investigated and a pyrazole derivative, **XI**, was obtained.

Pyrazoles are generally synthesized either via condensation of hydrazines with β-bifunctional reagents or by addition of diazomethane or nitrile-imines to activated double bond systems [1]. Although 1-acyl-1-substituted hydrazines seem to be interesting precursors for pyrazole derivatives through their condensation with bifunctional reagents, few examples for the synthesis of pyrazoles by this method have been reported [2—4]. We have an increasing interest in investigating the biological activity of pyrazole derivatives. For this purpose, samples of cyano-, ethoxycarbonyl- and perfluoroalkyl--pyrazole derivatives were required. The results of the experiments aimed at synthesizing these derivatives are presented here.

For the synthesis of 4-cyano-polyarylpyrazoles, it has been found that the nature of the reaction product of 1-benzoyl-1-phenylhydrazine (**I**) with benzoylacetonitrile depends on the reaction conditions. Thus, when **I** and benzoylacetonitrile were heated at 140—145 °C, compound **II** was the main

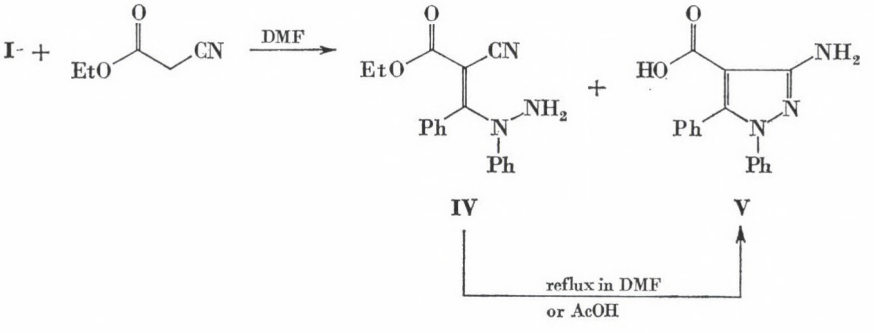


* To whom correspondence should be addressed

isolable product. On the other hand, heating at 160—180 °C afforded 1,3,5--triphenyl-4-cyanopyrazole, **III**, which had been prepared according to the literature, by other methods [5, 6].

Compound **II** could be converted into **III** by the action of ethanolic sodium hydroxide. The IR spectrum of **II** showed peaks at 2220, 2200 cm^{-1} (two cyano groups) and 1630 (CO group). The IR spectrum of **III** showed the cyano group at 2220 cm^{-1}.

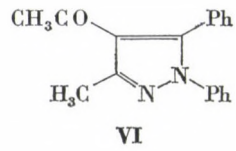
When **I** was boiled under reflux with ethyl cyanoacetate in DMF a mixture of the pyrazole **V** and the arylidene compound **IV** was obtained. The latter (**IV**) could be converted into the pyrazole **V** by prolonged reflux in DMF or acetic acid. The IR spectrum of **IV** showed peaks at 3220 cm^{-1} (NH_2), 2270 (CN) and 1650 (CO). The IR spectrum of **V** had peaks at 3320 cm^{-1} (NH_2), 2900—2000 (with the ragged appearance of the spectrum characteristic of a carboxylic group) and 1650 cm^{-1} (CO).



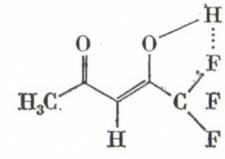
A number of heterocyclic compounds containing a perfluoroalkyl group, espacially CF_3, are of pharmaceutical and agrochemical interest [7]. However, the number of compounds of this kind is limited, because the introduction of a perfluoroalkyl group into a heterocyclic ring is usually not easy [8, 9]. In continuation of our previous work [10, 11] in which some fluorine-containing heterocycles were synthesized, we tried here the synthesis of perfluoroalkyl-pyrazoles.

The reaction of **I** with acetylacetone has been reported [3, 4] to give the pyrazole derivative **VI**. So we expected that **I** would cyclize with the fluorinated β-diketones **VIIa—e** to afford perfluoroalkylpyrazoles. However, in most cases acyclic hydrazones (**VIII**) were obtained and it was in one case only that a pyrazole derivative could be isolated.

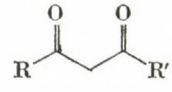
Thus, 1,1,1-trifluoropentan-2,4-dione (**VIIa**), which probably exists in the enol form **IX**, was allowed to react with **I** in ethanol at 40 °C to yield a product for which structure **VIIIa** seemed possible, based on elemental and spectral analyses.



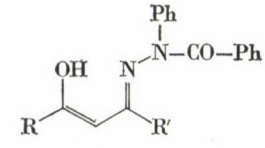
VI



IX



VII



VIII

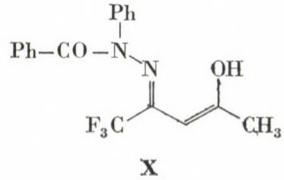
	R	R′
a:	CF_3	CH_3
b:	CF_3	C_6H_5
c:	C_2F_5	CH_3
d:	C_2F_5	C_6H_5
e:	CF_3	C_6H_4Cl-*p*

	R	R′
a:	CF_3	CH_3
b:	CF_3	C_6H_5
c:	C_2F_5	CH_3
d:	C_2F_5	C_6H_5

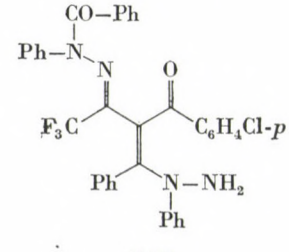
The IR spectrum of **VIIIa** had peaks at 1690 cm^{-1} (CO—Ph) and 1610 (C=N). Its ^{1}H-NMR spectrum ($CDCl_3$) showed signals at δ2.2 ppm (s, 3H, CH_3), δ5.5 (s, 1H, olefinic proton), δ7.1—7.6 (m, 10H, aromatic protons) and δ12.2 (broad s, 1H, OH, disappearing on D_2O exchange). The ^{19}F-NMR spectrum ($CHCl_3$) had one signal at δ-2.0 ppm for the CF_3 group, which is almost the same position as measured for the CF_3 in **VIIa**. Other theoretically possible structures, such as **X**, would require a much lower chemical shift for the CF_3 group in the ^{19}F-NMR spectrum of the product.

Compound **I** reacted with **VIIb** in ethanol in the presence of a catalytic amount of sulfuric acid to give the hydrazone **VIIIb** in a good yield.

The IR spectrum of **VIIIb** showed peaks at 1670 cm^{-1} (CO—Ph) and, 1610 (C=N). The ^{1}H-NMR spectrum ($CDCl_3$) had peaks at δ5.6 ppm (s, 1H,



X

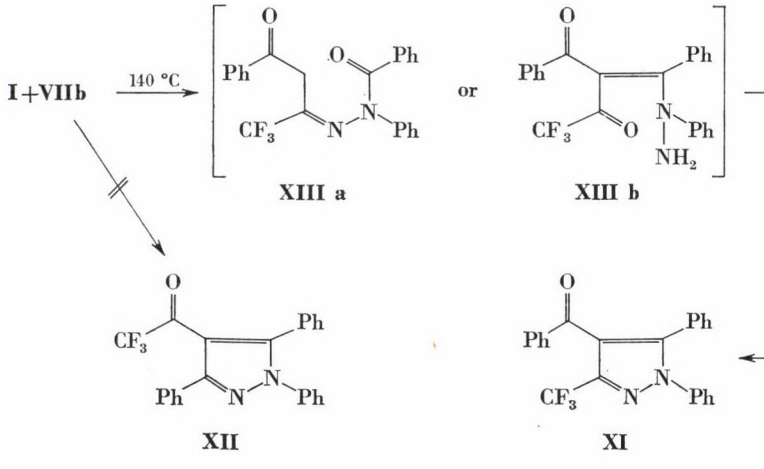


XIV

olefinic proton), δ6.9—7.8 (m, 15H, aromatic protons) and δ12.2 (broad s 1H, OH, absent after D_2O exchange). The ^{19}F-NMR spectrum ($CHCl_3$) showed the CF_3 signal at δ-1.83 ppm.

On the other hand, fusion of **I** and **VIIb** at 140 °C afforded a product of molecular formula $C_{23}H_{15}F_3N_2O$. Two structures, **XI** and **XII**, seemed possible for this compound. Structure **XI** was more favoured based on spectral evidence. Thus ^{19}F-NMR showed the CF_3 resonance at δ-18.3 ppm, which is different from that expected for a trifluoroacetyl group but is in agreement with a CF_3 group. The IR spectrum of the reaction product also revealed the C=O absorption at 1670 cm^{-1}, a much lower value than expected for a CF_3CO group (about 1780 cm^{-1}) [12]. The ^{1}H-NMR analysis also supported structure **XI**. Thus the aromatic protons are separated into a high-field 13-proton signal at δ7.2 ppm and a lower field 2-proton signal at δ7.6 ppm. If this product were **XII**, one would expect the four *ortho* protons of the phenyl groups at C_3 and C_5 to be shifted to lower field by the anisotropy of the carbonyl group. Moreover, the MS spectrum of the compound showed the molecular ion M^+ 392, as well as other fragment peaks at 315 (M^+-Ph), 105 (Ph—CO^+), 77 (Ph^+) and 69 (CF_3^+).

Compound **XI** can be formed via the intermediate **XIIIa** or **XIIIb**. Attempts to isolate such an intermediate remained unsuccessful. However, the intermediate role of **XIIIa** seems more likely in view of the ease of hydrazone formation under much milder conditions.



The diketones **VIIc, d** reacted with **I** on heating at 120—130 °C to give the hydrazones **VIIIc, d** in good yields.

The IR spectrum of **VIIIc** had peaks at 1690 cm^{-1} (CO—Ph) and 1610 (C=N). The ^{1}H-NMR ($CDCl_3$) showed signals at δ2.2 ppm (s, 3H, CH_3), δ5.5 (s, 1H, olefinic proton), δ6.8—7.8 (m, 10H, aromatic protons) and δ12.3

(broad s, 1H, OH, absent after D_2O exchange). The ^{19}F-NMR spectrum (acetone) indicated the C_2F_5 group as two signals at δ5.0 ppm (CF_3) and δ44.3 (CF_2) in the ratio of 3 : 2. Similarly, the spectral data of **VIIId** were in agreement with the assigned structure; IR: 1680 cm^{-1} (CO—Ph) and 1620 (C=N); ^{1}H-NMR (CCl_4): δ5.5 ppm (s, 1H, olefinic proton), δ6.6—7.2 (m, 15H, aromatic protons) and δ12.0 (broad s, 1H, OH); ^{19}F-NMR (CCl_4): δ3.6 ppm and 43.3 (ratio 3 : 2) for CF_3—CF_2 group.

On the other hand, the reaction of **I** and **VIIe** at 120 °C afforded a product to which structure **XIV** could be assigned according to elemental and spectral analyses.

The IR spectrum of **XIV** had a peak at 1660 cm^{-1} for a carbonyl group. The ^{1}H-NMR spectrum ($CDCl_3$) showed a multiplet at δ6.9—8.0 ppm for the aromatic protons. The ^{19}F-NMR spectrum (acetone) had one signal at δ-18.3 ppm, due to the CF_3 group.

Experimental

M.p.'s are uncorrected. IR spectra were taken in KBr with a Pye-Unicam SP 1000 Spectrophotometer. ^{1}H-NMR spectra were recorded on a Hitachi 60 MHz instrument using TMS as internal standard. ^{19}F-NMR spectra were taken with a Hitachi RF 24 Spectrometer using TFA as external standard.

Reaction of I with benzoylacetonitrile at 140—145 °C

A mixture of **I** (2.12 g; 10 mmol) and benzoylacetonitrile (1.45 g; 10 mmol) was heated at 140—145 °C for 1 h and then allowed to cool. The product was triturated with ethanol, dried and crystallized from acetic acid to give **II**, m.p. 291 °C; yield 30%.

$C_{31}H_{22}N_4O$ (466.55). Calcd. C 79.81; H 4.75. Found C 79.60; H 4.70%.

4-Cyano-1,3,5-triphenylpyrazole (III)

A mixture of **I** (2.12 g; 10 mmol) and benzoylacetonitrile (1.45 g; 10 mmol) was heated at 160—180 °C for 1 h and then left to cool. Trituration with ethanol gave **III**, crystallized from ethanol, m.p. 185 °C; yield 40%.

$C_{22}H_{15}N_3$ (321.39). Calcd. C 82.22; H 4.70; N 13.07. Found C 82.60; H 4.60; N 13.40%.

Reaction of II with ethanolic sodium hydroxide

A solution of **II** (2 g) in ethanol (50 mL) was mixed with 2 mL of 5 *M* NaOH solution. The reaction mixture was kept at room temperature for 1 h and then diluted with water. The solid obtained was filtered off, washed with water, dried and crystallized from ethanol to give **III** (m.p. and mixed m.p.).

Reaction of I with ethyl cyanoacetate

A solution of **I** (10 mmol) in DMF (30 mL) was treated with ethyl cyanoacetate (1.13 g; 10 mmol) and was then refluxed for 10 h. The DMF was removed in vacuum and ethanol was added. The resulting solid was filtered off and crystallized from DMF to give 3-amino-4--carboxy-1,5-diphenylpyrazole (**V**). Evaporation of the filtrate gave ethyl 2-cyano-3-phenyl-3--(1-phenylhydrazino)propenoate (**IV**).

Compound **V** was obtained in 40% yield, m.p. 250 °C.

$C_{16}H_{13}N_3O_2$ (279.30). Calcd. C 68.81; H 4.69. Found C 68.60; H 4.50%.

IV was crystallized from ethanol, m.p. 157 °C; yield 40%.

$C_{18}H_{17}N_3O_2$ (307.36). Calcd. C 70.34; H 5.57. Found C 69.80; H 5.40%.

Conversion of IV into V

Compound **IV** (2 g) was refluxed in DMF (20 mL) for 10 h. The solid that separated on cooling was filtered off and recrystallized from DMF to give **V** (m.p. and mixed m.p.).

5,5,5-Trifluoro-4-hydroxy-3-penten-2-one *N*-benzoyl-*N*-phenylhydrazone (VIIIa)

A solution of **I** (1.06 g; 5 mmol) and **VIIa** (0.77 g; 5 mmol) in ethanol (30 mL) was stirred at 40 °C for 30 min. The solid that separated was filtered off, washed with ethanol and dried to give 1.5 g of **VIIIa**. It was crystallized from ethanol, m.p. 157 °C.

$C_{18}H_{15}F_3N_2O_2$ (348.33). Calcd. C 62.07; H 4.34; N 8.04. Found C 62.04; H 4.39; N 8.09%.

4,4,4-Trifluoro-3-hydroxy-1-phenyl-2-buten-1-one *N*-benzoyl-*N*-phenylhydrazone (VIIIb)

A mixture of **I** (2.12 g; 10 mmol) and **VIIb** (2.16 g; 10 mmol) in 50 mL of ethanol containing 0.5 mL of *conc.* sulfuric acid was refluxed for 10 h. The ethanol was removed in vacuum and the remaining oily product was triturated with benzene. The resulting solid was filtered off and identified as the sulfate of **I**. The filtrate was chromatographed on silica gel using benzene as eluent. Evaporation of the benzene in vacuum afforded a solid, which was crystallized from *n*-pentane to give 2.1 g of **VIIIb**, m.p. 104 °C.

$C_{23}H_{17}F_3N_2O_2$ (410.40). Calcd. C 67.31; H 4.18; N 6.83. Found C 67.76; H 4.16; N 6.79%.

4-Benzoyl-1,5-diphenyl-3-trifluoromethylpyrazole (XI)

A mixture of **I** (2.12 g; 10 mmol) and **VIIb** (2.16 g; 10 mmol) was heated at 130—140 °C for 1 h and then left to cool. The oily product was dissolved in *n*-hexane and chromatographed on silica gel. The solid which separated after evaporating the *n*-hexane was crystallized from ethanol to give 1.25 g of **XI**, m.p. 127 °C.

$C_{23}H_{15}F_3N_2O$ (392.38). Calcd. C 70.40; H 3.85; N 7.14. Found C 70.13; H 3.95; N 7.20%.

Reaction of I with VIIc, d

A mixture of 10 mmol of **I** and 10 mmol of **VIIc** or **VIId** was heated at 120—130 °C for 1 h and then left to cool. The reaction mixture was triturated with petroleum ether, dried and crystallized. **VIIIc** was crystallized from aqueous ethanol; m.p. 108 °C; yield 71%.

$C_{19}H_{15}F_5N_2O_2$ (398.34). Calcd. C 57. 29; H 3.80; N 7.03; Found C 57.20; H 3.98; N 7.18%.

VIIId was crystallized from *n*-hexane; m.p. 104 °C; yield 55%.

$C_{24}H_{17}F_5N_2O_2$ (460.41). Calcd. C 62.61; H 3.72; N 6.08. Found C 62.33; H 3.59; N 6.19%.

Reaction of I with VIIe

A mixture of **I** (2.12 g; 10 mmol) and **VIIe** (2.5 g; 10 mmol) was heated at 120 °C for 1 h and then left to cool. The oily product was dissolved in *n*-hexane and chromatographed on silica gel. The solid which separated after evaporating the *n*-hexane was crystallized from aqueous ethanol to give **XIV**, m.p. 218 °C; yield 8%.

$C_{36}H_{26}F_3ClN_4O_2$ (639.08). Calcd. C 67.66; H 4.10; N 8.77. Found C 67.55; H 3.79; N 9.02%.

REFERENCES

[1] Behr, L. C., Fusco, R., Jarboe, C. H.: The Chemistry of Heterocyclic Compounds-Pyrazoles, Pyrazolines, Pyrazolidines, Indazoles and Condensed Rings (Ed. A. Weissberger), Interscience Publishers, New York 1967

[2] Alemagna, A., Bacchtti, R., Rossi, S.: Gazz. Chim. Ital., **93,** 748 (1963)
[3] El-Sayed, A. A., Ohta, M.: Bull. Chem. Soc. Jpn., **46,** 947 (1973)
[4] Al-Saleh, F. S., Khawaja, I. K., Joule, J. A.: J. Chem. Soc. Perkin Trans. 1, **1981,** 642
[5] Fusco, R., Justoni, R.: Gazz. Chim. Ital., **67,** 3 (1937)
[6] Cusmano, S., Tiberio, T.: Gazz. Chim. Ital., **86,** 507 (1956)
[7] See, e.g., Filler, R.: Advances in Fluorine Chemistry, Vol. **6,** 1, 1970; Filler, R.: Chem. Tech., **4,** 752 (1974)
[8] Kobayashi, Y., Kumadaki, A.: Yuki Gosei Kagaku Kyokai Shi, **29,** 126 (1971)
[9] Kobayashi, Y., Kumadaki, Y., Osawa, A.: Yuki Gosei Kagaku Kyokai Shi, **31,** 477 (1973)
[10] Hammouda, H. A., Ishikawa, N.: Bull. Chem. Soc. Jpn., **51,** 3091 (1978)
[11] Kawa, H., Hammouda, H. A., Ishikawa, N.: Bull. Chem. Soc. Jpn., **53,** 1694 (1980)
[12] Bellamy, L. J.: The Infrared Spectra of Complex Molecules, p. 141, Methuen & Co. Ltd., London 1964

Acta Chimica Hungarica 116 (1), pp. 29—37 (1984)

CARBOXYLATO DERIVATIVES OF MONO(CYCLOPENTADIENYL)TITANIUM(IV)

O. P. PANDEY, S. K. SENGUPTA* and S. C. TRIPATHI

(Department of Chemistry, University of Gorakhpur, Gorakhpur-273001, India)

Received April 19, 1983

Accepted for publication June 7, 1983

Preparation of titanium(IV) complexes of the types $CpTi(OOCR)Cl_2$ and $CpTi(OOCR)_2Cl$ has been carried out by reacting $CpTiCl_3$ and carboxylic acids (R = = C_7H_{15}, $C_{11}H_{23}$, $C_{13}H_{27}$, $C_{15}H_{31}$, $C_{17}H_{35}$ and $C_{21}H_{43}$; Cp = η^5-cyclopentadienyl) in the desired metal to ligand ratio in tetrahydrofuran in the presence of a base. These compounds have been characterized by elemental analysis, electrical conductance, magnetic susceptibility measurements and i.r. spectra. Ebullioscopic molecular weight determinations show them to be trimeric and monomeric, respectively, in benzene.

Despite the considerable interest in metal carboxylates [1, 2], very little has been reported with early transition metals [3—5]. Carboxylic acids can coordinate by several different bonding interactions depending upon reaction conditions, nature of metal ion and pH of the medium [6]. A number of papers on carboxylic acid derivatives of Ti(III) and Ti(IV) have appeared in the literature [7—9] but only one paper on mono(cyclopentadienyl)titanium(IV) with simple carboxylic acids has appeared so far [10]. Such a study appears to be useful in view of the fact that organometallic compounds of titanium are found to be capable of activating molecular nitrogen and also used as oxygen carriers of biological interest [11, 12]. In the present communication, we report the preparation and characterization of mono(cyclopentadienyl)-titanium(IV) derivatives with caprylic, lauric, myristic, palmitic, stearic and behenic acids.

Experimental

All experimental operations were carried out under strictly anhydrous condition, and glass apparatus with interchangeable joints was used. All the carboxylic acids used in the present investigations (caprylic, lauric, myristic, palmitic, stearic and behenic) were redistilled before use. Mono(cyclopentadienyl)titanium(IV) trichloride was prepared from Cp_2TiCl_2 and $TiCl_4$ in *p*-xylene [13]. THF (Baker AR) was dried by storage on sodium wire overnight and then refluxed until it a gave a blue colouration with benzophenone. It was finally dried by distilling over $LiAlH_4$. Triethylamine and *n*-butylamine were purified by the given methods [14].

Titanium was determined gravimetrically as TiO_2 and chloride as AgCl. The carbon and hydrogen analyses were carried out at Central Drug Research Institute, Lucknow.

Molecular weight determinations were carried out ebullioscopically in boiling benzene using a Gallenkemp (U.K.) ebulliometer. Conductance measurements were done in nitrobenzene using a Beckman conductivity Bridge Model No. RC-18A. Solid state infrared spectra were recorded on a Perkin-Elmer 621 grating spectrophotometer in KBr medium in the range

* To whom correspondence should be addressed

Table I

Reactions of $CpTiCl_3$ *with carboxylic acids in* 1 : 1 *molar ratio*

Reactants (Molar ratio)	Stirring time (h)	Product, colour and dec. temp. (°C)	Mol. wt. Found (Calcd.)	Found (Calcd.) %			
				Ti	C	H	Cl
$CpTiCl_3 + C_7H_{15}COOH + BuNH_2$ (1 : 1 : 1)	30	$CpTi(OOCC_7H_{15})Cl_2$ Orange, 180	970 (326.9)	14.4 (14.6)	47.5 (47.7)	6.1 (6.1)	21.5 (21.7)
$CpTiCl_3 + C_{11}H_{23}COOH + BuNH_2$ (1 : 1 : 1)	30	$CpTi(OOCC_{11}H_{23})Cl_2$ Yellow, 228	1140 (382.9)	12.5 (12.5)	53.0 (53.3)	7.1 (7.3)	18.2 (18.5)
$CpTiCl_3 + C_{13}H_{27}COOH + BuNH_2$ (1 : 1 : 1)	32	$CpTi(OOCC_{13}H_{27})Cl_2$ Yellow, 210	1225 (410.9)	11.6 (11.6)	55.1 (55.5)	7.4 (7.8)	17.2 (17.3)
$CpTiCl_3 + C_{15}H_{31}COOH + BuNH_2$ (1 : 1 : 1)	34	$CpTi(OOCC_{15}H_{31})Cl_2$ Brown, 150	1310 (438.9)	10.7 (10.9)	57.2 (57.4)	8.1 (8.2)	16.0 (16.2)
$CpTiCl_3 + C_{17}H_{35}COOH + BuNH_2$ (1 : 1 : 1)	34	$CpTi(OOCC_{17}H_{35})Cl_2$ Orange, 130	1400 (466.9)	9.9 (10.2)	59.0 (59.1)	8.4 (8.4)	15.2 (15.2)
$CpTiCl_3 + C_{21}H_{43}COOH + BuNH_2$ (1 : 1 : 1)	34	$CpTi(OOCC_{21}H_{43})Cl_2$ Orange, 250	1560 (522.9)	9.0 (9.2)	61.9 (62.0)	9.1 (9.2)	13.5 (13.6)

Table II

Reactions of $CpTiCl_3$ *with carboxylic acids in* 1 : 2 *molar ratio*

Reactants (Molar ratio)	Stirring time (h)	Product, colour and dec. temp. (°C)	Mol. wt. Found (Calcd.)	Found (Calcd.) %			
				Ti	C	H	Cl
$CpTiCl_3 + C_7H_{15}COOH + Et_3N$ (1 : 2 : 2)	24	$CpTi(OOCC_7H_{15})_2Cl$ Dark yellow, 260	430 (434.4)	11.0 (11.0)	57.8 (58.0)	7.8 (8.0)	8.0 (8.2)
$CpTiCl_3 + C_{11}H_{23}COOH + Et_3N$ (1 : 2 : 2)	24	$CpTi(OOCC_{11}H_{23})_2Cl$ Orange, 190	538 (546.4)	8.7 (8.8)	63.4 (63.7)	9.2 (9.3)	6.3 (6.5)
$CpTiCl_3 + C_{13}H_{27}COOH + Et_3N$ (1 : 2 : 2)	24	$CpTi(OOCC_{13}H_{27})_2Cl$ Orange, 280	598 (602.4)	7.7 (7.9)	65.3 (65.7)	9.8 (9.8)	5.9 (5.9)
$CpTiCl_3 + C_{15}H_{31}COOH + Et_3N$ (1 : 2 : 2)	24	$CpTi(OOCC_{15}H_{31})_2Cl$ Brown, 170	655 (658.4)	7.1 (7.3)	67.3 (67.4)	10.0 (10.2)	5.2 (5.4)
$CpTiCl_3 + C_{17}H_{35}COOH + Et_3N$ (1 : 2 : 2)	24	$CpTi(OOCC_{17}H_{35})_2Cl$ Dark yellow, 150	710 (714.4)	6.7 (6.7)	68.6 (68.9)	10.2 (10.5)	4.9 (5.0)
$CpTiCl_3 + C_{21}H_{43}COOH + Et_3N$ (1 : 2 : 2)	24	$CpTi(OOCC_{21}H_{43})_2Cl$ Orange, 175	821 (826.4)	5.6 (5.8)	71.0 (71.1)	11.0 (11.0)	4.2 (4.2)

4000—200 cm^{-1}. Magnetic measurements were performed by Gouy's method using copper sulphate as a calibrant. The electronic spectra of the complexes were taken on a Perkin-Elmer 4000 A°. Proton NMR spectra of the ligands and the complexes were recorded on a Perkin-Elmer R-32 spectrometer at a sweep width of 900 Hz.

Preparation of $CpTi(OOCR)Cl_2$

Freshly distilled carboxylic acids (1.0 mmol) were added to a solution of mono(cyclopentadienyl) titanium(IV) trichloride (1.0 mmol) in dry THF (~60 mL). To this *n*-butylamine (1.0 mmol) was added, the mixture was stirred for ~30—34 h. The complex which precipitated was filtered, whereas the soluble amine hydrochloride remained in the solution. The precipitate was dried and crystallized from benzene. Yield ~75—80%.

Preparation of $CpTi(OOCR)_2Cl$

To a mixture of mono(cyclopentadienyl) titanium(IV) trichloride (1.0 mmol) and carboxylic acid (2.0 mmol) dissolved in dry THF (~60 mL) triethylamine (2.0 mmol) was added. The mixture was stirred for 24 h. The separated $Et_3N \cdot HCl$ was removed by filtration and the solvent was removed under reduced pressure. The complex was crystallized from a THF/hexane mixture. Yield ~80%.

The analytical data of the complexes prepared are given in Tables I and II.

Results and Discussion

Reactions of $CpTiCl_3$ with different carboxylic acids viz. caprylic, lauric, myristic, palmitic, stearic and behenic acids in anhydrous tetrahydrofuran in the presence of *n*-butylamine or triethylamine may be represented by the following general equation;

$$CpTiCl_3 + RCOOH + \text{amine} \xrightarrow[\text{room temp.}]{\text{THF}} CpTi(OOCR)Cl_2\downarrow + \text{amine} \cdot HCl$$

$$CpTiCl_3 + 2RCOOH + 2\ \text{amine} \xrightarrow[\text{room temp.}]{\text{THF}} CpTi(OOCR)_2Cl + 2\ \text{amine} \cdot HCl\downarrow$$

All the above reactions proceed readily and the resulting compounds can be isolated in almost quantitative yields. The complexes are yellow to orange in colour, nonvolatile, extremely sensitive to hydrolysis and decompose on heating between 130 and 280 °C. Electrical conductance measured in nitrobenzene showed them to be essentially nonelectrolytes. Magnetic susceptibility values at room temperature show their diamagnetic nature. The ebullioscopic molecular weight determinations show the $CpTi(OOCR)Cl_2$ derivatives to be trimeric and $CpTi(OOCR)_2Cl$ monomeric in benzene, indicating the possibility of chlorine to be involved in the molecular association. The presence of two electronegative chlorine atoms in $CpTi(OOCR)Cl_2$ derivatives seems to increase the electropositive character of titanium and consequently, its electron acceptor tendency increases and thus probably causing intermolecular association. The $CpTi(OOCR)_2Cl$ derivatives, in which one chloride ion is replaced by a

bulky carboxylate group, are expected to possess comparatively less electropositive titanium thereby resulting in a decrease in their molecular association tendency.

Electronic spectra

The electronic spectra of all the carboxylato complexes of mono(cyclopentadienyl) titanium(IV) were recorded in chloroform. All complexes show a single band in the region 23800—24500 cm^{-1} which can be assigned to their charge-transfer band [15, 16] and is in accordance with their $(n—1)d^{\circ}$ ns° electronic configuration.

Infrared spectra

The important IR frequencies are given in Table III. Absorption bands occurring at $\sim$3000 cm^{-1} ν(C—H), $\sim$1430 cm^{-1} ν(C—C), $\sim$1020 cm^{-1} δ(—CH) and at $\sim$810 cm^{-1} δ(—CH) in the complexes indicate the presence of cyclopentadienyl moiety. All these bands are similar to those of mono(cyclopentadienyl)-titanium(IV) [4, 17]. Davison and Rakita have pointed out that above 3000 cm^{-1}, η^1-C_5H_5 groups should show four bands whereas η^5-C_5H_5 should show only one [18]. In the complexes reported in this paper, only one band near 3000 cm^{-1} indicates the pentahapto nature of cyclopentadienyl ring. However, in some areas of the spectrum, there is considerable overlap between bands due to cyclopentadienyl, bands due to alkyl groups and bands due to

Table III

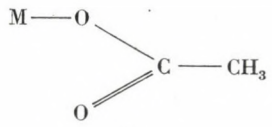
Characteristic infrared bands (cm^{-1})

Compound	$\nu_{asym.COO}$	$\nu_{sym.COO}$	$\Delta\nu$	ν(Ti—O)	ν(Ti—Cl)
$CpTi(OOCC_7H_{15})Cl_2$	1610s	1450s	160	530m	385w
	1550s				325w
$CpTi(OOCC_7H_{15})_2Cl$	1530s	1440s	90	520m	380m
$CpTi(OOCC_{11}H_{23})Cl_2$	1620s	1450s	170	500m	380w
	1530s		80		300w
$CpTi(IOOCC_{11}H_{23})_2Cl$	1520s	1440s	80	550m	400w
$CpTi(OOCC_{13}H_{27})Cl_2$	1600s	1440s	160	530m	420m
	1540s		100		350w
$CpTi(OOCC_{13}H_{27})_2Cl$	1525s	1435s	90	540m	360w
$CpTi(OOCC_{15}H_{31})Cl_2$	1620s	1450s	170	540m	400w
	1550s		100		330w
$CpTi(OOCC_{15}H_{31})_2Cl$	1530s	1440s	90	535m	370w
$CpTi(OOCC_{17}H_{35})Cl_2$	1620s	1420s	200	530m	400w
	1540s		80		320w
$CpTi(OOCC_{17}H_{35})_2Cl$	1520s	1450s	70	525m	375w
$CpTi(OOCC_{21}H_{43})Cl_2$	1620s	1455s	165	540m	410w
	1550s		95		310w
$CpTi(OOCC_{21}H_{43})_2Cl$	1530s	1435s	95	510m	365w

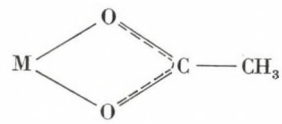
s = strong, m = medium, w = weak

carboxylato ligands, and care should be taken in making some assignments. Our conclusions are based on the data reported by Stammreich from Raman spectra and polarization measurements [19].

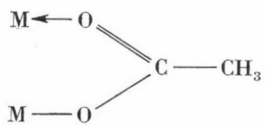
The most important IR stretching vibrations belong to that of carboxylato ligands. Nakamoto has explored [20] the possibilities of coordination of acetate ion to a metal atom as follows:



I



II



III

The effect of metal ion on the O—C—O stretching frequencies may be different for each structure mentioned above. In the carboxylato complexes symmetrial O—C—O stretching frequencies (ν_1) and asymmetrical O—C—O stretching frequency (ν_2) are of importance since their position and separation ($\Delta\nu = \nu_2 - \nu_1$) can help in determining the type of bonding of the metal [6].

In the acetate ion, the two C—O bands are supposed to be equivalent and the $\nu_{\text{asym.}}$ and $\nu_{\text{sym.}}$ frequencies appear at ca. 1578 and 1435 cm^{-1}. In bidentate coordination, the bonding of the carbonyl oxygen to the same metal ion causes O—C—O angle to decrease in comparison with that in the acetate ion. Consequently $\nu_{\text{asym.}}$ COO stretching frequency (ν_2) decreases [6, 21]. Coutts and Wailes have studied the IR spectra of carboxylato derivatives of bis(cyclopentadienyl)titanium(III)and found that the ($\nu_2 - \nu_1$) for acetato and benzoato derivatives is 65 and 80 cm^{-1}, respectively, and gave the usual bidentate (II) structure [7]. On the other hand bridging coordination is supposed to increase in the O—C—O angle resulting in the subsequent increase in the $\nu_{\text{asym.}}$ COO stretching frequency [22, 23]. Parashar and Rai have studied the IR spectra of chromium(III) carboxylato complexes and found that the ($\nu_2 - \nu_1$) is of the order of 180—170 cm^{-1} and gave the bridging (III) structure [24]. In view of this, since the IR spectra of all dicarboxylato derivatives of type $CpTi(OOCR)_2Cl$, exhibit the antisymmetric COO band at about 1530 cm^{-1} (lower than those reported for acetate ion, 1578 cm^{-1}) and symmetric COO band at about 1440 cm^{-1}, the behaviour of carboxylate groups in the present derivatives may tentatively be assigned as bidentate in nature. The difference between two COO bands i.e. $\Delta\nu$ has been found to be of the order of 80—90 cm^{-1}, which is similar to those found by Coutts and Wailes [7] and

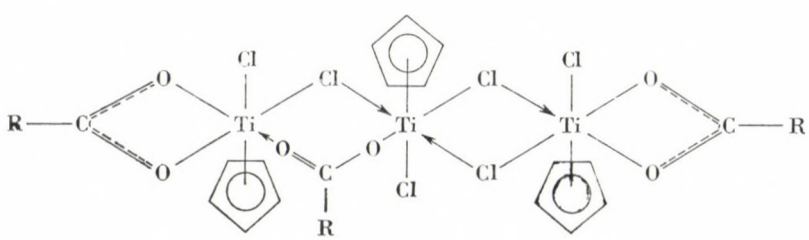
confirms the bidentate nature of the carboxylato groups. However, in the spectra of monocarboxylato derivatives of type $CpTi(OOCR)Cl_2$, the antisymmetric COO stretching band was found to split into two bands situated at $\sim$1620 cm^{-1} (higher than those reported for acetate ion, 1575 cm^{-1}) and $\sim$1550 cm^{-1} (lower than those reported for acetate ion, 1578 cm^{-1}). This type of splitting has been reported by many workers in a number of metal carboxylate complexes, due to the presence of bridging as well as bidentate carboxylate groups [25]. In view of this, the band observed at higher frequency may be attributed to bridging, while the lower frequency band to the bidentate carboxylate groups in the present complexes. The far infrared spectra of all these derivatives show medium bands at about 500—550 cm^{-1}, which may be assigned [20] to ν(Ti—O). In addition, monocarboxylato derivatives show weak bands in the regions of 380—420 and 300—350 cm^{-1} whereas dicarboxylato derivatives show only one band in the region 380—400 cm^{-1} assignable [16] to ν(Ti—Cl]. The presence of two bands in the (M—Cl) region in case of monocarboxylato derivatives indicates the presence of two types of chlorine atoms in these complexes.

^1H-*NMR spectra*

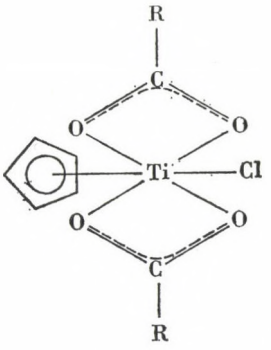
The proton NMR spectra of these complexes have been recorded in deuterated chloroform and DMF. The spectra are quite complicated due to the coupling between various alkyl groups attached to the carboxylate group and are not easy to interpret. However, a comparison of the spectra of ligands with that of the complexes can lead to following conclusions;

(1) A new signal in all carboxylato derivatives (absence in ligands) at δ 6.5 ppm may be assigned to the protons of cyclopentadienyl ring. The value is in the range reported [27] for other $C_5H_5Ti(IV)$ complexes with chelating ligands and is significantly upfield from the position in $CpTiCl_3$ (δ 7.07 ppm).

(2) The proton signals appearing in the region 4.5—5.0 ppm may be assigned [28] to the OH protons of carboxylate group in the ligands. However, the signals disappear in the spectra of the corresponding titanium complexes, indicating the deprotonation of the functional group.



(I)



(II)

Thus, on the basis of analyses, molecular weight determinations and spectral data, the following structures (**I** and **II**) may be proposed for monocarboxylato and dicarboxylato derivatives, respectively.

*

One of the author (S.K.S.) is thankful to University Grants Commission for providing financial assistance in the form of Minor Research Project. The authors are also thankful to Dr. Shyam Kumar for his help in preparing $CpTiCl_3$.

REFERENCES

[1] Garner, C. D., Hughes, B.: Adv. Inorg. Chem. Radiochem., **17,** 1 (1975)
[2] Doedens, R. J.: Prog. Inorg. Chem., **21,** 209 (1976)
[3] Nesmeyanov, A. N., Fedin, E. I., Nogina, O. V., Kochetkova, N. S., Dubovitskii, V. A., Petrovsky, P. V.: Tetrahedron Suppl., **8,** 389 (1966)
[4] Nesmeyanov, A. N., Nogina, O. V., Dubovitskii, V. A.: Izv. Akad. Nauk. SSSR, Otd. Khim. Nauk, **1962,** 1481
[5] Klanberg, F., Multterties, E. L., Guggenberger, L. J.: Inorg. Chem., **7,** 2272 (1968)
[6] Oldham, C.: Prog. Inorg. Chem., **10,** 223 (1968)
[7] Coutts, R. S. P., Martin, R. L., Wailes, P. C.: Aust. J. Chem., **26,** 941 (1973)
[8] Coutts, R. S. P., Wailes, P. C.: Aust. J. Chem., **20,** 1579 (1967)
[9] Chandra, K., Sharma, R. K., Garg, B. S., Singh, R. P.: J. Inorg. Nucl. Chem., **42,** 187 (1980); Sengupta, S. K., Baranwal, B. P.: Rev. Roum. de Chimie (In press)
[10] Razuvaev, G. A., Latyaeva, V. N., Lineva, A. N.: Zh. Obshch. Khim., **40,** 1804 (1970)
[11] Volpin, M. E., Shur, B. V.: Nature, **209,** 1236 (1966); Van Tamelen, E. E., Seeley, D., Schneller, S., Rudler, M., Cretney, W.: J. Am. Chem. Soc., **92,** 5251 (1970)
[12] Wailes, P. C., Coutts, R.S. P., Weigold, H.: "Organometallic Chemistry of Titanium, Zirconium and Hafnium", Academic Press, New York 1974
[13] Gorsich, R. D.: J. Am. Chem. Soc., **82,** 4211 (1960)
[14] Vogel, A. I.: "A Text Book of Practical Organic Chemistry", Longman, London 1948
[15] Dorain, P. B., Patterson, H. H., Jordon, P. C.: J. Chem. Phys., **49,** 3845 (1968)
[16] Kumar, S., Kaushik, N. K.: J. Inorg. Nucl. Chem., **43,** 2679 (1981)
[17] Fritz, H. P.: Adv. Organometal. Chem., **1,** 262 (1964)
[18] Davison, A., Rakita, P. E.: Inorg. Chem., **9,** 289 (1970)
[19] Stammreich, H.: personal communication to Fritz, H. P.: Adv. Organometal. Chem., **1,** 239 (1963)
[20] Nakamoto, K.: "Infrared Spectra of Inorganic and Coordination Compounds" Wiley Interscience, New York 1970
[21] Nakamura, K.: J. Chem. Soc. Japan, **79,** 1411 (1958)
[22] Grigorev, A. I.: Russ. J. Inorg. Chem., **8,** 409 (1963)

[23] Oldham, C., Sandford, W. F.: J. Chem. Soc. Dalton Trans., **1977,** 2068
[24] Parashar, G. K., Rai, A. K.: Synth. React. Inorg. Met.-Org. Chem., **8,** 427 (1978)
[25] Lever, A. B. P., Ogden, D.: J. Chem. Soc., A, **1967,** 2041
[26] Faniran, J. A., Patel, K. S., Mesubi, M. A.: Spectrochim. Acta, **31A,** 117 (1975)
[27] Alyea, E. C., Malek, A.: Inorg. Nucl. Chem. Lett., **13,** 587 (1977) and references therein
[28] Sharma, R. K., Singh, R. V., Tandon, J. P.: Synth. React. Inorg. Met.-Org. Chem., **10,** 221 (1980)

Acta Chimica Hungarica 116 (1), pp. 39—50 (1984)

AMINOPOLYCARBOXYLATES OF RARE EARTHS, XI

KINETICS OF METAL ION-EXCHANGE AND LIGAND EXCHANGE REACTIONS OF THE ETHYLENEGLYCOL-BIS-(2-AMINOETHYLETHER)--TETRAACETATE COMPLEX OF CERIUM(III)

E. BRÜCHER[1]*, I. BÁNYAI[2] and L. KRUSPER[1]

([1]Department of Inorganic and Analytical Chemistry, and [2]Department of Physical Chemistry, Kossuth Lajos University, H-4010 Debrecen, Hungary P.O.Box 10.)

Received April 28, 1983

Accepted for publication June 7, 1983

The metal ion exchange reaction between the complex Ceegta and Y^{3+} ions is relatively fast in the pH interval 4.6—6; it can be studied with a stopped-flow method. The rate of the reaction increases with increases in the Y^{3+} or H^+ ion concentrations, but a greater role is played by the exchange involving the direct encounter of the complex and Y^{3+} ions than by that taking place through the proton catalyzed dissociation of Ceegta.

At pH 5—6 the ligand exchange reaction between Ceegta and dtpa proceeds predominantly through the proton catalyzed dissociation of the complex, while in the interval 6—10 the most important process leading to exchange is the direct attack by the species $H_i$dtpa on the complex, with the formation of an intermediate mixed complex. A maximum is observed at pH 8—9.5 in the rate of the exchange; this was explain-by an interaction (presumably H-bonding) between an $H_i$dtpa species and the egta coordinated in the intermediate mixed ligand complex.

The rate of the metal ion exchange reaction of Ceegta is much higher, while that of its ligand exchange reaction is much lower than the corresponding rates of Ceedta; this was explained by the coordinative saturation of Ceegta.

Ethyleneglycol-bis-(2-aminoethylether)-tetraacetic acid (H_4egta), which contains eight donor atoms, is a complex forming agent frequently used in biology and in medical practice. The stability constants of egta with various transition metals, alkali metals and rare earth metals are well known [1], but very few data are available on the kinetic behaviour of the complexes. Only the kinetics of the isotope exchange reaction between $Ceegta^-$ and Ce^{3+} ions [2, 3] and the ligand exchange reaction between $Caegta^{2-}$ and egta [4] have been studied. At the same time, the kinetics of the metal ion exchange and ligand-exchange reactions of various complexes involving the hexadentate ligand ethylenediaminetetraacetate ($edta^{4-}$), which has a similar structure, have been investigated in great detail [5—14]. Thus, it is known that these exchange reactions take place through the proton catalyzed dissociation of the complexes and through the direct attack of the metal ions or ligands on the complexes. In the metal ion exchange reactions of the rare earth metal-(III) — edta complexes (Lnedta), the proton catalyzed dissociation of the complexes plays the major role, while the reactions proceeding through the

* To whom correspondence should be addressed

direct encounter of the metal ions and the complexes make only a slight contribution. As a consequence of the relatively high coordination number of the Ln^{3+} ions (generally 8—9), the Lnedta complexes are coordinatively unsaturated, whereas in the case of $Lnegta^-$ the number of functional groups in the ligand is nearly the same as the coordination number of the metal ion. Thus, if the kinetic behaviour of the $Lnegta^-$ complexes is studied, and the results are compared with those for the complexes $Lnedta^-$ interesting information may be obtained on the influence of the coordination saturation of the complexes on the kinetics of the metal ion exchange and the ligand exchange reactions. Accordingly, we have investigated the kinetics of the metal ion exchange reaction between $Ceegta^-$ and Y^{3+} ions, and the ligand exchange reaction between $Ceegta^-$ and the diethylenetriaminepentaacetate ligand ($dtpa^{5-}$).

Experimental

Chemicals of the highest analytical purity were used in the experiments. The KCeegta solution was prepared from equivalent amounts of $CeCl_3$ of 99.9% purity (Koch-Light) and H_4egta (Fluka). YCl_3 solution was prepared from Y_2O_3 of 99.9% purity (Fluka). The concentrations of the YCl_3 and $CeCl_3$ solutions, and solutions with the approximate compositions K_2H_2egta and K_3H_2dtpa, were determined by complexometric titration.

The exchange reaction between $Ceegta^-$ and Y^{3+} ions was followed at 277 nm (the position of one of the band maxima of Ceegta) with a Hitachi-Perkin-Elmer 139 spectrophotometer fitted with a stopped-flow head, and was recorded with a Tektronix memory-oscilloscope.

The ligand exchange between Ceegta and dtpa was studied in 4 cm cells at 300 nm (the position of one of the band maxima of Cedtpa) with a Beckman-DB-GT spectrophotometer.

The ionic strengths of solutions were kept constant (1 *M* KCl). The metal ion-exchange reaction was studied in solutions in which the pH was maintained constant with boric acid — mannitol or boric acid — pentaerythritol (0.01 *M* boric acid and 0.04 *M* mannitol or pentaerythritol) buffers.

With regard to the stability constants of Ceegta and Cedtpa ($\log K_{Ceegta} = 16.06$, $\log K_{Cedtpa} = 20.33$ [1]), with the use of a slight dtpa excess the ligand exchange reaction is virtually quantitative. The stability constant of Yegta is only about one order higher than that of Ceegta ($\log K_{Yegta} = 17.16$ [1]), and the Y^{3+} ions were therefore applied in a larger excess. Thus, both the ligand exchange and the metal ion exchange reaction can be regarded as being a pseudo first-order one, and the reaction rate can be given by the following simple relation:

$$-\frac{d[Ceegta]_t}{dt} = k_p[Ceegta]_t \qquad (1)$$

where $[Ceegta]_t$ is the total concentration of the Ceegta complexes, and k_p is a pseudo first-order rate constant. The k_p values were determined from the slopes of the linear plots of $\log (A_t - A_\infty)$ as a function of the reaction time. (A_t is the absorbance measured at time t after the beginning of the reaction, and A_∞ is that measured after the attainment of equilibrium.) The rate equations were established by examining the variations of k_p as functions of the pH, and the Y^{3+} ion and dtpa ligand concentrations.

Results and Discussion

Kinetics of exchange between Ceegta and Y^{3+} ions

The rate of the exchange reaction between the Ceegta complexes and Y^{3+} ions was studied in the pH interval 4.6—6 at various Y^{3+} ion concentrations. The resulting k_p values are shown in Fig. 1. It is seen that there is a

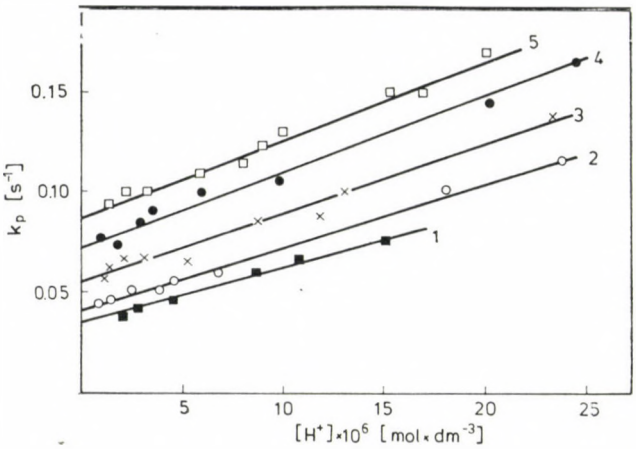


Fig. 1. Pseudo first-order rate constants k_p of metal ion exchange reaction between Ceegta and Y^{3+} ion. $[Ceegta]_t = 1.5\times10^{-3}$ mol dm^{-3}. $[Y^{3+}] = 1.25\times10^{-2}$ (1), 1.5×10^{-2} (2), 2×10^{-2} (3), 2.5×10^{-2} (4) and 3×10^{-2} (5) mol dm^{-3}

linear relation between reaction rate and H^+ ion concentration, i.e. the exchange is a process catalyzed by H^+ ions. The rate of exchange also increases with an increase in Y^{3+} ion concentration and the plots in Fig. 1 can be described by the relation

$$k_p = k_1 + k_2[H^+] \tag{2}$$

where k_1 and k_2 are constants. The values of k_1 and k_2 were calculated via the least squares principle and are depicted as functions of the Y^{3+} ion concentration in Figs 2 and 3.

In Fig. 2 it is seen that k_1 is directly proportional to the Y^{3+} ion concentration; $k_1 = k^a_{CeX}[Y^{3+}]$, where X = egta.

Although to only a slight extent, k_2 similarly increases with an increase in Y^{3+} ion concentration (Fig. 3); $k_2 = k^d_{CeHX} + k^a_{CeHX}[Y^{3+}]$. If these expressions for k_1 and k_2 are substituted into Eq. (2), the following expression is obtained for the rate of the metal ion exchange in Eq. (1);

$$-\frac{d[Ceegta]_t}{dt} = k^a_{CeX}[Ceegta]_t[Y^{3+}] + k^a_{CeHX}[Ceegta]_t[H^+][Y^{3+}] + k^d_{CeHX}[Ceegta]_t[H^+] \tag{3}$$

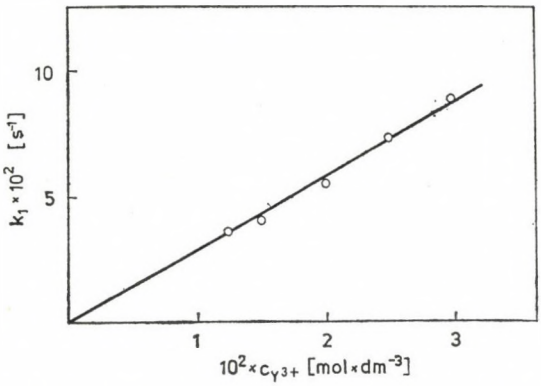


Fig. 2. Dependence of k_1 values in Eq. (2) on Y^{3+} ion concentration

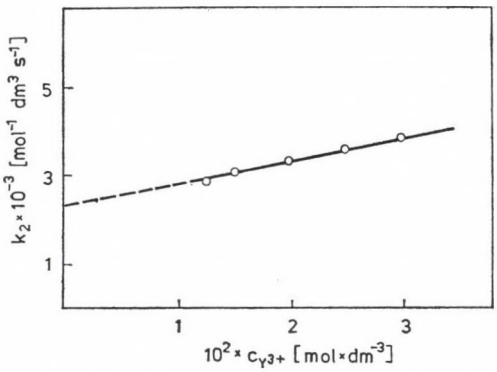


Fig. 3. Dependence of k_2 values in Eq. (2) on Y^{3+} ion concentration

The rate constants k^{a}_{CeX}, k^{a}_{CeHX} and k^{d}_{CeHX} were calculated from the data in Figs 2 and 3 via the least squares principle; $k^{a}_{CeX} = 3.0 \pm 0.15$ mol^{-1} dm^3 s^{-1}, $k^{a}_{CeHX} = (4.7 \pm 1.0) \times 10^4$ mol^{-2} dm^6 s^{-1}, and $k^{d}_{CeHX} = (2.4 \pm 0.4) \times 10^3$ mol^{-1} dm^3 s^{-1}. Rate equation (3) essentially coincides with that found in the study of the isotope exchange reaction between Ceegta$^-$ and labelled Ce^{3+} ions [2, 3]. but the rate constants differ appreciably; one of the reasons for this may be that Balcombe and Wiseall carried out their measurements at 5 °C and an ionic strength $I = 0.1$ mol dm^{-3} KNO_3.

On the basis of rate equation (3), the metal ion exchange reaction between Ceegta and Y^{3+} ions may proceed through the proton catalyzed dissociation of Ceegta, and the direct encounter of the Y^{3+} ion and the complex. The egta ligands formed in the relatively slow dissociation of Ceegta react very quickly with the Y^{3+} ions. The rate of exchange of Y^{3+} ions by direct attack on the Cegta complex (k^{a}_{CeX}) is 1—2 orders higher than the rates of similar (associa-

tive) metal ion exchange reations of Ceedta [16]. As a consequence of the comparatively high k^{a}_{CeX} value, exchange through the attack of the Y^{3+} ions always plays the major role in the reaction in the pH interval 4.6—6.

Kinetics of the ligand exchange reaction between Ceegta and dtpa

The kinetics of the ligand exchange reactions between $Ceegta^{-}$ and the ligands $H_i dtpa^{(5-i)-}$ were investigated in a fairly wide pH interval 5—10. The resulting pseudo first-order rate constants k_p are given in Fig. 4. The continuous lines are the k_p values calculated via the established rate equation (17). Similarly as observed for the $Tbedta^{-}$ — dtpa system [15], in neutral medium the rate of the ligand exchange reactions passes through a minimum in Fig. 4. At the same time, at higher pH, particularly when a larger dtpa ligand excess is applied, the k_p values display a definite maximum; with further increase of the pH, the k_p values increase slightly. On the basis of the results of earlier investigations [5—14], the increase in the reaction rate at lower pH (<6) can be interpreted by ligand exchange through the proton catalyzed dissociation of the complexes. The reaction rate increase observed with the increase of the dtpa concentration and the pH at higher pH can be explained by the more effective exchange occurring through the direct attack of the less protonated $H_i dtpai^{(5-i)-}$ species. It is substantially more difficult to interpret the maximum at pH 8—9.5, for a similar phenomenon has not previously been observed in studies on the exchange reactions of complexes involving aminopolycarboxylic acids.

In the establishment of the rate equation, the contributions of the reactions dependent on or independent of the dtpa concentration were first

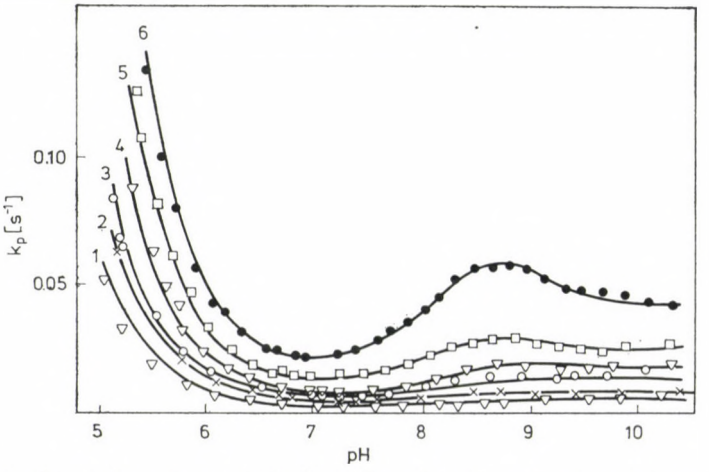


Fig. 4. Pseudo first-order rate constants k_p of ligand exchange reaction between Ceegta and dtpa. $[Ceegta]_t = 4\times10^{-4}$ mol dm^{-3}. $[dtpa] = 2.25\times10^{-3}$ (1), 3.75×10^{-3} (2), 6×10^{-3} (3), 7.5×10^{-3} (4), 1.5×10^{-2} (5) and 3.75×10^{-2} (6) mol dm^{-3}

separated [15]. The k_p values relating to the given pH were read off at 0.1—0.2 pH unit intervals from the plots fitted to the k_p values obtained at each dtpa concentration, and were then plotted as a function of the dtpa concentration. In the pH interval 5—7.5, k_p was found to increase linearly with the increase of the dtpa concentration. Some of these plots are presented in Fig. 5. Similarly as for the $Tbedta^-$ — dtpa system [15], the plots in this pH range could be described by the relation

$$k_p = k^d + k^a[\text{dtpa}]_t \tag{4}$$

where k^d contains the rate constants of the reactions involving dissociation of the complexes, while k^a contains those involving direct attack of the variously protonated species $H_i\text{dtpa}^{(5-i)-}$, and $[\text{dtpa}]_t$ is the total concentration of dtpa.

The curves in the pH interval 7.5—10 (Fig. 6) could be described by the relation

$$k_p = k^d + k^a[\text{dtpa}]_t + k^b[\text{dtpa}]_t^2 \tag{5}$$

The rate equation for the ligand exchange reaction was established from the k_p values in the pH interval 5—7.5 with the procedure used in the study of the $Tbedta^-$ — dtpa system [15]. The k^d values obtained as the intercepts in Fig. 5 (and calculated via the least squares principle) vary linearly with the H^+ ion concentration of the solution;

$$k^d = k^d_{CeX} + k^d_{CeHX}[H^+] \tag{6}$$

where $k^d_{CeX} = (2.3 + 0.5) \times 10^{-3}\ s^{-1}$ and $k^d_{CeHX} = (4.6 \pm 0.1) \times 10^3\ mol^{-1}\ dm^3\ s^{-1}$.

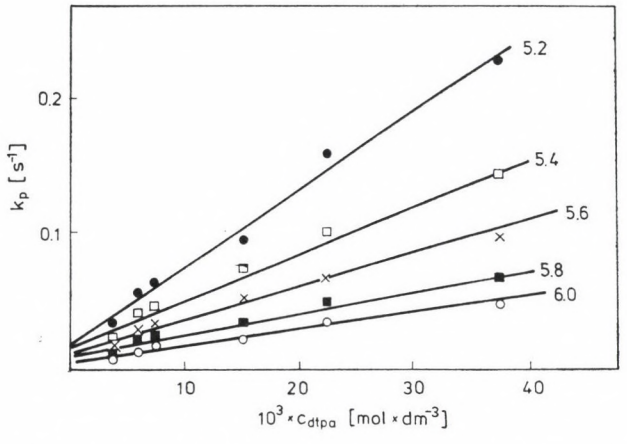


Fig. 5. Dependence of rate of ligand exchange on dtpa concentration

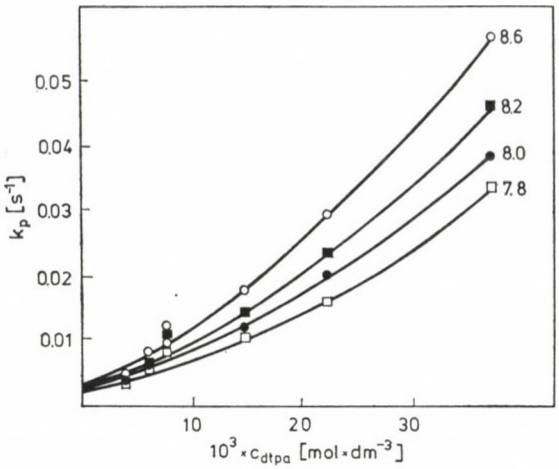


Fig. 6. Dependence of rate of ligand exchange on dtpa concentration

The variation of the k_p values at higher pH (Fig. 4) indicates that the ligand exchange also occurs via attack of the variously protonated species $H_i dtpa^{(5-i)i}$ on the complex. If the mole fractions of the species of composition $H_i dtpa$ ($H_i L$; $i = 0, 1, 2, \ldots, 5$) are denoted by x_0, $x_1, x_2, \ldots, x_5$ the rates k^a of the exchange reactions involving direct attack of the ligand species can be expressed by the following relation;

$$k^a = \sum_{i=0}^{i=z} k^a_{H_iL}\, x_i \tag{7}$$

where $k^a_{H_iL}$ is the rate constant of the exchange reaction involving attack of the species of composition $H_i dtpa$, and z is the number of protons in the species $H_i dtpa$ participating in the exchange.

The mole fraction values x_i can be given by taking into consideration the protonation product of the species $H_i dtpa$ ($\beta_i = [H_i dtpa]/[dtpa][H^+]^i$);

$$x_i = \frac{\beta_i [H^+]^i}{\sum_0^5 \beta_i [H^+]^i} \tag{8}$$

If the denominator of Eq. (8) is denoted by α_H, from Eqs (7) and (8) we arrive at the following relation;

$$k^a \cdot \alpha_H = \sum_{i=0}^{i=z} k^a_{H_iL} \beta_i [H^+]^i \tag{9}$$

When the $k^a \cdot \alpha_H$ values are plotted as a function of the H^+ ion concentration, the curve shown in Fig. 7 is obtained. This curve can be described as a cubic function of the H^+ ion concentration. Thus, in the pH interval 5—7.5 the

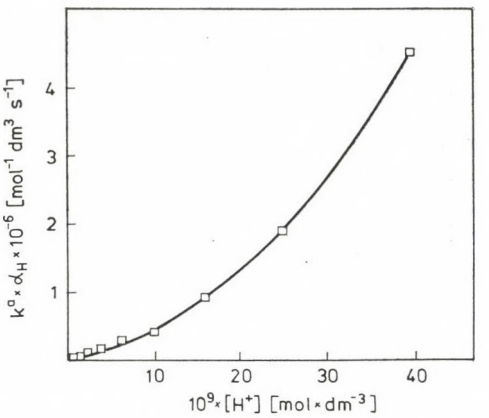


Fig. 7. Dependence of $k^a \cdot \alpha_H$ value on H^+ ion concentration

rate equation for the exchange reaction between Ceegta$^-$ and the dtpa ligand can be given as follows on the basis of Eqs. (1), (4), (6) and (9);

$$-\frac{d[\text{Ceegta}]_t}{dt} = [\text{Ceegta}]_t \left\{ k^d_{CeX} + k^d_{CeHX}[H^+] + \sum_{i=0}^{i=3} k^a_{H_iL}[H_i\text{dtpa}] \right\} \quad (10)$$

The rate constants $k^a_{H_iL}$ were calculated from the found $k^a \cdot \alpha_H$ values via Eq. (9) with the use of $z = 3$ and the known β_i values [1]. With linearization of the cubic function and the application of the least squares principle, calculated led to the following $k^a_{H_iL}$ values; $k^a_L = 1.33 \pm 0.3$ mol^{-1} dm^3 s^{-1}; $k^a_{HL} = 0.92 \pm 0.1$ mol^{-1} dm^3 s^{-1}; $k^a_{H_2L} = 0.2 \pm 0.02$ mol^{-1} dm^3 s^{-1}; $k^a_{H_3L} = 50 \pm 10$ mol^{-1} dm^3 s^{-1}.

On the basis of rate equation (10), the following assumptions may be made concerning the course of the ligand exchange reaction in the pH interval 5—7.5 The ligand exchange may take place by the fast reaction between $H_i$dtpa ligands and Ce^{3+} ions released in the relatively slow spontaneous (k^d_{CeX}) and the proton catalyzed (k^d_{CeHX}) dissociation of Ceegta$^-$. These reactions (and praticularly the exchange via the proton catalyzed dissociation of Ceegta$^-$) play a determining role in the pH range 5—6. In the case of the reactions at pH $\approx$ 6, as the pH increases a greater role is played by the exchange involving direct attack by the species H_3dtpa^{2-}, H_2dtpa^{3-}, Hdtpa^{4-} and dtpa^{5-} on Ceegta$^-$. During the reaction, the attacking ligand forms an intermediate mixed ligand complex with the Ceegta. In this resulting mixed ligand complex, the functional groups of the attacking dtpa progressively displace the functional groups of the egta ligand from the coordination sphere of the Ce^{3+} ion. The rate of exchange through direct attack of the $H_i$dtpa species is relatively low; this is clearly a consequence of the fact that the egta

ligand (with 8 donor atoms) occupies the vast majority of the coordination sites of the Ce^{3+} ion (the coordination number of the Ce^{3+} ion is probably 9 [17]), and thus the formation of the mixed ligand complexes is hindered, and proceeds only very slowly. The rate constants $k^{a}_{H_iL}$ expressing the effectiveness of the attack by the $H_i$dtpa species decrease in the sequence $k^{a}_{L} > k^{a}_{HL} > k^{a}_{H_2L}$, which understandably indicates that attack on the complex by the less protonated $H_i$dtpa species is more effective as concerns exchange. At the same time, it is surprising that $k^{a}_{H_3L} > k^{a}_{L}$. This result can be interpreted only if it is assumed that $k^{a}_{H_3L}$ does not express the effectiveness of the attack by the H_3dtpa^{2-} ligand, but rather the effectiveness of the direct reaction between the H_2dtpa^{3-} and the protonated complex CeHegta. The rate of this reaction is likewise proportional to the third power of the H^+ ion concentration. The correctness of the assumption is shown by the fact that, even at lower pH (where an appreciable role is played by the proton-catalyzed dissociation of the complexes), the k_p values in Fig. 4 display a definite increase as the dtpa concentration rises.

The rate of the ligand exchange reaction in the pH interval 7.5—10 is given by a quadratic function of the exchanging dtpa ligand concentration, as in Eq. (5). The occurrence of a term involving the square of the dtpa concentration can be explained if it is assumed that a $H_i$dtpa species may interact with the egta ligand coordinated in the mixed ligand complex Ceegta($H_j$dtpa) formed as intermediate, with a resulting increase in the rate of displacement of egta. As regards the nature of the interaction, we assume that this is intermolecular H-bonding between the egta ligand and the proton(s) of the attacking $H_i$dtpa ligand. Support for this assumption is provided by the fact that the maximum in the rate of ligand exchange lies in a pH interval where the concentrations of the species $Hdtpa^{4-}$ and H_2dtpa^{3-} are significant, while the concentration of $dtpa^{5-}$ is low. The ligand exchange probably proceeds as in the following reactions, with the participation of two $H_i$dtpa species;

$$\text{Ceegta(Hdtpa)} + \text{H}_2\text{dtpa} \rightarrow \text{Cedtpa} + \text{Hegta} + \text{H}_2\text{dtpa} \qquad (11)$$

$$\text{Ceegta(Hdtpa)} + \text{Hdtpa} \rightarrow \text{Cedtpa} + \text{Hegta} + \text{Hdtpa} \qquad (12)$$

$$\text{Ceegta(H}_2\text{dtpa)} + \text{H}_2\text{dtpa} \rightarrow \text{Cedtpa} + \text{H}_2\text{egta} + \text{H}_2\text{dtpa} \qquad (13)$$

$$\text{Ceegta(H}_2\text{dtpa)} + \text{Hdtpa} \rightarrow \text{Cedtpa} + \text{H}_2\text{egta} + \text{Hdtpa} \qquad (14)$$

Exchange processes (11) and (14) can not be distinguished, since they result in the appearance of the same terms in the rate equation. Accordingly, the value of k^b in Eq. (5) can be given as

$$k^b = k^b_2 x_1^2 + k^b_3 x_1 x_2 + k^b_4 x_2^2 \qquad (15)$$

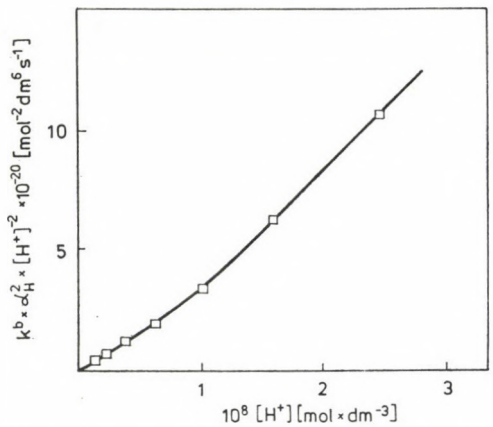


Fig. 8. Dependence of $k^b \cdot \alpha_H^2/[H^+]^2$ values on H^+ ion concentration

From Eqs (15) and (8);

$$\frac{k^b \alpha_H^2}{[H^+]^2} = k_2^b \beta_1^2 + k_3^b \beta_1 \beta_2 [H^+] + k_4^b \beta_2^2 [H^+]^2 \tag{16}$$

If the $k^b \alpha_H^2/[H^+]^2$ values are plotted as a function of the H^+ ion concentration, the curve given in Fig. 8 is obtained, which reveals that the first term on the right-hand side of Eq. (16) is approximately zero, i.e. $k_2^b \approx 0$. From the established k^b values and by linearization of Eq. (16), the calculated values of the constants k_3^b and k_4^b are as follows; $k_3^b = 92 \pm 10$ mol^{-2} dm^6 s^{-1}, and $k_4^b = 4.2 \pm 1.5$ mol^{-2} dm^6 s^{-1}.

From (16) and (11), the rate equation for the ligand exchange reaction between Ceegta and dtpa in the pH interval 5—10 is

$$-\frac{d[Ceegta]_t}{dt} = [Ceegta]_t \{k_{CeX}^d + k_{CeHX}^d [H^+] +$$

$$+ \sum_{i=0}^{i=3} k_{H_iL}^a [H_i dtpa] + k_3^b [Hdtpa]\ [H_2dtpa] + k_4^b [H_2dtpa]^2\} \tag{17}$$

Rate equation (17) gives a relatively good description of the rate of the ligand exchange in the whole of the pH interval examined; this is demonstrated by the reasonably good fit of the full-line plots calculated via Eq. (17) to the experimentally measured points in Fig. 4.

Conclusions

Similarly to the reactions of other aminopolycarboxylate complexes, the metal ion exchange and the ligand exchange reactions of the complex $Ceegta^-$ proceed through proton catalyzed dissociation and through the direct attack

of the exchanging metal ions or ligands on the complex. At the same time, the proportions of exchange occurring by associative and dissociative means differ considerably from those observed in the reactions of Ceedta$^-$ [16]. In the metal ion exchange reaction of Ceegta$^-$, the role of reactions involving direct attack by the exchanging Y^{3+} ions is very significant or determining in a wide pH interval; in contrast, the exchange reactions of Ceedta$^-$ proceed predominantly through proton catalyzed dissociation. The rate of the reaction taking place by direct attack of the exchanging metal ion is much higher in the case of Ceegta than for Ceedta (k^a_{CeX} values of 3.0 ± 0.15 and 0.022 mol^{-1} dm^3 s^{-1} [16], respectively). The situation is just the reverse for the ligand exchange reactions. The exchange involving the direct encounter of the Ceedta and $H_i$dtpa species is much faster than the similar reaction of Ceegta; thus, the values of k^a_L and k^a_{HL} are 1×10^7 and 1.3×10^3 [15], and 1.33 and 0.92 mol $^{-1}$ dm^3 s^{-1}, respectively. These results can be interpreted in term of the higher number of donor atoms in the egta ligand. The complex Ceegta is practically "saturated" coordinately, while Ceedta is "unsaturated". Consequently, the interaction between the central ion and the donor atoms of the ligand is somewhat stronger in Ceedta, and thus the bonds between the Ce^{3+} ion and the functional groups are presumably broken more easily and more frequently in Ceegta; this facilitates the attack by the exchanging metal ion, and the formation of the dinuclear intermediate. At the same time, in the case of ligand exchange the coordinatively almost saturated complex Ceegta forms an intermediate mixed ligand complex with the attacking $H_i$dtpa ligand only with difficulty; the corresponding reaction of Ceedta proceeds practically without any obstacle (the Ce^{3+} ion in Ceedta still possesses at least 3 free coordination sites).

These results demonstrate that the reactivity of a complex formed with polyfunctional ligands depends considerably on the coordinative saturation of the complex. The metal ion exchange reactions of complexes that are coordinatively saturated occur comparatively quickly via an associative mechanism, while their ligand exchange reactions take place relatively slowly. In the case of coordinatively unsaturated complexes the ligand-exchange reactions are fast, while the metal ion exchange reactions proceed comparatively slowly via an associative pathway.

REFERENCES

[1] Critical Stability Constants, Vol. **1,** Eds Martell, A. E. and Smith, K. M. Plenum Press. N. Y. 1974
[2] Wiseall, B., Balcombe, C. J. J.: Inorg. Nucl. Chem., **32,** 1751 (1970)
[3] Balcombe, C. J., Wiseall, B. J.: Inorg. Nucl. Chem., **35,** 2859 (1973)
[4] Mirti, P. J.: Inorg. Nucl. Chem., **41,** 323 (1979)
[5] Schwarzenbach, G., Ackermann, H.: Helv. Chim. Acta, **35,** 485 (1952)
[6] Margerum, D. W.: Record Chem. Progress (Kresge-Hooker Sci. Lib., **24,** 237 (1963)

[7] Margerum, D. W., Cayley, G. R., Weatherburn, D. C., Pagenkopf, G. K.: "Coordination Chemistry" Vol. **2**. Ed. Martell, A. E. ACS Monograph 174, Amer. Chem. Soc. Washington, 1976. p. 1.
[8] Kula, R. J., Reed, G. H.: Anal. Chem., **38,** 697 (1966)
[9] Schwartzfager, D. G., Carr, J. D.: J. Amer. Chem. Soc., **97,** 315 (1975)
[10] Sudmeier, K. L., Reilley, C. N.: Inorg. Chem., **5,** 1047 (1966)
[11] Kula, R. J., Rabenstein, D. L.: J. Amer. Chem. Soc., **89,** 552 (1967)
[12] Ryhl, A.: Acta Chem. Scand., **26,** 4001 (1972)
[13] Reed, G. H., Kula, R. J.: Inorg. Chem., **10,** 2050 (1971)
[14] Force, R. K., Marianelli, R. S., Carr, J. D.: Inorg. Chem., **15,** 2653 (1976)
[15] Brücher, E., Bányai, I.: J. Inorg. Nucl. Chem., **42,** 749 (1980)
[16] Brücher, E., Bányai, I.: Acta Chim. Acad. Sci. Hung., **95,** 147 (1977)
[17] Moeller, T., Martin, D. F., Thompson, Z. C., Randall, F.: Chem. Rev., **65,** 1 (1965)

Acta Chimica Hungarica 116 (1), pp. 51—62 (1984)

POLAROGRAPHIC STUDY ON THE KINETICS AND MECHANISM OF THE HYDROLYSIS OF 1,2-CYCLOHEPTANE DIONE DIOXIME

F. MÁNOK*, E. KŐSZEGI and CS. VÁRHELYI

(Faculty of Chemical Technology, Babes-Bolyai University, 3400-Cluj-Napoca, Str. Arany János No. 11., Romania)

Received February 4, 1983

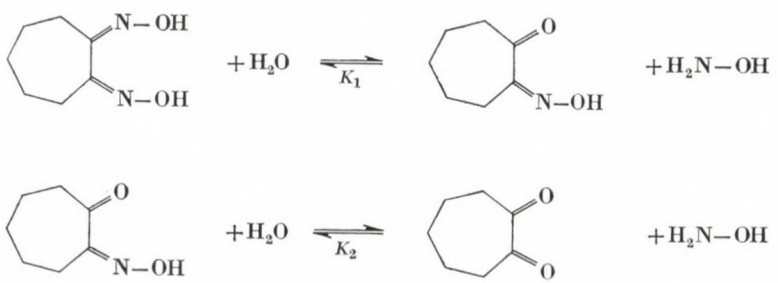
Accepted for publication June 28, 1983

In acidic aqueous solutions of 1,2-cycloheptane dione dioxime (heptoxime) the oxime groups are successively hydrolyzed and 1,2-cycloheptane dione monoxime and 1,2-.cycloheptane dione are formed. The kinetics of these reactions was studied polarographically both in the absence and presence of an excess of hydroxylamine in perchloric acid of various concentrations (0.05—0.2 *M*) at 20 °C. The protonization constant of the heptoxime was also determined from kinetic data. The mechanism of the first hydrolysis step is discussed.

1,2-cycloheptane dione dioxime (heptoxime : Heptox. H_2 : $C_7H_{12}N_2O_2$) is a well known reagent used for the gravimetric and spectrophotometric determination of Ni(II), Ni(IV) and Pd(II) in form of $[Ni(Heptox.H_2)]$, $[Ni(Heptox)_3]^{2-}$, $[Pd((Heptox.H)_2]$, etc. [1]. Co(III) and Rh(III) mixed chelates: $[Co(Heptox.H)_2X_2]^-$, $[Co(Heptox.H)X(amine)]^0$, $[Rh(Heptox.H)_2X_2]^-$ etc. are important from the point of view of co-ordination chemistry.

The UV spectroscopic investigations of Alibina and Peshkova [2] in neutral and acidic aqueous solutions of some aliphatic and alicyclic dioximes have shown that in acidic media hydrolysis processes occur with the liberation of hydroxylamine.

In the case of the heptoxime the following equilibria can be assumed



In a previous paper [3] the polarographic behaviour of 1,2,3-cyclohexane trione trioxime was studied in acidic media. These investigations proved that polarography can be used to study the hydrolysis of oxime derivatives.

* To whom correspondence should be addressed

Table I

Kinetic data on the hydrolysis of heptoxime at different acidities

$HClO_4$ M	Time min	Div_A	Div_B	[A°]	[B°]	[C]	[D°]
				$M \times 10^3$			
	10	62.8	1.5	0.94	0.038	0.022	0.082
	15	60.9	2.4	0.91	0.060	0.030	0.12
	20	59.0	3.2	0.88	0.080	0.040	0.16
	25	57.3	3.5	0.86	0.099	0.041	0.18
0.05	30	55.6	4.6	0.83	0.12	0.050	0.22
	35	54.0	5.3	0.81	0.13	0.060	0.25
	40	52.3	5.9	0.78	0.15	0.070	0.29
	45	50.8	6.5	0.76	0.16	0.080	0.32
	50	49.3	7.0	0.74	0.17	0.090	0.35
	10	62.4	1.6	0.94	0.039	0.021	0.10
	15	60.5	2.4	0.91	0.061	0.029	0.12
	20	58.5	3.2	0.88	0.081	0.039	0.16
	25	56.5	4.0	0.85	0.10	0.050	0.20
0.06	30	54.7	4.7	0.82	0.12	0.060	0.24
	35	52.9	5.5	0.79	0.14	0.070	0.28
	40	51.0	6.1	0.76	0.15	0.090	0.33
	45	49.5	6.7	0.74	0.16	0.100	0.36
	50	47.7	7.4	0.71	0.18	0.140	0.40
	10	61.0	2.3	0.91	0.057	0.033	0.12
	15	58.3	3.4	0.87	0.085	0.045	0.185
	20	55.8	4.3	0.844	0.11	0.050	0.21
0.10	25	53.3	5.2	0.80	0.13	0.070	0.27
	30	50.9	5.7	0.76	0.15	0.090	0.33
	35	48.6	6.6	0.73	0.17	0.100	0.37
	40	46.5	7.3	0.70	0.18	0.120	0.42
	45	44.5	7.8	0.67	0.20	0.130	0.46
	50	42.5	8.3	0.64	0.21	0.150	0.51
	10	58.9	2.6	0.88	0.065	0.055	0.18
	15	55.2	4.3	0.83	0.11	0.060	0.23
	20	51.9	5.6	0.78	0.14	0.080	0.30
	25	48.7	6.7	0.73	0.17	0.100	0.37
0.20	30	45.8	7.6	0.68	0.19	0.130	0.45
	35	43.0	8.5	0.64	0.22	0.140	0.50
	40	40.3	9.2	0.60	0.23	0.170	0.57
	45	38.1	9.8	0.57	0.25	0.18	0.61
	50	35.6	10.5	0.53	0.27	0.20	0.67

[A°] — total concentration of 1,2-cycloheptane dione dioxime
[B°] — total concentration of 1,2-cycloheptane dione monoxime
[C] — total concentration of 1,2-cycloheptane dione
[D°] — total concentration of hydroxylamine

In acidic solutions (0.05—0.2M $HClO_4$) the polarograms of the heptoxime have only a single wave with $E_{1/2} = -740$ mV (vs. SCE). The shape of this curve suggests a complicated, non uniform electrode process. The height of the wave, however, is proportional to the concentration of the dioxime. On

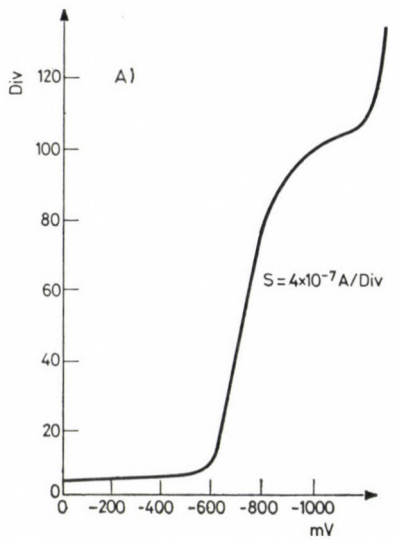


Fig. 1a. **Polarogram of 1,2-cycloheptane dione dioxime; $[HClO_4] = 0.1$ M**

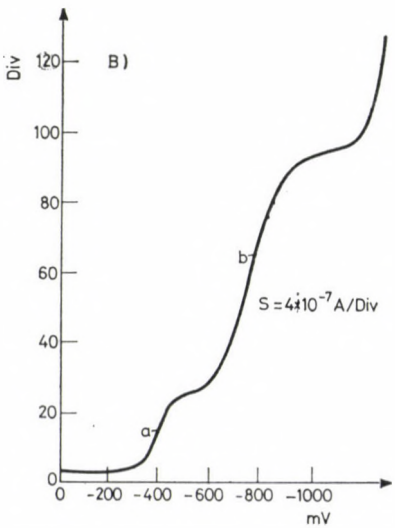


Fig. 1b. Polarogram of 1,2-cycloheptane dione dioxime and of its hydrolysis product after standing for 1 hour. $S = 4 \times 10^{-7}$ A/Div; $[HClO_4] = 0.1$ M; ionic strength: 0.2; $t = 20.0 \pm 0.01$ °C

standing a new polarographic wave appears at a more positive potential value ($E_{1/2}$ = —390—410 mV (vs. SCE)). The height of this second wave increases with time. After standing for 4—5 days an equilibrium sets in.

We suppose that the wave at more positive potential value corresponds to the reduction of 1,2-cycloheptane dione monoxime.

In order to prove this presumption, since pure 1,2-cycloheptane dione monoxime was not available, an analogous system: methyl-isopropylglyoxime and methyl-isopropyl dione monoxime was studied polarographically under the same experimental conditions (a mixture of $HClO_4$ and $NaClO_4$, ionic strength: 0.2 *M*).

The methyl-isopropyl dione monoxime is reduced in a single step at $E_{1/2}$ = —490 mV (vs. SCE). The height is proportional to the concentration of the monoxime, on standing it decreases only slowly. Methyl-isopropyl-glyoxime also gives a single step, proportional to the concentration, but it is considerably higher than the step of the monoxime: $E_{1/2}$ = 750 mV (vs. ESCE). These are in agreement with our previous presumptions and enable us to establish the concentration—wave height relationship also in the case of the 1,2-cycloheptane dione monoxime, by presuming that the ratios of the wave heights of the corresponding dioximes and monoximes have the same value in both systems, the system under investigation and that of comparison. From the change in time of the height of the 1,2-cycloheptane dione monoxime wave we could conclude that the end product of the hydrolysis, the corresponding diketone, is a polarographically inactive substance under the given experimental conditions.

In the presence of a 10—20 fold excess of hydroxylamine hydrochloride the dioxime is reformed: the height of the first wave ($E_{1/2}$ = —490 mV) decreases and that of the second one increases.

In our earlier paper [4] we investigated polarographically the equilibria in acidic aqueous 1,2-cycloheptane dione dioxime solutions. Following this

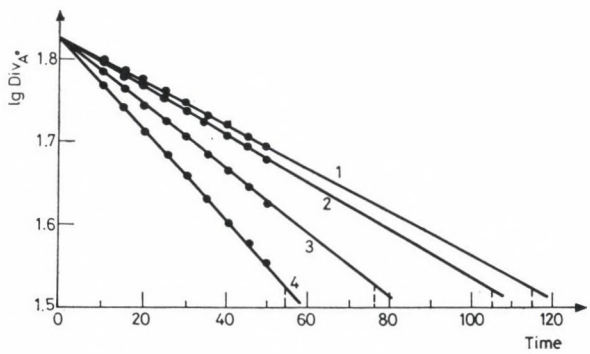


Fig. 2. Plot of the log Div_A versus time. 1 — $[HClO_4]$ = 0.05 *M*; 2 — $[HClO_4]$ = 0.06 *M*; 3 — $[HClO_4]$ = 0.1 *M*; 4 — $[HClO_4]$ = 0.2 *M*

study, in the present paper the results on the kinetics and mechanism of the hydrolysis of the same substance both in the presence and in the absence of hydroxylamine, are reported.

Experimental

Four acidic aqueous heptoxime solutions were prepared. Concentration of the heptoxime: 10^{-3} *M*. Acidity: 0.05—0.2 *M* $HClO_4$. Ionic strength: 0.2 *M* (with $NaClO_4$). The change with the time of the concentration of 1,2-cycloheptane dione dioxime and — monoxime was followed polarographically at 20 ± 0.01 °C under thermostated conditions.

The concentrations of the oximes were obtained using the following data:

Polarographic sensibility	Concentration of 1,2-cycloheptane dione monoxime	Concentration of 1,2-cycloheptane dione dioxime
3×10^{-7} A/Div	$\frac{\text{Division}\times10^{-3}}{39.5}$	$\frac{\text{Division}\times10^{-3}}{66.8}$
4×10^{-7} A/Div	$\frac{\text{Division}\times10^{-3}}{29.6}$	$\frac{\text{Division}\times10^{-3}}{50.1}$

The polarograms were taken on a Radelkis-Type-OH-120 polarograph by using a conventional polarographic cell with a saturated calomel reference electrode, connected to the cell by means of an agar-agar bridge (1 *M* KNO_3). The oxygen was eliminated from the solutions with purified methane. The dropping mercury electrode had a flow rate of 1.30 m s^{-1} and a drop time of 5.20 s in 0.20 *M* $NaClO_4$ solution and with a mercury reservoir height of 60 cm (at 20 °C).

Results and Discussion

Kinetics of the hydrolysis of 1,2-cycloheptane dione dioxime in diluted perchloric acid solution

The polarographic data on heptoxime and its hydrolysis products at different concentrations of $HClO_4$ are given in Table I.

By using the data from Table I the plot of lg Div_A versus time at various $HClO_4$ concentrations is given in Fig. 2.

The lg Div_A values at various acidities and times are presented in Table II.

It can be seen that lg Div_A values decrease linearly over a long period of time at all acidities studied. This means that the overall reaction is of pseudo first order. From the half life times ($t_{1/2}$) the rate constants k_1 at different acidities were calculated (Table III).

The k_1 values refer to the first step of the hydrolysis, i.e. to the formation of 1,2-cycloheptane dione monoxime.

Table II

lg Div_A *values in function of acidity and time*

Time min	lg Div_A			
	$[HClO_4]$ 0.05 *M*	$[HClO_4]$ 0.06 *M*	$[HClO_4]$ 0.10 *M*	$[HClO_4]$ 0.20 *M*
10	1.798	1.795	1.785	1.770
15	1.784	1.782	1.766	1.742
20	1.771	1.767	1.747	1.715
25	1.758	1.752	1.727	1.687
30	1.745	1.738	1.707	1.661
35	1.732	1.723	1.687	1.633
40	1.718	1.708	1.667	1.605
45	1.706	1.695	1.648	1.581
50	1.693	1.678	1.628	1.551

Table III

k_1 *and* $t_{1/2}$ *values for different acidities at* 20 °C

$[HClO_4]$ *M*	$t_{1/2}$ min	$k_1 \times 10^3$ min^{-1}
0.05	112.5	6.1
0.06	102.5	6.8
0.10	76.0	9.1
0.20	64.5	12.7

In this complicated system, considering the reverse reactions, four partial processes can be supposed

$$A^\circ \underset{k_{-1}}{\overset{k_1}{\rightleftarrows}} B^\circ + D^\circ \tag{1}$$

$$B^\circ \underset{k_{-2}}{\overset{k_2}{\rightleftarrows}} C + D^\circ \tag{2}$$

For these processes the following equations are valid:

$$\frac{d[A^\circ]}{dt} = -k_1[A^\circ] + k_{-1}[B^\circ]\,[D^\circ] \tag{3}$$

$$\frac{d[B^\circ]}{dt} = k_1[A^\circ] - k_2[B^\circ] + k_{-2}[C]\,[D^\circ] - k_{-1}[B^\circ]\,[D^\circ] \tag{4}$$

$$\frac{d[C]}{dt} = k_2[B^\circ] - k_{-2}\,[C]\,[D^\circ] \tag{5}$$

Table IV

Kinetic data for the calculation of k_2 and k_{-2} values
$[HClO_4] = 0.10\ M$

Time, min	$-m_A \times 10^6$	$m_B \times 10^6$	$\frac{m_A + m_B}{[B^\circ]} \times 10^3$	$\frac{[C]\,[D^\circ]}{[B^\circ]} \times 10^3$
25	7.23	3.62	27.3	0.144
30	6.90	3.14	25.1	0.191
35	6.59	2.89	22.0	0.236
40	6.31	2.78	19.2	0.276
45	6.03	2.48	18.0	0.327
50	5.76	2.33	16.3	0.380

By using the following notations:

$$\frac{d[A^\circ]}{dt} = m_A; \quad \frac{d[B^\circ]}{dt} = m_B; \quad \frac{d[C]}{dt} = m_C$$

one can write:

$$m_A + m_B + m_C = 0 \tag{6}$$

$$\frac{m_A}{[A^\circ]} = -k_1 + k_{-1}\frac{[B^\circ][D^\circ]}{[A^\circ]} \tag{7}$$

$$\frac{m_A + m_B}{[B^\circ]} = -k_2 + k_{-2}\frac{[C]\,[D^\circ]}{[B^\circ]} \tag{8}$$

From the slope of the $[A^\circ] = [A^\circ]$ (time) and $[B^\circ] = [B^\circ]$ (time) curves, by using relations (7) and (8), in principle we could compute all the four rate constants.

In spite of this, practically the k_1 and k_{-1} values cannot be determined separately in the case of hydrolysis reactions, since m_A changes linearly with $[A^\circ]$ in a large time interval, and further this change is slight.

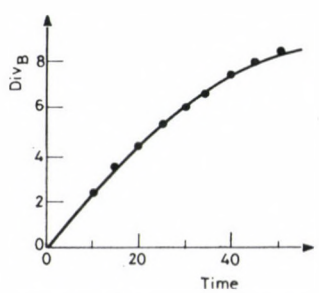


Fig. 3. Plot of Div_{B° — versus time. $[HClO_4] = 0.1\ M$; ionic strength: $0.2\ M$

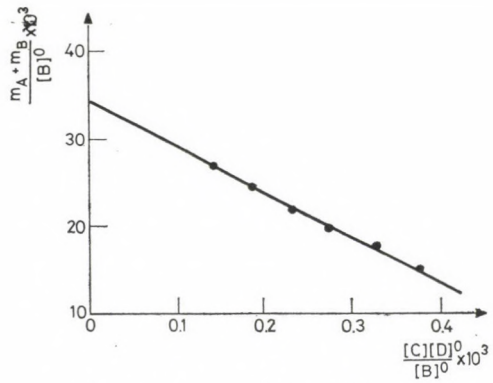


Fig. 4. Plot of $\frac{m_A + m_B}{[B^\circ]}$ versus $\frac{[C] \cdot [D^\circ]}{[B^\circ]}$; $[HClO_4] = 0.1\ M$

For the determination of k_2 and k_{-2} the plot of $[B^\circ] = [B^\circ]$ (time) versus time was used. The slopes of these curves were determined graphically ("mirror method") at different intervals of time (Fig. 3).

The experimental data in 0.1 M $HClO_4$ used for the calculation of k_2 and k_{-2} values, are presented in Table IV. m_A was computed by using $[A^\circ]$ values taken from Table I and the value of k_1 was determined earlier.

$$-m_A = k_1[A^\circ]$$

The plot of $\frac{m_A + m_B}{[B^\circ]}$ versus $\frac{[C]\ [D^\circ]}{[B^\circ]}$ gives a straight line (Fig. 4).

From the slope of this line and its intercept the k_2 and k_{-2} values were obtained:

$$-\text{tg}\ \alpha = k_{-2} = 51.6\ M^{-1}\ \text{min}^{-1}$$

$$k_2 = 3.46 \times 10^{-2}\ M^{-1}\ \text{min}^{-1}$$

The value of the equilibrium constant $K_2 = \frac{k_{-2}}{k_2} = 1.50 \times 10^{-3}$ obtained from the kinetic data, agrees well with that calculated from equilibrium data (4).

Kinetics of the formation of 1 2-cycloheptane dione dioxime in the presence of an excess of hydroxylamine

If a hydrolyzed heptoxime solution in equilibrium is treated with an excess of hydroxylamine hydrochloride the 1,2-cycloheptane dione monoxime

and — dioxime are reformed. This phenomenon proves that during the hydrolysis irreversible reactions, e.g. intramolecular transposition, do not occur.

For the study of these oximation reactions in equilibrium a hydrolysed 10^{-3} *M* heptoxime solution was used at 20 °C, in the presence of 0.1 *M* $HClO_4$. This solution was treated with an excess of $NH_2OH.HCl$: 21.1×10^{-3} *M*, by taking into account also the amount of NH_2OH resulting from the hydrolysis (ionic strength: 0.2 *M*).

The change of the concentration of the molecular species in the above system was recorded. The data obtained are given in Table V.

Plot of A° versus time enabled us to determine the rate constants k_1 and k_{-1}. The corresponding experimental data are presented in Table VI.

Table V

Concentration data on the molecular species in a hydrolyzed heptoxime solution in the presence of an excess of NH_2OH

Time, min	Div_A	Div_B	[A°]	[B°]	[C]	[D°]
			$M \times 10^3$			
0	9.6	23.7	0.14	0.60	0.26	21.12
25	28.6	10.1	0.57	0.34	0.09	20.52
30	31.8	9.1	0.64	0.31	0.05	20.41
35	34.3	8.3	0.68	0.28	0.04	20.36
40	36.5	7.6	0.73	0.26	0.01	20.28
45	38.2	7.0	0.76	0.24	0.00	20.24
50	39.3	6.5	0.78	0.22		20.22

$[HClO_4] = 0.1\ M$; $[A^\circ] + [B^\circ] + [C] = 10^{-3}\ M$

Table VI

Kinetic data for the determination of k_1 *and* k_{-1} at $[HClO_4] = 0.1\ M$

Time, min	m_A Div/min	$M_A \times 10^6$ $M\ min^{-1}$	$\frac{M_A}{[A^\circ]} \times 10^3$	$\frac{[B^\circ]\ [D^\circ]}{[A^\circ]} \times 10^3$
25	0.674	13.5	23.6	12.2
30	0.533	10.6	16.8	9.87
35	0.453	9.04	13.2	8.32
40	0.362	7.22	9.92	7.13
45	0.270	5.37	7.05	6.27
50	0.190	3.80	4.84	5.64

Plot of $\frac{m_A}{[A^\circ]}$ versus $\frac{[B^\circ]\,[D^\circ]}{A^\circ}$ gives also a straight line. From the slope of this line and its intercept with the ordinate axis k_1 and k_{-1} were calculated.

$$\text{tg}\,\alpha = k_{-1} = 2.46\ M^{-1}\ \text{min}^{-1}$$

$$k_1 = 9.6\times10^{-3}\ M^{-1}\ \text{min}^{-1}$$

These values are in a good agreement with the value of the formation constant K_1 obtained from the equilibrium study [4] $K_1 = 0.20$

$$K_1 = \frac{k_{-1}}{k_1} = 0.25$$

A very good agreement was also found concerning the k_1 values obtained from kinetic data ($k_1 = 9.6\times10^{-3}\ M^{-1}\ \text{min}^{-1}$) and those obtained by the

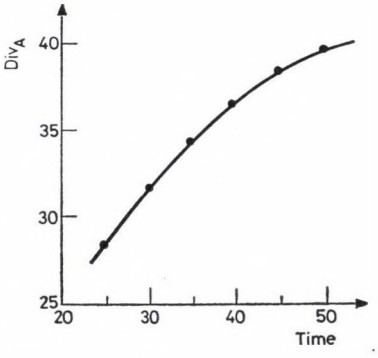


Fig. 5. Plot of Div_A versus time. $[HClO_4] = 0.1\ M$; $[NH_2OH \cdot HCl]_{initial} = 2.12\times10^{-2}\ M$

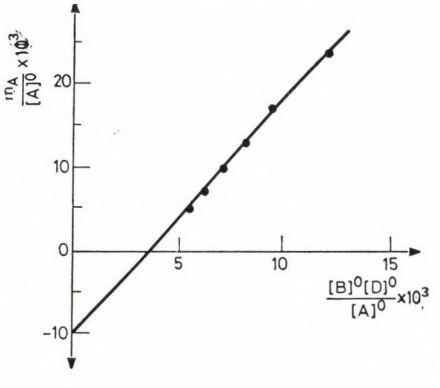


Fig. 6. Graphical determination of k_{-1} and k_1. Plot of $\frac{m_A}{[A^\circ]}$ versus $\frac{[B^\circ]\,[D^\circ]}{[A^\circ]}$. $[HClO_4] = 0.1\ M$; $[NH_2{-}OH \cdot HCl]_{initial} = 2.11\times10^{-2}\ M$

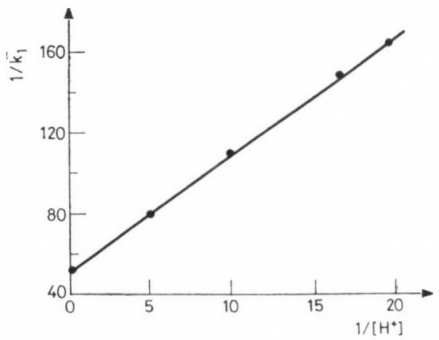
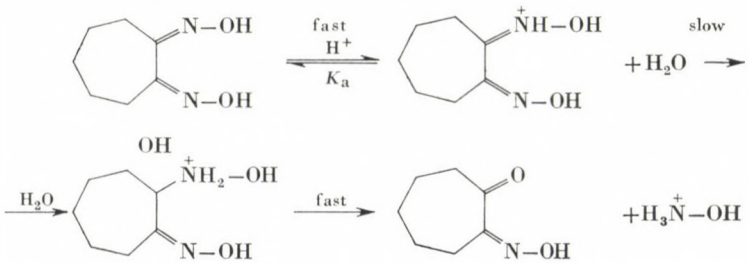


Fig. 7. Plot of $1/k_1$ versus $1/[H^+]$

hydrolysis of the heptoxime ($k_1 = 9.1 \times 10^{-3}\ M^{-1}\ \text{min}^{-1}$). The above mentioned kinetic data explain the good linearity of the graphical plot of lg Div_A vs. time in the case of the hydrolysis of heptoxime. One can demonstrate that the second member in the right hand side of equation (3) in the case of large time intervals can be dropped.

Mechanism of the dezoximation. Determination of the protonization constant of heptoxime from kinetic data

In order to elucidate the dependence of the k_1 values on the acidity of the heptoxime solutions the following mechanism can be suggested for the first step of the hydrolysis



The first step of the dezoximation is a fast protonization of an oxime group. The rate determining process is the slow addition of a water molecule to the double bond, followed by a fast dezoximation reaction.

The dependence of k_1 on the acidity of the solution can be

$$\frac{d[A^\circ]}{dt} = \frac{d[A]}{dt} + \frac{d[AH^+]}{dt} \tag{9}$$

$$\frac{d[A^\circ]}{dt} = -k_{01}[AH^+] = -k_{01}\frac{[H^+]}{K_a + [H^+]}[A^\circ] \tag{10}$$

Table VII

Kinetic data for the determination of the protonization constant K_a

$1/[HClO_4]$ M	$\frac{1}{k_1}$ min
20	164
16.66	148
10	110
5	79

Comparison of (10) with the equation;

$$\frac{d[A^\circ]}{dt} = -k_1 [A^\circ]$$

gives;

$$k_1 = k_{01} = \frac{[H^+]}{K_a + [H^+]} \tag{11}$$

and

$$\frac{1}{k_1} = \frac{K_a}{k_{01}} \cdot \frac{1}{[H^+]} + \frac{1}{k_{01}} \tag{12}$$

The plot of $1/k_1$ versus $1/[H^+]$ gives a straight line if our presumption is valid. The corresponding kinetic data are given in Table VII.

From the slope of the straight line and from its intercept the K_a and k_{01} values were obtained.

$$\text{tg}\,\alpha = \frac{K_a}{k_{01}} = 5.72$$

$$\frac{1}{k_{01}} = 52;\ k_{01} = 1.9 \times 10^{-2}\ M^{-1}\ \text{min}^{-1}$$

$$K_a = \frac{5.72}{52} = 0.11$$

The agreement between the K_a value determined from kinetic data ($K_a = 0.11$) and those from equilibrium measurements ($K_a = 0.12$) is very good.

REFERENCES

[1] Banks, C. V., Barnum, D. V.: J. Am. Chem. Soc., **80,** 3579 (1958)
[2] Alibina, A. N., Peshkova, V. M.: Vestnik Moskovsk. Univ. Ser II. Khim., **1970,** 337
[3] Mánok, F., Várhelyi, Cs., Benkő, A., Tarsoly-Magyari, M.: Monatsh. Chem., **109,** 1329 (1978)
[4] Mánok, F., Kőszegi, E., Várhelyi, Cs., Benkő, A.: Monatsh. Chem. (in press)

Acta Chimica Hungarica 116 (1), pp. 63—67 (1984)

PREPARATION, INFRARED ABSORPTION SPECTRA AND X-RAY POWDER DIFFRACTION PATTERNS OF MIXED (Ca + Ba + Pb) HYDROXYLAPATITES

P. N. PATEL[1]* and S. PANDEY[2]

([1]Post-Graduate Department of Chemistry, G. M. College, Sambalpur-768 004, India, [2]Department of Zoology, Women's College, Sambalpur-768 001, India)

Received May 13, 1983

Accepted for publication June 28, 1983

Homogeneous solid solutions of calcium, barium and lead hydroxylapatite have been prepared over the entire compositional range by the method of co-precipitation in aqueous media. Frequencies and assignments for the infrared absorption and the lattice constants of the solid solutions have been measured and found to vary linearly with composition between those of the pure end members.

Introduction

Calcium hydroxylapatite (CaHA), $Ca_{10}(PO_4)_6(OH)_2$, the principal inorganic constituent of human bones and teeth [1, 2] belongs to an isomorphous series of compounds known as apatites. Calcium hydroxylapatite (CaHA) also exists in nature as the mineral hydroxylapatite, which is similar if not identical to that in bone material, it can be prepared in aqueous solution [3, 4]. The ionic radii [5] of calcium (0.099 μm), barium (0.135 μm) and lead (0.120 μm) are close to each other to enable solid solutions to be formed between isomorphous substances containing these ions [5]. Apatite undergoes a series of cationic and anionic replacement reactions [6]. The $Ca^{2+} \rightarrow Ba^{2+}$ and/or Pb^{2+} replacement reactions in CaHA are of extreme biological significance and in view of its action on calcified tissue is interesting. They form the basis of incorporation of Ba^{2+} and Pb^{2+} into the human skeletal system according to the following equation;

$$Ca_{10}(PO_4)_6(OH)_2 + nBa^{2+} + mPb^{2+} \rightarrow Ca_{10-(n+m)}Ba_nPb_m(PO_4)_6(OH)_2 + \\ + (n + m)\,Ca^{2+}$$

where $n = 1$

Solid solutions of calcium, barium and lead hydroxylapatites were prepared separately earlier [7] by firing mixtures containing various proportions of calcium, barium and lead hydroxylapatite at about 1300 °C. These

* To whom correspondence should be addressed

samples prepared by the solid state reaction were however, found to be discontinuous and non-homogeneous.

Now an attempt has been made by the method of co-precipitation [8—10] to prepare the homogeneous solid solutions of mixed (Ca + Ba + Pb) hydroxylapatite over the entire compositional range.

Experimental

All chemicals used for the preparation of these samples were either AR (BDH) or E. MERCK extra pure grade. Water used in the preparation and for washing was boiled to remove CO_2, and then used immediately.

Preparation

Stoichiometric quantities of ammonium dihydrogen phosphate (Solution A) and a solution containing Ca^{2+}, Ba^{2+} and Pb^{2+} ions in the proportion desired for the solid solutions (Solution B) were prepared separately in carbon dioxide free doubly distilled water. The pH of these solutions was adjusted above 11 by the addition of ethylene diamine. The a part of solution B was put in a flask (2 dm^3) fitted with two separatory funnels and a delivery tube. Solution A and Solution B were poured individually into the separatory funnels and added dropwise to the content of the flask simultaneously. Precipitation was carried out in carbon dioxide free atmosphere and the mixture was stirred vigorously by bubbling CO_2-free air to prevent the formation of carbonatoapatites.

The precipitate and mother liquor were aged by boiling under reflux for 30 min to improve the homogeneity and crystallinity of the precipitate, and the maintenance of the desired pH during precipitation was ensured by testing the filtrate after separation of the precipitate, since any alteration of pH of the medium during precipitation leads to the formation of calcium deficient apatites [11]. The precipitate was washed thoroughly with doubly distilled water to free it from ammonium salts. Samples dried at 100 °C for few hours were analysed complexometrically and their molar volumes were determined by density method using toluene [12] as a solvent.

Infrared absorption techniques

Sample used for infrared studies was washed with acetone and dried on air. All the bands were recorded on a Grating Infrared Spectrophotometer model 577 (Perkin-Elmer) in KBr. A few milligrams of the sample was ground with two drops of Nujol in an agate mortar. About 50 mg of a fine polythylene powder (VESTOLENA 6016 Chem. Werke Huels, Germany) was added. The resulting paste was melted rapidly at about 140° and pressed between glass plates to a slightly wedge shaped film of an average thickness of 0.1 mm.

X-ray diffraction techniques

Samples dried at 110° for a few hours were used for X-ray diffraction. The X-ray diffraction pattern of the samples was obtained on a Siemens Powder diffractometer with a NaCl(Tl) counter employing CuK_α (Nickel filtered) radiation with a scanning speed of 1 degree (2Θ) per min (using tube voltage of 30 kV and 24 mA, respectively).

Lattice constant measurements

CaHA, BaHA and PbHA are hexagonal with two lattice constants a_0 and c_0. These were determined [13, 14] for all the samples by measuring the diffraction angle 2Θ of the three planes (312), (123) and (321). Each sample was thoroughly mixed with 25% NaCl (recrystallized from HCl) which served as a standard. So the observed values of $\sin\Theta$ for the solid solution lines could be corrected directly for absorption and instrumental errors. The lattice constant of NaCl at 26° was taken to be 0.56403 μm [15]. A least squares calculation on the corrected values of $\sin\Theta$ for the three reflections then gave the two parameters, a_0 and c_0, for

each sample. The diffraction lines were quite sharp and the diffraction angle was read by counting over the top of the peak with the scaling unit and estimating the position of maximum intensity from a plot of intensity against 2Θ. The average probable error in unit cell parameters is less than ± 0.05 μm.

Results and Discussion

The results of chemical analysis of the samples are given in Table I. Based on the fact that a mole of each sample has a total 10 g-atoms of calcium and/or barium and/or lead the molecular formula of the samples was calculated. The fact that the observed value of molar g-atom ratio of $\frac{Ca}{P}$, $\frac{Ba}{P}$, $\frac{Pb}{P}$ for the end members and $\frac{Ca + Ba + Pb}{P}$ were found to be equal to 1.664 (theoretical 1.67) is consistent with the formation of a homogeneous solid solution [12]. This was further supported by the closeness of the values of molar volume of the members and those of the intermediate samples which lie within the range of end members.

The formation of solid solutions can be further confirmed by the X-ray diffraction analysis. It is well established that all the members of the apatite series exhibit hexagonal-bipyramidal class — $6/m$ (space group $P6_{3/m}$) [16, 17]. Lattice parameters showed unit cell dilation consequent upon the introduction of larger ions Ba^{2+} (0.135 μm) and Pb^{2+} (0.120 μm) in place of Ca^{2+} (0.099 μm) ion in the apatite lattice. Such dilation with the proportion of Ca—Ba—PbHA

Table I

Chemical analysis of calcium, barium and lead hydroxylapatite and their solid solutions

Sample No.	Molecular Formula	G. atom ratio $\frac{Ca+Ba+Pb}{P}$	Lattice parameter (μm)		Unit cell volume $\frac{\sqrt{3}}{2} a^2c \times 10^3$	Frequency (cm^{-1})		
			a	c		PO_4^{3-} ν_4	PO_4^{-3} ν_3	OH^- ν_3
1	$Ca_{10}(PO_4)_6(OH)_2$	1.665	0.937	0.686	0.523	570	1075	3450
2	$Ca_{8.1}Ba_{1.1}Pb_{0.8}(PO_4)_6(OH)_2$	1.667	0.941	0.689	0.528	565	1070	3448
3	$Ca_{7.05}Ba_{1.05}Pb_{1.9}(PO_4)_6(OH)_2$	1.666						
4	$Ca_{5.95}Ba_{1.1}Pb_{2.95}(PO_4)_6(OH)_2$	1.663	0.950	0.696	0.544	565	1068	3445
5	$Ca_{5.0}Ba_{1.15}Pb_{3.85}(PO_4)_6(OH)_2$	1.658						
6	$Ca_{4.0}Ba_{0.95}Pb_{5.05}(PO_4)_6(OH)_2$	1.662	0.958	0.705	0.560	560	1065	3440
7	$Ca_{2.8}Ba_{1.15}Pb_{6.05}(PO_4)_6(OH)_2$	1.656						
8	$Ca_{2.1}Ba_{1.1}Pb_{6.8}(PO_4)_6(OH)_2$	1.663	0.966	0.715	0.578	555	1060	3435
9	$Ca_{1.2}Ba_{0.85}Pb_{7.95}(PO_4)_6(OH)_2$	1.666						
10	$Ba_{1.2}Pb_{8.8}(PO_4)_6(OH)_2$	1.655	0.979	0.727	0.603	550	1060	3435
11	$Pb_{10}(PO_4)_6(OH)_2$	1.664	0.986	0.738	0.621	545	1055	3436

was evident that the unit cell volume of the samples calculated on the basis of the experimentally determined lattice constant increased with the proportion of barium and lead content in Ca—Ba—PbHA. This, of course, is the real evidence for solid solution in this series and clearly shows that these preparations are not mixtures of two components or one component with the absorbed material.

The CaHA and its solid solutions with barium and lead have hexagonal crystalline structure and are interesting examples of solid state of fairly simple molecules of tetrahderal symmetry where bands become allowed due to relaxation of the molecular symmetry [18] selection rules due to the influence of site symmetry. The ideal symmetry of tribasic phosphate ion in the free or undistorted state is tetrahedral — a member of *Td* point group. Under this ideal symmetry condition only a few absorption bands corresponding to ν_4 (570 cm^{-1}) and ν_3 (1075 cm^{-1}) of PO_4^{3-} and ν_3 (3450 cm^{-1}) of OH^- were observed clearly. From the spectra of the samples, it could be seen that the ν_3 and ν_4 frequencies corresponding to PO_4^{3-} ion and ν_3 corresponding to OH^- ion are shifted to lower frequencies and the shape of the peaks was affected by the introduction of barium and lead ion into the samples. The shift of the ν_3 and ν_4 of PO_4^{3-} vibrations to lower frequencies may be due to the effect of binding energy and atomic mass. The lowering of frequency of ν_3 of OH^- indicates the presence of hydroxyl group in the apatite [19]. This hydroxyl group in hydroxylapatite lies in the internuclear axis coincident with six fold screw axis. In Barness expression [20]

$$\nu = \frac{1}{2\pi c}\sqrt{\frac{K}{\mu}}$$

which gives a relationship between frequency, atomic mass and force constant. The vibrational frequencies are dependent on the reduced mass μ of the participating atoms and restoring forces K between atoms, all other terms remaining constant. When the equilibrium distance between the positive and the negative atoms of the molecule is descreased K generally increases in the above equation. This equilibrium distance depends on the ionic radii of the participating atoms in the molecule. Substitution of Ca^{2+} with an ion like Ba^{2+} and/or Pb^{2+} gives rise to a stronger coordination of the PO_4^{3-} group through oxygen. This in turn weakens the P—O bond, lowering K (increasing P—O bond length) and the frequency is lowered. The PO_4^{3-} bonding is normally around 520 cm^{-1} and bonding modes do not shift very much under these conditions. But here the substitution is more complex, presumably because of the splitting of the triply degenerate mode at 600 cm^{-1} and thus there is an increase in the frequency from 520 cm^{-1} to 570 cm^{-1}. This theoretical explanation agrees well with the experimental data.

*

The authors are highly indebted to Prof. G. Ferraris of University of Torino (Italy) for X-ray data and Dr. M. M. Dhar F.N.A., C.D.R.T., Lucknow for infrared spectra. The financial support to the authors by the University Grants Commission is gratefull acknowledged.

REFERENCES

[1] Neuman, W. F., Neuman, M. W.: Chem. Revs., **53,** 1 (1953)
[2] Robinson, R. A.: J. Bone and Joint Surg., **34,** 389 (1952)
[3] Wallacys, R., Chaudron, G.: Compt. rend., **231,** 355 (1950)
[4] Hayek, E., Stadlmann, P.: Angew Chem., **67,** 327 (1955)
[5] Wells, A. F.: "Structural Inorganic Chemistry", P. 70, Oxford University Press, London 1950
[6] Van Wazer, J. R.: "Phosphorus and its Compounds" Vol. **1,** P. 530, New York, Interscience Publis ers, Inc.
[7] Van Wazer, J. R.: "Phosphorus and its Compounds" Vol. **2,** P. 1429, New York, Interscience Publishers 1966
[8] Patel, P. N.: J. Chem. Ind. (London), **20,** 804 (1978)
[9] Patel, P. N.: J. Ind. Chem. Soc., **56,** 410 (1979)
[10] Patel, P. N.: J. Chem. Ind. (London), **14,** 19 (1980)
[11] Berry, E. E.: J. Inorg. Nucl. Chem., **29,** 1585 (1967)
[12] Partington, J. R.: "An Advanced Treatise on Physical Chemistry" Vol. **3,** P. 121, Longman Green and Co. 1952
[13] Azaroff, L. V.: "Elements of X-ray Crystallography" Chapter **18,** London, McGraw Hill Book Co. 1968
[14] Cullity, M.: "Elements of X-ray Diffraction" pp. 309—313
[15] Straumanis, M., Levins, A. Z.: Phys., **109,** 728 (1938)
[16] Mehmel, M. Z.: Krist., **75,** 323 (1930); Naray-Szabó, I.: ibid., **75,** 387 (1930)
[17] Hentschel, H.: Z. Mineral Geol., **1923,** 609
[18] Nakamoto, K.: "Infrared Spectra of Inorganic and Co-ordination Compounds" P. 103, New York, John Wiley and Sons, Inc. 1966
[19] Engel, G., Klee, W. E.: J. Solid State Chem., **6,** 28 (1972)
[20] Barnes, R. B., Gore, R. C., Liddel, V., Williams, V. Z.: "Infrared Spectroscopy" Reinhold, New York 1944

Acta Chimica Hungarica 116 (1), pp. 69—75 (1984)

ION EXCHANGE KINETICS OF ALKALINE EARTHS ON Zr(IV) ARSENOSILICATE CATION EXCHANGER

ACTIVATION ENERGY AS A LINEAR FUNCTION OF THE IONIC MOBILITIES AND RADII

K. G. VARSHNEY*, S. AGRAWAL and K. VARSHNEY

(Analytical Laboratories, Chemistry Section, Faculty of Engineering & Technology, Aligarh Muslim University, Aligarh-202001, India)

Received May 17, 1983

Accepted for publication June 28, 1983

A new approach based on the Nernst–Planck equations has been applied to study the ion exchange kinetics for the exchange reactions of Mg(II), Ca(II), Sr(II) and Ba(II) with H^+-ions at various temperatures on the zirconium(IV) arsenosilicate phase. Under the conditions of particle diffusion, the rate of exchange was found to be independent of the metal ion concentration at and above 0.1 *M* in aqueous medium. Energy and entropy of activation were determined and found to vary linearly with the ionic radii and mobilities of alkaline earths, a unique feature observed for an inorganic ion exchanger. The results are useful for predicting the ion exchange processes occurring on the surface of an inorganic material of the type studied.

Introduction

Inorganic ion exchangers are useful for the separation of metals [1,2]. Although a large number of such materials have been prepared, only a few of them have been reported for their kinetic studies [3—21]. Moreover, the earlier approaches are based on the old 'Bt criterion' [22] which is useful only for ions having similar effective diffusion coefficients i.e. for the isotope exchange processes. In an ion exchange phenomenon, however, the fluxes of two different ionic species are coupled into one another [23], and, therefore, a single diffusion coefficient can not describe the actual process. This article, therefore, summarizes our efforts to apply the Nernst—Planck equations [24, 25] which take into account the exchange of ions having different mobilities to determine the various kinetic parameters. Zirconium(IV) arsenosilicate (ZAS) has been selected because of its fairly good stability, reproducibility and applicability in the analysis of some real samples [26, 27].

* To whom correspondence should be addressed

Experimental

Reagents and chemicals

Zirconyl chloride and arsenic acid used in this study were BDH (England) products while sodium silicate was the product of Riedel (DEHAENAG, Seelze Hannover). Other reagents and chemicals were of analaR grade.

Apparatus

A water-bath incubator shaker having a temperature variation of ± 0.5 °C was used in the equilibrium studies.

Synthesis of the ion exchange material

ZAS was prepared as earlier [26] by the following method: An aqueous (0.1 *M*) sodium silicate solution, made acidic (pH 0—1) by adding HCl, was mixed with an aqueous (0.1 *M*) zirconyl chloride solution and the pH of the mixture was raised to 8—10 by a slow addition of ammonium hydroxide with intermittent shaking to obtain a slurry. After filtration and washing with demineralized water (DMW), it was treated with a 1 : 1 (*V*/*V*) mixture of 0.5 *M* solutions of arsenic and nitric acids. This resulted in a gel which was digested at room temperature for 24 h and then separated by filtration. It was washed thoroughly to remove excess acid, dried at 45 °C and cracked into small granules by putting in DMW and then converted into the H^+-form using 1 *M* HNO_3. They were finally washed with DMW and dried as usual for further study. The Na^+-exchange capacity of the material was found to be 1.3 meq/dry g as determined by the column process.

Kinetic measurements

Ion exchange particles of mean radii 250 μm (55—65 mesh size) were used in this experiment. 20 mL fractions of the 0.1 *M* metal ion solution (Mg, Ca, Sr and Ba) were shaken with 200 mg of the exchanger in several stoppered conical flasks at the desired temperature (20, 30, 45 and 60 °C, ± 0.5 °C) for different time intervals. Supernatant liquid was immediately removed by filtering it through a Whatman No. 4 filter paper. Determinations were done by EDTA titrations [28] using Eriochrome Black T as an indicator. Each run was repeated at least six times.

Results and Discussion

A study of the concentration effect on the rate of exchange for Mg^{2+}—H^+ exchange at 30 °C shows that at concentrations <0.1 *M* the initial rate of exchange is proportional to [Mg(II)]. At concentrations ≥ 0.1 *M* it is found to be independent of the metal ion concentration. Under the conditions of particle diffusion control, a relatively large particle size of the exchanger and vigorous shaking, the fractional attainment of equilibrium may be given as

$$U(\tau) = \frac{\text{the amount of exchange at time } t}{\text{the amount of exchange at infinite time}}$$

A plot of $U(\tau)$ versus t (Fig. 1) indicates that the fractional attainment of equilibrium is faster at a higher temperature, an observation analogous to the other materials of this class. Although, this is a limited bath system, the equation applicable to an infinite bath can be used here because $CV \gg \bar{C}\bar{V}$ where C and $\bar{C}$ are the metal ion concentrations in the solution and the exchanger

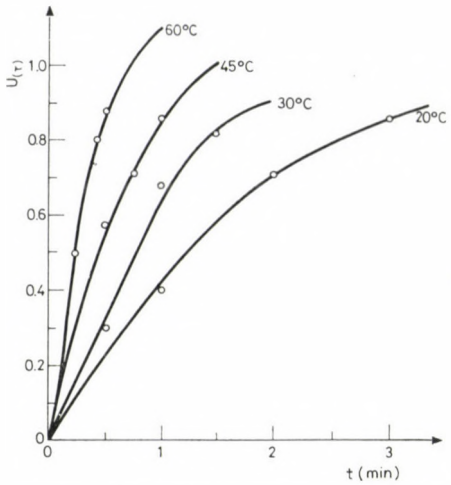


Fig. 1. Plot of $U(\tau)$ versus t for $Mg^{2+}-H^+$ exchange at different temperatures on ZAS

phases, respectively, while V and $\bar{V}$ are the volumes of these phases. The Nernst—Planck equations can be solved with some additional assumptions [23] which are valid for inorganic ion exchangers as the swelling changes and the specific interactions are not significant in this case. As a result we obtain a coupled interdiffusion coefficient $\bar{D}_{AB}$, the value of which depends on the relative concentrations of the counter ions 'A' and 'B' in the exchanger phase ($\bar{C}_A$ and $\bar{C}_B$). For $\bar{C}_A \ll \bar{C}_B$, the interdiffusion coefficient assumes the value $\bar{D}_A$, 'A' being the counter ion initially present in the ion exchanger phase. Since in the present study the exchanger is taken in the H^+ form, $\bar{D}_A$ may be replaced by $\bar{D}_H$.

Thus, on the basis of the Nernst—Planck equations the numerical results can be expressed by the explicit approximation [25]

$$U(\tau) = \left\{1 - \exp\left[\pi^2(f_1(\alpha)\,\tau + f_2(\alpha)\,\tau^2 + f_3(\alpha)\,\tau^3)\right]\right\}^{\frac{1}{2}} \qquad (1)$$

where $\tau \equiv \dfrac{\bar{D}_H\, t}{r_0^2}$,

mobility ratio, $\alpha \equiv \dfrac{\bar{D}_H}{\bar{D}_M}$, r_0 = particle radius and $\bar{D}_M$ is the interdiffusion coefficient of the metal ion. Under the conditions $1 \leq \alpha \leq 20$ and $\dfrac{Z_H}{Z_M} = \dfrac{1}{2}$ which are fulfilled in the present case, the three functions $f_1(\alpha)$, $f_2(\alpha)$ and $f_3(\alpha)$ can be expressed as

$$f_1(\alpha) = -\frac{1}{0.64 + 0.36\alpha^{0.668}}$$

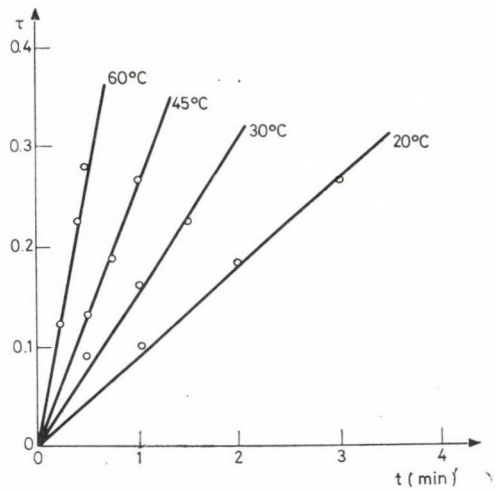


Fig. 2. Plot of τ versus t for $Mg^{2+}-H^{+}$ exchange at different temperatures on ZAS

$$f_2(\alpha) = -\frac{1}{0.96 - 2.0\,\alpha^{0.4635}}$$

$$f_3(\alpha) = -\frac{1}{0.27 + 0.09\,\alpha^{1.14}}$$

Each value of $U(\tau)$ will have a corresponding value of τ which is obtained by solving the equation (1) by graphical method. Plots of τ vs. t at the four different temperatures (Fig. 2) for Mg(II) ion are shown at a concentration 0.1 M which are straight lines passing through the origin. This confirms that the phenomenon is particle-diffusion controlled. Table I Slopes (S) of such lines for all the four alkaline earths are given in Table I which are related with $\bar{D}_H$ as follows;

$$S = \frac{\bar{D}_H}{r_0^2} \tag{2}$$

Table I

Slopes (S) of the various τ versus time plots for alkaline earths on ZAS

Migrating ion	$S\ (s^{-1})$			
	20 °C	30 °C	45 °C	60 °C
Mg(II)	1.50×10^{-3}	2.56×10^{-3}	4.42×10^{-3}	9.26×10^{-3}
Ca(II)	1.75×10^{-3}	2.78×10^{-3}	4.90×10^{-3}	11.10×10^{-3}
Sr(II)	1.34×10^{-3}	2.08×10^{-3}	4.35×10^{-3}	7.90×10^{-3}
Ba(II)	1.08×10^{-3}	1.79×10^{-3}	3.55×10^{-3}	7.20×10^{-3}

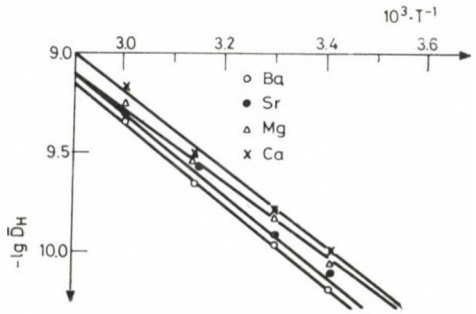


Fig. 3. $\log \bar{D}_H$ against T^{-1}

The values of $\log \bar{D}_H$ obtained by this equation were plotted against $1/T$. Straight lines are obtained for all the metal ions studied, as shown in Fig. 3, justifying the validity of the Arrhenius equation;

$$\bar{D}_H = D_0 \exp(-E_a/RT) \tag{3}$$

The pre-exponential constants D_0 are obtained from the intercepts of the lines and then the E_a values can be calculated by the use of this equation.

The entropy of activation (ΔS^*) is obtained by substituting D_0 into the following equation

$$D_0 = 2.72\, d^2 \frac{kT}{h} \exp\left(\frac{\Delta S^*}{R}\right) \tag{4}$$

where k and h are the Boltzmann and Planck's constants, d is the ionic jump distance taken [29] as 0.5 nm, R is the gas constant and T is taken as 273 °K. The values of D_0, E_a and ΔS^* are summarized in Table II. As the results show E_a increases with the ionic radii as usual. Positive entropy changes may be due to the deformation in the shape of the matrix because of the introduction

Table II

D_0, energy of activation and entropy of activation of alkaline earths on ZAS in H^+-form

Migrating ion	Ionic mobility $m^2 \cdot V^{-1} \cdot s^{-1} \cdot 10^8$	Ionic radii nm	Hydrated ionic radii nm	D_0 $m^2 \cdot s^{-1}$	E_a $kJ \cdot mol^{-1}$	ΔS^* $J \cdot K^{-1} \cdot mol^{-1}$
Mg(II)	5.5	0.078	0.310	1.36×10^{-4}	34.53	29.57
Ca(II)	6.2	0.106	0.200	2.93×10^{-4}	36.05	35.98
Sr(II)	6.2	0.127	0.180	3.85×10^{-4}	37.55	38.25
Ba(II)	6.6	0.143	0.150	4.47×10^{-4}	38.28	39.49

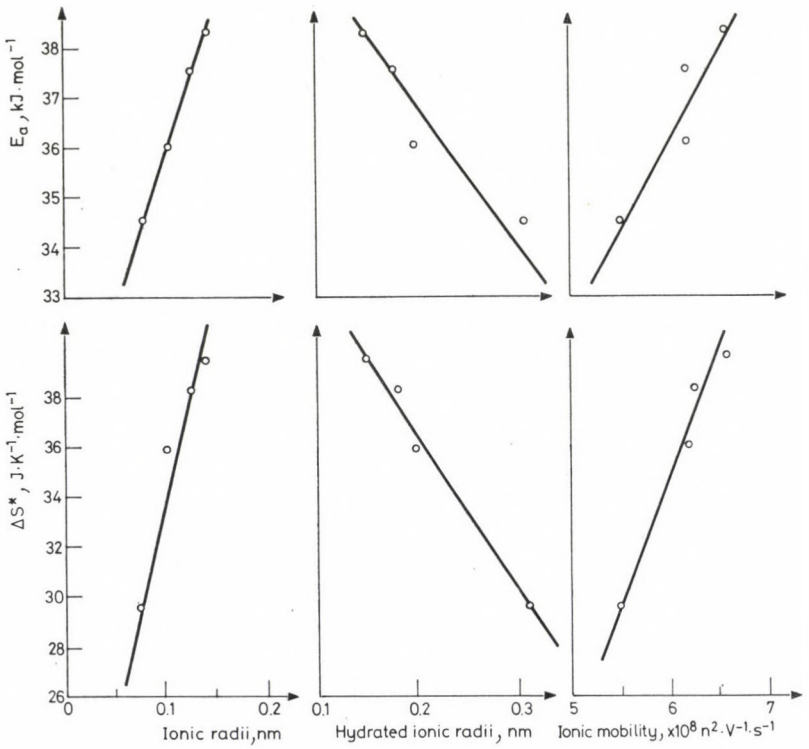


Fig. 4. Variation of E_a and ΔS^* with ionic radii, hydrated ionic radii and ionic mobilities of the alkaline earths on ZAS

of larger ions in place of the previously present H^+ ions in the matrix. A similar behaviour has also been observed earlier for the exchange of Co(III) amine complex cations on chromium ferrocyanide gel [17]. We found linear relations between E_a and ΔS^* values and the ion mobilities and radii of the alkaline earths as shown in Fig. 4.

*

The authors are thankful to Prof. Mohsin Qureshi for research facilities and to the CSIR (India) for financial assistance.

REFERENCES

[1] Nachod, F. C., Schubert, J.: Ion Exchange Technology, p. 287, Academic Press Inc. Publishers, New York 1956
[2] Clearfield, A., Nancollas, G. H., Blessing, R. H.: in Ion Exchange and Solvent Extraction, Vol. **5** (Eds J. A. Marinsky and Y. Marcus), Marcel Dekker, New York 1973
[3] Nancollas, G. H., Paterson, R.: J. Inorg. Nucl. Chem., **22,** 259 (1961)
[4] Harvie, S. J., Nancollas, G. H.: J. Inorg. Nucl. Chem., **30,** 273 (1968)
[5] Ruvarac, A. L., Vesely, V.: J. Inorg. Nucl. Chem., **32,** 3939 (1970)
[6] Clearfield, A., Medina, A. S.: J. Inorg. Nucl. Chem., **32,** 2775 (1970)
[7] Dyer, A., Ocon, F. T.: J. Inorg. Nucl. Chem., **33,** 3153 (1971)
[8] Ruvarac, A. L.: J. Chromatogr., **60,** 235 (1971)

[9] Choudhury, D., Mukherjee, S. K.: J. Inorg. Nucl., Chem., **33,** 1933 (1971)
[10] Ruvarac, A. L., Trtanj, M. I.: J. Inorg. Nucl. Chem., **34,** 3893 (1972)
[11] Alberti, G., Bertrami, R., Cascoila, M., Costantino, U., Gupta, J. P.: J. Inorg. Nucl. Chem., **38,** 843 (1976)
[12] Rawat, J. P., Thind, P. S.: J. Phys. Chem., **80,** 1384 (1976)
[13] Herman, R. G., Clearfield, A.: J. Inorg. Nucl. Chem., **38,** 853 (1976)
[14] Dyer, A., Gill. J. S.: J. Inorg. Nucl. Chem., **39,** 665 (1977)
[15] Bunzl, K.: J. Inorg. Nucl. Chem., **39,** 1049 (1977)
[16] Rawat, J. P., Singh, D. K.: J. Inorg. Nucl. Chem., **40,** 897 (1978)
[17] Saraswat, I. P., Srivastava, S. K., Sharma, A. K.: Can. J. Chem., **57,** 1214 (1979)
[18] Rawat, J. P., Khan, M. A.: J. Inorg. Nucl. Chem., **42,** 905 (1980)
[19] Singh, N. J., Mathew, J., Tandon, S. N.: J. Phys. Chem., **84,** 21 (1980)
[20] Singh, N. J., Tandon, S. N.: Ind. J. Chem., **19A,** 416 (1980)
[21] Varshney, K. G., Premadas, A.: Ind. J. Chem., **20A,** 841 (1981)
[22] Boyd, G. E., Adamson, A. W., Myers, L. S.: J. Am. Chem. Soc., **69,** 2836 (1947)
[23] Helfferich, F.: Ion Exchange, Ch. 6, Mc Graw-Hill, New York 1962
[24] Nernst, W. Z.: J. physik. Chem., **2,** 613 (1888); **4,** 129 (1889)
[25] Planck, M.: Ann. Phys. Chem., **39,** 161 (1890)
[26] Varshney, K. G., Agrawal, S., Varshney, K.: Sep. Sci. Technol., **18,** 59 (11983)
[27] Varshney, K. G., Agrawal, S., Varshney, K.: J. Liq. Chromatogr., **6,** 1535 (1983)
[28] Reilley, C. N., Schmid, R. W., Fawzys: J. Chem. Educ., **36,** 555 (1959)
[29] Barrer, R. M., Bartholomew, R. F., Rees, L. V. C.: J. Phys. Chem. Solids, **12,** 21 (1961)

Acta Chimica Hungarica 116 (1), pp. 77—80 (1984)

THERMODYNAMIC PROPERTIES OF BINARY MIXTURES PYRIDINE BASE AND *ISO*-ALIPHATIC ALCOHOLS

T. KASPRZYCKA-GUTTMAN* and H. WILCZURA

(Department of Chemical Technology, Warsaw University, 02-093 Warsaw, ul. Pasteura 1, Poland)

Received January 19, 1983
In revised form June 14, 1983
Accepted for publication July 13, 1983

Excess enthalpy of mixing H^E measured at 293.15 and 303.15 K and excess Gibbs energy G^E at 323.15 K are reported for binary mixtures of pyridine base and *iso*-aliphatic alcohols.

This work is continuation of our study on the excess enthalpies H^E and excess Gibbs energy G^E of mixtures consisting of pyridine base and *iso*-aliphatic alcohols.

We have our investigations H^E for binary systems: pyridine base (γ-picoline) and *iso*-aliphatic alcohols (2-propanol,2-butanol, *iso*-butanol, *tert*-butanol) at 293.15 and 303.15 K and excess Gibbs energy at 323.15 K for the same binary mixtures.

Experimental

The *iso*-aliphatic alcohols ($C_3 - C_4$) were purified as suggested by Weissberger [1]. The pyridine base, γ-picoline was dried over the potassium hydroxide and distilled with a laboratory column. Physical properties: density ϱ, molar volume V_{0i}, refractive index n_D, gas chromatographic analysis of the pure liquid at 298.15 K are given in Table I. The apparatus and the operational procedure for measuring properties have been described in [2, 3].

Results and Discussion

The results G^E and H^E were fitted to the equation:

$$Y^E[\mathrm{Jmol^{-1}}] = x_1 x_2 \sum_{i=1}^{4} C_i (x_1 - x_2)^{i-1} \qquad (1)$$

where $C_1, \ldots C_i$ are adjustable coefficients calculated by the method of least squares, x_1 and x_2 are mole fractions of aclohol and pyridine base. The values obtained are given in Table II, δ is the standard error defined by

$$\delta(Y^E)\,[\mathrm{Jmol^{-1}}] = [\Sigma(H^E_{\mathrm{exp.}} - H^E_{\mathrm{calc.}})^2\,(n-k)^{-1}]^{1/2} \qquad (2)$$

* To whom correspondence should be addressed

Table I

Physical properties of pure substances at 298.15 K

Substance	ϱ (gcm^{-3})	V_{0i} (cm^3 mole^{-1})	n_D	Degree of purity (per cent)
γ-picoline	0.95031	98.01	1.5023	99.99
2-propanol	0.78095	74.71	1.3747	99.99
2-butanol	0.60267	93.34	1.3978	99.99
iso-butanol	0.79435	91.98	1.3939	99.80
tert-butanol	0.78086	94.92	1.3823	99.9

Degree of purity (per cent) determined by gas chromatography.

Table II

Coefficients of equation (1) *for binary mixtures with the corresponding standard deviations* $\delta(Y^E)$ Jmol^{-1}

Mixtures	Y^E	T, K	C_1	C_2	C_3	C_4	$\delta(Y^E)$
γ-picoline +	H^E	293.15	621.21	45.57	−102.46	−68.09	0.53
2-propanol	H^E	303.15	691.47	213.95	−30.41	−171.15	0.56
	G^E	323.15	−3722.28	3900.66	−2930.78	182.47	4.19
γ-picoline +	H^E	303.15	−457.30	264.71	−94.00	−23.86	0.27
2-butanol	G^E	323.15	−2013.11	270.11	495.51	−1149.82	2.85
γ-picoline +	H^E	293.15	827.16	179.88	−34.43	−233.42	1.70
iso-butanol	H^E	303.15	636.38	152.98	42.28	340.88	0.79
	G^E	323.15	−2629.09	−968.66	507.01	−184.47	2.70
γ-picoline +	H^E	293.15	−196.42	773.64	51.73	793.46	0.15
tert-butanol	H^E	303.15	−633.08	1694.97	−432.63	1191.13	0.16
	G^E	323.15	−1538.13	948.58	−1855.83	2900.64	0.62

where k is the number of coefficients needed to represent the results adequately and the sum is taken over the set of n results.

The experimental results of the measurements of H^E and G^E for γ-picoline and *iso*-aliphatic alcohols binary mixtures were plotted in the system H^E or G^E vs. mole fraction of the pyridine base in Figs 1, 2.

G^E values for the γ-picoline + *iso*-alophatic alcohols (C_3—C_4) mixtures are negative and increase in the sequence;2-propanol < *i*-butanol < *tert*-butanol < 2-butanol.

The H^E values increase in the sequence for $x_1 = x_2 = 0.5$: *i*-butanol < < *tert*-butanol < 2-propanol < 2-butanol.

The studied systems feature significant deviations from the ideal solution laws due to the strong specific interactions.

The $-G^E$ vs. x_p and $\pm H^E$ vs. x_p relation is not symmetrical one. The lack of the symmetry of G^E and H^E results from the different kinds of association between the molecules of pure alcohols (the linear and cyclic associations should be taken into account) pure pyridine base and their mixtures, presumably.

The considerably greater value of G^E of the system with *i*-propanol in comparison the to other butyl alcohols is evidently connected with the change of the length of the carbon chain in *i*-propanol. The very likely consequence of this change is the increase of the mobility of particles, which facilitates the orientation of —OH groups toward nitrogen atoms in γ-picoline. The steric interaction between the groups of high volume may also influence the values of G^E and H^E measured. For the systems of picoline and *i*-alcohols this effect

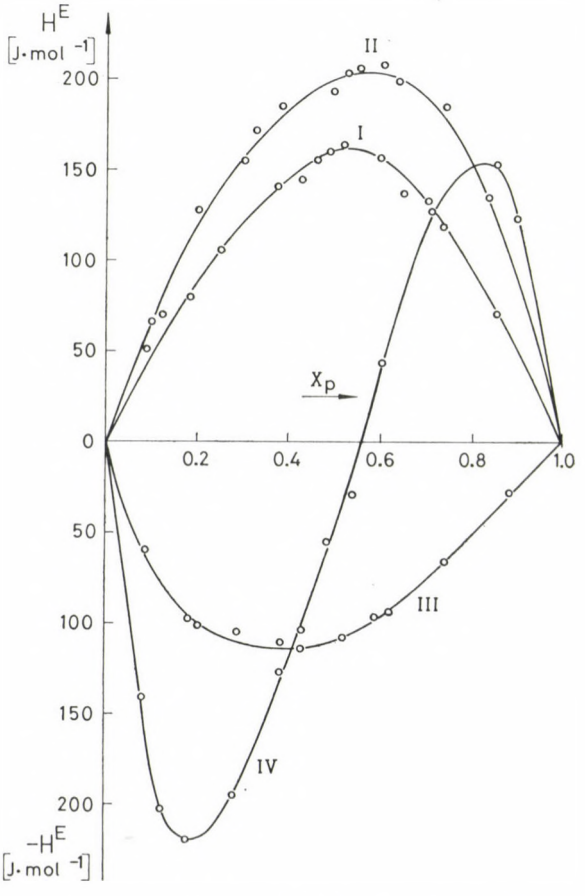


Fig. 1. Excess enthalpy of mixing H^E vs. x_p of the binary systems: I. γ-picoline + 2-propanol, II. γ-picoline + 2-butanol, III. γ-picoline + *iso*-butanol at 293.15 K and IV. *tert*-butanol + + γ-picoline at 313.15 K

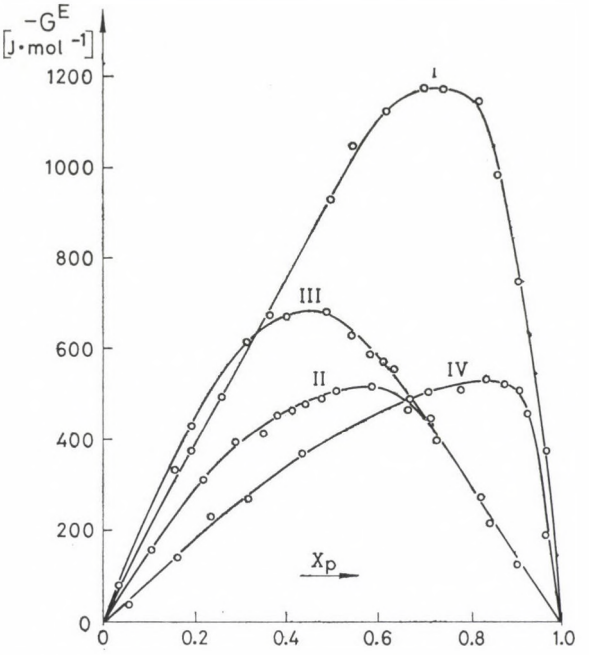


Fig. 2. Excess Gibbs energy G^E vs. x_p of the binary systems: I. γ-picoline + 2-propanol, II. γ-picoline + 2-butanol, III. γ-picoline + *iso*-butanol, IV. γ-picoline + *tert*-butanol at 323.15 K

is predominant in pure alcohols. The formation of hydrogen bond of the alcohol--alcohol type is considerably impeded in *t*-butanol, but may easily take place in *i*-butanol. This enables to explain the fact, that the values of G^E for *i*-butanol are greater than in the case of the remaining alcohols.

The decisive factors, which influence the values of G^E and H^E in the systems discussed, are: specific interactions, steric effects and the size of the molecule [4—7].

The overlap of the described effects is making difficult the clear-cut qualitative interpretation of the results obtained, thus the qualitative one is presented, at present. However, supported by the forthcoming experimental data the presented interpretation will be extended to quantitative one in the near future.

REFERENCES

[1] Weissberger, A. (ed): Organic Solvents, Moscow 1958
[2] Orszagh, A., Kasprzycka-Guttman, T.: Bull. Acad. Polon. Sci., **4**, 349 (1972)
[3] Orszagh, A., Kasprzycka-Guttman, T.: Proc. First Intern. Conf. Calorimetry and Thermodynamics, Warsaw, 1969, p. 861
[4] Perrin, D. D.: Dissociation Constants of Organic Bases in Aqueous Solution, London 1965
[5] Kiefer, M., Becker, F.:Proc. Intern. Conf. on Thermodynamics, Vienna, 1973., p. 145
[6] Cox, J. D.: Trans Faraday Soc., **56**, 349 (1960)
[7] Kowalski, B., Kasprzycka-Guttman, T.: Polish J. Chem., **54**, 1775 (1980)

Acta Chimica Hungarica 116 (1), pp. 81—87 (1984)

VISCOSITY OF BINARY SYSTEMS OF THE TYPE: CRESOL—PYRIDINE BASE

I. CHOJNACKA* and A. ORSZAGH

(Department of Chemistry, University of Warsaw, 02-093 Warsaw, Pasteura 1, Poland)

Received January 27 1983

In revised form June 20, 1983

Accepted for publication July 13, 1983

The viscosity, density and refractive index were determined — as a function of composition at 303 K — in eight binary systems: *m*-cresol (*p*-cresol) + pyridine, α-picoline, 2,6-lutidine 2,4,6-collidine. The viscosity isotherms were calculated for these systems according to the principle of molar additivity of viscosity, and of molar additivity of the lg of viscosity, as well as from so-called excess viscosity.

The components of the investigated systems of the type: cresol—pyridine base are characterized by complicated molecular interactions which are decisive of their properties. Thus they are so-called compound liquids forming complex sulutions [1]. The macroscopic effects measured are the resultant of many factors of energetic and structural nature. Structural factors presenting difficulties in direct experimental studies can be estimated from measurements of the parameters being a function of the structure of solution. Viscosity belongs to these parameters.

Experimental

The components of the binary systems were dried and purified by fractional distillations. Purity was checked by measurements of density, and refractive index, and by analytical gas chromatography. The substances used were 99.7 to 99.9 per cent pure.

The method of measurements has previously been published [2].

Results

Viscosity was calculated from the equation;

$$\eta = \left(C \cdot t - \frac{B}{t}\right) \cdot d,$$

where; η — viscosity, t — time of flow, d — density, B, C — constants.

* To whom correspondence should be addressed

Table I

Results of measurements of density, refractive index and viscosity
(measured and calculated)

x_1	$d \cdot 10^3$ kg/m^3	n_D	$\eta \cdot 10^3$ kg/ms	$\eta_a \cdot 10^3$ kg/ms	$\eta_i \cdot 10^3$ kg/ms	$\lg \eta^E$	x_1	$d \cdot 10^3$ kg/m^3	n_D	$\eta \cdot 10^3$ kg/ms	$\eta_a \cdot 10^3$ kg/ms	$\eta_i \cdot 10^3$ kg/ms	$\lg \eta^E$
1	2	3	4	5	6	7	1	2	3	4	5	6	7
		m-cresol + pyridine							*m*-cresol + 2,6-lutidine				
0.000	0.9725	1.5032	0.831				0.000	0.9170	1.4920	0.759			
0.125	0.9831	1.5144	1.135	1.999	1.137	0.000	0.126	0.9357	1.5025	1.098	1.946	1.053	0.018
0.250	0.9947	1.5245	1.615	3.168	1.555	0.016	0.250	0.9542	1.5113	1.668	3.114	1.452	0.060
0.375	1.0035	1.5308	2.361	4.335	2.126	0.045	0.375	0.9721	1.5205	2.773	4.289	2.009	0.140
0.500	1.0108	1.5319	3.663	5.503	2.908	0.100	0.500	0.9882	1.5286	5.194	5.468	2.780	0.271
0.625	1.0177	1.5348	5.557	6.669	3.975	0.145	0.625	1.0021	1.5335	8.907	6.644	3.844	0.365
0.749	1.0209	1.5360	7.666	7.834	5.431	0.149	0.766	1.0123	1.5362	11.842	7.969	5.540	0.330
0.874	1.0248	1.5361	9.297	8.998	7.421	0.098	0.875	1.0196	1.5365	11.977	8.999	7.358	0.212
1.000	1.0259	1.5360	10.174				1.000	1.0259	1.5360	10.174			
		m-cresol + α-picoline							*m*-cresol + 2,4,6-collidine				
0.000	0.9346	1.4953	0.708				0.000	0.9101	1.4940	0.806			
0.126	0.9517	1.5048	1.001	1.897	0.989	0.003	0.128	0.9289	1.5027	1.188	2.004	1.115	0.027
0.250	0.9687	1.5185	1.483	3.074	1.378	0.032	0.251	0.9464	1.5112	1.870	3.155	1.523	0.089
0.375	0.9841	1.5219	2.352	4.255	1.921	0.088	0.375	0.9651	1.5200	3.325	4.316	2.085	0.203
0.500	0.9981	1.5290	3.966	5.443	2.684	0.169	0.500	0.9815	1.5282	6.468	5.491	2.864	0.354
0.626	1.0082	1.5335	6.504	6.632	3.754	0.239	0.625	0.9962	1.5332	11.505	6.657	3.927	0.467
0.749	1.0153	1.5366	9.022	7.797	5.210	0.238	0.750	1.0081	1.5360	13.412	7.834	5.401	0.395
0.874	1.0214	1.5365	10.295	8.981	7.270	0.151	0.875	1.0185	1.5362	13.254	9.000	7.405	0.253
1.000	1.0259	1.5360	10.174				1.000	1.0259	1.5360	10.174			

p-cresol + pyridine

0.000	0.9725	1.5032	0.831			
0.123	0.9854	1.5197	1.162	2.098	1.145	0.006
0.250	0.9957	1.5183	1.735	2.386	1.587	0.039
0.375	1.0053	1.5245	2.437	4.663	2.195	0.046
0.499	1.0128	1.5303	3.650	5.932	3.024	0.082
0.616	1.0192	1.5342	5.682	7.127	4.093	0.143
0.750	1.0232	1.5358	7.954	8.494	5.785	0.138
0.875	1.0269	1.5360	9.929	9.770	8.030	0.092
1.000	1.0265	1.5357	11.050			

p-cresol + α-picoline

0.000	0.9346	1.4953	0.708			
0.125	0.9525	1.5047	1.001	2.001	0.998	0.000
0.250	0.9689	1.5137	1.505	3.291	1.406	0.030
0.375	0.9855	1.5220	2.367	4.587	1.984	0.077
0.500	0.9987	1.5290	3.946	5.879	2.797	0.150
0.625	1.0093	1.5332	6.584	7.169	3.941	0.223
0.757	1.0164	1.5350	9.449	8.535	5.664	0.222
0.875	1.0229	1.5352	11.052	9.758	7.841	0.149
1.000	1.0265	1.5357	11.050			

p-cresol + 2,6-lutidine

0.000	0.9170	1.4920	0.759			
0.125	0.9362	1.5023	1.080	2.047	1.061	0.007
0.250	0.9554	1.5118	1.651	3.332	1.483	0.046
0.375	0.9726	1.5202	2.745	4.618	2.072	0.122
0.500	0.9933	1.5298	5.212	5.901	2.894	0.247
0.625	1.0026	1.5333	8.905	7.191	4.047	0.342
0.749	1.0126	1.5348	12.351	8.467	5.642	0.340
0.875	1.0208	1.5352	12.834	9.765	7.910	0.210
1.000	1.0265	1.5357	11.050			

p-cresol + 2,4,6-collidine

0.000	0.9101	1.4940	0.806			
0.125	0.9282	1.5023	1.176	2.086	1.118	0.022
0.250	0.9473	1.5112	1.852	3.364	1.550	0.077
0.375	0.9652	1.5200	3.197	4.648	2.153	0.171
0.500	0.9830	1.5280	6.182	5.928	2.985	0.316
0.624	0.9982	1.5340	11.438	7.203	4.125	0.442
0.749	1.0096	1.5350	13.919	8.485	5.736	0.385
0.875	1.0190	1.5358	14.222	9.768	7.965	0.252
1.000	1.0265	1.5357	11.052			

x_1 — mole fraction of cresol

The relative error of the viscosity measurement did not exceed 0.2%. Results of measurements are given in Table I (columns 1, 2, 3, 4).

For all investigated systems, $\eta = f(x)$ was calculated according to:

1. the principle of molar additivity of viscosity [3]: $\eta_a = x_1\eta_1 + x_2\eta_2$,

2. the principle of molar additivity of the lg of viscosity [4—7]: $\lg \eta_i = x_1 \lg \eta_1 + x_2 \lg \eta_2$,

3. record was made of the behaviour of so-called excess viscosity [8, 9], being the difference between the viscosity logarithm measured and this logarithm calculated according to the principle of molar additivity of the lg of viscosity, as a function of composition:

$$\lg \eta^E = \lg \eta - \lg \eta_i;$$

where: x_1, x_2 — mole fraction of components, η_1, η_2 — viscosity of the pure components.

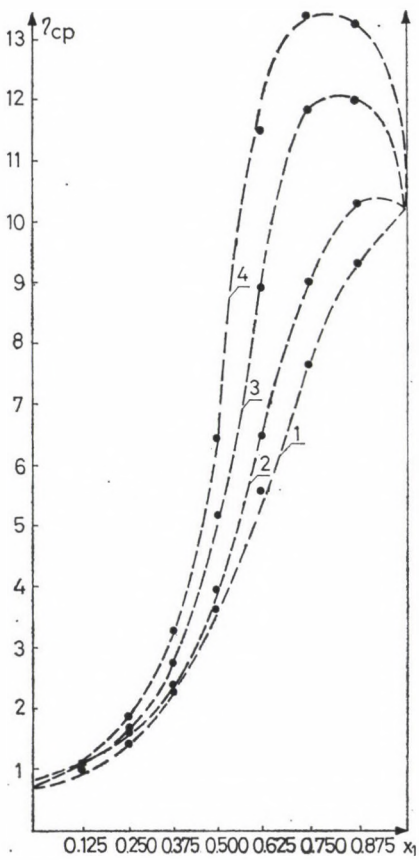


Fig. 1. Viscosity (η) of binary liquid systems: 1. *m*-cresol + pyridine, 2. *m*-cresol + α-picoline, 3. *m*-cresol + 2,6-lutidine, 4. *m*-cresol + 2,4,6-collidine

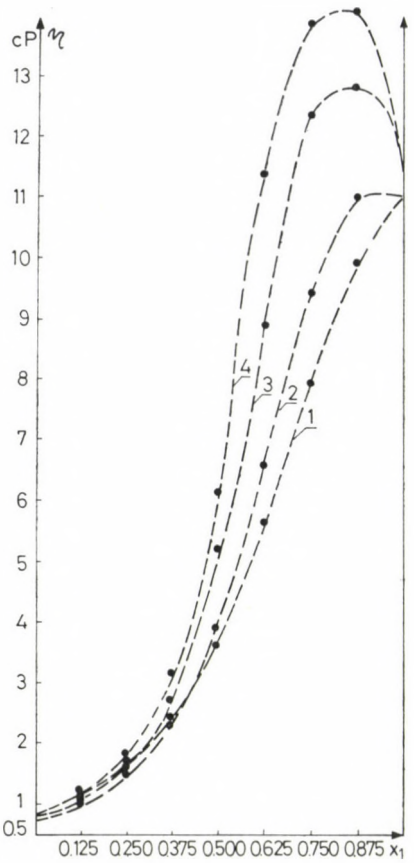


Fig. 2. Viscosity (η) of binary liquid systems: 1. *p*-cresol + pyridine, 2. *p*-cresol + α-picoline, 3. *p*-cresol + 2,6-lutidine, 4. *p*-cresol + 2,4,6-collidine

Results of calculations are presented in Table I (columns 5, 6, 7 — η_a, η_i, lg η^E, respectively).

Discussion

1. For all investigated binary systems, the course of $\eta = f(x)$ isotherms is curvilinear (Figs 1, 2). These isotherms, as compared with the calculated $\eta_i = f(x)$ ones, exhibit positive deviations, whereas when compared with the $\eta_a = f(x)$ isotherms they show deviations changing from negative (for compositions with a higher content of base) to positive ones (for compositions richer in cresols). With gradual transition to systems containing the consecutive pyridine base, the intersection point of $\eta = f(x)$ isotherms with $\eta_a = f(x)$ isotherms shifts in the direction of increasing concentrations of base from $x = 0.2$ to $x = 0.5$ mole fraction of base for systems containing pyridine and

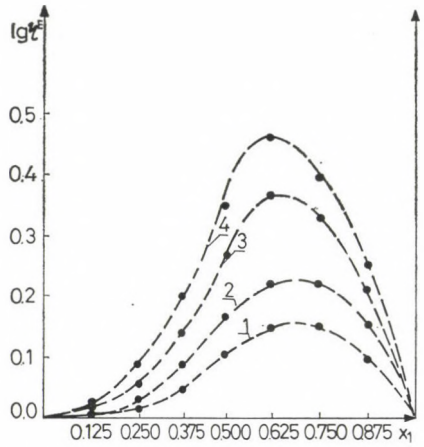


Fig. 3. Excess viscosity (lg η^E) of binary liquid systems: 1. *m*-cresol + pyridine, 2. *m*-cresol + + α-picoline, 3. *m*-cresol + 2,6-lutidine, 4. *m*-cresol + 2,4,6-collidine

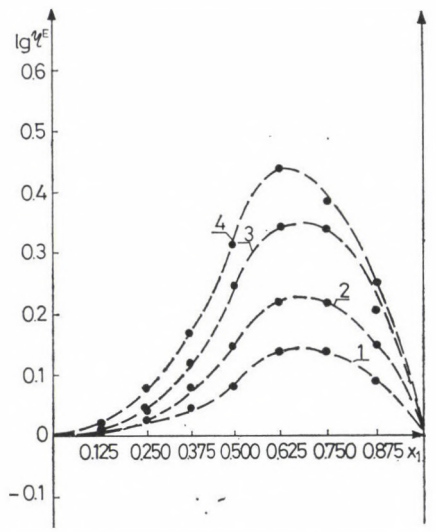


Fig. 4. Excess viscosity (lg η^E) of binary liquid systems: 1. *p*-cresol + pyridine, 2. *p*-cresol + + α-picoline, 3. *p*-cresol + 2,6-lutidine, 4. *p*-cresol + 2,4,6-collidine

2,4,6-collidine, respectively. The values of positive deviations change as follows: pyridine < α-picoline < 2,6-lutidine < 2,4,6-collidine; for systems with 2,6-lutidine and 2,4,6-collidine, the $\eta = f(x)$ isotherms exhibit pronounced maxima.

2. For all systems and all concentrations, the $\lg \eta^E = f(x)$ isotherms display positive deviation increasing as follows: pyridine < α-picoline < 2,6-lutidine < 2,4,6-collidine. The values of maxima on the isotherms increase in the same direction (Figs 3, 4).

3. The course of the $\lg \eta^{E} = f(x)$ isotherms indicates that the intermolecular interactions are strongest in systems with low concentrations of base (0.31—0.37 mole fraction of base).

All above conclusions are consistent with the course of the $d = f(x)$ and $n_D = f(x)$ isotherms which — being convex with respect to the composition axis — point to volume contraction and optical density increase, i.e. to the presence of phenomena parallelling the formation of complexes, associates and addition compounds [9, 10].

REFERENCES

[1] Malesinski, W., Baranowski, B., Buchowski, H., Stecki, J.: Theory of Liquid Solutions in Equilibrium State., PAN, Warsaw 1961
[2] Chojnacka, I., Orszagh, A.: Zh. Fiz. Khim. (in press)
[3] Dunstan, A. E.: Trans. Chem. Soc., **85,** 817 (1904); **87,** 11 (1905); Dunstan, A. E., Tholle, G. B.: Trans. Chem. Soc., **95,** 1556 (1909)
[4] Arrhenius, S.: J. Phys. Chem., **1,** 285 (1887)
[5] Glasston, S., Laidler, K. J., Eyring, H.: The Theory of Rate Processes, Wiley New York 1941
[6] Dejcz, A. Ja.: Zh. Fiz. Khim., **31,** 2336 (1957); **36-II,** 1777 (1962)
[7] Pospiechov, D. A.: Zh. Fiz. Khim., **30,** 228 (1956)
[8] Fried, V., Hala, E., Pick, J.: Coll. Chech. Chem. Comm., **24,** 400 (1959)
[9] Addison, C. C., Smith, B. C.: J. Chem. Soc., **1958,** 3664
[10] Michajlov, V., Kamarzin, A. A.: J. Gen. Chem. (Russ.), **29,** 1398 (1959)

Acta Chimica Hungarica 116 (1), pp. 89—94 (1984)

SYNTHESIS OF 1-ARYL-2-CARBAMOYL-1,4--DIHYDRO-3(2*H*)-ISOQUINOLINONES FROM 2-TRITYLCARBAMOYL DERIVATIVES

(SHORT COMMUNICATION)

E. ZÁRA-KACZIÁN and GY. DEÁK*

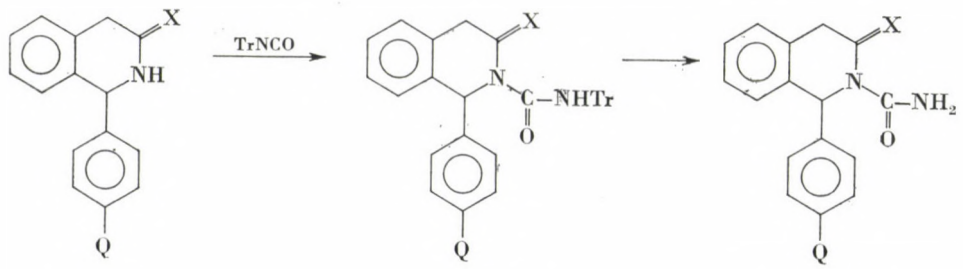
(Institute of Experimental Medicine of the Hungarian Academy of Sciences H-1450 Budapest, P.O. Box 67.)

Received March 15, 1983
Accepted for publication July 13, 1983

In continuation of our work on 1-aryl-2-alkyl- and 2-arylcarbamoyl-1,4--dihydro-3(2*H*)-isoquinolinones [1] having anticonvulsive activity, the unsubstituted carbamoyl derivatives were to be prepared.

Since the reaction of 2-ethoxycarbonyl-1-phenyl-1,4-dihydro-3(2*H*)-isoquinolinone with ammonia did not give the expected 2-carbamoyl derivative but via ring cleavage an urethane derivative was formed [2], and the reaction of 1-phenyl-1,4-dihydro-3(2*H*)-isoquinolinone with KNCO failed, the appropriate 2-tritylcarbamoyl compounds were prepared using trityl isocyanate (TrNCO) [3] and these were detritylated (Scheme 1).

This procedure was employed in the synthesis of the 2-tritylcarbamoyl derivatives (**4**, **5** and **7**) of 1-phenyl-1,4-dihydro-3(2*H*)-isoquinolinone (**1**) [4]



1-3 **4, 5, 7** **8, 9, 11**

	X	Q
1, 4, 8	O	H
2, 5, 9	O	NO_2
3, 7, 11	H_2	H

Scheme 1

* To whom correspondence should be addressed.

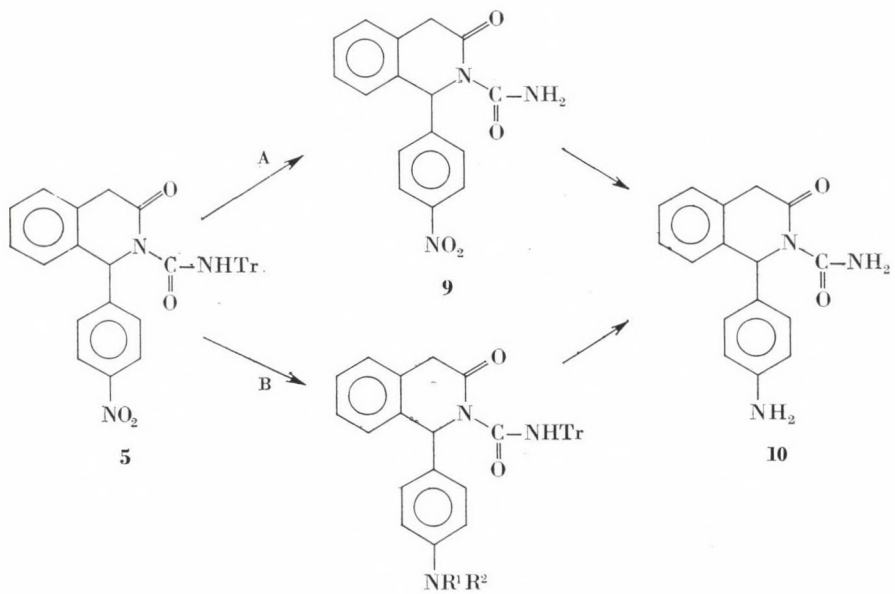
and 1-(*p*-nitrophenyl)-1,4-dihydro-3(2*H*)-isoquinolinone(**2**) [5], compounds prepared first in this laboratory, and also of 1-phenyl-1,2,3,4-tetrahydroisoquinoline(**3**), obtained by reducing **1** with metallic sodium [4].

Since TrNCO has low reactivity, its addition to the nitrogen atom in the also not very recative lactame(X=O) takes place only on extremely long refluxing in benzene solutions (Q=H, 60 h; Q=NH_2, 110 h). By increasing, however, the molar ratio of TrNCO to threefold amount, the reaction time can be significantly shortened (Q=H, 6 h). When using **3** as the starting material, the reaction with TrNCO is almost instantaneous.

Detritylation by catalytic hydrogenation failed, but it could be effected with HBr in glacial acetic acid at room temperature or with ethanolic hydrogen chloride in chloroform solution at the boiling point. The 2-carbamoyl derivatives **8**, **9** and **11** corresponding to the starting materials **1**, **2** and **3**, of which compound **11** has already been described in the literature [6], were thus prepared.

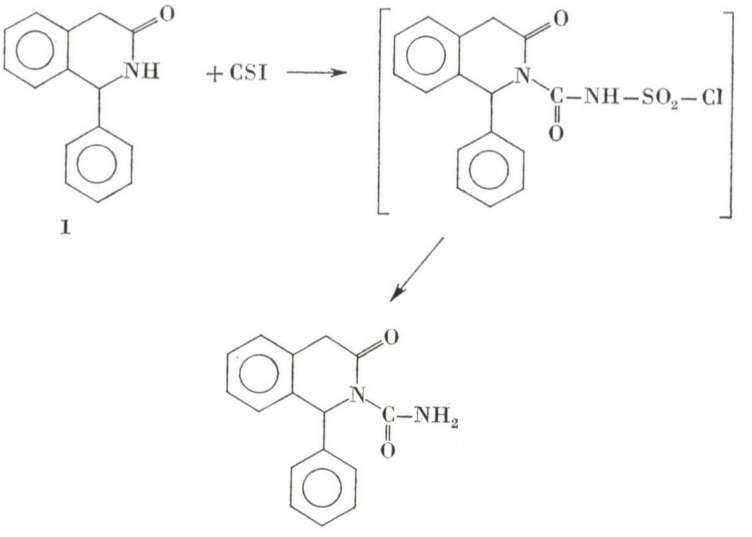
The synthesis of 1-(*p*-aminophenyl)-2-carbamoyl-1,4-dihydro-3(2*H*)-isoquinolinone **10** is possible in two ways starting from **5** (Scheme 2): (*A*) first detritylation is effected with subsequent catalytic reduction of the NO_2 group or (*B*) the reversed course is followed.

In pathway *B*, the detritylation of compound **6** may cause problems because of the presence of the amino group formed by the reduction of the



6 $R^1=R^2=H$
6a $R^1=H$, $R^2=Ac$

Scheme 2



Scheme 3

nitro group; on the effect of acetic acid, dehydrated with acetic anhydride, the acetylamino derivative **6a** separates almost immediately. When working in non dehydrated acetic acid, hydrogen bromide gives rise to the separation of the HBr salt of the starting compound **6**, causing difficulty. In this case only refluxing with ethanolic hydrogen chloride is practicable, but, unlike the other detritylation reactions, this requires a longer reaction time. Preparation of **10** by pathway *A* is therefore more economic, since the overall yield in the two reaction steps is 52% in this case, while by pathway *B* it is only 33%.

The refluxing of **1** with chlorosulfonyl isocyanate (CSI) in benzene solution did not yield the expected chlorosulfonylcarbamoyl derivative, but again the 2-carbamoyl derivative **8** was obtained (Scheme 3). This result is not surprising, since the decomposition to primary amide of *N*-chlorosulfonylamide, prepared by means of CSI has been reported in the literature [7]. It is interesting that this reaction failed with compound **2**, since the substance decomposed in the course of the reaction.

One of the compounds synthesized by us, 1-(*p*-aminophenyl)-2-carbamoyl-1,4-dihydro-3(2*H*)-isoquinolinone **10**, belongs to the "strong inhibiting action" group according to our earlier classification [8] ($p = 70$).

Experimental

M.p.'s were determined on a Büchi—Tottoli apparatus and are uncorrected. IR spectra were recorded in KBr pellets (Perkin-Elmer Model 377).

1-Phenyl-2-tritylcarbamoyl-1,4-dihydro-3(2*H*)-isoquinolinone (4)

1-Phenyl-1,4-dihydro-3(2*H*)-isoquinolinone (**1**) [4] (5.57 g; 0.025 mol) was refluxed with trityl isocyanate (24.1 g; 0.075 mol) [3] in anhydrous benzene (60 mL) for 6 h. The reaction mixture was cooled, the substance which separated was filtered with suction and washed with acetone (5×30 mL). The yellowish white product was shortly boiled with methanol (20 mL), filtered off and washed with hot methanol (3×10 mL). The resulting white solid (7.4 g) was recrystallized from ethyl acetate (320 mL) to obtain white crystals (7.2 g; 75.5%), m.p. 168—170 °C.

$C_{35}H_{28}N_2O_2$ (508.63). Calcd. C 82.65; H 5.55; N 5.51. Found C 82.63; H 5.76; N 5.48%.

IR (KBr): νNH 3450, 3260, νC=O 1740, 1685, Amide II 1550 cm^{-1}.

1-(*p*-Nitrophenyl)-2-tritylcarbamoyl-1,4-dihydro-3(2*H*)-isoquinolinone (5)

1-(*p*-Nitrophenyl)-1,4-dihydro-3(2*H*)-isoquinolinone (**2**) [5] (18.7 g; 0.07 mol) was refluxed with trityl isocyanate (22.15 g; 0.077 mol) in anhydrous benzene (570 mL), with stirring, for 100 h. The reaction mixture was cooled and the substance which separated was filtered off with suction (2.3 g, unchanged material). The filtrate was evaporated to dryness and treated with ether (150 mL). The solid product was filtered off and washed with ether (3×70 mL), then recrystallized from isopropanol (1300 mL) to obtain beige crystals (24.9 g; 77.8%, also considering the starting material recovered); m.p. 124—126 °C.

$C_{35}H_{27}N_3O_4$ (553.63). Calcd. C 75.93; H 4.91; N 7.59. Found C 76.12; H 5.19; N 7.60%.

IR (KBr): νNH 3250, 3170, νC=O 1720, 1670, Amide II + $\nu_{as}NO_2$ 1520 broad, ν_sNO_2 1350 cm^{-1}.

1-(*p*-Aminophenyl-2-tritylcarbamoyl-1,4-dihydro-3(2*H*)-isoquinolinone (6)

1-(*p*-Nitrophenyl)-1,4-dihydro-3(2*H*)-isoquinolinone (**5**) (5.5 g; 0.01 mol) was dissolved in glacial acetic acid (130 mL) and hydrogenated in the presence of 10% Pd/C catalyst (1 g) at atmospheric pressure (2 h, consumption: 800 mL of H_2). The catalyst was removed by filtration, washed with chloroform (3×10 mL), and the solvent was evaporated in vacuum (35 °C/2.7 kPa). The syrupy residue was dissolved in chloroform (50 mL), the chloroform was evaporated in vacuum, and this procedure was repeated several times. The resulting solid was washed with water (5×50 mL) and petroleum ether (10×10 mL) and dissolved in hot isopropanol (500 mL) to obtain beige crystals (3.7 g; 70.5%), m.p. 161—162 °C.

$C_{35}H_{29}N_3O_2$ (523.64). Calcd. C 80.28; H 5.58; N 8.03. Found C 80.34; H 5.59; N 8.07%.

IR (KBr): νNH 3470, 3380, 3220, 3180, νC=O 1715, 1665/1655, β_sNH_2 1625, Amide II 1520 cm^{-1}.

1-(*p*-Acetylaminophenyl)-2-tritylcarbamoyl-1,4-dihydro-3(2*H*)-isoquinolinone (6a)

1-(*p*-Aminophenyl)-2-tritylcarbamoyl-1,4-dihydro-3(2*H*)-isoquinolinone (**6**) (0.6 g; 0.0011 mol) was dissolved in anhydrous acetic acid (dehydrated with acetic anhydride) (12 mL) and allowed to react with a solution (0.23 mL) of HBr in glacial acetic acid (473.8 mg HBr/mL; 0.00136 mol) with stirring, at 17 °C. After 5 min, a white substance separated. Acetic acid was evaporated in vacuum (40 °C/2.7 kPa) and the residue washed with ether (5×10 mL) to obtain a white powder (0.5 g; 80%), m.p. 136—138 °C.

$C_{37}H_{31}N_3O_3$ (565.677). Calcd. C 78.56; H 5.52; N 7.42. Found C 78.16; H 5.82; N 7.16%.

IR (KBr): νNH 3370, 3250, νC=O 1720, 1670, Amide II 1620 (broad) cm^{-1}.

1-Phenyl-2-tritylcarbamoyl-1,2,3,4-tetrahydroisoquinoline (7)

1-Phenyl-1,2,3,4-tetrahydroisoquinoline (**3**) [4] (2.93 g; 0.014 mol) was refluxed with trityl isocyanate (3.99 g; 0.014 mol) in anhydrous benzene (35 mL) for 5 h. The solvent was evaporated in vacuum and the residual white powder (6.8 g) recrystallized from methanol to obtain white crystals (5.5 g; 82.4%), m.p. 199 °C.

$C_{33}H_{30}N_2O$ (494.642). Calcd. C 84.99; H 6.11; N 5.66. Found C 85.23; H 6.39; N 5.66%.

IR (KBr): νNH 3520, 3420, νC=O 1660/1640, Amide II and ν_{as} and ν_s N—C—N 1490 cm^{-1}.

1-Phenyl-2-carbamoyl-1,4-dihydro-3(2*H*)-isoquinolinone (8)

(a) From the 2-tritylcarbamoyl derivative

1-Phenyl-2-tritylcarbamoyl-1,4-dihydro-3(2*H*)- isoquinolinone (**4**) (17.8 g; 0.035 mol) was dissolved in a mixture of anhydrous chloroform (250 mL) and ethanol (90 mL) and refluxed with 23.3% ethanolic hydrogen chloride (59.5 mL) for 6 h. The solution was then evaporated to dryness in vacuum (40 °C/2.7 kPa), the residue was suspended in ether (30 mL), the ether was evaporated in vacuum and this procedure was repeated several times. The solid residue was suspended in ether, filtered off and washed with ether (5 × 50 mL) to obtain a white powder (9.5 g). After dissolution in hot ethyl acetate (300 mL), white crystals were obtained on cooling (5.9 g; 62%), m.p. 185—187 °C.

$C_{16}H_{24}N_2O_2$ (266.30). Calcd. C 72.16; H 5.30; N 10.52. Found C 72.35; H 5.43; N 10.68%.

IR (KBr): νNH 3350, 3200, νC=O 1710 .1685, Amide II 1575 cm^{-1}.

(b) From 1-phenyl-1,4-dihydro-3(2H)-isoquinolinone

1-Phenyl-1,4-dihydro-3(2*H*)-isoquinolinone (**1**) (2.23 g; 0.01 mol) was dissolved in a mixture of ethanol (17 mL) and anhydrous chloroform, and it was allowed to react with a solution of chlorosulfonyl isocyanate (2.83 g; 0.02 mol, 1.74 mL) in chloroform (10 mL) under cooling and stirring at 0 °C; the mixture was then allowed to stand at room temperature for 24 h. The solvent was evaporated in vacuum and the residue washed with benzene (3 × 10 mL) to obtain beige-white crystals (2.6 g). These were dissolved in chloroform (30 mL), diluted with benzene (20 mL) and subjected to chromatographic separation on Silicagel 40 column (70 g) using chloroform. Evaporation of the first 200 mL of the eluate gave white crystals (1.6 g), which efforded the pure product (0.95 g; 36%) on recrystallization from ethyl acetate; m.p. 188 °C. According to the IR spectrum, TLC and mixed m.p. tests, the compound was identical with an authentic sample of **8**.

Found C 72.04; H 5.5; N 10.48%.

2-Carbamoyl-1-(*p*-nitrophenyl)-1,4-dihydro-3(2*H*)-isoquinolinone (9)

1-(*p*-Nitrophenyl)-2-tritylcarbamoyl-1,4-dihydro-3(2*H*)-isoquinolinone (**5**) (5.5g; 0.01 mol) was dissolved in anhydrous acetic acid (120 mL) and allowed to react with a saturated glacial acetic acid solution of HBr containing 1.085 g (0.012 mol) of HBr, with stirring at 17 °C. The mixture was stirred at room temperature for 8 h. The trityl bromide which separated was filtered off with suction and washed with anhydrous acetic acid (2 × 5 mL). The filtrate was poured into ice-water (100 mL), extracted with chloroform (4 × 80 mL) and the combined chloroform solution was successively washed with water (2 × 100 mL) until free from acid, 5% $NaHCO_3$ solution (150 mL) and with water (2 × 80 mL); it was the dried over anhydrous Na_2SO_4. The solvent was evaporated in vacuum at room temperature, the residue rubbed with ether (100 mL), the powdery material was filtered off and washed with ether (2 × 10 mL). The product (2.0 g) was then recrystallized from ethanol to obtain yellowish-white crystals (1.8 g; 66.6%, also considering the starting material (0.7 g) recovered from the ethereal washing liquid); m.p. 158 °C.

$C_{16}H_{13}N_3O_4$ (311.50). Calcd. C 61.73; H 4.21; N 13.50. Found C 61.89; H 4.39; N 13.64%.

IR (KBr): νNH 3470, 3390, νC=O 1730, 1700, 1670, Amide II 1550, $\nu_{as}NO_2$ 1515, ν_sNO_2 1350 cm^{-1}.

1-(*p*-Aminophenyl)-2-carbamoyl-1,4-dihydro-3(2*H*)-isoquinolinone (10)

(a) Reduction of the nitro derivative (Pathway A)

2-Carbamoyl-1-(*p*-nitrophenyl)-1,4-dihydro-3(2*H*)-isoquinolinone (**9**) (6.0 g; 0.019 mol) was dissolved in glacial acetic acid (60 mL) and hydrogenated in the presence of prehydrogenated 10% Pd/C catalyst (1.0 g) at room temperature under atmospheric pressure (3 h, consumption: 1500 mL of H_2). The catalyst was then removed by filtration and washed with chloroform (3 × 10 mL). The solution was evaporated to dryness in vacuum (30 °C/2.7 kPa), the remaining oil was dissolved in ether (20 mL) and the ether was evaporated; this procedure was repeated several times. The resulting solid was suspended in ether (30 mL), filtered off and dissolved in hot ethanol (300 mL) to obtain pale pinkish white crystals (4.3 g; 79.7%), m.p. 189—190 °C.

$C_{16}H_{15}N_3O_2$ (281.32). Calcd. C 68.31; H 5.37; N 14.94. Found C 68.32; H 5.63; N 15.10%.
IR (KBr): νNH 3460, 3380, 3200, νC=O 1730, 1700, 1680, $\beta_s NH_2$ 1620, Amide II 1575 cm^{-1}.

(b) Detritylation of the amino derivative (Pathway B)

1-(*p*-Aminophenyl)-2-tritylcarbamoyl-1,4-dihydro-3(2*H*)-isoquinolinone (**6**) (1.2 g; 0.023 mol) was dissolved in anhydrous chloroform (18 mL), the solution diluted with ethanol (8 mL) and refluxed with 18% ethanolic hydrogen chloride (4.5 mL) for 20 h. The reaction mixture was evaporated to dryness in vacuum, the remaining orange oil was diluted with chloroform (40 mL) and the solution was shaken with 5% $NaHCO_3$ solution (3×20 mL) to liberate the base from the hydrochloride. The solution was then washed with water (4×20 mL) until neutral and dried. The solvent was evaporated in vacuum, the foamy residue dissolved in chloroform (5 mL) and subjected to chromatographic separation on Silicagel 40 coloumn (20 g) using chloroform (300 mL) and a chloroform-ethanol mixture (1 : 1, 100 mL). Evaporation of the latter eluate gave a pink residue (0.5 g); on recrystallization from ethanol white crystals separated (0.3 g; 47%), m.p. 187—188 °C.
$C_{16}H_{15}N_3O_2$ (281.32). Calcd. C 68.31; H 5.37; N 14.94. Found C 68.12; H 5.63; N 14.77%.
According to the IR spectrum, the TLC test and the mixed m.p., the substance was identical with that prepared according to Pathway *A*.

1-Phenyl-2-carbamoyl-1,2,3-tetrahydroisoquinoline (11) [6]

2-Tritylcarbamoyl-1-phenyl-1,2,3,4-tetrahydroisoquinoline (**7**) (4.9 g; 0.01 mol) was refluxed with 17% ethanolic hydrogen chloride (23 mL) in chloroform (50 mL) for 8 h. The solvent was evaporated in vacuum and the residue washed with petroleum ether (5×30 mL) to give a yellowish-white powder (3.0 g). After recrystallization from ethanol and water, white crystals (1.2 g; 48%) were obtained, m.p. 184 °C.
$C_{16}H_{16}N_2O$ (252.32). Calcd. C 76.16; H 6.39; N 11.10. Found C 76.20; H 6.26; N 10.97%.
IR (KBr): νNH 3430, 3370, 3220, νC=O 1640, Amide II 1590 cm^{-1}.

*

The authors express their thanks to Mrs. J. Haskó-Breuer for recording the infrared spectra and to Miss M. Fodor for the microanalyses. Excellent technical assistance of Mrs. Horváth-Gáll is gratefully acknowledged.

REFERENCES

[1] Zára-Kaczián, E., Deák, Gy., Gáll-Istók, K., Haskó-Breuer, J.: Acta Chim. Acad. Sci. Hung., **100,** 37 (1979)
[2] Zára-Kaczián, E., Deák, Gy.: Acta Chim. Acad. Sci. Hung., **98,** 247 (1978)
[3] Bredereck, H., Reif, E.: Chem. Ber., **81,** 426 (1948)
[4] Csürös, Z., Deák, Gy., Hoffmann, I., Török-Kalmár, A.: Acta Chim. Acad. Sci. Hung., **60,** 177 (1969)
[5] Deák, Gy., Gáll-Istók, K., Hazai, L., Sterk, L.: Synthesis, **1975,** 393
[6] Japan Kokai 7334, 180 (Cl. 16E433) 1973; Chem. Abstr., **79,** 31925r
[7] Foucaude, A., Gourion, Y.: Bull. Soc. Chim. France, **1971,** 1500
[8] Deák, Gy., Dóda, M., György, L., Hazai, L., Sterk, L.: J. Med. Chem., **20,** 1384 (1977)

Acta Chimica Hungarica 116 (1), pp. 95—102 (1984)

STRUCTURE OF THE SELF-CONDENSATION PRODUCTS OF LACTAMS

R. MAZURKIEWICZ

(Institute of Organic Chemistry and Technology, Silesian Polytechnical University, 44-101 Gliwice, Krzywoustego 4, Poland)

Received March 18, 1983
In revised form June 16, 1983
Accepted for publication July 13, 1983

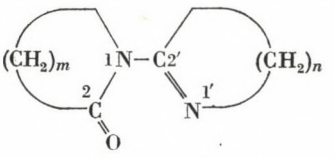
Based on investigations of the title compounds by means of spectroscopic methods as well as mass spectrometry, the products were found to have acylamidine structure. The IR spectra display two bands in the range 1800—1600 cm^{-1} ($\nu C{=}O$ and $\nu C{=}N$), which may overlap in the case of lactams having a larger than 5 membered rings. The ^1H-NMR and ^{13}C-NMR spectra prove that the symmetry of these compounds corresponds to that of acylamidines. The observed analogies in the fragmentation of the investigated compounds and respective *N*-substituted lactams confirm the acylamidine structure.

When amides or lactams are treated with reactive inorganic acid halides, such as phosgene, phosphorus oxychloride, or phosphorus pentachloride, imidoyl halides or amide halides are usually formed [1], though, under suitable conditions, other reactions may also take place. Thus, for instance, treament of lactams with the inorganic acid chlorides mentioned above, as well as with methyl dichlorophosphate or phosphorus pentoxide may give, in effect, self-condensation products with the general formula (2 ×lactam)-H_2O [2—8]. Such a reaction is particularly favoured by the use of an excess of lactam. These same substances may also be obtained in another way, e.g. by condensing lactams with lactim chloroformates [9] or lactim ethers [10], as well as by means of Beckmann rearrangement of the oximes of cyclic ketones [11—14].

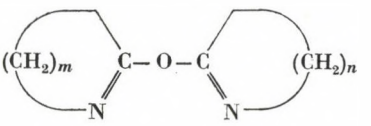
There are numerous patents concerning the application of these compounds as co-catalysts in the anionic polymerization of lactams. Although the discussed substances are very important in practice, their structure is still continually a subject of controversy; they are said to have the structure of acylamidines **A** [4—8, 10, 15, 16] or that of dilactim ethers **B** [2, 4, 9, 11—14, 17—19].

Meyer [3] converted the self-condensation product of ε-caprolactam into caprolactim methyl ether which,in his opinion, proves that the self-condensation product has the structure **IVB**. He did not provide, however, any other details concerning this transformation.

According to Bredereck and Bredereck [4] the self-condensation of 2-pyrrolidinone gives the acylamidine **IA**, whereas the same reaction of ε-caprolactam yields the dilactim ether **IVB**. According to these authors the observed



A



B

I $m = 3$; $n = 3$
II $m = 3$; $n = 5$
III $m = 4$; $n = 4$
IV $m = 5$; $n = 5$

differences in the behaviour of 2-pyrrolidinone and ε-caprolactam result from differences in the basicity of the oxygen atoms in these lactams.

It was the aim of the present investigations to solve the controversial problem of the structure of the self-condensation products of lactams.

Results and Discussion

The structures of the title substances have been investigated by means of spectroscopic methods (IR, ^{1}H-NMR, ^{13}C-NMR, UV) as well as mass spectrometry. The results obtained in this way have been gathered in Table I and in Figs 1 and 2.

Compounds **I** and **II** display in the range 1800—1600 cm^{-1} two distinct absorption bands in general interpreted as the νC=O and νC=N bands,

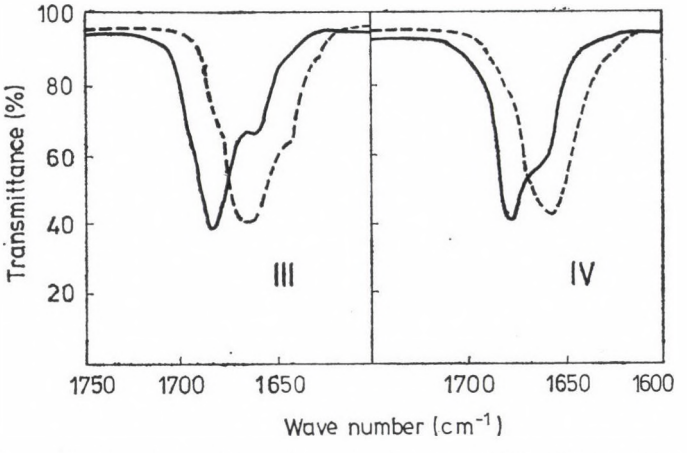


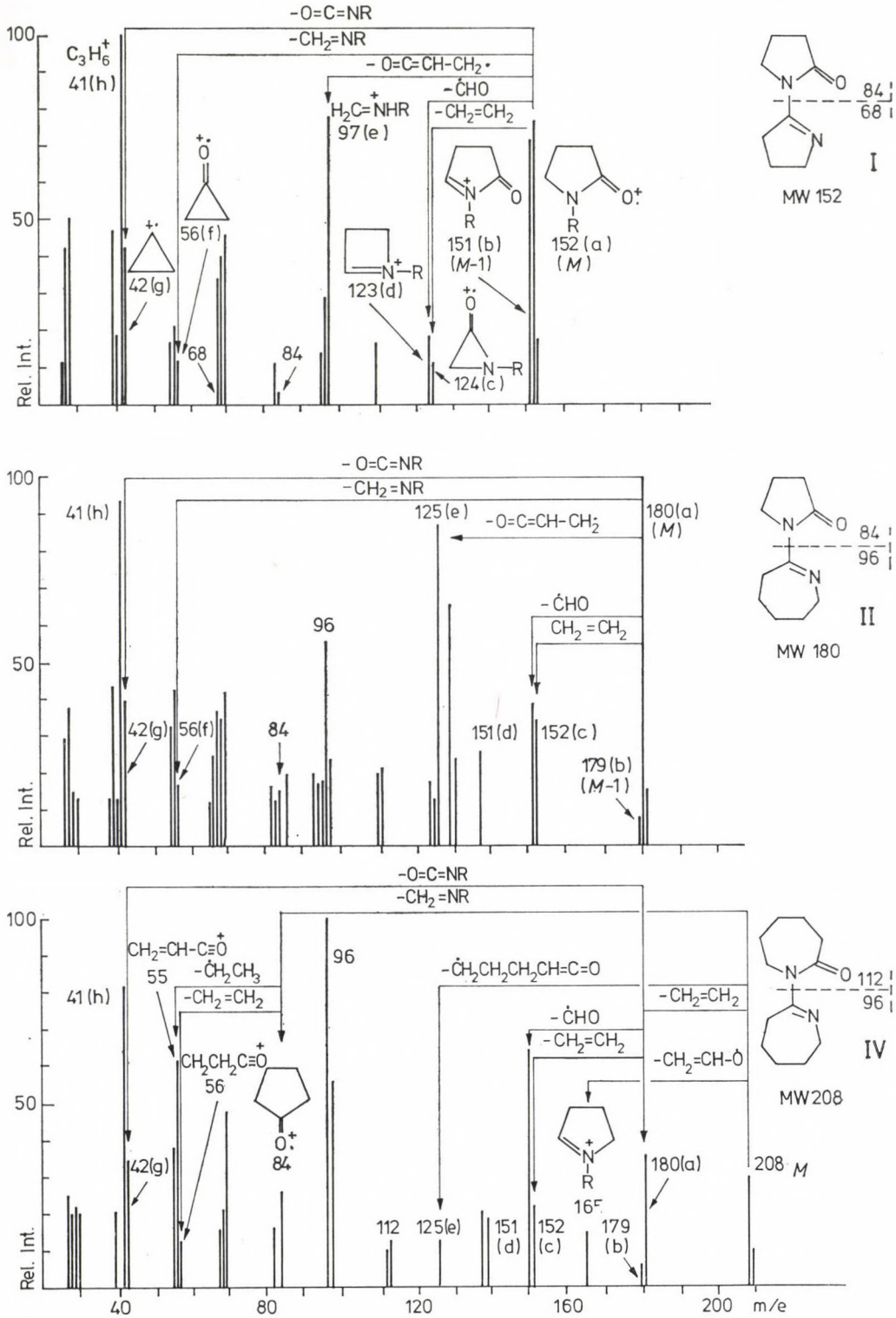
Fig. 1. Changes in the shape of the absorption band at 1700—1650 cm^{-1} as a rseult of a change in the polarity of the solvent. Concentration 0.1 mol/L, cell 0.047 mm. Full line — solution in cyclohexane. Broken line — solution in CH_2Cl_2

Table I

Spectral data of compounds **I**—**IV**

Compound	IR spectra[a] (cm^{-1})	^{1}H-NMR spectra[b] (δ(ppm), $CDCl_3$, int. standard — TMS)	^{13}C-NMR spectra[b] (δ(ppm), $CDCl_3$, int. standard — TMS)	UV spectra[c] λ_{max} (nm) / ε_{max}
I[d]	1717, 1616	3.84 (t; 2H, J = 7 Hz, H-5), 3.66 (t; 2H, J = 7 Hz, H-5′), 3.05 (t; 2H, J = 8 Hz, H-3′), 2.50 (t; 2H, J = 8 Hz, H-3), 2.30—1.76 (m; 4H, H-4, H-4′)	175.0, C-2; 163.8 C-2′; 55.8, 47.4, C-5, C-5′; 33.3, 32.9, C-3, C-3′; 23.4, 18.1, C-4, C-4′	223 / 13500
II	1702, 1648	3.76 (t; 2H, J = 8 Hz, H-5), 3.69—3.53 (m; 2H, H-7′), 3.20—3.03 (m; 2H, H-3′), 2.54 (t; 2H, J = 8 Hz, H-3), 2.09 (t; 2H, J = 8 Hz, H-4), 1.96—1.40 (m; 6H, H-4′, H-5′, H-6′)	175.4, C-2; 164.4, C-2′; 49.6, 48.1, C-5, C-7′; 33.9, 31.2, C-3, C-3′; 28.8, 26.9, 23.0, 17.5-not assigned	229 / 12600
III	1661	3.80—3.55 (m; 4H, H-6, H-6′), 2.78—2.25 (m; 4H, H-3, H-3′), 1.93—1.55 (m; 8H, H-4, H-5, H-4′, H-5′)	171.4, C-2; 162.2, C-2′; 48.2, 47.2, C-6, C-6′; 33.9, 29.2, C-3, C-3′; 23.3, 22.1, 21.0, 20.0-not assigned	226 / 9900
IV	1655	3.89—3.70 (m; 2H, H-7), 3.64—3.50 (m; 2H, H-7′), 2.73—2.48 (m; 4H, H-3, H-3′), 1.85—1.40 (m; 12H, H-4, H-5, H-6, H-4′, H-5′, H-6′)	175.5, C-2; 168.3, C-2′; 49.3, 47.7, C-7, C-7′; 37.6, 33.3, C-3, C-3′; 30.2 28.9, 28.5, 25.8, 22.7[e]-not assigned	231 / 10100

[a] Range 1800—1600 cm^{-1}, solution in CH_2Cl_2 0.1 mol/L, cell 0.047 mm. [b] The numbering of the atoms is seen from the formula **A** (above). [c] Solution in cyclohexane. [d] Similar spectral data for substance **I** have been given by Dannhardt [7]. [e] Probable coincidence of two signals


-O=C=NR
-CH2=NR
-O=C=CH-CH2·
-ĊHO
-CH2=CH2
C3H6+
41(h)
H2C=NHR
97(e)
56(f)
42(g)
68
84
123(d)
151(b)
(M-1)
152(a)
(M)
124(c)
Rel. Int.
100
50
I
MW 152
84
68
-O=C=NR
-CH2=NR
41(h)
125(e)
-O=C=CH-CH2
180(a)
(M)
-ĊHO
CH2=CH2
96
42(g)
56(f)
84
151(d)
152(c)
179(b)
(M-1)
II
MW 180
84
96
-O=C=NR
-CH2=NR
CH2=CH-C≡O+
55
-ĊH2CH3
-CH2=CH2
41(h)
96
-ĊH2CH2CH2CH=C=O
-CH2=CH2
-ĊHO
-CH2=CH2
-CH2=CH-Ȯ
CH2CH2C≡O+
56
42(g)
84
180(a)
208 M
112
125(e)
151
(d)
152
(c)
179
(b)
IV
MW208
112
96
40
80
120
160
200
m/e

whereas the IR spectra of substances **III** and **IV** have in this same range only one strong absorption band. This seems to be the main reason for attributing the structure of dilactim ether to substances **III** and **IV**, as done by numerous authors.

We have found that in the spectra of substances **III** and **IV**, recorded in non-polar solvents (hexane or cyclohexane), on the long-wave side of the discussed band there appears a distinct shoulder (Fig. 1). Therefore we may assume that in the case of these compounds the νC=O and νC=N bands overlap. Such an effect is to be expected based on the analysis of the influence of the ring size upon the position of these bands. Hall and Zbinden [20] have proved that the C=O group absorbs in 7-membered rings approximately 45 wave numbers lower than in 5-membered rings, and in 6-membered rings about 30 wave numbers lower than in that latter case. No adequately documented data are available concerning the influence of the ring size on the position of absorption maxima of the endocyclic C=N groups. The data provided in the paper by Pilotti et al. [21], dealing with lactim ethers, indicate that the endocyclic C=N group absorbs in 7-membered rings about 20 wave numbers higher than in 5-membered rings. A comparison of the positions of the νC=N bands in the spectra of compounds **I** and **II** leads to similar conclusions.

Taking into account the data quoted above it is to be expected that in the spectrum of compound **IV** the νC=O and νC=N bands will appear closer to each other by about 65 wave numbers than in the spectrum of substance **I**, and by about 45 wave numbers, in comparison with the spectrum of **II**, so that these two bands overlap.

It should be observed that also in the case of dilactim ethers we might expect the appearance of two absorption bands in the range 1800—1600 cm^{-1}, brought about by the splitting of the νC=N band due to mechanical coupling.

In the range about 1200—1040 cm^{-1}, in which dilactim ethers ought to display a strong absorption band due to antisymmetric vibrations of the C—O—C group, no adequately intense band could be detected. In the case of similar systems, as for instance acid anhydrides and divinyl ether, such an absorption band of a very high intensity is found at 1175—1045 cm^{-1} [22] and 1200 cm^{-1} [23], respectively.

Based on ^{13}C-NMR spectra of the investigated substances, a magnetic nonequivalence of the carbon atoms in both rings has been stated. An analogical magnetic nonequivalence of hydrogen atoms has been displayed when analyzing the ^{1}H-NMR spectra of compounds **I**, **II** and **IV** (the spectrum of

Fig. 2. Mass spectra of the substances **I**, **II** and **IV**. **I**; R = 1-pyrrolin-2-yl, **II** and **IV** R = = 4,5,6,7-tetrahydro-3*H*-azepin-2-yl. All ions with >10% relative abundance, together with other ions of special interest, are included

III is hardly legible). This indicates that the investigated products have the structure of acylamidines.

The same magnetic nonequivalence of the respective atoms might also be observed in the case of the planar *E, Z* conformation of a dilactim ether provided there is sufficiently slow topomerization of this conformation; this, however, seems to be little probable due to a considerably rapid conformational interchange, as found in the case of similar systems, for instance in the case of imides [24] and acid anhydrides [25].

The mass spectra of the investigated substances have not been studied so far, as it seems, except for substance **I**, which was recorded by Dannhardt [7]. The spectra of compounds **I**, **II** and **IV** are presented and interpreted in Fig. 2.

Taking into consideration the similarity of the structures of acylamidines and *N*-substituted lactams, the spectra have been interpreted to a large extent on the basis of the known fragmentation mechanisms of the respective *N*-substituted lactams [26—28]. To nearly all the fragments identified in the spectra of *N*-methyl-2-pyrrolidinone [26] or *N*-methyl-ε-caprolactam [28] there may be attributed analogical peaks in the spectra of the investigated substances.

In the spectrum of **I** there appear two peaks at *m/e* 68 and 84. Dannhardt [7] attributes the formulas C_4H_6N and C_4H_6NO to the respective ions. These ions are probably formed as a result of the cleavage of the C—N bond, whereas the charge may remain on the lactam fragment or within the azomethine group. Corresponding peaks occur also in the spectra of substances **II** and **IV**. Such a fragmentation mode has also been observed in the case of other amidines [29].

Thus it is possible to interpret satisfactorily the mass spectra of the investigated compounds assuming that they have acylamidine structure.

Taking into account all the presented data concerning the structure of the self-condensation products of lactams, it might be said that the investigated substances have acylamidine structure.

Experimental

M.p.'s are uncorrected. The analyses were consistent with the structures of the products. IR spectra were recorded with a Zeiss UR-20 spectrophotometer. ^{1}H-NMR spectra were taken with a Varian XL-100 instrument, at 20 °C. ^{13}C-NMR spectra were recorded with a Bruker HFX 90 spectrometer operating at 22.63 MHz, at 25 °C. UV spectra were recorded on a Zeiss Specord UV/VIS spectrophotometer. MS measurements were carried out with a Gas Chromatograph-Mass Spectrometer LKB 2091. The ionizing energy was maintained at 70 eV. The samples were introduced into the ion source by direct evaporation.

1-(1-Pyrrolin-2-yl)-2-pyrrolidinone (I)

The title compound was prepared from 2-pyrrolidinone (34 g; 0.40 mol) making use of Bredereck and Bredereck's method [4]. The crude product was crystallized from hexane, to obtain **I** (17.7 g; 58%) as white flakes, m.p. 60—60.5 °C (*lit.* [4] m.p. 61 °C).

1-(4,5,6,7-Tetrahydro-3*H*-azepin-2-yl)-2-pyrrolidinone (II)

Compound **II** was obtained, in the way described by Glickman and Miller [10], from caprolactim methyl ether (9.5 g; 0.075 mol) and 2-pyrrolidinone (5.85 g; 0.069 mol). The crude product obtained after distillation (b.p. 93—95 °C/ 20 Pa, *lit.* [10] b.p. 78—81 °C/13.3 Pa) was crystallized from hexane and then sublimed (50 °C, 6.6 Pa) to yield white crystalline **II** (4.17 g; 34%), m.p. 54.5—56 °C (*lit.* [10] m.p. 56.5—58.5 °C).

1-(3,4,5,6-Tetrahydropyridin-2-yl)-2-piperidinone (III)

General descriptions of preparing compound **III** from 2-piperidinone and phosgene or by Beckmann rearrangement of cyclopentanone oxime have been given by Hechelhammer [2] and Junji and Fumio [11, 12], respectively. These authors did not report the yield, nor the physical properties of the resulting products. Our attempts at repeating these syntheses resulted in both cases in the formation of a self-condensation product in a poor yield, amounting only to a few per cent. This same product (IR, TLC) was obtained by us in a good yield by applying an original method of synthesis, as described below.

To a solution of 2-piperidinone (9.2 g; 0.093 mol) in 20 mL of dry benzene, cooled to 0 °C, diphenyl chlorophosphate (12.6 g; 0.047 mol) was added. The mixture was allowed to stand for 18 h at room temperature, and then heated for 6 h at a temperature of 75 °C. The reaction mixture was diluted with 30 mL of benzene, then 60 mL of 20% aqueous K_2CO_3 solution was added, with cooling at the same time by means of ice-water; finally the whole mixture was vigorously stirred for 10 min. After the separation of the organic layer, the water layer was twice extracted with 40 mL of benzene. The combined organic layers were dried (K_2CO_3), the benzene evaporated and the remainder distilled to obtain **III** (3.7 g; 44%) as an oil, b.p. 92 °C/8.0 Pa, $n_D^{20} = 1.518$.

$C_{10}H_{16}N_2O$ (180.26). Calcd. C 66.63; H 8.95; N 15.54. Found C 66.55; H 9.08; N 15.33%.

1-(4,5,6,7-Tetrahydro-3*H*-azepin-2-yl)-hexahydro-2*H*-azepin-2-one (IV)

The title compound was obtained as described by Bredereck and Bredereck [4] from ε-caprolactam (45 g; 0.40 mol). The crude product, obtained after distillation (27.3 g; 66%, b.p. 105—106 °C/20 Pa, *lit.* [4] b.p. 98—100 °C/8.0 Pa, *lit* [5] b.p. 113 °C/5.3 Pa), was crystallized from hexane to yield white crystalline **IV**, m.p. 31—32 °C (*lit.* [5] m.p. 30—32 °C).

REFERENCES

[1] Ronnett, R.: The Chemistry of the Carbon-Nitrogen Double Bond (Ed. S. Patai), Chapter 13, Interscience Publ., London 1970
[2] Hechelhammer, W.: German Pat., 917,669 (1955)
[3] Meyer, H. R.: Kunstst.-Plast., **3,** 160 (1956)
[4] Bredereck, H., Bredereck, K.: Ber., **94,** 2278 (1961)
[5] von Reinisch, G., Dietrich, K., Dargazanli, F.: J. Prakt, Chem., **311,** 455 (1969)
[6] Razodovskaya, L. V., Grapov, A. F., Mel'nikov, N. N.: Zh. Obshch. Khim., **42,** 1277 (1972)
[7] Dannhardt, G.: Arch. Pharm., **311,** 294 (1978)
[8] Ney, W. O., Jr., La Mar Zollinger, J.: U.S. Pat. 3,057,874 (1962)
[9] Hechelhammer, W.: German Pat. 948,973 (1956)
[10] Glickman, S. A. Miller, E. S.: U.S. Pat. 3,040,004 (1962)
[11] Junji, T., Fumio, I.: Japan Pat. 7,436,668 (1974); Chem. Abstr., **81,** P 91073 (1974)
[12] Junji, T., Fumio, I.: Japan Pat. 7,456,972 (1975); Chem. Abstr., **83,** P 59749 (1975)
[13] Rákóczi, J., Siska, J., Mitke, G.: Hung. Pat. 152,966 (1965)
[14] Beck, I., Rákóczi, J., Török, J.: Acta Chim. (Budapest) **75,** 63 (1972)
[15] Prajsner, B.: Zesz. Nauk. Pol. Sl. Chemia, **20,** 60 (1963)
[16] Botta, A.: Justus Liebigs Ann. Chem., **1976,** 336
[17] Hendrik, B. E., Piet, J., Warnier, J. M. M., Brouweis, J. A. L.: German Pat. 2,901,891 (1977)
[18] Kohan, M. I.: U.S. Pat. 3,141,006 (1964)
[19] Inventa, A. G. für Forschung und Patentverwertung: Fr. Pat. 1,419,921 (1965)
[20] Hall, H. K., Zbinden, R.: J. Am. Chem. Soc., **80,** 6428 (1958)

[21] Pilotti, A., Reuterhall, A., Torssel, K.: Acta Chem. Scand., **23,** 820 (1969)
[22] Colthup, J.: J. Opt. Soc. Amer., **40,** 397 (1950)
[23] Horák, M., Papousek, D.: Infracervená Spektra a Struktura Molekul, p. 310, Academia, Praha 1976
[24] Noe, E. A., Raban, M.: J. Am. Chem. Soc., **97,** 5811 (1974)
[25] Noe, E. A., Raban, M.: J. Chem. Soc. Chem. Commun., **1974,** 479
[26] Duffild, A. M., Budzikiewicz, H., Djerassi, C.: J. Am. Chem. Soc., **86,** 5536 (1964)
[27] Duffild, A. M., Budzikiewicz, H., Djerassi, C.: J. Am. Chem. Soc., **87,** 2913 (1965)
[28] Mitera, J., Kubelka, V.: Org. Mass Spectrom., **5,** 651 (1971)
[29] Grutzmacher, H. F., Kuschel, H.: Org. Mass Spectrom., **3,** 605 (1970)

Acta Chimica Hungarica 116 (1), pp. 103—109 (1984)

KINETICS OF EXCHANGE OF TRANSITION METALS ON ZIRCONIUM(IV) AND THORIUM(IV) PHOSPHOSILICATE CATION EXCHANGERS

K. G. VARSHNEY* and U. SHARMA

(Analytical Laboratories, Chemistry Section, Faculty of Engineering & Technology, Aligarh Muslim University, Aligarh-202001, India)

Received April 2, 1983
In revised form June 17, 1983
Accepted for publication July 13, 1983

Kinetics of the exchange reactions of Mn^{2+}, Fe^{2+}, Co^{2+} and Ni^{2+} ions on Zr(IV) and Th(IV) phosphosilicate cation exchangers has been studied at 25, 32, 50 and 65 °C under the conditions favourable to the particle diffusion mechanism only and the rate of exchange has been found to be independent of the metal ion concentration at and above 0.01 *M* in aqueous medium on both the materials. Various kinetic parameters such as self-diffusion coefficient (D_0), energy of activation (E_a) and entropy of activation (ΔS^*) have been calculated which are useful for predicting the ion exchange phenomenon taking place.

Introduction

Inorganic ion exchangers are generally used for the metal separations. They are superior to the organic resins as they are resistant to heat and radiations. To understand the mechanism underlying in an ion exchange process its kinetic studies are essential which have been done mostly on the crystalline and amorphous zirconium phosphate [1—5], zirconium oxide [6], tantalum and tin arsenates [7, 8], ceric phosphate [9] and zirconium, iron and tin antimonates [10—12]. Moreover, these studies are based on the old Bt criterion [13] which is not very useful for an ion exchange process because of the different effective diffusion coefficients taking part in such a case. Here, the Nernst—Planck [14, 15] equations are more appropriate. Since the kinetic studies are rarely made [16—18] on double salts, the following pages summarize our study on zirconium(IV) and thorium(IV) phosphosilicates (ZPS and TPS) as cation exchangers, taking transition metal ions as exchanging species with H^+ ions.

Experimental

Reagents and chemicals

Zirconyl chloride and thorium nitrate were of B.D.H. (England) while sodium silicate was a Riedel (DEHAENAG, Seelze Hannover) product. All other reagents and chemicals were of AnalaR grade.

* To whom correspondence should be addressed

Apparatus

A water bath incubator shaker having a temperature variation of ± 0.5 °C was used for the equilibrium studies.

Synthesis of the ion exchange materials

To a definite volume of a 0.1 *M* sodium silicate ($Na_2SiO_3 \cdot 3H_2O$) solution *conc.* HCl (5 mL per 100 mL Na-silicate solution) and a definite volume of 0.1 *M* zirconium oxychloride ($ZrOCl_2 \cdot 8H_2O$) solution were added. The pH of the mixture was made 9—10 by adding NH_4OH and the resultant slurry was allowed to stand overnight. It was filtered, washed with DMW and mixed with a fixed volume of a H_3PO_4—HNO_3 mixture (1 *M* in terms of each acid). The gel thus obtained was kept overnight, filtered out, washed thoroughly with DMW, dried at 45 °C in an air oven and was cracked in DMW to form small granules. The granules were then placed in 1 *M* HNO_3 to convert them into the H^+-form and were finally washed and dried at 45 °C before use for further study. TPS was prepared in a similar manner by taking thorium nitrate $Th(NO_3)_4 \cdot 6H_2O$ instead of zirconium oxychloride. The Na^+-ion exchange capacities of these materials (ZPS and TPS) were found to be 2.19 and 1.66 meq/dry g, respectively.

Kinetic measurements

The rates of exchange of metal ions were determined by the limited bath technique. 20 mL fractions of the 0.01 *M* metal ion solutions of the divalent transition metals (Mn^{2+}, Fe^{2+}, Co^{2+} and Ni^{2+}) were shaken with 200 mg of the exchanger beads (mean radius 120 μm; 100—150 mesh size) in some stoppered conical flasks at the desired temperature (25, 32, 50 and 65 °C ± 0.5 °C) for different time intervals as mentioned in Fig. 2. Supernatant liquid was immediately removed by filtering through a Whatman No. 4 filter paper and the determinations were done by EDTA titrations [19] using Eriochrome Black T as an indicator.

Results and Discussion

A study of the concentration effect on the rate of Mn^{+2}—H^+ exchange at 25 °C shows that at concentrations <0.01 *M* the initial rate of exchange is proportional to $[Mn^{2+}]$. At concentrations ≥ 0.01 *M* it is found to be independent of the metal ion concentration. Under the conditions of a particle diffusion control, a relatively large particle size of the exchanger and vigorous shaking the fractional attainment of equilibrium may be given as,

$$U(\tau) = \frac{\text{the total amount of exchange at time '}t\text{'}}{\text{the amount of exchange at infinite time}} \qquad (1)$$

A plot of $U(\tau)$ versus t (Fig. 1) for Mn^{2+} ion on ZPS and TPS indicates that the fractional attainment of equilibrium is faster at a higher temperature, an observation analogous to the other materials of this class. Although this is a limited bath system, the equation applicable to an infinite bath can be used here because $CV \gg \bar{C}\bar{V}$ where C and $\bar{C}$ are the metal ion concentrations in the solution and exchanger phases, respectively. V and $\bar{V}$ are the volumes of these two phases. The Nernst—Planck equations can be solved with some additional assumptions [20], which are valid for inorganic ion exchangers as the swelling changes and the specific interactions are not significant in this

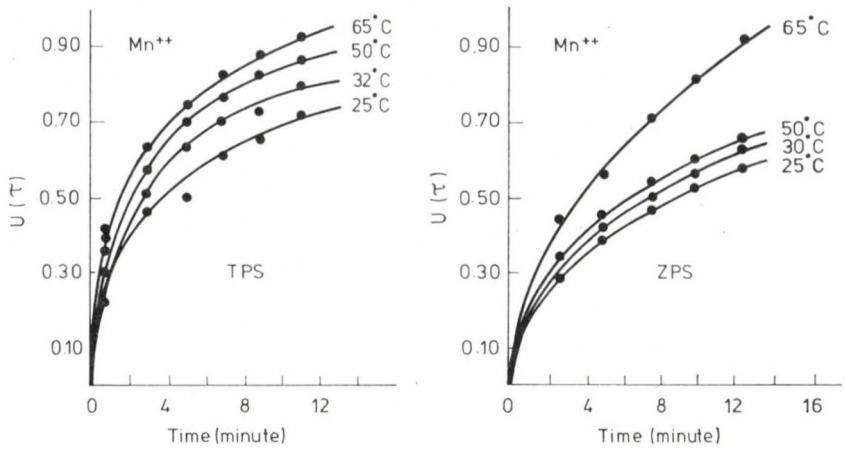


Fig. 1

case. As a result we obtain a coupled interdiffusion coefficient $\bar{D}_{AB}$, the value of which depends on the relative concentrations of the counter ions A and B in the exchanger phase ($\bar{C}_A$ and $\bar{C}_B$). For $\bar{C}_A \ll \bar{C}_B$ the interdiffusion coefficient assumes the values $\bar{D}_A$, A being the counter ion initially present in the ion exchanger phase. Since in the present case the exchanger is taken in H^+ form, $\bar{D}_A$ may be replaced by $\bar{D}_H$.

Thus, on the basis of the Nernst—Planck equations

$$U(\tau) = 1 - \exp\left\{[\pi^2(f_1(\alpha)\ \tau + f_2(\alpha)\ \tau^2 + f_3(\alpha)\ \tau^3)]\right\}^{\frac{1}{2}} \tag{2}$$

where

$$\tau = \frac{\bar{D}_H t}{r_0^2}$$

and the mobility ratio $\alpha = \dfrac{\bar{D}_H}{\bar{D}_M}$, r_0 = particle radius and $\bar{D}_M$ is the interdiffusion coefficient of the metal ion. Under the conditions $1 \leq \alpha \leq 20$ and $Z_H/Z_M = 1/2$ as in the present case, the three functions $f_1(\alpha)$, $f_2(\alpha)$ and $f_3(\alpha)$ can be expressed [21] as:

$$f_1(\alpha) = -\frac{1}{0.64 + 0.36\,\alpha^{0.668}} \tag{a}$$

$$f_2(\alpha) = -\frac{1}{0.96 - 2.0\,\alpha^{0.4635}} \tag{b}$$

and

$$f_3(\alpha) = -\frac{1}{0.27 + 0.09\,\alpha^{1.14}} \tag{c}$$

Each value of $U(\tau)$ will have a corresponding value of τ which is obtained on solving equation (2) by graphical method. The plots of τ vs. t at the four different temperatures (Fig. 2) on ZPS and TPS for the Mn^{2+} ions are shown at a concentration 0.1 M which are straight lines passing through the origin. It confirms a particle diffusion controlled phenomenon. The slopes (S) of such lines for all the four transition metals on ZPS and TPS are given in Table I, which are related with $\bar{D}_H$ as follows:

$$S = \frac{\bar{D}_H}{r_0^2} \tag{3}$$

The plots of — log $\bar{D}_H$ vs. $1/T$ are straight lines as shown in Fig. 3, thus varifying the Arrhenius relation:

$$\bar{D}_H = D_0 \, e^{(E_a/RT)} \tag{4}$$

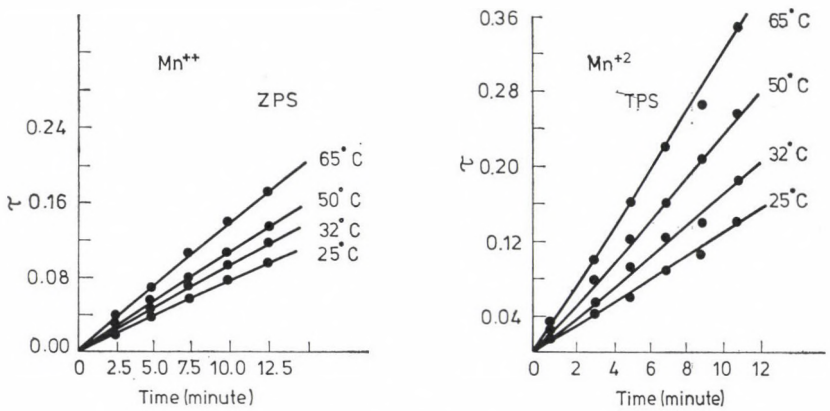


Fig. 2

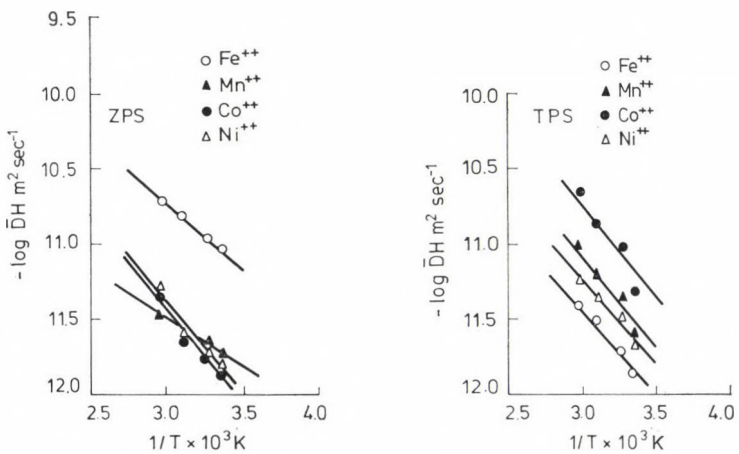


Fig. 3

Table I

Slopes of the various τ versus time plots for transition metals on Zr(IV) *and* Th(IV) *phosphosilicates*

Migrating ion	Slopes (s^{-1})							
	On ZPS				On TPS			
	25 °C	35 °C	50 °C	65 °C	25 °C	35 °C	50 °C	65 °C
Mn^{2+}	1.27×10^{-4}	1.55×10^{-4}	1.77×10^{-4}	2.44×10^{-4}	1.83×10^{-4}	3.16×10^{-4}	4.16×10^{-4}	5.33×10^{-4}
Fe^{2+}	6.38×10^{-4}	7.77×10^{-4}	1.11×10^{-4}	14.44×10^{-4}	1.00×10^{-3}	1.33×10^{-4}	2.16×10^{-4}	2.66×10^{-4}
Co^{2+}	1.00×10^{-4}	1.27×10^{-4}	1.72×10^{-4}	3.11×10^{-4}	3.33×10^{-4}	5.00×10^{-4}	9.44×10^{-4}	16.11×10^{-4}
Ni^{2+}	1.11×10^{-4}	1.33×10^{-4}	1.72×10^{-4}	3.33×10^{-4}	1.66×10^{-4}	2.33×10^{-4}	3.16×10^{-4}	4.00×10^{-4}

Table II

Self-diffusion coefficient, energy of activation and entropy of activation of transition metals on Zr(IV) *and* Th(IV) *phosphosilicates*

Migrating ion	Ionic mobility (m^2 volt^{-1} s^{-1})	Ionic radii (nm)	D_0, E_a and ΔS^* values					
			On ZPS			On TPS		
			D_0 (m^2 s^{-1})	E_a (kJ mole^{-1})	ΔS^* (JK^{-1} mole^{-1})	D_0 (m^2 s^{-1})	E_a (KJ mole^{-1})	ΔS^* (JK^{-1} mole^{-1})
Mn^{2+}	55×10^{-9}	9.1×10^{-2}	3.55×10^{-10}	13.07	−77.29	2.51×10^{-8}	22.21	−47.88
Fe^{2+}	54×10^{-9}	6.7×10^{-2}	8.41×10^{-9}	16.85	−31.83	5.01×10^{-9}	19.86	−55.28
Co^{2+}	55×10^{-9}	8.2×10^{-2}	1.88×10^{-8}	23.52	−44.27	6.68×10^{-8}	22.60	−33.74
Ni^{2+}	52×10^{-9}	7.8×10^{-2}	1.99×10^{-8}	23.25	−43.79	1.00×10^{-8}	20.51	−49.53

D_0 is then obtained by extrapolating these lines and observing the intercepts at the origin. E_a values are then calculated from equation (4) putting the value of $\bar{D}_H$ corresponding to the T value as 273 °K in the graph. Finally ΔS^* values are obtained from the expression:

$$D_0 = 2.72\, d^2 \frac{kT}{h} \exp\,(\Delta S^*/R) \tag{5}$$

where d is the ionic jump distance [22] taken as 0.5 nm and k and h are the Boltzmann and Planck constants, respectively. T is taken as 273 °K. The values of D_0, E_a and ΔS^* are summarized in Table II.

*

The authors are thankful to Prof. Mohsin Qureshi for the research facilities and to the C.S.I.R., India for the financial assistance.

REFERENCES

[1] Ruvarac, A. L., Veseley, V.: J. Inorg. Nucl. Chem., **32,** 3939 (1970)
[2] Ruvarac, A. L.: J. Chromatogr., **60,** 235 (1971)
[3] Clearfield, A., Medina, A. S.: J. Inorg. Nucl. Chem., **32,** 2775 (1970)
[4] Alberti, G., Costantino, U., Bertrami, R., Cascoila, M., Gupta, J. P.: J. Inorg. Nucl. Chem., **38,** 843 (1976)
[5] Nancollas, G. H., Paterson, R.: J. Inorg. Nucl. Chem., **22,** 259 (1961)
[6] Ruvarac, A. L., Trtanj, M. I.: J. Inorg. Nucl. Chem., **34,** 3893 (1972)
[7] Rawat, J. P., Thind, P. S.: J. Phys. Chem., **80,** 1384 (1976)
[8] Rawat, J. P., Khan, M. A.: J. Inorg. Nucl. Chem., **42,** 905 (1980)
[9] Herman, R. G., Clearfield, A.: J. Inorg. Nucl. Chem., **38,** 853 (1976)
[10] Methew, J., Tandon, S. N.: Can. J. Chem., **55,** 3857 (1977)
[11] Rawat, J. P., Singh, D. K.: J. Inorg. Nucl. Chem., **40,** 897 (1978)
[12] Singh, N. J., Tandon, S. N., Ind. J. Chem., **19A,** 416 (1980)
[13] Boyd, G. E., Adamson, A. W., Myers, L. S.: J. Am. Chem. Soc., **69,** 2836 (1947)
[14] Nernst, W. Z.: Physik Chem., **2,** 613 (1888); **4,** 129 (1889)
[15] Planck, M.: Ann. Phys. Chem., **39,** 161 (1890)
[16] Choudhuri, D., Mukherjee, S. K.: J. Inorg. Nucl. Chem., **33,** 1933 (1971)
[17] Singh, N. J., Mathew, J., Tandon, S. N.: J. Phys. Chem., **84,** 21 (1980)
[18] Varshney, K. G., Permadas, A.: Ind. J. Chem., **20A,** 841 (1981)
[19] Reilley, C. N., Schmid, R. W. E.: J. Chem. Educ., **36,** 555 (1959)
[20] Helfferich, F.: Ion-Exchange, McGraw-Hill Book Company, New York, p. 268. (1962)
[21] Helfferich, F.: Ion-Exchange, Mc Graw-Hill Book Company, New York, p. 271 (1962)
[22] Barrer, R. M., Bartholomew, R. F., Rees, L. V. C.: J. Phys. Chem. Solids, **12,** 21 (1961)

ACTA PHYSICA

ACADEMIAE SCIENTIARUM HUNGARICAE

EDITOR-IN-CHIEF

I. KOVÁCS

VOLUME 52 CONTENTS NUMBER 2

A. P. Kajwadkar and *L. K. Sharma:* Solutions of Wave Equation for the Superposed Potential with Application to Charmonium Spectroscopy

T. Margaritisz and *K. Szegő:* The Nucleon Form Factors in the Geometrodynamical Model

R. G. Kulkarni and *K. Andhradev:* Negative Parity Levels in ^{195}Pt Via Coulomb Excitation

B. J. Reddy and *K. B. N. Sarma:* Absorption Spectra of Mn^{2+} in Manganoan Clinozoisite

A. M. Ghodgaonkar and *K. Ramani:* Estimation of Dissociation Energies of Weakly Bound Molecules

A. Natarajan and *S. Somasundaram:* Normal Coordinate Analysis of the Tetrafluoro-1,3 Dithietane

A. Taszner and *J. Wojtkowiak:* Gain Measurements in the $He-I^+$ Laser

P. Singh and *S. Antony Raj:* An Approximate Variational Solution of Boundary Layer Flow when Free Stream Varies as Power Function

Bhimsen K. Shivamoggi: A Nearly Exact Helical-Wave Solution to the Equations of Slightly Dissipative Magnetohydrodynamics

G. Adler: Modification of the MHD Equations to Reduce Numerical Instability in the Simulation of Slow Plasma Motions

A. H. Abou El Ela and *N. Abdelmohsen:* Electrical Properties of $AgTlSe_2$ Semiconductor in the Liquid State

A. H. Abou El Ela, S. Mahmoud and *M. A. Mahmoud:* Electrical Conduction of Thin Bismuth Films

M. F. Kothata, E. A. Mahmoud and *M. K. El-Mously:* An X-Ray Study of the Se—Te System

S. C. Jain and *C. M. Kachhava:* Certain Characteristics of Copper Pair

B. Krishnan and *A. Srinivasa Rao:* Structural Studies on a Human Bladder Stone — PMR and IR Studies

Papers in English. Published in two volumes (4 issues each) annually.
Subscription rate per vol ume: $40.00

AKADÉMIAI KIADÓ

Publishing House of the Hungarian Academy of Sciences

Budapest

Distributed by KULTURA, Hungarian Foreign Trading Co , P.O.B. 149, H-1389 Budapest

ACTA GEODAETICA, GEOPHYSICA ET MONTANISTICA

ACADEMIAE SCIENTIARUM HUNGARICAE

EDITOR-IN-CHIEF
A. TÁRCZY-HORNOCH

EDITOR
J. VERŐ

VOLUME 17 NUMBER 2

CONTENTS

Ádám, J.—Halmos, F.—Varga, M.: On the concepts of combination of Doppler satellite and terrestrial geodetic networks

Ádám, J.—Tarcsai, Gy.: Doppler location equations for platform localization using satellites

Csernyák, L.—Steiner, F.: Amplifying residual filters

Csernyák, L.—Steiner, F.—Zilahi-Sebes, L.: A short note to prescribed w-properties

Abdelhamid Kamal Hassan: Comparison between results of the gyro-azimuths determined with old and new gyrotheodolites

Kardos, I.—Borza, T.—Vass, T.: Laser ranging observations at the Satellite Geodetic Observatory (SGO)

Krasnobaeva, A. G.—Diakonov, B. P.—Astafiev, P. F.—Batalova, O. V.—Vishnev, V. S.—Gavrilova, I. E.—Zhuravlyova, R. B.—Kirillov, S. K.: Magnetotelluric data on the geoelectric structure in the North-Eastern part of the Baltic Shield

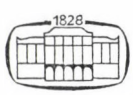
Raspopov, O. M.—Afanasyeva, L. T.: Localization of the Pc5-source and of the auroral oval

Rösler, R.—Lindner, H.: Ableitung von Feldtransformationen für Profile von Potentialfeldanomalien

Немеши, Л.—Богнар, Е.—Лавдансурен—Хорван—Майкут, Т.—Том, Ч.: Комплексная геофизическая разведка в пустыне Гоби.

Gasco, J. C.—Febrer, J. M.—Demicheli, J.—Fournier, H. G.: Zarate MT sounding and upper mantle resistivity

Papers in English, German and Russian. Published in one volume (4 issues) annually.
Subscription rate per volume $40.00



AKADÉMIAI KIADÓ
Publishing House of the Hungarian Academy of Sciences
Budapest

Distributed by KULTURA, Hungarian Foreign Trading Co., P.O.B. 149, H-1389 Budapest

Text

The text of the paper should be concise. The description of new compounds (in the Experimental) must include the complete analytical data. Special attention must be paid to structural formulas given within the text. Complicated (non-linear) formulas should be drawn on separate sheets of paper and their position in the text should be clearly marked. The numbering of formulas and equations (in parentheses on the right-hand side) is only needed if they are referred to in the text. Units should conform to the International System of Units (SI). In nomenclature the rules of the I.U.P.A.C. are accepted as standard. Symbols for physical quantities are printed in italic type and should, therefore, be underlined in the manuscript.

References

References should be numbered in order of appearance in the text (where the reference number appears in brackets) and listed at the end of the paper. The reference list, too, should be typed double-spaced. Journal titles are to be abbreviated as defined by the Chemical Abstracts Service Source Index.

Examples:

[1] Brossi, A., Lindlar, H., Walter, M., Schneider, O.: Helv. Chim. Acta, **41**, 119 (1958)
[2] Parr, R. G.: Quantum Theory of Molecular Electronic Structure. Benjamin, New York 1964
[3] Warshel, A.: in Modern Theoretical Chemistry, Vol. 7, Part A (Ed. G. A. Segal), Plenum Press, New York 1977

Tables

Each table should be given a Roman number and a brief informative title. Structural formulas should not be used in column headings or in the body of tables.

Figures

Figures should be numbered consecutively with Arabic numerals. Their approximate place should be indicated in the text on the margin. All figures must be identified on the back by the author's name and the figure number in pencil. Standard symbols (such as circles, triangles, squares) are to be used on line-drawings to denote the points determined experimentally. Line-drawings must not contain structural formulas and comments. Spectra or relevant segments thereof, chromatograms, and X-ray diffraction patterns will be reproduced only if concise numerical summaries are inadequate to replace them. Drawings and graphs should be prepared in black ink on good-quality white or tracing paper. Photographs should be submitted on glossy paper as high-contrast copies. Xerox or similar copies are not suitable for reproduction, but may be used for duplicate copies.

Redrawn illustrations will be sent to the authors for checking. No corrections of figures will, therefore, be accepted in the proofs.

Submission of manuscript

After having completed the corrections suggested by the referees and editors, the final manuscript should be submitted in duplicate, in a form ready for publication. If the corrected manuscript is not returned to the editors *within six weeks*, the intended publication of the paper will be regarded as withdrawn by the authors.

Page charge will not be assessed for the publication, however, authors, from overseas countries must contribute to the postage of correspondence by sending, together with the manuscript, international postal coupons to the value of U.S. $ 10.—

Proofs and reprints

A set of proofs will be sent to the submitting author. The proofs must be returned within 48 hours of receipt. Late return may cause a delay in the publication of the paper. 100 reprints will be supplied to the authors free of charge.

Periodicals of the Hungarian Academy of Sciences are obtainable at the following addresses:

AUSTRALIA
C.B.D. LIBRARY AND SUBSCRIPTION SERVICE
Box 4886, G.P.O., *Sydney N.S.W. 2001*
COSMOS BOOKSHOP, 145 Ackland Street
St. Kilda (Melbourne), Victoria 3182

AUSTRIA
GLOBUS, Höchstädtplatz 3, *1206 Wien XX*

BELGIUM
OFFICE INTERNATIONAL DE LIBRAIRIE
30 Avenue Marnix, *1050 Bruxelles*
LIBRAIRIE DU MONDE ENTIER
162 rue du Midi, *1000 Bruxelles*

BULGARIA
HEMUS, Bulvar Ruszki 6, *Sofia*

CANADA
PANNONIA BOOKS, P.O. Box 1017
Postal Station "B", *Toronto, Ontario M5T 2T8*

CHINA
CNPICOR, Periodical Department, P.O. Box 50
Peking

CZECHOSLOVAKIA
MAD'ARSKÁ KULTURA, Národní třida 22
115 66 Praha
PNS DOVOZ TISKU, Vinohradská 46, *Praha 2*
PNS DOVOZ TLAČE, *Bratislava 2*

DENMARK
EJNAR MUNKSGAARD, Norregade 6
1165 Copenhagen K

FEDERAL REPUBLIC OF GERMANY
KUNST UND WISSEN ERICH BIEBER
Postfach 46, *7000 Stuttgart 1*

FINLAND
AKATEEMINEN KIRJAKAUPPA, P.O. Box 128
SF-00101 Helsinki 10

FRANCE
DAWSON-FRANCE S. A., B. P. 40, *91121 Palaiseau*
EUROPÉRIODIQUES S. A., 31 Avenue de Versailles, *78170 La Celle St. Cloud*
OFFICE INTERNATIONAL DE DOCUMENTATION ET LIBRAIRIE, 48 rue Gay-Lussac
75240 Paris Cedex 05

GERMAN DEMOCRATIC REPUBLIC
HAUS DER UNGARISCHEN KULTUR
Karl Liebknecht-Straße 9, *DDR-102 Berlin*
DEUTSCHE POST ZEITUNGSVERTRIEBSAMT
Sraße der Pariser Kommüne 3–4, *DDR-104 Berlin*

GREAT BRITAIN
BLACKWELL'S PERIODICALS DIVISION
Hythe Bridge Street, *Oxford OX1 2ET*
BUMPUS, HALDANE AND MAXWELL LTD.
Cowper Works, *Olney, Bucks MK46 4BN*
COLLET'S HOLDINGS LTD., Denington Estate
Wellingborough, Northants NN8 2QT
WM. DAWSON AND SONS LTD., Cannon House
Folkstone, Kent CT19 5EE
H. K. LEWIS AND CO., 136 Gower Street
London WC1E 6BS

GREECE
KOSTARAKIS BROTHERS INTERNATIONAL BOOKSELLERS, 2 Hippokratous Street, *Athens-143*

HOLLAND
MEULENHOFF-BRUNA B.V., Beulingstraat 2,
Amsterdam
MARTINUS NIJHOFF B.V.
Lange Voorhout 9–11, *Den Haag*
SWETS SUBSCRIPTION SERVICE
347b Heereweg, *Lisse*

INDIA
ALLIED PUBLISHING PRIVATE LTD., 13/14
Asaf Ali Road, *New Delhi 110001*
150 B-6 Mount Road, *Madras 600002*
INTERNATIONAL BOOK HOUSE PVT. LTD.
Madame Cama Road, *Bombay 400039*
THE STATE TRADING CORPORATION OF INDIA LTD., Books Import Division, Chandralok
36 Janpath, *New Delhi 110001*

ITALY
INTERSCIENTIA, Via Mazzé 28, *10149 Torino*
LIBRERIA COMMISSIONARIA SANSONI, Via Lamarmora 45, *50121 Firenze*
SANTO VANASIA, Via M. Macchi 58
20124 Milano
D. E. A., Via Lima 28, *00198 Roma*

JAPAN
KINOKUNIYA BOOK-STORE CO. LTD.
17-7 Shinjuku 3 chome, Shinjuku-ku, *Tokyo 160-91*
MARUZEN COMPANY LTD., Book Department, P.O. Box 5050 Tokyo International, *Tokyo 100-31*
NAUKA LTD. IMPORT DEPARTMENT
2-30-19 Minami Ikebukuro, Toshima-ku, *Tokyo 171*

KOREA
CHULPANMUL, *Phenjan*

NORWAY
TANUM-TIDSKRIFT-SENTRALEN A.S., Karl Johansgatan 41–43, *1000 Oslo*

POLAND
WĘGIERSKI INSTYTUT KULTURY, Marszałkowska 80, *00-517 Warszawa*
CKP I W, ul. Towarowa 28, *00-958 Warszawa*

ROUMANIA
D. E. P., *Bucureşti*
ILEXIM, Calea Grivitei 64–66, *Bucureşti*

SOVIET UNION
SOJUZPECHAT — IMPORT, *Moscow*
and the post offices in each town
MEZHDUNARODNAYA KNIGA, *Moscow G-200*

SPAIN
DIAZ DE SANTOS, Lagasca 95, *Madrid 6*

SWEDEN
ALMQVIST AND WIKSELL, Gamla Brogatan 26
101 20 Stockholm
GUMPERTS UNIVERSITETSBOKHANDEL AB
Box 346, *401 25 Göteborg 1*

SWITZERLAND
KARGER LIBRI AG, Petersgraben 31, *4011 Basel*

USA
EBSCO SUBSCRIPTION SERVICES
P.O. Box 1943, *Birmingham, Alabama 35201*
F. W. FAXON COMPANY, INC.
15 Southwest Park, *Westwood Mass. 02090*
THE MOORE-COTTRELL SUBSCRIPTION AGENCIES, *North Cohocton, N. Y. 14868*
READ-MORE PUBLICATIONS, INC.
140 Cedar Street, *New York, N. Y. 10006*
STECHERT-MACMILLAN, INC.
7250 Westfield Avenue, *Pennsauken N. J. 08110*

YUGOSLAVIA
JUGOSLOVENSKA KNJIGA, Terazije 27, *Beograd*
FORUM, Vojvode Mišića 1, *21000 Novi Sad*

Index: 26.007

Acta Chimica Hungarica

VOLUME 116, NUMBER 2, JUNE 1984

EDITOR-IN-CHIEF
F. MÁRTA

MANAGING EDITOR
GY. DEÁK

ASSISTANT EDITOR
L. HAZAI

EDITORIAL BOARD
M. T. BECK, R. BOGNÁR, GY. HARDY, K. LEMPERT, B. LENGYEL, K. POLINSZKY, E. PUNGOR, G. SCHAY, Z. G. SZABÓ, P. TÉTÉNYI

Akadémiai Kiadó, Budapest

ACTA CHIM. HUNG. ACASA2 116 (2) 111—191 (1984) HU ISSN 0231-3146

ACTA CHIMICA HUNGARICA

A JOURNAL OF THE HUNGARIAN ACADEMY OF SCIENCES

Acta Chimica publishes original reports on all aspects of chemistry in English.

Acta Chimica is published in three volumes per year, each volume consisting of four issues, by

AKADÉMIAI KIADÓ

Publishing House of the Hungarian Academy of Sciences
H-1054 Budapest, Alkotmány u. 21.

Manuscripts and editorial correspondence should be addressed to

Acta Chimica
H-1450 Budapest P.O. Box 67

Subscription information

Orders should be addressed to

KULTURA Foreign Trading Company
H-1389 Budapest P.O. Box 149

or to its representatives abroad

Acta Chimica is indexed in Current Contents

NOTICE TO AUTHORS

Acta Chimica publishes original papers on all aspects of chemistry in English. Before preparing a manuscript for submission to this journal authors are advised to consult recent issues.

Form of manuscript

Manuscripts, tables and illustrations should be submitted in triplicate. Manuscripts should be typewritten double spaced (25 lines, 50 characters per line including spaces). The *title page* should include (1) the title of the paper, (2) the full names of the author(s) in the sequence to be published; apply an asterisk to designate the name of the author to whom correspondence should be addressed, (3) name and address of the institution where the work was done. If the paper is part of a series, reference to the previous communication must be given as a footnote.

Abstract

A summary is printed at the head of each paper. This should not exceed 200 words and should state briefly the principal results and major conclusions of the work. It should be suitable for use by abstracting services.

CONTENTS

PHYSICAL AND INORGANIC CHEMISTRY

Electrochemical behaviour of the benzimidazoles, **G. Korányi, E. Szebényi-Győri, A. Vélin-Prikidánovics, J. Brlik** 131
Comparison of some quantum chemical methods estimating hydration effects on the hydrogen fluoride — ammonia proton transfer reaction, **J. Ángyán, G. Náray-Szabó** 141
Influence of the chemical potential of transition metals on their adsorptive and catalytic properties, **P. J. Pomonis** 163

ORGANIC CHEMISTRY

New 17-spirosteroids, IV. Synthesis and examination of steroid 17*S*-spirodioxolanes, **K. Szilágyi, S. Sólyom, L. Toldy** 111
New 17-spirosteroids, V. Preparation and investigation of steroid-17-spiro-1',3',2'-oxazaphospholidines and -1',3',2'-dioxaphospholanes, **S. Sólyom, K. Szilágyi, L. Toldy** 125
The structure of deoxyluteins, **M. Baranyai, L. Radics, M. Kajtár, J. Kajtár, Gy. Bujtás, J. Szabolcs** 153
Design and synthesis of inhibitory analogues of LH—RH with increased antiovulatory potency, **I. Mező, J. Seprődi, J. Erchegyi, A. Horváth, K. Nikolics, I. Teplán, S. Vigh, M. Kovács, B. Flerkó, D. H. Coy, E. Pedroza, M. V. Nekola, A. V. Schally** 173

BOOK REVIEWS 189

Acta Chimica Hungarica 116 (2), pp. 111–123 (1984)

NEW 17-SPIROSTEROIDS, IV*

SYNTHESIS AND EXAMINATION OF STEROID 17S-SPIRODIOXOLANES

K. SZILÁGYI**, S. SÓLYOM and L. TOLDY

(Institute for Drug Research, H-1325 Budapest, P.O. Box 82)

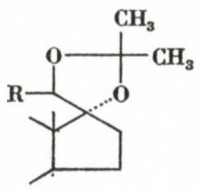
Received February 16, 1983

Accepted for publication September 8, 1983

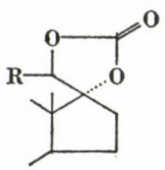
New 17*S*-spirodioxolanes with androstane, oestrane and 13β-ethylgonane skeleton have been synthesized by cyclization in different ways of known and new 17α--hydroxymethyl-17β-hydroxysteroids obtained by the alkaline hydrolysis of 17*S*--spirooxiranes. Some of the products had significant peroral antialdosterone activity.

Earlier papers dealt with the synthesis and biological tests of such 17-spirosteroids having antialdosterone activity, which, unlike the known and biologically active spirosteroids of γ-lactone type (e.g., spironolactone [1]), contain nitrogen atom [3, 4] or nitrogen and sulfur atoms [5] in the spiro ring, in addition to the β-oriented oxygen atom required for the antialdosterone effect [2]. In the present work new spirosteroids will be described which contain a further oxygen atom, besides the β-oriented oxygen, in the spiro ring.

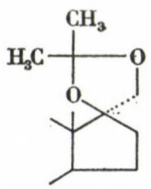
Of these 17-spirodioxolane steroids, some pregnane derivatives **I** [6, 7, 8] and **II** [9, 10], as well as representatives of the **III.** [11, 12] adrostane and 1,3,5--(10)-oestratriol derivatives have already been known, but no investigations on their activity have been reported yet.



I



II



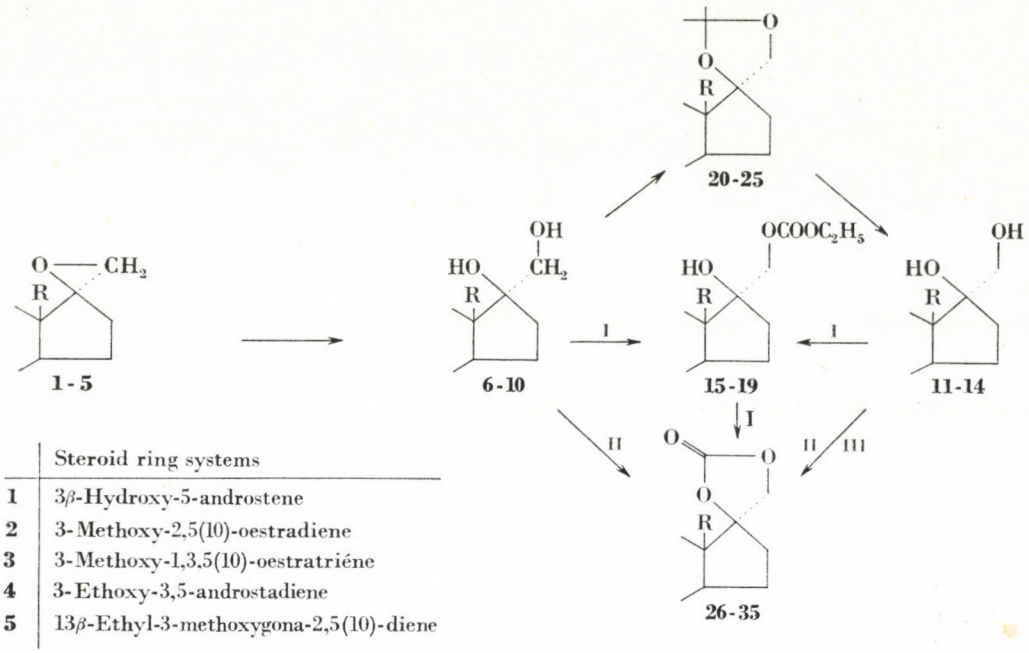
III

R = CH_3
CH_2OH
CH_2Br

The new 17*S*-spirodioxolanes have been prepared by the cyclization of 17α-hydroxymethyl-17β-hydroxy derivatives with androstane, oestrane and 13β-ethylgonane skeleton. The diols used as starting materials were obtained by the alkaline hydrolysis of the known 17*S*-spirooxiranes **1—5** (Scheme 1).

* Part III. S. Sólyom, K. Szilágyi, L. Toldy: Justus Liebigs Ann. Chem., **1983**, 1001

** To whom correspondence should be addressed



	Steroid ring systems
1	3β-Hydroxy-5-androstene
2	3-Methoxy-2,5(10)-oestradiene
3	3-Methoxy-1,3,5(10)-oestratriéne
4	3-Ethoxy-3,5-androstadiene
5	13β-Ethyl-3-methoxygona-2,5(10)-diene

Scheme 1

Ring cleavage of 17*S*-spirooxiranes can be readily effected with many nucleophilic reagents [16], but their alkaline hydrolysis takes place relatively slowly [11, 17]. In alkaline hydrolysis in alcoholic media, the formation of the 17α-alkoxymethyl-17β-ol derivative was also observed [11] as a competitive reaction, beside the steroid diol.

Berti et al. [18] examined the conditions of alkaline hydrolysis of non-steroid epoxides and observed an increased rate of hydrolysis in dimethyl sulfoxide medium due to the high polarity of the solvent and its weak solvation effect on the anion.

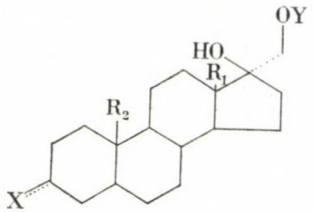
In view of this fact, the alkaline hydrolysis of **1**—**5** was effected with potassium hydroxide in 85% aqueous dimethyl sulfoxide. In this way the rate of hydrolysis was increased, and higher yields were attained in the preparation of the steroid diols **6**—**10** (Table I) by avoiding the competitive reaction.

The advantage of the method was also shown by the fact that, although Ponsold et al. failed in hydrolyzing the sterically hindered 13β-ethylgona-3,5(10)-diene-17*S*-spirooxirane **5** with 40% aqueous sodium hydroxide in alcohol [19], the hydrolysis of this compound could be accomplished under the above conditions, in medium yield.

The 3-oxo-4-ene steroid diols (**11**—**13**) were prepared by hydrolysis of the corresponding acetonide derivatives (**21**, **24**, **25**, Table II) with aqueous hydrochloric acid (Scheme 2).

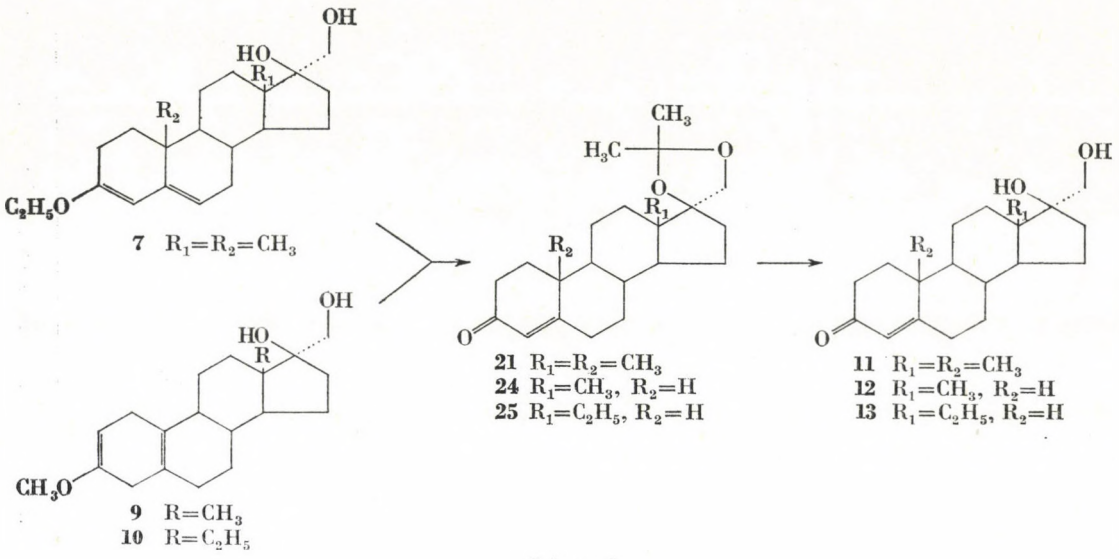
Table I

17α-Hydroxymethyl-17β-hydroxysteroids and O-ethoxycarbonyloxy derivatives



No.	R_1	R_2	X	Y	Unsaturation	Starting compd.	Mp. °C ([Lit.], Mp., °C)	Formula	Calcd. % Found % C:	Calcd. % Found % H	Yield, %
6	CH_3	CH_3	βOH	H	5	**1** [13]	204–7[a] ([11], 216)	$C_{20}H_{32}O_3$	74.95 74.89	10.07 9.81	95
7	CH_3	CH_3	C_2H_5O	H	3.5	**2** [14]	170–2[a]	$C_{22}H_{34}O_3$	76.25 76.58	9.89 10.37	88
8	CH_3	—	CH_3O	H	1,3,5(10)	**3** [15]	163–5[b] ([16], 168–71)	$C_{20}H_{28}O_3$	75.91 75.86	8.91 8.78	81
9	CH_3	—	CH_3O	H	2,5(10)	**4** [15]	191–7[a] ([19], 193–4)	$C_{20}H_{30}O_3$	75.43 75.38	9.49 9.32	87
10	C_2H_5	—	CH_3O	H	2,5(10)	**5** [3]	166–7[a]	$C_{21}H_{32}O_3$	75.85 75.82	9.70 9.74	54
11	CH_3	CH_3	O	H	4	**21**	186–198[a] ([11], 193)	$C_{20}H_{30}O_3$	75.43 75.38	9.49 9.53	56
12	CH_3	H	O	H	4	**9** **24**	137–8[c] ([19], 139–41)	$C_{19}H_{28}O_3$	74.94 74.86	9.27 9.35	55 60
13	C_2H_5	H	O	H	4	**25**	146–8[oc]	$C_{20}H_{30}O_3$	75.43 75 37	9.49 9.67	51
14	CH_3	CH_3	O	H	4.6	**7**	233–5[c]	$C_{20}H_{28}O_3$	75.91 76.05	8.91 8.64	77
15	CH_3	CH_3	βOH	CO_2Et	5	**6**	58–63[d]	$C_{23}H_{36}O_5$	70.37 70.49	9.24 9.33	37
16	CH_3	CH_3	OCO_2Et	CO_2Et	5	**6**	88–90 [e]	$C_{26}H_{40}O_7$	67.21 67.47	8.67 8.36	42
17	CH_3	CH_3	C_2H_5O	CO_2Et	3.5	**7**	oil[f]	$C_{25}H_{38}O_5$			97
18	CH_3	CH_3	O	CO_2Et	4	**11**	oil[f]	$C_{23}H_{34}O_5$			93
19	CH_3	—	CH_3O	CO_2Et	1,3,5(10)	**8**	oil[f]	$C_{23}H_{32}O_5$			90

[a] From ethanol. [b] From methanol. [c] From ethyl acetate. [d] From diisopropyl ether. [e] From diisopropyl ether/acetone. [f] The crude product was used for further steps.



Scheme 2

The diol **11** with 3-oxo-4-ene structure was prepared first according to the literature method [11] starting from the triol **6** (Table I), protecting the glycol functional group at C-17 by converting it into the acetonide (**20**) and oxidizing the C-3 hydroxyl according to Oppenauer (**21**); the acetonide protective group was then removed by hydrolysis.

Intermediate **21** and, via this, **11** was synthesized more efficiently from 3-ethoxy-3,5-androstadienediol (**7**). Simultaneously with the formation of the acetonide of **7**, the hydrolysis of the enol ether group and the isomerization of the C_5—C_6 double bond also took place, thus acetonide **21**, the precursor of **11** was obtained in one step (Scheme 2).

Diols **12** and **13** were prepared according to the above method, starting from the 3-methoxy-2,5(10)-dienediols **9** and **10**, respectively, via the acetonide derivatives **24** and **25** of 19-nor-3-oxo-4-ene structure (Scheme 2).

The diol **14** of 3-oxo-4,6-diene structure was synthesized by oxodizing **7** with chloranil in aqueous acetone.

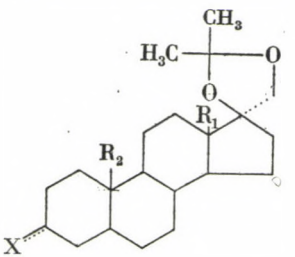
The above and some other acetonides were prepared by the known method, i.e., by the reaction of the **6**—**10** and **14** diols with excess acetone in the presence of catalytic amounts of perchloric acid (Table II).

Cyclization of the diols **6**—**14** (Table I) was effected by the methods usually employed for the formation of the dioxolanone ring [20] (Scheme 1).

Method I [9]: The steroid diols were ethoxycarbonylated with ethyl chloroformate in pyridine, with subsequent cyclization of the 17α-ethoxycarbonyloxy derivatives in the presence of a base. This method was employed in the preparation of spirodioxolanones **26**, **27**, **28**, **32** and **29** (Table III) from

Table II

Steroid-17S-spiro-2',2'-dimethyl-1', 3'-dioxolanes

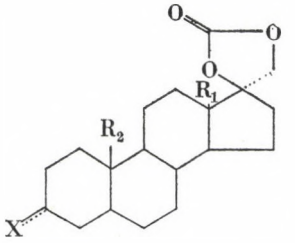


No.	R_1	R_2	X	Unsaturation	Starting compd.	Mp., °C ([Lit.], mp. °C)	$[\alpha]_D^{25}$	Formula	Calcd. % Found % C:	Calcd. % Found % H:	Yield, %
20	CH_3	CH_3	βOH	5	**6**	94—8[a] ([11], 106)	—	$C_{23}H_{36}O_3$	76.60 76.32	10.10 9.85	82
21	CH_3	CH_3	O	4	**7** **20**	188—92[b] ([11], 193)	+62.6°	$C_{23}H_{34}O_3$	77.05 77.13	9.56 9.66	70 58
22	CH_3	CH_3	O	4.6	**14**	180—3[e]	+12.30°	$C_{23}H_{32}O_3$	77.48 77.24	9.04 9.08	75
23	CH_3	—	CH_3O	1,3,5(10)	**8**	97—8[d] ([12], 97—8)	+28.10°	$C_{23}H_{32}O_3$	77.48 77.43	9.04 9.31	62
24	CH_3	H	O	4	**9**	140—1[d]	+12.70°	$C_{22}H_{32}O_3$	76.70 76.79	9.36 9.15	72
25	C_2H_5	H	O	4	**10**	137—9[e]	+ 9.3°	$C_{23}H_{34}O_3$	77.05 77.23	9.56 9.60	64

[a] From 50% acetone water. [b] From ether. [c] From 90% alkohol. [d] From methanol. [e] From diisopropyl ether.

Table III

Steroid-17S-spiro-1',3'-dioxolan-2'-ones and their derivatives



No.	R_1	R_2	X	Unsaturation	Starting compd.	Method	Mp., °C	$[\alpha]_D^{20}$	Formula	Calcd. % Found % C	Calcd. % Found % H	Yield %
26	CH_3	CH_3	βOH	5	**15**	I	222—7[a]	−93.5°	$C_{21}H_{30}O_4$	72.79 72.32	8.72 9.00	57
27	CH_3	CH_3	OCO_2Et	5	**16** **6**	I II	165—8[b]	−78.4°	$C_{24}H_{34}O_6$	68.87 68.91	8.18 8.36	59 82
28	CH_3	CH_3	C_2H_5O	3,5	**17** **7**	I II	170—2[b]	−166.7°	$C_{23}H_{32}O_4$	74.15 74.36	8.66 8.76	51 71
29	CH_3	—	CH_3O	1,3,5(10)	**19**	I	167—171[b]	+10°	$C_{21}H_{26}O_4$	73.65 73.73	7.65 7.84	62
30	CH_3	—	CH_3O	2,5(10)	**9**	II	172—4[b]	+47.2°	$C_{21}H_{28}O_4$	73.22 73.17	8.19 7.94	73
31	C_2H_5	—	CH_3O	2,5(10)	**10**	II	246—8[c]	+32.7°	$C_{22}H_{30}O_4$	73.71 73.65	8.44 8.69	53

32	CH_3	CH_3	O	4	**18** **11** **28**	I II, III IV	174–6[b]	+78.6°	$C_{21}H_{28}O_4$	73.22 73.19	8.19 7.28	56 50, 69 90
33	CH_3	H	O	4	**12** **30**	III IV	192[b]	+24.1°	$C_{20}H_{26}O_4$	72.69 72.72	7.93 7.68	69 73
34	C_2H_5	H	O	4	**13** **31**	III IV	201–4[b]	+20.7°	$C_{21}H_{28}O_4$	73.22 73.19	8.19 8.22	46 25
35	CH_3	CH_3	O	4,6	**14** **32**	II, III V	227–9[a]	+40.15°	$C_{21}H_{26}O_4$	73.65 73.50	7.65 7.73	58, 62 56
36	CH_3	CH_3	βAcO	5	**26**	VI	170–4[a]	−95.61°	$C_{23}H_{32}O_5$	71.16 71.38	8.30 8.68	67
37d	CH_3	CH_3	HON	4	**32**	VII	273–5[c]	—	$C_{21}H_{29}NO_4$	70.16 70.19	8.73 8.03	60
38d	CH_3	H	HON	4	**33**	VII	259–61[c]	—	$C_{20}H_{27}NO_4$	69.53 69.47	7.88 7.61	72
39d	C_2H_5	H	HON	4	**34**	VII	270–6[b]	—	$C_{21}H_{29}NO_4$	70.16 70.23	8.13 8.11	60
40d	CH_3	CH_3	HON	4,6	**35**	VII	285–290[a]	—	$C_{21}H_{27}NO_4$	70.56 70.54	7.61 7.63	63

[a] From methanol. [b] From ethanol. [c] From ethyl acetate. [d] Mixtures of *syn-anti* isomers.

diols **6**, **7**, **8** and **11**, respectively, via the intermediates **15**, **16**, **17**, **19** and **18** (Table I).

During ethoxycarbonylation of the triol **6** (Table I), the C-3 hydroxyl group was also carbethoxylated partly, and **16** was formed, in addition to **15** (Table I). Cyclization of this mixture yielded **26** and **27** as a mixture (Table III). Both mixtures, **15** and **16**, and **26** and **27**, could only be separated by the column chromatographic technique. Compounds **26** and **27** can be obtained in higher yields by the cyclization of pure **15** and **16**, respectively.

Method II [20]: The steroid diols were heated in excess diethyl carbonate in the presence of catalytic amounts of sodium metal to convert them into spirodioxolanes in a single step.

When sodium hydroxide was used instead of sodium metal as catalyst, the end-product was obtained in a shorter reaction time, but in a lower yield. In this case, the corresponding oxirane was also isolated, beside the expected dioxolanone.

Starting from the diols **6**, **7**, **9**, **10** and **14** (Table I), the spiro derivatives **27**, **28**, **30**, **31**, **32** and **35** were prepared according to this method (Table III).

Table IV

IR- and ^{1}H-NMR data of new 17α-hydroxymethyl-17β-hydroxysteroids and their ethoxycarbonyloxy derivatives

	IR(KBr), cm^{-1}			^{1}H-NMR ($CDCl_3$)δ, (ppm)			
	νOH	νC=O	νC=C	Me-18, 19 s, 3H	CH_3—CH_2 t, 3H	CH_2—OH 2xd, 2x1H	Other signals
7	3300 (b)	—	1655 1630	0.93 1.00	1.30	3.55 3.20	H-4,6: 5.3—5.0 m, 2H CH_3—CH_2: 3.78 q, 2H C—*OH*: 3.3—2.8 b, 2H
10	3200— 3600	—	1700 1670	0.97 —	0.97	3.80 3.40	H-2: 4.61 t, 1H O—CH_3: 3.56 s, 3H
13[a]	3300— 3600	1670	1640 1620	— —	1.00	3.70 3.33	C—*OH*: 2.4 b, 2H H-4: 5.78 s, 1H
14	3420	1660	1625	0.94 1.12	—	3.45 3.20	CH_2—*OH*: 4.30 t, 1H C—*OH*: 3.94 s, 1H H-6,7: 6.12 s, 2H
15	3200— 3600	1745	— 1265[b]	0.97 1.06	1.33	— —	H-6: 5.33 m, 1H CH_2—O: 4.5—3.8 m, 4H
16	3500	1740	— 1270[b]	0.90 1.02	1.33	— —	H-6: 5.35 m, 1H CH_2—O: 4.4—3.9 m, 4H CH_3: 1.3 t, 6H

[a] The ^{1}H-NMR spectra were obtained in DMSO-d_6
[b] νC—O—C

Table V

IR- and ^{1}H-NMR data of steroid-17S-spiro-dioxolanones

	IR (KBr) cm^{-1}			Other bands	^{1}H–NMR($CDCl_3$)δ(ppm)		Other signals
	νC=O spiro	νC=O	νC=O		Me-18, 19 s, 3H	CH_2—O 2xd, 2x1H	
26	1790 (b)	—	—	νOH: 3500	0.96	5.53	H-6: 5.35 dd, 1H
					1.03	4.05	H-3: 3.50 m, 1H
27	1800	1740	—	νC–O–C: 1270	0.92	4.6	H-6: 5.30 m, 1H
				1260	1.00	3.8	CH_3–CH_2: 1.25 t, 3H
28	1800	—	1660	—	0.98	4.55	H-4,6: 5.3–5.0 m, 2H
			1630		(s, 6H,	4.08	CH_3–CH_2: 3.8 q, 2H
					H-18,19)		CH_3–CH_2: 1.28 t, 3H
29	1800	—	—	νAr: 1600	0.98	4.60	H-1: 7.19 d, 1H
				1500	—	4.10	H-2: 6.72 dd, 1H
							H-4: 6.66 d, 1H
							CH_3–O: 3.77 s, 3H
30	1805	—	1695	—	0.97	4.50	H-2: 4.6 s, 1H
			1665		—	4.00	CH_3–O: 3.50 s, 3H
31[a]	1800	—	1686	—	—	4.62	H-2: 4.64 t, 1H
			1658		—	4.16	CH_3–O: 3.48 s, 3H
							CH_3–CH_2: 0.92 t, 3H
32	1800	1670	1620	—	1.00	4.55	H-4: 5.73 s, 1H
					1.20	4.05	
33	1795	1668	1618	—	1.05	4.55	H-4: 5.85 s, 1H
					—	4.05	
34	1805	1660	—	—	—	4.50	H-4: 5.80 s, 1H
					—	4.00	CH_3–CH_2: 1.02 t, 3H
35	1800	1660	1620	—	1.10	4.52	H-6,7: 6.08 s, 2H
					1.14	4.05	H-4: 5.80 s, 1H

[a] The ^{1}H-NMR spectra were obtained in $CDCl_3$-DMSO-d_6

Method III [10]: The spirodioxolanes **32**, **33**, **34** and **35** (Table III) were again obtained in one single step by effecting the condensation of the diols **11**, **12**, **13** and **14** (Table I) with 20% phosgene in toluene in pyridine solution.

Compounds **32**, **33** and **34** (Table III) can be prepared more favourably by the hydrolysis reaction in aqueous hydrochloric acid of compounds **28**, **30** and **31** (Table III) having enol ether structure. Compound **35** was also prepared by oxidizing **32** with chloranil.

Based on structure-activity considerations, some further derivatives have been prepared by acylation and oximation; these are shown in Table III.

Characteristic IR and NMR data of the new steroid diols and ethoxycarbonyl derivatives (Table I) are shown in Table IV, those of the spirodioxolanones (Table III) are summarized in Table V.

The aldosterone blocking activity of the new spirosteroids was examined in rats according to the Kagawa method [21]. Compounds **27**, **33** and **39** had significant activity, yet it was weaker than that of the reference substance, spironolactone.*

* The activity tests were made int the Institute for Drug Research. The results have not been published yet.

Experimental

M.p.'s were determined with a Küstner microscope and are uncorrected. Optical rotation was measured in chloroform ($c = 0.5$) with a LEP-OPTON polarimeter.

The IR spectra were recorded with a Perkin-Elmer 457 instrument, the ^{1}H-NMR spectra were obtained with a Varian A-60D spectrometer in $CDCl_3$, using TMS as internal standard. The UV spectra were recorded in 96% alcohol with a Cary 118C spectrophotometer.

The thin-layer chromatograms were run on Kieselgel G of 0.05 mm layer thickness. The developing mixtures were benzene : methanol : acetone = 8 : 1 : 1 (I) and chloroform : ethyl acetate = 7 : 3 (II). Detection of the spots was effected by spraying with 50% aqueous phosphoric acid and heating at 120 °C for 5 min followed by illumination with UV light of 366 nm wave length.

(A) 17α-Hydroxymethyl-17β-hydroxysteroids (6—14)

General method, employing alkaline hydrolysis of 17*S*-spirooxiranes (6—10)

The steroid-17*S*-spirooxirane (10 mmol) was suspended in DMSO (85 mL) and a solution of potassium hydroxide (1.68 g; 30 mmol) in water (15 mL) was added. The mixture was stirred at 100 °C for 1—2.5 h. (In the case of oxirane **5**, the reaction time was 2.5—3 h.) When the starting oxirane could no longer be detected by TLC (in developing mixture I), the reaction mixture was cooled to room temperature, neutralized with 5% acetic acid and poured into ten volumes of water. After stirring for 30 min the precipitate was filtered off, washed with water and dried. The crude product was purified for analysis by recrystallization.

Physical and analytical data of the steroid diols **6**—**10** prepared by alkaline hydrolysis of oxiranes **1**—**5** are summarized in Table I.

Preparation of steroid diols of 3-oxo-4-ene type (11—13)

17α-Hydroxymethyl-3-oxo-4-androsten-17β-ol (11)

Compound **21** (3.58 g; 10 mmol) was dissolved in 90% ethanol (100 mL) containing 5*N* hydrochloric acid (1.8 mL) and the solution was kept at 60 °C for 3 h. It was then concentrated to one-third of its volume and the solvent was replaced by water. The precipitate which separated was filtered off and washed with water until neutral reaction. The crude product (2.75 g; 86%) (m.p. 182—185 °C) was dissolved in hot alcohol and the solution concentrated to half of its volume to obtain the crystalline end-product (1.78 g; 56%), m.p. 186—190 °C (*lit.* [11] m.p. 193 °C); $\lambda_{max} = 241$ nm ($\varepsilon = 16250$).

17α-Hydroxymethyl-3-oxo-4-oestren-17β-ol (12)

(*a*) Compound **9** (3.18 g; 10 mmol) was dissolved in dimethyl formamide (57 mL) and a solution of conc. hydrochloric acid (2.85 mL) in dimethyl formamide (15 mL) was added dropwise under nitrogen atmosphere. The solution was stirred at room temperature for 1 h, then it was poured into saturated Na_2SO_4 solution (600 mL), with stirring. The precipitate was extracted with dichloromethane. The dichloromethane solution was washed with water until neutral reaction, dried over $MgSO_4$ and evaporated to dryness. The evaporation residue (2.9 g) was recrystallized from ethyl acetate to obtain **12** (1.68 g; 55%), m.p. 137—138 °C (*lit.* [19] m.p. 139—141 °C); $\lambda_{max} = 239$ nm ($\varepsilon = 15770$).

(*b*) Compound **24** (3.44 g; 10 mmol) was hydrolyzed on the analogy of **11**. The crude product (2.49 g; 81%) was recrystallized to obtain the end-product (1.86 g; 60%) which was identical with that prepared according to method (*a*); m.p. 137—138 °C.

13β-Ethyl-17α-hydroxymethyl-3-oxo-4-gonen-17β-ol (13)

Compound **25** (3.58 g; 10 mmol) was hydrolyzed according to **11**. The crude product (3 g) was recrystallized from ethyl acetate to give **13** (1.56 g; 51%), m.p. 146—148 °C; $[\alpha]_D^{20}$ +18.6°; $\lambda_{max} = 239$ nm ($\varepsilon = 16200$).

17α-Hydroxymethyl-3-oxo-4,6-androstadien-17β-ol (14)

Compound **7** (3.47 g; 10 mmol) was dissolved in methanol (70 mL) containing 5% water and chloranil (2.52 g; 10.2 mmol) was added. The suspension was stirred at room temperature in darkness until the starting material could no longer be detected by TLC (developing mixture II). The reaction mixture was added to a mixture of water (160 mL) and 30% aqueous sodium hydroxide (3.5 mL). After stirring for 30 min the precipitate was filtered off and washed with water until neutral reaction. The crude product (2.96 g) was recrystallized from ethyl acetate to obtain **14** (2.46 g; 77%), m.p. 233—235 °C; $[\alpha]_D^{20}$ +24.6°; λ_{max} = 283 nm (ε = 23130).

(B) General method for the preparation of 17α-ethoxycarbonyloxymethyl-17β--hydroxysteroids (15—19)

The appropriate 17α-hydroxymethyl-17β-hydroxysteroid derivative (10 mmol) was dissolved in tenfold amount of anhydrous pyridine and ethyl chloroformate (2.6 mL; 27 mmol) was added dropwise, with stirring, at +5—10 °C. The reaction mixture was stirred at +5 °C until the starting material could no longer be detected by TLC (developing mixture I). The reaction mixture was poured into ice-water (500 mL) and it was extracted with dichloromethane. The dichloromethane solution was washed with 2% aqueous hydrochloric acid, then with water, dried over $MgSO_4$ and evaporated to dryness.

Compounds **15** and **16** could be recrystallized, but compounds **17—19** could not be isolated in the crystalline state. On standing or crystallization, cyclization partly took place and only the corresponding spirodioxolanones could be isolated as crystals.

17α-Ethoxycarbonyloxymethyl-5-androstene-3β,17β-diol (15) and 17α-ethoxycarbonyloxymethyl-3-ethoxycarbonyloxy-5-androsten-17β-ol (16)

Starting from **6** (3.20 g; 10 mmol) and employing the above general procedure, a crude product consisting of a mixture of **15** and **16** (4.02 g) was obtained. This was subjected to chromatographic separation on a silica gel column (400 g). The eluent was a 9 : 1 mixture of benzene and acetone; in this way **16** (2.28 g) was obtained, which was crystallized from a mixture of *n*-hexane and petroleum ether; m.p. 88—90 °C $[\alpha]_D^{20}$ −66.9°; λ_{max} = 203 nm (ε = 3300).

Elution was continued with a 7 : 3 mixture of benzene and acetone to isolate **15**. The crude product (1.6 g) was recrystallized from isopropyl ether to give the crystalline end-product (1.47 g), m.p. 58—63 °C; $[\alpha]_D^{20}$ −68.47°; λ_{max} = 203 nm (ε = 6990).

(C) General method for the preparation of steroid-17*S*-spiro-4'-(2',2'-dimethyl--1',3'-dioxolane) derivatives (20—25)

The appropriate steroid diol (10 mmol) was stirred in anhydrous acetone (160 mL) containing 70% perchloric acid (0.5 mL) at room temperature until the starting material could no longer be detected by TLC in the reaction mixture (developing system II) (1—3 h). The mixture was neutralized with potassium carbonate, filtered, and the filtrate was evaporated to dryness. The evaporation residue was purified by recrystallization or column chromatography.

The acetonide derivative **21** was also prepared by the literature method [11], oxidizing compound **20** according to Oppenauer. The substance obtained in this manner proved to be identical with that synthesized from the diol **7** according to the general method, as shown by the spectral data.

Physical constants and analytical data of **20—25** prepared from diols **6—10** and **14** are shown in Table II.

(D) Preparation of spirodioxolanones

I. General procedure for the cyclization of 17α-ethoxy-carbonyloxymethyl-17β-hydroxysteroids

The starting compound (10 mmol) was dissolved in five parts of anhydrous alcohol and two parts of 0.1 *N* alcoholic sodium hydroxide solution was added by drops. The mixture was allowed to stand at room temperature for 30 min. The resulting crystalline mass was

diluted with water to tenfold volume and neutralized with 1 *N* hydrochloric acid, with stirring and cooling. The crude product was isolated by filtration or extraction with dichloromethane, then purified by recrystallization.

This method was employed in the preparation of compounds **26**, **27**, **28**, **32** and **29**, starting from compounds **15**, **16**, **17**, **18** and **19**, respectively (Table III).

II. Reaction of 17α-hydroxymethyl-17β-hydroxysteroids with diethyl carbonate

A suspension of the appropriate steroid diol in tenfold amount of diethyl carbonate was refluxed in the presence of catalytic amounts of sodium metal (50—80 mg for 10 mmol of the diol), until no starting material could be detected by TLC (developing mixture I) (1—15 h). The solvent was evaporated under reduced pressure and the residue was mixed with water. The crude product was filtered off or extracted and purified by recrystallization.

This method was employed in the preparation of spirodioxolanones **27**, **28**, **30**, **31**, **32** and **35** starting from diols **6**, **7**, **9**, **10** and **14**, respectively (Table III).

III. Condensation of 17α-hydroxymethyl-17β-hydroxysteroids with phosgene

The steroid diol (10 mmol) was dissolved in anhydrous pyridine (50 mL) and 20% phosgene solution in toluene (20 mL) was added to it dropwise, with stirring at 0 — +5 °C. The mixture was stirred at +5 °C for 30 min then poured into ice water (500 mL). It was extracted with dichloromethane and the organic phase was washed with 2% aqueous hydrochloric acid then with water. After drying over $MgSO_4$, the solution was evaporated to dryness and the crude product was purified by recrystallization.

This method was employed in the preparation of derivatives **32**, **33**, **34** and **35** starting from diols **11**, **12**, **13** and **14**, respectively (Table III).

IV. Hydrolysis of steroid spirodioxolanone derivatives of enol ether structure

The starting material (1 g) was suspended in methanol (10 mL) and heated to 40 °C. A mixture of *conc.* hydrochloric acid (0.5 mL) and water (0.5 mL) was then added dropwise, in nitrogen atmosphere. After heating for 30 min and stirring, the reaction mixture was poured into ice-water (150 mL). The crystalline precipitate was filtered off, washed with water until neutral reaction, dried and purified by recrystallization.

Compounds **32**, **33**, and **34** were thus prepared by the hydrolysis of compounds **28**, **30** and **31**, respectively (Table III).

V. Dehydrogenation with chloranil

3-Oxo-4,6-androstadiene-17*S*-spiro-4'-(1',3'-dioxolan-2'-one) 35

Compound **32** (3.44 g; 10 mmol) was dissolved in methanol (80 mL) and refluxed with chloranil (2.6 g; 10.6 mmol) under stirring for 3 h. The mixture was concentrated to one-third volume and mixed with water (70 mL). The product was extracted with dichloromethane. The dichloromethane solution was washed with 1 *N* sodium hydroxide containing 3% sodium dithionite, then with water, dride over $MgSO_4$ and evaporated to dryness. The crude product (3.2 g) was recrystallized from methanol to obtain **35** (1.98 g; 56%), which was identical with the substance prepared according to methods II or III; m. p. 226—229 °C; $[\alpha]_D^{20}$ 38.9°; $\lambda_{max} = 281$ nm ($\varepsilon = 22560$).

VI. 3β-Acetoxy-5-androstene-17*S*-spiro-4'-(1',3'-dioxolan-2'-one) 36

A suspension of **26** (1.17 g; 3.3 mmol) in acetic anhydride (3 mL) was stirred at 80 °C, until the dissolution of the starting material. After cooling, the reaction mixture was poured into ice-water (30 mL), the precipitate was filterd off and washed with water until neutral reaction. The crude product (1.2 g, 92%) was recrystallized from methanol to obtain **36** (0.87 g; 67%), m.p. 170—174 °C; $[\alpha]_D^{20}$ −95.61°.

VII. Oxime derivatives of 17*S*-spirodioxolanones (37—40)

The 3-oxo-steroid (6 mmol) was suspended in alcohol (20—30 mL), a solution of hydroxylamine hydrochloride (8 mmol) and sodium acetate (9 mmol) in water (2.5 mL) was added and the mixture was refluxed with stirring, for 1—2 h. The solvent was evaporated and the

residue rubbed with water. The crude product was filtered off, washed with water until neutral reaction, and purified by recrystallization.

Physical constants and analytical data of compounds **37**, **38**, **39** and **40** prepared from compounds **32**, **33**, **34** and **35**, rsepectively, according to this procedure, are shown in Table III.

*

The authors' thanks are due to Dr. P. Sohár and to Dr. P. Dvortsák for assistance in evaluating the IR and ^{1}H-NMR spectra, and to Dr. A. Szabó for recording the UV spectra.

REFERENCES

[1] Funder, J. W., Feldman, D., Highland, E., Edelman, I. S.: Biochem. Pharmacol., **23,** 1493 (1974)
[2] Hess, J. H.: J. Org. Chem., **27,** 1096 (1962)
[3] Sólyom, S., Zubovics, Z., Toldy, L.: Acta Chim. Acad. Sci. Hung., **100,** 89 (1979)
[4] Sólyom, S., Szilágyi, K., Toldy, L.: Steroids, **35,** 2572 (1980)
[5] Sólyom, S., Szilágyi, K., Toldy, L.: Justus Liebigs Ann., Chem., **1983,** 1001
[6] Schubert, A., Schwarz, S.: Experientia, **21,** 499 (1965)
[7] Lewbart, M. L., Schneider, J. J.: J. Org. Chem., **34,** 3505 (1969)
[8] Lewbart, M. L., Schneider, J. J.: J. Org. Chem., **34,** 3513 (1969)
[9] Lewbart, M. L.: J. Org. Chem., **37,** 1233 (1972)
[10] Lewbart, M. L.: J. Org. Chem., **41,** 78 (1976)
[11] Bertin, D., Nedelec, L.: Bull. Soc. Chim. France, **1964,** 2140
[12] Miller, Th. C.: J. Org. Chem., **34,** 3829 (1969)
[13] Kirk, D. N., Wilson, M. A.: J. Chem. Soc. (C) **1971,** 414
[14] Warnant, J., Jolly, J.: D. P. 2 404 947 (6.2.1973); Chem. Abstr., **81,** 136383g
[15] Hübner, M., Noack, J.: J. Prakt. Chem., **314,** 667 (1972)
[16] Ponsold, K., Hübner, M., Kasch, H., Noack, J.: Z. Chem., **11,** 106 (1971)
[17] Ponsold, K., Hübner, M., Schnabel, R., Strecke, J.: Arzneim.-Forsch., **24,** 896 (1974)
[18] Berti, G., Macchia, M., Macchia, F.: Tetrahedron Lett., **38,** 3421 (1965)
[19] Ponsold, K., Hübner, M., Schade, W., Oettel, M., Freund, R.: Pharmazie, **33,** 792 (1978)
[20] Houben-Weyl: Methoden der Org. Chemie, Ed. 4, Vol. **VIII,** p. 107 (1952)
[21] Kagawa, C. M. et al.: J. Pharmacol. Exp. Ther., **126,** 123 (1959)

Acta Chimica Hungarica 116 (2), pp. 125—129 (1984)

NEW 17-SPIROSTEROIDS, V*

PREPARATION AND INVESTIGATION OF STEROID-17-SPIRO-1',3',2'--OXAZAPHOSPHOLIDINES AND -1',3',2'-DIOXAPHOSPHOLANES

S. SÓLYOM**, K. SZILÁGYI and L. TOLDY

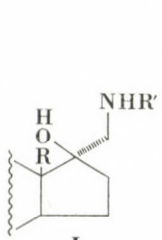
(Pharmaceutical Research Institute H-1045 Budapest, Szabadságharcosok u. 47—49.)

Received February 16, 1983

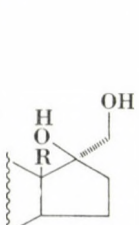
Accepted for publication May 16, 1983

Steroid-17*S*-spiro-1',3',2'-oxazaphospholidines and -1',3',2'-dioxaphospholanes were prepared from steroid-17α-methylaminomethyl-17β-ols and from a 17α-hydroxymethyl-17β-ol with *N,N*-disubstituted phosphoric acid amide dichlorides. Of the compounds formed as diastereomeric pairs some were separated by chromatography. The isomers can practically not be distinguished on the basis of their ^{1}H-NMR spectra.

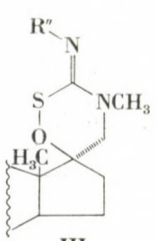
In the course of a research for new compounds with aldosterone antagonist action, the following compounds of spirosteroid type have been synthesized so far from 17α-alkylaminomethylsteroid-17β-ols (**I**) and 17α-hydroxymethylsteroid-17β-ols (**II**), using various ring closing reagents: 17-spiro-6'--perhydro-1',2',4'-oxathiazines **III** [2], 17-spiro-5'-(2'-imino)-oxazolidines **IV** [2], 17-spiro-5'-(2'-thioxo)-oxazolidines **V** [2], 17-spiro-5'-(2'-oxo)-oxazolidines **VI** [3], 17-spiro-5'-(1',2',3'-oxathiazolidine)-2'-oxides **VII** [4] and 17-spiro-4'--(2'-oxo)-1',3'-dioxolanes **VIII** [1]. Some of the compounds had noteworthy biological action, and this justified the extension of our work to other structures.



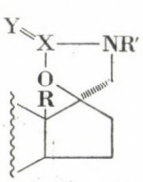
I



II



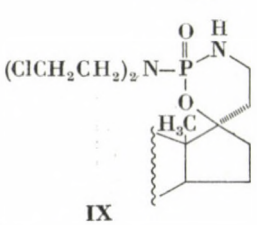
III



IV (X=C; Y=NR'')
V (X=C; Y=S)
VI (X=C; Y=O)
VII (X=S; Y=O)



VIII



IX

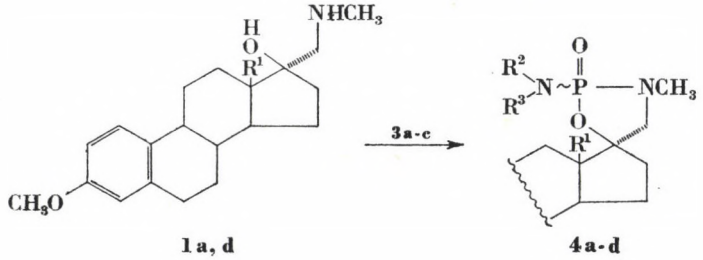
* Part IV: See Ref. [1]

** To whom correspondence should be addressed

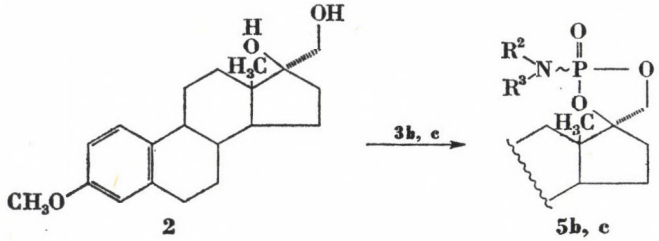
This paper describes the preparation of heterocyclic spirosteroids containing phosphorus.

Some six-membered, phosphorus containing heterocyclic spirosteroids (**IX**) have been reported in the literature [5]. These compounds contain the molecule of cyclophosphamide [2-bis-(2-chloroethyl)-amino-1-oxa-3-aza-2--phosphacyclohexane-2-oxide], a compound of well known cytostatic effect [6], as the spiro substituent. No data were found on the biological action of compounds of type **IX**. Similarly, there is no indication whether these derivatives are formed as diastereomeric pairs, as expected because of the chirality of the phosphorus atom with four different ligands.

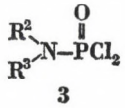
In the course of the synthesis of new spirosteroids the aim of our work was to prepare and investigate yet unknown five-membered analogues having similar structure to **IX**, such as 17-spiro-1',3',2'-oxazaphospholidines (**4**) and 17-spiro-1',3',2'-dioxaphospholanes (**5**), the latter containing an oxygen atom instead of the nitrogen in the ring. The attachment of nitrogen mustard to the steroid carrier was expected to result first of all in tumour inhibiting effect. Similar endeavours are also known from the literature [5, 7].



1a, d **4a-d**



2 **5b, c**



3

	R^1	R^2	R^3
a	Me	Me	Me
b	Me	Me	$ClCH_2CH_2-$
c	Me	$ClCH_2CH_2-$	$ClCH_2CH_2-$
d	Et	$ClCH_2CH_2-$	$ClCH_2CH_2-$

The reactions of the steroid aminoalcohols **1** and of the diol **2** with *N,N*-disubstituted phosphoric acid amide dichlorides (**3**) in the presence of triethylamine yielded compounds **4** and **5**. The formation of the spiro ring was supported by the missing NH and OH absorptions in the IR spectra of the products.

Owing to the chirality of the phosphorus atom, compounds **4** and **5** were expected to form as diastereomeric pairs. Indeed, with the exception of **5b**, the formation of the isomers can be readily observed by thin-layer chromatography, and in the case of **4b**—**d** the isomers can be even separated by column chromatography.

The ^{1}H-NMR spectra of the diastereomers scarcely differ from each other, though in the case of the analogous steroid-17-spiro-1',2',3'-oxathiazolidine-2'-oxides (**VII**) definite differences could be observed, because of the anisotropy of the S=O group, in the angular $\delta CH_3(18)$, the spiro ring δNCH_3 and δNCH_2 signals, and on this basis also the steric position of the SO group could be inferred [4].

In the ^{1}H-NMR spectra of compounds **4a**—**c** there is only a slight difference (2—3 Hz) between the diastereomers in the position of the spiro ring δNCH_3 signal. In the case of **4d** even this difference is absent. The anisotropic effect of the P=O group on the angular $CH_3(18)$ and spiro ring NCH_2 protons is no longer observable. Similarly, the presence of the P=O isomers did not double the $\delta CH_3(18)$ signal in the case of the spirodioxaphospholanes **5**; thus, e.g., **5c** while being apparently homogeneous according to the ^{1}H-NMR spectrum, was shown by TLC to be a mixture of the two isomers.

For this reason ^{1}H-NMR investigations alone do not allow conclusions to be drawn on the P=O isomeric conditions of the diastereomers **4** and **5**. For the time being, the separated diastereomers are distinguished on the basis of differences in polarity, observed in a suitable chromatographic system (see Experimental).

Compounds **4** and **5** did not reveal any noteworthy endocrinous or tumour inhibiting effect in biological tests.

Experimental

M.p.'s were determined on a Küstner microscope and are uncorrected. ^{1}H-NMR spectra were taken with a VARIAN EM-390 instrument in $CDCl_3$ using TMS as internal standard; the values are given in δ ppm units. Optical rotation was measured at $c = 0.5$ in $CHCl_3$. The conditions of TLC were: neutral Al_2O_3 (Merck, Typ T); layer thickness: 0.05 mm; solvent mixture: $CHCl_3$–ethyl acetate (3 : 1), detection: *conc.* sulfuric acid and heating at 110 °C.

Column chromatography was effected on neutral Al_2O_3 (Brockmann II) with a mixture of $CHCl_3$–ethyl acetate (3 : 1).

Steroid-17-spiro-1',3',2'-oxazaphospholidines

3-Methoxy-1,3,5(10)-estradiene-17*S*-spiro-5'-[2'-oxo-2'-(*N*,*N*-dimethyl)amino-3'-methyl-1',3',2'-oxazaphospholidine] (4a)

To a solution of 3.24 g (20 mmol) of **3a** [8] in 30 mL of dry methylene chloride, the solution of 3.29 g (10 mmol) of **1a** [9] in a mixture of 40 mL dry tetrahydrofuran and 2.8 mL triethylamine were added dropwise, with stirring, at room temperature. After stirring for 3 h the precipitate was filtered off, and washed with tetrahydrofuran. The combined solutions were evaporated, and the residue was dissolved in saturated sodium hydrogen carbonate solution and chloroform. The extract in chloroform was washed with water, dried and the solvent evaporated. The residual oily substance was dissolved in dichloromethane, filtered through 30 g of neutral Al_2O_3, and the column was exhaustively washed with the solvent. Evaporation, gave 2.11 g of a mixture of crystals and oil, from which 1.5 g crystalline substance could be isolated by trituration with petroleum ether. According to TLC the product was a mixture of two isomers (R_f: 0.7 and 0.6).

For analytical purposes it was recrystallized from acetone; m.p. 134—137 °C (about 1 : 1 mixture of the isomers).

$C_{23}H_{35}N_2PO_3$ (418.50). Calcd. P 7.40; N 6.69. Found P 7.30; N 6.82%.

^{1}H-NMR: δCH_3 (18): 0.98 s (3H); δNCH_3 (spiro ring): 2.60 and 2.56 (diastereomers) d (3H), $J_{P,CH_3} \sim 9$ Hz; δNCH_3: 2.67 d (6H), $J_{P,CH_3} \sim 11$ Hz; δOCH_3: 3.76 s (3H); δH-2, H-4: 6.6—6.8 m (2H); δH-1: 7.20 d (1H).

3-Methoxy-1,3,5(10)-estratriene-17*S*-spiro-5'-[2'-oxo-2'-(*N*-methyl-*N*-β-chloroethyl)amino-3'-methyl-1',3',2'-oxazaphospholidine] (4b)

Using 6.30 g (30 mmol) of **3b** [10] and 4.95 g (15 mmol) of **1a**, the procedure was the same as for **4a**. The crude product was purified on a chromatographic column. The less polar isomer was eluted first (R_f 0.70): 1.0 g; after recrystallization from ethyl acetate, m.p. 142—143 °C; $[\alpha]_D^{20}$ 0°.

$C_{24}H_{36}ClN_2O_3P$ (466.98). Calcd. P 6.63; N 6.00. Found P 6.20; N 6.07%.

^{1}H-NMR: δCH_3 (18): 0.98 s (3H); δNCH_3: 2.58 d (3H), $J_{P,CH_3} \sim 8$ Hz; δNCH_3: 2.69 d (3H), $J_{P,CH_3} \sim 8$ Hz; δOCH_3: 3.73 s (3H); δH-2, H-4: 6.5—6.8 m (2H); δH-1: 7.20 d (1H).

Continued elution gave 0.96 g of an isomeric mixture, and then 1.03 g of the more polar (R_f 0.55) pure isomer. After recrystallization from acetone it has m.p. 176—177 °C; $[\alpha]_D^{20}$ +18.6°.

^{1}H-NMR: δNCH_3: 2.65 d (3H), $J_{P,CH_3} \sim 9$ Hz; δNCH_3: 2.70 d (3H), $J_{P,CH_3} \sim 9$ Hz; δOCH_3: 3.76 s (3H); the other peaks were identical with those given for the less polar isomer.

3-Methoxy-1,3,5(10)-estratriene-17*S*-spiro-5'-[2'-oxo-2'-bis-(β-chloroethyl)amino-3'-methyl-1',3',2'-oxazaphospholidine] (4c)

Using 7.8 g (30 mmol) of **3c** [11] and 4.95 g (15 mmol) of **1a**, the procedure was the same as for **4a**. Treatment of the crude product with acetone gave 2.17 g of crystalline substance, consisting mainly of the more polar ($R_f \sim 0.55$) isomer. After recrystallization from acetone, m.p. 192—193 °C; $[\alpha]_D^{20}$ +13.08°.

$C_{25}H_{37}Cl_2N_2O_3P$ (515.45). Calcd. Cl 13.75. Found Cl 13.62%.

^{1}H-NMR: δCH_3 (18): 0.97 s (3H); δNCH_3: 2.66 d (3H), $J_{P,CH_3} \sim 9$ Hz; δOCH_3: 3.74 s (3H); δH-2, H-4: 6.5—6.8 m, (2H); δH-1: 7.18 d(1H).

The mother liquors were combined, evaporated to dryness and the residue was chromatographed on a column, to obtain 2.45 g of the less polar ($R_f \sim 0.70$) isomer. After recrystallization from acetone, m.p. 168—170 °C; $[\alpha]_D^{20}$ —13.70°.

^{1}H-NMR: δNCH_3: 2.62 d (3H), $J_{P,CH_3} \sim 9$ Hz; δOCH_3: 3.73 s (3H); the other peaks were identical with those given for the more polar isomer.

13β-Ethyl-3-methoxy-1,3,5(10)-gonatriene-17*S*-spiro-5'-[2'-oxo-2'-bis(β-chloroethyl)amino-3'-methyl-1',3',2'-oxazaphospholidine] (4d)

Using 1.78 g (5.2 mmol) of **1d** [4] and 2.10 g (8.1 mmol) of **3c**, the procedure was the same as above. The crude product was chromatographed. The less polar isomer ($R_f \sim 0.80$) was 0.68 g (m.p. 116—118 °C), on recrystallization from methanol (0.51 g) it had m.p. 76—77 °C; $[\alpha]_D^{20}$ —27.8°. Continued elution gave 0.40 g of the isomeric mixture;

$C_{26}H_{39}Cl_2N_2O_3P$ (529.47). Calcd. Cl 13.39; P 5.85. Found Cl 13.44; P 5.75%.

^{1}H-NMR: δCH_3-CH_2 (13): 0.97 t (3H); δNCH_3: 2.67 d (3H), $J_{P,CH_3} \sim 9$ Hz; δOCH_3: 3.70 s (3H); δH-2, H-4: 6.5–6.8 m (2H); δH-1: 7.15 d (1H).

Further elution yielded 0.45 g of the more polar isomer ($R_f \sim 0.51$), m.p. 200 °C. After recrystallization from ethanol: 0.41 g; m.p. 204–205 °C; $[\alpha]_D^{20}$ 0 °C.

Steroid-17-spiro-1',3',2'-dioxophospholanes

3-Methoxy-1,3,5(10)-estratriene-17*S*-spiro-4'-[2'-oxo-2'-(*N*-methyl-*N*-β-chloroethyl)amino--1',3',2'-dioxaphospholane] (5b)

To a solution of 3.15 g (15 mmol) of **3b** in 30 mL of dry dichloromethane, a solution of 2.37 g (7.5 mmol) of **2** [1, 12] and of 5.6 g of triethylamine in 30 mL of dry tetrahydrofuran was added dropwise, with stirring at 10 °C. The reaction mixture was allowed to warm to room temperature and let to stand for 24 h. The precipitate which formed was filtered off and the filtrate evaporated. The residue was triturated with 2.5% sodium hydrogen carbonate solution and extracted with dichloromethane. The organic phase was washed with water, dried and evaporated. The crude product was recrystallized from ethanol to yield 0.83 g; m.p. 200–204 °C (homogeneus in TLC, $R_f = 0.9$).

$C_{23}H_{33}ClNO_4P$ (453.92). Calcd. C 60.85; H 7.32; N 3.09; P 6.83. Found C 60.94; H 7.98; N 3.25; P 6.8%.

^{1}H-NMR: δCH_3 (18): 0.99 s (3H); δNCH_3: 2.75 d (3H), $J_{P,CH_3} \sim 9$ Hz; δOCH_3: 3.73 s (3H); δOCH_2: 3.90 dd (1H), $J_{P,CH_2} \sim 5$ Hz and 4.54 dd (1H), $J_{P,CH_2} \sim 16$ Hz; δH-2, H-4: 6.5–6.8 m (2H); H-1: 7.18 d (1H).

3-Methoxy-1,3,5(10)-estratriene-17*S*-spiro-4'-[2'-oxo-2'-bis-(β-chloroethyl)amino-1'-3',2'--dioxaphospholane] (5c)

Using 5.82 g (22.4 mmol) of **3c** and 3.56 g (11.2 mmol) of **2**, the procedure was analogous to that of **5b**. The crude product was recrystallized from ethanol; the yield was 3.7 g m.p. 166–175 °C. TCL showed the presence of two spots R_f 0.95 and 0.90.

$C_{24}H_{34}Cl_2NO_4P$ (502.40). Calcd. Cl 14.11; P 6.17. Found Cl 14.19; P 6.05.

^{1}H-NMR: δCH_3 (18): 1.03 s (3H); δOCH_3: 3.75 s (3H); δOCH_2: 4.00 dd (1H), $J_{P,CH_2} \sim$ ~ 5 Hz and 4.57 dd (1H), $J_{P,CH_2} \sim 16$ Hz; δH-2, H-4: 6.5–6.8 m (2H); δH-1: 7.20 d (1H).

*

The authors' thanks are due to Dr. Péter Dvortsák for the evaluation of the PMR spectra.

REFERENCES

[1] Szilágyi, K., Sólyom, S., Toldy, L.: Acta Chim. Acad. Sci. Hung., **116,** 111 (1984)
[2] Sólyom, S., Zubovics, Z., Toldy, L.: Acta Chim. Acad. Sci. Hung., **100,** 89 (1979)
[3] Sólyom, S., Szilágyi, K. Toldy, L.: Steroids, **35,** 361 (1980)
[4] Sólyom, S., Szilágyi, K., Toldy, L.: Justus Liebigs Ann. Chem. **1983,** 1001
[5] Foster, E. L., Blickenstaff, R. T.: Steroids, **27,** 353 (1976)
[6] Zon, G.: Cyclophosphamide Analogues, in: Progress in Medicinal Chemistry, Vol. **19,** p. 205, Elsevier Biomedical Press, 1982
[7] Masnyk, I. J.: Steroids, **19,** 771 (1972)
[8] Harvey, R. B., Mayhood, J. E.: Can. J. Chem., **33,** 1552 (1955)
[9] Ponsold, K., Hübner, M., Schnabel, R., Strecke, J.: Arzneim. Forsch., **24,** 896 (1974)
[10] U.S. Pat. 3,732,340; Chem. Abstr., **79,** P 18772u (1973)
[11] Brit. Pat. 1,030,836; Chem. Abstr., **65,** 5366h (1966)
[12] Hörhold, C., Hübner, M., Ponsold, K., Schnabel, R., Schubert K.: Pharmazie, **30,** 35 (1975)

Acta Chimica Hungarica 116 (2), pp. 131—140 (1984)

ELECTROCHEMICAL BEHAVIOUR OF THE BENZIMIDAZOLES

G. KORÁNYI[1]*, E. SZEBÉNYI-GYŐRI[1], A. VÉLIN-PRIKIDÁNOVICS[1] and J. BRLIK[2]

([1]Technical University, Budapest, Department of Applied Chemistry, H-1521 Budapest, Egry J. u. 20—22. and [2]Technical University, Budapest, Department of General and Analytical Chemistry, H-1521 Budapest, Gellért t. 4.)

Received April 20, 1983

Accepted for publication July 13, 1983

The anodic oxidation of 2-aminobenzimidazole — a metabolite of certain fungicide agents — was studied by cyclic voltammetry, and controlled potential electrolysis is $MeCN/LiClO_4$ (0.1 *M*) solution at Pt working electrode. Evaluation of the c.v. experiments showed that the electrode process can be described as a quasi-reversible one-electron transfer coupled to a second order dimerization reaction. The macro-scale controlled potential electrolysis at the first anodic peak (+1.52 V vs. Ag/AgI reference electrode) supported the results of the c.v. experiments. The starting material dimerized to a *s*-tetrazine derivative (m.p. 184—185 °C) with a molecular weight of 266, with no hydrogen atoms lost in the coupling reaction. The structure of the dimer was established by mass-spectrometric data and a mechanism for the oxidation pathway was proposed.

Anodic oxidation of 2-aminobenzimidazole

The electrochemical investigation on the benzimidazoles has not received considerable attention, in spite of the importance of these compounds in polymer chemistry and in biological systems. The benzimidazole polymers and co-polymers are characterized by high thermal stability with semiconducting properties and resistance to hydrolytic and oxidative media [1—3].

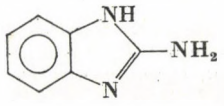
The chlorine resistant polybenzimidazole reverse osmosis permselective membrane is capable of desalting seawater in a single pass to yield potable water [4]. Benzimidazole derivatives containing sulfur are useful as anthelmintics and antimicrobial agents [5, 6]. Several hundred of substituted 2-aminobenzimidazoles are described as systemic fungistates, fungicides, acaricides and curatives for many crop diseases [7, 8].

Oxidation of benzimidazole by ozone gave diozonides [9], by air 2,2'-azobenzimidazole [10], by H_2O_2 4,5-imidazoledicarboxylic acid [11], by periodate oxidation as well as in neutral DMF the benzimidazole nucleus remained untouched [12, 13], while in acidic media the reaction center was the imidazole ring. Oxidation by PbO_2 might yield $\Delta^{2,2'}$-bisizobenzimidazoly-

* To whom correspondence should be addressed

lidene, quinoxalino [2,3-*b*]-quinoxaline or 2,2'-bibenzimidazole [14]. Photochemical irradiation produced the dehydrodimers [15].

The present work stems from a general programme orientated towards the investigations on the electrochemical behaviour of the benzimidazoles, using first the 2-amino-benzimidazole (**1**) "a metabolite for certain fungicide agents" as model compounds.



1

This compound was chosen on the basis of its ready availability and the potential biolgical activity of its oxidation products, which are difficult to be obtained by other synthetic routes. It was anticipated that the anodically generated 2-aminobenzimidazole cation radicals would couple to form dimeric species in a fashion analogous to the structurally similar imidazoles, as well as other *N*-heterocycles [16], and the dimer formation sheds some light on the reactivity of the biologically important benzimidazole nucleus and is thus reported herein.

Experimental

Chemicals

2-Aminobenzimidazole was prepared by the method described by Pierron [17]. Reagent grade acetonitrile was purified by distilling repeatedly from phosphorous pentoxide [18] and stored on molecular sieves (0.3 nm) under nitrogen atmosphere. The supporting electrolyte was $LiClO_4$ a Fluka product. In the reference electrode tetrabutyl-ammonium-iodide (TBAI) was employed as supporting electrolyte, also a Fluka product.

Apparatus and procedure

In the voltammetric tests the polarizing unit was a Radelkis Mod. OH-405 potentiostat connected with an Electroflex function generator Mod. EF-1808. The current-voltage curves were recorded on an EMG Mod. NE-230 X—Y recorder; in these experiments a cell of suitable geometry was employed [19]. The working microelectrode was a platinum sphere. In the macroscale controlled potential electrolyses a Radelkis Mod. OH-405 potentiostat with an associated coulometer (Radelkis) Mod. OH-404/c were used. In these tests a H-cell similar to that described by Lund [20] was employed using a platinum sheet working electrode (geometrical area 2×2 cm) and a carbon rod auxiliary electrode, the latter separated from the main compartment by two coarse sintered glass discs. Stirring was accomplished by using a magnetic stir bar, as well as by degassing with nitrogen gas during the electrolysis. The concentration of the starting material was $2.15 \cdot 10^{-2}$ *M*.

Both in the voltammetric and in the coulometric experiments all the reported potential values are referred to an Ag/AgI reference electrode. (Solvent: CH_3CN supporting electrolyte: 0.1 *M* TBAI.) All experiments were carried out at room temperature.

After completion of the electrolyses the CH_3CN solvent was stripped off by evaporation under vacuum. The solid residue was taken up with water and extracted with $CHCl_3$, and the chloroform soluble portion was chromatographed on a column of 50 cm length packed with Kieselgel 40 (70—230 mesh, ASTM) eluent was $CHCl_3/CCl_4$/MeOH 8 : 5 : 1.

The MS spectra were obtained by JEOL made JMS-01SG-2 type mass spectrometer by peak matching technique and photoplated detection. Thin-layer chromatography of the

product was performed with 0.25 mm thickness of the Silicagel 60 layer and $CHCl_3/CCl_4/MeOH$ 8 : 5 : 1 as developing solvent. R_f values for **1** : 0.19 for the product (**2**) : 0.65. M.p. values for **1**: 222—24 °C, for **2**: 184—185 °C.

Results and Discussion

In acetonitrile solvent 2-aminobenzimidazole (**1**) exhibits two consecutive oxidation steps on a single cycle as shown by the cyclic voltammetric curve reported in Fig. 1; the peak potentials lie at +1.52 and 1.98 V, respectively, at a potential scan rate of 0.1 Vs^{-1}. The first of these waves corresponds to the initial oxidation of **1**, while the further anodic wave apparently is due to

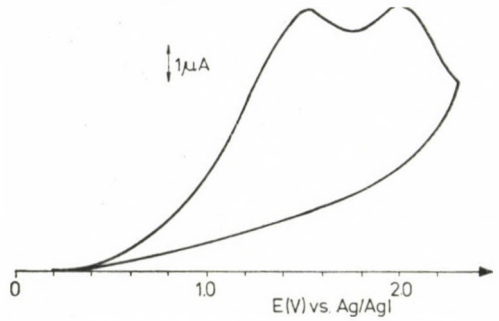


Fig. 1. Cyclic voltammogram of 2-aminobenzimidazole (2.15×10^{-2} *M*) in $MeCN/LiClO_4$ at platinum, sweep rate = 0.1 Vs^{-1}

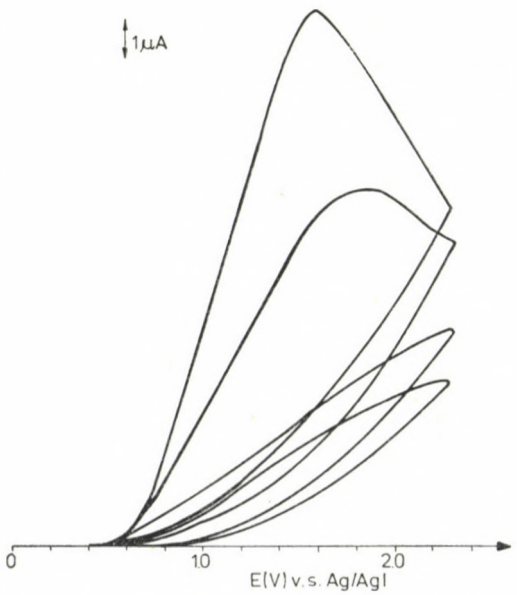


Fig. 2. Multicyclic voltammogram of 2-aminobenzimidazole (2.15×10^{-2} *M*) in $MeCN/LiClO_4$ at platinum, at 0.4 Vs^{-1}

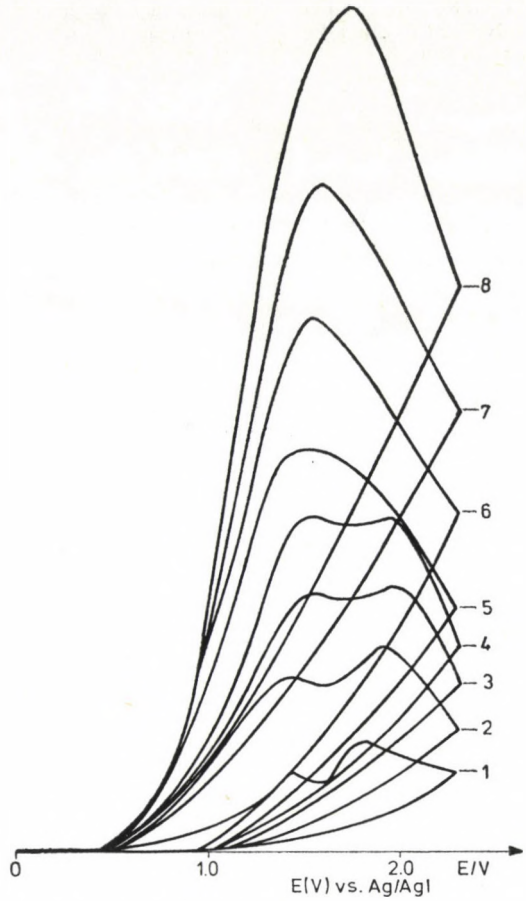


Fig. 3. Effect of sweep rate on the cyclic voltammograms of 2.15×10^{-2} *M* 2-aminobenzimidazole in MeCN/$LiClO_4$ at platinum. Sweep rates: (1) 0.01 Vs^{-1}; (2) 0.04 Vs^{-1}; (3) 0.10 Vs^{-1}; (4) 0.15 Vs^{-1}; (5) 0.25 Vs^{-1}; (6) 0.40 Vs^{-1}; (7) 0.60 Vs^{-1}; (8) 1.00 Vs^{-1}

the oxidation of a product formed from the initially generated species. After the first scan the peak heights diminished considerably (see the multicyclic voltammogram in Fig. 2) due probably to a conducting polymer formation at the electrode surface like in the case of other structurally similar *N*-heterocycles [21].

Cyclic voltammetric tests were performed at the first scan by varying the potential scan rate in the range 0.01—1.0 $V \cdot s^{-1}$ (Fig. 3) and the concentration in the range 0.5—2.2 $\cdot 10^{-2}$ *M*. These data are summarized in Tables I and II. Evaluation of the CV data was performed according to the Nicholson—Shain criteria [22]. The anodic peak potential shifts anodically with increasing scan rate. The plot of the first anodic peak (I_a) current vs. the square root of the scan rate as well as the $i_{I_a}/(v^{1/2} \cdot c)$ were found to be constant within 3%.

The ratio between the height of the second anodic peak (II_a) and that of the first one decreased at increasing scan rate and above 0.4 Vs^{-1} scan rate peak II_a completely disappeared, which may indicate that the subsequent chemical step is not too fast.

Table I

Anodic and cathodic peak potentials; ratio of cathodic to anodic current peaks and the ratio of anodic peak current to the square root of scan rate times the molar concentration for the electrochemical oxidation of 2-aminobenzimidazole in $MeCN/LiClO_4$ *at platinum*

v (Vs^{-1})	$E_{p_{I_a}}$ (V)	$E_{p_{II_a}}$ (V)	$E_{p_{I_c}}$ (V)	$I_{p_c}/I_{p_{I_a}}$	$I_{p_{I_a}}/V^{1/2}\,c \cdot 10^{-2}$ ($A\,s^{1/2}\,V^{-1/2}\,mol^{-1}$)
0.01	1.445	1.79			0.101
0.04	1.45	1.92			0.107
0.10	1.52	1.984			0.101
0.15	1.52	1.95			0.107
0.25	1.525		0.95	0.066	0.101
0.4	1.568		0.90	0.134	0.104
0.60	1.61		0.85	0.158	0.107
1.00	1.77		0.75	0.167	0.104

Table II

Molar concentration; scan rate, anodic peak potential and current for the electrochemical oxidation of 2-aminobenzimidazole in $MeCN/LiClO_4$ *at platinum*

c ($mol\,L^{-1}$)	v (Vs^{-1})	$E_{p_{I_a}}$ (V)	$i_{p_{I_a}}$ (μA)	$E_{p_{II_a}}$ (V)	$i_{p_{II_a}}$ (μA)
0.5375×10^{-2}	0.10	1.50	3.1	2.2	5.4
0.5375×10^{-2}	0.40	1.65	6.8	2.1	7.4
	1.00	1.80	9.0		
	0.10	1.50	4.7		
1.075×10^{-2}	0.40	1.69	9.0		
	1.00	1.82	14.3		
	0.10	1.51	5.4		
1.6125×10^{-2}	0.40	1.70	8.8		
	1.00	1.90	14.6		
	0.10	1.53	6.9		
2.15×10^{-2}	0.40	1.78	13.6		
	1.00	2.00	20.2		

Wave clipping — that is reversal of the scan direction at a potential between peaks I_a and II_a (ca. + 1.9 V) showed one new cathodic peak (I_c) (Fig. 4). This indicates that peak I_c is associated with the reduction of the species formed in the first oxidation step. The intensity of the reduction peak I_c increases with increasing scan rate; that is, at higher scan rate the clipped voltammogram resembled the reversible case, however at slow scan rate the electrode process appeared totally irreversible.

As far as the first oxidation process is concerned, since reversibility can be reached by increasing scan rate, the electron transfer from **1** to the electrode

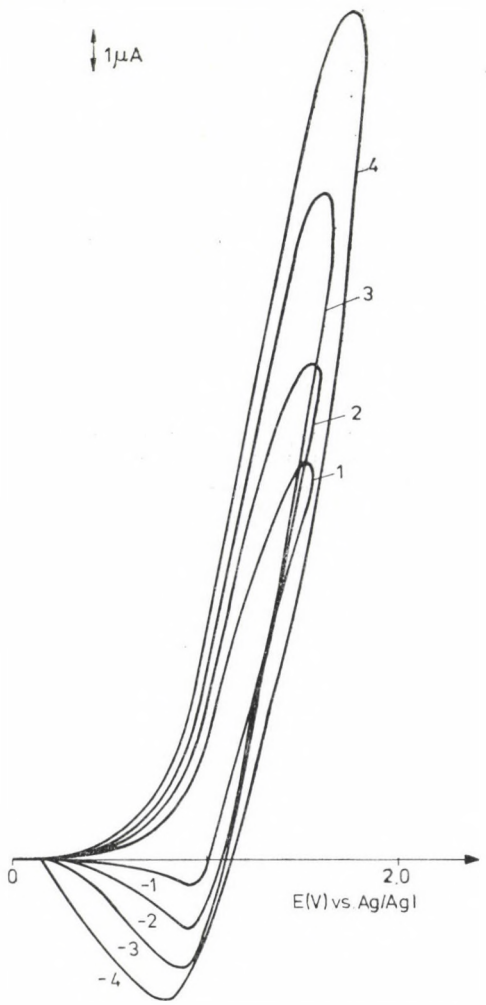


Fig. 4. Clipped voltammograms (scan reversed after the first anodic peak) of 2-aminobenzimidazole (2.15×10^{-2} *M*) in MeCN/$LiClO_4$ at platinum. Scan rates: (1) 0.25 Vs^{-1}; (2) 0.40 Vs^{-1}; (3) 0.60 Vs^{-1}; (4) 1.00 Vs^{-1}

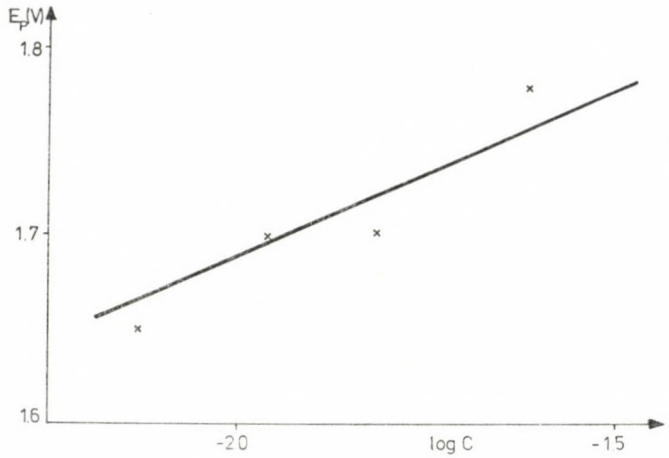


Fig. 5. Variation of the cyclic voltammetric peak potential I_a of 2-aminobenzimidazole with log c in MeCN/$LiClO_4$ at platinum. Scan rate: 0.4 Vs^{-1}

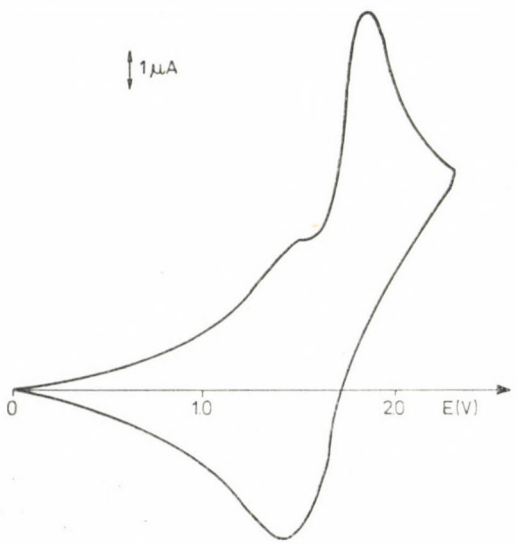


Fig. 6. Cyclic voltammogram of the isolated electrolysis product of 2-aminobenzimidazole [3] in MeCN/$LiClO_4$ platinum. Scan rate = 0.4 Vs^{-1}

to form the cation radical appears to be fast and reversible. On the other hand in the region where the peak is irreversible, the peak potential shows a linear variation with log c of about 150 mV per decade (Fig. 5) and the ratio between cathodic and anodic peak current is smaller than unity. These facts suggest that irreversibility might be due to a bimolecular chemical reaction following the first electron transfer [23, 24]. Therefore the electrode process can be described as a quasi-reversible one-electron step coupled to a chemical step.

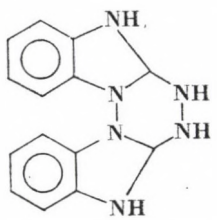
A coulometrically determined n value for this oxidation lends additional support for having a one-electron process, the n value being 1.03 (corrected for background current).

Changes in concentration shifted peak potential plots anodically along the scan rate axis (Table II), therefore the coupled chemical reaction can be described as a second order dimerization process, for a first order reaction curves would have not been affected by changes in concentration [25].

From a comparison of the cyclic voltammograms of **1** and its electrolysis products (Fig. 6), it may be seen that the oxidation wave for this product corresponds fairly closely with the further anodic wave II_a in the cyclic voltammogram of **1** (Fig. 1), there being an approximately 50 mV cathodic shift of the former with respect to the latter. This shift is most probably due to the presence of protons in the unreduced mixture.

Conclusion

A controlled potential electrolysis at the potential of the first anodic peak ($E = 1.52$ V) confirms the results of the c.v. experiment. Long-term electrolyses lead to the product described in the Experimental section subsequently characterized as the dimer of **1**:



2

The nature of the species finally formed in the electrochemical reaction with a product yield of 43% was determined by mass-spectral characterization of the isolated electrolysis product. The fragmentation patterns of the mass-spectral data (listed in Table III) with a molecular ion at 266 are consistent with the structure of **2**; it appears that the compound indeed is the dimer of **1**; exact masses for the parent ion and several fragments calculated correctly matched with double focussing mass-spectral observed peaks.

The composition $C_{14}H_{14}N_6$ indicates that the electrolysis product **2** is a stable *s*-tetrazine derivative: apparently no further oxidation or gross structural changes in the basic benzimidazole nucleus have occurred during the dimerization process except a new tetrazine ring formation. However, since imidazole itself is a heteroaromatic system with amphoteric properties [26]

Table III

The mass-spectral data of the electro-oxidation product of **2***-aminobenzimidazole*

m/z	Relative intensities %	Chemical formula	Fragments
266	16.5	$C_{14}H_{14}N_6$	M^+
265	100.0	$C_{14}H_{13}N_6$	$M\text{-}H^+$
236	6.8	$C_{14}H_{12}N_4$	$M\text{-}30^+$
233	8.8	$C_{14}H_9N_4$	$M\text{-}33^+$
223	25.1	$C_{13}H_{11}N_4$	$M\text{-}43^+$
222	14.7	$C_{13}H_{10}N_4$	$M\text{-}44^+$
191	36.3		$M\text{-}75^+$
43	10.3	CN_2H_3	$M\text{-}223^+$

in the anodic oxidation pathway a proton transfer was coupled to electron transfer.

From the isolated product and with the help of the obtained c.v. data the following scheme (Fig. 7) is suggested for the interpretation of the electrochemical oxidation of **1** at the platinum anode.

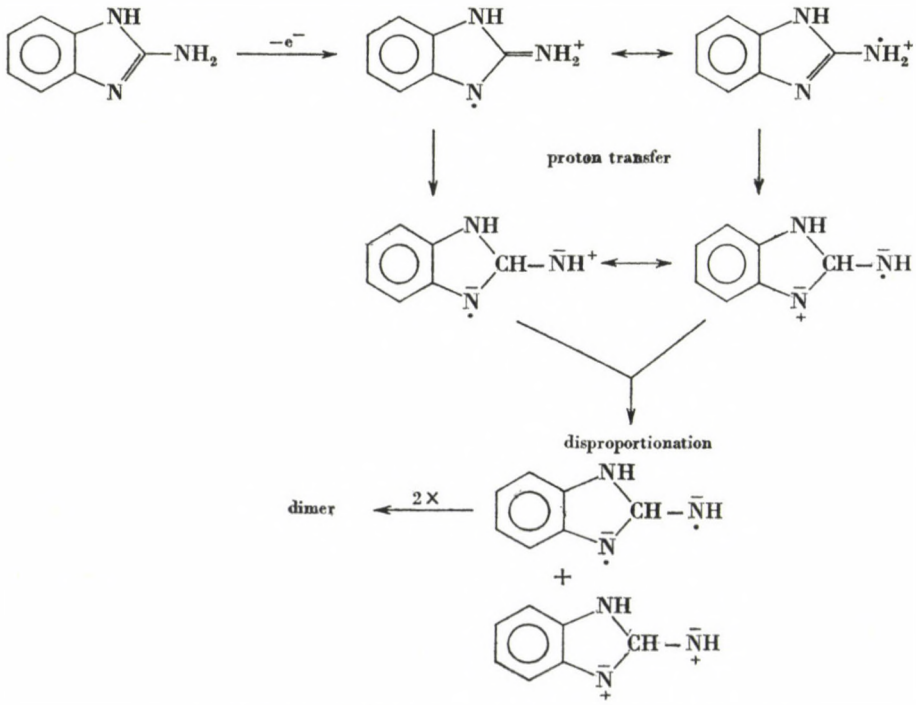


Fig. 7. Proposed scheme for the formation of the dimer **2**

The first step would consist of a quasi-reversible heterogeneous electron transfer yielding cation radicals existing in two resonance structures. Then proton transfers are involved in the oxidation pathway followed by a disproportionation reaction producing a dication and a biradical. The coupling of two biradicals leads to the final *s*-tetrazine ring containing symmetric dimer **2**. The dication was therefore electrochemically produced by a one-electron oxidation step, but without the formation of this dication no dimerization would have occurred.

REFERENCES

[1] Kray, R. J., Winter, R. A. E.: Ger. Off., 2.131 179 (1971)
[2] Babe, S. G., De Abajo, J.:Rev. Plast. Mod., **22,** 182 (1971)
[3] D'Alcilo, G. F.: U.S., 3 763 107 (1973)
[4] Davis, H. J., Soehugen, J. W.: Gov. Rep. Announce Index U.S., **81/24,** 5098 (1981)
[5] Rastogi, R., Sharma, S., Iyer, R. N.: Eur. J. Med. Chem.-Chim. Ther., **14,** 489 (1978)
[6] Benzimidazole derivatives containing sulfur (Chinoin) Belg. 866910
[7] Klopping, H. L.: Fr. 1,523 597 (1968)
[8] Lukens, H. R., Williams, C. B., Levison, S. A., Dandliker, W. B., Murayama, D., Baron, R. L.: Environ. Sci. Technol., **11,** 292 (1977)
[9] Tynpalo, N. F., Yahobi, V. A., Steoanyan, A. A., Budemaya, L. F., Korozerov, A. Z.: Ukr. Khim. Zh., **42,** 394 (1976)
[10] Pozharskii, A. F., Zvezdina, E. A., Andreichikov, Yu. P., Simonov, A. M., Anisimova, V. A., Popova, S. F.: Khim. Geterosikl. Soedin, **1970,** 1267
[11] Schubert, H., Lehmann, G., Otterpohl, G.: Ger. (East) 73,768 (1970)
[12] Edward, C., Heath, S. R.: Methods Carbohydrate Chem. (Roy, L. Whistler and M. L. Wolrom editors, Academic Press, Inc. New York, **2,** 489 (1963)
[13] Subbotin, V. A., Sosokin, I. M., Fedyainov, N. Y., Rumatsov, V. I.: Khim. Geterosikl. Soedin, **1978,** 516
[14] Hill, J. H. M.: J. Org. Chem., **28,** 1931 (1963)
[15] Cole, E. R., Crank, G., Sheikh, A.-S.: Tetrahedron Lett., **1973,** 2650; **1973,** 2987
[16] Sümmermann, W., Baumgärtel, H.: Coll. Czech. Chem. Comm., **36,** 575 (1971); Lang, U., Baumgärtel, H.: J. Electroanal. Chem., **78,** 133 (1977)
[17] Pierron, P.: Ann. Chim. Phys., **15,** 193 (1908)
[18] Ambrose, J. F., Nelson, R. F.: J. Electrochem. **Soc., 115,** 1159 (1968)
[19] Brown, E. R., Large, R. F., Weissberger, B. W. (Eds): Physical Methods of Chemistry, Part **IIA,** Electrochemical Methods, Vol. **1.** Wiley-Interscience, New York 1971, p. 518
[20] Lund, H.: Österreich. Chem. Z. **68,** 43 (1967)
[21] Tourillon, G., Garnier, F.: J. Electroanal. Chem., **135,** 173 (1982)
[22] Nicholson, R. S., Shain, I.: Anal. Chem., **36,** 760 (1964)
[23] Savéant, J. M., Vianello, E.: C. R. Acad. Sci. (Paris), **256,** 2597 (1963); Electrochim. Acta, **12,** 629, 1545 (1967)
[24] Andrieux, C. P., Nadjo, L., Savéantl, J. M.: J. Electroanal. Chem. **26,** 147 (1970)
[25] Olmstead, M. L., Hamilton, R. G., Nicholson, R. S.: Anal. Chem., **41,** 2 (1969)
[26] Hülhagen, R., Baumgärtel, H.: J. Electroanal. Chem., **98,** 119 (1979)

Acta Chimica Hungarica 116 (2), pp. 141—151 (1984)

COMPARISON OF SOME QUANTUM CHEMICAL METHODS ESTIMATING HYDRATION EFFECTS ON THE HYDROGEN FLUORIDE — AMMONIA PROTON TRANSFER REACTION*

J. ÁNGYÁN and G. NÁRAY-SZABÓ**

(Chinoin Pharmaceutical and Chemical Works, H-1325 Budapest, P.O. Box 110)

Received May 24, 1983

Accepted for publication July 13, 1983

The proton transfer energy curve for the hydrogen fluoride — ammonia system was studied in vacuum and in a hydrated form. Both systems were treated in the framework of the semiempirical CNDO/2 method which allows to compare various hydration models. Stabilization energies due to six surrounding water molecules were calculated at various levels of approximations. Simple approaches to estimate the electrostatic and polarization interaction energies were considered and tested for their reliability. To calculate stabilization energies between the canonical and ion-pair structures of the hydrogen-bonded complex both Coulombic and mutual polarization interactions should be accounted for. However, these two types of interaction are insufficient if quantitative agreement with CNDO/2 supermolecule results is desired. If only the trend of changes is needed simple Coulombic models yield surprisingly good results.

Introduction

Proton transfer plays an important role in several chemical, biochemical and biological events [1]. In spite of the spectacular success of quantum chemistry in treating elementary chemical processes, proton transfer reactions remain a difficult problem to handle [2]. Large basis sets and careful geometry optimization of the reaction species are needed even if semiquantitative agreement with experiment is desired. Since initial, final, or both products of the reaction are highly polar or even charged, environmental effects play a decisive role in most cases. Water is the most important solvent in chemistry and in biological media, so the study of the effect of hydration on proton transfer reactions is of outstanding importance. Water molecules interact rather strongly with polar solutes, that is why the specific interactions of the first hydration shell with the solute should be included in all realistic models.

The supermolecule approach [3] can be straightforward way to account for these interactions but the rapidly increasing computational work as the size of the system is enlarged makes the inclusion even of the first hydration shell in most cases impracticable. Approximations are needed which can

* An abridged version of this study has been published in Theoret. Chim. Acta (Berl.), **64**, 27 (1983)

** To whom correspondence should be addressed

account for the most important environmental effects, while keeping the size of quantum chemically treated system within reasonable limits. A great variety of computational schemes have been proposed in the literature but, to our knowledge, no comparative analysis of these methods was published. The aim of the present paper is to analyse and compare some of the current methods applied to the hydration of a thoroughly investigated [4—9] hydrogen-bonded complex the FH . . . NH_3 system.

All calculations were done at the CNDO/2 level of approximation [10]. Though this procedure, like all ZDO methods, is not able to describe the interaction energies and geometrics of hydrogen bonded complexes accurately it may be used for comparative purposes.

Model and Methods

The first hydration shell of the FH . . . NH_3 complex was modelled by six water molecules. They were arranged in a hydrogen bonded position in such a way that three of them were oriented to the lone pairs of the fluorine, three other were directed by an oxygen lone pair of the hydrogens of the ammonia (Fig. 1). We took the geometrical parameters from the paper of Schuster and co-workers [5], and we held the model fixed throughout the proton translocation. Conclusions concerning protonation equilibria, drawn from such type of rigid models should be handled with care, as it was pointed out by several authors [5, 7]. To find the minimal energy structures of the hydrated complex both the variation of the F—N distance [7] and the relaxation of the hydration shell geometry [5] in the course of the proton transfer must be considered; the proton potential curves obtained in rigid models give only an arbitrary intersection of the true potential energy hypersurface. However, for our purposes, to compare results obtained within the framework of different approximate methods, the rigid geometry model suits well.

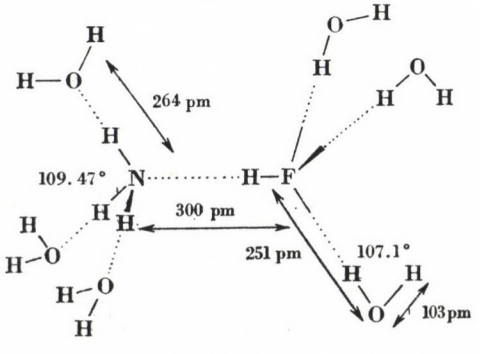


Fig. 1. Geometrical model of the hydrated FH...NH_3 system

The interaction energy between the hydrogen bonded $FH \ldots NH_3$ complex and its hydration shell can be decomposed to several contributions. Different decomposition schemes had been proposed depending on the nature of the wave function approximation used [11, 12]. In spite of some discrepancies, all these schemes agree that the most important components of the intermolecular interaction energy are the Coulombic, polarization, charge transfer and exchange repulsion interactions. Dispersion forces arise only in methods which treat intermolecular electron correlation explicitly.

Despite of the fact that semiempirical ZDO theories, like the CNDO/2 give often qualitatively correct description of the total interaction energy, decomposition of these ZDO supermolecule interaction energies may be completely erroneous and misleading [13]. Therefore we do not attempt to fit separately the approximate calculational procedures to the corresponding interaction energy components coming from an energy decomposition of the CNDO supermolecule interaction energy. Rather we prefer to consider the total CNDO/2 result as a reference, and we try to analyse the physical meaning of the approximations in the computation of the Coulombic and polarization interactions, as the most important contributions responsible for the effect of the solvent on the proton potential curve. In the following we shortly recapitulate the current approximation schemes.

Electrostatic interactions

The electrostatic interaction energy is the Coulomb interaction of the unperturbed charge distributions of the isolated subsystems (i.e. the solvent S, and the solute M):

$$E_{es} = \iint \mathrm{d}\mathbf{r}_1 \, \mathrm{d}\mathbf{r}_2 \, \varrho_S(\mathbf{r}_1) \, \varrho_M(\mathbf{r}_2) \; |\mathbf{r}_1 - \mathbf{r}_2|^{-1} \tag{1}$$

where $\varrho_S(\mathbf{r})$ and $\varrho_M(\mathbf{r})$ are the total (electronic and nuclear) charge density functions of the solvent and of the solute:

$$\varrho_M(\mathbf{r}) = \left\langle \Psi_M^0 \left| -\sum_{i=1}^{n} \delta(\mathbf{r} - \mathbf{r}_i) + \sum_{A=1}^{N} Z_A \, \delta(\mathbf{r} - \mathbf{r}_A) \right| \Psi_M^0 \right\rangle. \tag{2}$$

The charge density functions can be replaced by some appropriate model distributions. The simplest approaches useful for CNDO/2 wave functions are the atomic point charge (PC) and the atomic point charge-point dipole (PCD) models;*

$$\varrho^{PC}(\mathbf{r}) = \sum_{A=1}^{N} \left[Z_A - \sum_{\mu \in A} P_{\mu\mu} \right] \delta(\mathbf{r} - \mathbf{r}_A) \equiv \sum_{A=1}^{N} q_A \, \delta(\mathbf{r} - \mathbf{r}_A) \tag{3}$$

* The formal definition of equivalent charge density is used for the atomic hybridization dipoles, see e.g. [26].

$$\varrho^{\mathrm{PCD}}(\mathbf{r}) = \sum_{A=1}^{N}\left[q_A - \operatorname{div}\sum_{\mu,\nu\in A} P_{\mu\nu}\langle\chi_\mu|\mathbf{r}-\mathbf{r}_A|\chi_\nu\rangle\right]\delta(\mathbf{r}-\mathbf{r}_A) \equiv$$
$$\equiv \sum_{A=1}^{N}[q_A - \operatorname{div}\mu_A^{\mathrm{hibr.}}]\,\delta(\mathbf{r}-\mathbf{r}_A). \tag{4}$$

There are arguments for and against the use of the simple point charge model distributions. The effective atomic charge q_A (the sum of the nuclear and the net Mulliken charges) have a privileged role in the SCF LCAO theories as basic quantities governing the electrostatic interactions [10, 14]. However, an often cited objection is, that such point charge models fail to reproduce the total multiple moments of the molecule, even the total dipole moment [15]. Consideration of atomic dipoles means a refinement in the description of the electrostatic interactions, and by the way, the "exact" total dipole moment can be recovered in CNDO-like ZDO theories.

The electrostatic interaction energy according to the above charge density models reads as follows:

$$E_{\mathrm{es}}^{\mathrm{PC}} = \sum_{A=1}^{Nm}\sum_{B=1}^{Ns} q_A q_B\, T(\mathbf{r}_A - \mathbf{r}_B) \tag{5}$$

$$E_{\mathrm{es}}^{\mathrm{PCD}} = \sum_{A=1}^{Nm}\sum_{B=1}^{Ns}\left[q_A q_B\, T(\mathbf{r}_A,\mathbf{r}_B) - (q_B\,\mu_A^{\mathrm{hibr.}} - q_A\,\mu_B^{\mathrm{hibr.}})\times\right.$$
$$\left.\times\,\mathbf{T}(\mathbf{r}_A,\mathbf{r}_B) - \mu_A^{\mathrm{hibr.}}\cdot\overline{\overline{T}}(\mathbf{r}_A,\mathbf{r}_B)\,\mu_B^{\mathrm{hibr.}}\right]. \tag{6}$$

The three terms in Eq. (6) correspond to the charge–charge, charge–dipole and dipole–dipole interactions, respectively. The usual definition of the $T(\mathbf{r}_A, \mathbf{r}_B)$ interaction tensors is [22]:

$$T(\mathbf{r}_A,\mathbf{r}_B) = |\mathbf{r}_A - \mathbf{r}_B|^{-1} \equiv |\mathbf{r}_{AB}|^{-1} \tag{7/a}$$

$$\mathbf{T}(\mathbf{r}_A,\mathbf{r}_B) = \mathbf{r}_{AB}\,|\,\mathbf{r}_B\,|^{-3} \tag{7/b}$$

$$\overline{\overline{T}}(\mathbf{r}_A,\mathbf{r}_B) = (3\,\mathbf{r}_{AB}\cdot\mathbf{r}_{AB} - |\,\mathbf{r}_{AB}\,|^2\,\mathbf{1})\,|\,\mathbf{r}_{AB}\,|^{-5}. \tag{7/c}$$

Another possible way to determine the electrostatic interaction energy makes use of the electrostatic potential $V_{\mathrm{S}}(\mathbf{r})$ created by the solvent molecules [16]:

$$E_{\mathrm{es}} = \int \mathrm{d}\mathbf{r}_1\,\varrho_{\mathrm{M}}(\mathbf{r}_1)\int \mathrm{d}\mathbf{r}_2\,\varrho_{\mathrm{S}}(\mathbf{r}_2)\,|\,\mathbf{r}_1 - \mathbf{r}_2\,|^{-1} \equiv \int \mathrm{d}\mathbf{r}_1\,\varrho_{\mathrm{M}}(\mathbf{r}_1)\,V_{\mathrm{S}}(\mathbf{r}_1). \tag{8}$$

The electrostatic potential can be computed exactly from the wave function of the solute system. In the present study we adapted the bond increment method [17—19], which constructs the approximate wave function of very large systems using the transferability of the strictly localized bond orbitals [18].

A "quantum chemical" representation of the solute charge density $\varrho_M(\mathbf{r})$ (i.e. a method based on an atomic basis function expansion) would require the evaluation of the intermolecular Coulomb integrals. To avoid this tedious computational work, it is preferred to use one of the above approximate charge distributions of the solute. PC and PDC models lead to the following interaction energy expressions:

$$E^{VPC} = \sum_{A=1}^{Nm} q_A V_S(\mathbf{r}_A) \tag{9}$$

$$E^{VPCD} = \sum_{A=1}^{Nm} [q_A V_S(\mathbf{r}_A)(\mathbf{r}_A) - \mu_A^{hibr.} \cdot \operatorname{grad} V_S(\mathbf{r}_A)]. \tag{10}$$

Polarization of the solute

The above approximations neglect the redistribution of the solvent and solute charge densities. First we consider the polarization of the solute charge distribution under the influence of the electrostatic field of the solvent molecules. The electrostatic potential of the solvent can be introduced into the molecular Hamiltonian as an effective core [6], and the solution of this modified Schrödinger equation provides the polarized solute wave function, while the energy expectation value contains the electrostatic, and partly, the polarization interaction energy with the solvent.

The Fock operator in the CNDO/2 framework is the following [23]:

$$F_{\mu\nu} = F^0_{\mu\nu} - [S_{\mu\nu} V(\mathbf{r}_A) - \langle \chi_\mu | \mathbf{r} - \mathbf{r}_A | \chi_\nu \rangle \operatorname{grad} V(\mathbf{r}_A)] \delta_{AB} \quad \mu \in A, \; \nu \in B\,. \tag{11}$$

Polarization of the solvent

In the case of highly polar solutes, like the hydrogen bonded complex $FH \ldots NH_3$, the polarization of the solvent plays also an important role besides the above mentioned Coulombic effect. At this point it should be noted that the term "polarization" is used in two senses when speaking about solvent effects. The *orientational polarization*, which is of crucial importance in polar solutions, is taken into account in our model by considering an ordered, oriented first hydration shell around the solute. This structured model has some advantages with respect to the continuum theories of solvent effects, where specific solute–solvent interactions cannot be properly handled.

Another sense of the term "polarization" means the redistribution of electron density (*electronic polarization*) in the solvent molecules, i.e. the solvent charge density is not treated as a rigid one, but instead, induced dipole moments are also taken into account. This effect is included automatically in sophisticated calculations, like the supermolecule approach. However, as we

should like to avoid the explicit quantum mechanical treatment of solvent molecules, further approximations and models would be desirable.

The polarization density $\mathbf{P}(\mathbf{r})$ in the solvent (we mean here only the electronic polarization) is related to the $\mathbf{D}(\mathbf{r})$ electric displacement field via the $\bar{\bar{\chi}}(\mathbf{r})$ dielectric susceptibility density, according to the following relation [20]:

$$\mathbf{P}(\mathbf{r}) = \bar{\bar{\chi}}(\mathbf{r}) \left[\mathbf{D}(\mathbf{r}) + \int \mathrm{d}\mathbf{r}' \, \bar{\bar{T}}(\mathbf{r}, \mathbf{r}') \, \mathbf{P}(\mathbf{r}) \right]. \tag{12}$$

The displacement field arising from the solute is:

$$\mathbf{D}(\mathbf{r}) = - \operatorname{grad} \left\{ \langle \Psi_{\mathrm{M}} | \int \mathrm{d}\mathbf{r}' \, T(\mathbf{r}, \mathbf{r}') \, \hat{\varrho}(\mathbf{r}') \, | \Psi_{\mathrm{M}} \rangle \right\}. \tag{13}$$

Multipolar expansion of the solute charge density around an arbitrary origin $\mathbf{R}_0$ within the volume occupied by the solute leads to the expression [24] (for the neutral dipolar case):

$$\mathbf{D}(\mathbf{r}) \approx \bar{\bar{T}}(\mathbf{r}, \mathbf{R}_0) \cdot \mathbf{M} \tag{14}$$

where $\mathbf{M}$ is the total dipole moment:

$$\mathbf{M} = \langle \Psi_{\mathrm{M}} | \int \mathrm{d}\mathbf{r} \, \hat{\varrho}(\mathbf{r}) \cdot \mathbf{r} \, | \Psi_{\mathrm{M}} \rangle \, . \tag{15}$$

Neglecting many-body contributions we get for the polarization potential contribution in the Hamiltonian the following approximate expression:

$$V_{\mathrm{POL}}(\mathbf{r}) = - \int \mathrm{d}\mathbf{r}' \, \mathbf{T}(\mathbf{r}, \mathbf{r}') \, \bar{\bar{\chi}}(\mathbf{r}') \, \bar{\bar{T}}(\mathbf{r}', \mathbf{R}_0) \, \mathbf{M} \equiv - \mathbf{g}(\mathbf{r}, \mathbf{R}_0) \cdot \mathbf{M}. \tag{16}$$

A reasonable approximation to the susceptibility density is to take a sum of effective atomic polarizabilities:

$$\bar{\bar{\chi}}(\mathbf{r}, \mathbf{R}_0) = \sum_s \bar{\bar{\alpha}}_s \, \delta(\mathbf{r} - \mathbf{r}_s) \tag{17}$$

where the sum runs over the solvent atoms. Thus the following formula is obtained for the $\mathbf{g}(\mathbf{r}, \mathbf{R}_0)$ vectorial reaction field factor:

$$\mathbf{g}(\mathbf{r}, \mathbf{R}_0) = \sum_s \mathbf{T}(\mathbf{r}, \mathbf{r}_s) \, \bar{\bar{\alpha}}_s \, \bar{\bar{T}}(\mathbf{r}_s, \mathbf{R}_0). \tag{18}$$

Introduction of this additional term into the effective solute Hamiltonian leads to a nonlinear Schrödinger equation [25]:

$$\left[H(\Psi)\right] \Psi = \left[H^{\circ} + V + V_{\mathrm{POL}}(\Psi)\right] \Psi = E_{\mathrm{eff}} \, \Psi. \tag{19}$$

The expectation value of the above Hamiltonian $E_{\mathrm{eff}} = \dfrac{\langle \Psi | H(\Psi) | \Psi \rangle}{\langle \Psi | \Psi \rangle}$ does not contain the amount of work spent by the solute to set up the $\mathbf{P}(\mathbf{r})$ polarization density in the solvent. E_{eff} describes the molecule as an open system in thermodynamical sense. However, when equilibrium processes,

like proton transfer is studied, the polarization work [27, 28]:

$$W_{\mathrm{POL}} = -\frac{1}{2}\frac{\langle \Psi | V_{\mathrm{POL}}(\Psi) | \Psi \rangle}{\langle \Psi | \Psi \rangle} \tag{20}$$

must be included.

The correct energy functional, associated to the entire solute–solvent model system has to be taken as:

$$E(\Psi) = E_{\mathrm{eff}}(\Psi) + W_{\mathrm{POL}}(\Psi) \tag{21}$$

First order perturbation theory applied to the nonlinear Schrödinger equation [29] leads to the following estimate of the environmental stabilization energy of the solute:

$$\sum_{m}^{Nm} \left\{ q_m \left[V_{\mathrm{s}}(\mathbf{r}_m) + \frac{1}{2} V_{\mathrm{POL,s}}(\mathbf{r}_m) \right] + \right.$$
$$\left. + \mu_m \left[\mathrm{grad}\, V_{\mathrm{s}}(\mathbf{r}_m) + \frac{1}{2} \mathrm{grad}\, V_{\mathrm{POL,s}}(\mathbf{r}_m) \right] \right\}. \tag{22}$$

Alternatively, the nonlinear Schrödinger equation can be solved variationally (INSCRF: inhomogeneous self consistent reaction field method) [23—25]. In this case the solute wave function is polarized by the solvent static and polarization charge densities as well, so this method seems to be the best balanced one.

Results and Discussion

We summarized the approximations discussed in this paper, in Table I. To compare their efficiency we computed the differences in interaction energies with the hydration shell for proton positions, $R_{\mathrm{H...F}} = 180$ and 100 pm,

Table I

Hierarchy of approximations analyzed in this paper

Numbers refer to differences in interaction energies with the hydration shell for $R_{\mathrm{H...F}} = 180$ and 100 pm, respectively (in kJ/mol)

Solute \ Solvent	Point charges	PC + hybr. dipoles	El. stat. pot.	El. pot. + pot.	CNDO/2
Point charges	PC Eq. (5) 89	—	VPC Eq. (9) 181	—	—
PC + hybr. dipoles	—	PCD Eq. (6) 198	VPCD Eq. (10) 153	ELPOL Eq. (19) 194	—
CNDO/2	PCSCF Eq. (11) 89	—	ELPSCF Eq. (11) 172	INSCRF Eq. (21) 231	SUPER 339

Table II

Energy change (in kJ/mol) *in the free and hydrated* $FH\ldots NH_3$ *system as the function of the proton position* ($R_{H\ldots F}$ *in* pm).

From each entry 110,000 kJ/mol is subtracted. The total CNDO/2 energy of the hydration shell $E(6H_2O)$ is −312.671 kJ/mol. Δq denotes the aomunt of electrons (in millielectrons) shifted from the solute to the hydration shell

$R_{H\ldots F}$	$-E_{vac}$	$-E_{PC}$	$-E_{VPC}$	$-E_{INSCRF}$	$-E_{super}+E(6H_2O)$	Δq
200	414	568	723	891	953	102
190	523	660	799	953	1006	96
180	582	701	822	965	1000	86
170	625	727	830	961	975	71
160	672	758	843	962	959	57
150	734	805	875	985	967	44
140	817	875	932	1033	1004	35
130	917	964	1011	1105	1067	28
120	1021	1050	1099	1188	1144	24
110	1107	1141	1174	1260	1210	21
100	1138	1168	1197	1290	1227	19
90	1058	1083	1110	1203	1134	18

respectively. These distances correspond to local equilibria as obtained by the INSCRF method. In Table II we give the energy as a function of $R_{H\ldots F}$ for the free $FH\ldots NH_3$ system and for the hydrated case as calculated by four of the methods mentioned in Table I. Interaction energies are calculated from the entries in Table II, e.g. $E_{PC}^{int} = E_{vac} - E_{PC} = 119$ and 30 kJ/mol for $R_{H\ldots F} = 180$ and 100 pm, respectively. To spare room we do not give data for all potential curves in Table II for which the interaction energies in Table I are calculated. Note that atomic point charges of Eqs (5), (6), (9) and (10) are not obtained from the conventional CNDO/2 procedure, rather we used fully transferable bond polarities, as defined in Ref. [18]. Graphs of potential curves, given numerically in Table II, are depicted in Fig. 2.

Our results indicate that it is the inhomogeneous SCRF method alone which is able to reproduce the double minimum character of the potential curve obtained for the supermolecule, though the agreement is by far not quantitative (cf. Fig. 2). All other methods underestimate the change in the interaction energy so strongly that the second minimum appears only as a (somewhat more pronounced) shoulder which is already present on the E_{vac} curve. However, if only trends are desired even the simplest method yields satisfactory results. We have found the following empirical relationships

between interaction energies, as calculated by the PC, VPC and INSCRF approximations, respectively, and the reference calculation (see Table I).

$$E^{\text{int}}_{\text{SUPER}} = 1.38\, E^{\text{int}}_{\text{INSCRF}} - 1.164 \qquad r = 0.9992 \qquad (23/a)$$

$$= 1.81\, E^{\text{int}}_{\text{VPC}} \quad - 0.202 \qquad r = 0.9998 \qquad (23/b)$$

$$= 3.66\, E^{\text{int}}_{\text{PC}} \quad - 0.230 \qquad r = 0.9997 \qquad (23/c)$$

The high value of their correlation coefficient in Eq. (23) justifies the application of simple point-charge or electrostatic potential [21] models in estimating interaction energy changes for polar complexes. For larger intermolecular distance, as in the present model, the point charge and electrostatic potential methods work equally well. However, the former may yield erroneous results for the orientation dependence of the interaction energy since the directionality of the electrostatic potential coming from lone pairs is not adequately reproduced. The bond increment method [17—19] which allows to calculate molecular electrostatic potentials and interaction energies very rapidly, do

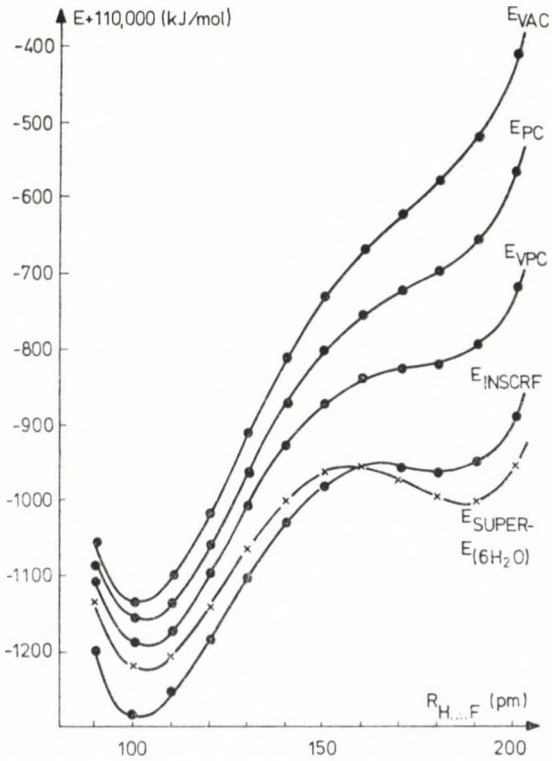


Fig. 2. Potential curves for the proton transfer reactions as obtained by various approximations. Subscripts refer to the notations of Table I

not suffer from the above drawback. A potential application of the regression relations in Eq. (23) is correction of approximate results to estimate interaction energies obtainable by the supermolecule approach.

Interaction energy differences, as given in Table I, provide some information on the overall reliability of the investigated approximations. The point-charge method is useless if quantitative agreement with the supermolecule results is needed. As it is seen in Fig. 2 the E_{vac} curve is only slightly modified if using point charges to model environmental effects. Even if these charges are directly included into the Hamiltonian (PCSCF) no better agreement is achieved since in the CNDO/2 parametrization the simplified electronic interaction integrals behave in larger distances as Coulombic point-charge interactions. Consideration of charge–dipole and dipole–dipole interactions is important (cf. PCD in Table I). Using electrostatic potentials a much better agreement is observed than for the point-charge model (cf. VPC in Table I and the E_{VPC} curve in Fig. 2). Consideration of hybridization dipoles or inclusion of the electrostatic potential into the model Hamiltonian brings nothing, the results get even "worse" (cf. VPCD and ELPSCF in Table I). The best agreement is obtained using INSCRF though even this yields only 70 per cent of the total interaction energy. It is seen that self-consistency is important here, the static ELPOL approximation gives a smaller interaction energy.

The failure of the INSCRF method to give a quantitative agreement with the supermolecule approach is primarily due to the neglect of charge transfer which is quite large and which changes considerably with the hydrogen-fluorine distance (cf. Table II). A fair correlation between the amount of charge transfer (Δq in millielectrons) and the interaction energy (in kJ/mol) in the supermolecule approach is observed.

$$\Delta q = 0.196\, E^{int}_{SUPER} + 0.14 \qquad r = 0.9951 \tag{24}$$

Combining one of Eqs (23a—c) and Eq. (24) it is possible to estimate the amount of charge transfer from approximately calculated interaction energies.

*

We are indebted to Dr. P. R. Surján (Budapest) for comments on the manuscript.

REFERENCES

[1] Gandour, R. D., Schowen, R. L. Eds.: Transition States of Biochemical Processes, New York, Plenum Press 1978
[2] Čársky, P., Urban, M.: Ab Initio Calculations: Methods and Applications in Chemistry, Lecture Notes in Chemistry, Vol. **16,** Berlin, Springer, 1980, p. 197.
[3] Pullman, A., Pullman, B.: Quart, Rev. Biophys., **7,** 505 (1975)
[4] Yamabe, S., Kato, S., Fujimoto, H., Fukui, K.: Theoret. Chim. Acta (Berl.), **30,** 327 (1973)
[5] Schuster, P., Jakubetz, W., Beier, G., Meyer, W., Rode, B. M.: The Jerusalem Symposia in Quantum Chemistry and Biochemistry, Vol. **6,** Chemical and Biochemical Reactivity. Bergmann, E. D., Pullman, B., ed. Jerusalem, 1974, p. 257.

[6] Noell, J., Morokuma, K.: Chem. Phys. Lett., **36,** 465 (1975)
[7] Noell, J., Morokuma, K.: J. Phys. Chem., **80,** 2675 (1976)
[8] Kollman, P. A., Kuntz, I. D.: J. Am. Chem. Soc., **98,** 6820 (1976)
[9] Miertus, S., Bartos, J.: Coll. Czech. Chem. Comm. **45,** 2308 (1980)
[10] Pople, J. A., Beveridge, D. L.: Approximate Molecular Orbital Theory, New York, McGraw Hill 1970
[11] Schuster, P.: Intermolecular Interactions: From Diatomics to Biopolymers, Pullman, B., ed. Wiley, London, 1978., p. 363.
[12] Morokuma, K., Kitaura, K.: Chemical Applications of Atomic and Molecular Electrostatic Potentials, Politzer, P., Truhlar, D. C., eds. New York, Plenum Press, 1981., p. 215.
[13] Schuster, P., Karpfen, A., Beyer, A.: Molecular Interactions, Orwille-Thomas, W. J., Ratajczak, H., eds. London, Wiley 1979
[14] Mayer, I.: Int. J. Quant. Chem., **23,** 341 (1983)
[15] Claverie, P.: Intermolecular Interactions: From Diatomics to Biopolymers, Pullman, B., ed. London, Wiley, 1978., p. 63.
[16] Scrocco, E., Tomasi, J.: Topics Curr. Chem., **42,** 95 (1973)
[17] Náray-Szabó, G.: Int. J. Quant. Chem., **16,** 265 (1979)
[18] Náray-Szabó, G., Grofcsik, A., Kósa, K., Kubinyi, M., Martin, A.: J. Comput. Chem., **2,** 58 (1980)
[19] Náray-Szabó, G.: Quantum Chemistry Program Exchange, **13,** 395 (1980)
[20] Tapia, O.: Intermolecular Interactions, Vol. **3,** Chap. 2, Ratajczak, J., Orwille-Thomas, W. J. eds. Chichester, Wiley 1982
[21] Weinstein, H., Osman, R., Green, J. P., Topiol, S.: Chemical Applications of Atomic and Molecular Electrostatic Potentials, Politzer, P., Truhlar, D. C., eds. New York, Plenum Press, 1981, p. 309.
[22] Buckingham, A. D.: Adv. Chem. Phys., **12,** 107 (1967)
[23] Tapia, O., Johannin, G.: J. Chem. Phys., **75,** 3624 (1981)
[24] Sanhueza, J. E., Tapia, O.: THEOCHEM, **6,** 131 (1982)
[25] Sanhueza, J. E., Tapia, O., Laidler, W. G., Trsic, M.: J. Chem. Phys., **70,** 3096 (1979)
[26] Bertaut, E. F.: J. Phys., **39,** 1331 (1978)
[27] Tapia, O.: Theoret. Chim. Acta (Berl.), **47,** 157 (1978)
[28] Linder, B.: Adv. Chem. Phys., **12,** 225 (1967)
[29] Surján, P. R., Ángyán, J.: Phys. Rev. **A, 28,** 45 (1983)

Acta Chimica Hungarica 116 (2), pp. 153—161 (1984)

THE STRUCTURE OF DEOXYLUTEINS

M. BARANYAI[1], L. RADICS[2], M. KAJTÁR[3], J. KAJTÁR[3], GY. BUJTÁS[2] and J. SZABOLCS[1]*

([1]University Medical School, H-7643 Pécs, Szigeti út 12, [2]Central Research Institute for Chemistry, H-1525 Budapest, P.O. Box 17, [3]Institute of Organic Chemistry, Eötvös University, H-1445 Budapest, P.O. Box 325)

Received June 15, 1983

Accepted for publication July 26, 1983

Based on mass, IR, ^{1}H- and ^{13}C-NMR, UV-VIS and CD spectral studies, constitutions and absolute configurations pictured in formulae **1**—**3** were assigned to deoxylutein I ((3*R*)-3-hydroxy-3',4'-didehydro-β,β-carotene), deoxylutein II ((3*R*,6'*R*)-3-hydroxy-3',4'-didehydro-β,γ-carotene) and deoxylutein III ((3*R*,6'*R*)-3-hydroxy-2',3'-didehydro-β,ε-carotene).

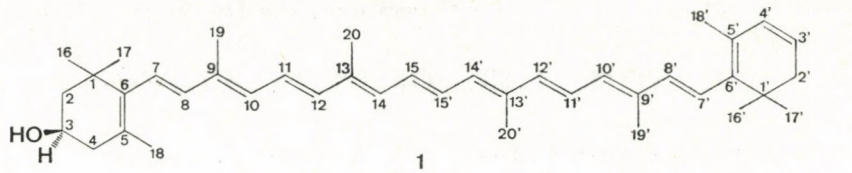
Although deoxyluteins (**1**—**3**), the dehydration products of lutein (**4**), have been known for a long time [1—3], the constitutions proposed for them, have not yet been confirmed, neither has their stereochemistry been clarified. During an investigation of the absolute configuration of lutein by Eugster and co-workers [4], the problem of the uncertain structures of deoxylutein II (**2**) and III (**3**) arose again. Therefore, we prepared deoxyluteins I, II and III (**1**—**3**) by Zechmeister's original procedure [1] and reinvestigated their structures by today's spectroscopic methods. Our results have proved the earlier tentative constitutions **1**—**3** [2, 3] and led to assigning absolute configurations to the chiral centres.

Results and Discussion

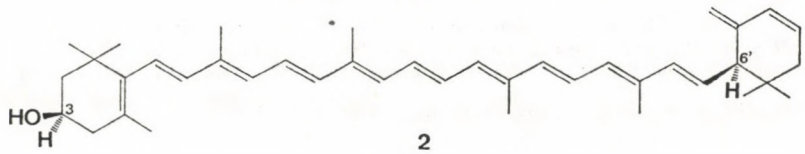
Mass spectra

The mass spectra of **1**—**3** show identical molecular ions [m/e = 550 (100%); $C_{40}H_{54}O$ requires 550] and the same fragments indicating the presence of a hydroxyl group [(M-18): 1%, 1%, 1%, resp.] and of the polyene chain [(M-92): 25%, 18%, 16%, resp.; (M-106): 3.5%, 19%, 7%, resp.] in the molecules. The relative intensities of the (M-92) and the (M-106) peaks are, however, significantly different in the mass spectra of the three isomers, their values being of 7.1, 0.9 and 2.3 for **1**, **2** and **3**, respectively. The higher values (7.1 and 2.3) correspond to those found in the mass spectra of other bicyclic carotenoids [5—7], whereas the one of 0.9 refers to an unusual feature in the structure of **2**.

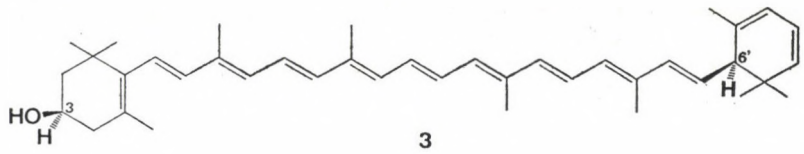
* To whom correspondence should be addressed



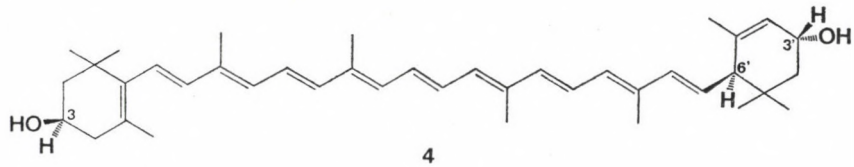
1



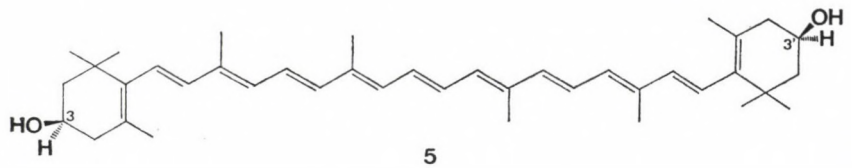
2



3



4



5

IR spectra

The IR spectra of **1**, **2** and **3** (see Experimental) show great similarities and are indicative of the presence of a hydroxyl group in the molecules (bands around 3600 and 3440 cm^{-1}).

^1H- and ^{13}C-NMR spectra

The constitutions of the isomeric deoxyluteins **1**—**3** were readily deducible from their 100 MHz ^1H-NMR spectra. The site of dehydration, expectedly common for each of these products, became evident by the absence of the C-3'H carbinyl proton resonance occurring at 4.25 ppm in the parent **4**. Partial structures pertinent to the various deoxy-end-groups were ascertained through ^1H-[^1H] double resonance experiments providing direct infor-

Table I

Relevant ^{1}H-NMR *parameters*[a] *of deoxy-end-groups in isomers* **1**—**3** *and in lutein* (**4**)

	2'H_A	2'H_B	3'H	4'H	6'H	7'H	18'H
(**1**)	1.46	1.54	[b]	5.70 $J_{3',4'}$ 9.5	—	5.74 $J_{7',8'}$ 16.5	1.74
(**2**)	[b]	[b]	6.62 $J_{3',4'}$ 10	5.72 $J_{2',4'}$ 3.5	2.65 $J_{6',7'}$ 8.8	5.65 $J_{7',8'}$ 16.5	4.8
(**3**)	5.32 $J_{2',3'}$ 9	—	5.73 $J_{3',4'}$ 5	5.59 $J_{4',18'}$ 1.2	2.24 $J_{6',7'}$ 8.7	6.22 $J_{7',8'}$ 16.5	1.73
(**4**)	1.38 $J_{2'A,4'}$ 0.5	1.64 $J_{2'B,4'}$ 1.1	4.25 $J_{3',4'}$ 3	5.56[c] $J_{4',6'}$ 1.5	2.41 $J_{6',7'}$ 8.8	5.42 $J_{7',8'}$ 16.5	1.64

[a] In dilute $CDCl_3$ solns. Chemical shifts in ppm from internal TMS; coupling constants n Hz.

[b] Not measured. [c] In Ref. [4] this resonance has been erroneously reported as due to C-7H.

mation on spin-coupled proton sequences. The relevant ^{1}H-NMR parameters thus derived are shown in Table I.

Examination of these data reveals that, in accordance with earlier suggestions based on UV-VIS spectral studies [3], the most prominent structural characteristic of **1** is the extension of the primary polyene system over the deoxy-end-group involving the C-3', C-4', C-5' and C-6' carbon atoms. This follows, in particular, from the lack of a C-6'H resonance in the spectrum of **1** and the characteristic changes in the chemical shift values of C-3'H, C-4'H and C-7'H (with respect to those in **4**). As evidenced by the missing C-18' methyl signal (1.64 ppm in **4**) and the occurrence at 4.8 ppm of a vinylic $=CH_2$ resonance, isomer **2** features an endocyclic $\Delta^{5',18'}$ double bond. Conjugated with it is another unsaturated bond comprising of C-3' and C-4', a finding which is reflected by the coupling pattern of pertinent proton resonances. Deoxylutein III (**3**), finally, has a deoxy-end-group with a conjugated diene sequence involving carbon atoms C-2', C-3', C-4' and C-5', a structural property clearly reflected by the chemical shifts and coupling data reported in Table I.

Full support for these conclusions was obtained from the analysis of the carbon-13 NMR spectra of **1**—**3**. The assigned ^{13}C chemical shift data for the parent lutein (**4**) and the three isomeric deoxy derivatives are collected in Table II. The assignment of resonances to individual carbon atoms in the isomers followed from the known assignments for lutein [8], and from the results of single-frequency-off-resonance and single-frequency selective ^{13}C-[^{1}H] double resonance experiments. From the examination of these data it follows that, in agreement with chemical expectations and other spectral results, the β-end of the parent carotenoid remains unchanged upon dehydration. The variations in carbon-13 chemical shifts of the ε-end resonances, on the other

Table II

^{13}C chemical shifts[a] of lutein (4) and its three isomeric deoxy-derivates (1 — 3)

		C-1	C-2	C-3	C-4	C-5	C-6	C-7	C-8	C-9	C-10
Lutein[b]	β-end	36.76	48.41	64.34	42.61	126.69	137.26	125.81	137.92	135.48	131.03
	ε-end	34.00	44.89	63.46	125.97	135.55	54.77	129.13	137.35	134.88	130.52
Deoxylutein I[c]	β-end	37.14	48.53	65.09	42.62	126.19	137.81	125.60	138.53	135.65	131.35
	deoxy-end	34.02	39.99	125.09	130.03	126.71	138.73	125.53	137.29	135.92	131.54
Deoxylutein II[c]	β-end	37.13	48.55	65.09	42.63	126.20	137.84	125.61	138.52	135.61	131.36
	deoxy-end	33.49	38.64	128.43[d]	129.24[d]	145.72	55.54	127.77	136.68	135.46	130.72
Deoxylutein III[c]	β-end	37.15	48.55	65.09	42.63	126.19	137.83	125.60	138.56	135.60	131.36
	deoxy-end	34.88	134.59	122.16	117.65	137.21	55.82	127.99	135.98	135.68	130.52

		C-11	C-12	C-13	C-14	C-15	C-16	C-17	C-18	C-19	C-20
Lutein[b]	β-end	124.88	137.27	136.09	132.44	129.99	28.63	30.27	21.55	12.61	12.68
	ε-end	124.80	137.27	136.14	132.44	129.99	23.72	29.56	22.68	12.98	12.68
Deoxylutein I[c]	β-end	124.92	137.61	136.45	132.34	130.14	28.76	30.29	21.61	12.81	12.81
	deoxy-end	124.86	137.56	136.55	132.64	130.08	26.82	26.82	20.32	12.75	12.65
Deoxylutein II[c]	β-end	124.91	137.63	136.37	132.65	130.14	28.77	30.30	21.61	12.80	12.80
	deoxy-end	125.01	137.35	136.50	132.43	130.01	25.35	28.48	113.01	13.12	12.80
Deoxylutein III[c]	β-end	124.90	137.64	136.34	132.66	130.16	28.77	30.30	21.61	12.80	12.80
	deoxy-end	125.04	137.21	136.52	132.39	129.97	25.80	26.73	22.16	13.12	12.80

[a] In ppm from internal TMS. [b] In $CDCl_3$ — DMSO (2 : 1) solvent mixture. [c] In $CDCl_3$. [d] Assignment may be reversed.

hand, correspond to changes in hybridization and degree of conjugation of carbon atoms exactly in the way as expected from the ^{1}H-NMR-derived partial structures **1**—**3**.

UV-VIS spectra

The electronic absorption spectra obtained for the isomeric deoxyluteins (see Experimental) agree with those described in the literature [3] and are consistent with the structures postulated by the NMR data. The bathochromic shift of about 20 nm shown by the maximum and shoulders in the spectrum of **1** with respect to the almost identical spectra of **2** and **3** refer to the longer chromophoric system of conjugated double bonds in **1**. The absorption band of **1** displays a less definite vibrational fine structure than do those of **2** and **3** (cf. Ref. [3]). This difference may be accounted for by a higher conformational mobility of the molecules of **1**, also reflected in the CD spectra (see below).

CD spectra

The CD spectra (recorded in methanol) of the three deoxyluteins (**1**—**3**) together with those of lutein (**4**) and zeaxanthin (**5**) [9] are shown in Fig. 1. The spectra of **2** and **3** are almost identical, whereas that of **1** is of much

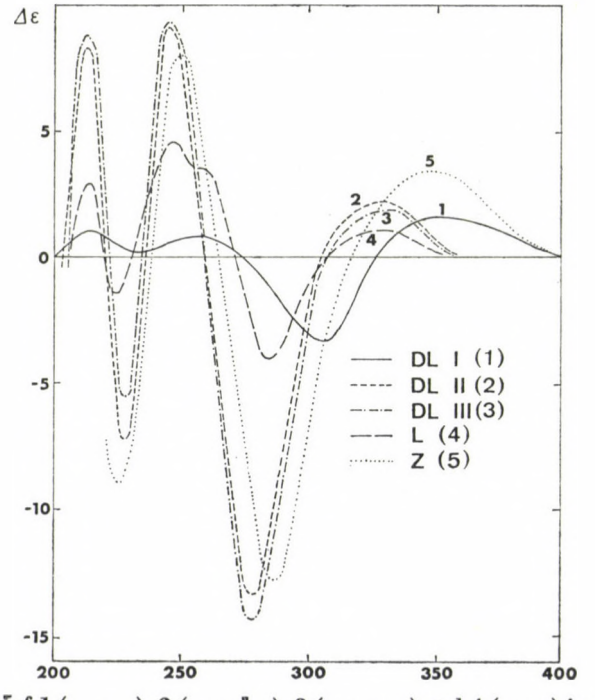


Fig. 1. CD spectra of **1** (———), **2** (— —), **3** (—·—·—) and **4** (— —) in methanol, and of **5** (. . . . . .) in dioxan [10]

lower intensity and, in accordance with the UV-VIS spectra, displays the corresponding bands red-shifted by about 20 nm. The negative maximum at 228 nm in the CD spectra of **2** and **3** is apparently missing from that of **1**. However, the minimum found at 230 nm between the two positive maxima at 255 and 215 nm in the spectrum of **1** may be correlated with a hidden negative maximum of low intensity. Thus the sign pattern of CD bands can be regarded as identical for all the three deoxyluteins.

In their sign patterns, the CD spectra of deoxyluteins I—III are similar also to that of zeaxanthin (**5**). Owing to the different lengths of the conjugated polyene chains in the four molecules, however, the bands of **2** and **3** are blue-shifted, whereas those of **1** red-shifted, with respect to the positions of the corresponding bands of zeaxanthin. In the case of **2** and **3**, even the CD band intensities are almost identical with those of the zeaxanthin spectrum. (Similar results have been found for **2** by Eugster and co-workers [4].) The intensities of the weak CD bands of **1**, on the other hand, are less than a half of those of the zeaxanthin bands.

The origin of the optical activity of carotenoids was discussed recently by Noack and Thomson [9], and by Sturzenegger, Buchecker and Wagniere [10]. According to their reasoning, the rotational strengths due to the $\pi \rightarrow \pi^*$ transitions of carotenoid molecules arise from a well-defined inherent chirality imposed upon the chromophoric polyene chain by the one or two cyclic end-groups, the more or less fixed conformation of which is determined by the configurations of the chiral centres within the rings. Although the geometry of the polyene chain cannot be completely fixed in solution, one of the various conformations is favoured by the configurations of the chiral centres, and it is this predominating conformer that mainly determines the chiroptical properties. In zeaxanthin molecules containing two identical chiral end-groups, the helicities imparted by these rings upon the two halves of the polyene chain are of the same sense, and thus the chromophore has $\mathbf{C_2}$ symmetry. The *co-operativity* of the effects of the two end-groups results in an increased stabilization of the helical conformation of the chromophoric system and gives rise to relatively intense CD bands. This type of structure is called *homodichiral* [10, 11]. It has been shown experimentally [9] as well as theoretically [10] that carotenoids of this type exhibit conservative CD spectra of relatively high intensity. The conservative character and, at the same time, high intensity of the CD spectrum of a carotenoid is, therefore, indicative of a unique sense of helicity along the whole chromophoric chain fixed by the cooperative effects of two chiral end-groups.

According to the above reasoning, the CD spectra of deoxyluteins II and III (**2** and **3**), which are in their sign patterns as well as intensities almost identical with that of zeaxanthin, indicate not only the (3*R*) configuration of the zeaxanthin-end-group in these two molecules, but also the fixed chirality of

the deoxy-end-group. At present there are no experimental data available on the conformation of the latter rings and on their spatial disposition with respect to the polyene chain, nevertheless, it can be taken for granted that the helicity imposed by these chiral end-groups upon the one half of the chromophoric system is of the same sense as that effected by the zeaxanthin-end-group in the other. The molecules of **2** and **3** can thus be called *pseudo-homodichiral*, implying that, though the two chiral end-groups are different, the helicities of the two halves of the polyene chain are of the same sense, i.e. the chromophore itself has C_2 symmetry.

Our conclusion that the chiral centres of the deoxy-end-groups in deoxyluteins II and III are of fixed configuration and *not* racemised (cf. Ref. [4]), receives support from the very low intensity of the CD spectrum of deoxylutein I (**1**) in which one of the end-groups is achiral.

According to Noack and Thomson [9], the CD spectra of monochiral carotenoids are determined in their sign pattern by the single chiral end-group and should be of half intensity with respect to the corresponding homodichiral analogs (cf. also Rf. [11]). There are many examples among monochiral carotenoids (e.g. β-cryptoxanthin [9], rubixanthin [9], agelaxanthin A [12]) which, indeed, display "half-zeaxanthin" CD spectra. Our own experiences with deoxylutein I showing a greater reduction of the intensity of CD bands can be explained by a destabilizing effect exerted by the "achiral"end-group on the helical conformation of the chromophore. The deoxy-ring of **1** possessing no chiral centre can adopt two enantiomeric chiral conformations which will impose enantiomeric helicities upon the neighbouring part of the polyene chain. The possibility of different (enantiomeric) conformations in the one half of the polyene chain imparts an enhanced conformational mobility to the molecule as a whole, and thus destabilizes the unique sense of helicity even of that half of the chromophore which is connected to the optically active end-group. This effect can be regarded as a "negative" cooperativity between the end-groups, the one of which is achiral, that results in the weakening of the optical activity of the substance.

Since the sign pattern of the weak bands in the CD spectrum of deoxylutein I (**1**) (which, nevertheless, is close to conservative in character) is identical with the sign pattern of the zeaxanthin spectrum, the single chiral centre at C-3 in the zeaxanthin-end-group of **1** must also be of (*R*) absolute configuration.

The configuration of chiral centre 6' in deoxyluteins II and III can be deduced by comparing their CD spectra with that of lutein (**4**) of known absolute configuration [4] (see Fig. 1). Lutein ((3*R*,3'*R*,6'*R*)-3,3'-dihydroxy-β,ε-carotene) and 3'-epilutein ((3*R*,3'*S*,6'*R*)-3,3'-dihydroxy-β,ε-carotene) exhibit CD spectra (classified by Wagniere and co-workers [10] as being close to conservative) which are identical in sign pattern, but somewhat different in

the absolute as well as relative intensities of the bands (see data in Ref. [10]). This suggests the assumption that it is the chiral centre 6' (and not the 3') whose configuration determines the conformation of the ε-end-ring and, through this, the helicity of the neighbouring half of the chromophoric chain in these molecules. The difference between the two spectra may probably be attributed to the different conformational stabilities of the ε-rings of the two epimers leading to different conformational equilibria in solution. Nevertheless, the CD spectra of lutein and, particularly, of 3'-epilutein are similar to those of deoxyluteins II and III. From this similarity of the chiroptical properties it can be concluded that the configuration of the chiral centre 6' in every one of these four compounds is the same, i.e. (*R*), as established for lutein by Eugster [4]. In any case, it is reasonable to suppose that the dehydration process leading to deoxyluteins II and III does not interfere directly with chiral centre 6' of lutein, and thus leaves its configuration unchanged.

As the result of our chiroptical studies, it can be stated that the chiral centres of deoxyluteins I—III preserve the absolute configurations of the respective centres in the parent lutein. The correct structures of the three isomeric dehydration products of lutein are, therefore, those pictured in formulae **1**—**3**.

Experimental

Preparation

Deoxylutein I (**1**; 24 mg, m.p. 134 °C), deoxylutein II (**2**; 130 mg, m.p. 149 °C) and deoxylutein III (**3**; 23 mg, m.p. 158 °C) were prepared from lutein (**4**; 735 mg, from *Helianthus annuus*) according to the method of Zechmeister and Sease [1]. The routine procedures used after chromatography have been described previously [13]. Melting points were determined on a Boetius hot stage apparatus.

Mass spectra

The spectra were taken by an AEI MS 902 mass spectrometer at 70 eV, trap current 100 μA, ion accelerating voltage 8 kV, using a direct insertion probe at a source temperature of 180 °C.

IR spectra

Infrared spectra were recorded on a Zeiss (Jena) UR 10 Spectrophotometer.

Deoxylutein I (1), ν, cm^{-1} (KBr): 3430 s, 3020 m, 2950 s, 2915 s, 1550 w, 1460 w, 1445 m, 1382 w, 1358 m, 1036 m, 1000 w, 964 s.

Deoxylutein II (2), ν, cm^{-1} ($CHCl_3$): 3607 m, 3445 w, 3030 m, 2990 s, 2958 s, 2928 s, 2860 s, 1565 m, 1465 w, 1442 m, 1392 m, 1382 m, 1362 s, 1005 m, 970 s, 888 s.

Deoxylutein III (3), ν, cm^{-1} ($CHCl_3$): 3610 m, 3435 w, 3030 s, 2965 s, 2920 s, 2865 s, 1565 m, 1470 w, 1430 s, 1400 m, 1390 w, 1370 m, 1035 s, 1000 w, 974 s, 890 s.

NMR spectra

^1H (100.1 MHz) and ^{13}C (25.16 MHz) NMR spectra were recorded in the Fourier transform mode using a Varian XL-100-15 FT NMR instrument equipped with Varian Disk System Accessory.

Deoxylutein I (1), ^1H-NMR ($CDCl_3$): 1.04 s (CH_3 16', 17'); 1.07 s (CH_3 16, 17); 1.74 m (CH_3 18, 18'); 1.88 m (CH_3 19'); 1.96 m (CH_3 19, 20, 20'); 1.2—2.55 (methylene protons); 3.98 m (H C-3); 5.70 m (H C-4'); 5.74 m (H C-7'); 6—6.8 (vinyl protons).

Deoxylutein II (2), ^{1}H-NMR ($CDCl_3$): 0.88 s (CH_3 16'); 0.90 s (CH_3 17'); 1.07 s (CH_3 16, 17); 1.73 m (CH_3 18); 1.92 m (CH_3 19'); 1.96 m (CH_3 19, 20, 20'); 1.24—2.52 m (methylene protons); 2.66 m (H C-6'); 3.98 m (H C-3); 4.82—4.88 m (=CH_2 18'); 5.65 m (H C-7'); 5.72 m (H C-4'); 6—6.8 m (vinyl protons).

Deoxylutein III (3), ^{1}H-NMR ($CDCl_3$): 0.94 s (CH_3 16'); 1.01 s (CH_3 17'); 1.07 s (CH_3 16, 17); 1.73 m (CH_3 18, 18'); 1.88 m (CH_3 19'); 1.96 m (CH_3 19, 20, 20'); 1.25—2.4 m (methylene protons); 2.23 m (H C-6'); 3.98 m (H C-3); 5.32 m (H C-2'); 5.59 m (H C-4'); 5.73 m (H C-3'); 6—6.8 m (vinyl protons).

UV-VIS spectra

The visible parts of the absorption spectra were measured in benzene solution on a Perkin-Elmer 402 instrument.

Deoxylutein I (1), λ, nm ($\varepsilon \cdot 10^{-3}$): 506 (105.0) sh, 478 (124.0), 450 (101.0) sh.

Deoxylutein II (2), λ, nm ($\varepsilon \cdot 10^{-3}$): 486 (127.5), 456 (140.5), 432 (98.5).

Deoxylutein III (3), λ, nm ($\varepsilon \cdot 10^{-3}$): 489 (126.0), 459 (139.0), 434 (98.0).

CD spectra

The CD spectra were taken in methanol solution at room temperature on a Roussel-Juan Dichrographe III (Jobin-Yvon), in quartz cells of different lengths.

Deoxylutein I (1), λ, nm ($\Delta\varepsilon$): 355 (+1.6), 325 (0), 305 (−3.4), 274 (0), 255 (+0.9), 231 (+0.2) min, 213 (+1.0), 200 (0).

Deoxylutein II (2), λ, nm ($\Delta\varepsilon$): 330 (+2.3), 306 (0), 278 (−13.4), 260 (0), 245 (+9.1), 235 (0), 228 (−7.3), 220 (0), 213 (+8.3), 203 (0).

Deoxylutein III (3), λ, nm ($\Delta\varepsilon$): 333 (+1.9), 305 (0), 278 (−14.4), 260 (0), 243 (+9.3), 235 (0), 228 (−5.6), 220 (0), 213 (+8.8), 204 (0).

Lutein (4), λ, nm ($\Delta\varepsilon$): 328 (+1.0), 308 (0), 283 (−4.1), 271 (0), 260 (+3.4) sh., 246 (+4.6), 230 (0), 225 (−1.5), 220 (0), 214 (+3.0), 207 (0).

*

The authors wish to thank Miss É. Nyers for her skillful assistance in the chromatographic work.

REFERENCES

[1] Zechmeister, L., Sease, J. W.: J. Am. Chem. Soc., **65,** 1951 (1943)
[2] Zechmeister, L., Petracek, F. J.: Arch. Biochem. Biophys., **61,** 243 (1956)
[3] Zechmeister, L.: Fortschr. Chem. Org. Naturst., **15,** 62 (1958)
[4] Buchecker, R., Hamm, P., Eugster, C. H.: Helv. Chim. Acta, **57,** 631 (1974)
[5] Enzell, C. R.: Pure and Appl. Chem., **20,** 497 (1969)
[6] Carnevale, J., Cole, E. R., Nelson, D., Shannon, J. S.: Biomed. Mass Spectrom., **1978,** 641
[7] Vetter, W., Englert, G., Rigassi, N., Schwieter, U. in Isler, O. (Ed): Carotenoids, Chapter 4. Birkhäuser Verlag, Basel 1971
[8] Baranyai, M., Molnár, P., Szabolcs, J., Radics, L., Kajtár-Peredy, M.: Tetrahedron, **37,** 203 (1981)
[9] Noack, K., Thomson, A. J.: Helv. Chim. Acta, **62,** 1902 (1979)
[10] Sturzenegger, V., Buchecker, R., Wagnière, G.: Helv. Chim. Acta, **63,** 1074 (1980)
[11] Bartlett, L., Klyne, W., Mose, W. P., Scopes, P. M., Galasko, G., Mallams, A. K., Weedon, B. C. L., Szabolcs, J., Tóth, G.: J. Chem. Soc. (C) **1969,** 2527
[12] Buchecker, R., Eugster, C. H., Litchfield, C.: Helv. Chim. Acta, **60,** 2780 (1977)
[13] Molnár, P., Szabolcs, J.: Acta Chim. Acad. Sci. Hung., **99,** 155 (1979)

Acta Chimica Hungarica 116 (2), pp. 163–172 (1984)

INFLUENCE OF THE CHEMICAL POTENTIAL OF TRANSITION METALS ON THEIR ADSORPTIVE AND CATALYTIC PROPERTIES

P. J. POMONIS

(Department of Chemistry, University of Ioannina, Ioannina, Greece)

Received April 1, 1983

Accepted for publication July 27, 1983

The adsorptive and catalytic properties of transition metals seem to be strongly influenced by the chemical potential of the electrons in the solid. High values of chemical potential result in weak adsorption, as measured by the enthalpy of adsorption, and high rates of catalytic reaction. On the contrary, low values of chemical potential result in strong adsorption and reduced reaction rates. These observations are explained in the context of adsorption time which depends on the enthalpy of adsorption.

Introduction

In examining the processes taking place on solid–gas interfaces the influence of both phases should be taken into account. The question nevertheless remains: is there any single physical quantity which controls from the part of the solid, as well as from that of the gas, the surface properties like adsorption and catalysis?

A candidate for such a key role might be the chemical potential μ of electrons of both solid and gas molecules.

This hypothesis is founded on the following arguments [1, 2, 3]. Because the chemical potentials of solid and gas are not equal, electronic charge will be transferred from the substance with larger μ to the substance with smaller μ in order to make the chemical potentials equal ever. To be more precise, the change ΔG_{A-M} of the free energy of two subsystems A and M having chemical potentials μ_A and μ_M, respectively, and exchanging during contact $q_A = -q_M$ charges will be

$$(-\Delta G_{A-M}) = \mu_M q_M + \mu_A q_A = (-q_A)(\mu_A - \mu_M). \tag{1}$$

If $\mu_A < \mu_M$ then transition to equilibrium means $(-\Delta G_{A-M}) > 0$, therefore, $q_A > 0$ and the number of charges in the subsystem A increases. If $\mu_A > \mu_M$, the opposite will be the case. Supposing that during the described process $T \cdot \Delta S_{A-M} \ll \Delta H_{A-M}$ then Eq. (1) can be written in the form

$$(-\Delta H_{A-M}) = (-q_A)(\mu_A - \mu_M). \tag{2}$$

The main correction to Eq. (2) should be some electrostatic potentials q_A^2/r related to the Madelung energy [3] in the case of solid formation or to the image forces [4] in the case of adsorption. Equation (2) is written in the general form

$$(-\Delta H_{A-M}) = (-q_A)(\mu_A - \mu_M) + \frac{(-q_A)^2}{r} . \qquad (3)$$

There are now two points which should be noticed about Eq. (3). First $(-q_A)$ is expected to be proportional to $(\mu_A - \mu_M)$ [2, 3] but the exact nature of this dependence in not quite clear. Second, the values of chemical potentials μ_A and μ_M, as well of r, are needed in order to have an exact solution of Eq. (3).

Now in the case of solid–gas processes we are interested in, let us consider that A is the non-metal and M the metal. Unfortunately, the values of μ_A are not known for the non-metallic elements, let alone the heteroatomic molecules. On the contrary the chemical potentials μ_M of electrons in transition metals have been recently calculated [2, 3, 5] based on the electron density of the solid. Then Eq. (3) is written in the form

$$(-\Delta H_{A-M}) = a - b\mu_M \qquad (4)$$

which contains only the parameter μ_M which is known for metals, and the constants a and b substitute the unknown terms $(-q_A)\mu_A + (-q_A)^2/r$ and $(-q_A)$ respectively.

Equation (4) is a simplified form of (3) and can be used to test similar processes. Namely we shall check to what extent the enthalpy of formation $(-\Delta H_{O-M})$ of the transition metal oxides, calculated per metal atom, is related to μ_M via relation (4). Similarly we shall examine if the integral heats of adsorption of simple gases on transition metals can be described by the same equation. Finally we shall investigate to what extent the rates of catalytic reactions over transition metals show any dependence on the chemical potential of the corresponding solid.

Before proceeding to the treatment of the data we should notice that the values of μ_M used in this text are those cited in [6] and calculated in the following way. Alonso and Girifalco give [3] the values $(\mu_M - \mu_{Sc})$, where μ_{Sc} is referred to the chemical potential of Scandium. To have an absolute value of μ_M we need the value of μ_{Sc} which was taken as 2 eV based on the relation between μ_{Sc} and Pauling's electronegativity given by Hodgess and Stott [2]. It is noteworthy that even a mistake of 10—20% in the calculation of μ_{Sc} does not affect the rather qualitative discussion which follows. The values of μ_M used in the next are (in eV): Sc = 2.00, Ti = 2.95, V = 3.76, Cr = 4.57, Mn = 5.66, Fe = 5.76, Co = 6.74, Ni = 6.60, Y = 2.27, Zr = 3.22, Nb = 4.71 Mo = 5.25, Tc = 6.46, Ru = 8.09, Rh = 8.50, Pd = 7.69, Ta = 4.84, W = = 4.84, Ir = 8.22, Pt = 8.77.

Discussion

Adsorption

Figure 1 shows the enthalpy of formation ($-\Delta H_{O-M}$) of transition metal oxides calculated per metal atom as well as the integral heats of adsorption ($-\Delta H_{ads}$) of the gases O_2, CO_2, CO, N_2 and H_2 on transition metals versus the corresponding chemical potential. The ($-\Delta H_{O-M}$) is included in the figure since this quantity has often been used as a measure of comparison with catalytic activity [7, 8, 9]. Besides, its relation with the heats of adsorption of gases on metals has been well established [10, 11]. The data of ($-\Delta H_{ads}$) are taken from Ref. [11].

From Fig. 1 we observe that the heats of adsorption of simple molecules on metallic surfaces are high at low values of chemical potential of metals. The same is also true for the heats of formation of oxides per metal atom. Both ($-\Delta H_{O-M}$) and ($-\Delta H_{ads}$) depend on μ_M in a way described in a first approximation by Eq. (4).

This kind of dependence can be easily explained in terms of Eq. (2) or 3). Namely, at the point where ($-\Delta H_{A-M}$) $\rightarrow 0$, according to (2), $\mu_A \rightarrow \mu_M$,

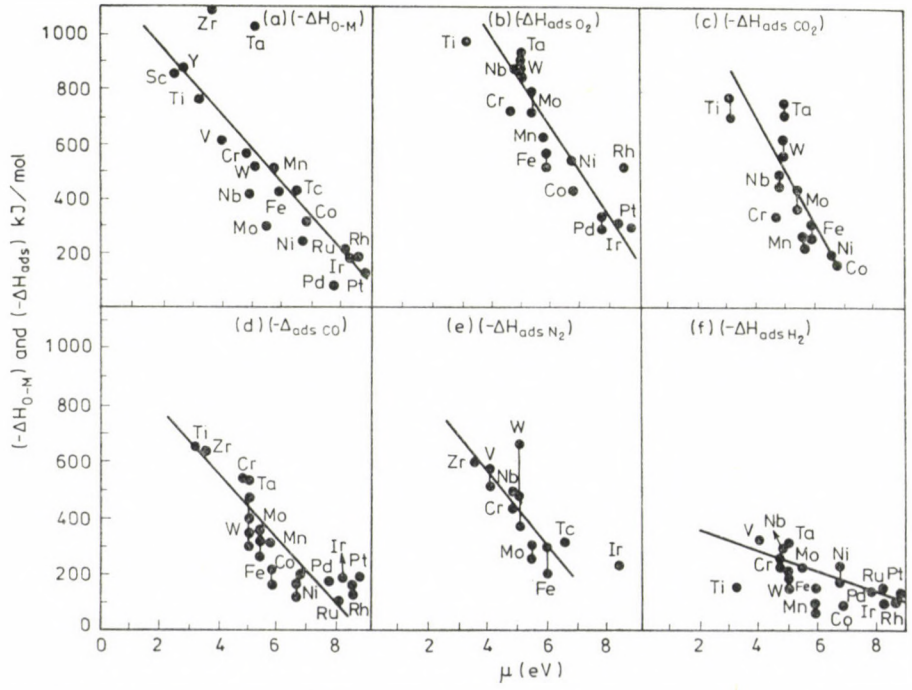


Fig. 1. (a) Enthalpy of formation ($-\Delta H_{O-M}$) of transition metal oxides calculated per metal atom versus the chemical potential μ of the corresponding metal. (b), (c), (d), (e) and (f): enthalpies of adsorption ($-\Delta H_{ads}$) of the gases O_2, CO_2, CO, N_2 and H_2 on metals versus μ. ($-\Delta H_{ads}$) date are from Figs 1a, 4, 3a, 5a and 2a, respectively, of Ref. [11]

while according to (3), $(\mu_A - \mu_M) \to (q_A)/r$. If the condition $(-\Delta H_{A-M}) \to 0$ is a result of infinitely small difference in the chemical potentials of A and M this should result in an infinitely small tranfer of charges between them. Therefore, both $(\mu_A - \mu_M)$ and $(-q_A)$ tend to zero. According to this analysis, we observe from Figs 1a and 1b that the chemical potential of oxygen should probably be around 9 to 10 eV on the scale used here. Although this number should not be taken very seriously, it can be suggested that the far smaller chemical potential of elements like Sc and Y results in high values of the $(\mu_A - \mu_M)$ term in Eq. (3) or small values of the $b\mu_M$ term in Eq. (4), therefore, $(-\Delta H_{O-M})$ and $(-\Delta H_{ads,\,O_2})$ are high. On the contrary, the large values of the chemical potential of elements like Pt and Rh result in small values of the $(\mu_A - \mu_M)$ term in (3) or large values of the $b\mu_M$ term in (4) and, therefore, $(-\Delta H_{O-M})$ and $(-\Delta H_{ads,\,O_2})$ are low.

The slope of lines in Fig. 1 according to Eq. (4) is equal to the charge transferred between the metal and the non-metal. Although the picture is only indicative, we observe that as we move from $O_2 \to N_2 \to H_2$, in other words to elements with lower electronegativities, the slope of lines, and therefore the charge transferred, decreases. Such a result is expectable since smaller electronegativities are associated with smaller values of chemical potentials of metals [2, 3, 5]. If the same trend is valid for non-metals, then as we move from oxygen to nitrogen and finally to hydrogen, the difference $(\mu_A - \mu_M)$ decreases and $(-q_A)$ as depended on $(\mu_A - \mu_M)$, also drops.

Nevertheless the constant slope of lines drawn in Fig. 1 suggests a constant number of charges transferred, let us say, during the adsorption of O_2, regardless of the metal participating in the process. This result is considered only as tentative. Actually, the sets of data in Fig. 1 show some trend to increase faster than first order but slower than a second order relation as μ_M decreases. This signifies a dependence of $(-\mu_A)$ on the difference $(\mu_A - \mu_M)$ as noticed previously [2, 3]. So, according to Eq. (2), we can write:

$$(-\Delta H_{A-M}) = (\mu_{A-}\mu_M)^{\alpha}(\mu_A - \mu_M) = (\mu_A - \mu_M)^{1+\alpha} \tag{5}$$

where $(\mu_A - \mu_M)^{\alpha} = (-q_M)$ and $0 < \alpha < 1$. According to (3), we have

$$(-\Delta H_{A-M}) = (\mu_A - \mu_M)^{1+\alpha} + \frac{(\mu_A - \mu_M)^{2\alpha}}{r} = \\ = (\mu_A - \mu_M)^{1-\alpha}\left(1 + \frac{1}{r(\mu_A - \mu_M)^{1-\alpha}}\right). \tag{6}$$

For r equal to 2 or 3 a.u., $(\mu_A - \mu_M)$, assumsing values between 1 and 10 eV and α around 0.5, the second trem in Eq. (6) takes values from 1.5 to 1.1. Therefore, the main part in Eq. (6) seems to be the first one which is similar

to Eq. (5). Unfortunately, the data do not allow us a precise knowledge of μ_A and therefore α. So this subject cannot be considered settled for the moment and we shall proceed to the analysis of the results based, to a first approximation, on relations (2), (3) and (4).

Catalysis

Catalytic activity data are shown in Figs 2, 3, 4 and 5 versus the chemical potential of the metal acting as catalyst.

Figure 2 includes catalytic activity data presented by Balandin in a review article on the "Multiplet Theory of Catalysis" [12]. These data were presented [12] as plots of activity $= f$ (heat of metal sublimation, L_s) except the data in Fig. 2(a), where the plot was activity $= f$ (heat of formation of metal formate). All the plots drawn in Ref. [12] showed there the well known "volcano-shape curves" with the exception of data shown in Fig. 2 (1) where straight lines of positive slope were drawn.

Figure 3 shows catalytic activity data presented by Bond in the last chapter of his well-known monograph "Catalysis by Metals" [10]. The catalytic activity data presented in Fig. 3 (a) and 3 (b) were plotted in [10] versus L_s while the data shown in 3 (c) were plotted versus ΔH_{ads} at $\Theta \to 0$. In the first two cases straight lines of positive slope were obtained while in the third, a line with a negative slope was drawn.

Figure 4 includes data presented by Tanaka and Tamaru [7]. The three sets of data shown in this figure were drawn in Ref. [7] versus $(-\Delta H_{O-M})$ and showed a "volcano shape curve".

Finally, Fig. 5 includes catalytic activity data presented by Tétényi [13] and drawn versus μ of the corresponding metal catalyst.

From Figures 2, 3, 4 and 5 we observe that the catalytic activity, as measured by the reaction rate R, or the rate constant k, or the remperature T_r necessary to achieve a certain rate or conversion, is favored at high values of μ. Some scatter of data or complete lack of trends [Figs 2(e), 2(j), 2(l), 4(b), 4(c)] might be due to different reasons, like surface contamination or requirements other than electronic (i.e. geometric) for a special reaction. But on the whole, the general increase of activity with μ_M is unmistakable. Our task now is to search for an explanation for the trends appearing in Figs 2, 3, 4 and 5, which obey the equation

$$\text{Catalytic activity} = a' + b'\mu_M \tag{7}$$

This can be done in conjunction with the adsorption data presented in Fig. 1 and described by Eq. (4) in the following way. The adsorption trends shown in Fig. 1 and described by Eq. (4) are expected to hold not only for the molecules included in this figure but also for other molecules as well, which are the

reactants or products of the reactions shown in Figs 2, 3, 4 and 5. Strong adsorption, as measured by high values of $(-\Delta H_{ads})$ and resulting from the low values of μ_M, poisons the surface which is unable to accept and catalyze the arriving reactants anymore. A semiquentitate explanation of this can be offered using the "adsorption time" suggested by de Boer [14]

$$\tau = \tau_0 \, e^{(-\Delta H_{ads})/RT} . \tag{8}$$

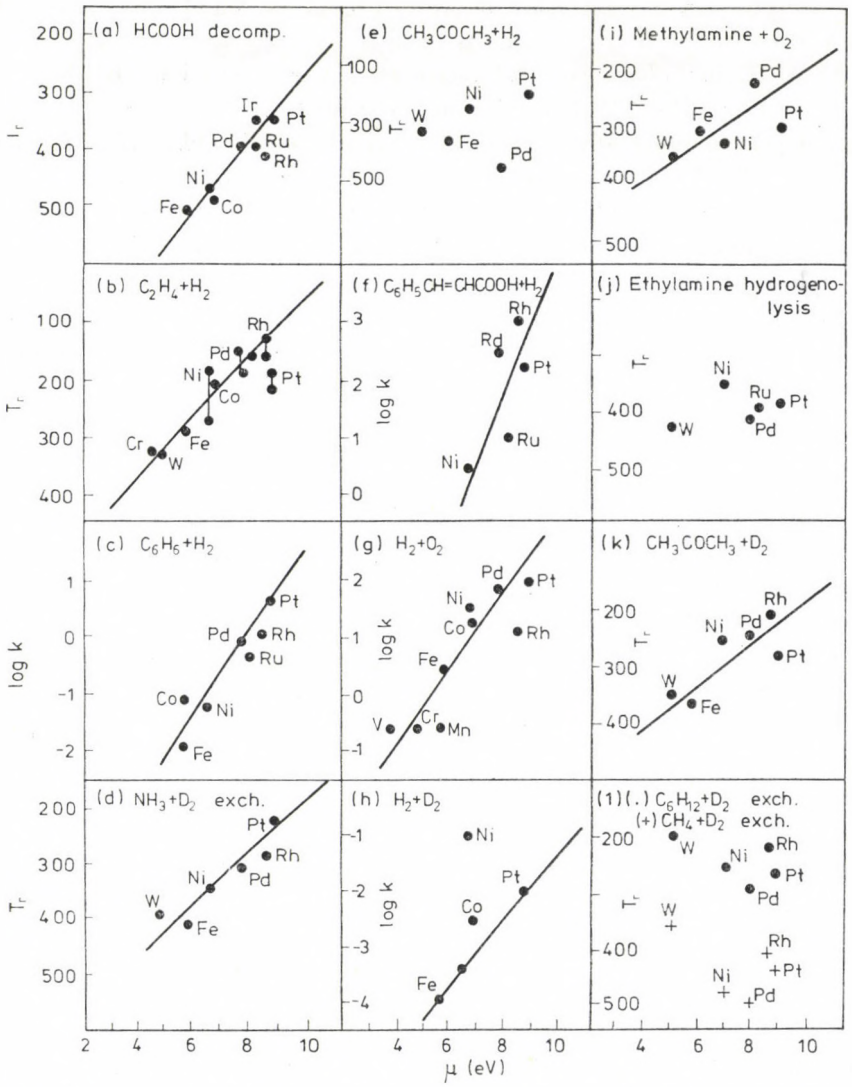


Fig. 2. Catalytic activity data for various reactions on transition metals versus the chemical potential of the corresponding solid. Catalytic activity data are from Figs 63, 64, 65, 66, 67 and 68 of Ref. [12]. T_r is the temperature required to achieve a certain degree of conversion and k is the rate constant

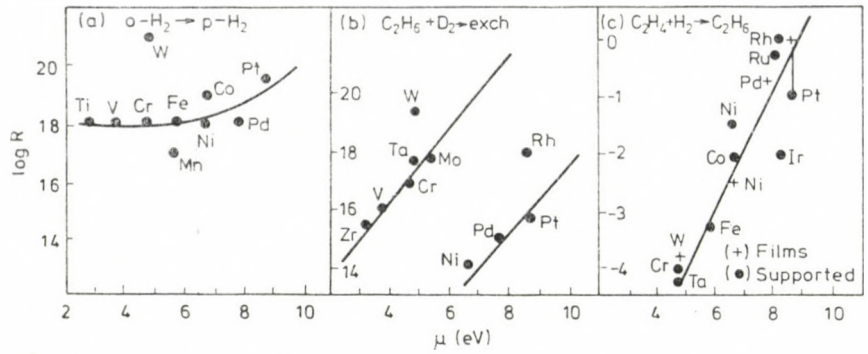


Fig. 3. Catalytic activity for different reactions on various metals versus μ. Catalytic activity data are from Figs 6, 7 and 9 of chapter 21 of Ref. [10]. R is reaction rate

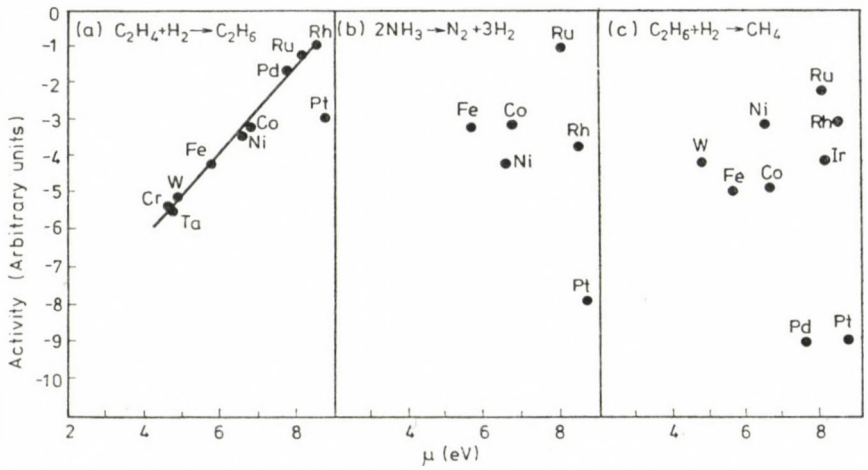


Fig. 4. Catalytic activity data for the reactions shown on transition metals versus μ. Catalytic data are from Ref. [7]

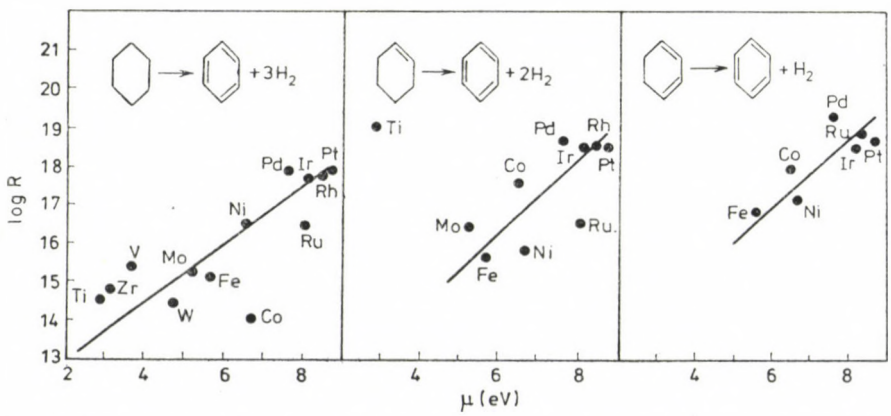


Fig. 5. Catalytic acativity data for the reactions shown on transition metals versus μ. Catalytic data are from Ref. [13]

The adsorption time τ is defined as the time during which a molecule remains adsorbed on the surface while τ_0 is related to the time of oscillation of the adsorbed molecule perpendicular to the surface.

Then substitution of Eq. (4) into (8) results in

$$\tau = \tau_0 \, e^{(a - b\mu_M)/RT} \tag{9}$$

or

$$\tau = \tau_0' e^{-b\mu_M/RT} \tag{10}$$

where $\tau_0' = \tau_0 \exp(a/RT)$. We assume now that the adsorption and reaction steps are fast. Then the rate-determining step should be desorption. During time t the regeneration of the surface will take place t/τ times which will be equal to the rate R of the reaction:

$$R = \frac{t}{\tau} = \frac{t}{\tau_0} e^{b\mu_M/RT} = kf(c) \tag{11}$$

where $f(c)$ is a function of concentrations. Taking logarithms

$$\log R = \log\left(\frac{t}{\tau_0}\right) + \frac{b}{2.3RT}\mu_M = \log k + \log\left[f(c)\right] \tag{12}$$

or

$$\log R = a' + b'\mu_M = \log k + C \tag{13}$$

where $a' = \log(t/\tau_0')$, $b' = b/2.3RT$ and $\log[f(c)] = C$. Equation (13) is similar to relation (7) which describes the majority of relations between catalytic activity (as measured by $\log R$, $\log k$, or T_r) and μ_M and which are shown in Figs 2, 3, 4 and 5.

At this point it should be said that not all kinds of catalytic reactions on transition metals obey Eq. (7). For example the data given by Dobrovolszky, Tétényi, and Paál [15] for the conversion of cyclohexanone and cyclohexanol do not show any correlation with the chemical potential of the metal catalyst. This might be due to the large number of products obtained or to requirements other than electronic (i.e. spatial) of the said reaction. The same lack of correlation appears also in the data of Ko and Garden for ethane hydrogenolysis [16] and of Tétényi, Guczi and Sárkány [17] for the same reaction. Again the reasons might be geometric requirements which may be important in controlling the activity and/or selectivity of a particular metal for a certain reaction. Such a case has been discussed [18] for the hydrogenolysis of 3-methylpentane and methylcyclopentane where it has been shown that the surface geometry may be of considerable importance in accommodating molecules and thus facilitating surface reactions.

It seems that factors other than electronic, i.e. geometric, appear to be important in reactions of demanding character, like the fission of C—C bond. Such a case is apparent in the data of Ref. [17] where the rates fo the reactions $CH_4 + D_2 \rightarrow$ exchange and $C_2H_6 + D_2 \rightarrow$ exchange do show a dependence on μ, similar to that described by Eq. (7) but ethane hydrogenolysis [17] does not show any such dependence. Also from the data presented in Figs 2, 3, 4 and 5, it seems that the non-applicability of relation (7) (Figs 2e-acetone hydrogenation, 2j-ethylamine hydrogenolysis, 21-$C_6H_{12} + D_2 \rightarrow$ exchange, $CH_4 + D_2 \rightarrow$ exchange, 4b-NH_3 decomposition and 4c-ethane hydrogenolysis) is always connected to fission of C—C or N—N bond or adsorption of rather complex molecules. These kinds of reactions seem to necessitate both electronic and geometric requirements in order to proceed.

Conclusions

The results presented above and the explanations offered provide an alternative way of looking into problems of adsorption and catalysis by metals. The examples presented could probably be multiplied from data in the literature. But it should also be said that these explanations are not expected to be a panacea for all the problems arising in the field. It seems that electronic factors in catalysis on metals are valid, but always within the constrains imposed by the spatial requirements of molecules adsorbed on the surface.

Nevertheles, the proposed approach provides a tool which might be proved useful in the formulation of electronic theories of catalysis on metals, a fact lacking for the moment, as well as some possible connection with the corresponding electronic theories of catalysis on semiconductors. A detailed discussion of this matter, including the accuracy and the applicability of the proposed correlations, as well as their relationship with those already known, will be the subject of some future work.

*

The author wishes to thank one of the referees for valuable suggestions which contributed to the improvement of this article.

REFERENCES

[1] Kireev, P. S.: "Semiconductor Physics", Mir Publishers 1975
[2] Hodgess, C. H., Stott, M. J.: Phill. Mag., **26,** 375 (1979)
[3] Alonso, J. A., Girifalco, Phys. Rev. B, **19,** 3889 (1979)
[4] Welder, G.: "Chemisorption", Butterworths London 1976
[5] Miedema, A. R., de Boer, F. R., de Chatel, P. F.: J. Phys. F (Metal Phys.), **3,** 1558 (1973)
[6] Pomonis, P. J.: React. Kinet. Catal. Lett., **21,** 29 (1982)
[7] Gates, B. C., Katzer, J. R. A., Schuit, G. C.: in "Chemistry of Catalytic Processes", McGraw-Hill London 1979
[8] Morooka, Y., Morikawa, Y., Ozaki, A.: J. Catal., **7,** 23 (1976)
[9] Vijh, A.: J. Catal., **33,** 395 (1974)

[10] Bond, G. C.: "Catalysis by Metals", Academic Press New York 1962
[11] Toyoshima, I., Somorjai, G. A.:Catal. Rev., **19,** 105 (1979)
[12] Balantin, A. A.: Adv. Catal., **19,** 1 (1969)
[13] Tétényi, P.: Acta Chim. Acad. Sci. Hung., **107,** 237 (1981)
[14] De Boer, J. H.: Adv. Catal., **8,** 18 (1956)
[15] Dobrovolszky, M., Tétényi P., Paál, Z.: Acta Chim. Acad. Sci. Hung., **107,** 343 (1981)
[16] Ko, E. I., Garden, L.: J. Catal., **68,** 233 (1981)
[17] Tétényi, P., Guczi, L., Sárkány, A.: Acta Chim. Acad. Sci. Hung., **97,** 221 (1978)
[18] Paál, Z., Tétényi, P.: Nature, **267,** 234 (1977)

Acta Chimica Hungarica 116 (2), pp. 173—187 (1984)

DESIGN AND SYNTHESIS OF INHIBITORY ANALOGUES OF LH–RH WITH INCREASED ANTIOVULATORY POTENCY

I. Mező[1], J. Seprődi[1], J. Érchegyi[1], A. Horváth[1], K. Nikolics[1]*, I. Teplán[1], S. Vigh[2], M. Kovács[2], B. Flerkó[2], D. H. Coy[3], E. Pedroza[3], M. V. Nekola[3] and A. V. Schally[3]

([1]1st Institute of Biochemistry, Semmelweis University Medical School, H-1444 Budapest ,P.O. Box 260,
[2] Institute of Anatomy, Medical School, Pécs, H-7624, Szigeti út 12,
[3] Department of Medicine, Tulane University School of Medicine and V.A. Hospital New Orleans, LA 70112, U.S.A.)

Received May 20, 1983

In revised form July 19, 1983

Accepted for publication August 9, 1983

Structure biological activity relationships in fifty-four LH–RH inhibitory ana logues have been studied. The syntheses of most of the peptides are described. An additiv effect of combinations of substitution is found — at least in a limited range — amon the LH–RH inhibitory analogues.

Introduction

Although the molecular factors increasing the agonistic and/or antagonistic properties of LH–RH have been investigated for many years and, for a better understanding of the hormone's mechanism of action, extensive

Abbreviations are in accord with the recommendations of the IUPAC-IUB Commission on Biochemical Nomenclature [J. Biol. Chem., **247**, 977 (1972)].

Other abbrevations are the following:

Glp	pyroglutamic acid
dehydro-Lys	2,6-diamino-4-hexynoic acid
Cpa (*p*-Cl-Phe)	4-chlorophenylalanine
Fpa (*p*-F-Phe)	4-fluorophenylalanine
p-Br-Phe	4-bromophenylalanine
p-Me-Phe	4-methylphenylalanine
o-Cl-Phe	2-chlorophenylalanine
p-NO_2-Phe	4-nitrophenylalanine
HO-Succ	monosuccinoyl-
EtCO	propionyl-
BOC	*t*-butyloxycarbonyl-
Z	benzyloxycarbonyl-
DCC	dicyclohexylcarbodiimide
BHA	benzhydrylamine
Tos	tosyl-
DIC	diisopropylcarbodiimide

* To whom correspondence should be addressed

structure–activity studies have been done, the greatest attention has always been focused on the search for long-acting superactive and antagonistic analogues.

It has been shown that superactive derivatives can only be obtained by the substitution of the glycines in position 6 and 10 [1]. On the other hand, the optimization of antagonistic analogues of LH–RH, inhibiting the releasing effect of endogenous LH–RH, has still to be investigated.

The omission of histidine in LH–RH yielded the first set of antagonistic analogues inhibiting the effect of exogenous LH–RH both in cell culture [2] and in vivo [3]. Further studies have shown that more active antagonistic analogues can be derived from the decapeptide if histidine in position 2 is substituted by D-Phe [4]; if L-Trp is substituted by D-Trp [1]; if Gly in position 6 is substituted by D-amino acids [1] and if, in addition, from peptides with these combined substitutions, semidimeric [5] or dimeric [6, 7, 8] structures are prepared. As a result of these modifications in the native structure of LH–RH, antagonistic derivatives have been obtained which can efficiently inhibit the release of pituitary LH also in human studies [9].

For a better understanding of the mechanism of action of LH–RH and its analogues it was desirable to prepare radio labelled derivatives, too. The substitution with Cpa (*p*-Cl-Phe) [10] offers two advantages: first, from peptides containing a "precursor" aminoacid like this, a fully biologically active compound labelled with tritium in a stable position can be prepared in one step immediately before its application, as we demonstrated earlier with other peptides [11, 12, 13, 14, 15]. Second, from the biological activity of the precursor peptides, some conclusions can be drawn concerning the biological role of the substituent in *para* position.

We have found that the D-Cpa^2 substitution increases the inhibitory activity of a certain series of LH–RH antagonists by a factor of about 7, as compared with the D-Phe^2 analogues. In addition to this, it was found that D-Glp^1 [16], acetyl-dehydro-Pro^1 [17] and especially acetylated aromatic D-amino acid substitutions in position 1 [18], also greatly enhanced the antiovulatory potency. Combining these findings with the D-Cpa^2 substitution, we succeeded in preparing derivatives with extremely high antagonistic effect.

In this paper a short review is given of the guidelines, experimental details and results of our work on improving the antiovulatory activity of these analogues.

Results and Discussion

From the aspect of the agonistic and antagonistic effects of LH–RH analogues, one of the most interesting structural factors is the role of D-amino acids in position 6. The side chain of the D-amino acid in position 6 standing

opposite from the center of the quasicyclic molecule [19] may form an additional binding interaction contributing to the biological efficiency. In this position even bulky side chain substituents [20] do not decrease the specific recognition and biological activity of LH–RH analogues. Therefore it could well be expected that the side chain functional group (like the epsilon amino group of lysine) can be substituted by various peptides without any risk of decreasing the binding activity of the parent analogue. We have reported [5] that an antagonistic pentadecapeptide of LH–RH having two N termini shows a significantly higher antiovulatory activity than the corresponding D-Lys^6 decapeptide.

As this effect gets lost when the epsilon amino group of D-lysine^6 is substituted by other peptides, the increase cannot be ascribed merely to the depolarization of the side chain amino group of lysine. Aromatic D-amino acids in position 6 were found to increase the inhibitory activity of LH–RH analogues much more than the aliphatic D-Lys^6 substitution (**1**, **2** Table I). Thus, according to our expectation, the Y-shaped analogue containing D-*p*-

Table I

Antiovulatory activities of Y-shaped and oligomeric analogues of D-Phe^2*(or* D-Cpa^2*)*,D-Trp^3,D-Lys^6*(or p-amino-*D-Phe^6*)*-LH–RH

No.	Analogue	% Antiovulatory activity ** Dose (μg/rat) 1500	1000	500	250	100	Ref.
1	D-Phe^2,D-Trp^3,D-Cpa^6-LH–RH*		80				[6]
2	D-Phe^2,D-Trp^3,D-Lys^6-LH–RH	0					[6]
3	Glp-D-Phe-D-Trp-Ser-Tyr¬ D-Phe^2,D-Trp^3,D-Lys^6-LH–RH		80				[5]
4	Glp-D-Phe-D-Trp-Ser-Tyr¬ D-Phe^2,D-Trp^3,$\Delta^{4'5}$-D-Lys^6-LH-RH		30				
5	Glp-D-Phe-D-Trp-Ser-Tyr——¬ D-Phe^2,D-Trp^3,*p*-amino-D-Phe^6-LH–RH		100	60			[6]
6	Glp-D-Cpa-D-Trp-Ser-Tyr——¬ D-Cpa^2,D-Trp^3,*p*-amino-D-Phe^6-LH–RH			90	90	20	[6]
7	Succinyl-bis(D-Phe^2,D-Trp^3,D-Lys^6-LH–RH			40			[6]
8	Succinyl-bis-Gly(D-Phe^2,D-Trp^3,D-Lys^6-LH–RH)			40			
9	Muconyl-bis(D-Phe^2,D-Trp^3,D-Lys^6-LH–RH)			40			
10	Terephthaloyl-bis(D-Phe^2,D-Trp^3,D-Lys^6-LH–RH)		100				[6]
11	Isophthaloyl-bis(D-Phe^2,D-Trp^3,D-Lys^6-LH–RH)			60			[6]
12	2,2'-Biphenyl-dicarboxylyl--bis(D-Phe^2,D-Trp^3,D-Lys^6-LH–RH)			50			
13	1,2,3-Propanetricarboxylyl--tris(D-Phe^2,D-Trp^3,D-Lys^6-LH–RH)	0	0				[6]
14	1,3,5-Benzenetricarboxylyl--tris(D-Phe^2,D-Trp^3,D-Lys^6-LH–RH)	0	0				[6]

* D-Cpa = *p*-Chloro-D-phenylalanine

** % Antiovulatory activity $= 100 \times \left(1 - \frac{\text{No. of rats ovulated}}{\text{No. of rats treated}}\right)$

-NH_2-Phe in position 6 (**5**) also proved to be significantly more active than the corresponding D-Lys^6 analogue (**3**) reported upon earlier [5].

The decreased antiovulatory potency of the D-dehydro-Lys^6 analogue (**4**), possibly being due to the aliphatic side chain of the D-amino acid, also seems to corroborate this finding.

Assuming that the extra branched chain can form additional binding to the receptor, we prepared the simplest dimers of antagonists in different series to investigate this effect [6, 7, 21]. The D-Lys^6 analogues can be simply dimerized with the pentafluorophenyl esters of the corresponding dicarboxylic acids, and in this way covalent bonds of different lengths with aliphatic, aromatic, rigid or flexible character can be formed between the two molecules of the antagonistic peptides. Dimerization increased the antiovulatory potency of the corresponding D-Lys^6 analogues (**2:7—12; 17:19—21**) (Tables I—III) by 5—7 times, and again this type of analogues proved to be twice as active as the most effective decapeptide analogue prepared at that time: D-Phe^2, D-Trp^3,D-Phe^6-LH–RH [1]. This effect cannot be explained by the increased resistance toward enzymes [22] and it is not intensive enough to indicate the formation of two hormon-receptor complexes simultaneously. Possibly the extra side chain may be capable of getting into an additional non-specific interaction with the receptor. For the trimeric derivatives (**13**, **14**) (Table I) remaining inactive in contrast to the dimers, it may be assumed that the tridecapeptide chains, being in extremely close sterical proximity, hinder attachment to the receptor.

Parallel with these oligomer studies we further investigated the effect of different groups substituting the benzene ring of the D-Phe in position 2. While D-Cpa^2,D-Ala^6-LH–RH was inactive in vivo, some modest increase in the inhibitory activity of D-Fpa^2,D-Ala^6-LH–RH [23] was reported. This observation, however, has not been utilized for improving some of the new series of inhibitors.

The idea of the D-Cpa substitution in positions 2 and 6 originated from the possibility of tritium labelling [10, 11]. However, due to the increased activity of the analogues obtained [6, 24], tritium exchange was not carried out by this route. In accordance with our expectations, the D-Cpa^6 substitution (**1**) did not bring any significant change in the efficiency of the molecule as compared to the D-Phe^6 analogue [1]. On the other hand, a dramatic effect was observed in different series of analogues in case of D-Cpa in position 2 (**22** $<$ **25**; $A <$ **36**; **5** $<$ **6**) (Tables I, IV, **VII**). The chlorine atom in this position increased the inhibitory activity of the antagonistic analogues by about six-fold on the average.

To investigate the role of aromatic ring substituents, we inserted different D-Phe derivatives into position 2. It was found that while in the D-Glp^1, X^2,D-Trp^3,D-Lys^6 series the effect of Cl and F atoms substituting the D-Phe^2

Table II

*The effect of p-halogeno-*D*-Phe-substitution of* D-Glp[1],X[2],D-Trp[3],D-Lys[6]-LH–RH *on the antiovulatory activity*

No.	Analogue	% Antiovulatory activity Dose (μg/rat)				Ref.
		1500	1000	500	250	
15	D-Glp[1],D-Phe[2]-D-Trp[3]-D-Lys[6]-LH–RH	100		25		[7]
16	/*p*-F *		60			
17	/*p*-Cl		60			[7]
18	/*p*-Br		30			[7]

* *p* refers to the *para* substitution of Phe in the Tables

Table III

The effect of dimerization of D-Glp[1],D-Cpa[2],D-Trp[3],D-Lys[6]-LH–RH *on the antiovulatory activity*

No.	Analogue	% Antiovulatory activity Dose (μg/rat)			Ref.
		500	250	125	
19	Isophthaloyl-bis(D-Glp[1],D-Cpa[2],D-Trp[3],D-Lys[6]-LH–RH)		100	53	[7]
20	*trans*-1,2-cyclohexanoyl-bis-(D-Glp[1],D-Cpa[2],D-Trp[3],D-Lys[6]-LH–RH)	100	50		
21	*trans*-1,4-cyclohexanoyl-bis-(D-Glp[1], D-Cpa[2],D-Trp[3],D-Lys[6]-LH–RH)	100	44		

in *para* position was the same (**16**=**17**) and relatively high as compared with the case of Br atom (**18**) (Table II), the order of efficiency of halogens reversed in the D-Phe[1],X[2],D-Trp[3],D-Phe[6] series; the Cl and even Br were significantly more favourable from the point of inhibitory activity than the F substitution (**25** > **29** > **23**) (Table IV).

The difference between the Cl and F atoms in *para* positions is undoubtedly more expressed in the Ac-D-Phe[1],X[2],D-Trp[3],D-Phe[6] series (**24**, **26**) (Table IV), where the D-Fpa[2] compound is inactive in the dose tested, while the D-Cpa[2] derivative is fully active in a dose of 31 μg. It is interesting to note that the single para substitution by fluorine or chlorine of D-Phe[2] in parallel compounds results in different inhibitory activity of the LH–RH analogues. As more efficient compounds were developed, the *para*-chloro substitution turned out to be significantly more advantageous, as shown in Table V.

While in the D-Ala[6] series the D-Fpa[2] substitution is significantly more active than the D-Cpa[2] in 6×1 mg dose, as it was shown earlier [23], now we have found in the series of those analogues that blocked ovulation at a very

low dose level that D-Cpa substitution was significantly better than D-Fpa substitution.

Thus we can conclude that the aromatic D-amino acids used in the antagonistic analogues of LH–RH generally conserve their properties contributing to the antiovulatory activity, while various substitutions in the aromatic ring may produce changes of different degree. Another example for this divergent effect is that in the Ac-X^1,D-Cpa^2,D-Trp^3,D-Trp^6 series Ac-D-Trp^1 is a more favourable substitution than Ac-D-Phe^1 (**48** $>$ **36**). This is inconsistent with the fact [18] that in the Ac-X^1,D-Phe^2,D-Trp^3,D-Trp^6 series the opposite effect can be observed.

An antiovulatory potency of one order of magnitude greater has been found in some series with *N*-acetyl derivatives, as compared with analogues

Table IV

Antiovulatory activity of D-Phe^1,X^2,D-Trp^3,D-Phe^6-LH–RH *analogues and their acyl derivatives*

No.	Analogue	% Antiovulatory activity Dose (μg/rat)							Ref.
		1000	500	250	125	62	31	15	
22	H-D-Phe^1,D-Phe^2,D-Trp^3,D-Phe^6-LH–RH	0							[7]
23	*p*-F			10					[7]
24	Ac — *p*-F						0		
25	*p*-Cl		100	82	11				[7]
26	Ac — *p*-Cl					100	100	55	[7]
27	Suc — *p*-Cl		100		80	55			[8]
28	TFA — *p*-Cl	0							[8]
29	*p*-Br			50					[7]
30	*p*-NO_2		40						
31	D-Trp		25						
32	Ac — D-Trp				0				

Table V

The antiovulatory potency of D-Fpa^2- *and* D-Cpa^2-*substituted inhibitory analogues of* LH–RH

Compound	Dose	% Antiovulatory activity	
		X = Fpa	X = Cpa
D-Glp^1,X^2,D-Ala^6-LH–RH	6×1 mg	100	0
D-Glp^1,X^2,D-Trp^3,D-Lys^6-LH–RH	1 mg	60	60
D-Phe^1,X^2,D-Trp^3,D-Phe^6-LH–RH	0.25 mg	10	80
Ac-D-Phe^1,X^2,D-Trp^3,D-Phe^6-LH–RH	0.031 mg	0	100

Table VI

Antiovulatory activity of inhibitory LH–RH *analogues*

No.	Analogue	% Antiovulatory activity Dose (μg/rat)						Ref.
		1000	250	125	62	31	15	
33	D-Glp[1],D-Cpa[2],D-Trp[3],D-Trp[6]-LH–RH		30					[7]
34	Ac-L-Phe[1]				10			
35	H-D-Phe[1]			0				[8]
36	Ac-D-Phe[1]				100	64	20	[8]
37	Pr-D-Phe[1]				100	50		
38	Boc-D-Phe[1]		0					
39	Succ-bis-D-Phe[1]	10						

having free N termini (**35** < **36**; **25** < **26**) (Table IV). Since the propionyl (**37**) and the monosuccinoyl (**27**) groups also have a positive effect, this acetyl group is not absolutely essential for the antagonistic activity. When testing compounds containing trifluoroacetyl (**28**) and BOC (**38**) groups, it must be taken into consideration that their very low activity can be due not only to the electronic effect of the acyl-type groups, but also to the expressed apolar character of the molecules. Indeed, both derivatives show unprecedently low solubility in propyleneglycol, PEG-400 or corn oil, thus their effectivity may be significantly influenced by the kinetics and degree of absorption.

Comparing the D-Glp[1] analogue with the Ac-D-Phe[1] (**33** < **36**) (Table VI) in the X[1],D-Cpa[2],D-Trp[3],D-Trp[6] series, it can be seen that the Ac-D-Phe[1] substitution shows better results, presumably as a consequence of the aromatic interaction of the side chains. To study the electronic or sterical effects on the aromatic character, we prepared some D-Phe[1] derivatives in this series too.

First the Ac-D-Phe[1] substitution (**36**) was changed to its optical antipode (**34**). In this case, the antiovulatory potency decreased by 10 times, indicating the important role of configuration in this position. This phenomenon seems to contradict the findings (**25**) that the Ac-L-Pro[1],D-Phe[2],D-Trp[3],D-Trp[6] analogue is better than the corresponding Ac-D-Pro[1] analogue. Again, this provides another example for the antagonistic character of the molecule being determined by all components and by the joint conformation of all amino acids.

As Ac-L-Phe[1] [25] did not prove to be a useful substitution, we applied Ac-D-Phe in position 1 [26] and, since the acetylation of the N termini contributed to the biological activity to the highest degree, we prepared some derivatives of D-Phe[2] substituted in its aromatic ring in the Ac-D-Phe[1],X[2],

D-Trp[3]-D-Trp[6] series too. Similarly to the D-Phe[1]-substituted analogues (see later), it was found in every case that the peptides with D-phenylalanines substituted in *para* position had higher antiovulatory potency than the D-Phe[2]-containing peptides ($A < 36$; $A < 42$). However, no clear structure–activity relationship can be observed between any property of the substituent and its biological efficiency. Comparing the D-Cpa-containing compound (**40**) with analogue *A* (Table VII.), it can be seen that the decrease in antiovulatory potency in case of *ortho* substitution may be caused by unfavourable sterical effects. This also indicates the importance of the *para* position of the Cl atom in this aromatic ring.

By exchanging the hydrogen in *para* position of D-Phe[1] for halogens or a methyl group ($36 < 46 = 47 < 44 < 45 < 48$ and $A < 43$) (Tables VII,

Table VII

The effect of Phe-ring substitution of Ac-D-Phe[1],D-Phe[2],D-Trp[3],D-Trp[6]-LH–RH *on the antiovulatory activity*

No.	Analogue	% Antiovulatory activity Dose (μg/rat)					Ref.
		250	125	62	31	15	
A	Ac-D-Phe[1],D-Phe[2],D-Trp[3],D-Trp[6]-LH–RH	100	30[a]				[26]
36	*p*-Cl			100	64	20	[8]
40	*p*-Cl *		0				[29]
41	*p*-Me				20		[29]
42	*p*-OH				10		[29]
43	*p*-Cl		90				

[a] Dose = 100 μg
* *o*- refers to the *ortho* substitution of Phe in the Tables

Table VIII

The effect of X[1] *substitution of* Ac-X[1],D-Cpa[2],D-Trp[3],D-Trp[6]-LH–RH *on the antiovulatory activity*

No.	Analogue	% Antiovulatory activity Dose (μg/rat)			Ref.
		62	31	15	
36	Ac-D-Phe[1],D-Cpa[2],D-Trp[6]-LH-RH	100	63	20	[8]
44	*p*-Cl			70	[27]
45	*p*-F			80	[27]
46	*p*-Br			50	[27]
47	*p*-Me			50	[27]
48	Ac-D-Trp			90	[27]

Table IX

The effect of substitution in position **1** *of* Ac-X[1],D-Cpa[2],D-Trp[3],D-Phe[6],D-Ala[10] *on the antiovulatory activity*

No.	Analogue	% Antiovulatory activity Dose (μg/rat)					Ref.
		50	30	25	10	5	
49	Ac-D-Trp[1],D-Cpa[2],D-Trp[3],D-Phe[6],D-Ala[10]-LH–RH				100	60	[31]
50	Ac-D-Phe[1]		100	70			
51	Ac-Sar[1]	50		30			[31]
52	Ac-Gly[1]	60		30			[31]

Table X

The antiovulatory activity of inhibitory analogues of LH–RH-*containing "preferred" substitutions as tested in single dose and long-term dose injections.*

For experimental details, see text

Analogue	% Antiovulatory activity					
	Single dose, μg/rat				Long-term (12 days) dose, μg/day	
	10	5	2	1	10	5
49 Ac-D-Trp[1],D-Cpa[2],D-Trp[3],D-Phe[6],D-Ala[10]- -LH–RH	100	60			40	
53 Ac-D-Trp[1],D-Cpa[2],D-Trp[3],D-Lys[6],D-Ala[10]- -LH–RH		100	100	40		100

VIII), an equally modest increase in activity can be obtained but, as in the case of substituents in position 2 (see above), no direct correlation between the properties and effect of the substituents can be established [27]. The compound with Ac-D-Trp[1] (**48**) has the most outstanding inhibitory effect among the analogues listed in Table VIII. It was also found that D-Phe[6] substitution is more favourable than D-Trp[6] in the D-Phe[1],D-Cpa[2],D-Trp[3],X[6] series (**25** > **35**) and in the Ac-D-Phe[1],D-Cpa[2],D-Trp[3],X[6] series (**26** > **36**).

Based on the substitutions presented and comparing the efficiencies of individual amino acid substitutions in increasing the antiovulatory potency of LH–RH analogues, one can conclude that favourable modifications are:

(a) Ac-D-Trp in position 1,

(b) D-Cpa in position 2,

(c) D-Phe (better than D-Trp) in position 6.

As a working hypothesis, we assumed a certain degree of additivity of the individual substitutions, as already observed in the case of other peptide

Table XI

Amino acid analyses and R_f values of peptides

Compound	Ser	Glu	Pro	Gly	Leu	Tyr	Phe	Lys	Trp	Arg		R_f			
1	1.03	0.97	0.91	1.00	0.92	0.83	0.94			0.94	1.03+	0.85[A],	0.50[B],	0.30[G],	0.20[J]
2	0.92	1.08	1.06	1.00	0.95	0.99	0.98	0.97	0.88	0.97		0.40[A],	0.20[B],	0.70[D],	0.50[G]
4	1.86	2.10	1.00	1.00	1.00	1.86	2.15			0.96		0.90[A],	0.55[B],	0.99[D],	0.15[J]
6	2.14	2.14	0.98	1.04	0.92	1.75			0.92	1.05	2.06+	0.75[A],	0.45[B],	0.80[D],	0.80[G]
7	0.90	1.13	1.05	1.00	1.01	0.99	0.99	0.95	0.89	1.02		0.55[A],	0.25[B],	0.80[D],	0.50[G]
8	0.96	1.15	1.04	1.96	1.05	0.96	1.00	0.95		1.03		0.30[B],	0.70[A],	0.90[D],	0.53[G]
9	0.95	1.05	1.00	1.00	0.95	0.90	0.95	0.96		0.95		0.80[A],	0.30[B],	0.70[D],	0.05[J]
10	0.87	1.06	1.00	1.00	1.09	1.01	0.99	1.00	0.82	1.00		0.70[A],	0.40[B],	0.65[G],	0.20[J]
11	0.95	1.15	1.05	1.00	1.02	0.98	0.99	0.97	0.90	1.05		0.70[A],	0.25[B],	0.90[D],	0.50[G]
12												0.75[A],	0.30[B],	0.40[D],	0.90[G]
13	0.87	1.08	1.06	1.14	1.01	1.00	1.00	0.80		1.02		0.60[A],	0.20[B],	0.70[D],	0.50[G]
14	0.92	1.12	1.06	1.02	1.01	0.99	0.99	1.01		1.01		0.55[A],	0.20[B],	0.70[D],	0.50[G]
16	0.92	0.99	0.96	1.00	1.00	0.95		0.94	1.05	0.97		0.53[A],	0.13[B],	0.52[C],	0.50[G]
17	0.90	1.06	1.00	1.00	1.02	0.95		0.96	1.05	0.96		0.56[A],	0.14[B],	0.53[C],	0.81[D]
18	0.90	1.05	0.96	1.00	1.00	0.95		0.96	1.07	1.97*		0.52[A],	0.15[B],	0.53[C],	0.52[G]
19	0.89	1.06	0.98	1.00	1.02	0.99		0.95	0.94	1.04		0.61[A],	0.28[B],	0.61[C],	
20	0.91	1.08	0.97	1.00	1.00	0.97		0.95	0.94	0.96		0.65[A],	0.25[B],	0.62[C],	0.61[G]
21	0.91	1.08	0.98	1.00	1.02	0.99		0.90	0.94	1.04		0.60[A],	0.27[B],	0.60[C],	0.79[D]
22	0.90		1.00	1.05	1.05	0.96	3.07		0.95	1.00		0.78[A],	0.43[B],	0.59[C],	0.49[E]
23	0.90		1.03	1.05	1.00	0.98	1.95		0.93	1.10		0.81[A],	0.45[B],	0.59[C],	0.51[E]
25	0.86		0.94	1.00	1.01	0.98	1.93		0.90	0.98		0.81[A],	0.46[B],	0.59[C],	0.52[E]
26	0.88		0.98	1.06	1.06	1.00	2.05		0.88	1.06		0.66[A],	0.53[B],	0.14[E],	0.76[F]
27	0.88		0.98	1.00	1.09	1.06	1.98		0.87	1.01		0.70[A],	0.51[B],	0.96[D],	0.70[G]

28	0.87	0.97	1.03	1.00	0.97	1.18**		1.03	0.94+	0.82^{A},	0.52^{B},	0.68^{C},	0.57^{E}
29	0.83	0.94	1.00	1.01	0.98	1.84	0.80	1.84*		0.81^{A},	0.47^{B},	0.59^{C},	0.54^{E}
30										0.66^{A},	0.39^{B},	0.64^{C},	0.80^{D}
31	0.91	0.97	1.00	1.00	0.96	1.97	2.10	0.97		0.64^{A},	0.38^{B},	0.63^{C},	0.72^{F}
32	0.89	1.00	0.99	1.02	1.00	2.00	1.95	0.96		0.65^{A},	0.51^{B},	0.12^{E},	0.75^{F}
35	0.91	0.97	1.07	1.09	0.98	0.97	1.80	1.01		0.66^{A},	0.54^{B},	0.64^{C},	0.15^{F}
36	0.93	1.02	1.03	1.09	1.00	1.02	1.90	1.01		0.71^{A},	0.63^{B},	0.66^{C},	0.26^{F}
38	1.05	1.01	1.00	1.02	0.94	0.95	1.92	0.98	0.96+	0.80^{A},	0.65^{B},	0.85^{G},	0.60^{J}
39	0.89	1.04	1.00	1.09	1.07	2.14	0.94	1.04		0.77^{A}			
43	1.00	0.98	1.01	1.00	1.01	0.96	2.07	1.05		0.82^{A},	0.81^{B},	0.12^{E},	0.75^{F}
50	0.95	0.98		1.00	0.96	1.96	0.97	1.02	1.01+++	0.74^{A},	0.76^{G},	0.60^{I},	0.60^{J}

\+ Cpa was estimated only in special cases
++ Asp, +++ Ala

* *p*-bromophenylalanine was estimated with Arg together
** 36 h hydrolysate; low Phe content due to acid stability of TFA group

A *n*-BuOH : AcOH : H_2O : EtOAc — 1 : 1 : 1 : 1
B *n*-BuOH : AcOH : H_2O — 4 : 1 : 5 up
C *n*-BuOH : Pyr : AcOH : H_2O — 15 : 10 : 3 : 12
D EtOAc : Pyr : AcOH : H_2O — 5 : 5 : 1 : 3
E EtOAc : Pyr : AcOH : H_2O — 20 : 5 : 1 : 3
F 2-PrOH : cc.NH_4OH : H_2O — 15 : 1 : 14
G 2-PrOH : 1*N* AcOH — 2 : 1
H $CHCl_3$: AcOH — 95 : 5
I *n*-BuOH : AcOH : H_2O — 4 : 1 : 1
J EtOAc : Pyr : AcOH : H_2O — 60 : 20 : 6 : 11

hormones [28]. Thus we designed an analogue combining the above substitutions, of which we expected increased ovulation inhibition, provided additivity was valid. The resulting analogue, Ac-D-Trp[1],D-Cpa[2],D-Trp[3],D-Phe[6],D-Ala[10]--LH–RH (**49**) [27, 29] proved to be very effective and inhibited ovulation in a significantly lower dose than any of the analogues reported earlier. Our working hypothesis was thus confirmed and it can be assumed that, at least within a limited range, additivity arising of the combination of certain substituents is in effect.

In the series of acyl-X[1],D-Cpa[2],D-Trp[3],D-Phe[6],D-Ala[10] we investigated the contribution of the acyl group to the ovulation inhibitory effect of the analogues. Larger lipophilic groups decreased the inhibitory effectivity of the peptides [30], which is in good agreement with observations of Rivier et al., [31] who found a similar tendency in the acyl-dehydro-Pro[1],D-Cpa[2], D-Trp[3,6],*N*MeLeu[7]-LH–RH series.

In the csae of position 1, we found the presence of aromatic D-amino acids not to be an absolute requirement, however, bulky aromatic amino acids significantly increase the inhibitory potency of the peptides (**49** > **50** > > **51** = **52**) (Table IX). Ac-Gly[1] substitution yielded a significantly less active compound than in the X[1],D-Cpa[2],D-Trp[3,6]-LH–RH series [32].

More recently, photoaffinity labelling has been widely used for studying hormone–receptor interactions [33, 34], for which a very convenient approach is the introduction of the nitrophenyl-azidosulfenyl group via the ε-amino group of lysine [35]. It had earlier been reported that in the case of LH–RH inhibitory analogues, the side chain of D-Lys[6] can be acylated without loss of activity [5, 26]. Thus, an analogue containing D-Lys[6] substitution could serve as a suitable starting compound for photoaffinity labelling. Our earlier studies [6, 7] found dimers of D-Lys[6]-containing antagonists to show higher antiovulatory potency than the corresponding monomeric compounds.

According to the rationale discussed above, i.e. combining several substitutions with expected additivity, we exchanged D-Phe[6] for D-Lys[6] while leaving substituents 1,2,3 and 10 identical with compound **49**, and prepared Ac-D-Trp[1],D-Cpa[2],D-Trp[3],D-Lys[6],D-Ala[10]-LH–RH (**53**). The analogue, which is water-soluble shows extremely high antiovulatory activity. In rats, a 2 μg single dose fully blocks ovulation and even a 1 μg injection leads to 40% inhibition of ovulation (Table X).

The compound has a further outstanding characteristic. While analogue **49** during long-term application (12 days) in a 10 μg daily dose could prevent ovulation only in 40% of the animals, analogue **53** during 12 days in 5 μg daily dose, i.e. only 2.5 times the fully inhibitory single dose, completely inhibited ovulation in all 10 animals of the experiment. Vaginal smears of the rats showed constant estrus with occasional signs of methestrus. Such an observation was made only with Ac-dehydro-Pro[1],D-Cpa[2],D-Trp[3,6],*N*Meleu[7]-

-LH–RH which in a 20 μg single dose fully inhibits ovulation and in 10 μg results in 50% blockade of ovulation [37]. However, during long-term application for 14 days, a daily dose of 1 mg was required, i.e. 50 times the fully effective single dose, for maintaning signs of estrus, while, daily 500 μg only partially inhibited ovulation.

Conclusion

The results obtained with analogue **53**, i.e. substitution of an aromatic D-amino acid by D-Lys[6] increased the inhibitory potency in contrast to the effect observed with analogues **33** and **17**, leading to the following conclusions.

Although there is additivity of substituent combination in a given series of analogues, this is likely to be restricted to certain combinations. A specific substitution which may be very advantageous in one series of LH–RH antagonists, may not be so in another series. Thus, the effectiveness of a certain substituent is basically dependent on the structure of the whole molecule, i.e. the combination with other substitutions.

Other examples, in this work, like the aromatic halogen substitutions of D-Phe[2] in several series of acetyl-L-amino acids and acetyl-D-amino acids also support these conclusions.

Experimental

The amino acids used for the syntheses were generally of L-configuration; only D-configuration is stated. Amino acids were resolved by selective enzymatic hydrolysis of their TFA derivatives [27]. DL-*p*-Chlorophenylalanine was resolved by chemical means [10].

The syntheses of compounds **3** [5], **41**–**43** and **45**–**49** [27], **50** and **52**–**53** [31] have been described elsewhere.

The following side chain protecting groups were used: Arg, tosyl; D-Lys, 4-chloro-Z; Tyr, for **1**–**14** 2-bromo-Bzl, for **15**–**49** unprotected [38], for **50**–**54** benzyl; Ser, benzyl; D-*p*-NH_2-Phe, NPS.

All peptides were prepared by the Merrifield method on BHA resin by a previously described procedure [39]. Crude peptides were cleaved from the resin by liquid HF at 0 °C for 45–60 min. Purification of compounds **1**–**6** was carried out in the following way: first eluted on a column of Sephadex G 25 F in 0.2 *M* AcOH solution then on a partition column of Sephadex G 50 in BuOH-Pyr-AcOH–H_2O (7 : 1 : 2 : 10) solvent system, and finally the products were purified on Sephadex G 50 F in 50% AcOH. Purification of compounds **15**–**54** was carried out by gel filtration on Sephadex G 25F column (2.5×100 cm) in 50% acetic acid. The fractions were pooled and evaporated, then applied on to silica gel column (2×150 cm) equilibrated with ethyl acetate–pyridine–acetic acid–water (20 : 5 : 1 : 3) or equilibrated with *n*-butanol–acetic acid–water (4 : 1 : 1 or 5 : 1 : 1). The separations were followed by thin-layer chromatography on SiO_2 plates.

The fractions containing the desired peptides, as estimated by thin-layer chromatography using appropriate visualizing reagents (ninhydrin, Ehrlich, chlorine–*o*-toluidine), were pooled, evaporated and lyophilized. Homogeneity of the final products was checked by TLC developed in four different solvent systems in loads of approximately 30 to 50 μg. Purifications were continued until homogeneous peptides were obtained. Final yields of approximately 10 to 25% based on the starting BOC-amino acid-resin were typically achieved. Amino acid analyses were performed in a Beckman Model 119 and JEOL JCL-5AH amino acid analyzer

on samples hydrolyzed (110 °C, 24 h) in 4 *M* methanesulfonic acid. The amino acid analyses and R_f values can be seen in Table XI. Optical rotations were determined by a PERKIN-ELMER 241 polarimeter.

The branched chain peptides (**4, 5, 6**) were prepared by the usual solid phase technique, except that BOC-D-Phe(NH-NPS) and BOC-dehydro-D-Lys (ε-BOC) were incorporated in the 6 position. Simultaneous removal of the NPS and BOC groups with TFA/33% in dichloromethane allowed the remaining part of the peptide (in 1 mmol scale) to be extended from two points.

General procedure for dimerization of peptides with pentafluorophenyl active esters

Synthesis of dicarboxylic acid active esters

The dicarboxylic acid (1 mmol) and pentafluorphenol (2 mmol) were dissolved in 2 mL of DMF and DCC (2.2 mmol), was added at 0 °C. The reaction mixture was stirred for 2 h then the precipitated urea derivative was filtered off and the DMF was evaporated. The crude material was crystallized from ether or ethyl acetate.

Dimerization of D-Lys^6 analogues of LH—RH

The LH–RH analogue (10 μM) containing D-Lys in position 6 (**2, 17**) was dissolved in 1 mL of DMF and to this solution 1 equivalent of freshly prepared di- or tricarboxylic acid active ester was added at 0 °C. The conversion could be readily followed by TLC. After stirring the reaction mixture for 12 h, the solvent was evaporated in vacuum. In order to remove the small molecular weight fractions, the crude material was eluted on a column of Sephadex G50 in 50% AcOH. The tri- and dimeric compounds moved faster then the monomer in every case. In some cases the molecular weight was determined from the electrophoretic mobility of the peptides, or by HPLC method [22]. In the case of peptide **7** the relative glycine content of the analogue directly proved the dimeric structure. Dimerization of the compounds of the D-Lys^6-series proved to be an easy reaction, the yield exceeded 60 – 70%. Attempted dimerization of the H-D-Phe^1 compound by the *N*-terminal using pentafluorophenyl isophthalate was unsuccessful. **The monosuccinyl derivative (27)** was isolated when dimerization was attempted using succinyl dichloride as dicarboxylic acid derivative.

In the case of compound **12**, 2,2'-biphenyldicarboxylic acid bis-*p*-nitrophenyl ester was used, because the bis-pentafluorophenyl ester did not lead to sufficient dimerization.

Succinyl-bis(D-Phe^1, D-Cpa^2, D-Trp^3, D-Phe^6-LH–RH) (39) was synthesized by a special solid phase synthesis. After deprotection of the corresponding LH–RH-decapeptide-resin, it was allowed to react with a three-fold excess of dipentafluorophenyl succinate for 24 h in DMF. The excess of the active ester was removed by filtration. The resin did not give positive ninhydrin test. The resulting "active ester-resin" was compled with a large excess of D-Phe^1, D-Cpa^2,D-Trp^3,D-Phe^6,LH–RH (**25**) in DMF. The excess of **25** was removed and the dimeric peptide was cleaved from the resin in the usual way. The purification of the dimer was carried out in 80% acetic acid because of the low solubility of compound **39**.

Bioassay

All peptides were assayed for antiovulatory activity in adult female rats. Only those rats exhibiting at least two consecutive 4-day cycles were used. All peptides were administered s.c. in propylene glycol-saline, PEG 400, or corn oil at noon on the day of proestrus. All rats were autopsied on the morning of estrus and the absence of ova was ascertained under a microscope.

REFERENCES

[1] Coy, D. H., Vilchez-Martinez, J. A., Schally, A. V.: in Peptides, 1976. pp. 463. (Ed.: Loffet, A.) Editions de l'Université de Bruxelles, Brussels 1977

[2] Vale, W., Grant, G., Rivier, J., Monahan, M., Amoss, M., Blackwell, R., Burgus, R. Guillemin, R.: Science, **176,** 933 (1972)

[3] Coy, D. H., Vilchez-Martinez, J. A., Coy, E. J., Arimura, A., Schally, A. V.: J. Clin. Endocrinol. Metab., **37,** 331 (1973)

[4] Rees, R. W. A., Foell, T. J., Chai, S., Grant, N.: J. Med. Chem., **17,** 1016 (1974)
[5] Seprődi, J., Coy, D. H., Vilchez-Martinez, J. A., Pedroza, E., Schally, A. V.: J. Med. Chem., **21,** 276 (1978)
[6] Seprődi, J., Coy, D. H., Teplán, I., Schally, A. V.: in Peptides, 1978, p. 499. Wrocław University Press, Poland 1979
[7] Coy, D. H., Mező, I., Pedroza, E., Nekola, M. V., Vilchez-Martinez, J., Piyachaturawat, P., Schally, A. V., Seprődi, J., Teplán, I : in Peptides: Structures and Biological Function. Proceedings of 6th American Peptide Symposium, p. 775. (Ed.: Gross, E., Meienhofer, J.) Pierce Chem. Co., Rockford 1979
[8] Coy, D. H., Seprődi, J., Vilchez-Martinez, J. A., Pedroza, E., Gardner, J., Schally, A. V.: in Central Nervous System Effects of Hypothalamic Hormones and Other Peptides, p. 317. (Ed.: Collu, E., Barbeau, A., Ducharme, J. R., Rochefort, J. G.). Raven Press, New York 1979
[9] Gonzalez-Barcena, D., Kastin, A. J., Coy, D. H., Nikolics, K., Schally, A. V.: Lancet, **2,** 997 (1977)
[10] Kovács, J., Teplán, I., Mező, I.: Acta Chim. **84,** (Budapest) 109 (1975)
[11] Mező, I., Teplán, I., Seprődi, J., Morgat, J. L., Fromageot, P., Tóth, G., Sirokmán, F.: J. Lab. Comp. Radiopharm., **14,** 557 (1978)
[12] Seprődi, J., Teplán, I., Magocsi, M., Medzihradszky, K.: Acta Chim. Acad. Sci. Hung., **104,** 227 (1980)
[13] Bienert, M., Klauschenz, E., Ehrlich, A., Katzwinkel, S., Niedrich, H., Tóth, G., Teplán, I.: J. Lab. Comp. Radiopharm., **14,** 577 (1978)
[14] Bienert, M., Klauschenz, E., Ehrlich, A., Katzwinkel, S., Niedrich, H., Tóth, G., Teplán, I.: J. Lab. Comp. Radiopharm., **16,** 673 (1979)
[15] Kéri, Gy., Teplán, I.: J. Lab. Comp. Radiopharm., **15,** 153 (1978)
[16] Rivier, J. E., Vale, W.: Life Sci., **23,** 869 (1978)
[17] Rivier, C., Rivier, J., Vale, W.: Science, **210,** 94 (1980)
[18] Channabasavaiah, K., Stewart, J. M.: Biochem. Biophys. Res. Commun., **86,** 1266 (1979)
[19] Seprődi, J., Coy, D. H., Vilchez, J. A., Pedroza, E., Huang, W., Schally, A. V.: J. Med. Chem., **21,** 993 (1978)
[20] Sandow, J., König, W., Geiger, R., Uhmann, R., von Rechenberg, W.: in Control of Ovulation, p. 49. (Ed: Crighton, D. B. et al.) Butterworths, London—Boston 1978
[21] Coy, D. A., Mező, I., Pedroza, E., Nekola, M. V., Schally, A. V., Murphy, W., Meyers, C. A.: in Polypeptide Hormones, p. 185. (Ed.: Beers, R. F. Jr., Bassett, E. G.) Raven Press, New York 1980
[22] Nikolics, K., Teplán, I.: in Königsteiner Chromatographie Symp., **4,** 32 (1979)
[23] Beattie, C. W., Corbin, A., Foell, T. J., Garsky, V., McKinley, W. A., Rees, R. W., Sarantakis, D., Yardley, J. P.: J. Med. Chem., **18,** 1247 (1975)
[24] Nikolics, K., Bieglmayer, C., Spona, J., Seprődi, J., Teplán, I.: Peptides, **2,** 65 (1981)
[25] Humphries, J., Wasiak, T., Wan, Y. P., Folkers, K., Bowers, C. Y.: Biochem. Biophys. Res. Commun., **85,** 709 (1978)
[26] Érchegyi, J., J., Coy, D. H., Nekola, M. V., Coy, E. J., Shally, A. V., Mező, I., Teplán, I.: Biochem. Biophys. Res. Commun., **100,** 915 (1981)
[27] Érchegyi, J., Coy, D. H., Nekola, M. V., Pedroza, E., Coy, E. J., Mező, I., Schally, A. V.: Peptides, **2,** 251 (1981)
[28] Sawyer, W. H., Grzonka, Z., Manning, M : Mol. Cell. Endocrinol,. **22,** 117 (1981)
[29] Mező, I., Seprődi, J., Érchegyi, J., Teplán, I., Coy, D. H., Schally, A. V.: in Drugs Biochemistry and Metabolism. Suppl. 1. (Ed.: Klebovich, J., Laszlovszky, I., Rosdy, B.) Biochem. Section Hung. Chem. Soc., Budapest 1981
[30] Mező, I., Seprődi, J., Érchegyi, J., Teplán, I., Kovács, M., Flerkó, B.: Peptides, **4,** 149 (1983)
[31] Rivier, J., Rivier, C., Perrin, M., Porter, J., Vale, W.: in Peptides 1980, p. 566. (Ed. Brunfeldt, K.) Scriptor, Copenhagen 1981
[32] Spatola, A. F., Agarwal, N. S.: Biochem. Biophys. Res. Commun., **97,** 1571 (1980)
[33] Bayley, A., Knowles, J. R.: Methods Enzymol., **46,** 69 (1977)
[34] Chaudry, V., Westheimer, F. H.: Ann. Rev. Biochem., **48,** 293 (1979)
[35] Muramoto, K., Ramachandran, J.: Biochemistry, **19,** 3280 (1980)
[36] Ling, N. C., Rivier, J. E., Monahan, M. W., Vale, W. W.: J. Med. Chem., **19,** 937 (1976)
[37] Rivier, C., Rivier, J., Vale, W.: Endocrinol., **108,** 1425 (1981)
[38] Coy, D. H., Branyas, N.: Int. J. Pept. Protein Res., **14,** 339 (1979)
[39] Coy, D. H., Coy, E. J., Schally, A. V., Vilchez-Martinez, J. A., Debeljuk, L., Carter, W. A., Arimura, A.: Biochemistry, **13,** 323 (1974)

BOOK REVIEWS

Advances in Polymer Science, Vol. **48**

Springer-Verlag, Berlin, Heidelberg, New York, 1983

The volume contains two articles, both of them dealing with new methods of polymer investigations developed from the classical technique of light scattering.

W. Burchard: Static and Dynamic Light Scattering from Branched Polymers and Biopolymers. (125 pages, with 242 references)

For branched macromolecules in dilute solution, the shape of the molecules is measured by static light scattering; the internal mobility and the translational motion of the mass centre can be obtained by dynamic light scattering. The following quantities are measured by the two light scattering techniques: the mass average molecular mass M_m, the z-averages of the mean square radius of gyration $(S^2)_z$, the particle scattering factor $P_z(q)$, the translational diffusion coefficient D_z, and the reduced first cumulant Γ/q^2.

The article present various techniques for the calculation of the measurable quantities, extends the theory from the regularly branched chains to randomly branched polymers.

The review is a very good summary of the possibilities and applicability of light scattering to branched polymers. The results, in particular the conditions of gelation and the conformation, are important determining properties of the macromolecules.

Gray D. Patterson: Photon Correlation Spectroscopy of Bulk Polymers. (35 pages, 63 references)

Bulk polymers show slowly relaxing fluctuations in density and optical anisotropy near the glass transition. Photon correlation spectroscopy (PCS) is used for the study of these phenomena. The dynamic light scattering theory is applied for polymers. Experimental data are collected on the dynamics of fluctuations near the glass transition in polymers.

The method is a valuable technique in the study of the dynamics of glass transition. The paper summarizes the results of all published data on the subject of PCS of bulk polymers, and gives a good stimulation for further studies.

Research Institute
for the Plastics Industry,
Budapest

G. Bodor

Proceedings of the Fifth Tihany Symposium on Radiation Chemistry

Ed.: J. Dobó, P. Hedvig, and R. Schiller, Akadémiai Kiadó, Budapest, 1983, p. 1142

The Radiation Chemistry Symposia convened at Tihany or at various localities near Lake Balaton, have earned international acceptance and reputation in the course of the last twenty years. Already the first of these symposia (Tihany, 1962), held not long after the easing up on the "embargo" of nuclear sciences, was a meeting of radiation chemistry scientists from Eastern and from Western Europe, and was a dialogue by direct discussions of participants. The increasingly high repute of the further occasions in this series (Tihany 1966, Balatonfüred 1971, Keszthely 1976, Siófok 1982), with the participation of colleagues also from overseas, has been merited by this straight dialogue maintained by lively professional debates and, last but not least, by the fact that the Hungarian Academy of Sciences published, in book form, the text of lectures as well as the discussions within a very short time following the symposia.

In this instance, seven months after its end, the complete subject matter of the last i.e. Fifth Tihany Symposium has been issued in two volumes. The English text of all the 145 lectures, together with questions and answers, is printed in this book of 1142 pages. The two bulky volumes contain five chapters, viz.

General problems, 179 pages,
Aqueous and inorganic systems, 242 pages.
Organic materials, 288 pages,
Polymers, 296 pages,
Biological problems, 115 pages.

In the first chapter, which deals with general problems, we find interesting studies about electron capture processes, behaviour of solvated electrons, charge-transfer reactions as elementary processes of radiation chemistry as well as data relevant to exotic phenomena like the dependence of the β-hyperfine coupling constant of muon-electrons on temperature and the consequence of this. Several papers are about the formation of a positronium.

Innumerable questions of theory are still unanswered concerning the radiation chemistry of aqueous solutions and inorganic systems. Professor Schuler's study, at the head of Chapter 2, concerning reactions of ·OH radicals with scavengers provoked a debate which lasted perhaps longer than the lecture itself. Techniques of pulse radiolysis, and pulse photoelectron emission induced by a laser, produced new data and explanations which were received with great attention. Likewise, results rich in information concerning gamma-radiolysis of aqueous solutions, which had been achieved by a combination of computerized mass spectrometry and gas chromatography data commanded deep interest.

The basic-research character of such and similar papers in this book is obvious. It should not be forgotten however, that these researches help to elucidate, among other things, details of fundamental processes involved in radiation-induced changes that occur inside living cells. On the other hand, these studies closely affect the highly important and rapidly expanding field of such radiation technologies as preserving of foodstuff or the rather promising technique of waste water treatment.

Similarly pertinent to pure science is the majority of papers in Chapter 3, concerning the radiation chemistry of organic compounds. Experiments with a radiation source like a linear accelerator of 45 MeV delivering 11 ns electron pulses, or an electron-synchroton, are indeed far from industrial applications. But the systems studied are important aliphatic or aromatic hydrocarbons or chlorinated hydrocarbons. The radiation chemistry of various sulfohydryl compounds (thiols) is important because of their protective effects against radiation. New results achieved with organic chemical dosimeters (alanine and glutamine dosimeter, alcoholic chlorobenzene dosimeter dissolved in trimethylpentane) are applicable in measuring techniques in connection with industrial processes.

Chapter 4, about the radiation chemistry of synthetic polymers, is the closest to industrial radiation chemistry. The study reported by Professor Silverman is a good example of the fact that also in the chemical background of radiation technologies already long applied by industries, further results can be achieved by thorough research. Silverman and his team have shown, by means of a high-resolution ^{13}C-NMR method, that in the course of radiation crosslinking of polyolefins the reactions between terminal vinyl groups and secondary alkyl radicals are prominently important besides the union of secondary alkyl radicals which was considered to be the most important reaction of the gel formation process. The proposed new reaction mechanism explains why gel formation that takes place in the amorphous phase of solid polyethylene can be effected with the help of relatively small radiation doses.

The book contains several very interesting papers about crosslinking of polyolefins and PVC. The more and important polymer emulsions, e.g. acrylate polymer latexes, also can be prepared by means of radiation chemical techniques which yield products having greater molecular mass, and less residual monomer content, as it has been reported by the members of research teams of the Karpov Institute of worldwide renown. Less was said about radiation homopolymerization and graft-polymerization. Production by irradiation of combinations of synthetic polymers with cellulose and cellulose-based systems seems to be interesting.

This is the first time that radiation chemical reactions of biological substances were included in the programme of a Tihany symposium. The short, concluding chapter which deals with these, consists mainly of discussions focused on questions pertinent to the chemistry of polymers.

Likewise it is the first time in the series of Tihany Radiation Chemistry Symposia that the book which contains the proceedings is made photographically from camera ready typescript pages. It is to the credit of the devoted care of the editors that through their correcting

unintelligible parts, re-typing several papers, uniformly presenting the discussions the book has become a homogeneous, well constructed work at a high level both of contents and exterior.

In this book we read — in professor Charlesby's paper about the application of the pulse NMR technique in the study of crosslinking by radiation methods — that radiation chemical research follows two distinct paths. On the one hand it dissects increasingly complex fundamental processes of radiation chemistry and from the point of view of a rapidly decreasing time-scale, on the other hand, it reveals the practical application of radiation technologies on levels of increasingly finer details. A survey of this book as a whole seems to suggest that in the last Tihany symposia reports on fundamental research are accorded ever greater prominence, as evidenced by the majority of research papers of high quality offered by authors from Middle or Eastern Europe. True, a considerable part of these efforts is clearly linked to industrial radiation chemistry, viz. sterilization by irradiation of medical appliances made of plastics; production of materials of use in atomic power plant; crosslinking of substances to be used in the electrical industry and packaging. Unfortunately, the most dynamically expanding field of radiation chemical technologies: the surface coating is hardly mentioned in this book. This is regrettable because the practice of the solvent-free and energy saving application of polymer systems (like polyester-acrylates, epoxy-acrylates, silicone-acrylates) for the electron beam curable (EBC) coating of surfaces like paper, wood, metals, and plastics has progressed much farther than the elucidation of the chemical mechanisms pertinent to.

This is, of course, no fault of the editors or of the publisher, the book being proceedings of a series of lectures delivered.

This book, unreservedly recommended to every expert and student of radiation and photochemistry, proves that the specialists now traditionally convening at this delightful spot of Middle-Europe do excel in several fields of fundamental and applied radiation chemistry.

Research Institute of the Plastics Industry,
Budapest

T. CZVIKOVSZKY

PRINTED IN HUNGARY

Akadémiai Kiadó és Nyomda, Budapest

Text

The text of the paper should be concise. The description of new compounds (in the Experimental) must include the complete analytical data. Special attention must be paid to structural formulas given within the text. Complicated (non-linear) formulas should be drawn on separate sheets of paper and their position in the text should be clearly marked. The numbering of formulas and equations (in parentheses on the right-hand side) is only needed if they are referred to in the text. Units should conform to the International System of Units (SI). In nomenclature the rules of the I.U.P.A.C. are accepted as standard. Symbols for physical quantities are printed in italic type and should, therefore, be underlined in the manuscript.

References

References should be numbered in order of appearance in the text (where the reference number appears in brackets) and listed at the end of the paper. The reference list, too, should be typed double-spaced. Journal titles are to be abbreviated as defined by the Chemical Abstracts Service Source Index.

Examples:

[1] Brossi, A., Lindlar, H., Walter, M., Schneider, O.: Helv. Chim. Acta, **41**, 119 (1958)
[2] Parr, R. G.: Quantum Theory of Molecular Electronic Structure. Benjamin, New York 1964
[3] Warshel, A.: in Modern Theoretical Chemistry, Vol. 7, Part A (Ed. G. A. Segal), Plenum Press, New York 1977

Tables

Each table should be given a Roman number and a brief informative title. Structural formulas should not be used in column headings or in the body of tables.

Figures

Figures should be numbered consecutively with Arabic numerals. Their approximate place should be indicated in the text on the margin. All figures must be identified on the back by the author's name and the figure number in pencil. Standard symbols (such as circles, triangles, squares) are to be used on line-drawings to denote the points determined experimentally. Line-drawings must not contain structural formulas and comments. Spectra or relevant segments thereof, chromatograms, and X-ray diffraction patterns will be reproduced only if concise numerical summaries are inadequate to replace them. Drawings and graphs should be prepared in black ink on good-quality white or tracing paper. Photographs should be submitted on glossy paper as high-contrast copies. Xerox or similar copies are not suitable for reproduction, but may be used for duplicate copies.

Redrawn illustrations will be sent to the authors for checking. No corrections of figures will, therefore, be accepted in the proofs.

Submission of manuscript

After having completed the corrections suggested by the referees and editors, the final manuscript should be submitted in duplicate, in a form ready for publication. If the corrected manuscript is not returned to the editors *within six weeks*, the intended publication of the paper will be regarded as withdrawn by the authors.

Page charge will not be assessed for the publication, however, authors, from overseas countries must contribute to the postage of correspondence by sending, together with the manuscript, international postal coupons to the value of U.S. $ 10.—

Proofs and reprints

A set of proofs will be sent to the submitting author. The proofs must be returned within 48 hours of receipt. Late return may cause a delay in the publication of the paper. 100 reprints will be supplied to the authors free of charge.

Periodicals of the Hungarian Academy of Sciences are obtainable at the following addresses:

AUSTRALIA
C.B.D. LIBRARY AND SUBSCRIPTION SERVICE
Box 4886, G.P.O., *Sydney N.S.W. 2001*
COSMOS BOOKSHOP, 145 Ackland Street
St. Kilda (Melbourne), Victoria 3182

AUSTRIA
GLOBUS, Höchstädtplatz 3, *1206 Wien XX*

BELGIUM
OFFICE INTERNATIONAL DE LIBRAIRIE
30 Avenue Marnix, *1050 Bruxelles*
LIBRAIRIE DU MONDE ENTIER
162 rue du Midi, *1000 Bruxelles*

BULGARIA
HEMUS, Bulvar Ruszki 6, *Sofia*

CANADA
PANNONIA BOOKS, P.O. Box 1017
Postal Station "B", *Toronto, Ontario M5T 2T8*

CHINA
CNPICOR, Periodical Department, P.O. Box 50
Peking

CZECHOSLOVAKIA
MAD'ARSKÁ KULTURA, Národní třida 22
115 66 Praha
PNS DOVOZ TISKU, Vinohradská 46, *Praha 2*
PNS DOVOZ TLAČE, *Bratislava 2*

DENMARK
EJNAR MUNKSGAARD, Norregade 6
1165 Copenhagen K

FEDERAL REPUBLIC OF GERMANY
KUNST UND WISSEN ERICH BIEBER
Postfach 46, *7000 Stuttgart 1*

FINLAND
AKATEEMINEN KIRJAKAUPPA, P.O. Box 128
SF-00101 Helsinki 10

FRANCE
DAWSON-FRANCE S. A., B. P. 40, *91121 Palaiseau*
EUROPÉRIODIQUES S. A., 31 Avenue de Versailles, *78170 La Celle St. Cloud*
OFFICE INTERNATIONAL DE DOCUMENTATION ET LIBRAIRIE, 48 rue Gay-Lussac
75240 Paris Cedex 05

GERMAN DEMOCRATIC REPUBLIC
HAUS DER UNGARISCHEN KULTUR
Karl Liebknecht-Straße 9, *DDR-102 Berlin*
DEUTSCHE POST ZEITUNGSVERTRIEBSAMT
Sraße der Pariser Kommüne 3–4, *DDR-104 Berlin*

GREAT BRITAIN
BLACKWELL'S PERIODICALS DIVISION
Hythe Bridge Street, *Oxford OX1 2ET*
BUMPUS, HALDANE AND MAXWELL LTD.
Cowper Works, *Olney, Bucks MK46 4BN*
COLLET'S HOLDINGS LTD., Denington Estate
Wellingborough, Northants NN8 2QT
WM. DAWSON AND SONS LTD., Cannon House
Folkstone, Kent CT19 5EE
H. K. LEWIS AND CO., 136 Gower Street
London WC1E 6BS

GREECE
KOSTARAKIS BROTHERS INTERNATIONAL BOOKSELLERS, 2 Hippokratous Street, *Athens-143*

HOLLAND
MEULENHOFF-BRUNA B.V., Beulingstraat 2,
Amsterdam
MARTINUS NIJHOFF B.V.
Lange Voorhout 9–11, *Den Haag*
SWETS SUBSCRIPTION SERVICE
347b Heereweg, *Lisse*

INDIA
ALLIED PUBLISHING PRIVATE LTD., 13/14
Asaf Ali Road, *New Delhi 110001*
150 B-6 Mount Road, *Madras 600002*
INTERNATIONAL BOOK HOUSE PVT. LTD.
Madame Cama Road, *Bombay 400039*
THE STATE TRADING CORPORATION OF INDIA LTD., Books Import Division, Chandralok
36 Janpath, *New Delhi 110001*

ITALY
INTERSCIENTIA, Via Mazzé 28, *10149 Torino*
LIBRERIA COMMISSIONARIA SANSONI, Via Lamarmora 45, *50121 Firenze*
SANTO VANASIA, Via M. Macchi 58
20124 Milano
D. E. A., Via Lima 28, *00198 Roma*

JAPAN
KINOKUNIYA BOOK-STORE CO. LTD.
17-7 Shinjuku 3 chome, Shinjuku-ku, *Tokyo 160-91*
MARUZEN COMPANY LTD., Book Department, P.O. Box 5050 Tokyo International, *Tokyo 100-31*
NAUKA LTD. IMPORT DEPARTMENT
2-30-19 Minami Ikebukuro, Toshima-ku, *Tokyo 171*

KOREA
CHULPANMUL, *Phenjan*

NORWAY
TANUM-TIDSKRIFT-SENTRALEN A.S., Karl Johansgatan 41–43, *1000 Oslo*

POLAND
WĘGIERSKI INSTYTUT KULTURY, Marszałkowska 80, *00-517 Warszawa*
CKP I W, ul. Towarowa 28, *00-958 Warszawa*

ROUMANIA
D. E. P., *Bucureşti*
ILEXIM, Calea Grivitei 64–66, *Bucureşti*

SOVIET UNION
SOJUZPECHAT – IMPORT, *Moscow*
and the post offices in each town
MEZHDUNARODNAYA KNIGA, *Moscow G-200*

SPAIN
DIAZ DE SANTOS, Lagasca 95, *Madrid 6*

SWEDEN
ALMQVIST AND WIKSELL, Gamla Brogatan 26
101 20 Stockholm
GUMPERTS UNIVERSITETSBOKHANDEL AB
Box 346, *401 25 Göteborg 1*

SWITZERLAND
KARGER LIBRI AG, Petersgraben 31, *4011 Basel*

USA
EBSCO SUBSCRIPTION SERVICES
P.O. Box 1943, *Birmingham, Alabama 35201*
F. W. FAXON COMPANY, INC.
15 Southwest Park, *Westwood Mass. 02090*
THE MOORE-COTTRELL SUBSCRIPTION AGENCIES, *North Cohocton, N. Y. 14868*
READ-MORE PUBLICATIONS, INC.
140 Cedar Street, *New York, N. Y. 10006*
STECHERT-MACMILLAN, INC.
7250 Westfield Avenue, *Pennsauken N. J. 08110*

YUGOSLAVIA
JUGOSLOVENSKA KNJIGA, Terazije 27, *Beograd*
FORUM, Vojvode Mišića 1, *21000 Novi Sad*

Acta Chimica Hungarica

VOLUME 116, NUMBER 3, JULY 1984

EDITOR-IN-CHIEF
F. MÁRTA

MANAGING EDITOR
GY. DEÁK

ASSISTANT EDITOR
L. HAZAI

EDITORIAL BOARD
M. T. BECK, R. BOGNÁR, GY. HARDY, K. LEMPERT, B. LENGYEL, K. POLINSZKY, E. PUNGOR, G. SCHAY, Z. G. SZABÓ, P. TÉTÉNYI

Akadémiai Kiadó, Budapest
ACTA CHIM. HUNG. ACASA2 116 (3) 193–324 (1984) HU ISSN 0231-3146

ACTA CHIMICA HUNGARICA

A JOURNAL OF THE HUNGARIAN ACADEMY OF SCIENCES

Acta Chimica publishes original reports on all aspects of chemistry in English.

Acta Chimica is published in three volumes per year, each volume consisting of four issues, by

AKADÉMIAI KIADÓ

Publishing House of the Hungarian Academy of Sciences
H-1054 Budapest, Alkotmány u. 21.

Manuscripts and editorial correspondence should be addressed to

Acta Chimica
H-1450 Budapest P.O. Box 67

Subscription information

Orders should be addressed to

KULTURA Foreign Trading Company
H-1389 Budapest P.O. Box 149

or to its representatives abroad

Acta Chimica is indexed in Current Contents

NOTICE TO AUTHORS

Acta Chimica publishes original papers on all aspects of chemistry in English. Before preparing a manuscript for submission to this journal authors are advised to consult recent issues.

Form of manuscript

Manuscripts, tables and illustrations should be submitted in triplicate. Manuscripts should be typewritten double spaced (25 lines, 50 characters per line including spaces). The *title page* should include (1) the title of the paper, (2) the full names of the author(s) in the sequence to be published; apply an asterisk to designate the name of the author to whom correspondence should be addressed, (3) name and address of the institution where the work was done. If the paper is part of a series, reference to the previous communication must be given as a footnote.

Abstract

A summary is printed at the head of each paper. This should not exceed 200 words and should state briefly the principal results and major conclusions of the work. It should be suitable for use by abstracting services.

CONTENTS

PHYSICAL AND INORGANIC CHEMISTRY

Application of organic compounds as thermochemical agents in spectral analysis, **A. Delijska, Chr. Pravčeva, I. Donchev** 235
Xanthate anions as salts of oxinato bis(η^5-idenyl)titanium(IV)/zirconium(IV) chelates **R. K. Bajaj, G. S. Sodhi, N. K. Kaushik, K. N. Johri** 261
A complete CNDO force field of furan, **J. Bánki, F. Billes, A. Grofcsik** 283

ORGANIC CHEMISTRY

Synthesis and reactions of 2,2-diphosphono-1,3-benzodioxoles, **H. Gross, I. Keitel, B. Costisella** 229
Synthesis and characterization of 1-phenyl-3-formamidino thiocarbamide complexes with some bivalent metal ions, **B. Singh, B. P. Yadava, R. C. Aggarwal** 251
Condensation and ring closure reactions of phthalazinone derivatives, **S. A. Mahgoub, A. M. Fahmy, M. M. Aly, M. Z. A. Badr** 267
Spectroscopic study of the donor behaviour of benzidine derivatives towards aromatic nitro compounds, **Y. M. Issa, A. L. El-Ansary, M. Gaber, R. M. Issa** 273
Diels-Alder reaction of 3(2*H*)-isoquinolinones, II. Studies on the lactam–lactim tautomerism of 3(2*H*)-isoquinolinones, **L. Hazai, Gy. Deák, A. Schnitta, J. Haskó-Breuer, E. Horváth** 303

ANALYTICAL CHEMISTRY

Behaviour of metal carbonates in spectroscopic arc, I. Preliminaries. Role of instability of carbonates, **Z. L. Szabó, É. Bertalan, E. Tatár** 193
Behaviour of metal carbonates in spectroscopic arc, II. Investigation of $CaCO_3$. The effect of carbon powder mixed to the sample on the chemical behaviour of the main component, **Z. L. Szabó, É. Bertalan, E. Tatár** 209
The application of addition methods in spectrographic analysis, II, **O. Filo** 245
Application of a new potentiometric evaluation method for the determination of the concentration of monovalent weak bases, **G. Pethő** 293

BOOK REVIEWS 315

PRINTED IN HUNGARY
Akadémiai Kiadó és Nyomda, Budapest

Acta Chimica Hungarica 116 (3), pp. 193—207 (1984)

BEHAVIOUR OF METAL CARBONATES IN SPECTROSCOPIC ARC, I

PRELIMINARIES. ROLE OF INSTABILITY OF CARBONATES

Z. L. SZABÓ[1]*, É. BERTALAN[2] and E. TATÁR[1]

([1]Institute of Inorganic and Analytical Chemistry, Eötvös L. University, H-1088 Budapest, Múzeum krt. 4/b. and
[2] Hungarian Geological Survey H-1143 Budapest, Népstadion u. 14.)

Received April 8, 1983

Accepted for publication August 25, 1983

Seven kinds of metal carbonates of different stability were studied in a.c. polarized arc, in Ar atmosphere, on mixtures with carbon powder of a molar fraction of 0.3 metal carbonate. The higher the thermal stability of the carbonate, the lower quantities of carbon oxides, measured by gas analytical methods [14] were produced in the arc. The less stable carbonates suffer simple thermal decomposition, while in the case of Li_2CO_3 and $BaCO_3$, carbon powder have a direct reducing effect. Under the conditions of the arc a substantial volume of CO was formed too, mainly according to the equation $CO_2 + C = 2\ CO$. Of the less stable carbonates, unstable metal oxides were formed, giving rise to further oxidation reactions. In the case of several carbonates, carbide formation could also be proved by gas analytical methods. Processes proceeding in the arc, their place, the depth of the reaction zone, etc., could be calculated and followed on the basis of data measured. Model substances for further investigations were chosen on the bases of these experiences.

In our earlier investigations [1—13] the behaviour of metal oxides in carbon powder mixture was studied by an a.c. polarized arc excitation. This is essentially a pulsing direct current, having the advantage of high momentary current, but without an excessive glowing of the electrode because of the short burning periods. The amounts of gaseous substances, carbon dioxide carbon monoxide and oxigen produced by the arc were measured by our titrimetric gas analytical methods [14]. The investigations were carried out both in flowing and stationary Ar atmosphere to eliminate the interfering side processes, e.g. reactions with the gas atmosphere. Results obtained at different arc parameters were compared with the spectral line intensities of the simultaneously evaporated metal vapours, and with the changes of these intensities. Several facts were established concerning the gas producing reactions and their effect on spectral line intensity and on the state of the plasma. According to the findings, reactions exert in the arc three essential effects, of which two are well known from literature, too:

1. They change with their energy consumption or production the energy of the arc.

2. Compounds and metals of different evaporation are formed.

* To whom correspondence should be addressed

3. The reactions change by their gas production the composition of the discharge gas atmosphere and of the plasma.

All the three effects influence the intensity of the spectral lines.

The aim of our present series of papers is a further elucidation of the above phenomena, since the formation of carbon dioxide is to be expected also during the decomposition of carbonates. Using carbon auxiliary substances (auxiliary electrode, carbon powder additives mixed to the sample), there is also a possibility of carbon monoxide formation both from the substance filled in the boring of the electrode and in the plasma. Our results are thought to be useful in the spectral analysis of geological samples and carbonate compounds, as experiments and results of this character are missing in the technical literature.

First, seven kinds of carbonates were selected from several metal carbonates for the experiments. Suitable model substances were sought for our further investigations, which give in the arc, readily measurable amounts of carbon oxides, while on the other hand we expected from these experiments useful information on the decomposition in the arc of metal carbonates of different stability.

Only regular carbonates came into consideration for our experiments. Basic carbonates could not be used because their structural water causes further interfering reactions. This possibility was proved earlier [1], since from the adsorptively bound water content of carbon carrier electrodes, not dried before the investigation, carbon oxides were formed in readily measurable amount on excitation. Thus, the composition of the carbonates used was previously checked.

In further investigations the quality of the carbonates, the composition of their mixture with carbon powder, the polarity of the carrier electrode, the current and in a few cases the burning time of the arc were changed. In several cases arc voltage and electrode temperature were measured. The loss in mass of the substances filled in the cavity of the holding electrode caused by the arc was measured, and the results were compared with mass loss, arising from the loss of gases during reactions, calculated from the results of gas analysis. This was also suitable for checking the sputtering of the substances from the cavity of the electrode. (Electrodes with plastic fastening [15] could not be used in the investigations, because the resin mixed to the sample causes further reactions.) Results obtained on changing the arc parameters (current, carbon powder ratio, etc.) were compared with the changes of spectral line intensities simultaneously measured to study also this effect of the reactions. Flowing Ar gase atmosphere was used for the elimination of interfering parallel electrode surface reactions and other ones.

In our present first paper the role of the instability of metal carbonates is studied in an arc of given current, measuring the quantities of carbon

dioxide and carbon monoxide produced in the arc. Spectral pure graphite powder was added to our samples, but at a lower ratio than usual. In analytical practice the carbon powder is generally mixed in a mass ratio from 1 : 1 to 5 : 1 with the sample On the basis of the results obtained with metal oxides we have the opinion that in the investigation of metal carbonates also suitable the amount of carbon powder calculated in atomic ratio or molar fraction [2], if possible reactions are studied. Carbon powder, besides providing for current conduction and dilution, and playing a certain equalizing role may also be a chemical reactant. In our first investigations, to keep the atomic ratio of carbon sufficiently low, carbon powder mixtures of 0.3 molar fraction metal carbonate content were used for the experiments. (The mass ratio 1 : 1 would have meant in general a molar ratio of 1 : 9, and the mass ratio of 1 : 5 to 1 : 100 to the advantage of carbon powder in the case of most of the carbonates investigated.) A molar fraction of 0.3 does not yet produce a strong dilution in our investigation of brief exposure time.

Experimental

Model substances

$CaCO_3$ (marble), $MgCO_3$ (magnesite), $BaCO_3$ $MnCO_3$, $LiCO_3$, $CdCO_3$ and $PbCO_3$ reagents of analytical pure grade. Their metal content was checked by chelatometry and gravimetry, their carbonate content by acidimetric determination of CO_2 after eliberation with acid. Metal : carbonate molar ratios obtained are contained in Table I.

Electrode materials

Amorphous carbon electrode marked RW II, manufactured by Ringsdorff Werke G.m.b.H. These glow stronger in the arc than graphitic ones, so that their reactions and effects are easier to observe.

Table I

Metal to carbonate ratio of the starting model substances

Metal carbonate	Molar ratio
$BaCO_3$	1 : 1.005
Li_2CO_3	2 : 0.998
$CaCO_3$	1 : 0.996*
$MgCO_3$	1 : 1.019*
$MnCO_3$	1 : 0.997
$CdCO_3$	1 : 0.996
$PbCO_3$	1 : 1.004

* While marble was $CaCO_3$ of 99.4% purity, magnesite contained a few per cent (about 4%) of other components, among these also $CaCO_3$

Carrier electrode

Electrode of 6 mm ∅ and 22 mm length with a tap of 3.7 extrenal ∅ and 4 mm height at one end. The diameter of the boring in the tap is 2.7 mm, its depth 4 mm. Through two sides of the wall of the boring, at 1 mm from the bottom of the crater there is also a cross-bore of the wall of the boring of 1 mm ∅ to facilitate the easy departure of gases evolved in the interior of the filling, and to hinder the sputter of the sample from the electrode (so-called "ventillating electrodes" [1]).

Counterelectrode

Electrode of the same dimensions, without boring, fitted with a tap.

Carbon powder additive

Graphitic carbon powder type SU-601 manufactured by Elektrokarban Topolčany, Czechoslovakia, for the preparation of the carbon powder mixtures containing 0.3 mole fraction of metal carbonate.

Preparation of the electrodes

The electrode filled with the sample was weighed on an analytical balance and kept before excitation for at least 3 hours in a drying box at 135 °C. Taken out from this, it was placed without delay in Ar atmosphere.

Excitation

With a.c. polarized arc ignited at maximum voltage, connecting the carrier electrodes in separate series both as anodes and cathodes. Average current of the arc 7 A (the momentary strength of the pulsating direct current is about twice of it), burning time 10 s. The reason of this relatively short burning time is that in the case of the less stable compounds the most part of the reactions proceeds already during this time. At longer burning time reactions are not controlled by the chemical nature of the samples but by the amount of the substance filled in the electrode.

Gas atmosphere

Ar at a flow rate of 860 cm^3/min controlled by the capillary of given dimensions.

Gas cell

Quartz tube of 50 cm^3 volume sealed at the top and bottom with hard rubber rings, and stainless steel top and bottom, widning conically inwards. Stainless steel tubes holding the electrodes have conical end at the inside and conduct also the gas stream, because their internal ends reaching into the cell are perforated at the sides. The gas is sucked through the cell and the capillary by a 600 cm^3 gas analytical titration flask containing also gas analytical reagents [1], and evacuated before.

Principle of the gas analytical measurements

Carbon dioxide is absorbed in a standard barium hydroxide solution. Its excess is titrated with acid. Carbon monoxide is oxidized in the presence of silver ion catalyst by potassium permanganate to carbon dioxide. The excess of the permanganate is measured. We refer for details of these methods to an earlier communication [14].

Results and Discussion

Figure 1 shows the carbon dioxide amounts measured for the mixtures of various metal carbonates and carbon powder in the order of the stability of the carbonates. For their characterization the initial decomposition temper-

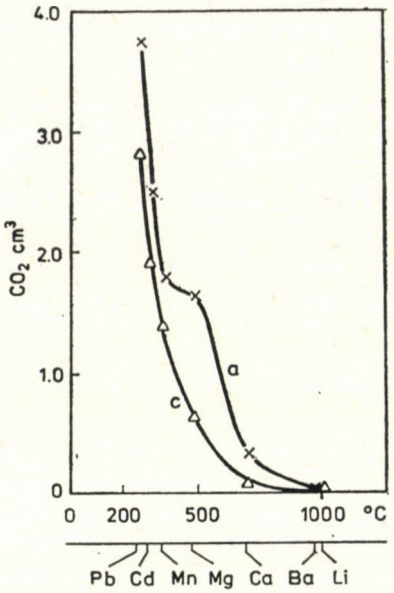


Fig. 1. Change is amount of CO_2 produced in the arc with the thermal stability of metal carbonates (*a* anoddic, *c* cathodic excitation)

ature of the single carbonates determined by thermal analysis was taken [16—17]. The horizontal axis of further figures too, features these values. For $CdCO_3$ we have only an estimated value 300 °C, because data in the literature differ from one another.

It can be seen from the figure that both in anodic (a) and in cathodic (c) excitation the CO_2 production of the arc rapidly decreases with increasing stability of the carbonates, though in anodic excitation values for $MnCO_3$ and $MgCO_3$ do not lie along the curve determined by the other points.

The curves indicate that here we have actually a simple thermal decomposition in the bulk of the filling according to equation

$$MeCO_3 = MeO + CO_2 \qquad (1)$$

because the amorphous carbon electrode connected as anode is always glowing stronger in its whole mass than the cathode [12, 18].

According to Fig. 2 simultaneously a substantial amount of CO is also formed in the arc. Moreover, it will be noted that the trend of the curves is similar to the change in CO_2 values, but the points belonging to the single carbonates give rather wavy curves. It was thought that these great differences can be attributed to the fact that though in the case of carbonates of different molecular masses mixtures of identical composition with respect to their molar fraction can be filled into the cavities of identical dimension of

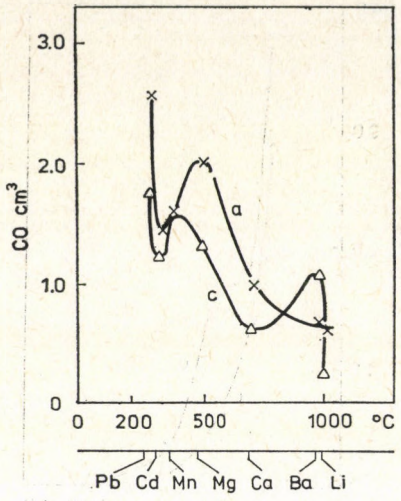


Fig. 2. Change in amount of CO produced in the arc with the thermal stability of metal carbonates (*a* anodic, *c* cathodic excitation)

the carrier electrodes, the quantities of the mixtures are different with respect to their total mass. This was accounted for by the normalization of gas analytical results. For this purpose the volume of the gases formed was divided by the really amount of the carbonate in the mixture (mass *g*) filled into the electrodes, expressed in mole number from case to case.

$$M_{\mathrm{MeCO_3}} \frac{g}{Mt_{\mathrm{MeCO_3}}}$$

where $Mt_{\mathrm{MeCO_3}}$ is the molecular mass of the carbonate. The normalized values marked with square brackets are:

$$[\mathrm{CO_2}] - \frac{[\mathrm{CO_2}]\,\mathrm{cm^3}}{M_{\mathrm{MeCO_3}}} \quad \text{and} \quad [\mathrm{CO}] = \frac{\mathrm{CO\ cm^3}}{M_{\mathrm{MeCO_3}}}.$$

Thus, essentially the gas production of 1 g · mol of carbonate under the given experimental conditions was calculated. This would give in the case of total decomposition according to Equation (1) the normal gas volume of CO_2:

$$[\mathrm{CO_2}]_t = 2.23 \times 10^3\ \mathrm{cm^3}$$

if no other side ractions were present.

However, such side or parallel reaction is also the formation of CO. In principle, CO can be formed in the arc by four ways:

1. CO_2 primarily formed is further decomposed in the arc:

$$CO_2 = CO + O \tag{2}$$

and oxygen partly oxidizes the auxiliary carbon substances, such as carbon powder and carbon electrodes, and carbon vapours in the plasma:

$$C + O = CO \quad \text{and} \quad C + 2\,O = CO_2 \tag{3}$$

However, this process can only be of very small extent, as part of the oxygen atoms were to be recombined into O_2 molecules, however, oxygen was scarcely measurable in the gas space. This problem will be treated in detail in our next paper.

2. CO_2 formed in the decomposition (1) reacts at higher temperatures with the carbon auxiliary substances:

$$CO_2 + C = 2\,CO \tag{4}$$

This is in essence Boudouard's equilibrium reaction, which can be taken already at 1000 °C as complete, and can proceed in the filling itself, but also in a plasma zone of appropriate temperature. In this way two mol of CO were to be formed from each mol of decomposed carbonate, since each of our model substances contained one carbonate group.

3. Carbon powder may directly reduce the carbonates in the filling under formation of oxides and metals:

$$MeCO_3 + C = MeO + 2\,CO \tag{5}$$

or presumably in the burning spot of the arc:

$$MeCO_3 + 2\,C = Me + 3\,CO. \tag{6}$$

4. Combination of the above reactions with possible carbide formation, similarly in the filling:

$$x\,MeCO_3 + y\,C = Me_xC_{(y-2x)} + (3x)CO, \tag{7}$$

or more simply:

$$MeCO_3 + x\,C = MeC_{(x-2)} + 3\,CO. \tag{8}$$

As compared to the above, the last three reactions increase the CO product of the arc, because in these three mol of CO (is) formed from each mol of decomposed carbonate.

Change of data reffered to $[CO_2]$ and [CO] values normalized in the way described is shown in the order of the reactivity (stability) of the metal carbonates in Figs 3 and 4, given in 10^{-4} units. The points of the $[CO_2]$ curves obtained by excitation of both polarities follow well the average curves, with

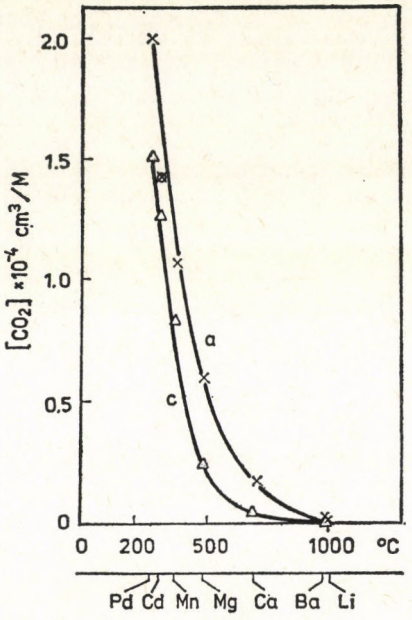


Fig. 3. CO_2 amount normalized to 1 mol of carbonate as a function of the stability of carbonates (*a* anodic, *c* cathodic excitation)

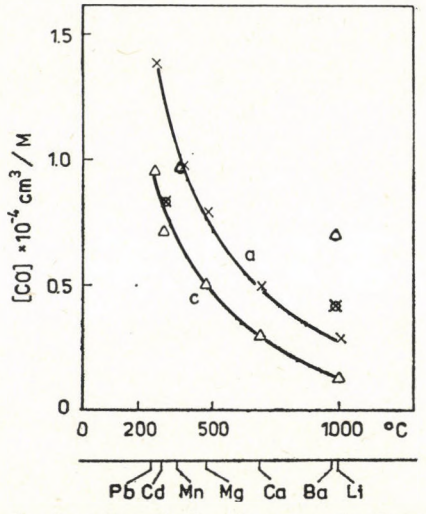


Fig. 4. CO amount normalized to 1 mol of carbonate as a function of the stability of the carbonates (*a* anodic, *c* cathodic excitation)

the exception of the lower values obtained for $CdCO_3$ upon anodic excitation, and perhaps the values obtained for $MnCO_3$ upon cathodic excitation. Evidently these normalized values, too, decrease asymptotically with increasing stability of the carbonates. For $BaCO_3$ and Li_2CO_3 of high stability only volumes of ca. 0.01 cm^3 of CO_2 could be measured.

On the other hand, curves plotted from [CO] data differed in the case of three carbonates. Here too, values obtained in the anodic investigation of unstable $CdCO_3$ are considerably lower than expected. However, it could be observed that particularly CdO formed in the cavity of the anode hotter in its whole mass, strongly sublimes and precipitates on the cooler internal top of the cell in form of a yellow substance, before it can further react with carbon.

$BaCO_3$ gives at both electrode polarities considerably higher [CO] values than expected, and here the value obtained by cathodic excitation is higher. According to certain data in the literature [19], $BaCO_3$ mixed with carbon powder reacts at lower temperatures according to Eq. (5) than that of decomposition of $BaCO_3$:

$$BaCO_3 + C = BaO + 2\ CO \tag{9}$$

It was found also in our thermoanalytical investigations* that while the thermal decomposition of pure $BaCO_3$ begins at 1000 °C and maximal decomposition rate can be observed at 1200 °C, in a mixture with carbon powder of 0.3 molar fraction of $BaCO_3$ the above reaction can proceed already at a temperature lower by about 200 °C. Thus, instead of reactions (1) and (4), CO formation according to Eq. (9) becomes predominant and CO_2 formation by spontaneous thermal decomposition of $BaCO_3$ is negligible.

At the same time, carbide formation according to reaction (8):

$$BaCO_3 + 4\ C = BaC_2 + 3\ CO \tag{10}$$

could also be proved. The ignition residue remaining in the cavity of the electrode heated as cathode with a 10 A arc (for easier detection) was hydrolyzed with perchloric acid according to the reaction scheme:

$$BaC_2 + 2\ HClO_4 = Ba(ClO_4)_2 + C_2H_2 \tag{11}$$

and 0.083 cm^3 acetylene could be measured by gas chromatography,** which means according to reaction (10) that simultaneously three times as much CO is formed. This process proceeds decisively at the cathode, and increases the CO production to a higher extent. According to our earlier observations, conclusions drawn from measuring results, direct proof [20, 21], and also according to certain data in the literature [22], the temperature of the burning spot

* We thank Mrs. Péter Gábor and Dr. László Pöppl for thermal analyses.
** We thank Dr. Jenő Trompler, Dr. László Maros, Mrs. Jenő Hollós for the gas chromatographic analyses.

of the arc is higher at the cathode, than at the anode. Thus in the burning spot and its immediate environment the possibility of reactions (9) and (10) is also higher, but at the same time at the anode, hotter in its total mass, CO production also increases, but to a lesser extent. Owing to the lower temperature of the burning spot formed at the anode, only 0.057 cm^3 of C_2H_2 could be measured under similar circumstances. At the same time, at 10 A cathodic excitation 1.86, at anodic one 1.69 cm_3 of CO was measured. Thus the contribution of reaction (10) to CO production is in anodic excitation only 10% of the total quantity, while in cathodic one 13% of the orginally higher CO quantitiy. Taking into consideration the 1 : 3 ratio of formation of C_2H_2 and CO, this means that reaction (9), proceeding parallel to reaction (10), where carbon has similarly a direct reducing effect, is contributing at a higher ratio.

Similar carbide formation, but of a considerably smaller extent could be detected also in the case of the $CaCO_3$ mixture of 0.3 molar fraction. Here 0.021 and 0.018 cm^3 C_2H_2 were obtained while in the case of $MgCO_3$ decomposing still easier into CO_2, C_2H_2 amounts of only about 0.001 cm^3 could be detected.

Carbide formation could also be detected in the carbon powder mixtures of $MnCO_3$. In the hydrolysis of carbide formed in the reaction

$$7\ MnCO_3 + 17\ C = Mn_7C_3 + 21\ CO \tag{12}$$

or

$$3\ MnCO_3 + 7\ C = Mn_3C + 9\ CO \tag{13}$$

methane was evolved according to the reactions

$$Mn_7C_3 + 14\ HClO_4 = 7\ Mn(ClO_4)_2 + 3\ CH_4 + H_2 \tag{14}$$

and

$$Mn_3C + 6\ HClO_4 = 3\ Mn(ClO_4)_2 + CH_4 + H_2 \tag{15}$$

in very low amounts of 0.001—0.002 thousandth cm^3, and here too, more in cathodic excitation.

Special attention was given to Li_2CO_3, because it is often used in the spectral analysis of powder shaped samples also mixed with carbon powder as carrier distillation agent and as spectroscopic buffer [23—26] because of the low ionization potential of metal vapours getting into the plasma. Here carbide formation was not expected, because the measured CO values are much lower than in the case of $BaCO_3$ (0.61 upon anodic, and 0.25 cm^3 upon cathodic excitation), and neither was the mutual ratio of CO amounts obtained with anodic and cathodic polarity of holding electrode inverted. In several tests C_2H_2 really could not be safely detected. Owing to the similarly very low CO_2 amounts (0.02 and 0 cm^3), recation (5) is thought to be probable.

Looking reversely, with decreasing stabilities the ascent of both pairs of curves relevant to the carbon oxides becomes steeper. In this the fact may

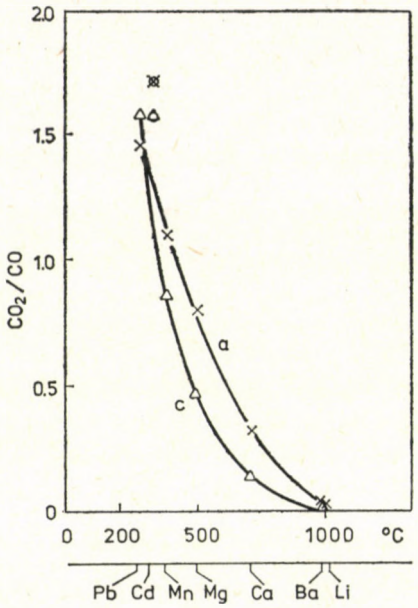


Fig. 5. Ratio of the measured volumes of the two carbon oxides as a function of the stability of the metal carbonates (*a* anodic, *c* cathodic excitation)

also play a role that metal oxides formed during decomposition are in the same order less and less stable [4]. This creates further possibilities of oxidation, on account of which the total quantity of carbon oxides increases, and moreover, parallel recations are shifted more and more in the direction of CO_2 formation. This can be clearly seen in Fig. 5, where the volume ratio of carbon oxides measured is plotted against the order of stability of carbonates. The volume ratio CO_2/CO is characteristic, besides of temperature conditions, also of the oxidation conditions of the electrode gap [4, 27], because CO_2 in the numerator of the ratio contains the carbon of higher oxidation state. Therefore, if conditions become more oxidative in the system, ratios must change to the advantage of CO_2.

The extent of increased reaction can be characterized by data of the "summarized basic reaction". According to our assumption this summarized reaction can be calculated from Eqs (1) and (4) in the following way. Since, according to Eq. (1), from 1 mol of metal carbonate the same amount of CO_2 is formed, but this can partly produce in reaction (4) twice as much CO,

$$\text{"summarized reaction"} = CO_2 + \frac{1}{2} CO \text{ cm}^3 \qquad (16)$$

which essentially gives the total amount of carbonate decomposed in the first step of reaction (1). If these values are also normalized, dividing them by the

number of moles, which can be filled in the cavity of the electrodes, increasing decomposition abilities approach the value of 2.23×10^4 cm^3, the normal volume of CO_2 (Fig. 6). In the case of lead carbonate this value is even surpassed which proves that probably already is the cases of $MnCO_3$ and $CdCO_3$ the reaction proceeds to an increasing extent according to reaction schemes

$$MeO + C = Me + CO \tag{17}$$

and

$$2\ MeO + C = 2\ Me + CO_2 \tag{18}$$

Earlier these reactions were experimentally proved in the investigation of metal oxides (3). Values obtained by the excitation of $BaCO_3$ at both polarities and of $MnCO_3$ by cathodic excitation are also higher than expected, indicating carbide formation and the fact that this process is of greater extent at the cathode. Scattering points lie nearer to the curve, if we calculate in these cases with the formula:

$$\text{"summarized reaction"} = CO_2 + \frac{1}{3} CO \text{ cm}^3,$$

taking into consideration that according to Eqs (10) and (11) from each mole of carbonate not two moles of CO, but reffered to the carbide formed, a threefold quantity of CO is formed. Owing to this, calculated with Eq. (12), for the total reaction the limiting value would not be the normal molar volume, but one and a half times its value. The problems of carbide formation will be discussed in following papers.

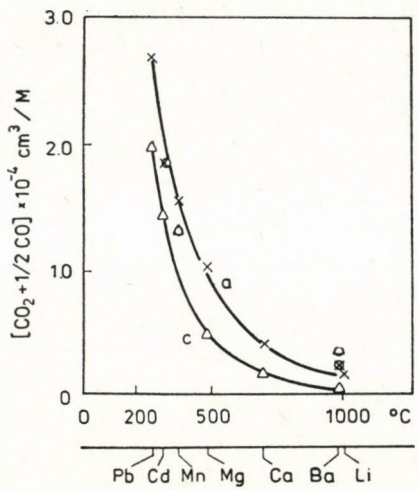


Fig. 6. Change of the "summarized basic reaction" with the stability of the metal carbonates (*a* anodic, *c* cathodic excitation)

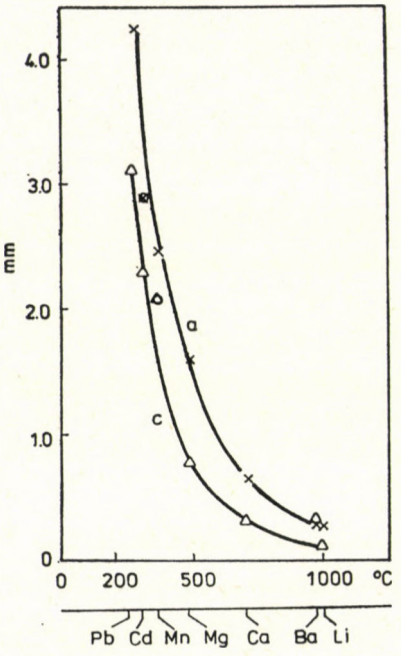


Fig. 7. Calculated depth of the reaction zone (*a* anodic, *c* cathodic excitation)

Knowing the composition of the samples and the mass of the substance filled in the cavity of the electrode for each probe, from the data of gas analysis the layer thickness can be calculated in which gas forming reactions still proceed under the given experimental conditions (7 A, 10 s). This similarly requires data on the quantities formed during the summarized basic reaction. Assuming that in this zone reaction is complete, and that at constant arc parameters the rate of heat transport is identical for all the carbonates because of the buffering role of carbon powder, results shown in Fig. 7 are obtained. Since these data are derived from results of gas analysis too, and are not independent values, it is evident that they follow the course of the curve of the summarized basic reaction, but on another scale. Anyway, a further obvious finding is that proceeding toward less stable substances the reaction zone in the electrode filling increasingly extends downwards, starting from the 0.1—0.2 mm deep zone of the Li_2CO_3 mixture, which essentially is the burning spot of the arc and its near environment, because the less stable carbonates can undergo reactions also in the lower, relatively cooler layers. Even below the deepest reaction zone (the case of $PbCO_3$) there must remain some unreacted substance, which was also found after breaking the top of electrode. This shows that the choosing of the arc parameters, the using of the short burning time belonging to the given current were correct, because thus the extent of the reaction is

controlled by the properties of the single substances, and not by their amounts filled in the boring. In anodic excitation of $PbCO_3$ the depth of the reaction zone is unrealistically larger than the true 4.0 mm deep boring of the electrode. This supports again findings in conjunction with Fig. 6, though not with independent data, but by another way of thought.

The sputtering of the substances from the bore of the electrode by the pulsing arc could be also checked with the aid of results obtained by gas analysis. Mass losses determined directly on an analytical balance (m) and the total $CO_2 + CO$ mass losses calculated from the gaseous products are compared in Fig. 8 for the anodic (a) and cathodic (c) excitation of the samples. It will be noted that measured data are always higher, and the difference between measured and calculated values increases on proceeding towards less stable substances. This indicates that gaseous products formed in increasingly large volume blow out part of the powder sample even from the so called "ventillating electrodes" with cross-boring. The smallest differences were obtained for Ca, Ba and Li carbonates, for which the reactions are also moderate. This is the fourth observable effect of chemical reaction in finely pulverized samples.

On the basis of these results the following model substances were chosen for our further investigations: fairly stable $CaCO_3$, the less stable $MgCO_3$ still producing stable oxides, $MnCO_3$ of low stability producing also unstable

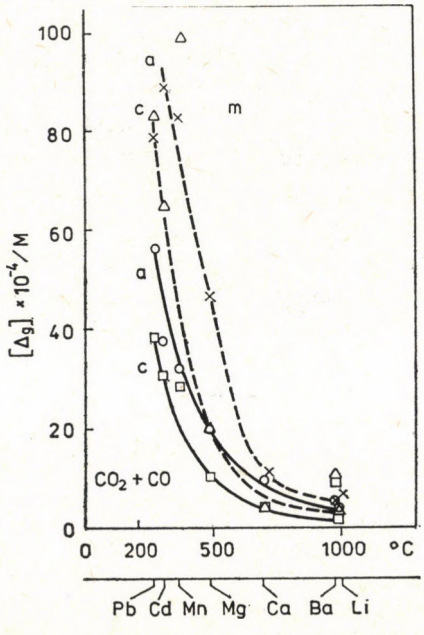


Fig. 8. Mass losses measured (m) and calculated ($CO_2 + CO$) in the bore of the electrode (a anodic, c cathodic excitation)

oxides, and $BaCO_3$ of different behaviour in its carbon powder mixtures.

In the further parts of our series of communications we will report on the results of these experiments.

REFERENCES

[1] Szabó, Z. L., Dobolyi-Fejérdy, H.: Acta Chim. Acad. Sci. Hung., **96,** 189 (1978)
[2] Szabó, Z. L., Dobolyi-Fejérdy, H.: Acta Chim. Acad. Sci. Hung., **96,** 201 (1978)
[3] Szabó, Z. L., Dobolyi-Fejérdy, H.: Acta Chim. Acad. Sci. Hung., **97,** 1 (1978)
[4] Szabó, Z. L., Dobolyi-Fejérdy, H.: Acta Chim. Acad. Sci. Hung., **97,** 13 (1978)
[5] Szabó, Z. L., Dobolyi-Fejérdy, H.: Acta Chim. Acad. Sci. Hung., **97,** 27 (1978)
[6] Szabó, Z. L., Dobolyi-Fejérdy, H.: Acta Chim. Acad. Sci. Hung., **97,** 111 (1978)
[7] Szabó, Z. L., Dobolyi-Fejérdy, H.: Acta Chim. Acad. Sci. Hung., **97,** 125 (1978)
[8] Szabó, Z. L., Dobolyi-Fejérdy, H.: Acta Chim. Acad. Sci. Hung., **97,** 137 (1978)
[9] Szabó, Z. L., Dobolyi-Fejérdy, H.: Acta Chim. Acad. Sci. Hung., **98,** 147 (1978)
[10] Szabó, Z. L., Dobolyi-Fejérdy, H.: Acta Chim. Acad. Sci. Hung., **98,** 157 (1978)
[11] Szabó, Z. L., Bertalan, É.: Acta Chim. Acad. Sci. Hung., **102,** 371 (1979)
[12] Szabó, Z. L., Bertalan, É.: Acta Chim. Acad. Sci. Hung., **102,** 383 (1979)
[13] Szabó, Z. L., Bertalan, É.: Acta Chim. Acad. Sci. Hung., **103,** 391 (1979)
[14] Szabó, Z. L., Tóth, I.: Acta Chim. (Budapest), **73,** 363 (1972)
[15] Papp, L., Szarvas, P.: Publication of the 12th MESZEV, Aggtelek, 1969, p. 175.
[16] Duval, C.: Inorganic Thermogravimetric Analysis. Elsevier Publishing Co. London 1963
[17] Barin, I., Knacke, O., Kubaschewski, O.: Thermochemical Properties of Inorganic Substances, Supplement, Springer Verlag. Berlin, Heidelberg, New York 1977
[18] Pöppl, L., Szabó, Z. L.: Acta Chim. (Budapest) **79,** 27 (1973)
[19] McKetta, J. J., Cunningham, W. A.: Encyclopedia of Chemical Processing and Design, Vol. **4.** Marcel Dekker. New York, Basel 1977
[20] Szabó, Z. L., Pöppl, L.: Acta Chim. (Budapest) **77,** 125 (1973)
[21] Szabó, Z. L.: Acta Chim. (Budapest) **85,** 13 (1975)
[22] Zalesskii, A. M.: The Electric Arc (in Hungarian). Műszaki Könyvkiadó. Budapest 1968
[23] Marinkovic, M.: Bull. Boris Kidric Inst. Nucl. Sci., **14,** 305 (1963)
[24] Rekalic, M., Vukanovic, V.: Appl. Spectr., **28,** 244 (1974)
[25] Maessen, F. J. M. J., Elgersma, J. W., Boumans, P. W. J. M.: Spectrochim. Acta, **31B,** 179 (1976)
[26] Flórián, K., Zimmer, K.: Magy. Kém. Folyóirat, **86,** 24 (1980)
[27] Szabó, Z. L.: Spectrochim. Acta, **29B,** 231 (1974)

Acta Chimica Hungarica 116 (3), pp. 209—227 (1984)

BEHAVIOUR OF METAL CARBONATES IN SPECTROSCOPIC ARC, II

INVESTIGATION OF $CaCO_3$. THE EFFECT OF CARBON POWDER MIXED TO THE SAMPLE ON THE CHEMICAL BEHAVIOUR OF THE MAIN COMPONENT

Z. L. SZABÓ[1]*, É. BERTALAN[2] and E. TATÁR[1]

([1] Institute of Inorganic and Analytical Chemistry, Eötvös L. University, H-1088 Budapest, Múzeum krt. 4/b. and [2] Hungarian Geological Survey, H-1143 Budapest, Népstadion u. 14.)

Received April 8, 1983

Accepted for publication August 25, 1983

The decomposition reaction of $CaCO_3$ and consecutive and possibly parallel reactions were investigated in a.c. polarized arc. The results showed that the carbonate is primarily decomposed into metal oxide and carbon dioxide. The latter reacts partly still in the electrode filling, but probably mainly in the plasma with carbon powder and carbon vapours, respectively, to yield in this secondary reaction carbon monoxide. The ratio of carbon monoxide formation diminishes with decreasing ratio of carbon powder. The temperature of the electrode plays a decisive role in the reactions, which was proved by comparative measurements with copper carrier electrodes heating up less, and by direct measurements with a thermocouple. After suitable preparation the formation of CaC_2 was also studied by gas chromatography.

In the first part of present series of our papers [1] aspects and reasons of the selection of the model substances were given. $CaCO_3$ (marble) was chosen because of its relatively high thermal stability, and the high stability of its oxide formed during the moderate decomposition. Thus, a relatively small amount of carbon dioxide is formed in the arc, which changes only slightly the composition of the initial pure Ar atmosphere. It became evident from data of the publication cited that current of 7 A used is too low for measuring with desired accuracy the small amounts of carbon oxides to be expected in the case of powder mixtures of extreme composition. Therefore, we worked with an a.c. polarized arc, essentially a pulsating d.c. arc of 10 A average current, i.e. higher than earlier. The momentary current is about double of this in the ca. 1/200 s burning periods of the arc ignited at maximum voltage.

Investigations began as a function of the molar fraction of $CaCO_3$ on mixtures of the carbonate with carbon powder.

Similar investigations were undertaken already earlier with several metal oxides, and it was found that an evaluation according to molar fraction is the most suitable for the characterization of reaction conditions, and also for

* To whom correspondence should be addressed

the comparison of the different compounds [2]. Carbon oxides measured with our gas analytical method [3] yielded maximum curves [4], and the position of the maxima fell between the molar ratios 1 : 1 and 2 : 1 of metal oxide : carbon powder, optimal for the formation of the two carbon oxides. This indicated that carbon oxides are formed even in the case of the relatively unstable CuO mainly by reduction with carbon. We wished to investigate whether there is a similar phenomenon in the case of $CaCO_3$, too. As in principle the formation of oxygen gas in the arc is also possible, for checking certain presumed reactions a few oxygen determinations were also carried out by our titrimetric method [3]. (According to this manganese(II)-hydroxide prepared under oxygen-free conditions is oxidized by oxygen formed in the arc, and manganese in higher oxidation state can be measured iodometrically.) The loss in mass of the samples by arc excitation was also measured and compared with the (CO_2 + CO) loss of mass, calculated from gas analytical results. In some cases the change in average temperature of the electrode was checked with an iron-constantan thermocouple. For this purpose the head of the thermocouple was placed into a horizontal hole of 1 mm ∅ and of 2 mm depth, bored 1 mm below the sample filling into the side of the 6 mm thick electrode body. Though this did not measure directly the temperature of the sample but lower values, it could be used well for comparing data of the characterization of the changes.

Other experimental conditions (flowing Ar atmosphere, etc.) were the same as described in our first publication [1]. Measuring points in our results represent average values of several (often 8—15) parallel measurements, because as found already earlier, the single values measured vary considerably on account of the spontaneous course of the reactions.

Checking of the marble sample

The marble used for the investigations contained, according to the gravimetric ($CaC_2O_2 \cdot H_2O$) and chelatometric measurements, on the basis of the metal content an average of 99.2% of $CaCO_3$. Carbon dioxide was eliberated with acid, sucked into a gas analytical flask, flashed in with Ar gas stream, absorbed in a closed system in a standard $Ba(OH)_2$ solution measured the excess of which was by acidimetry titrated under a layer of pentane. In this way a $CaCO_3$ content of 99.6% was obtained. This corresponds to a Ca : CO_3 molar ratio of 1 : 1.004, so that only a few tenth of a per cent of other metal compounds could be contained in the sample. This was checked by qualitative spectral analysis. In the sample magnesium, silicon, iron, manganese and copper were found in detectable amounts. The sample practically did not contain water, because after drying 1 g of finely pulverized substance at 135 °C for 8 hours, no measurable loss in mass was found.

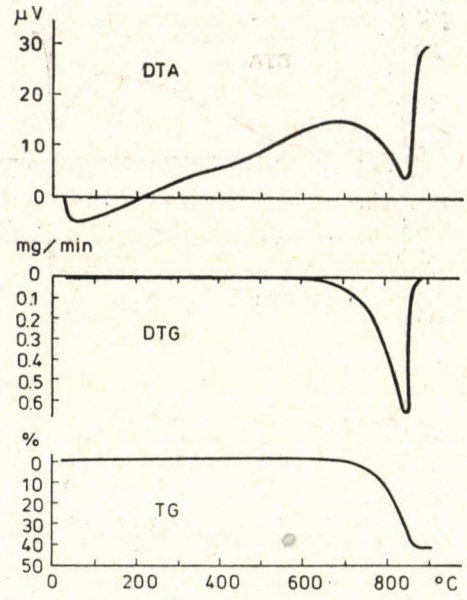


Fig. 1. Thermoanalytical curves of pure $CaCO_3$

The thermal behaviour of the pure substance was checked by thermal analysis.* Experimental conditions:

Apparatus: Mettler TA-1 thermoanalyzer;
Temperature interval: 20—900 °C;
Heating rate: 10 °C/min (upon our request an unusually high value to approach closer the arc conditions);
Atmosphere: Ar flowing at a rate of 4.55 dm^3/h;
Weight of sample: 11.40 mg marble sample.

The DTG curve in Fig. 1 shows that transformation begins already at 610 °C at a very low rate, however, decomposition important also from the practical point of view can be observed on the basis of the TG curve only at about 680 °C. Thermal dissociation proceeds completely until 870 °C, the whole mass of the sample is converted into CaO and CO_2. CaO formed is stable in a wide temperature range [5]. Decrease in mass in 43.4%, while the value calculated for the pure substance is 44.0% showing a good agreement. According to the DTA curve, decomposition is an endothermic process.

Figure 2 shows the thermoanalytical curves of a $CaCO_3$ + C powder mixture of $n = 0.3$ metal carbonate molar fraction, recorded under identical experimental conditions. The mass of the sample was in this case 10.14 mg.

* We thank Dr. László Pöppl for the thermoanalytical investigations.

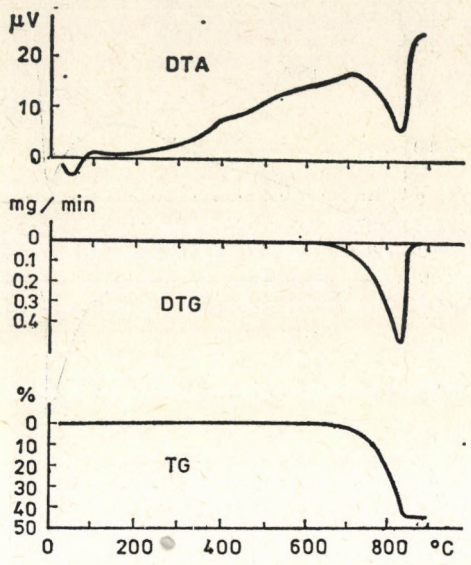


Fig. 2. Thermoanalytical curves of carbon powder mixture of 0.3 $CaCO_3$ molar fraction

It can be seen from the diagram that in the case of the mixture with carbon powder, decomposition begins already at a temperature lower by a few degrees, at 590 °C. However, as compared to pure marble, no new peak appears in the picture. This shows that up to 900 °C carbon powder plays only the role of a diluent and plays a part in the heat conduction of the sample because of the high heating rate. This fact supports the conclusion drawn also from other curves to be discussed later, viz. that up to the given temperature carbon powder virtually does not directly react with the carbonate, it has no reducing effect.

Investigation of the reactions by changing the ratio of carbon powder in the sample

Figure 3 shows in anodic (a) and cathodic (c) connection of the carbon electrode holding the sample the amounts of CO_2 formed by the action of the arc as a function of the carbon powder ratio of the sample. This is given as molar fraction of $CaCO_3$ (n). As expected on the basis of the thermoanalytical curves, CO_2 is formed from the carbonate by simple thermal decomposition. This reaction was proved also by a qualitative experiment. The powder mixture of 0.3 molar fraction of carbonate was shaken with freshly boiled and cooled distilled water. The pH of the solution obtained was 6.5. Filling a mixture of identical composition into the boring of an RW II carbon carrier electrode connected as anode, it was ignited with an average current of 17 A for 10 s.

Shaking the substance remained in the cavity similarly with freshly boiled distilled water, the pH of the solution was 10.0. This result, together with data in Fig. 3 proves the reaction

$$CaCO_3 = CaO + CO_2 \qquad (1)$$

proceeding in the filling by the action of the arc.

The CO production of the arc is shown in Fig. 4. From Figs 3 and 4 the following could be established:

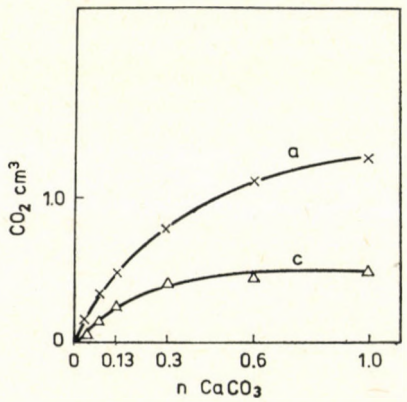


Fig. 3. Amount of CO_2 formed in the arc as a function of the $CaCO_3$ molar fraction (n) in the carbon powder mixtures: *a:* anodic, *c:* cathodic excitation

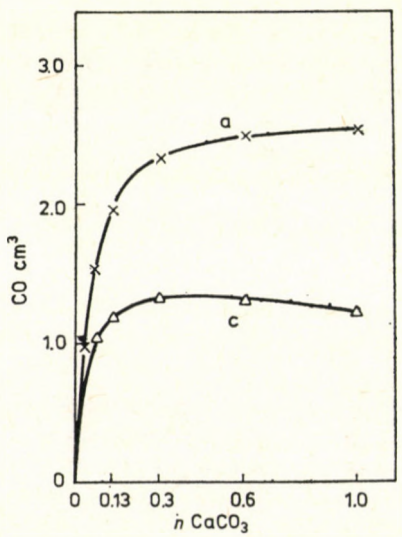


Fig. 4. Amount of CO formed in the arc as a function of the $CaCO_3$ molar fraction (n) in the carbon powder mixtures; *a:* anodic, *c:* cathodic excitation

1. The amounts of both carbon oxides are higher when the holding electrode is connected as anode, as compared to the cathodic one. The reason for this is that, when connected as anode, the RW II carbon electrode glows in its whole mass visibly stronger (see also Fig. 11), so that in anodic excitation the reaction is generally more intensive. A further proof of this can be found

Table I

Gas analytical results measured with RW II carbon and copper auxiliary electrodes; a anodic, *c* cathodic excitation

n $CaCO_3$		CO (cm^3)		CO_2 (cm^3)		Loss of mass (g)	
		RW II	Cu	RW II	Cu	RW II	Cu
0.3	a	5.25	0.23	0.75	0.07	0.0107	0.0012
	c	4.22	0.41	0.58	0.12	0.0072	0.002
1.0	a	6.30	0.21	1.43	0.18	0.0162	0.0017
	c	—	0.26	—	0.24	—	0.0017

in Table I, comparing data obtained on the one hand with the poor heat conductor and thus stronger glowing RW II carbon electrodes, and on the other hand with the good heat conductor copper carrier electrodes relatively colder also during arcing. To stress differences, here exceptionally a current of 17 A was used too, and samples of two different (0.3 and 1.0) $CaCO_3$ molar fraction excited both anodically (a) and cathodically (c).

Though with samples of identical composition no difference is to be expected in the temperature of the burning spot of the arc burning on the sample itself in the case of the two types of carrier electrodes, using copper electrode very small amounts of both carbon oxides were measured, as compared to results obtained with the carbon electrode. It follows from this that in the carbon electrode the filling is also heated up more strongly, and to a greater extent in anodic excitation. Therefore, in this case the reaction zone is deeper than in cathodic excitation. In the colder copper electrode the decomposition of the carbonate can proceed only at the burning spot of the arc and its near environment. The lower reaction zone is absent [6]. (In RW II carbon the whole mass of the sample is heated up more strongly, so that a second, lower zone is also formed below the environment of the burning spot, where the main part of the carbonate is thermally decomposed. Naturally, the two zones are not sharply separated from one another.) For this very reason, in the copper electrode the reaction is stronger in cathodic excitation because of the presumably higher temperature of the burning spot of the arc than in anodic excitation.

2. With the carbon electrode about twice as much carbon monoxide is formed in the arc as carbon dioxide, though mainly the formation of CO_2 was to be expected as a result of thermal decomposition. This proves that further conversions play also an important role. Owing to the large amount of CO formed, of these the process

$$CO_2 + C = 2\ CO \tag{2}$$

is the most probable, proceeding predominantly in the filling of the electrode, but partly in the plasma, where the reaction

$$CO_2 = C + 2\ O \tag{3}$$

must also be taken into consideration. The reaction

$$CaO = Ca + O \tag{4}$$

is essentially the evaporation of the sample at the burning spot of the arc, while decomposition

$$CO = C + O \tag{5}$$

may proceed in the hotter zones of the plasma. Oxigen formed in this way is recombined in the cooler zones of the plasma partly with the evaporated atomic calcium and partly with the carbon vapours to oxides, but the recombination of the oxygen atoms to oxygen molecules is also possible. For at least a partial verification of these processes, oxygen determinations were also undertaken [3] on substances of $n = 0.3$ and 1.0 (pure $CaCO_3$) molar fraction at 7 and 17 A current both upon anodic and cathodic excitation, with an arc drawn for 10 s. Results are given in Table II. Though these amounts are close to the magnitude of measuring error, the average values were accepted as orientative data, as we did not obtain negative results in parallel measurements.

Table II

The volume of O_2 obtained at the RW II auxiliary carbon electrodes;
a anodic, *c* cathodic excitation

n $CaCO_3$	O_2 (cm^3)			
	7 A		17 A	
	a	c	a	c
0.3	0.004	0.005	0.004	0
1.0	0.002	0.003	0.004	0.002

Table III

The volume of O_2 obtained with copper auxiliary electrodes; a anodic, c cathodic excitation

n $CaCO_3$	O_2 (cm^3)	
	a	c
0.1	0.003	0.015
1.0	0.09	0.03

The very low values make it likely that reaction (3) must be subordinate, because if CO were to be formed only by this way, about 1 cm^3 of oxygen should have been obtained according to the reaction. However, owing to relatively quick cooling, the recombination of oxygen with carbon vapours cannot be complete, but must nevertheless be considerable, which was proved again with copper auxiliary electrodes. Data relevant to excitation at 17 A are summarized in Table III. It will be noted that e.g. in the case of pure $CaCO_3$ the volume of oxygen measured is by an order of magnitude higher than in the case of the carbon electrode. With samples of 0.3 molar fraction of $CaCO_3$ the arc burns also on the mixture made electrically conductive by carbon powder, so that more oxygen is formed at the burning spot of higher temperature of the cathode. In the cathodic excitation of the sample containing no carbon, the arc burns mainly at the end of the carrier electrode and thus the sample is less heated. Therefore, in this case more oxygen was obtained in the anodic excitation of the sample. Increased values, as compared to the carbon electrode prove at the same time the plasma reaction, since in the absence of carbon vapours oxygen atoms can mainly recombine with themselves in the plasma, and much less with copper vapours evaporating from the auxiliary electrode and less active than carbon.

In the same way, process (4) must be also of small extent, because in the investigation of CuO [7], considerably less stable than CaO, only a few tenth of a cm^3 of oxygen was formed in the absence of the reaction partner carbon under similar conditions. Neither can a larger contribution by reaction (5) be expected, because according to data in the literature [8] in the plasma of atmospheric pressure only an average of 10^{17} particles/cm^3 can be found per species in the zones of higher temperature. Considering all this, the main reaction of CO formation is at high probability process (2):

$$CO_2 + C = 2\,CO.$$

This equilibrium reaction depending on temperature (the known Boudouars equilibrium) is shifted at 400 °C still completely to the advantage of CO_2

while at 1000 °C practically to the complete advantage of CO. However, under the conditions of the arc one cannot speak of an equilibrium system. CO_2 formed in the interior of the filling, leaving upwards, passes hotter and hotter zones still containing carbon powder, so that the reaction is shifted more and more in the direction of CO formation, even if not in an extent corresponding to equilibrium. This proves also that more CO is formed than CO_2.

3. It can be seen from Figs 3 and 4 that carbon powder in the electrode filling has primarily a diluting effect and a physical one furthering the heating up of the sample on account of its thermal conductivity and high sublimation temperature, which regulate the temperature of the site of heat transmission, concretely of the burning spot of the arc. Indeed, no characteristic sharp maximum appears on the curves at any particular molar ratio as in the case of metal oxides [4]. Thus in this case the direct reaction

$$CaCO_3 + C = CaO + 2\ CO,$$

is hardly likely, because according to this equation curves for CO should have revealed a maximum at a molar ratio of 1 : 1, i.e. at $n = 0.5$.

For further comparison, data of the $CaCO_3 + C$ mixture shown in Figs 3 and 4 were plotted again in Figs 5 and 6 as a function of the per cent composition of the mixture. This gives further information. The two pairs of curves relevant to the two kinds of carbon oxides show with respect to shape an opposite tendency. With increasing carbonate content, reaction (1), i.e. the thermal decomposition of the carbonate increases, but the simultaneous decrease of carbon powder diminishes the ratio of reaction (2), the reduction of CO_2 by carbon. This becomes evident from Fig. 7, where the

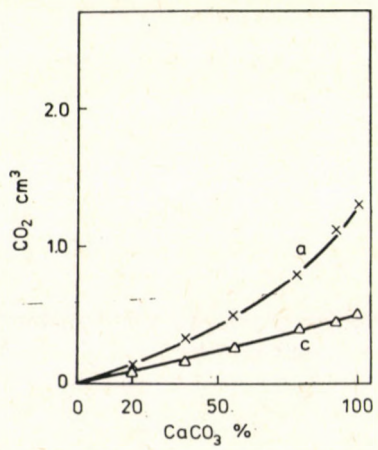


Fig. 5. Data of Fig. 3 as a function of the per cent $CaCO_3$ content of the carbon powder mixtures; *a:* anodic, *c:* cathodic excitation

"summarized basic reaction" [1] is plotted as a function of the mass per cent of $CaCO_3$. In plotting these data it has been taken into consideration that twice as much CO has been formed in reaction (2) than the volume of CO_2 consumed. Thus essentially the volume of total CO_2 formed in the first step by thermal decomposition, i.e. $CO_2 + 1/2$ CO was obtained. In anodic excitation,

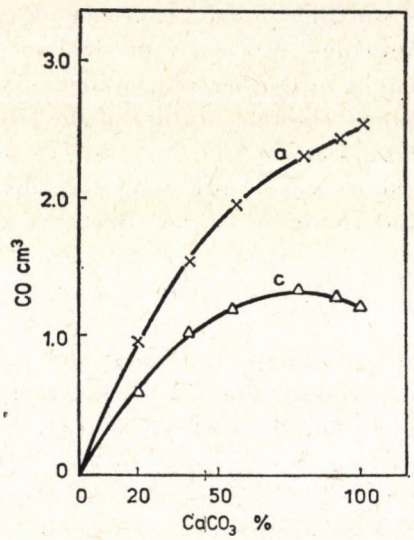


Fig. 6. Data of Fig. 4 as a function of the per cent $CaCO_3$ content of the carbon powder mixtures; *a:* anodic, *c:* cathodic excitation

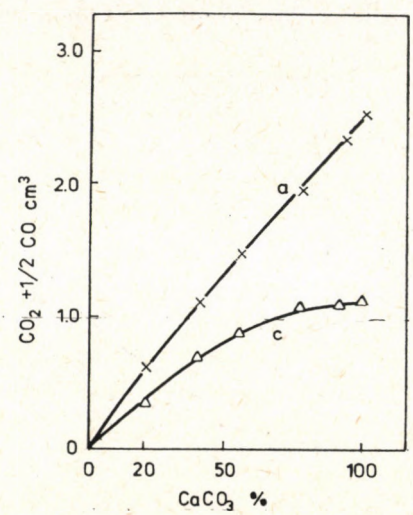


Fig. 7. Change of the "summarized basic reaction" ($CO_2 + 1/2$ CO) as a function of the mass per cent of $CaCO_3$; *a:* anodic, *c:* cathodic excitation

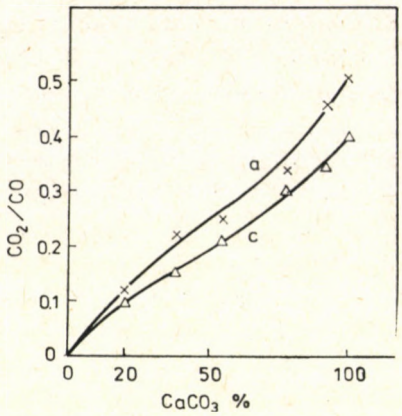


Fig. 8. Volume ratio of CO_2/CO as a function of the composition of the powder mixtures; *a:* anodic, *c:* cathodic excitation

disregarding the initial section of the curve, this amount increases linearly within a wide concentration range. Thus the volume of CO_2 formed in the first step is directly proportional to the carbonate content of the sample, which proves again reaction (1) and excludes reaction (6). Simultaneously with the increase of carbonate content in the mixture the amount of carbon powder is decreasing. If the carbon powder had a chemical role, the curve would bend back with decreasing carbon content. However, considering that this curve is the resultant of two curves of opposite tendency, it may be assumed that in mixtures of lower carbon content, reaction (2) is hindered by carbon powder deficiency and this brings about the opposite trends of the two curves. In cathodic excitation the bending back of the curve may be caused by the fact that in cathodic excitation the temperature of the burning spot of the arc decreases with decreasing carbon powder content, or decreases more than in anodic excitation, because the arc burns on a sample of steadily decreasing evaporation temperature. Heating, heat conduction and evaporation mechanisms are also different in anodic and cathodic excitation, and even the ratio is uncertain in which the area of the burning spots is divided between the surface of the sample and the edge of the carrier electrode. In the case of a 100% carbonate sample, in cathodic excitation electrons are decisively emitted by the carbon carrier electrode, so that the arc may "fixed" to the edge of the electrode.

The volume ratio of the two carbon oxides, that is the CO_2/CO ratio is shown in Fig. 8, similarly as function of the composition of the powder mixtures. The ascent of the curves is steep and almost linear, showing again the importance of thermal decomposition, increasing with increasing carbonate content of the sample, i.e. merely the diluting role of carbon powder. Moreover, if follows from the increase of the ratios that with decreasing amount

of carbon powder in the mixture for the reduction of CO_2 according to reaction (2) conditions of reduction become less favourable in the arc, and the ratio of the two carbon oxides is shifted to the advantage of CO_2, containing carbon of higher oxidation state. That reaction (2) is nevertheless of great importance, becomes evident from the fact that even in the case of pure ($n = 1{,}0$) $CaCO_3$ sample only a ratio of 0.5 is obtained. Since the sample is in contact now only with the wall of the carbon electrode, but does not contain carbon powder, this reaction can proceed only with carbon vapours coming from the carrier electrode into the plasma to a greater extent. According to experimental findings [9], more carbon vapour from the burning spot of higher temperature formed by the arc at the cathode, as compared to that at the anode, in the cathodic excitation of the sample the CO_2/CO ratios are lower, conditions are more reducing.

From the mass of the substance filled in the electrode borings and from the "summarized basic reaction" characteristic of the total amount of the gases produced, the depth of the reaction zone on changing the carbon powder ratio could be calculated, in which reaction accompanied by gas evolution proceeds, assuming that the substance is completely decomposed in the zone. It can be seen from data in Fig. 9 that on replacing the carbon powder of better heat conductivity with $CaCO_3$, the depth of the reaction zone steadily decreases at practically identical current and at identical burning time of the arc. Moreover, in anode carrier electrode of higher average temperature in its

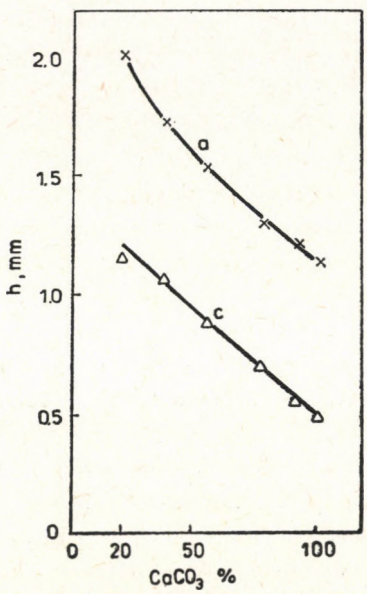


Fig. 9. Depth of the decomposition zone (mm) as a function of carbonate content; *a:* anodic, *c:* cathodic excitation

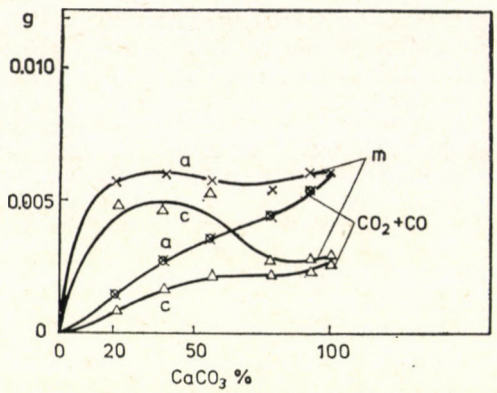


Fig. 10. Loss of mass of the samples measured after arc excitation (*m*) and calculated from gas analytical results (CO_2 + CO) as a function of the mass per cent of $CaCO_3$; *a:* anodic, *c:* cathodic excitation

whole mass (see later Fig. 11) the depth of the reaction zone is larger for carbon powder mixtures of the same composition. Decrease in cathodic excitation is nearly linear, but in the case of the anode of higher temperature a slightly bend back is obtained on the curve, probably because of the greater temperature gradients.

In Fig. 10 the loss in mass of the samples during the burning of the arc, directly measured on an analytical balance (*m*) and the loss in mass calculated from gas analytical results (CO_2 + CO) are compared. It can be seen that the very fine carbon powder of mixtures richer in carbon is sputtered more strongly than marble. Moreover, it can be noted from data relative to pure marble ($n = 1.0$) that only a very small amount of CaO was decomposed and evaporated, so that reaction (4) can be of very small extent, as measured and calculated data are nearly identical. The difference between them is 0.0001 and 0.0004 g in anodic and cathodic excitation, respectively, which may include also the mass of substance sputtered from the boring of the electrode. The sum of these losses is less than, or equal to, 1 *w/w* % of the weighed in carbonate. Anyway, it can be seen that the difference is greater in cathodic excitation, as presumably a larger amount of CaO is evaporated.

It has been said already that our method of excitation was a.c. polarized arc. This was achieved by igniting the a.c. arc only in each second half period at maximum voltage. In this way arc duration of about 1/200 s was followed by a cooling period of 3/200 s. Thus during the total excitation time of 10 s 500 discharges of 1/200 s occur. Dividing the losses in mass observed by 500, in each discharge the evaporation of 10^{-7} to 10^{-6} g of substance is to be expected. This value agrees well with an earlier observation [10] in the measuring of the oxygen consumption of the arc in O_2 + Ar atmosphere with a rotating disc metal aluminium electrode (and a stationary copper auxiliary counter-

electrode with conical end). There too, 10^{-7} to 10^{-6} g of Al was oxidized and evaporated in the arc in each discharge, depending on the exciting conditions. At the same time mass data called attention to the fact that although very finely pulverized samples are generally used because of homogenity problems, suitably an optimal degree of pulverization will be used to diminish problems of reproducibility caused by sputtering.

Carbide formation in the sample by the action of the arc was also investigated. This carbide formation can only be of very small extent and occurs probably only at the high-temperature burning spot of the arc, because when the ignition residue was hydrolyzed with acid after the arc excitation of the samples, even in the optimal case only a very small volume of acetylene (in anodic excitation 0.018 cm^3, in cathodic 0.039 cm^3) could be measured by a very sensitive gas chromatographic method.* This proves also the parallel reaction

$$CaCO_3 + 4\,C = CaC_2 + 3\,CO \qquad (7)$$

for which the optimal case mentioned was represented by the molar fraction 0.2 $CaCO_3$, corresponding to a molar ratio of 1 : 4 carbonate : C according to Eq. (7). However, this percentage is of no importance in view of other reactions producing carbon oxide. Since carbide formation is higher at cathodic excitation, this proves repeatedly that in the case of an amorphous carbon electrode the temperature of the burning spot of the arc at the cathode is higher than that of the burning spot at the anode.

The average temperature of the electrodes during the burning of the arc was measured. Results for a carbon powder mixture containing 55.5% of

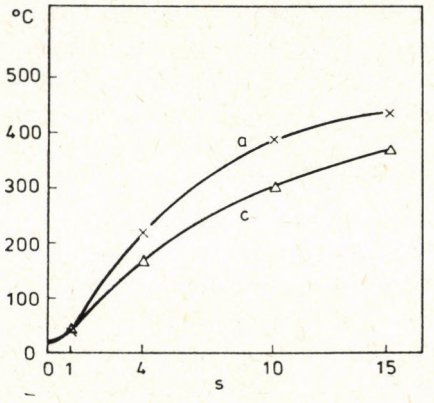


Fig. 11. Change in the average temperature of the electrodes with a mixture of $n = 0.13$ $CaCO_3$ content during the burning of the arc; *a:* anodic, *b:* cathodic excitation

* We thank for gas chromatographic measurements Dr. Jenő Trompler, Dr. László Maros, and Mrs. Dr. Jenő Hollós.

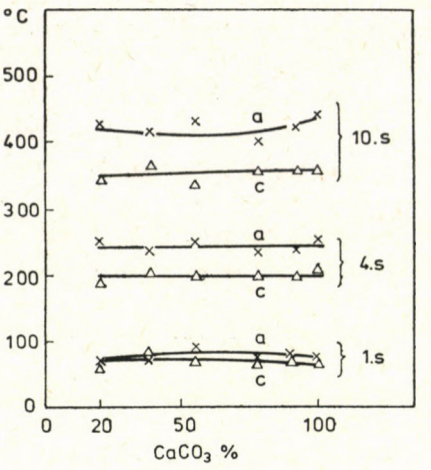


Fig. 12. Relationship between the average temperature of the electrodes and the $CaCO_3$ content of the sample at various moments of arc excitation; *a:* anodic, *c:* cathodic excitation

$CaCO_3$ ($n = 0.13$) are shown in Fig. 11. The pair of electrode temperature vs. arc duration curves starts flatter, because the measuring site of temperature is rather far, at a distance of 5 mm from the site of heat transmission, i.e. from the burning spot of the arc. The whole mass of the electrode begins to get hotter after 1—2 s, and as mentioned already, in anodic excitation to a higher extent. With increasing arc duration the temperature of the electrode increases too, because here the rate of heat transfer is still higher than that of heat loss. However, with increasing electrode temperature the temperature gradients in the system increase too, both in the solid and the gaseous phases, owing to which heat losses become disproportionately higher. Thus, curves begin to bend back.

During the first period of arc burning only the top layer of the filling is sufficiently hot for the proceeding of reactions (1) and (2). Thus, CO_2 formed can rapidly leave the carbon powder environment. With advancing time the reaction zone extends downwards, and CO_2 covers an increasingly long path between carbon particles in an increasingly hot environment. Thus, on account of the longer time and of the temperature-dependence of the Boudouard equilibrium (because the upper layers become continuously hotter) reaction (2) becomes more prominent in time. Later, however these upper layers become poorer in carbon powder just because of reaction (2), which hinders a further increase in the extent of reaction (2) and the increase in temperature of the electrode is not linear.

Temperature curves of similar character are obtained also with pure marble, indicating that in the change of temperature of the electrode actually the ratios of heating up and heat loss are decisive, besides heat conduction

changing according to the composition of the mixture the heat conditions of the carrier electrode are decisive (see also earlier experiments with Cu-electrode). To support this statement, the effect of the ratio of the carbon powder in the mixture on the average temperature of the electrode was also investigated. According to Fig. 12, particularly after longer burning times, the points of the curves are located somewhat higher, though changes are not very convincing. Nevertheless, it can be seen that proceeding towards mixtures poorer in carbon powder, the originally not too high heat conduction of carbon powder

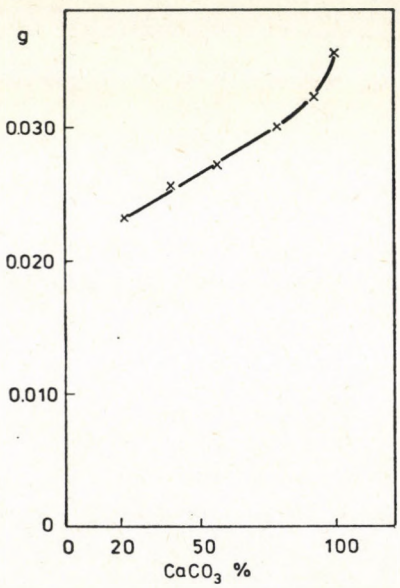


Fig. 13. Mass of mixtures filled in the cavity of the electrodes as a function of the composition of the sample

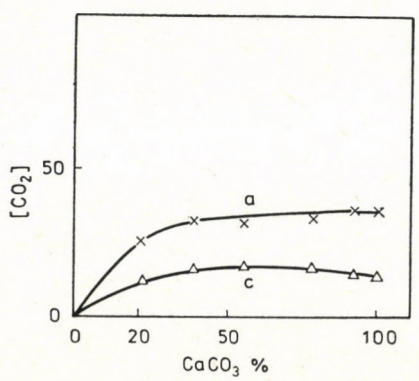


Fig. 14. Volume of CO_2 calculated (normalized) for 1 g of $CaCO_3$ as a function of the sample composition; *a:* anodic, *c:* cathodic excitation

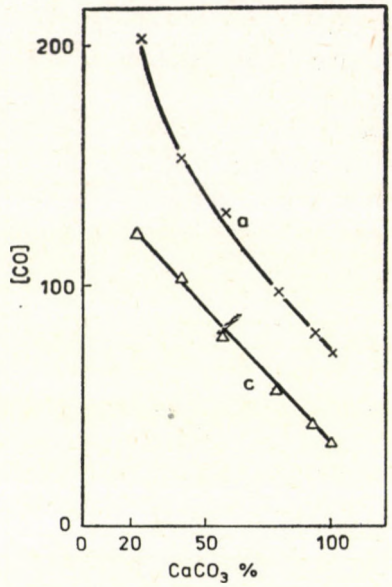


Fig. 15. Volume of CO calculated (normalized) for 1 g of $CaCO_3$ as a function of sample composition; *a:* anodic, *c:* cathodic excitation

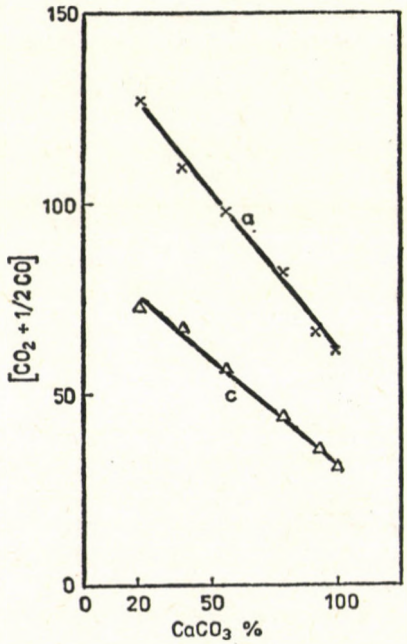


Fig. 16. Extent of the "summarized basic reaction" calculated (normalized) for 1 g of $CaCO_3$ as a function of sample composition; *a:* anodic, *c:* cathodic excitation

is exchanged for the still lower heat conduction of the carbonate. (Changes are more marked in stationary Ar atmosphere, where the cooling effect of the flowing gas is absent.)

So far, in the evaluation of our results the fact was taken into consideration only in the calculation of the depth of the reaction zone that with increasing carbonate content larger and larger masses of sample mixture fit in electrode cavities of the same size (Fig. 13). If, however, gas analytical results measured are normalized by dividing them by the mass of $CaCO_3$ in grams, filled into the bore of the holding electrode and contained in the mixture, i.e. values are referred to 1 g of $CaCO_3$ contained in the sample of given composition, according to Fig. 14 the change in amount of CO_2 produced in the arc ($[CO_2]$) reveals a saturation character, contrary to curves in Fig. 5. Thus, though initially the CO_2 production of the arc increases with increasing carbonate content, this is later compensated by the decrease in magnitude of the reaction zone. Figure 15 shows the change of similarly normalized CO amounts ([CO]) as function of the per cent carbonate content of the mixture. It is easy to note that reaction (2) becomes more and more repressed with decreasing carbon powder ratio, conditions of reduction become less favourable in the arc. The tendency of the curves follows the changes in depth of the reaction zone.

If the values of the "summarized basic reaction" are normalized in a similar way ($[CO_2 + 1/2\ CO]$) which gives the measure of primary decomposition assumed according to reaction (1), it can be seen that the curves obtained (Fig. 16) can be superimposed on those in Fig. 9. It is natural, because these data are not independent of one another. In spite of this, in the filling the reaction described by equation (1)

$$CaCO_3 = CaO + CO_2$$

is the primary process, and the reaction described by Eq. (2)

$$CO_2 + C = 2\ CO$$

is only following this. Disregarding slight carbide formation, here $CaCO_3$ is not directly reduced by carbon powder.

Knowing the above data and results, in our next communication the effect of the reactions and of the carbon powder ratio on the spectral behaviour of the $CaCO_3$ matrix will be discussed.

REFERENCES

[1] Szabó, Z. L., Bertalan, É., Tatár, E.: Acta Chim. Hung. (in press)
[2] Szabó, Z. L., Dobolyi-Fejérdy, H.: Acta Chim. Acad. Sci. Hung., **96**, 201 (1978)
[3] Szabó, Z. L., Tóth, I.: Acta Chim. Acad. (Budapest) **73**, 363 (1962)
[4] Szabó, Z. L., Dobolyi-Fejérdy, H.: Acta Chim. Acad. Sci. Hung., **96**, 125 (1978)

[5] Duval, G.: Inorganic Thermogravimetric Analysis. Elsevier Publishing Co., London 1963
[6] Szabó, Z. L., Dobolyi-Fejérdy, H.: Acta Chim. Acad. Sci. Hung., **97,** 1 (1978)
[7] Szabó, Z. L., Bertalan, É.: Acta Chim. Acad. Sci. Hung., **102,** 371 (1979)
[8] Boumans, P. W. J. M.: Theory of Spectrochemical Excitation, Hilger and Watts Ltd., London, 1966, p. 320
[9] Szabó, Z. L., Pöppl, L.: Acta Chim. (Budapest) **77,** 123 (1973)
[10] Szabó, Z. L., Tóth, I.: Acta Chim. (Budapest) **73,** 373 (1972)

Acta Chimica Hungarica 116 (3), pp. 229—233 (1984)

SYNTHESIS AND REACTIONS OF 2,2-DIPHOSPHONO-1,3-BENZODIOXOLES+*

H. GROSS**, I. KEITEL and B. COSTISELLA

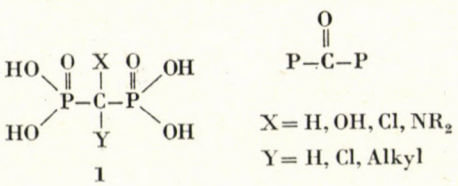
(Central Institute for Organic Chemistry, Academy of Sciences of the GDR, 1199 Berlin, Rudower Chaussee 5, GDR)

Received March 10, 1983

Accepted for publication July 26, 1983

Dealkylation with trimethylsilyl bromide or acid hydrolysis of 2,2-bis(diethylphosphono)-1,3-benzodioxole (**3**) yields a stable acetal of the carbonyldiphosphonic acid: 2,2-diphosphono-1,3-benzodioxole (**5**). The latter is split by conc. hydrobromic acid; with bromine in aqueous solution the 5,6-dibromo derivative **6** is formed.

gem-Diphosphonic acids of type **1** with substituents X and Y are remarkable for their complexing behaviour. Increasing interest is attached to these compounds in the diagnostics and therapy of certain skeletal diseases [1]



1

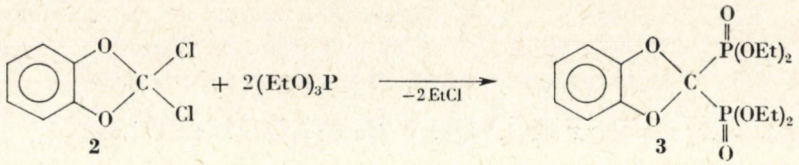
Particularly interesting properties as complex ligands could be expected from methanediphosphonic acids in which X and Y are members of a ring system. The prospects, however, for synthesizing a compound of type **1** containing a carbon ring were poor, since *gem*-dihalides with the corresponding structure would not react with phosphites in the desired manner [2]. On the other hand, dihalides with heterosubstituents acting as donors in positions X and Y should allow the synthesis of suitable products.

As the first representative of this group of compounds we now synthesized 2,2-diphosphono-1,3-benzodioxole, **5**. The starting material was 2,2-bis(diethylphosphono)-1,3-benzodioxole (**3**) which had been obtained earlier from pyrocatechol dichloromethylene ether **2** and triethyl phosphite [3]. By the use of

+ Dedicated to Professor Rezső Bognár, with best wishes on the occasion of his 70th birthday.

* α-Substituierte Phosphonate, 45; Part 44. In: Gross, H., Keitel, I., Costisella, B., Mikolajczyk, J., Midura, W.: Phosphorus and Sulfur, **16**, 257 (1983)

** To whom correspondence should be addressed

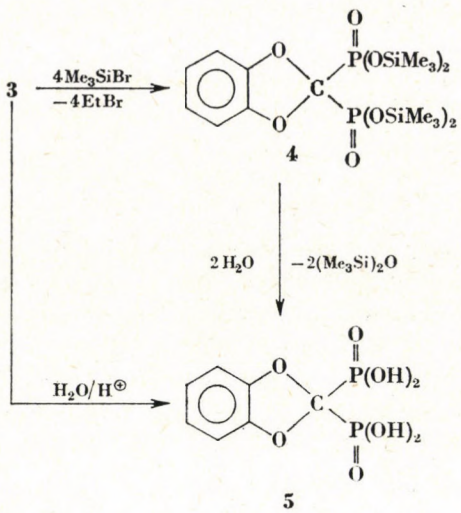


2 3

an excess of triethyl phosphate and prolonging the reaction period, the yield of **3** could be almost doubled.

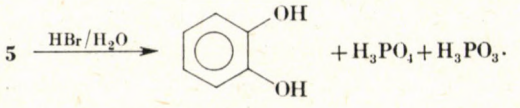
The benzodioxole derivative **3** can be regarded as an acetal of tetraethylcarbonyldiphosphonate.

However, phosphonates with acetal structure on the α-C atom are difficult to transform into the corresponding acids, since alkyl acetals suffer complete decomposition with splitting off the P—C bond if subjected to acid hydrolysis [4] and, under such conditions, also aryl acetals give usually poor yields [5]. For this reason, first the mild dealkylation technique by trimethylsilyl bromide [6] was tried to transform compound **3** into the diphosphonic acid **5**. On boiling **3** with an excess of this reagent, the trimethylsilyl ester was formed; it could subsequently be hydrolyzed, without isolation, by shaking with water, into the diphosphonic acid **5**. However,

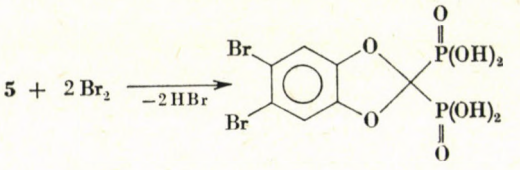


2,2-diphosphono-1,3-benzodioxole **5** turned out to be relatively stable to conc. hydrochloric acid, so that compound **5** was finally obtained in high yields also by boiling the tetraethyl ester **3** with conc. hydrochloric acid. The products prepared by either processes contained, as determined by ^{31}P-NMR tests, slight amount of phosphorus acid.

Compound **5** was largely decomposed by 48% hydrobromic acid: after boiling for 4 hours, pyrocatechol, phosphoric acid and phosphorous acid, in addition to unchanged **5**, were isolated or detected by NMR, but no carbonyl-



diphosphonic acid was found. Three further, not yet identified signals of decomposition products of the diphosphonic acid **5** were also found in the ^{31}P-NMR spectrum. In contrast, the acetal structure of the diphosphonic acid **5** proved to be stable to bromine: when an aqueous solution of **5** was heated with bromine, ring bromination took place, and 5,6-dibromo-2,2--diphosphono-1,3-benzodioxole (**6**) was obtained in a yield of 71%, in pure



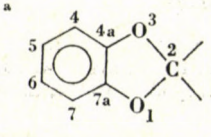
6

form, without any contamination by phosphorous acid. The structures of the diphosphonic acids **5** and **6** could be unequivocally confirmed by ^{31}C-NMR-spectroscopy (Table I). The triplets at 111.5 ppm and 114.9 ppm, are charac-

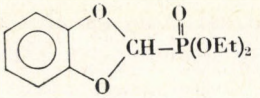
Table I

^{13}C—NMR spectral data of substituted 1,3-benzodioxoles[a]

Compound	solvent	Chemical shifts δ, ppm (Coupling constants *J*, Hz)					
		C[2] (J_{PC})	C[4a,7a]	C[4,7]	C[5,6]	CH_2 (MNE)d	CH_3 (MNE)d
3	$CDCl_3$	110.0 t	147.3	108.9	122.4	64.85	16.45
		(182.2)				(3.6)	(2.7)
						64.70	16.30
						(3.6)	(2.7)
3	C_6D_6	111.4 t	148.0	109.1	122.7	64.80	16.55
		(178.8)				(3.4)	(2.3)
						64.60	6.40
						(3.4)	(2.3)
5	D_2O	111.5 t	148.6	110.6	124.0	—	
		(174.4)					—
6	D_2O	114.9 t	149.6	114.7	116.6	—	—
		(168.6)					

[a] 

teristic: they are due to coupling with two equivalent phosphorus nuclei. The typical triplet was also observed in the spectrum of the tetraethyl ester **3**. The coupling constants (J_{PC}) found were of the order of magnitude observed for P—C-couplings in compounds with analogous acetal structure, e.g. in the diethyl ester **7** [7].



7

Investigations on the suitability of the new diphosphonic acids **5** and **6** as complex ligands, particularly as ligands for ^{99m}Tc to be utilized in bone scintillography will be reported later elsewhere.

Experimental

^{13}C- and ^{31}P-NMR spectra were recorded with a Varian CFT 20 spectrometer (standards: ^{13}C TMS internal, ^{31}P H_3PO_4 external).

2,2-Bis(diethylphosphono)-7,3-benzodioxole (3)

A mixture of **2** (19.1 g; 0.1 mol) and triethyl phosphite (35.6 g; 0.215 mol) was heated for 5h to 150—160 °C. The pyrocatechol carbonate formed as a by-product was then removed by distillation in vacuum (water jet pump), and the residue was distilled in high vacuum. A yield of 25.4 g (65%) of compound **3** was obtained, b.p. 155—158 °C/0.01 Torr; $n_D^{25} = 1.4905$; *(lit.* [3] b.p. 156—180 °C/0.01 Torr; $n_D^{25} = 1.4886$).

2,2-Diphosphono-1,3-benzodioxole (5)

(a) A mixture of **3** (19.7 g; 0.05 mol) and trimethylsilyl bromide (76.5 g; 0.5 mol) was heated for 4 h on a boiling water bath. Low-boiling components were removed in water-jet pump vacuum, and water (50 mol) was added to the oily residue, with shaking. The precipitated hecxamethyl-disiloxane was separated and the aqueous solution evaporated in vacuum. The crystals obtained were dried for 2 h at 50—60 °C in high vacuum to give 13.5 g (87%) of **5**, m.p. 165—167 °C.

$C_7H_8O_8P_2 \cdot 2\,H_2O$ (318.1). Calcd. C 26.43; H 3.80; H_2O 11.3. Found C 25.88; H 3.62; H_2O 11.8%.

(b) Conc. hydrochloric acid (10 mL) was added to **3** (3.94 g; 0.01 mol) and the mixture was refluxed for 2.5 h. After cooling, the mixture was evaporated in vacuum and the crystals were dried by pressing on clay to obtain 2.8 g (88%) of **5**, m.p. 164—167 °C.

Reaction of 5 with hydrobromic acid

Compound **5** (1 g) was refluxed for 4 h with 48% hydrobromic acid and the solution was evaporated. The residue crystallized partially. The filter-pressed crystals were identified as pyrocatechol (crude m.p. 93—98 °C, mixed m.p.: no depression). Another part of the residue was dissolved in water and the ^{31}P-NMR data were recorded.

$\delta = 0$ ppm (H_3PO_4), 2.0 ppm and 5.2 ppm (unidentified), 5.4 ppm H_3PO_3 ($J_{PH} = 685$ Hz), 6.4 ppm (**5**), 8.5 ppm (unidentified).

5,6-Dibromo-2,2-diphosphono-1,3-benzodioxole (6)

Compound **4** (3.18 g; 0.01 mol) was dissolved in water (5 mL) and heated to 50 °C. Bromine (3.18 g; 0.02 mol) was added dropwise, with stirring, and the mixture was kept for 15 min at this temperature. After cooling, it was evaporated on a rotary evaporator, the crystals

that separated were pressed on clay and dissolved in water; the solution was treated with active carbon, filtered and evaporated in vacuum. The crystals were dried on clay in air to yield 3.4 g (71%) of **6**, m.p. 185—187 °C; recrystallized from a small amount of water, m.p. 188—189 °C.

$C_7H_6Br_2O_8P_2$ 2 H_2O (475.9). Calcd. C 17.67; H 2.12; H_2O 7.57. Found C 17.58; H 2.31; H_2O 7.32%.

REFERENCES

[1] (a) Subramanian, G., Balir, R. J., Kallfelz, E. A., Thomas, F. D., McAfee, J. G.: J. Nucl. Med., **14,** 640 (1973); (b) Subramanian, G., McAfee, J. G., Blair, R. J., Thomas, F. D.: Proc. Symp. Medical Radionuclide Imaging IAEA, Vol. **II,** p. 83, Vienna, 1977; (c) Fleisch, H., Russell, R. G. G., Simpson, B., Mühlbauer, R. C.: Nature, **223,** 211 (1969); (d) Schenk, R., Merz, W. A., Mühlbauer, R. C., Russell, R. G. G., Fleisch, H.: Calcif Tissue Res., **11,** 196 (1973); (e) Alexandre, C., Meunier, P. J.: Lyon Med., **237,** 56. (1977); (f) Douglas, D. L., Russel,, R. G., Preston, Ch. J., Prenton, M. A., Duckworth, T., Kanis, J. A., Preston, F. E., Woodhead, S. St.: The Lancet, **1980,** 1044; (g) Unterspann, S.: Eur. J. Nucl. Med., **1,** 151 (1976); (h) Unterspann, S., Finck, W.: Dt. Gesundh.-Wesen, **36,** 2205 (1981); (i) Heaney, R. P., Saville, P. D.: Clin. Pharmacol. Ther., **1976,** 593

[2] Sasse, K., in: Houben-Weyl, Methoden der Organischen Chemie, Band **12/1,** p. 436. G. Thieme Verlag, Stuttgart 1963

[3] Gross, H., Engelhardt, G., Freiberg, J., Bürger, W., Costisella, B.: Justus Liebigs Ann. Chem., **707,** 35 (1965)

[4] Razumov, A. J., Moskva, V. V.: Zb. Obshch. Khim., **35,** 1595 (1965)

[5] Gross, H., Costisella, B.: J. Prakt. Chem., **313,** 265 (1971)

[6] Gross, H., Böck, Ch., Costisella, B., Gloede, J.: J. Prakt. Chem., **320** 344 (1978)

[7] Costisella, B., Gross, H.: J. Prakt. Chem., **319,** 8 (1977)

Acta Chimica Hungarica 116 (3), pp. 235—243 (1984)

APPLICATION OF ORGANIC COMPOUNDS AS THERMOCHEMICAL AGENTS IN SPECTRAL ANALYSIS

A. DELIJSKA[1]*, CHR. PRAVČEVA[2] and I. DONCHEV[1]

([1] Research and Projecting Institute NIPRORUDA, Stambolijski 205, Sofia 1309, Bulgaria and [2] Research Institute of Ferrous Metallurgy, Sofia 1770, Bulgaria)

Received March 15, 1983

Accepted for publication July 27, 1983

The possibilities of applying teflon, tetramethyl-, tetraethyl-, and tetrabutylammonium iodide, bromosuccinimide, sodium diethyldithiocarbamate and sodium oxalate as thermochemical agents in spectral analysis have been studied. The experiments were carried out with a d.c. arc on a C and a SiO_2 matrix, containing a variety of added elements. The influence of these organic compounds on the evaporation of the elements was investigated together with their influence on the anode and plasma temperatures and the line intensity. The evaluation of the results shows that the presence of organic additives influences the process within the plasma and in the electrode cavity.

NaDDTC was further investigated as an additive to the Fe_2O_3 matrix. The anode and plasma temperatures as well as the line intensity in the prsesence of NaDDTC and SiO_2 were determined. An attempt to explain the data obtained on the basis of thermochemical reactions, anode and plasma temperature was made. On the basis of these considerations a spectrographic method for determination of As, Bi, Ge, Sb, Sn, Tl, Zn in materials with high iron content was developed.

Organic compounds are comparatively less used as thermochemical agents in spectral analysis than inorganic compounds. Teflon [4, 13—15], C_2Cl_6, C_3Cl_8 [10—13] were applied to influence the process in the bearing electrode. In previous investigations [1] the effect of some organic compounds on Group 4, 5 and 6 elements was examined and $(C_2H_5)_4NI$ was applied to determine impurities in MoO_3 [2].

The purpose of this study is to investigate better the possibilities for using organic compounds as additives in spectral analysis by tracing their influence on the processes in the electrode cavity, the anode and plasma temperature and the intensity of the spectral lines.

Experimental

A Zeiss spectrograph Q24 was used in conjunction with an external optical system, consisting of 3 quartz lenses; the diaphragm of the internal lense was 3.2 mm; the slit width — 0.010 mm; arc source — a d.c. arc of 10A; electrodes — graphite type RWIII, 6 mm in diameter, the lower electrode (anode) had a sample cavity 4×6 mm, while the upper electrode (cathode) had a conically rounded end.

* To whom correspondence should be addressed

Photographic plates — ORWO WU-3.

Synthetic sample — matrix; graphite or SiO_2, to which 0.1% and 0.01% of the oxides of Ag, As, B, Be, Al, Bi, Ca, Cd, Co, Cu, Fe, Ge, Mg, Mn, Mo, Ni, Si, Sn, Ti, V, Zn were added.

A mixture of 20 mg synthetic sample and 20 mg organic compound was added to the anode cavity. Only the teflon was introduced to the bottom of the electrode, without being mixed.

Spectral lines — the most sensitive and interference — free lines of the elements were used.

The temperature at a level of 3 mm below the bottom of the anode cavity was measured with the aid of a Pt/Pt-Rh thermocouple, while the temperature at the bottom was calculated using Fourier's law of heat conduction [5]. The arc plasma temperature was measured by the two line method using Zn 307.6/328.3 nm and Zn 307.6/307.2 nm lines.

The behaviour of the oxides of some elements in the presence of different organic compounds was also investigated by using X-ray analysis of the residues obtained after burning a matrix, containing 10% of the oxides of the examined elements, and the corresponding organic additive.

The preliminary investigation was carried out with 16 aliphatic hydrocarbons, which are solid at room temperature and have comparatively high boiling points. Taking into account the column stability and the behaviour at burning, teflon, tetramethylammonium iodide, tetraethylammonium iodide, tetrabutylammonium iodide, bromosuccinimide, sodium diethyldithiocarbamate and sodium oxalate were selected for further investigation.

Results and Discussion

Influence of the organic additive on the evaporation process

Comparing the curves "$\log I - t_s$", with and without additive, the results can be generalized as follows:

— Teflon acts as a strongly fluorinating substance. This is especially pronounced for the graphite matrix, with less volatile elements like Al, B, Be, Mo, V, etc., which form more volatile fluorides. In the presence of teflon these elements enter the plasma during the first 60 s. On the contrary, with elements forming less volatile fluorides, as for example alkaline earth metals and iron, the evaporation is delayed. When the elements are added to the SiO_2 matrix, their evaporation is not accelerated, the matrix element only enters the plasma in larger quantities than in the absence of teflon. The character of evaporation of the matrix and the additive elements is not considerably changed when graphite is added to SiO_2 (1 : 1).

— Tetraalkylammonium iodide (TAAI). The boiling and decomposition points of TAAI increase with increasing molecular weight. As the products of its decomposition contain iodide, a iodination effect can be expected. This is noticeable especially with elements like Ag, Cu and Sn. Because of the fact that the examined matrices are indifferent to TAAI, the evaporation curves for graphite and SiO_2 are similar.

— Bromosuccinimide (BrSI). When BrSI is introduced to the two kinds of samples, the curves "$\log I - t_s$" for most of the elements have the same character as they do without organic additive. Only the entering of the volatile elements (As, Sn, Sb, Pb, Zn) into the plasma is increased. The

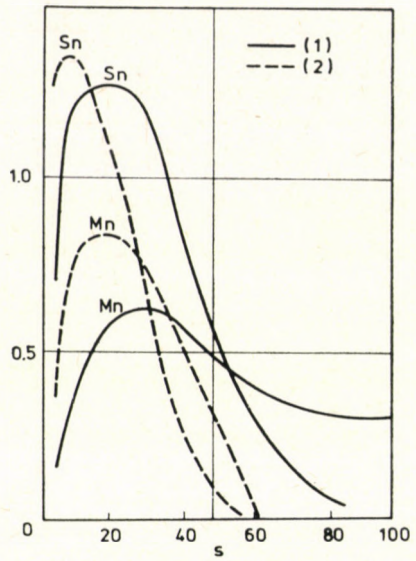


Fig. 1. Line intensity as a function of exposure time for Sn 283.99 nm and Mn 293.30 nm with a C and a SiO_2 matrix; (1) with additive, (2) without additive

observed behaviour of Mn is interesting — in the presence of BrSI it evaporates for 60 s (Fig. 1).

— Sodium diethyldithiocarbamate (NaDDTC). The presence of loosely connected sulfur in NaDDTC leads to a sulfiding action. This effect was proved by X-ray diffraction analysis. In the residues after an exposure of 5 s, PbS, MoS and ZnS were found. NaDDTC also accelerates the entering into the plasma of elements such as Bi and Ge.

— Sodium oxalate. With this compound obvious participation in thermochemical reaction cannot be proved.

Influence of the organig additive on the anode and plasma temperature

Usually when an organic additive is introduced, the anode temperature decreases and the extent of its decrease depends on the thermal stability of the additive (Fig. 2). The combination of teflon with SiO_2 is an exception; the anode temperature in this case is almost the same as without an additive and this can be explained by the exothermic reaction between fluorine and the matrix.

The influence of the organic compounds on the plasma temperature is shown for both matrices in Table I. As is seen in the table, teflon and BrSI give comparatively high plasma temperatures, which is favourable for elements with higher optimal conditions of excitation. TEAI and TBAI have different

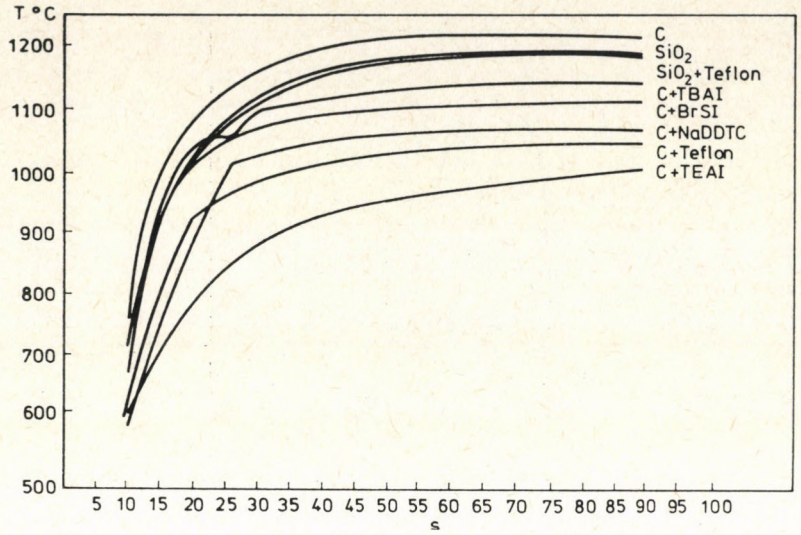


Fig. 2. Anode temperature (T °C) as a function of exposure time (s)

influences on the anode temperature, while they cause analogous temperatures in the plasma. The organic compounds containing sodium create a so-called "alkaline plasma", which has the lowest temperature and is favourable for the determination of elements with relatively lower excitation and ionization

Table I

Plasma temperatures measured with and without organic additive with a C *and a* SiO_2 *matrix*

Additive	Plasma temperature (K)	
	C	SiO_2
NONE	7100	6600
TEFLON	7000	6500
BrSI	6800	6700
TBAI	6650	6550
TEAI	6650	6500
NaDDTC	5700	5600

potentials. These changes in the anode and plasma temperatures allow the choice of such temperature conditions which are favourable for the corresponding matrix and element to be determined.

Influence of the organic additive on the line intensity

To investigate the influence of the organic additives on the integral line intensity of some elements, the values of the coefficients K were calculated:

$$K = \frac{\log I \text{ with additive}}{\log I \text{ without additive}} .$$

Some of the results are given in Figs 3 and 4. As can be seen in Fig. 3, when teflon is added to a graphite matrix, the line intensity of the elements decreases. For a mixture on SiO_2 basis the line intensity of the matrix element is considerably increased. In this case, teflon increases the line intensity of the impure elements as well, with the exception of iron with a difference in the increase, depending on the element. When other organic compounds are added, no matter what the matrix is, the influence on the line intensity of different elements is analogous.

In Fig. 4 it is shown that with the increase of the molecular weight of TAAI the line intensity also increases. BrSI has a positive effect on the values of K for Ag, Mn, Sn. The organic compounds, containing sodium, increase log I for elements like Pb, Sn and decrease it for Fe and Sb. The difference between the influence of $Na_2C_2O_4$ and the sulfur containing NaDDTC definitely affects the line intensity of Ge.

On the basis of these investigations the following conclusions can be made.

Teflon is recommended for use with a matrix that cannot be fluorinated or which forms less volatile fluorides, while the analysed elements form more volatile fluorides.

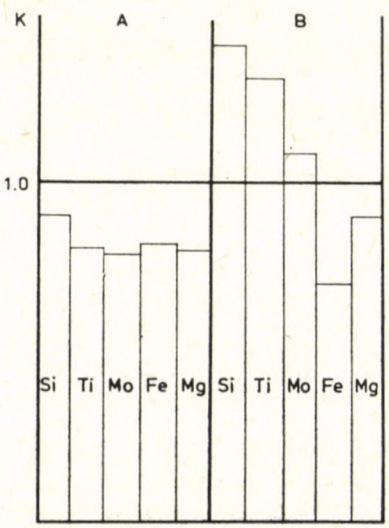


Fig. 3. Influence of teflon additive on the K-value; A—C matrix, B—SiO_2 matrix

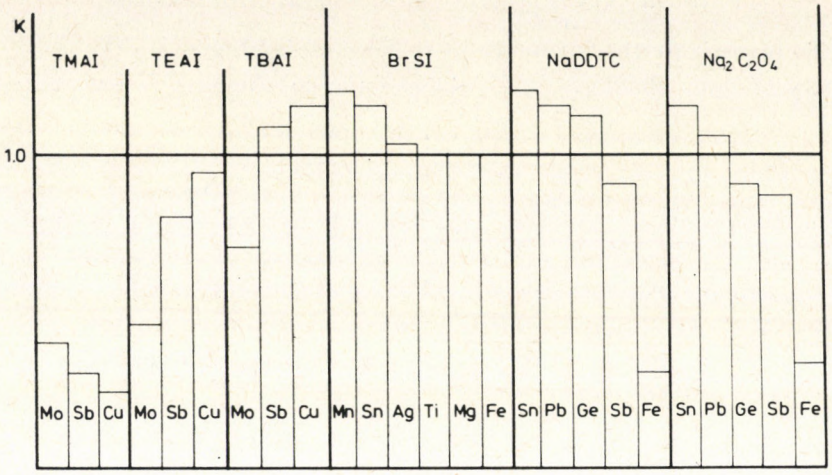


Fig. 4. Influence of TAAI, BrSI, NaDDTC and $Na_2C_2O_4$ additives on the *K*-value

When TAAI is used, the rate with which the elements enter the plasma is increased and the line intensity in the direction TBAI-TEAI-TMAI is decreased, the last compound being unfavourable because in its presence the elements move too fast from the electrode. That is why TEAI and TBAI must be used in milder conditions of evaporation for matrices with lower boiling point, respectively, for a matrix, which, because of chemical reactions with these additives, remains in the electrode cavity [2].

BrSI can be used instead of graphite powder. In the cases when a comparatively lower plasma temperature is required, a sodium containing organic compound can be used successfully and the sulfiding action of NaDDTC would be especially favourable in many cases. As a rule the decomposition of all organic compounds results in gaseous products, which favour the accelerated entry of the elements into the plasma.

In order to confirm the results obtained as well as the conclusions which they lead to, the application of one of the organic compounds was studied. NaDDTC was chosen on account of the possibility to control in this case the processes in the electrode cavity and the plasma temperature simultaneously. The decrease of the line intensity of iron and increase of the line intensity of a number of elements in its presence directed us towards investigating the possibility of application of NaDDTC as an additive in the analysis of products with high iron content.

First, experiments with a synthetic sample of Fe_2O_3 matrix were carried out. The apparatus and the experimental conditions were the same, only the plasma temperature measurements were carried out by using couples of iron lines [6]: Fe 317.54/319.20 nm, Fe 323.30/323.50 nm and Fe 323.00/324.60 nm.

It was established that when adding NaDDTC to the matrix Fe_2O_3 (1 : 1), the measured anode temperature remained unchanged (900 °C) for 60 s and after that it slowly increased. During this time the elements capable of forming volatile sulfides in these conditions, enter the plasma. But the intensity of the interfering matrix element also increases after a minimum at the 55th second. To increase the plasma temperature (measured 5100K) SiO_2 was added to NaDDTC, all the more that SiO_2 is often present in the natural samples. Optimal conditions for obtaining maximal line intensity for the impurity elements were observed when 12.5% SiO_2 was introduced in the mixture. Under these conditions (Fig. 5) the plasma temperature increases to 5800K, which is optimal for gaining maximal line intensity of a number of elements. The temperature in the electrode cavity in this case reaches 1000 °C for 20 s and remains constant. Regardless of the higher temperature in the electrode cavity, iron volatilization is suppressed to a higher degree than when only NaDDTC is added. For clarifying the behaviour of the matrix element, X-ray diffraction analyses of the residues after 5, 10 and 60 s exposition time were made. The results obtained are given in Table II. As can be seen from the table, in the absence of SiO_2 the reduction of Fe_2O_3 to less volatile iron metal (b.p. 3000 °C) is accelerated and nevertheless when only NaDDTC is added

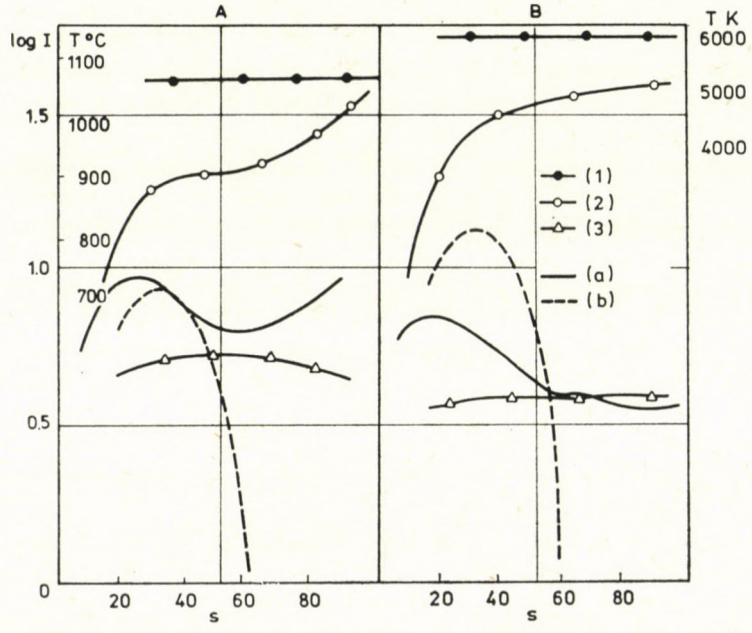


Fig. 5. Plasma temperature T(K) (1), anode temperature T °C (2) and the line intensity of the buffer element NaI 285.28 nm (3), the matrix element FeII 258.59 nm (a) and the analyzed element SnI 283.99 nm (b) versus burning time; A — with addition of NaDDTC, B — with addition of NaDDTC and SiO_2 (3 : 1)

Table II

X-Ray diffraction analysis of the residue after burning a mixture of Fe_2O_3 *and an organic additive* (1 : 1)

Additive	Prooved phases after exposition time		
	5 s	10 s	60 s
NaDDTC	Fe_3O_4, FeO	FeO, Fe_3O_4	αFe, FeO, γFe_2O_3
NaDDTC and SiO_2 (3 : 1)	Fe_3O_4, γFe_2O_3	γFe_2O_3, FeO	FeO, γFe_2O_3, αFe

Phases are arranged in a row according to their concentration decrease

the line intensity of iron is increased. The more pronounced depression of iron volatilization in the electrode cavity when SiO_2 is introduced, can be explained possibly with the forming of a melt at the very first 5—10 s. Delayed entering of Fe into the plasma has been observed by the authors when SiO_2 was introduced to a buffer KNO_3 (1 : 1). With this buffer, used in the analysis of products containing iron [7, 8], are compared with the line intensity of some elements when a NaDDTC : SiO_2 (3 : 1) buffer is used (Fig. 6). It is seen that for some elements, such as Ge and Sn, the addition of the sulfur containing reagent improves the element sensitivity.

On the basis of the results obtained a spectrographic method for the determination of As, Bi, Ge, Pb, Sb, Sn, Tl, Zn in iron ores and iron containing products was developed.

During the preparation of this paper, the results obtained and reported [3, 9] were confirmed and applied for some other matrices [16].

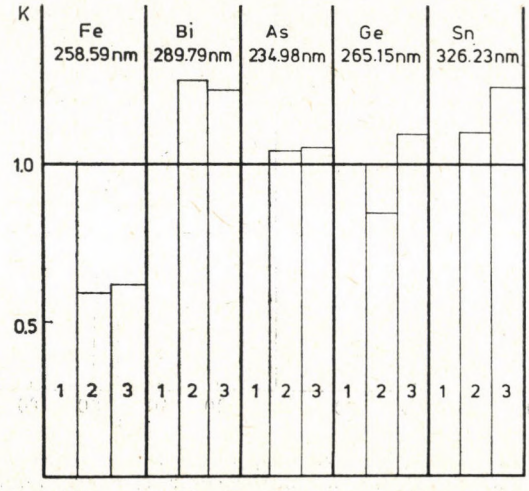


Fig. 6. Influence of the additive on *K*-value; 1. without additive, 2. with addition of KNO_3 and SiO_2 (1 : 1), 3. with addition of NaDDTC and SiO_2 (3 : 1)

REFERENCES

[1] Delijska, A., Pravčeva, Ch., Tončev, N.: Spectrochim. Acta, **318,** 121 (1976)
[2] Delijska, A., Pravčeva, Ch.: Z. anal. Chem., **281,** 281 (1976)
[3] Delijska, A., Pravčeva, Ch.: XX CSI, Prague, No. 44., (1977)
[4] Izmajlova, D., Zakharia, B.: Zh. Anal. Khim., **27,** 2134 (1972)
[5] Kántor, T., Pungor, E.: J. Therm. Anal., **6,** 521 (1974)
[6] Morozova, N., Startsev, G.: Izv. Akad. Nauk SSSR, Ser. Fiz., **7,** 929 (1962)
[7] Pravčeva, Ch., Ganev, P., Delijska, A.: Cont. rend. Acad. Bulg. Sci., **24,** 893 (1971)
[8] Pravčeva, Ch., Ganev, P., Delijska, A., Ninova, V.: Z. anal. Chem., **254,** 16 (1971)
[9] Pravčeva, Ch., Delijska, A.: XX CSI Prague, No. 45., (1977)
[10] Rautschke, R., Dowe, Ch., Isensee, G., Herbeck, J.: Z. anorg. allog Chem., **413,** 127 (1975)
[11] Rautschke, R., Nada, N.: Chemie Anal., **21,** 23 (1976)
[12] Rautschke, R., Grote, U.: Z. Chem., **7,** 346 (1977)
[13] Rautschke, R.: Wiss. Z. Karl Marx Univ. Leipzig, Math. Naturwiss. R., **28,** 415 (1979)
[14] Schaeps, R., Mazukiewicz, M., Nickel, H.: Z. anal. Chem., **281,** 273 (1976)
[15] Tarassevich, N., Semenenko, K., Khromova, G.: Zh. Anal. Khim., **26,** 2149 (1971)
[16] Türker, R., Dogan, M.: 7th CANAS, June 14—18, 1982, Sopron, Hungary, Abstract D 32

Acta Chimica Hungarica 116 (3), pp. 245—249 (1984)

THE APPLICATION OF ADDITION METHODS IN SPECTROGRAPHIC ANALYSIS, II*

O. FILO

(Department of Chemistry, Faculty of Metallurgy of the Technical University, 043 85 Košice, Švermova 9, Czechoslovakia)

Received May 23, 1983

Accepted for publication August 3, 1983

The agreement of the parameters of the analytical calibration line obtained by the addition methods and by the method of least squares was studied. It was found that background correction largely improves the numerical agreement of parameters. A favourable effect of background correction on accuracy and precision of concentration determination was also observed.

Introduction

In a previous paper [1] we reported the course of calculating the unknown concentration c_X applying the addition method. The determination of c_X allows to calculate the parameters A and B of the analytical calibration line [1]:

$$\Delta Y = A + B \cdot \log c_X \tag{1}$$

This is actually a generalization of the addition methods, insofar as the calculated values of the parameters A and B can be utilized to determine the unknown concentration c_X in samples with matrix of similar composition.

The objective of this work was to compare the parameters A and B of the analytical calibration line obtained by the method of least squares [2, 3] and by the addition method utilizing more than two additions procedure. In the following we studied the application possibilities of the addition method to determine unknown concentrations and the effect of background correction on the accuracy and precision of concentration determinations.

Experimental

The experimental data were obtained with the technique applied in [4]. Spectral analysis was performed with synthetic model substances of the following composition:

SiO_2	50.0%
Al_2O_3	16.0%
Fe_2O_3	7.0%
MgO	4.0%
CaO	6.0%
Na_2CO_3	7.0%

* Part I cf. [1]

Table I

Experimental conditions

Spectrograph	Grating spektrograph PGS-2 $m = 2$: $D = 0.37$ nm/mm
Wave length range	270 to 350 nm
Projection	three-lense, Zeiss
Aperture of intermediate diaphragm	3.2 mm
Slit width	0.040 mm
Material of electrodes	Graphite manufactured by Elektrokarbon, Topolčany
Support electrode	SU-304
Counter electrode	SU-201
Graphite powder	SU-602
Electrode distance	4.0 mm
Emulsion	ORWO WU-3
Developer	ORWO F-43, 10 min, 20 °C
Excitation	a.c. arc
Choke resistance	250 ohm
Primary voltage	220 V
Current strength	5...6 A
Exposure time	60 s
Pre-excitation	10 s

Spectral lines used	Ni	305.08 nm
		344.63 nm
	V	318.34 nm
		318.40 nm
	Pd	302.79 nm
		346.08 nm

The analytical elements added to the model sample were Ni and V in the form of their oxides. In such way, we prepared seven calibration samples with Ni concentrations in the range $3.28\times10^{-3}\%$ to $6.74\times10^{-2}\%$ and V concentrations in the range $1.07\times10^{-3}\%$ to $2.20\times10^{-2}\%$. Pd was used as a reference element in the form of PdO, in a concentration of 0.04%. The spectral lines of the elements applied are presented in Table I [4, 5].

The samples used for spectral analysis were obtained by mixing the calibrating samples with $BaCO_3$ and graphite powder in a ratio of 6 : 2 : 2. The experimental conditions are listed in Table I [4].

Each spectrum was taken four times. Optical density values were determined with a Zeiss-Jena MD-100 microdensitometer. The density values were used to calculate the ΔY values of the individual calibration samples and the parameters A and B of the analytical calibration line, by a program developed by Flórián [6].

The ΔY values obtained were utilized in the addition method computations for more than two additions procedure by means of the relations represented in [1], using the program developed by Holländer [7]. We considered the lowest concentration of the analytical element as unknown, and the concentrations of the further calibration samples, reduced, of course, by the "unknown" concentration, as additions. The addition method allowed to compute, besides the unknown concentration, the parameters A and B of the analytical calibration line. The computation were first carried out without background correction, and then with background correction for, both spectral lines.

Results

By combining the utilized spectral lines of the analytical elements and the spectral lines of the reference element, we obtained a total of eight pairs of homologous lines. The parameters A and B, the determined "unknown"

Table II

Parameters of the analytical calibration line and unknown concentration c_X determined for the line pair Ni 344.63/Pd 346.08

Background correction	Mode of computation	A	s_A	B	s_B	c_X, %	s_{c_X}
None	Least squares	1.23	0.04	0.83	0.02	—	—
	Addition	1.49	0.58	1.05	0.43	0.00629	0.00436
Applied	Least squares	1.40	0.04	0.95	0.02	—	—
	Addition	1.37	0.58	0.97	0.32	0.00387	0.00223

Note: Ni concentration of the calibration sample with the lowest Ni concentration: Ni, % = 0.00328

Table III

Parameters of the analytical calibration line and unknown concentration c_X determined for the line pair V 318.40/Pd 346.08

Background correction	Mode of computation	A	s_A	B	s_B	c_X, %	s_{c_X}
None	Least squares	1.88	0.05	0.91	0.02	—	—
	Addition	1.93	0.67	0.97	0.30	0.00148	0.00079
Applied	Least squares	2.08	0.06	1.01	0.02	—	—
	Addition	2.06	0.60	1.02	0.27	0.00126	0.00062

Note: Vanadium concentration of the calibration sample with the lowest vanadium content: V, % = 0.00107

concentration c_X and the standard deviations of the mean values are listed in Table II for the Ni 344.63/Pd 346.08 pair, and in Table III for the V 318.40/Pd 346.08 pair. These pairs of lines exhibit perfect homology [4, 8].

The results presented in Tables II and III allow the comparison of the values A and B and the standard deviations of the means obtained by the addition method with the values obtained by using the method of least squares [2, 3, 6]. Since identical calibration samples were used for both techniques (in the addition method we determined the concentration of the sample with the lowest content of the analytical element), we were able to evaluate the accuracy and precision of concentration determination making use of the addition method. The criterium of accuracy is numerical agreement of the prepared calibration sample's concentration with the measured concentration. Precision is characterized by the standard deviation of the mean value: s_{c_X}.

The effect of background correction on the agreement of the values studied, on the parameters A and B can also be evaluated from the data in the tables. We did not perform statistical evaluation of the agreement of A and B, in view of the relatively high numerical values of s_A and s_B in the case of the addition method.

Besides the two homologous spectral line pairs the results of which are presented in Tables II and III, the lines given in Table I yield further six pairs. We determined their parameters A and B, the values of c_X and the standard deviation of the means. The results are not shown in this paper, since they are fully analogous to those listed in Tables II and III.

Discussion of the results

The results presented in Tables II and III indicate that the parameters A and B of the analytical calibration line obtained by more than two addition procedure of the addition method are numerically comparable to the values computed with the method of least squares. Agreement is substantially better when background correction is applied.

The standard deviations s_A and s_B are higher by about one order of magnitude in the case of the addition method. It should, however, be noted that the mode of calculation was different [1, 2, 3]. In the case of the addition method, standard deviation has its origin in repeated parallel measurements while in the method of least squares standard deviation belongs to one single value of the parameter.

When making use of the method of least squares it is assumed that only the values of the variable ΔY in Eq. (1), that is, in the equation of the analytical calibration curve, are liable to error whereas the values of the variable c_X are error-free. This assumption is, however, questionable, owing to the mode of preparation of the calibration samples. (Sample contains relatively small concentration of the analytical element which is repeatedly reduced.) In consequence of the assumption mentioned the standard deviation values s_A and s_B appear significantly more favourable.

To judge the accuracy and precision of concentration determination with the addition method, the calibration sample with the lowest amount of analytical element was used as the unknown. When background correction was applied, numerical agreement with the concentration of the prepared sample improved substantially. Background correction also improves the standard deviation of the mean concentration values s_{c_X}.

Concentrations determined with the addition method were higher in all cases, for all pairs of spectral lines, than the concentrations in the corresponding calibration samples. Presumably this phenomenon is due to the effects which

cause the upward deviation of the calibration line in the lower concentration ranges [9, 10]. From this view, it might probably be of interest to investigate the effect of the so-called two-gamma correction.

List of symbols

ΔY — logarithm ratio of spectral line intensities of the analytical and the reference element

A, B — parameters of the analytical calibration line

c_X — unknown concentration

s_A — standard deviation of the mean value of A

s_B — standard deviation of the mean value of B

s_{c_X} — standard deviation of the mean unknown concentration

REFERENCES

[1] Filo, O., Holländer: I.: Acta Chim. Hung., **113,** 317 (1983)
[2] Flórián, K., Lavrin, A., Matherny, M.: Chem. Zvesti, **27,** 623 (1973)
[3] Matherny, M., Ondáš, J.: Anal. Chim. Acta, **133,** 51 (1981)
[4] Filo, O., Matherny, M.: Acta Chim. Hung., **98,** 13 (1978)
[5] Zaydel, A. N., Prokofev, V. K., Raysky, S. M., Slavny, V. A., Shreyder, E. J.: Tables of Spectral Lines (in Russian), Nauka, Moscow 1969
[6] Flórián, K.: Computer program AP/82. Personal communication
[7] Holländer, I.: Personal communication
[8] Filo, O.: Dissertation. VSB, Ostrava 1972
[9] Zimmer, K., Szabó, E.: Proc. XV. Coll. Spectroscop. Internat. Madrid 1969. Vol. IV, p. 55. Iberica, Tarragona 1970
[10] Heltai, Gy., Zimmer, K., Flórián, K.: Acta Chim. Hung., **106,** 239 (1981)

Acta Chimica Hungarica 116 (3), pp. 251—259 (1984)

SYNTHESIS AND CHARACTERIZATION OF 1-PHENYL-3-FORMAMIDINO THIOCARBAMIDE COMPLEXES WITH SOME BIVALENT METAL IONS*

B. SINGH, B. P. YADAVA and R. C. AGGARWAL**

(Department of Chemistry, Banaras Hindu University, Varanasi 221 005, India)

Received March 21, 1983

In revised form July 11, 1983

Accepted for publication September 1, 1983

The complexes with the chemical compositions ML_2Cl_2 [M = Co(II), Ni(II), Cu(II), Zn(II), Cd(II) and Hg(II)], VOL_2SO_4, $CoLCl_2$ and $M'(L-H)_2$ [M' = Co(II), Ni(II), Cu(II)], L = 1-Phenyl-3-formamidino thiocarbamide (PFTC), have been prepared and characterized by analytical data, molar conductance, magnetic susceptibility, electronic, infrared, ESR, X-ray powder diffraction and NMR spectral studies. Some of the complexes have been tested for antifungal activity.

Introduction

Metal complexes with ligands containing sulphur and nitrogen as donor atoms have been extensively used as pesticides [1] and fungicides [2, 3]. A number of copper(II) complexes have been reported to be effective fungicides [4—8]. The toxicological importance of —N—C—S moiety have been well established in many fungicides and pesticides [9]. The survey of the literature shows that there is no previous report on metal complexes of 1-phenyl-3-formamidino thiocarbamide. Complete absence of previous work on transition metal complexes of PFTC, varied bonding and stereochemical possibilities offered by these complexes because of the presence of as many as five potential bonding sites and possibility of thione-thiol tautomerism in the ligand and their potential applications as antifungal and antibacterial agents, have prompted us to undertake synthesis and structural studies of VO(IV), Co(II), Ni(II), Cu(II), Zn(II), Cd(II) and Hg(II) complexes with the above ligand.

Experimental

Materials

All the chemicals used in the present study were of BDH or equivalent grade. PFTC was prepared by the method [10] reported earlier.

* Part of the work has been published in the proceedings of XIV National Seminar on Crystallography, IIT, Kharagpur (India), Dec. 20—23, 1982.

** To whom correspondence should be addressed.

Acta Chim. Hung. 116 1984

Table I

Analytical data, colour, melting point, molar conductance and magnetic moment of PFTC ocmplexes

Complexes	Colour	M.P. °C	Found (calcd.) %				Λ^{-1} M (ohm^{-1} cm^{-2} mol^{-1})	μ_{eff} (B.M.)
			Metal	Cl	S	N		
VOL_2SO_4	Dirty green	210[d]	8.70 (9.25)	—	16.92 (17.42)	19.50 (20.32)	12.51	1.59
CoL_2Cl_2	Green	165[d]	11.13 (11.37)	13.29 (13.70)	11.95 (12.35)	22.40 (22.62)	10.75	4.46
$CoLCl_2$	Brown	166[d]	18.00 (18.18)	21.57 (21.90)	9.12 (9.90)	17.00 (17.28)	8.10	2.62
NiL_2Cl_2	Pink	170[d]	10.82 (11.34)	13.42 (13.71)	12.12 (12.36)	21.28 (21.63)	144.0	Diamagnetic
CuL_2Cl_2	Grey	155[d]	11.97 (12.15)	12.96 (13.58)	12.00 (12.24)	21.50 (21.43)	140.6	Diamagnetic
ZnL_2Cl_2	White	195	12.51 (12.46)	13.56 (13.54)	11.81 (12.20)	20.81 (21.35)	13.61	Diamagnetic
CdL_2Cl_2	Ligh yellow	200[d]	19.00 (19.67)	12.50 (12.42)	10.75 (11.20)	18.95 (19.60)	12.98	Diamagnetic
HgL_2Cl_2	Yellow	140[d]	30.83 (30.41)	10.87 (10.76)	9.43 (9.70)	16.71 (16.98)	10.34	Diamagnetic
$Co(L-H)_2$	Brown	165[d]	13.50 (13.23)	—	14.50 (14.38)	24.70 (25.17)	4.20	1.20
$Ni(L-H)_2$	Red	220[d]	13.63 (13.20)	—	14.47 (14.39)	25.28 (25.18)	2.28	Diamagnetic
$Cu(L-H)_2$	Brown	190	13.07 (12.12)	—	13.99 (14.23)	24.75 (24.91)	9.00	1.10

d = decomposition temperature

Synthesis of complexes

The addition compounds, $CoLCl_2$, VOL_2SO_4 and ML_2Cl_2 [M = Co(II), Ni(II), Cu(II), Zn(II), Cd(II) and Hg(II)] were prepared by adding solution of appropriate metal salt (1 mmol) in 10 mL of ethanol or methanol to the solution of 2 mmol of the ligand in 10 mL ethanol at room temperature. The complexes were almost immediately precipitated except ZnL_2Cl_2 which was obtained by keeping the reaction mixture overnight. CoL_2Cl_2 was isolated from the filtrate of $CoLCl_2$ by concentrating it or by addition of solvent ether to it.

The deprotonated complexes $M'(L-H)_2$ [M' = Co(II), Ni(II) and Cu(II)] were obtained by adding 1 mmol of the appropriate metal acetate in 10 mL water to 2 mmol of the ligand in 15 mL ethanol and the complexes thus precipitated were digested on water bath for half an hour to ensure complete deprotonation.

The resulting complexes were suction filtered, washed with water (in case of deprotonated complexes only), ethanol or methanol, ether and finally dried in vacuum.

Analysis of the complexes

The complexes were analyzed for metal content using literature procedures [11]. Chloride was estimated as AgCl, sulphur as $BaSO_4$ and nitrogen microanalytically. The analytical data are given in Table I.

Physical measurements

Electrical conductance of the complexes in DMF at 10^{-3} *M* concentration was measured with a WTW conductivity meter. Magnetic susceptibility of the complexes was measured at room temperature on a Cahn—Faraday electrobalance using $HgCo(NCS)_4$ as calibrant and was corrected for diamagnetism [12] using Pascal's constants. Molar conductance and magnetic moment data are included in Table I. The UV and visible spectra of ligand as well as complexes in Nujol were recorded on a Cary-14 Spectrophotometer while the IR spectra of ligand as well as the complexes were recorded on a Perkin-Elmer Spectrophotometer Model-621 in Nujol (4000—200 cm^{-1}) and in KBr (4000—400 cm^{-1}). ESR spectra of CuL_2Cl_2 in chloroform solution were recorded at room temperature and 77 K on a Varian X-band spectrometer Model E-4 using DPPH as a *g* marker. The X-ray powder photograph for CuL_2Cl_2 was obtained on a Philips X-ray generator using nickel filtered CuK_α-radiation and a Guinier FR-552 camera. The indexing of X-ray diffraction lines was done by ITQ's method [13a]. The observed and computed *Q* values for tetragonal symmetry along with the corresponding *hkl* values are listed in Table II. The ^{1}H-NMR spectra of ZnL_2Cl_2 and ligand were recorded on a Varian A-60D spectrometer in DMSO-d_6 at 45° using TMS as an internal reference standard.

Table II

Observed and computed Q, hkl values for $Cu(PFTC)_2Cl_2$

Powder pattern line	*Q* obsd.	*Q* comp.	*hkl*	Powder pattern line	*Q* obsd.	*Q* comp.	*hkl*
1	0.0165	0.0164	110	12	0.0743	0.0739	301
2	0.0176	0.0175	111	13	0.0786	0.0776	109
3	0.0212	0.0208	112	14	0.0842	0.0831	312
4	0.0292	0.0263	113	15	0.0881	0.0886	108
5	0.0326	0.0326	200	16	0.0953	0.0949	217
6	0.0366	0.0357	105	17	0.0969	0.0973	109
7	0.0389	0.0372	202	18	0.1232	0.1237	324
8	0.0405	0.0410	210	19	0.1308	0.1312	400
9	0.0543	0.0560	116	20	0.1360	0.1356	402
10	0.0613	0.0603	205	21	0.1512	0.1520	332
11	0.0706	0.0704	008	22	0.1773	0.1770	328

Table III

Antifungal activity for ligand and complexes

Compound	Concentration				
	100 ppm	200 ppm	400 ppm	800 ppm	1000 ppm
Ligand (PFTC)	28.33	80.50	100	100	100
$Cu(PFTC)_2Cl_2$	17.79	67.97	74.94	100	100
$Co(PFTC)_2Cl_2$	0.94	1.16	44.31	77.26	100
$Ni(PFTC)_2Cl_2$	42.38	48.32	73.54	100	100

The antifungal activity of the complexes and the ligand was carried out at different concentrations by food-poison technique against *Rhizoctonia solani* Kuhn, an amnivorous root pathogen of various crop plants as described by Schmitz [13b]. The number of replication for each concentration was three with suitable control. After 72 hr of incubation at 25 ± 1 °C the colony diameter was measured and the percent inhibition was calculated as follows:

$$\text{Percent inhibition} = \frac{X - Y}{X} \times 100$$

where X = diameter of the colony in control plates and
Y = diameter of the colony in test plates at different concentrations. The antifungal activity shown by ligand and complexes is summarized in Table III.

Results and Discussion

The ligand PFTC forms two types of complexes viz., addition compounds ML_2Cl_2, $CoLCl_2$ and deprotonated complexes $M'(L-H)_2$ as indicated by analytical data (Table I). All the complexes decompose in 140—220 °C temperature range while ZnL_2Cl_2 and $Cu(L-H)_2$ melt at 195 and 190 °C, respectively. The complexes are insoluble in water and common organic solvents such as methanol, ethanol, carbon tetrachloride but most of them are soluble in DMF and DMSO.

The molar conductance values for all the complexes are low suggesting their non-electrolytic [14] nature except NiL_2Cl_2 and CuL_2Cl_2 which have molar conductivities 144.0 and 140.6 $ohm^{-1}\,cm^2\,mol^{-1}$, respectively, indicating 1 : 2 electrolytic behaviour of the above complexes.

Magnetic moments

The nickel(II) complexes are diamagnetic showing square planar geometry around Ni^{2+} ions. The magnetic moments of $CoLCl_2$ (2.62 B. M.) and CoL_2Cl_2 (4.46 B. M.) indicate square planar and tetrahedral geometry [12] around Co^{2+} ions in the complexes, respectively. The anomalous μ_{eff} values of $Co(L-H)_2$ (1.20 B. M.) and $Cu(L-H)_2$ (1.10 B. M.) may be attributed to super exchange or metal–metal interaction [15] while that of VOL_2SO_4 (1.59

B. M.) to V = O...V interaction [16]. CuL_2Cl_2 is diamagnetic indicating it to be either dimeric/polymeric copper(II) complex [17, 18] or a copper(I) complex. However, the visible and ESR spectra discussed later suggest that it is a dimeric copper(II) complex.

Electronic spectra

The electronic spectrum of the ligand in ethanol shows two strong bands at 35970 cm^{-1} (ε, 29,600) and 47,170 cm^{-1} (ε, 22,2220) which may be assigned to $\pi \rightarrow \pi^*$ and/or $n \rightarrow \pi^*$ transitions. The corresponding bands in the complexes are observed in 31,250 – 36,365 and 40,000 – 45,455 cm^{-1} regions. Three bands, observed at 12,120, 16,395 and 28,570 cm^{-1} in the spectrum of VOL_2SO_4, attributable to $d_{xy} \rightarrow d_{yz}$, d_{xz} and $d_{x^2-y^2}$ transitions, indicate the square pyramidal [19, 20] geometry of the complex. Electronic spectrum of CoL_2Cl_2 yields bands at 4880, 5480, 6515 (ν_2) and 12,905, 14,600, 15,750 cm^{-1} (ν_3) assignable to $^4A_2 \rightarrow {}^4T_1(F)$ and $^4T_1(P)$ transitions indicating tetrahedral [21] coordination around Co^{2+} ion. The ligand field parameters calculated [22] for the complex are $10Dq$, 2723 cm^{-1}; B' 754 cm^{-1}; β 0.78; β° 22% and LFSE, 38.90 kJ/mol.

The electronic spectrum of $CoLCl_2$ shows a strong band at 18,690 cm^{-1} and three split bands at 14,925, 15,875 and 16,260 cm^{-1} while that of $Co(L-H)_2$ yields a strong band at 18,180 cm^{-1} and two weak bands at 15,385 and 17,390 cm^{-1} in the visible region which can be assigned to $^2A_{1g} \rightarrow {}^2E'_{2g}$ transition assuming square planar [23, 24] geometry of the complexes. NiL_2Cl_2 exhibits a strong band at 19,610 cm^{-1} and a more intense band at 27,780 cm^{-1} while $Ni(L-H)_2$ yields corresponding bands at 21,050 and 28,570 cm^{-1} which may be assigned to ν_2 and ν_3 arising from $^1A_{1g} \rightarrow {}^1A_{2g}$ and $^1A_{1g} \rightarrow {}^1B_{1g}$ transitions, respectively, on the basis of square planar [25] geometry of the complexes. Both the complexes exhibit an additional well-defined band (at 10,810cm^{-1}) to a lower energy than ν_2 which is referred to as ν_1 and is probably a spin-forbidden transition [25]. The two bands observed at 16,130 and 22,220 cm^{-1} in the spectrum of $Cu(L-H)_2$ are attributed to d – d transitions in square planar [26] geometry while a band at 25,000 cm^{-1} is characteristic of dimeric [27, 28] nature of the complex. CuL_2Cl_2 is one of few copper(II) complexes in which the spin paramagnetism is completely quenched ($\mu_{eff} = 0$) at room temperature. The diamagnetism indicates that there is strong spin–spin interaction between two cupric ions. This may take place by the direct overlap of the singly occupied d-orbitals on two cupric ions or by superexchange phenomenon. Herris and co-workers [18] explained diamagnetism of dark green copper(II) complex with diazoaminobenzene on the basis of metal–metal interaction and attributed two bands at 14,925 and 18,870 cm^{-1} observed in the visible region of electronic spectrum of the above complex to d – d transitions in square

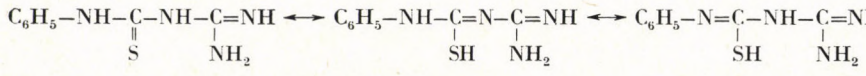
planar geometry around copper(II) ion. Electronic spectrum of our grey diamagnetic complex CuL_2Cl_2, yields a band at 14,285 cm^{-1} and we are inclined, after the above workers, to assign it to d—d transition in square pyramidal environment of copper(II) [29].

ESR spectral studies

Although, CuL_2Cl_2 is diamagnetic in the solid state, it is paramegnetic in solution as is evident from its chloroform solution ESR spectra studied at room and liquid nitrogen temperatures. The various ESR parameters[a] computed from the spectra are as follows$_8$ A_{II}, 180 Gauss; A_I, 62.16 Gauss; A_{iso}, 101.44 Gauss-g_{II}, 2.1809; g_I, 2.0196 and g_{av}, 2.0734. The paramagnetic behaviour of the complex in solution is presumably due to weakening [30] of electron spin–spin interaction between two cupric ions.

Infrared spectral studies

The appearance of a band at 2410 cm^{-1} in acetonitrile solution spectrum of PFTC indicates the existence of thione–thiol tautomerism [31] in the ligand in solution.



The infrared spectrum of PFTC shows bands at 3440, 3385, 3275 and 3195 cm^{-1}. The first two bands are assigned to $\nu(=N-H)$ and the remaining two bands to $\nu(NH)$. The position of these bands either remains unchanged or shows slight positive shift in the spectra of VOL_2SO_4, CoL_2Cl_2, ZnL_2Cl_2, CdL_2Cl_2 and HgL_2Cl_2 indicating that nitrogen of NH or NH_2 groups are not involved in bonding. The bands in $\nu(NH)$ region become either broad or shift to lower frequency in spectra of $CoLCl_2$, NiL_2Cl_2, CuL_2Cl_2, $Co(L-H)_2$, $Ni(L-H)_2$ and $Cu(L-H)_2$ which indicate that nitrogen is involved in bonding in these complexes. The $\nu(C=N)$ band [32] occurring at 1655 cm^{-1} in the ligand is observed in 1650—1695 cm^{-1} region in the complexes showing that azomethine nitrogen is not involved in coordination to the metal ion. A band at 1605 cm^{-1} in the spectrum of ligand assigned to $\beta(NH_2)$ is observed in 1590—1600 cm^{-1} region in $CoLCl_2$, NiL_2Cl_2, CuL_2Cl_2 and $M'(L-H)_2$ and in 1610—1630 cm^{-1} region in the remaining complexes indicating coordination of NH_2 in bonding in the former complexes and its non-involvement in the latter.

The thioamide(IV) band [33] (mainly due to $\nu(C=S)$) at 745 cm^{-1} shifts to lower frequency (715—730) in the complexes suggesting bonding through

[a] ESR parameters refer to 77 K; $g_{av} = (g_{II} + g_I)/3$.

thione sulphur in all the addition compounds. A band at 720 cm^{-1} in the spectra of deprotonated complexes may be assigned to ν(C—S) of M—S—C group. The appearance of four bands at 1225, 1075, 1025 and 970 cm^{-1} in vanadyl sulphate complex is in accord with bidentate chelating [34] nature of the sulphato ion. A strong band at 970 cm^{-1} is assignable to ν(V=O) [35]. However, the ν_1 band of the chelating sulphato group also occurs in the same region making this assignment rather uncertain.

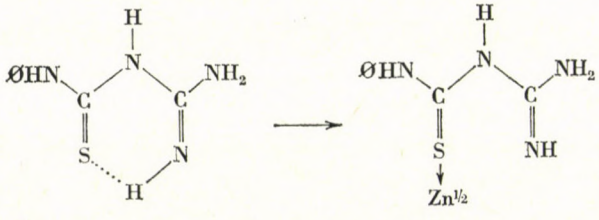
A non-ligand band observed in the 300—360 cm^{-1} region in all the complexes and that in 240—280 cm^{-1} region in spectrum of $CoLCl_2$, $NiLCl_2$, CuL_2Cl_2 and deprotonated complexes are tentatively assigned to ν(M—S) [34] and ν(M—N) [36] modes, respectively.

X-Ray diffraction studies

The powder X-ray diffraction lines have been successfully indexed for tetragonal symmetry. The lattice parameters computed for the above symmetry of the complex are $a = b = 11.071$ Å, $c = 29.104$ Å, $\varrho = 1.02$ g cm^{-3}, ϱ(cal) = $= 0.97$ g cm^{-3} and $z = 4$.

^{1}H-NMR spectral studies

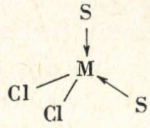
The ^{1}H-NMR spectrum of the ligand in DMSO-d_6 displays singlets at δ3.83 (NH_2 protons), δ 9.33 (=NH proton) and a multiplet δ 6.7—7.8 (C—NH—C and C—NH- protons). The spectrum of ZnL_2Cl_2 shows singlet at δ 3.83 for NH_2 protons and multiplet at δ 6.7—7.8 (for =NH, C—NH—C and C—NH-) protons. The shielding (upfield shift) of =NH, proton in complex suggests the involvement of proton in hydrogen bonding in the ligand which is broken in complex. The signal due to NH_2 protons (δ 3.83) remains unchanged in the complex indicating that NH_2 group of the ligand is not involved in bonding.



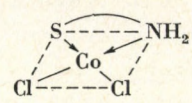
Antifungal activity

It is observed from Table III that the activity increases with concentration and becomes 100% for ligand, CuL_2Cl_2, NiL_2Cl_2 and CoL_2Cl_2 at 400, 800, 800 and 1000 ppm, respectively.

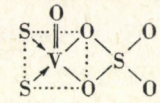
Based on analytical data and physicochemical studies following structures are tentatively proposed for the complexes.



ML_2Cl_2

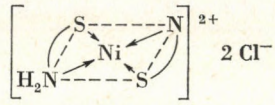


$CoL\,Cl_2$

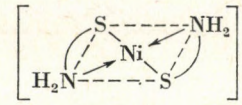


VOL_2SO_4

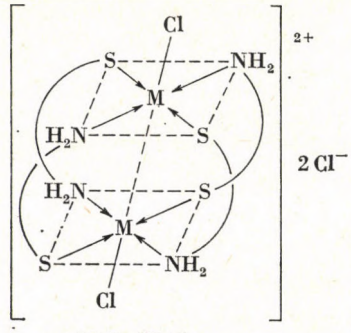
M = Co(II), Zn(II), Cd(II), or Hg(II)



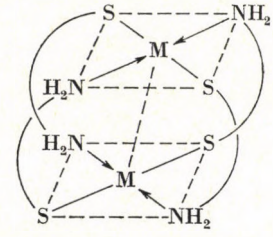
$[NiL_2]Cl_2$



$Ni(L-H)_2$



$[CuL_2Cl]_2Cl_2$



$M(L-H)_2$, M = Co(II) or Cu(II)

*

The authors wish to thank Prof. B. M. Shukla, Head of Chemistry Department, Banaras Hindu University, for providing laboratory facilities. One of them (B. P. Y.) is thankful to UGC, New Delhi, for award of Teacher Research Fellowship. Sincere thanks are also due to RSIC, IIT Madras for running ESR spectra of the complexes.

REFERENCES

[1] Johnson, C. W., Joyner, J. W., Perry, R. P.: Antibiotics and Chemotherapy, **2**, 636 (1952)
[2] Gansman, H. W., Rhykerd, C. I., Hinderliter, H. R., Scott, E. S., Andrieth, L. F.: Bot. Gazz., **114**, 292 (1953)
[3] Benos, B. G., Gingras, B. A., Bayley, C. H.: Appl. Microbiol., **8**, 353 (1961)
[4] Agrawal, S. P., Rai, R. A.: Trans. Met. Chem., **1**, 238 (1976)
[5] Herman, G.: J. Med. Chem., **17**, 824 (1974)
[6] Herman, G., Larry, S.: Can. J. Microbiol., **21**, 1317 (1975)
[7] Ganorkar, M. C., Reddy, G. V.: Proceedings of the Annual Convention of Chemists, Kurukshetra University, 16., 1979
[8] Bailar, J. C., Emeleus, J. H., Nyholm, R., Trotman-Dickenson, A. F.: Comprehensive Inorganic Chemistry, Vol. **3** Pergamon Press, New York, 3., 1973
[9] Dash, B. C., Mahapatra, G. N.: J. Indian Chem. Soc., **44**, 939 (1967)
[10] Kurzer, F., Sanderson, P. M.: J. Chem. Soc., **1959**, 3240
[11] Vogel, A. I.: A Text book of Quantitative Inorganic Analysis, ELBS and Longmans, 3rd Ed. (1973)

[12] Figgis, B. N., Lewis, J.: The Modern Coordination Chemistry, Edited by Lewis and Wilkins, R. G., Interscience, New York, 403 (1960)
[13a] Azaroff, L. V., Burger, M. J.: The Powder Method in X-ray Crystallography, McGraw Hill, New York, 119 (1958)
[13b] Schmitz, H.: Ind. Eng. Chem. Analyt., **4,** 361 (1930)
[14] Geary, W. J.: Coord. Chem. Rev., **7,** 81 (1971)
[15] Yamada, S., Niskihava, H., Tsuchida, T.: Bull. Chem. Soc. Japan, **33,** 1278 (1960)
[16] Syamal, A.: Coord. Chem. Rev., **16,** 309 (1975)
[17] Khuller, I. P., Agarwala, U.: Can. J. Chem., **53,** 1165 (1975)
[18] Harris, C. M., Hoskins, B. F., Martin, R. L.: J. Chem. Soc., **1959,** 3728
[19] Stocklosa, H. J., Wasson, J. R., McCormick, B. J.: Inorg. Chem., **13,** 592 (1974)
[20] Farmer, R. L., Urbach, F. L.: Inorg. Chem., **13,** 587 (1974)
[21] Cotton, F. A., Goodgame, D. M. L., Goodgame, M.: J. Am. Chem. Soc., **83,** 4690 (1961)
[22] Lever, A. B. P.: J. Chem. Ed., **45,** 711 (1968)
[23] Nishida, Y., Kida, S.: J. Inorg. Nucl. Chem. Lett., **7,** 325 (1971)
[24] Singh, P. P., Shukla, U. P., Makhija, R., Rivest, R.: J. Inorg. Nucl. Chem., **37,** 679 (1975)
[25] Lever, A. B. P.: Inorganic Electronic Spectroscopy, Elsevier, Amsterdam, 343 (1964)
[26] Scacconi, L., Ciampolini, M.: J. Chem. Soc., **1964,** 276
[27] Kato, M., Jonassen, H. B., Fanning, J. C.: Chem. Rev., **1964,** 6499
[28] Harris, C. M., Martin, R. L.: Proc. Chem. Soc., **1958,** 259
[29a] Pignedoli, A., Peyronal, G.: Gazz. Chim. Ital., **92,** 745 (1962)
[29b] Simmons, C. J., Lundeen, M., Seff, K.: Inorg. Chem., **17,** 1429 (1978)
[29c] Mckezie, E. D.: J. Chem. Soc., A., **1970,** 3095
[29d] Hathaway, B. J., Tomlinson, A. A. G.: Coord. Chem. Rev., **5,** 1 (1970)
[30] Churchil, M. R., Davies, G., El-Sayed, M. A., El-Shazly, M. F., Hutchinson, J. P., Rupich, M. W.: Inorg. Chem., **19,** 201 (1980)
[31] Sadler, P. W.: J. Chem. Soc., **1961,** 957
[32] Kurzer, F.: Tetrahedron, **32,** 1031 (1976)
[33] Pignedoli, A., Peyronel, G.: Spectrochim. Acta, **34A,** 1005 (1978)
[34] Nakamoto, K.: Infrared and Raman Spectra of Inorganic and Coordination Compounds, 3rd Ed. Wiley Interscience, New York 1978
[35] Selbin, J., Holmes, L. H. Jr., McGlynn, S. P.: J. Inorg. Nucl. Chem., **25,** 1359 (1963)
[36] Ohkaku, N., Nakamoto, K.: Inorg. Chem., **10,** 798 (1971)

Acta Chimica Hungarica 116 (3), pp. 261—265 (1984)

XANTHATE ANIONS AS SALTS OF OXINATO BIS(η^5-INDENYL)TITANIUM(IV)/ZIRCONIUM(IV) CHELATES

R. K. BAJAJ, G. S. SODHI, N. K. KAUSHIK and K. N. JOHRI*

(Department of Chemistry, University of Delhi, Delhi-110 007, India)

Received June 17, 1983

Accepted for publication September 2, 1983

A number of ionic chelates of the type, $[(\eta^5\text{-}C_9H_7)_2ML]^+[ROCS_2]^-$ (where R = Me, Et, *n*-Pr, *i*-Pr, *n*-Bu, *i*-Bu, M = Ti(IV), Zr(IV); and L is the conjugate base of oxine) have been synthesized and characterized by elemental analyses, electrical conductance and IR and ^{1}H-NMR spectral studies.

Introduction

During the course of our recent investigation we have elucidated that the coordination of two nitrogen and two oxygen atoms to $(\eta^5\text{-R})(\eta^5\text{-R}')M(IV)$ moiety would lead to the weakening of the metal-ring bonds [1—4] R = C_4H_4N, R′ = C_5H_5, C_9H_7; R = C_5H_5, R′ = C_9H_7; M = Ti, Zr]. In order to investigate whether or not the coordination of two oxygen and two nitrogen atoms around $(\eta^5\text{-}C_9H_7)_2M(IV)$ moiety (M = Ti, Zr) would produce a similar weakening of metal ring bonds, we studied the interaction of $(\eta^5\text{-}C_9H_7)_2MCl_2$ with oxine in aqueous medium. We failed to isolate a derivative in which two oxinate groups coordinate to $(\eta^5\text{-}C_9H_7)_2M(IV)$ moiety. However, ionic complexes of the type $[(\eta^5\text{-}C_9H_7)_2ML]^+ Cl^-$ (L is the conjugate base of oxine), in which only one bidentate oxinate ligand is coordinated to the metal ion were readily obtained. Such complexes possess low solution energies, as is evident from the ease of their preparation. This suggested that a number of xanthate ions present in aqueous solution might be isolated as salts of these complexes. The present communication describes the preparation and characterization of these complexes.

Results and Discussion

The method used for preparing and isolating $[(\eta^5\text{-}C_9H_7)_2ML]^+[ROCS_2]^-$ complexes yields materials of good purity as judged from satisfactory elemental analyses and spectroscopic data. The complexes are green in colour. They

* To whom correspondence should be addressed

Table I

Analytical data and physical characteristics

Compound	Decomposition temp. (°C)	Conductivity data Λ ($ohm^{-1}\,cm^2\,mole^{-1}$)	Anal. % Found (Calcd.)	
			N	S
(1)	(2)	(3)	(4)	(5)
$[(\eta^5\text{-}C_9H_7)_2TiL]^+[MeOCS_2]^-$	62	29.2	2.73 (2.65)	12.01 (12.10)
$[(\eta^5\text{-}C_9H_7)_2TiL]^+[EtOCS_2]^-$	68	26.8	2.43 (2.58)	11.66 (11.78)
$[(\eta^5\text{-}C_9H_7)_2TiL]^+[n\text{-}PrOCS_2]^-$	70	26.4	2.65 (2.51)	11.58 (11.49)
$[(\eta^5\text{-}C_9H_7)_2TiL]^+[i\text{-}PrOCS_2]^-$	98	25.6	2.63 (2.51)	11.40 (11.49)
$[(\eta^5\text{-}C_9H_7)_2TiL]^+[n\text{-}BuOCS_2]^-$	152	24.2	2.32 (2.45)	11.09 (11.21)
$[(\eta^5\text{-}C_9H_7)_2TiL]^+[i\text{-}BuOCS_2]^-$	148	29.6	2.30 (2.45)	11.11 (11.21)
$[(\eta^5\text{-}C_9H_7)_2ZrL]^+[MeOCS_2]^-$	93	28.2	2.58 (2.44)	11.04 (11.18)
$[(\eta^5\text{-}C_9H_7)_2ZrL]^+[EtOCS_2]^-$	152	25.4	2.21 (2.39)	10.79 (10.92)
$[(\eta^5\text{-}C_6H_7)_2ZrL)^+[n\text{-}PrOCS_2]^-$	160	30.2	2.23 (2.33)	10.53 (10.66)
$[(\eta^5\text{-}C_9H_7)_2ZrL]^+[i\text{-}PrOCS_2]^-$	89	28.8	2.45 (2.33)	10.51 (10.66)
$[\eta^5\text{-}C_9H_7)_2ZrL]^+[n\text{-}BuOCS_2]^-$	128	26.8	2.16 (2.28)	10.50 (10.42)
$[\eta^5\text{-}C_9H_7)_2ZrL]^+[i\text{-}BuOCS_2]^-$	87	24.6	2.12 (2.28)	10.29 (10.42)

are soluble in acetone, THF and partially soluble in halogenated hydrocarbons. Conductivity measurements reveal that the complexes are 1 : 1 electrolytes in nitrobenzene. The analytical data and physical characteristics of the complexes are given in Table I.

The C⋯N bond in the oxinate group shows a very intense IR absorption frequency at $\sim$1320 cm^{-1}. Since this bond possesses partial double bond characteristics, it is expected that its vibrational frequency should occur in the 1450—1500 cm^{-1} range [5]. In fact free oxine shows an intense absorption in the region. The occurrence of this band at lower energy in the present complexes indicates considerably less double bond character of C⋯N bond in the oxinate group. It may be assumed that the lone pair of electrons on nitrogen is involved in the formation of a coordinate bond with the metal ion which causes a drift of ring electrons towards nitrogen, making the double bond formation of the C⋯N bond considerably less as compared to the free oxine. The presence of an intense band at $\sim$1320 cm^{-1}, thus indicates that the oxinate ligand is chelating in all the complexes.

Magee and Gordan [6] studied the IR spectra of oxine and a number of metal oxinates. In free oxine, they attributed the absorption in the $\sim$1500 cm^{-1} region to ν(C⋯C) and ν(C⋯N) stretching frequencies. No absorption frequency was observed at 1320 cm^{-1} in this case. The IR spectra of the metal oxinates exhibited an absorption around $\sim$1320 cm^{-1}. However, these authors did not give any explanation of this fact.

The ν(C⎓S) bond in the xanthate group absorbs at 1060 cm^{-1} while the (C—O) stretching frequency shows an absorption at ~1270 cm^{-1} [7]. The ν(C—O—C) stretching vibration appears at ~1195 cm^{-1}.

The ν(C⎓H) aromatic stretching frequency due to the indenyl and the oxinate group results in a broad absorption band at ~3000 cm^{-1}. The ν(C⎓C) aromatic stretching absorbs at around 1435 cm^{-1}. The C—H out-of-plane deformation due to the π-ring system results in weak to medium intensity bands in 800—850 cm^{-1} region [9]. The C—H out-of-plane deformation due to the oxinate group occurs at ~770 cm^{-1}. A weak band at ~1075 cm^{-1} is attributed to the C—H in plane deformation of the η^5-indenyl group. This stretching frequency of the oxine group absorbs at 1225 cm^{-1}[6].

The in-plane oxine ring deformation shows an absorption at ~750 cm^{-1} [10]. The η^5-indenyl ring stretching frequency results in an absorption at ~1360 cm^{-1} [9]. The C—O stretching frequency shows an intense absorption centered around the 1115 cm^{-1} region [9]. A doublet is observed at 500 $\pm$ 35 cm^{-1}. The absorption at higher frequency is attributed to the C—O in-plane bending [10] and that at lower frequency to M—O stretching vibrations [9]. The characteristic IR frequencies together with their assignments are presented in Table II.

The ^{1}H-NMR spectra of the complexes were recorded in deuterated acetone. The C(2) proton of the oxinate group, in case of metal complexes, shows a signal at δ 9.05 ppm (q, $J = 4$ and 1.8 Hz). This is downfield as

Table II

Relevant IR *spectral data*

Compound	ν(C=S)	ν(C—O)	ν(C—H) in plane deformation	ν(C—H) out of plane deformation
(1)	(2)	(3)	(4)	(5)
$[(\eta^5\text{-}C_9H_7)_2TiL]^+[MeOCS_2]^-$	1070	1270, 1110	1085, 1210	820, 780
$[(\eta^5\text{-}C_9H_7)_2TiL]^+[EtOCS_2]^-$	1040	1265, 1120	1095, 1220	815, 785
$[(\eta^5\text{-}C_9H_7)_2TiL]^+[n\text{-}PrOCS_2]^-$	1060	1270, 1115	1090, 1220	815, 780
$[\eta^5\text{-}C_9H_7)_2TiL]^+[i\text{-}PrOCS_2]^-$	1070	1275, 1110	1095, 1220	810, 780
$[(\eta^5\text{-}C_9H_7]_2TiL]^+[n\text{-}BuOCS_2]^-$	1065	1280, 1105	1085, 1215	810, 775
$[(\eta^5\text{-}C_9H_7)_2TiL]^+[i\text{-}BuOCS_2]^-$	1060	1275, 1110	1090, 1220	825, 790
$[(\eta^5\text{-}C_9H_7)_2ZrL]^+[MeOCS_2]^-$	1050	1280, 1105	1095, 1225	815, 780
$[(\eta^5\text{-}C_9H_7)_2ZrL]^+[EtOCS_2]^-$	1070	1270, 1110	1090, 1220	820, 785
$[(\eta^5\text{-}C_9H_7)_2ZrL]^+[n\text{-}PrOCS]^-$	1055	1270, 1115	1085, 1210	815, 780
$[(\eta^5\text{-}C_9H_7)ZrL]^+[i\text{-}PrOCS_2]^-$	1065	1265, 1125	1085, 1215	810, 770
$[(\eta^5\text{-}C_9H_7)_2ZrL]^+[n\text{-}BuOCS_2]^-$	1060	1260, 1120	1090, 1220	825, 785
$[(\eta^5\text{-}C_9H_7)_2ZrL]^+[i\text{-}BuOCS_2]^-$	1070	1275, 1110	1095, 1225	815, 780

compared to the value of δ 8.73 ppm for the free oxine. Hence it supports the conclusion that the oxinate group is chelating. The signal due to the remaining protons of the oxinate group results in a complex multiplet in the range δ 7.3—8.1 ppm.

The possibility of oxinate ligand binding by simple hard sphere coulombic interaction to $(\eta^5\text{-}C_9H_7)_2M(IV)$ moiety is ruled out because in such a case bis oxinate complex may be isolated. Such a structure would maximize the coordination number of the metal ion and simultaneously maximize the total metal–ring overlap. Since the π-clouds are used in the formation of metal–ring bonds and would exert less of a steric effect as the equatorial ligands, this configuration cannot be described as unstable on the basis of steric effects. However, applying the Balihausen and Dahl's theory [11] to the present complexes, it can be assumed that two strongly directed metal hybrids which are used in $(\eta^5\text{-}C_9H_7)_2MCl_2$ are binding one oxinate ligand. Coordination of two oxygen and two nitrogen atoms in the XY plane by strong covalent bond would result in the weakening of the metal–ring bonds and would be energetically unfavourable. The Ti—O and Ti—N bonds have appreciable covalent character, since only one oxinate ligand interacts.

Experimental

Nitrobenzene was purified for conductance measurements by the method described by Fay and Lowry [12]. Conductance measurements were made on a Digital Direct Reading Conductivity Meter 304. Solid state IR spectra were recorded in KBr pellets in the 4000—200 cm^{-1} range using a Perkin-Elmer 621 grating spectrophotometer, ^{1}H-NMR spectra were recorded at a sweep width of 900 Hz with a Perkin-Elmer R-32 spectrophotometer. Chemical shifts are expressed relative to an internal reference of TMS (1% by volume). Bis(η^5-indenyl)titanium(IV) dichloride and bis(η^5-indenyl)zirconium dichloride were prepared by the reaction of titanum(IV) chloride or zirconium(IV) chloride with sodium indenide in THF [13].

Preparation of complexes

An aqueous solution of $[(\eta^5\text{-}C_9H_7)_2ML]^+$ Cl^- was obtained by stirring an aqueous solution of $(\eta^5\text{-}C_9H_7)_2MCl_2$ with a slight excess of solid oxine in about 100 mL double distilled water. After about 3 h, the contents were shaken with about 25 mL benzene. The aqueous phase was collected and added separately to the aqueous solutions of potassium xanthates. The green precipitates were filtered and washed with water followed by petroleum ether. These were reprecipitated from an acetone solution by the addition of petroleum ether.

REFERENCES

[1] Sodhi, G. S., Kaushik, N. K.: Inorg. Nucl. Chem. Lett., **17,** 211 (1981)
[2] Sodhi, G. S., Sharma, A. K., Kaushik, N. K.: J. Organomet. Chem., **238,** 177 (1982)
[3] Sodhi, G. S., Kaushik, N. K.: Bull. Soc. Chim. France, **1982,** 95
[4] Sodhi, G. S., Kumar, S., Kaushik, N. K.: Acta Chim. Hung. (In press)
[5] Chatt, J., Luncanson, L. A., Venanzi, L. M.: Suomen Kemi, **29,** 75 (1956); C. A., **51,** 559 (1951)
[6] Magee, R. J., Gordan, L.: Talanta, **10,** 851 (1963)
[7] Watt, G. W., McCormick, B. J.: Spectrochim. Acta, **21,** 553 (1965)

[8] Little, L. H., Poling, G. W., Leja, J.: Can, J. Chem., **39,** 745 (1961)
[9] Doyle, G., Tobias, R. S.: Inorg. Chem., **6,** 1111 (1967); **7,** 2484 (1960)
[10] Tackett, J. E., Sawyer, O. T.: Inorg. Chem., **3,** 692 (1964)
[11] Balehausen, C. I., Dahl, J. P.: Acta Chem. Scand., **15,** 1333 (1961)
[12] Fay, R. C., Lowry, R. N.: Inorg. Chem., **6,** 1512 (1967)
[13] Samuel, E., Setton, R.: J. Organomet. Chem., **10,** 257 (1967)

Acta Chimica Hungarica 116 (3), pp. 267—272 (1984)

CONDENSATION AND RING CLOSURE REACTIONS OF PHTHALAZINONE DERIVATIVES

S. A. MAHGOUB, A. M. FAHMY, M. M. ALY and M. Z. A. BADR*

(Department of Chemistry, Faculty of Science, Assiut University, Assiut, Egypt)

Received March 21, 1983

In revised form July 31, 1983

Accepted for publication September 8, 1983

2-Phenyl-4-hydrazinophthalazin-1-one undergoes several condensation and/or cyclization reactions on treatment with different carbonyl compounds, including acetic anhydride, phthalic anhydride, pyruvic acid, diethyl ketomalonate, diethyl oxalate, acrylonitrile, benzoyl chloride, formic acid, or with other reagents that can afford cyclization, such as carbon disulfide or nitrous acid. Structural elucidation of the products was based on results of elemental analysis and spectral studies.

Human metabolities of 1-hydrazinophthalazine, a common hypotensive agent, have received considerable attention [1—6]. It was proposed that the compound undergoes enzymatic acetylation to give 1-(2-acetylhydrazino)-phthalazine [5]. Other workers [2, 6] showed that enzymatic acetylation, instead, leads to 3-methyl-*s*-triazolo[3,4-*a*]phthalazine. 4-Hydrazinophthalazinones undergo condensation reactions [7, 8] with carbonyl compounds and are cyclized [7] with nitrous acid to 6-hydroxytetrazolo [4,5-*a*]phthalazinone. The ease of ring closure seems to be a common feature in reactions of phthalazine series where triazine [2] and tetrazole [9] ring systems are formed.

In the present paper we investigate the susceptibility of 2-phenyl-4--hydrazinophthalazin-1-one (**1**) towards condensation and cyclization reactions with different reagents as shown in Chart 1.

Refluxing **1** with acetic anhydride gave 2-phenyl-4-(1,2-diacetylhydrazino)phthalazin-1-one (**2**). Its structure was inferred from the IR spectrum which had absorption bands characteristic of NH at 3300 cm^{-1}, two $COCH_3$ at 1742, 1700 cm^{-1} and the phthalazine CO at 1665 cm^{-1}. Furthermore the NMR spectrum (Me_2SO-d_6) showed δ2.26 (s, 3H, N_1-$COCH_3$), 2.45 (s, 3H, N_2-$COCH_3$), 6.3 (s, NH) and 7.4—8.5 (m, 9H, ArH).

Reaction of **1** with phthalic anhydride in refluxing dimethylformamide yielded *N*-(4-amino-2-phenyl-phthalazin-1-one)phthalimide (**3**). Its IR spectrum revealed the absence of NH_2, whereas absorption bands characteristic of NH at 3240 cm^{-1} and the phthalimide ring at 1720 cm^{-1} were observed.

* To whom correspondence should be addressed

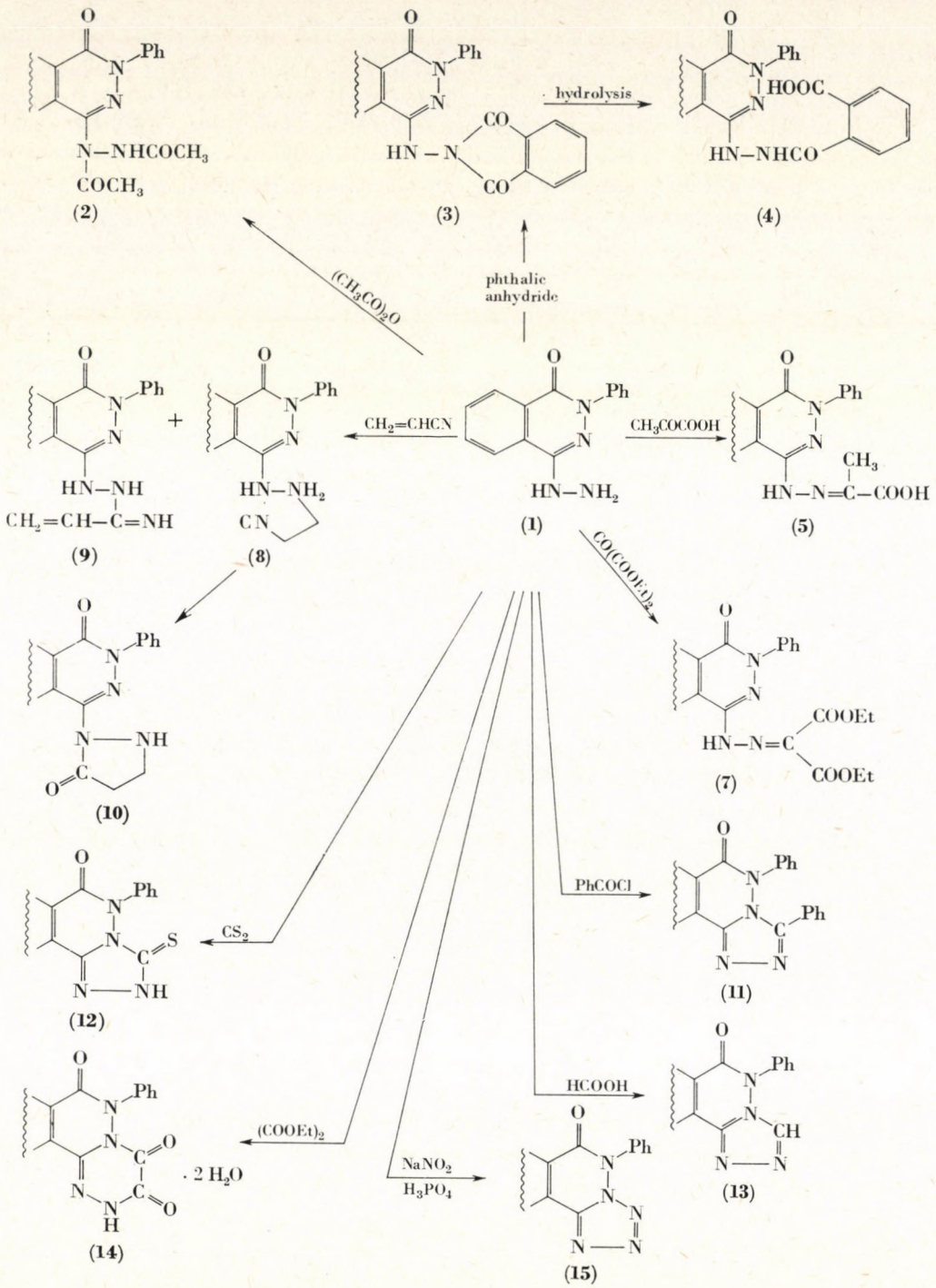

hydrolysis
phthalic anhydride
$(CH_3CO)_2O$
$CH_2=CHCN$
$CH_3COCOOH$
$CO(COOEt)_2$
CS_2
PhCOCl
HCOOH
$(COOEt)_2$
$NaNO_2$
H_3PO_4
$\cdot 2\,H_2O$
(1)
(2)
(3)
(4)
(5)
(7)
(8)
(9)
(10)
(11)
(12)
(13)
(14)
(15)

Chart 1

Further convincing proof for the structure was obtained from the alkaline hydrolysis on heating with sodium ethoxide in ethanol when 2-phenyl-4--(2-monophthaloylhydrazino)phthalazin-1-one (**4**) was isolated. The IR spectrum of **4** showed overlapping absorption bands at 3225, 3400 and 3600 cm^{-1} attributable to NH, CONH and associated OH, respectively, in addition to a strong absorption band at 1720 cm^{-1} characteristic of carboxylic CO.

Treatment of **1** with pyruvic acid in ethanol solution afforded 2-phenyl--4-(2-pyruvic acid hydrazone) phthalazin-1-one (**5**) whose IR spectrum had absorption bands attributed to NH and associated OH at 3150—3240 cm^{-1}, together with a strong absorption band at 1625 cm^{-1} for carboxylic CO. The NMR (Me_2SO-d_6) showed δ 1.9 (s, 3H, $-CH_3$), 7.1—8.4 (m, 9H, ArH), 9.7 (s, NH) and 12.55 (s, OH). Similarly, treatment of **1** with sodium pyruvate gave the sodium salt (**6**) from which the acid (**5**) was isolated on acidification, as confirmed by m.p., m.m.p. and coincidence of the infrared spectrum with that of an authentic sample.

Compound **1** also underwent condensation with diethyl ketomalonate affording 2-phenyl-4-(2-diethyl-carboxylmalonate hydrazone)-phthalazin-1-one (**7**). Its infrared spectrum had absorption bands corresponding to NH at 3170 cm^{-1} and ester CO at 1740 cm^{-1}. Furthermore, the molecular ion peak appeared at *m/e* 408, in agreement with the molecular formula $C_{21}H_{20}N_4O_5$.

2-Phenyl-4-hydrazinophthalazin-1-one (**1**) is known to possess high reactivity towards highly polarized alkene systems attached to strong electron-withdrawing groups [10]. We were prompted to investigate the reaction with acrylonitrile in aqueous pyridine under reflux, where two modes of condensation have been observed involving addition of the hydrazide group either to the olefinic bond or the cyano group of acrylonitrile, forming 2-phenyl-4--(2-cyanoethylhydrazino)phthalazin-1-one (**8**) and 2-phenyl-4-(2-1-acryl-imidylhydrazino)phthalazin-1-one (**9**), respectively. The IR spectrum of **8** exhibited characteristic absorptions for NH at 3280 cm^{-1}, CN at 2245 cm^{-1}, whereas that of **9** showed absorption bands for NH at 3380 cm^{-1}, C=NH at 3280 cm^{-1}, C=C at 1670 cm^{-1} and C=N at 1630 cm^{-1}. Moreover, when **8** was refluxed with dilute hydrochloric acid, it underwent hydrolysis followed by simultaneous cyclization forming 2-phenyl-4-(pyrazol-5-one-1-yl) phthalazin-1-one (**10**), as shown by examination of the IR absorption spectrum, which revealed the absence of the 2245 cm^{-1} band, characteristic of CN, and the appearance of a new band at 1740 cm^{-1} characteristic of the pyrazolone ring [11].

On the other hand, 2-phenyl-4-hydrazinophthalazin-1-one (**1**) underwent some cyclization reactions which lead to the formation of triazole, triazine and other ring systems. Thus refluxing **1** with benzoyl chloride produced 3,5-diphenyl-*s*-triazolo[3,4-*a*]phthalazin-(5*H*)-6-one (**11**), whose IR spectrum revealed the absence of NH band, while an absorption band characteristic of CO at 1675 cm^{-1} was present.

Similarly, refluxing **1** with carbon disulfide gave 5-phenyl-*s*-triazolo-[3,4-*a*]phthalazin-(5*H*)-6-one-3-thione (**12**). Its infrared spectrum showed absorptions characteristic of C=S at 1510 cm^{-1}, NH at 3075 cm^{-1} and C=O at 1680 cm^{-1}. Moreover, the absence of an absorption band at 2600 cm^{-1} characteristic of SH band revealed its existence as the thione tautomer. Its molecular ion peak appears at *m/e* 294, in agreement with the molecular formula $C_{15}H_{10}N_4SO$.

The refluxing of **1** with formic acid in ethanol solution resulted in the formation of 5-phenyl-*s*-triazolo[3,4-*a*]phthalazin-(5*H*)-6-one (**13**). The IR spectrum revealed the absence of NH and NH_2 groups.

On refluxing **1** with diethyl oxalate in ethanol, 6-phenyl-2-*H*-*as*-triazino-[3,4-*a*]phthalazine (5*H*)-3,4,7-trione dihydrate (**14**) was obtained. Its IR spectrum showed overlapping absorption bands in the region 1750 – 1650 cm^{-1} attributable to CONH and CO, in addition to a broad absorption at 3600 – 3300 cm^{-1} characteristic of water.

Treatment of **1** with sodium nitrite and phosphoric acid afforded 5-phenyl-tetrazolo[5,1-*a*]phthalazin-(5*H*)-6-one (**15**). This structure was assigned on the basis of the IR spectrum, which revealed the absence of NH and NH_2 groups. Furthermore, the molecular ion peak appeared at *m/e* 263, in agreement with the molecular formula $C_{14}H_9N_5O$.

Experimental

All m.p.'s are uncorrected. IR spectra were recorded on a Unicam SP 200 G instrument using the nujol mull technique. NMR spectra were taken with a Varian EM-390-90 MHz spectroscope. Mass spectra were obtained with an AEIMS 902 mass spectrophotometer.

2-Phenyl-4-hydrazinophthalazin-1-one (1)

It was prepared according to the literature [8] in 80% yield, as colourless needles from aqueous ethylene glycol, m.p. 188 – 190 °C.

2-Phenyl-4-(1,2-diacetylhydrazino)phthalazin-1-one (2)

It was made from **1** (1 g; 0.0004 mol) in excess freshly distilled acetic anhydride (10 mL) by refluxing for 2 h. The solid obtained in 65% yield was crystallized from ethanol to give colourless crystals, m.p. 222 °C.

$C_{18}H_{16}N_4O_3$. Calcd. C 64.27; H 4.80; N 16.66. Found C 65.00; H 5.00; N 16.58%.

N-(4-Amino-2-phenylphthalazin-1-one)phthalimide (3)

It was prepared from **1** (1 g; 0.0004 mol) and phthalic anhydride (0.83 g; 0.0056 mol) in dimethylformamide (10 mL) by refluxing for 30 min. The solid obtained on cooling was filtered off, washed with ethanol and crystallized from glacial acetic acid to yield colourless crystals, m.p. 233 °C, 60% yield.

$C_{22}H_{14}N_4O_3$. Calcd. C 69.10; H 3.69; N 14.65. Found C 67.98; H 4.06; N 14.60%.

2-Phenyl-4-(2-monophthaloylhydrazino)phthalazin-1-one (4)

It was synthesized by refluxing **1** (1 g) with sodium methoxide (0.05 g sodium in 5 mL ethanol) for 10 h, followed by acidification with HCl. The solid obtained in 70% yield was crystallized from ethanol; m.p. 162 °C.

$C_{22}H_{16}N_4O_4$. Calcd. C 65.99; H 4.03; N 13.99. Fund C 66.02; H 4.08; N 13.8%

2-Phenyl-4-(2-pyruvic acid hydrazone)phthalazin-1-one (5)

It was prepared by stirring a mixture of **1** (1 g) and pyruvic acid (0.16 mol) in ethanol (10 mL) at 25 °C. The solid obtained (85%, yield) was crystallized from glacial acetic acid, colourless crystals, m.p. 230 °C.

$C_{17}H_{14}N_4O_3$. Calcd. C 63.35; H 4.35; N 17.4. Found C 63.71; H 4.40; N 17.34%.

Sodium salt of 2-phenyl-4-(2-pyruvic acid hydrazone)-phthalazin-1-one (6)

It was similarly prepared using sodium pyruvate (0.2 g) instead of pyruvic acid. The solid obtained in 85% yield crystallized from ethanol as yellowish crystals, m.p. > 360 °C. On acidification with HCl it afforded the acid **5**, m.p. and m.m.p. 230 °C.

2-Phenyl-4-(2-diethylcarboxymalonate hydrazone)-phthalazin-1-one (7)

It was synthesized by stirring diethylketomalonate (0.19 g) in ethanol (10 mL) with **1** (0.5 g) at 25 °C for 18 h, followed by reflux for 2 h. The compound which precipitated on cooling was filtered off and crystallized from ethanol as pale yellow crystals, m.p. 125 °C, yield 75%.

$C_{21}H_{20}N_4O_5$. Calcd. C 61.76; H 4.90; N 13.72. Found. C 61.82; H 4.94; N 13.68%.

2-Phenyl-4-(2-cyanoethylhydrazino)phthalazin-1-one (8) and 2-phenyl-4-(2,1'-acrylimidyl-hydrazino)phthalazin-1-one (9)

They were made from **1** (2.5 g; 0.01 mol) and acrylonitrile (3 mL) in a mixture of pyridine (30 mL) and water (10 mL) by heating under reflux for 3 h. The reaction product was treated with dilute HCl and extracted with ether. The ether extract was dried ($MgSO_4$), evaporated to dryness and the residual oil treated with hot water and filtered. The filtrate was evaporated to give colourless crystals, recrystallized from ethanol, m.p. 149—150 °C, yield ca. 60%, whereas the brown residue was crystallized from ethanol as deep brown crystal, m.p. 205 °C, yield ca. 40%.

8: $C_{17}H_{15}N_5O$. Calcd. C 66.87; H 4.95; N 22.9. Found. C 66.91; H 5.00; N 22.87%.

9: $C_{16}H_{15}N_5O$. Calcd. N 22.9. Found. N 22.86%.

2-Phenyl-4-(pyrazol-5-one-1-yl)phthalazin-1-one (10)

It was obtained by hydrolysis of **8** (0.5 g; 0.003 mol) on refluxing with 20% HCl (10 mL) for 2 h. Crystallization from ethanol afforded colourless crystals in 70% yield, m.p. 210 °C.

$C_{17}H_{14}N_4O_2$. Calcd. C 66.65; H 4.61; N 18.29. Found C 66.72; H 4.66; N 18.26%.

3,5-Diphenyl-*s*-triazolo[3,4-*a*]phthalazin-(5*H*)-6-one (11)

It was formed through refluxing **1** (1 g; 0.004 mol) with excess benzoyl chloride for 2 h. The product obtained in 75% yield crystallized from glacial acetic acid as colourless crystals, m.p. 235—237 °C.

$C_{21}H_{14}N_4O$. Calcd. C 74.54; H 4.17; N 16.56. Found. C 74.63; H 4.19; N 16.53%.

5-Phenyl-*s*-triazolo[3,4-*a*]phthalazin-(5*H*)-6-on-3-thione (12)

It was prepared by refluxing **1** (1 g) in carbon disulfide (10 mL) for 30 min. The solid obtained was crystallized from ethanol to give colourless crystals, m.p. 260 °C, yield 90%.

$C_{15}H_{10}N_4SO$. Calcd. C 61.22; H 3.40; S 10.88. Found. C 62.00; H 4.00; S 10.86%.

5-Phenyl-*s*-triazolo[3,4-*a*]phthalazin-(5*H*)-6-one (13)

It was made from a mixture of **1** (1 g; 0.004 mol) and formic acid (0.5 g; 0.01 mol) in ethanol (10 mL) by refluxing for 6 h. Th solid obtained in 60% yield was crystallized from ethanol-water mixture to give colourless crystals, m.p. 220 °C.

$C_{15}H_{10}N_4O$. Calcd. C 68.69; H 3.84; N 21.37. Found. C 68.72; H 3.86; N 21.34%.

6-Phenyl-2-*H*-*as*-triazino[3,4-*a*]phthalazin-(5*H*)-3,4,7-trione dihydrate (14)

It was obtained in 80% yield by refluxing **1** (1 g) and diethyloxalate (1.46 g; 0.01 mol) in ethanol (30 mL) for 2 h. The excess of the ester was distilled off and the solid obtained was crystallized from ethanol to give colourless crystals, m.p. 195 °C (dec.).

$C_{16}H_{10}N_4O_3$. Calcd. C 58.89; H 4.32; N 17.17. Found C 57.98; H 4.4%.

5-Phenyltetrazolo[5,1-*a*]phthalazin-(5*H*)-6-one (15)

It was obtained in 80% yield from the interaction of **1** (1 g) in *conc.* phosphoric acid (10 mL) and sodium nitrite solution (6.5 mL, 5*N*) at 0 °C, on allowing the mixture to stand at room temperature for 2 h. The solid obtained crystallized from ethanol as colourless crystals, m.p. 129°.

$C_{14}H_9N_5O$. Calcd. C 63.87; H 3.45; N 26.61. Found. C 63.70; H 3.43; N 26.62%.

REFERENCES

[1] Litwin, A., Hess, E. V., McManus, J., Zimmer, H.: Anthritis Rheum., **16,** 217 (1973)
[2] Zimmer, H., McManus, J., Novinson, T., Hess, I. V., Litwin, A.: Arzneim. Forsch., **20,** 1586 (1970)
[3] Zimmer, H., Kokosa, J., Gartiez, D. A.: Arzneim.-Forsch., **23,** 1028 (1973)
[4] Douglas, C. O., Hogan, R.: Proc. Soc. Exp. Biol. Med., **100,** 446 (1959)
[5] McIssac, W. M., Kanda, J.: Pharmacol. Exp. Ther., **143,** 7 (1964)
[6] Edwards, S., Marquardt, F. H.: Hoppe-Seyler's Z. Physiol. Chem., **350,** 85 (1969)
[7] Koehler, W., Bubner, M., Ulbricht, G.: Chem. Ber., **100,** 1073 (1967)
[8] Drain, D. J., Seymour, D. E.: J. Chem. Soc., **1955,** 852
[9] Stolle, R., Storch, H.: J. Prakt. Chem., **135,** 128 (1932)
[10] Hoffmann, U., Jacobi, B.: Chem., Zntr., **1933,** 279
[11] Zaher, H. A., Jahine, H., Sherif, O., Mohammady, R.: Indian J. Chem., **18** , 316 (1979); Bellamy, L. J.: The Infrared Spectra of Complex Molecules, p. 269 Methuen, London 1960

Acta Chimica Hungarica 116 (3), pp. 273—281 (1984)

SPECTROSCOPIC STUDY OF THE DONOR BEHAVIOUR OF BENZIDINE DERIVATIVES TOWARDS AROMATIC NITRO COMPOUNDS

Y. M. ISSA[1]*, A. L. EL-ANSARY[1], M. GABER[2] and R. M. ISSA[2]

(Chemistry Department, Faculty of Science, [1]Cairo University, [2] Tanta University, Cairo A. E. Egypt)

Received July 11, 1983

Accepted for publication September 15, 1983

The solid CT complexes of three benzidine derivatives with nine tri- and dinitrobenzenes are prepared and investigated by elemental analysis, IR, electronic absorption and proton magnetic resonance spectroscopy. The results of microanalysis revealed that strong acceptors can form 1 : 1 and 1 : 2 complexes, while weak acceptors form only the 1 : 1 type (donor : acceptor). The spectral changes revealed that acidic acceptors form complexes with $\pi - \pi^*$ electronic interaction and proton transfer, while non acidic acceptors yield complexes having the $\pi - \pi^*$ transition.

Introduction

Molecular complexes of the donor–acceptor type were recently the subject of a vast number of investigations. Most of the complexes investigated with aromatic nitro compounds as acceptors utilized aniline derivatives, substituted benzenes or condensed ring system compounds as donors [1—5]. The interest in such studies led either in the evaluation of ionisation potentials of donor or electron affinities of the acceptors or the existence of the phenomena of structural colour isomerism as well as the nature of bonding between the donor and acceptor molecules. Studies of the latter type pointed out the importance of the existence of a donating π-electron system for CT complex formation.

In the present work, the solid complexes of some dinitro- and trinitro benzenes with benzidine derivatives are prepared and investigated by elemental analysis, IR, ^{1}H-NMR and electronic absorption spectroscopy aiming to throw some light on the donor behaviour of these molecules.

Experimental

The compounds used in the present investigation were pure laboratory grade chemicals from BDH.

The details for the preparation of the CT complexes and the recording of the spectra are as described earlier [4, 5]. Some compounds were subjected to carbon, hydrogen and

* To whom correspondence should be addressed

Table I

Reults of elemental analysis of some 1 : 2 (donor : acceptor) *complexes*

Acceptor	Formula	Carbon %		Hydrogen %		Nitrogen %	
		Cal.	Found	Cal.	Found	Cal.	Found
CT complexes of benzidine:							
II	$C_{26}H_{20}N_6O_{14}$	51.3	49.8	3.31	2.80	13.8	13.4
IV	$C_{24}H_{20}N_6O_{10}$	51.2	51.6	3.65	4.00	15.2	14.7
VI	$C_{24}H_{16}N_8O_{12}Cl_2$	42.4	43.5	2.37	2.20	16.5	15.9
VIII	$C_{24}H_{20}N_6O_8$	52.4	51.9	3.60	3.70	20.4	21.0
CT complexes of *o*-dianisidine:							
I	$C_{26}H_{22}N_8O_{16}$	44.5	44.7	3.10	2.90	15.9	15.6
III	$C_{28}H_{24}N_6O_{14}$	50.6	50.7	3.60	3.50	12.7	12.4
V	$C_{26}H_{22}N_8O_{14}$	46.6	47.1	3.30	3.20	16.7	17.4
VIII	$C_{26}H_{24}N_6O_{10}$	53.8	54.0	4.20	4.00	14.5	14.2
IX	$C_{26}H_{22}N_6O_{10}Cl_2$	48.1	47.9	3.40	3.60	12.9	12.7
CT complexes of diaminobenzidine:							
III	$C_{26}H_{22}N_8O_{12}$	48.9	49.5	3.50	3.60	17.5	18.7
V	$C_{24}H_{20}N_{10}O_{12}$	45.0	43.4	3.10	2.90	21.9	20.4
VII	$C_{26}H_{26}N_8O_8$	53.9	54.4	4.10	4.40	19.4	19.7
VIII	$C_{24}H_{22}N_8O_8$	52.4	51.1	4.00	3.70	20.4	21.0

nitrogen determinations. The results of analysis are always in confirmity with those required for 1 : 1 and 1 : 2 (donor : acceptor) complexes (Table I).

The donors used are benzidine (**a**), *o*-dianisidine (**b**) and diaminobenzidine (**c**) while the acceptors utilized are picric aicd (**I**), 3,5-dinitrosalicylic acid (**II**), 3,5-dinitrobenzoic acid (**III**), 2,4-dinitrophenol (**IV**), trinitrobenzene (**V**), picryl chloride (**VI**), 2,4-dinitrotoluene (**VIII**), *m*-dinitrobenzene (**VIII**) and 1-chloro-2,4-dinitrobenzene (**IX**).

The IR spectra were obtained by the aid of a UNICAM SP 1100 infrared spectrophotometer using the KBr-disc technique. The ^{1}H-NMR spectra were obtained by the aid of a Perkin Elmer R 34–220 Hz Spectrophotometer. The electronic absorption spectra were recorded on a UNICAM SP 8000 spectrophotometer using the Nujol Mull technique.

Results and Discussion

The infrared spectra

Charge-transfer complexes with non-acidic acceptors (Tables II and III)

This class of compounds is formed by using acceptors (**V**—**IX**). The IR spectra of this class of compounds display some interesting changes as compared to those of their free constituents. The γ_{CH} bands of the acceptors display a shift to lower wavenumbers whereas those of the donors display an

opposite shift; which is characteristic of charge transfer of the $\pi-\pi^*$ type [1, 4, 5]. For 1 : 1 complexes, the γ_{CH} bands of the donors undergo splitting or broadening indicating a difference in the energy of the two rings in this class of compounds since only one ring is involved in the CT interaction. The shift of the bands of the other ring not contributing to CT is due to enhanced migration of π-electrons to the donating ring under the influence of the positive hole left after the electron transfer.

The NO_2 bands of the acceptor molecules display a peculiar behaviour. The asym. NO_2 bands display a shift to lower wavenumbers which is in accordance with the increased π-electron density on the ring of the acceptor molecule.

Table II

Important bands in the IR spectra of CT complexes with strong acidic acceptors

Donor	Ratio	Colour	m.p. °C	νNH^2 asym	νNH^2 sym	asym NO_2	sym NO_2	γCH acceptor
Complexes with picric acid								
Bands of free acceptor						1550, 1540, 1530	1350	919, 874
a	1 : 1	reddish brown	195	3450	3340	1540, 1535	1345, 1335	910, —
	1 : 2	greenish yellow	217			1550, 1540	1350, 1340	915, —
b	1 : 1	yellow	205	3480	3270	1545, 1535	1340, 1335	912, —
	1 : 2	canary yellow	211			1548, 1535sh	1345, 1340	915, —
c	1 : 1	magenta red	175	3400	3250	1540, 1535	1343, 1338	913, 780
	1 : 2	brown	160	3420	3320	1540, 1535	1345, 1340	913, 780
Complexes with dinitrosalicylic acid								
Bands of free acceptor						1540, 1530	1344	925, 825
a	1 : 1	light brown	206	3480	3350	1533	1340	915, 815
	1 : 2	greenish yellow	210			1535	1345	920, 818
b	1 : 1	yellow	174	3460	3320	1530	1343	918, 815
	1 : 2	canary yellow	230			1535	1345	920, 818
c	1 : 1	greenish brown	208	3480	3390	1535	1340	920, 815
	1 : 2	olive green	155	3430	3320	1530	1343	925, 818
Complexes with dinitrobenzoic acid								
Bands of free acceptor						1555, 1540	1350	823, 808, 727
a	1 : 1	violet	195	3490	3360	1545, 1540	1340	815, — , 725
	1 : 2	pale violet	200			1550, 1540	1345	818, —, 725
b	1 : 1	pale cream	185	3460	3390	1545, 1535	1340	815, 805, 723
	1 : 2	pale cream	190			1550, 1540	1348	820, 805, 725
c	1 : 1	violet	179	3480	3380	1550, 1540	1345	815, 807, 720
	1 : 2	brick red	190	3480	3390	1550, 1545	1345	818, 805, 723

Acta Chim. Hung. 116, 1984

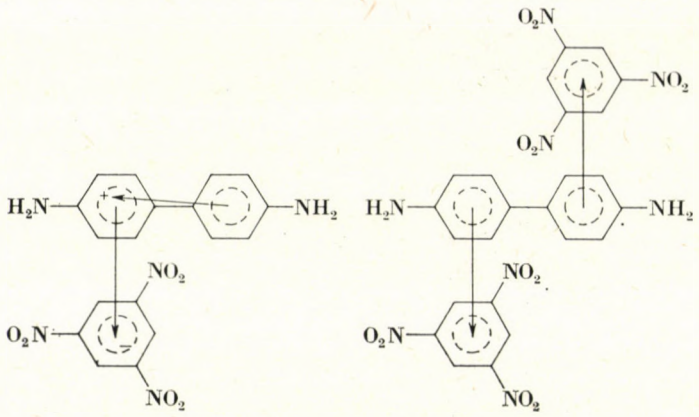
Table III

Important bands in the IR spectra of CT complexes with non acidic trinitrobenzenes and weak acidic dinitrobenzenes

Donor	Ratio	Colour	m.p. °C	νNH_2 asym.	νNH_2 sym.	Asym. NO_2	Sym. NO_2	γCH Acceptor
		Complexes with picrylchloride						
		Bands of free acceptor				1553, 1540	1348	—, 788
a	1 : 1	red	240	3440, 3400	3380, 3330	1540, 1530	1340, 1335	910, —
a	1 : 2	magenta red	243*	3380	3340	1545, 1533	1345, 1339	915, —
b	1 : 1	brown	223	3440, 3400	3380, 3340	1543, 1530	1340, 1330	—, 770
b	1 : 2	reddish brown	240	3450	3370	1545, 1535	1343, 1335	—, 780
c	1 : 1	brown	190	3480, 3430	3380, 3350	1540, 1533	1345, 1330	910, 775
c	1 : 2	reddish brown	233	3420	3360	1545, 1535	1345, 1335	915, 780
		Complexes with trinitrobenzene						
		Bands of free acceptor				1552	1347	
a	1 : 1	dark violet	135	3480, 3420	3390	1544, 1538	1340	907
a	1 : 2	violet	119	3470	3350	1548, 1535	1333	913
b	1 : 1	dark violet	138	3480, 3440	3390, 3370	1540, 1530	1335	910
b	1 : 2	dark violet	138	3460	3380	1543, 1533	1338	915
c	1 : 1	dark violet	195	3460, 3400	3380, 3360	1535	1335	908
c	1 : 2	reddish violet	198	3440	3380	1540	1340	915
		Complexes with 2,4-dinitrophenol						
		Bands of free acceptor				1540, 1520	1350	928, 825
a	1 : 1	olive green	133	3460	3350	1535	1340	920, —
a	1 : 2	greenish yellow	111*	—	—	1535	1343	920, —
b	1 : 1	greenish yellow	124	3440	3350	1530	1345	920, 820
b	1 : 2	yellow	133	—	—	1533	1345	925, 823
c	1 : 1	greenish brown	153	3460	3370	1530	1340	918, 818
c	1 : 2	dark brown	210*	—	—	1535	1343	925, 823

* charing near the melting

Also the sym. NO_2 bands show a shift to lower wavenumbers. Hence, $n-\pi^*$ interaction is to be excluded. The magnitude of the band shifts is generally higher in the 1 : 1 complexes due to the inhibited resonance between the two benzidine rings in the 1 : 2 complexes. The interaction of benzidine with trinitrobenzene in the 1 : 1 and 1 : 2 complexes can be represented as:



Charge-transfer complexes with acidic acceptors (Table IV)

These complexes are formed when the donors under investigation are allowed to react with acceptors (**I**—**IV**). The IR spectra of these complexes are characterized by a group of bands within the 2400—3000 cm^{-1} range which are not present in the spectra of the free donors or acceptors. These bands can be assigned to the stretching mode of the group ($-N^+H_3$) which is formed through the transfer of a proton from the acidic center of the acceptor to the nitrogen of the donor. This assumption is based on the disappearance of the bands due to the phenolic OH-groups of acceptors **I**, **II**, **IV** and carboxylic group of acceptor **III**. The two C=O bands of acceptor **II** appear as a single band denoting the disappearance of the rotational isomerism, occurring in the free acceptor, on complex formation. The C=O band of the acceptor **III** is no more observed in the spectra of CT complexes, being replaced by the two bands near 1500 cm^{-1} corresponding to the carboxylate ion. In the spectra of the 1 : 1 complexes the ν_{NH_2} bands appear with low intensity while in those of the 1 : 2 compounds these bands disappear more or less completely. The $-N^+H_3$ bands have much higher intensity in the 1 : 2 complexes.

The γ_{CH} bands of the acceptors are shifted to lower values whereas those of the donors shifted to higher ones. These bands display an identical behaviour as in CT complexes in the 1 : 1 and 1 : 2 compounds.

The asym. and sym. NO_2-bands shift to lower values as compared to those of the free acceptor as a result of the increased polarization of the NO_2

Acta Chim. Hung. 116, 1984

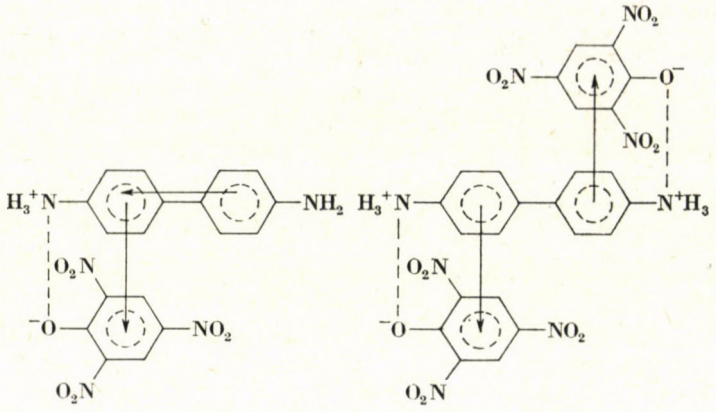
Table IV

Important bands in the IR spectra of CT complexes with non acidic dinitrobenzenes

Donor	Ratio	Colour	m.p. °C	νNH_2 asym.	νNH_2 sym.	Asym. NO_2	Sym. NO_2	γCH Acceptor
		Complexes with dinitrotoluene						
		Bands of free acceptor				1555, 1540	1352	920, 825
a	1 : 1	violet	71	3480, 3400	3370, 3340	1545, 1530	1345	910, 822
a	1 : 2	pale violet	C	3450	3340	1550, 1535	1338	915, 818
b	1 : 1	dark brown	50	3480, 3405	3370, 3330	1545, 1535	1345	915, 815
b	1 : 2	brown	87	3470	3380	1550, 1535	1348	920, 818
c	1 : 1	dark violet	145	3470, 3430	3370, 3340	1538, 1530	1345	915, 815
c	1 : 2	violet	137	3480	3390	1540, 1535	1350	920, 820
		Complexes with *m*-dinitrobenzene						
		Bands of free acceptor				1545	1352	920, 905
a	1 : 1	violet	125	3490	3390	1532, 1525	1342	908, 890
a	1 : 2	light violet	127*	3450	3390	1535, 1528	1345	910, 895
b	1 : 1	dark violet	87*	3480, 3440	3395, 3380	1535, 1525	1340	910, 895
b	1 : 2	reddish violet	58	3480	3390	1540, 1530	1348	915, 900
c	1 : 1	dark violet	145	3480, 3400	3360, 3320	1540, 1530	1345	910, 895
c	1 : 2	violet	198*	3460	3380	1545, 1530	1345	819, 900
		Complexes with 1-chloro-2,4-dinitrobenzene						
		Bands of free acceptor				1550, 1533	1353, 1335	
a	1 : 1	brick red	228	3450, 3420	3390, 3350	1540, 1525	1345, 1325	
a	1 : 2	reddish brown	233	3380	3330	1545, 1528	1350, 1332	
b	1 : 1	brick red	211*	3490, 3480	3395, 3380	1540, 1523	1340, 1325	
b	1 : 2	buff	240	3480	3390	1542, 1528	1343, 1330	

C charing, * charing near the melting

groups. Thus, complexes of this class are formed through $\pi-\pi^*$ bonding and proton transfer, hence the CT complexes formed belong to compounds of salt type [2, 4]:



The electronic absorption spectra

The electronic absorption spectra of CT complexes formed on using acceptors **I**–**V** are characterized by only one CT band within the wave length range 330—425 nm. The band observed would be assigned to the $\pi - \pi^*$ CT interaction, which is substantiated by calculating the energy of the CT interaction (E_{CT}) using the relation given by Briegleb [7]. The values determined from the CT bands amounts to 3.8—2.9 eV compared to 3.1—2.8 eV calculated from the equation for the CT complexes with trinitrotoluene. The absence of $n - \pi^*$ band reveals that $n - \pi^*$ interaction would be of low contribution to the bonding in the CT complex or even absent.

The CT bands of the 1 : 2 complexes are situated at shorter wave length in comparison to those of the 1 : 1 type as a result of the blocking of the resonance between the two rings in the former type of compounds.

The NMR spectra (Table V)

A substantial support for the results obtained from the IR and electronic spectra is gained by considering the changes of the NMR spectra of some of the molecular complexes under investigation in comparison to those of their constituents.

As a matter of fact the signals due to the aromatic protons of the donor parts are shifted downfields while those of the acceptor parts exhibit a reverse displacement. Such shifts are due to the decreased electron density on the donor rings and its increase on the acceptor ones which results from the intermolecular $\pi - \pi^*$ CT interaction. However, the magnitude of the shift

Table V

NMR signals for CT complexes of benzidine and o-dianisidine with some dinitrobenzene derivatives

Ratio / Position of	Signals of acceptor				Signals of donor			
	H 1	3	5	6	2	3 & 5	6	NH_2
Complexes of benzidine								
Complexes with 2,4-dinitrophenol								
free A or D	10.8[a]	9.20	8.50	7.30	6.65	7.30	6.65	3.40
1 : 1	—	9.12	8.42	7.18	6.70	7.37	6.70	3.35, 2.60[b]
1 : 2	—	9.15	8.45	7.24	6.72	7.40	6.72	—, 2.65
Complexes with 2,4-dinitrotoluene								
free A or D	2.75[c]	8.84	8.27	7.58	6.65	7.30	6.65	3.40
1 : 2	2.73	8.75	8.25	7.48	6.68	7.32	6.68	3.62
Complexes with *m*-dinitrobenzene								
free A or D	8.53	9.10	8.60	7.88	6.65	7.30	6.65	3.40
1 : 2	8.45	9.03	8.55	7.78	6.75	7.35	6.75	3.65
Complexes with 2,4-dinitrochlorobenzene								
free A or D	—	8.86	8.38	7.82	6.65	7.30	6.65	3.40
1 : 1	—	8.80	8.33	7.75	6.68	7.35	6.68	3.80, 3.35
1 : 2	—	8.83	8.35	7.78	6.70	7.37	6.70	3.75
Complexes of *o*-dianisidine								
Complexes with 2,4-dinitrochlorobenzene								
free A or D	—	8.86	8.38	7.82	3.90[d]	6.95	6.75	3.75
1 : 1	—	8.76	8.36	7.76	3.85 3.95	7.00	6.80	3.80, 3.70
1 : 2	—	8.78	8.38	7.78	3.95	7.08	6.83	3.80

[a] OH group, [b] N^+H_3 group, [c] CH_3 group and [d] OCH_3 group

in the signals of the aromatic protons varies with the stoichiometry of the complex. The shift of the acceptor signals to higher fields is of higher magnitude in the 1 : 1 complex while for the signals of the donors, the shifts is higher in case of the 1 : 2 complexes.

The NMR spectra of the CT complexes with 2,4-dinitrophenol, as an example of CT complexes of acidic acceptors are deprived from the signals due to the OH-group appearing at 10.8 ppm for the free acceptor. The NH_2

signals exhibit a peculiar behaviour. The free donors exhibit a broadened signal at 3.8—2.4 ppm with integrations corresponding to four protons. In the spectra of the 1 : 1 complexes, two signals are observed at 3.9—3.6 and 2.6—2.4 ppm with integrations equivalent to two and three protons, respectively. The latter one would be assigned to the $-N^+H_3$ group formed through the transfer of the proton from the acceptor to the donor. In the spectra of the 1 : 2 complexes, the NH_2 signals disappeared almost completely while the signal at 2.6—2.4 ppm increases in height to a value approaching six protons, being thus due to two $-N^+H_3$ groups.

For the complexes of benzidine and *o*-dianisidine with acceptor (**IX**), as an example for neutral acceptors, the NH_2 signal is splitted into two groups situated at lower and higher fields in the spectra of the 1 : 1 complexes while those of the 1 : 2 complexes exhibit only one signal with integration equivalent to four protons (Table V). This behaviour denotes that the two rings have identical energy states in the free and 1 : 2 complexes while in the 1 : 1 complexes the two rings have different energy states.

REFERENCES

[1] Kross, R. D., Fassel, V. A.: J. Amer. Chem. Soc., **79,** 38 (1957)
[2] Briegleb, G., Della, H.: Z. phys. Chem. (Frankfurt), **24,** 359 (1960)
[3] Kortum, G., Braun, W.: Z. phys. Chem. (Frankfurt), **28,** 362 (1961)
[4] Issa, R. M., El-Essawey, M. M.: Z. phys. Chem. (Leipzig), **253,** 96 (1973); Acta Chim. (Budapest) 341 (1976); **92,** 263 (1977)
[5] Issa, R. M., Issa, Y. M., Hindawey, A. M.: Indian J. Chem., **19Ä,** 615 (1980); Monatsh., Chem., **111,** 1114 (1980); J. Ind. Chem. Soc., **57,** 216 (1980)
[6] Matsunaga, Y. et al.: Bull. Chem. Soc. Japan, **46,** 714 (1973); **53,** 3085 (1980)
[7] Briegleb, G.: Z. Angew. Chem., **72,** 401 (1960); **76,** 326 (1964)

Acta Chimica Hungarica 116 (3), pp. 283—292 (1984)

A COMPLETE CNDO FORCE FIELD OF FURAN

J. BÁNKI[1], F. BILLES[2]* and A. GROFCSIK[2]

([1]Department of Organic Chemistry, Slovak Technical University, CS-81237, Bratislava, Janska 1, Czechoslovakia, [2]Department of Physical Chemistry, Technical University Budapest, H-1521 Budapest, Budafoki út 8.)

Received July 12, 1983

Accepted for publication September 21, 1983

The force field of furan has been calculated quantumchemically. The geometry was optimized by the CNDO/2 force method. A good agreement has been found between experimental and calculated geometries.

The force method has been applied for force and force constant calculations using both experimental and calculated geometries. No significant difference has been found between the two force constant sets. This result was surprising since the differences in some **G** matrix elements were quite large.

Six scaling factors (four for in-plane, two for out-of-plane vibration models) have been applied to achieve a reasonable force field reproducing the fundamentals of furan and its six deuterated derivatives with a small deviation. The fitting of the force fireld to these seven molecules has yielded an average deviation of 28 cm^{-1} for in-plane and 11 cm^{-1} for out-of-plane vibrations.

The TED matrix has been used for the prediction of the sensitivities of the individual fundamentals to the position of substitution. The effectivity of the prediction has been demonstrated on 2-furancarboxaldehyde.

Introduction

The infrared and Raman spectra of furan have been studied extensively [1—8]. Despite the simplicity of the molecule, the assignment of some of the fundamentals is ambiguous in the literature. Recent analyses of the infrared and Raman spectra of furan in the gas phase, liquid state and in CCl_4 solution [9] basically confirms the assignment of Rico and coworkers [4].

The usual way of interpreting vibrational spectra is the normal coordinate analysis based on the determination of harmonic force constants [10]. The aim of the present work is to determine the complete force field for furan by quantum chemical methods. A reliable force field of the parent compound would help to interpret the vibrational spectra of the derivatives, too. Since the present paper is the first member of a series on quantum chemical calculations of force constants of furan derivatives, for the sake of comparability of the force fields, the CNDO/2 force method [11] was chosen similarly to the case of larger molecules. Studies on different molecules show that the CNDO/2 method overestimates most of the force constants, the errors are, however,

* To whom correspondence should be addressed

systematic, and they can be taken into account by using empirical scaling factors [12—15]. Thus the "theoretical" force constants are scaled by empirical factors which are fitted to the vibrational frequencies. The basic difference from classical force constant calculations is that the number of the empirical parameters is much less, and the scaling factors are more transferable to different molecules than the force constants.

Calculations

For quantum chemical calculations one needs a complete set of non-redundant coordinates. Since the errors of the CNDO/2 method are different for stretching and deformational force constants, mixing of the stretching and bending motions in one coordinate would spoil the transferability of the scaling factors. Thus it is advantageous to define the coordinates in such a way that they represent either purely stretching or purely deformational motions. Coordinates meeting the above requirements are shown in Table I.

The reference geometry for the quantum chemical calculations can be either the experimental or the calculated equilibrium state of the molecule. There is a controversy in the literature about the most suitable geometry in such calculations. Some authors suggest that only the force constants determined in the calculated equilibrium configuration have real physical meaning [16]. Others argue that the errors in the calculated force constants are the smallest if the experimental geometry is used [17]. To solve this problem satisfactorily, one needs a systematic study of the force fields of many molecules. Nevertheless, we found it useful to compute the force field of furan in both experimental and CNDO/2 optimized equilibrium geometries.

A full geometry optimization on the molecule was performed by using the CNDO/2 force method, and our results agreed with those given in [18]. The experimental bond lengths and angles were taken from [19]. The agreement between calculated and experimental geometries is reasonably good. The C—C, C=C and C—O bond lengths are well reproduced, with a maximum error of 1 pm, while the calculated C—H bond lengths are 3—4 pm longer then the experimental ones. The discrepancies in bond angles are less than 3 degrees.

According to the CNDO/2 force method, the forces on the atoms were calculated analytically for appropriately distorted nuclear configurations around the reference geometry. The force constants were then evaluated numerically from the change in the forces. For the calculation of the in-plane force constants, the forces acting on the atoms were determined for both the positive and the negative displacements of nine independent in-plane internal coordinates. For the out-of-plane force constants, the forces in four additional displacements were sufficient. (In the latter case there is no sense in calculat-

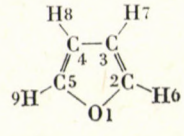
ing the forces in both the negative and the positive displacements, since a negative out-of-plane displacement produces the same geometry as a positive one.) The maximum atomic displacement in the calculations was about 0.5 pm.

Table I

Internal coordinates of furan

R_i	Internal coordinate
R_1	$\nu(O_1-C_2)$
R_2	$\nu(C_2=C_3)$
R_3	$\nu(C_3-C_4)$
R_4	$\nu(C_4=C_5)$
R_5	$\nu(C_5-O_1)$
R_6	$\nu(C_2-H_6)$
R_7	$\nu(C_3-H_7)$
R_8	$\nu(C_4-H_8)$
R_9	$\nu(C_5-H_9)$
R_{10}	$\beta(O_1-C_2-H_6)-\beta(C_3=C_2-H_6)$
R_{11}	$\beta(C_2=C_3-H_7)-\beta(C_4-C_3-H_7)$
R_{12}	$\beta(C_5=C_4-H_8)-\beta(C_3-C_4-H_8)$
R_{13}	$\beta(O_1-C_5-H_9)-\beta(C_4=C_5-H_9)$
R_{14}	$\beta(C_2-O_1-C_5)+\cos 144^\circ\,[\beta(O_1-C_2=C_3)+\beta(O_1-C_5=C_4)]+$ $+\cos 72^\circ\,[\beta(C_2=C_3-C_4)+\beta(C_3-C_4=C_5)]$
R_{15}	$(1-\cos 72^\circ)\,[\beta(O_1-C_2=C_3)-\beta(O_1-C_5=C_4)]+$ $+(\cos 144^\circ-\cos 72^\circ)[\beta(C_2=C_3-C_4)-\beta(C_3-C_4=C_5)]$
R_{16}	$\gamma(H_6-C_3-O_1-C_2)$
R_{17}	$\gamma(H_7-C_4-C_2-C_3)$
R_{18}	$\gamma(H_8-C_5-C_3-C_4)$
R_{19}	$\gamma(H_9-O_1-C_4-C_5)$
R_{20}	$\tau(C_2=C_3-C_4=C_5)+\cos 144^\circ\,[\tau(C_3-C_4=C_5-O_1)+\tau(O_1-C_2=C_3-C_4)]+$ $+\cos 72^\circ\,[\tau(C_4=C_5-O_1-C_2)+\tau(C_5-O_1-C_2=C_3)]$
R_{21}	$(1-\cos 72^\circ)\,[\tau(C_3-C_4=C_5-O_1)-\tau(O_1-C_2=C_3-C_4)]+$ $+(\cos 144^\circ-\cos 72^\circ)[\tau(C_4=C_5-O_1-C_2)-\tau(C_5-O_1-C_2=C_3)]$

The numbering of atoms is as follows:



ν, stretching; β, in-plane bending; τ, torsion; γ, out-of-plane bending. The normalization factors are not given.

The Cartesian forces calculated by the CNDO/2 force method were transformed into the coordinate system given in Table I. To obtain the in-plane force constants, the differences of the forces in the negative and positive displacements were divided by the differences of the corresponding coordinates. The out-of-plane force constants were obtained by dividing the forces by the coordinates with negative signs.

No significant difference was found between the force constants calculated for the experimental geometry and those obtained for the optimal equilibrium geometry. On the other hand, the differences in certain G matrix elements are quite large in the two different geometries. For this reason we found it more appropriate to use the force constants calculated for the experimental equilibrium geometry than those for the theoretical one.

Owing to the systematic errors, the force constants obtained from CNDO/2 wave functions cannot be immediately used for predicting vibrational spectra. Most of the errors can be corrected, however, by using empirical scaling factors. The values of the scaling factors needed for the diagonal elements of the force constant matrix primarily depend on the type of the coordinate. For the off-diagonal elements of the force constant matrix the geometric means of the scaling factors of the corresponding diagonal elements are used.

In our preliminary calculations the scaling factors were taken from the literature [13, 14, 15, 20]. The calculated frequencies using the corrected force constants showed a reasonably good correlation with the experimental ones, indicating that the scaling factors belonging to similar internal coordinates are transferable to different molecules. The optimum values of the scaling factors were determined by summarizing the squared deviations of the calculated and experimental frequencies. The observed fundamentals of gaseous furan and six deuterated derivatives [4] were used in the fitting procedure.

Results and Discussion

We tried to obtain a physically realistic force constant set by using the smallest possible number of independent scaling factors. So we applied four and two parameters for the in-plane and out-of-plane force constants, respectively. Our scaling factors (together with those in similar studies for different molecules) are as follows: 0.389 (0.35—0.395) for the C—C and C—H stretching, 0.243 for the C—O stretching, 0.681 (0.63—0.8) for the CH in-plane bending, 1.467 (1.2—1.43) for the ring in-plane bending, 0.540 (0.58—0.62) for the ring torsion and 0.802 (0.66—0.80) for the CH out-of-plane bending coordinates.

The CNDO/2 force constants corrected by the above scaling factors are given as lower triangular matrices in Tables II and III.

Table II

In-plane force constants of furan

	1														
1	5.148	2													
2	0.608	8.084	3												
3	−0.081	0.746	6.356	4											
4	0.173	−0.195	0.746	8.084	5										
5	0.264	0.173	−0.081	0.608	5.148	6									
6	0.166	0.180	0.008	−0.046	−0.003	5.426	7								
7	0.010	0.169	0.167	0.011	−0.035	0.0	5.393	8							
8	−0.035	0.011	0.167	0.169	0.010	0.003	−0.002	5.393	9						
9	−0.003	−0.046	0.008	0.180	0.166	0.002	0.003	0.0	5.426	10					
10	0.137	−0.126	−0.006	−0.013	−0.028	0.020	0.004	−0.003	0.004	0.449	11				
11	0.012	0.143	−0.129	0.010	−0.006	−0.004	0.011	0.007	−0.004	0.003	0.393	12			
12	−0.006	0.010	−0.129	0.143	0.012	−0.004	0.007	0.011	−0.004	0.008	−0.008	0.393	13		
13	−0.028	−0.013	−0.006	−0.126	0.137	0.004	−0.003	0.004	0.020	0.010	0.008	0.003	0.449	14	
14	0.082	−0.206	0.214	−0.206	0.082	0.190	−0.069	−0.069	0.190	0.089	−0.057	−0.057	0.089	1.959	15
15	0.191	−0.043	0.0	0.043	−0.191	−0.151	0.222	−0.222	0.151	−0.001	−0.010	0.010	0.001	0.0	1.750

The stretching force constants are given in 10^2 Nm^{-1}, the stretching–bending interactions in 10^{-8} $Nrad^{-1}$, the bending force constants in 10^{-18} $Nmrad^{-1}$

Table III

Out-of-plane force constants of furan

	16					
16	0.320	17				
17	−0.027	0.382	18			
18	0.006	−0.020	0.383	19		
19	0.031	0.006	−0.027	0.320	20	
20	−0.098	0.177	−0.177	0.098	0.536	21
21	−0.125	0.071	0.071	−0.125	0.0	0.396

All the force constants are given in 10^{-18} Nmrad^{-2}

Table IV

Normal vibrations of furan

	i	exp.	ν_i / cm^{-1} calc.	TED (%)
	1	3169	3150	$\nu CH_{6,9}$ (54), $\nu CH_{7,8}$ (46)
	2	3140	3134	$\nu CH_{7,8}$ (54), $\nu CH_{6,9}$ (46)
	3	1490	1529	$\nu C{=}C$ (62), βring(17), $\beta CH_{7,8}$ (16)
	4	1384	1419	$\nu C{-}C$ (44), νCO (10), $\beta CH_{6,9}$ (27), $\beta CH_{7,8}$ (16)
a_1	5	1140	1183	$\nu C{=}C$ (30), $\nu C{-}C$ (20), νCO (10), $\beta CH_{6,9}$ (36)
	6	1066	1043	$\beta CH_{7,8}$ (62), $\nu C{-}C$ (22)
	7	995	951	νCO (70), $\beta CH_{7,8}$ (14), $\beta CH_{6,9}$ (12)
	8	780	888	β ring(70)
	9	863	855	$\gamma CH_{7,8}$ (100)
a_2	10	727	732	$\gamma CH_{6,9}$ (86)
	11	613	614	τ (100)
	12	837	826	$\gamma CH_{7,8}$ (52), $\gamma CH_{6,9}$ (48)
b_1	13	743	749	$\gamma CH_{6,9}$ (52), $\gamma CH_{7,8}$ (42)
	14	601	586	τ (100)
	15	3160	3147	$\nu CH_{6,9}$ (80), $\nu CH_{7,8}$ (20)
	16	3130	3122	$\nu CH_{7,8}$ (80), $\nu CH_{6,9}$ (20)
	17	1555	1583	$\nu C{=}C$ (76)
b_2	18	1266	1271	$\beta CH_{7,8}$ (38), $\beta CH_{6,9}$ (32), νCO (22)
	19	1180	1163	$\beta CH_{6,9}$ (52), νCO (36), β (11)
	20	1041	1056	$\beta CH_{7,8}$ (52), $\beta CH_{6,9}$ (10), $\nu C{=}C$ (22), νCO (10)
	21	872	858	β ring(70), νCO (28)

The experimental and calculated frequencies of furan and its six deuterated derivatives are shown in Table IV. All the calculated C—H and C—D stretching frequencies are smaller than the experimental ones. For the rest of the stretching modes the calculated frequencies are higher than the experimental values. Using different scaling factors for the C—C and C—H force constants, a better fit could have been obtained but it was not our purpose to increase the number of parameters. On the other hand, it was necessary to use a different scaling factor for the C—O stretching force constants; the CNDO/2 method overestimates these force constants much more than the C—C and C—H ones.

The average deviation of the calculated and experimental frequencies of the seven molecules are 28 cm^{-1} and 11 cm^{-1} for the in-plane and out-of-plane vibrations, respectively. Using the frequencies of furan alone in the fitting procedure, the average deviations were only 17 cm^{-1} and 8 cm^{-1}, respectively. These figures indicate that the assignment of some of the deuterated compounds might not be correct. To check the assignment, however, would only be possible if more detailed experimental data were available than in [4]. In general, the frequency shifts caused by the deuteration are well reproduced by the calculations, showing that the derived force constant set is physically well established.

Table V contains the experimental and calculated frequencies of furan, together with the elements of TED (total energy distribution) matrix [21]. Contributions of less than 10% are not included in Table V.

The TED matrix elements indicate the character of each normal vibration. As is expected, the bands above 3100 cm^{-1} are purely C—H stretching vibrations. In the case of the skeletal and CH deformation vibrations the calculations provide some valuable information which is not available experimentally. According to the TED matrix of Table V, the fundamentals 3, 4, 5, 7 and 17 are basically skeletal bending vibrations. In the vibrations 4, 5 and 7, CH in-plane motions also participate. The fundamentals 7, 18, 19 and 20 are mainly CH in-plane deformations, with contributions from some skeletal stretchings. Normal vibrations 8 and 21 are deformations of the skeleton.

Among the six out-of-plane vibrations, two with the lowest frequencies (11 and 14) are torsions of the skeleton, the others are CH out-of-plane bending modes.

Further analysis of the TED matrix gives some insight into the expected effects of substitution. Some of the skeletal normal vibrations are practically not influenced by substitution. These are vibrations 11, 14 and 21. Substitution has only a secondary effect on these modes, that is the change in electron density distribution might affect the force constants of the skeleton and distort the ring geometry causing changes in the corresponding G matrix elements. So the fundamental frequencies of these modes are practically independent

Table V

Experimental and calculated frequencies of furan and its deuterated derivatives (cm^{-1})
(parentheses refer to non-observed bands)

Species	Furan		—2—5D_2		—3—4D_2		—D_4		Species	—2D_1		—3D_1		—2—3—5D_3	
	meas.	calcd.	meas.	calcd.	meas.	calcd.	meas.	calcd.		meas.	calcd.	meas.	calcd.	meas.	calcd.
	3169	3150	3145	3141	3155	3142	2388	2349		3164	3149	3164	3148	3139	3134
	3140	3134	2364	2329	2361	2333	2350	2313		3145	3138	3159	3142	2380	2343
	1490	1529	1436	1492	1484	1525	1424	1488		3133	3124	3134	3128	2362	2326
a_1	1384	1419	1357	1380	1442	1383	1315	1330		(2362)	2325	2354	2321	2342	2304
	1140	1183	1077	1098	1098	1156	1054	1079		1552	1578	1546	1569	1516	1553
	1066	1043	1018	1022	1053	977	920	913		1456	1508	1484	1527	1432	1489
	995	951	910	894	886	893	791	751		1370	1402	1367	1402	1322	1357
	870	888	781	750	732	726	727	724	a'	1228	1255	1240	1246	1171	1211
	(863)	855	(849)	852	780	772	(725)	750		1169	1170	1171	1171	1070	1088
a_2	727	732	644	664	(666)	693	572	588		1086	1086	1121	1162	1017	1051
	613	614	524	517	527	526	(498)	484		1045	1042	1061	1049	933	915
										1004	998	1020	968	903	872
	837	826	799	798	806	794	700	694		915	902	886	893	849	844
b_1	743	749	679	675	605	592	597	592		868	856	864	850	790	756
	601	586	506	488	587	586	500	486		811	788	774	767	754	746
	3160	3147	3134	3128	3155	3142	2371	2337		860	854	849	840	828	831
	3130	3122	(2360)	2322	2344	2310	2327	2295		814	811	800	789	709	715
	1555	1582	1553	1569	(1524)	1552	1490	1537	a''	738	743	729	736	666	672
b_2	1266	1271	1212	1241	1227	1224	1142	1186		658	668	646	663	582	589
	1180	1163	1060	1066	1148	1162	975	923		601	601	602	586	515	501
	1041	1056	902	864	872	857	857	841		516	502	547	549	499	486
	872	858	860	850	830	807	776	772							

Table VI

2-Furancarboxaldehyde fundamentals and frequency shifts relative to furan (cm^{-1})

i	ν_i trans/cis	$\Delta\nu_i$ trans/cis	Predicted sensitivity
1	3150	−19	$\alpha \approx \beta$
2	1277	−1863	$\alpha \approx \beta$
3	1473/1479	−17/−11	β, skeletal
4	1399	15	$\alpha > \beta$, skeletal
5	947/933	−193/−207	α
6	1085	20	β
7	1011/1018	16/23	$\alpha \approx \beta$ small, skeletal
8	746	−124	$\alpha \approx \beta$ small, skeletal
9	882	19	β
10	245/280	−482/−447	α
11	639/623	−26/10	characteristic
12	825	−12	$\beta > \alpha$
13	756/759	13/16	$\alpha > \beta$
14	515	−6	characteristic
15	3144	−16	$\alpha > \beta$
16	3128	−2	$\beta > \alpha$
17	1577	22	skeletal
18	1242/1272	−24/6	$\beta \approx \alpha$
19	213	−967	α
20	1155/1164	114/123	$\beta > \alpha$
21	888	16	characteristic

aldehyde

ν(C—H)	2804/2841
ν(C—O)	1694
β(CH)	1365/1394
β(CO)	495/498
γ(CH)	830
τ(CC)	145/184

of the quality and number of the substituents and are characteristic of the furan ring.

The frequencies of the rest of the skeletal modes (3, 4, 5, 7, 8 and 17) depend more or less on substitution.

Some modes are expected to be sensitive to α substitution (5, 10 and 19) others to β substitution (3, 6 and 9) while many of them (1, 2, 4, 7, 8, 12, 13, 15, 16, 18 and 20) can be influenced by both.

As an example, Table VI shows the assigned fundamentals of 2-furancarboxaldehyde based on our own measurements. The numbers of the first column refer to the corresponding fundamentals of furan in Table V. The frequency shifts demonstrate the predicted sensitivities. A more detailed analysis of the vibrational spectrum of 2-furancarboxaldehyde will be published separately.

REFERENCES

[1] Thompson, H. W., Temple, R. B.: Trans. Faraday Soc., **41**, 27 (1945)
[2] Lecomte, J.: Bull. Soc. Chim. France, **13**, 415 (1946)
[3] Bak, B., Brodersen, S., Hansen, L.: Acta Chem. Scand., **9**, 749 (1955)
[4] Rico, C., Barrachina, M., Orza, J. M.: J. Mol. Spectry., **24**, 133 (1967)
[5] Sidorov, N. K., Kalashnikova, L. P.: Optika Spektrosk., **24**, 469 (1968)
[6] Evsejeva, L. A., Finkel, A. G., Sverdlov, L. M., Pronina, L. V.: Zh. Prikl. Spektrosk. **10**, 614 (1969)
[7] Loisel, J., Pinan-Lucarre, J. P., Lorenzelli, V.: J. Mol. Struct., **17**, 341 (1973)
[8] Loisel, J., Lorenzelli, V.: Spectrochim. Acta, **23A**, 2203 (1967)
[9] Volka, K., Bánki, J., Achmidt, K.,Stibor, I., Ksandr, Z.: Scientific Papers of the Prague Institute of Chemical Technology, **H14**, 169 (1979)
[10] Wilson, E. B., Decius, J. C., Cross, P. C.: Molecular Vibrations. McGraw-Hill, New York 1955
[11] Pulay, P., Török, F.: Mol. Phys., **25**, 1153 (1973)
[12] Kozmutza, K., Pulay, P.: Theor. Chim. Acta, **37**, 67 (1975)
[13] Török, F., Hegedüs, A., Kósa, K., Pulay, P.: J. Mol. Struct., **32**, 93 (1976)
[14] Pulay, P., Fogarasi, G.: J. Mol. Struct., **39**, 275 (1977)
[15] Panchenko, Yu. N., Pulay, P., Török, F.: J. Mol. Struct., **34**, 283 (1976)
[16] Gribov, L. A., Novosadov, P. K., Timonin, V. N.: Optika Spektrosk., **29**, 671 (1970)
[17] Schwendemann, R. H.: J. Chem. Phys., **44**, 2115 (1966)
[18] Török, F., Hegedüs, A., Pulay, P.: Theor. Chim. Acta, **32**, 145 (1973)
[19] Bak, B., Christiansen, E., Dixon, W. B., Hansen, N. L., Rastrup, A. J., Schottländer, M.: J. Mol. Spectry, **9**, 124 (1962)
[20] Grofcsik, A., Billes, F., Fogarasi, G.: J. Mol. Struct., **56**, 277 (1979)
[21] Pulay, P., Török, F.: Acta Chim. Acad. Sci. Hung., **47**, 273 (1966)

Acta Chimica Hungarica 116 (3), pp. 293—301 (1984)

APPLICATION OF A NEW POTENTIOMETRIC EVALUATION METHOD FOR THE DETERMINATION OF THE CONCENTRATION OF MONOVALENT WEAK BASES

G. PETHŐ

(Pharmacy Centre of the Municipial Council, H-1374 Budapest, P.O.Box 590)

Received June 1, 1983

In revised form August 18, 1983

Accepted for publication October 3, 1983

The practical application of a potentiometric method, suitable for the determination of the concentration of weak bases and acids in aqueous medium, is described. (The method was developed independently by Paál and Szalai, and by Pethő).

In the application of the method the sought concentration is calculated from the differences of electromotive force values, using all the points of titration. Neither the equilibrium constant, nor the normal potential of the system are needed for the calculations, thus the calibration of the measuring instrument is unnecessary, only the slope of the response curve of the glass electrode must be determined.

The reliability of the method is characterized by the theoretical error of the method and by the error propagation of the data measured.

The determination of weak electrolytes in aqueous medium is a rather frequent, and often difficult task in analytical chemistry. The reason for this is that the equilibrium constant of the reaction forming the basis of the determination, most often a protonation and deprotonation reaction,does not reach the generally accepted value of 10^7, which is (naturally, depending on concentration, temperature and ionic stength) the minimum of the applicability of direct titration [1, 2].

In addition to the evaluation method of Gran [3,] considered almost classical in the determination of weak acids and bases in aqueous medium, the so-called "linearization methods" [4—9] are used; recently more and more often computer-aided methods are employed [10—18]. A method based on coordination chemical considerations is also known [19].

However, these evaluation methods require an exact knowledge of the equilibrium constant and of the formal potential (E') of the potentiometric measuring cell. These data are often unknown, and cannot be determined with the accuracy needed for evaluation.

By the application of the potentiometric method developed by Paál and Szalai [20] and by Pethő [21], these two data are dispensable in the evaluation of titration, since the differences between the values of electromotive force, recorded at the titration points, are used for the calculations. The potential

of the glass electrode at the i-th titration point is:

$$E_i = E' + S \log [H^+]_i \tag{1}$$

The difference between the potentials measured at points $i = 1$ and $i = 2$, chosen arbitrarily, is:

$$E_2 - E_1 = S \log \frac{[H^+]_2}{[H^+]_1} . \tag{2}$$

In the titration of a weak base (B), the reaction is the following:

$$B + H^+ \rightleftharpoons BH^+, \tag{3}$$

its equilibrium constant being:

$$K = \frac{[BH]_i}{[B]_i [H^+]_i} . \tag{4}$$

Let us assume that in the long period of titration the acid is present only in the BH^+ form, and the concentration of the not yet titrated base is equal to the concentration of the free base. Using the mass balance equations of the base and the acid, expressing $[H^+]$ from Eq. (4) and substituting it into Eq. (2), (omitting the deduction) we have:

$$c_B = c_H \frac{v_1 v_2 (A - 1)}{v_0 (A v_1 - v_2)} \tag{5}$$

where c_B is the concentration of the base, c_H the concentration of the titrant solution, v_0 the initial volume of titration, and v_1 and v_2 are two chosen volumes of the titrant solution. In this expression

$$A = \text{num log} \frac{E_2 - E_1}{S} . \tag{6}$$

In the titration of acids the formula is slightly modified:

$$c_{HA} = c_{OH} \frac{v_1 v_2 (A - 1)}{v_0 (A v_2 - v_1)} \tag{7}$$

where c_{OH} is the concentration of the alkali titrant solution.

It is seen that formulas (5) and (7) do not contain the value of either K or E'.

Practical application of the method

Paál and Szalai calculate the unknown concentration in a titration section determined by the accurately or approximately known equilibrium constant and by the concentration to be determined.

According to the evaluation method reported here, all the measuring points are used. (Naturally, v_2 is always larger than v_1). Thus series of numbers, determined by the variables v_1 and v_2 are obtained from the titration data. Such series are shown in Table I.

The Table makes possible several statements, important from the point of view of the method:

1. In the case of fixed v_1, the calculated c_B values first decrease with increasing v_2 (with the exception of the negative values), then, passing through the minimum marked by italicized, they increase again.

2 The minima are not sharp, the accuracy of rounding-off affects their number.

3. If v_1 has a value yielding only a monotonic increasing number series, then, in the absence of a minimum, no usable c_B values can be obtained from the number series.

4. Deviation of the minima from the average is a small value (see also part on error analysis).

5. c_B data belonging to very small v_1 consumptions are the least reliable.

Figure 1 shows some $c_B = f(v_2)$ functions obtained from another titration, where the statements made above can be readily detected.

The calculations should yield, in principle, results close to the real c_B values in the long section of titration. However, values differing from these

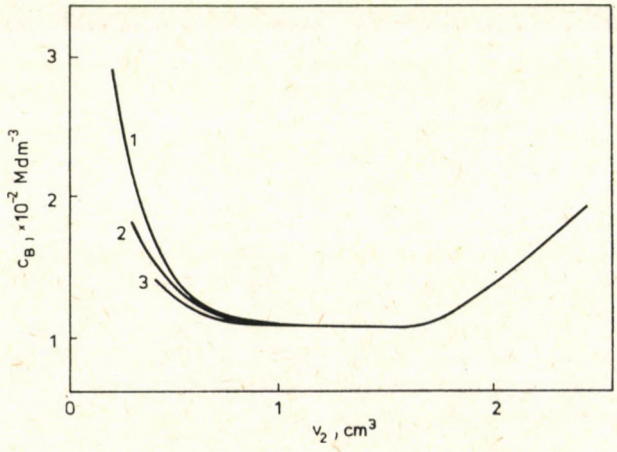


Fig. 1. $c_B = f(v_2)$ functions obtained in the titration of 0.01 mol/dm^3 amidazophene (20 cm^3) by means of 0.1 mol/dm^3 hydrochloric acid. Values of v_1: (1) 0.1 cm^3; (2) 0.2 cm^3; (3) 0.3 cm^3

Acta Chim. Hung. 116, 1984

Table I

c_B values (in $\cdot 10^{-2}$ mol/dm^3) *calculated from the titration of* 20 cm^3 *sodium sulfacetamide with* 0.1 mol/dm^3 *hydrochloric acid*

V_2, cm^3	v_1, cm^3													
	0.1	0.2	0.3	0.4	0.5	0.6	0.7	0.8	0.9	1.0	1.1	1.2	1.3	1.4
0.2	—13.54													
0.3	3.180	1.506												
0.4	1.794	1.216	1.402											
0.5	1.487	1.151	1.050	1.057										
0.6	1.337	1.112	1.042	1.042	1.029									
0.7	1.251	1.088	1.036	1.034	1.025	1.023								
0.8	1.186	1.063	1.023	1.020	1.011	1.004	0.988							
0.9	1.154	1.057	1.026	1.024	1.018	1.016	1.013	1.035						
1.0	1.121	1.045	1.020	1.017	1.012	1.010	1.007	1.014	0.997					
1.1	1.099	1.038	1.018	1.016	1.012	1.010	1.008	1.013	1.004	1.010				
1.2	1.079	1.031	1.014	1.013	1 010	1.008	1.006	1.009	1.003	1.005	1.002			
1.3	1.065	1.026	1.013	1.012	1.009	1.008	1.007	1.009	1.005	1.007	1.006	1.009		
1.4	1.051	1.020	1.009	1.008	1.00	1.005	1.004	1.005	1.002	1.003	1.001	1.001	0.995	
1.5	1.039	1.015	1.007	*1.006*	*1.004*	*1.003*	*1.002*	*1.003*	*1.001*	*1.001*	*1.000*	*1.000*	0.997	0.999
1.6	1.032	1.014	1.007	1.007	1.005	1.005	1.004	1.005	1.003	1.004	1.003	1.003	1.002	1.004
1.7	1.025	*1.011*	*1.006*	*1.006*	1.005	1.004	1.004	1.004	1.003	1.004	1.003	1.003	1.003	1.004
1.8	1.021	*1.011*	1.008	1.007	1.007	1.006	1.006	1.007	1.006	1.006	1.006	1.006	1.006	1.007
1.9	*1.018*	1.012	1.010	1.009	1.009	1.009	1.009	1.009	1.009	1.009	1.009	1.009	1.009	1.009
2.0	1.021	1.018	1.016	1.016	1.016	1.016	1.016	1.016	1.016	1.016	1.016	1.016	1.016	1.016
2.1	1.040	1.038	1.038	1.038	1.038	1.038	1.038	1.038	1.038	1.038	1.038	1.038	1.038	1.038
2.2	1.060	1.075	1.075	1.075	1.075	1.075	1.075	1.075	1.075	1.075	1.075	1.075	1.075	1.075
2.3	1.120	1.119	1.119	1.119	1.119	1.119	1.119	1.119	1.119	1.119	1.119	1.119	1.119	1.119
2.4	1.166	1.65 1	1.165	1.165	1.165	1.165	1.165	1.165	1.165	1.165	1.165	1.165	1.165	1.165
2.5	1.212	1.212	1.212	1.212	1.212	1.212	1.212	1.212	1.212	1.212	1.212	1.212	1.212	1.212

Table II

Results of determining some weak bases

Compound	pK_b	$c_{B'}$ mol/dm³	$c_{HCl'}$ mol/dm³	Confidence interval
Monosodium malate	10.6	0.1	0.1	$1.000 \cdot 10^{-1} \pm 5.1 \cdot 10^{-4}$ ($n = 34$; $P = 0.99$)
Amidazophene	8.7	0.1	0.1	$9.979 \cdot 10^{-2} \pm 4.6 \cdot 10^{-5}$ ($n = 40$; $P = 0.99$)
		0.01	0.1	$1.001 \cdot 10^{-2} \pm 2.3 \cdot 10^{-5}$ ($n = 39$; $P = 0.99$)
Sodium lactate	10.1	0.1	0.1	$1.018 \cdot 10^{-1} \pm 4.2 \cdot 10^{-4}$ ($n = 33$; $P = 0.99$)
Sodium sulfacetamide	9.0	0.01	0.1	$1.009 \cdot 10^{-2} \pm 2.9 \cdot 10^{-5}$ ($n = 74$; $P = 0.99$)
		0.01	0.01	$9.993 \cdot 10^{-3} \pm 3.0 \cdot 10^{-5}$ ($n = 51$; $P = 0.99$)
Sodium acetate	9.2	0.1	0.1	$9.807 \cdot 10^{-2} \pm 1.3 \cdot 10^{-4}$ ($n = 36$; $P = 0.99$)
		0.01	0.1	$9.502 \cdot 10^{-2} \pm 5.9 \cdot 10^{-5}$ ($n = 34$; $P = 0.99$)
Pyridine	8.9	0.01	0.1	$1.066 \cdot 10^{-2} \pm 1.5 \cdot 10^{-5}$ ($n = 56$; $P = 0.99$)

are obtained in the initial section of the titration curve as well as in the part close to the equilibrium point, since hydrogen ions formed during the hydrolysis of the base at the beginning of the titration change the values of E_i. This change is not equally reflected in E_1 and E_2; in this method this effect gives rise to a positive deviation. The diminishing of hydrolysis (with proceeding titration) decreases the value of c_B.

Before the equivalence point, another effect comes into play: in this section the concentration of free hydrogen ion should be less and less neglected. As a result of this, a positive deviation is again observed.

Thus, the concentration sought is best given by the average of the minimal c_B values in the columns.

This paper presents the results calculated from the titration of a few weak bases. Numerical data are summarized in Table II. The intervals obtained are narrow, showing the reliability of the method.

Characterization of the theoretical error of the method

In order to characterize the theoretical error, the points of the theoretical potentiometric titration curve were used.

First it had to be investigated whether, by using without neglection the material balance equations, the theoretical c_B value can be recovered.

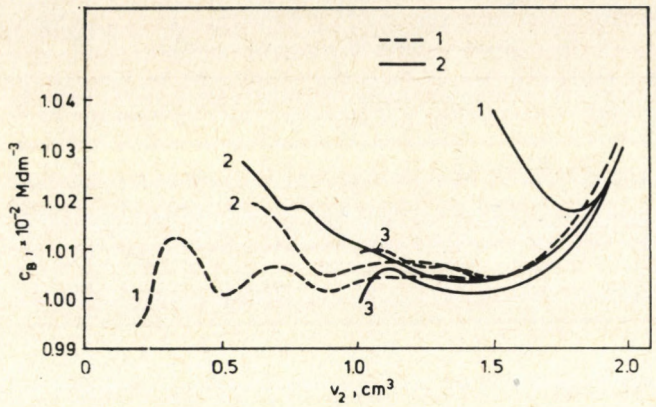


Fig. 2. Theoretical (1) and measured (2) $c_B = f(v_2)$ functions ($K = 10^5$; $v_0 = 20$ cm^3; $c_H = 0.1$ mol/dm^3; $S = 59.1$ mV/pH). Values of v_1: (1) 0.1 cm^3; (2) 0.5 cm^3; (3) 0.9 cm^3

The points of the theoretical titration curve can be obtained from the following equation (omitting deduction):

$$K[H^+]_i^2 + \left[\frac{K(c_B v_0 - c_H v_i)}{v_0 + v_i} + 1\right][H^+]_i - c_H \frac{v_i}{v_0 + v_i} = 0 \qquad (8)$$

and the values of c_B can be calculated by the equation

$$c_B = \frac{v_{1,t} v_{2,t}}{v_0} \cdot \frac{(c_{H,1} - [H^+]_1)(c_{H,2} - [H^+]_2)(A-1)}{A v_{1,t}(c_{H,1} - [H^+]_1) - v_{2,t}(c_{H,2} - [H^+]_2)}. \qquad (9)$$

In the latter formula the meaning of A is the same as given by expression (6); $v_{1,t}$ and $v_{2,t}$ are the total volumes, $c_{H,1}$ and $c_{H,2}$ the total acid concentrations, and $[H^+]_1$ and $[H^+]_2$ the free hydrogen ion concentrations at the titration points $i = 1$ and $i = 2$, respectively.

Results calculated for several systems with Eq. (9) exactly yielded the expected c_B values along the full section of the titration curves (from 0 to 100% degree of titration). Systems of this kind were: $K = 10^3$, 10^4, 10^5, 10^6; $c_B = 0.1$, 0.01, 0.001 mol/dm^3 and $c_H = 0.1$, 0.01 mol/dm^3, in several variations.

Naturally, for the characterization of the method the shape of the $c_B = f(v_2)$ function, calculated with Eq. (5), involving neglections, had to be also calculated.

It was found in each case that in the initial section of titration the c_B values varied in the vicinity of the expected value, because of the 0.1 mV rounding-off of the potential values calculated from the theoretical $[H^+]_i$. Later, in accordance with practice, the c_B values began to increase. Figure 2

shows some theoretical functions, as well as some results, measured under the same conditions (K, c_B, c_H, S) as used for the calculation of theoretical data.

Thus, in principle, the expected c_B data can be recovered with good approximation, with the exception of the section in the vicinity of the equivalence point.

Characterization of experimental error, error propagation

The error propagation can be characterized by the partial differential equations [22] of formula (5), which are the following:

$$\frac{\partial c_B}{\partial c_H} = \frac{v_1 v_2 (A-1)}{v_0 (A v_1 - v_2)} \tag{10}$$

$$\frac{\partial c_B}{\partial v_1} = \frac{c_H v_2 (A-1)}{v_0 (A v_1 - v_2)} - \frac{c_H v_1 v_2 A (A-1)}{v_0 (A v_1 - v_2)^2} \tag{11}$$

$$\frac{\partial c_B}{\partial v_2} = \frac{c_H v_1 (A-1)}{v_0 (A v_1 - v_2)} + \frac{c_H v_1 v_2 (A-1)}{v_0 (A v_1 - v_2)^2} \tag{12}$$

$$\frac{\partial c_B}{\partial v_0} = -\frac{1}{v_0^2} \cdot \frac{c_H v_1 v_2 (A-1)}{A v_1 - v_2} \tag{13}$$

$$\frac{\partial c_B}{\partial E_2} = \frac{c_H v_1 v_2}{v_0} \cdot \frac{A \ln 10}{S} \cdot \frac{(A v_1 - v_2) - v_1 (A-1)}{(A v_1 - v_2)^2} \tag{14}$$

$$\frac{\partial c_B}{\partial E_1} = -\frac{\partial c_B}{\partial E_2} \tag{15}$$

$$\frac{\partial c_B}{\partial S} = \frac{c_H v_1 v_2}{v_0} \cdot \frac{A \ln 10}{S^2} \cdot \frac{v_1 (A-1) - (A v_1 - v_2)}{(A v_1 - v_2)^2} \cdot (E_2 - E_1). \tag{16}$$

When plotting the effect of the parameters, the volume difference $v_2 - v_1$ can be chosen as the independent variable, in view of the method of calculation.

Since the same $v_2 - v_1$ value may result as the difference of many volumes, the members of this volume difference had to be made in some way more exact. As the results are always given at minimal c_B values, the value of v_2 will be suitably marked out at the place where the c_B minimum is obtained within a column.

In Figs 3 and 4, showing the effect of the measuring error of the parameters on c_B, the values of v_2 are given by the volumes belonging to $c_{B,\,min}$ in Table I.

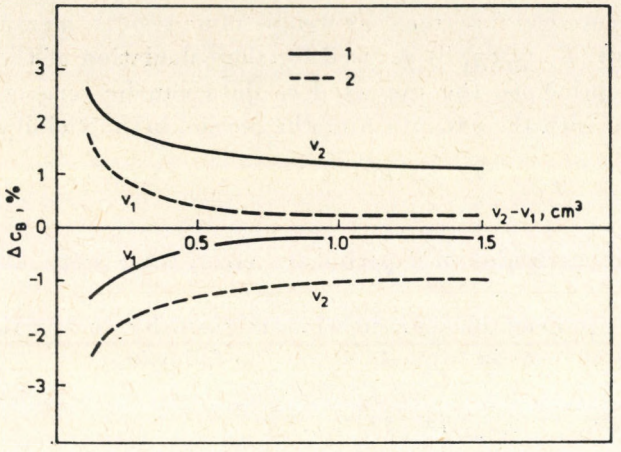


Fig. 3. Effect of parameters v_1 and v_2 on the c_B values; (1) means a change of + 1 rel. % and (2) — 1 rel. %

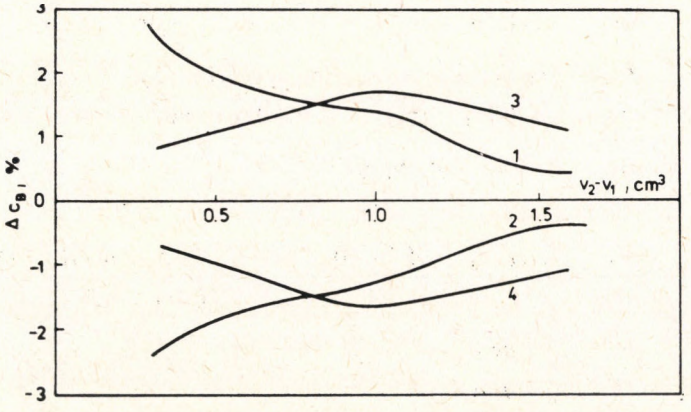


Fig. 4. Effect of parameters E_1, E_2 and S on the c_B values; (1) E_1(+1 mV) and E_2 (−1 mV); (2) E_1 (−1 mV) and E_2 (+1 mV); (3) S (+1 mV); (4) S (−1 mV) change in parameter

The effects of c_H and v_0 are not given separately in the Figures, because these two parameters are directly and inversely proportional to c_B, respectively.

It should be pointed out that of the parameter effects even the relatively coarse error (± 1 mV) of the two potential data and of the slope of the electrode response does not cause a considerable error. This was fully supported by the simulated error of the experimental results.

The accuracy of the method is characterized also by Table III, containing the standard deviation of all the data measured in solutions of $c_B = 0.1$ mol/dm^3 and $c_B = 0.01$ mol/dm^3 concentration. (Other data of titration, such as v_0, c_H naturally do change, but the great number of parallel results makes possible this kind of characterization of the method.)

Table III

Standard deviation (S) of the measured data

c_B, mol/dm³	S, %	n
0.1	±0.49	170
0.01	±0.70	229

In the first case the 170 data were obtained from the results of 12 titrations, in the second (299 pairs of points of evaluation) from the results of 17 titrations.

Experimental

For the measurement of hydrogen ion concentration a pH-meter Type RADELKIS OP 208; with digital display, and glass electrode, RADELKIS OP 7180 and RADIOMETER G 202 C, were used. As reference electrode a RADELKIS OP 830 calomel electrode, connected in a Wilhelm bridge [23], was employed.

Ionic stength was adjusted in each titration by means of potassium nitrate to a value of $I = 0.3$ mol/dm³.

Measurements were carried out in a thermostat (VEB MLW TB 25) at 25 °C and under mixing with a magnetic stirrer.

A RADELKIS OP 930 automatic burette was used for the addition of the titrant solution, and the results were calculated by means of a PTK 1096 minicomputer (HÍRADÁSTECHNIKAI SZÖVETKEZET, Budapest).

REFERENCES

[1] Laitinen, H. A., Harris, W. E.: Chemical Analysis, 2nd ed., p. 44., McGraw-Hill, New York 1975
[2] Meites, L., Goldman, J. A.: Anal. Chim. Acta, **29,** 472 (1963)
[3] Gran, G.: Analyst, **77,** 661 (1952); Acta Chem. Scand., **4,** 559 (1951)
[4] Liteanu, C., Cörmös, D.: Talanta, **7,** 25 (1960)
[5] Buffle, J., Parthasarathy, N., Monnier, D.: Anal. Chim. Acta, **59,** 427 (1972)
[6] Buffle, J.: Anal. Chim. Acta, **59,** 439 (1972)
[7] Parthasarathy, N., Monnier, D., Buffle, J.: Anal. Chim. Acta, **59,** 447 (1972)
[8] Charakova, P., Budevsky, O.: J. Electroanal. Chem., **73,** 369 (1976)
[9] Ingman, F., Still, E.: Talanta, **13,** 1431 (1966)
[10] Ivaska, A., Wänninen, E.: Anal. Lett., **6,** 961 (1973)
[11] Briggs, T. N., Stuehr. J. E.: Anal. Chem., **46,** 1517 (1974)
[12] Ivaska, A.: Academic Dissertation, Abo, Finland 1975
[13] Ivaska, A., Nagypál, I.: Magy. Kém. Foly., **86,** 84 (1980)
[14] Johansson, A., Johansson, S.: Analyst, **103,** 305 (1978)
[15] Johansson, A., Gran, G.: Analyst, **105,** 802 (1980)
[16] Gran, G., Johansson, A., Johansson, S.: Analyst, **106,** 1109 (1981)
[17] Gran, G., Johansson, A.: Analyst, **106,** 231 (1981)
[18] Wang, Bao-Jing, Wu, Wan-Hua, Fan, Xing-Xue: Hua-tung. Hua Kung Hsueh Yuan Hsueh Pao, **2,** 91 (1980)
[19] Burger, K., Pethő, G., Noszál, B.: Anal. Chim. Acta, **118,** 93 (1980)
[20] Paál, T., Szalai, H.: Analyst, **107,** 839 (1982)
[21] Pethő, G.: Dissertation for the degree Cand. Chem. Sci., p. 91., Budapest 1982
[22] Korn, G. A., Korn, T. M.: Matematikai Kézikönyv Műszakiaknak (Mathematical Handbook for Engineers), Műszaki Kiadó, Budapest 1975
[23] Forsling, J. W., Hietanen, S., Sillén, L. G.: Acta Chem. Scand., **6,** 905 (1952)

Acta Chimica Hungarica 116 (3), pp. 303—313 (1984)

DIELS–ALDER REACTION OF 3(2*H*)-ISOQUINOLINONES, II*

STUDIES ON THE LACTAM–LACTIM TAUTOMERISM OF 3(2*H*)-ISOQUINOLINONES

L. HAZAI, GY. DEÁK**, A. SCHNITTA, J. HASKÓ-BREUER and E. HORVÁTH

(Institute of Experimental Medicine, Hungarian Academy of Sciences, H-1450 Budapest, P.O.Box 67)

Received August 2, 1983

Accepted for publication October 11, 1983

The literature dealing with the tautomerism of 3(2*H*)-isoquinolinones (3-isoquinolinols) has been surveyed. The λ_{max} bands in the UV spectra indicating the lactam or lactim structure of the compounds prepared by us, and the main characteristics of the IR spectra are summarized in tabular form. Variations in the lactam—lactim ratio with the polarity of the solvent and depending on the substituents in the compounds were examined. It has been found that the lactam form is present also in nonpolar solvents; owing to its quinonoid structure, it can be regarded as a diene capable of participating in Diels—Alder reactions. Preparation procedures for some model compounds, not described hitherto, are given.

Introduction

3(2*H*)-Isoquinolinones[+] or 3-hydroxyisoquinolines, a group of compounds which has been little studied as shown by the literature, can be represented by two formulas of the tautomeric forms:



A *B*

It is obvious that the lactam form *A* can be regarded as a potential diene owing to its *ortho*-quinonoid structure and, assuming that the equilibrium is not shifted to *B* in 100%, the compound should be able to participate in Diels–Alder reactions.

The tautomerism of these compounds was discussed comprehensively by Katritzky [1, 2]. 3(2*H*)-Isoquinolinones were assumed to exist in the

* Part I.: Hazai, L., Deák, Gy., Tóth, G., Schnitta, A., Szőllősy, Á., Tamás, J.: Acta Chim. Hung., **113**, 237 (1983)

** To whom correspondence should be addressed

[+] The name "3(2*H*)-isoquinolinone" will be used further on, irrespective of the fact that the compound may exist exclusively in form *A* or *B* in the crystalline state or in solution.

3-hydroxy form, on the basis of chemical evidence (solubility in alkali) [3] and the IR spectra [4] (νOH 3413 cm^{-1}). These results have been questioned by other researchers [5] and, on the basis of the IR and UV spectra, furthermore, the pK_a values, they considered the lactam structure more probable. Later, thorough studies of the UV spectra revealed [6] that 3(2*H*)-isoquinolinone, as well as the 1-methyl- and 6,7-dimethoxy-1-methyl derivatives occur in tautomeric equilibrium with the 3-hydroxy form, the latter being predominant in the majority of solvents containing no hydroxyl group, whereas in water the lactam is the predominating tautomer. In ethanol and chloroform both forms are present simultaneously. IR and NMR studies [7] confirmed these results, and theoretical considerations based on MO calculations [8] also showed this probability. By an investigation of the UV spectra, Jones [9] also obtained similar results. In his opinion, 1-phenyl- and 1,4-diphenyl-3(2*H*)--isoquinolinone exist mainly in the lactim form in ethanol, but in the case of the 1-methyl analogues, the isoquinolinone form is predominating. 1-Chloro--3(2*H*)-isoquinolinone, however, occurs in the 3-hydroxy form in all solvents, as supported by the UV and IR spectra [6, 10] and also in the crystalline

Table I

UV spectra of 3(2H)-isoquinolinones published in the literature [9]

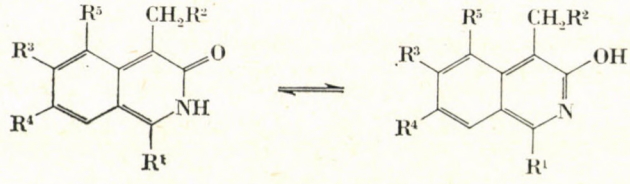
	Solvent	λ_{max} (nm) lactim	λ_{max} (nm) lactam	ε lactim	ε lactam
3(2*H*)-Isoquinolinone	anhydrous ethanol	344	405	2100	1970
	diethyl ether	341		3560	
	ethanol-diethyl ether 1 : 1	343	410	2800	527
	95% ethanol	347	405	1720	2560
3-Methoxyisoquinoline	anhydrous ethanol	399		3660	
2-Methyl-3(2*H*)-isoquinolinone	anhydrous ethanol	410		4990	
1-Methyl-3(2*H*)-isoquinolinone	anhydrous ethanol	345	412	1900	3230
	diethyl ether	344		4570	
	ethanol-diethyl ether 1 : 1	345	414	3180	1790
	95% ethanol	350	410	1590	4240
1-Methyl-3-methoxyisoquinoline	anhydrous ethanol	340		4170	
1,2-Dimethyl-3(2*H*)-isoquinolinone	anhydrous ethanol	416		5340	
	diethyl ether	444		4420	
1-Phenyl-3(2*H*)-isoquinolinone	anhydrous ethanol	350	420	5970	2210
	ethanol-diethyl ether 1 : 1	350	420	7140	1020
	diethyl ether	350		8150	
1,4-Diphenyl-3(2*H*)-isoquinolinone	anhydrous ethanol	360	435	8390	3150
	ethanol-diethyl ether 1 : 1	362	435	11200	990
	diethyl ether	360		12700	
	xylene*	345	450	7330	276

* Our own measurement in xylene, see compound **4** in Table IIa; $\varepsilon_{lactam}/\varepsilon_{lactim}$: 0.03777

state, as shown by X-ray diffraction analysis [11]. In Table I, the results obtained by Jones [9] are shown, providing a good survey of the lactam—lactim tautomerism. Deák et al. [12, 13] examined 4-benzyl-1-phenyl-3(2*H*)--isoquinolinone to find that in both the crystalline state and carbon tetrachloride solution this compound exists in the 3-hydroxy form, whereas in ethanol solution, as shown by the UV spectra (λ_{lactim} : 357 nm, λ_{lactam}: 438 nm), both isomers can be detected. In the IR spectrum, the characteristic features are the broad band with partial maxima between 3200 and 2100 cm^{-1}, the absence of the lactam band at 1670 cm^{-1}, and a strong band at 1620 cm^{-1} ($\nu C{=}N$). In carbon tetrachloride solution, the band assigned to the hydroxyl group is found at 3465 cm^{-1}, thus the 3-hydroxy form can justly be assumed.

Table IIa

UV spectra of compounds synthesized in the authors' laboratory (in 95% ethanol)



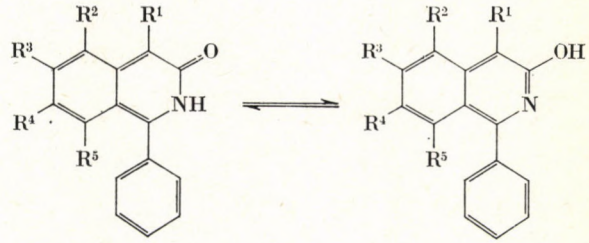
N°	R^1	R^2	R^3	R^4	R^5	λ_{max} (ε) lactam	λ_{max} (ε) lactim	$\varepsilon_{lactam}/\varepsilon_{lactim}$
1[1]	C_6H_5	C_6H_5	H	H	H	438 (3685)	357 (5350)	0.69
2	C_6H_5	C_6H_5	CH_3O	CH_3O	H	421 (6605)	321 (15250)	0.433
3[1]	4-Cl—C_6H_5	C_6H_5	H	H	H	419 (1640)	341 (5980)	0.275
4[2]	C_6H_5	H	H	H	H	425 (4060)	354 (5210)	0.795
4	C_6H_5	H	H	H	H	436 (360)*	340 (5490)*	0.066*
5[2]	C_6H_5	H	H	H	CH_3	413 (3315)	344 (4301)	0.72
6[2]	C_6H_5	CH_2R^2 : H	H	H	CH_3	404 (4559)	337 (5848)	0.78
7[3]	4-Py	4-Py	H	H	H	434 (1166)	359 (8270)	0.14
7	4-Py	4-Py	H	H	H	—**	397 (8550)**	lactim**
7	4-Py	4-Py	H	H	H	440 (5500)***	375 (7440)***	0.74***
8[3]	3-Py	3-Py	H	H	H	430 (899)	350 (7192)	0.125
9	4-Py	3-Py	H	H	H	422 (340)	343 (6020)	0.565
10	4-Py	H	H	H	H	419 (221)	339 (4600)	0.048

Py: abbreviation for the pyridyl group
* in xylene
** in 0.1 *N* NaOH
*** in 0.1 *N* HCl
[1] For preparation, see Ref. [12]
[2] For preparation, see Ref. [15]
[3] For preparation, see Ref. [14]

Acta Chim. Hung. 116, 1984

Table IIb

UV spectra of compounds with anellated benzene ring, synthesized in the authors' laboratory+ (in 95% ethanol)



N°	R¹	R²	R³	R⁴	R⁵	benzo	λ_{max} (ε) lactam	λ_{max} (ε) lactim	$\frac{\varepsilon_{lactam}}{\varepsilon_{lactim}}$
11*	$CH_2C_6H_5$	—CH=CH—CH=CH—		H	H	[f]	411 (5650)	344 (3090)	1.83
12*	H	—CH=CH—CH=CH—		H	H	[*f*]	410 (4820)	337 (2760)	1.75
13*	CH_3	—CH=CH—CH=CH—		H	H	[*f*]	411 (7950)	326 (5102)	1.56
14*	$CH_2C_6H_5$	H	H	—CH=CH—CH=CH—		[*h*]	385 (5619)	333 (4205)	1.34
15*	CH_3	H	H	—CH=CH—CH=CH—		[*h*]	394 (6306)	331 (2476)	2.55

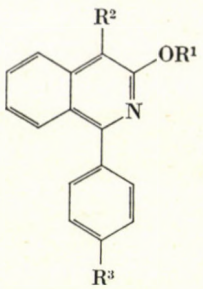
—CH=CH—CH=CH—: benzo-anellation

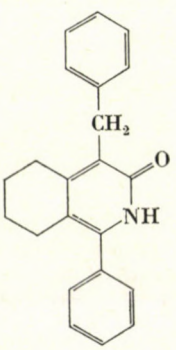
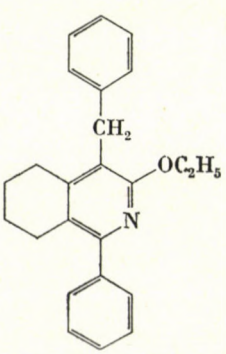
+ In benzo[*f*]- and [*h*]-isoquinolinones, as seen from the Table, the lactam form is prediominating. Jones and Wife stated that 1,4-diphenyl--benzo[*g*]-isoquinolin-3-ol [16], showing bands at 433 nm ($\varepsilon = 6690$) and at 560 nm ($\varepsilon = 340$) in alcohol solution, exists in about 90% in the lactim form. The unusually high wavelength values were assigned by preparing compounds with fixed lactam (*N*-Me) and lactim (*O*-Me) structure, and their UV examination. The IR spectra recorded in the crystalline state also correspond to the structures

* For preparation, see Ref. [15]

Table III

UV spectra of compounds with fixed lactim structure and of 5,6,7,8-*tetrahydro derivatives*
(in 95% ethanol)



N°	R¹	R²	R³	λ_{max} (ε)
16[1]	C_2H_5	$CH_2C_6H_5$	H	354 (9450)
17	$CH_2CH{=}CH_2$	CH_3	H	360 (9110)
18[2]	CH_3CO	$CH_2C_6H_5$	$NHCOCH_3$	360 (11200)*
19	CH_3SO_2	CH_3	H	330 (7810)
20[1]				328 (11650) *lactam*
21[1]				306 (1535) *lactim*

* in xylene
[1] For preparation, see Ref. [13]
[2] For preparation, see Ref. [12]

Investigations of the UV and IR spectra of the new 3(2*H*)-isoquinolinones prepared in our laboratory: tautomeric conditions

In the following, the characteristic bands in the UV (Tables II, III) and IR (Table IV) spectra will be summarized which are suitable for differentiating between the lactam and lactim tautomeric forms. In Table III the compounds with fixed lactim structure and the 5,6,7,8-tetrahydro derivatives saturated in ring A are shown.

The compounds listed in Table IIa exist mainly in the lactim form in 95% alcohol of polar nature, whereas in the compounds anellated with benzene

Table IV

Characteristic IR bands of 3(2H)-isoquinolinones synthesized in the authors' laboratory (in KBr)

N°		ν_{max} (cm^{-1})	Note
1	1620	3200—2100*	—
2	1620	3100—2200*	—
3	1620	3200—2200*	—
4	1620	3100—2100*	—
5	1610	3200—2100*	—
6	1635, 1620	3510, 3400, 3100—2200*	probably a mixture of lactam and lactim
7	1620 (also in $CHCl_3$)	3200—2100*, 3525 ($CHCl_3$)	OH group
8	1620	3100—2200*	—
9	1620	3100—2200*	—
10	1625	3100—2000*	—
11	1620	3100—2100*	—
12	1640, 1620 (sh)	3100—2300*	may be a lactam—lactim mixture
13	1630	3400 (broad), 3040, 2920, 2860	may be lactam
14	1630, 1620	3100—2300*	may be a mixture
15	1630 (sh), 1620	3100—2300*	may be a mixture
16	1620		—
17	1610	1545, 1310, 1180, 1150, 1090	—
18	1760, 1670, 1610		—
19	1620	1590, 1550, 1360, 1190, 1170, 1130	—
20	1660	3400 (sharp)	in CCl_4
21	1560	1420, 1320, 1210, 1180, 1090	—

* Broad band, with characteristic partial maxima

ring the lactam tautomer is predominating (Table IIb). It is important that, according to the spectra recorded in *xylene*, even in this solvent compounds can occur in the lactam form, too (see foot-note to Table I, and compound **4** in Table IIa), since this means that the *o*-quinonoid structure is present also in such a solvent which is generally used in Diels–Alder reations. In the case of derivatives containing a pyridine ring, the lactim form is significantly predominating. In alkaline media, the chromophore systems of the anions of these compounds (the electron distribution) is similar to that of the lactim form (Table IIa, compound **7**), while in acids the spectrum resembles that recorded in ethanol, with the difference that the lactam/lactim ratio is higher than in alcohol. In Table III, the spectra of compounds with fixed lactim structure are shown and it can be seen that these compounds, in accordance with the structural formula, *do not* contain the isomer with diene structure. Compound **20**, the 5,6,7,8-tetrahydro derivative, exists in the lactam form both in the crystalline state and in solvents (still, it can be *O*-acylated [13]). It must be noted that the difference between **20** and **21** is much more characteristic in the IR spectra than in the UV spectra, though the latter are otherwise well suitable to differentiate between the lactam and lactim types.

The IR spectra of the compounds are shown in Table IV. In the crystalline state the lactim structure is characterized by the $\nu C{=}N$ band at 1620 cm^{-1} and the region between 3200—2100 cm^{-1} with partial maxima [12]. The majority of our compounds has this structure, as also shown by the spectra. In some compounds the possibility of the presence of a lactam—lactim mixture exists (**6**, **12**, **14**, **15**); in the compounds anellated with benzene ring the establishment of the tautomeric form is difficult from the IR spectra, and solubility reasons prevented the recording of the solution spectra. In some cases the solution spectra could also be obtained, e.g., for compound **7**; here the band characteristic of the hydroxyl group appeared at 3525 cm^{-1}. The spectra of isoquinolines with fixed lactim structure are unambiguous, and this also applies to the 5,6,7,8-tetrahydro derivatives, as mentioned above.

Synthesis of model compounds

The syntheses of the majority of isoquinolinones prepared in our laboratory have been published previously, and pertaining papers are referred to in the Tables.

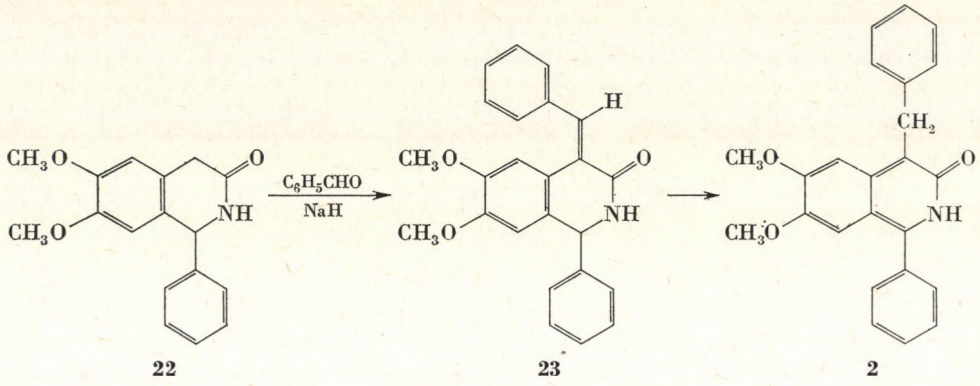
Here the syntheses of the newly prepared compounds are described for the substances whose spectral data are listed in the Tables.

The dimethoxy derivative **2** was synthesized on the analogy of the previous compounds [12, 15] (Scheme 1).

The condensation reaction was considerably slower than with the 5,6-unsubstituted isoquinolinone; it can be assumed that the electron-donating

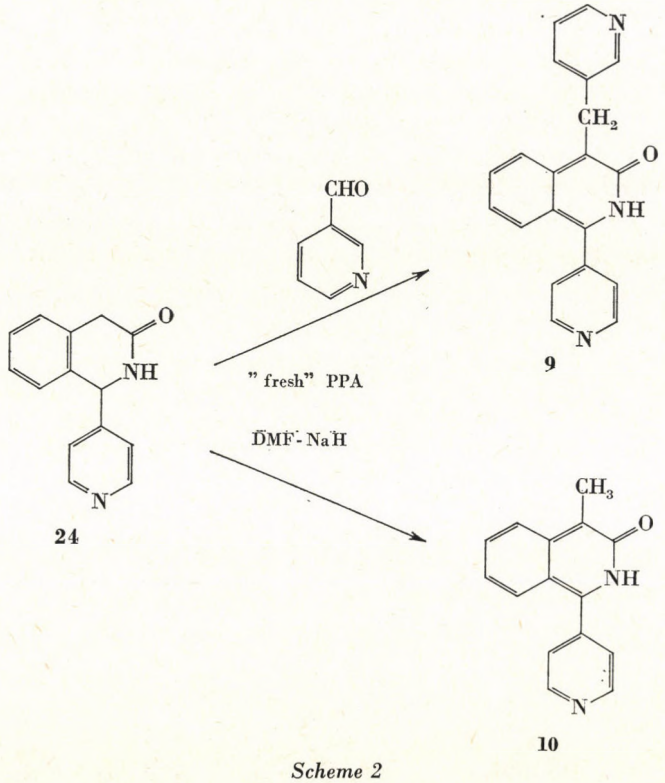
character of the 7-methoxy group is not favourable for the formation of the carbanion at the C-4 methylene.

In the former case, 4-benzyl-1-phenyl-3(2*H*)-isoquinolinone, unsubstituted in the carbocyclic ring, was obtained in benzene at 50 °C for 6 h in 51.4% yield [12]; in contrast, **22** was made to react with benzaldehyde in toluene at



22 **23** **2**

Scheme 1



24 **9** **10**

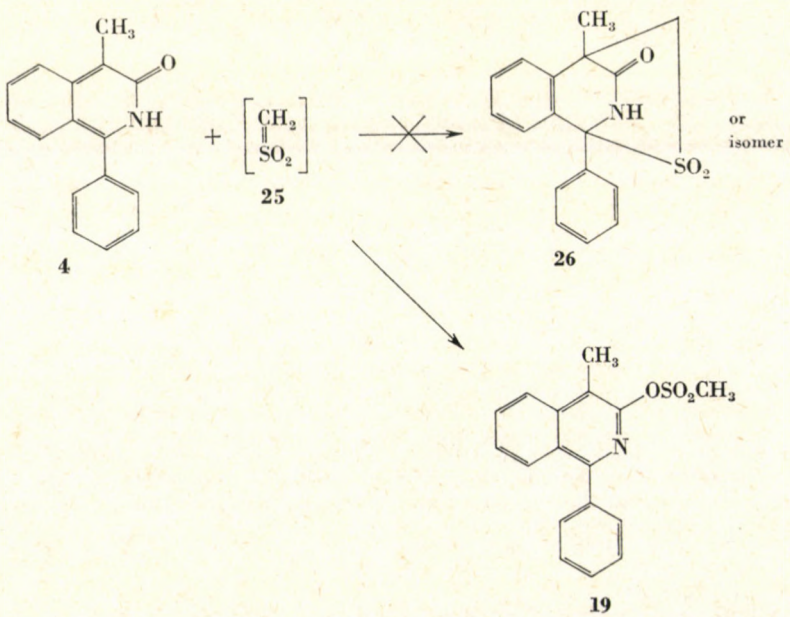
Scheme 2

100 °C for 15 h to obtain **2** in 48% yield, after the processing of the reaction mixture. The reaction was monitored by TLC and stopped at the proper time to isolate the intermediate **23** (at 60 °C, after 2 h reaction time, in 19% yield). The ^{1}H-NMR investigation of **23** has shown that, similarly to 4-benzylidene-isoquinolinones described earlier [13], the vinyl proton is located also here in *cis* position to the carbonyl group, that is, the *E* isomer can be isolated.

It was reported earlier [14] how the composition of polyphosphoric acid affected the outcome of the reaction of benzyl cyanide with pyridine-carboxaldehydes. On the basis of these results, compound **9** was synthesized by the reaction of 1-(4-pyridyl)-1,4-dihydro-3(2*H*)-isoquinolinone (**24**) and 3-pyridinecarboxaldehyde (nicotinaldehyde) in freshly prepared PPA, while compound **10** was obtained by means of a reaction with NAH-DMF [15] (Scheme 2).

Of the compounds with fixed lactim structure (Table III), the syntheses of the allyl ether **17** and the methanesulfonic ester derivative **19** are described in this paper. The isoquinoline **17** was prepared by the alkylation of **4** [15] with allyl bromide, via the silver salt, on the basis of an analogous method reported [17]; the syntheses of **16** and **18** were published earlier ([13] and [12], respectively).

In the course of investigations on some "in situ" produced dienophiles, the reaction between **4** and, among others, the sulfene **25** [18] was attempted. The sulfene generated by the reaction of methanesulfonyl chloride with tri-



4 25 26 19

Scheme 3

ethylamine, did not give an adduct with **4**, instead the *O*-methanesulfonyl derivative **19** was obtained (Scheme 3). The structure was confirmed by the IR spectrum; as the molecular formula of **26** is the same as that of **19**, analytical results cannot be accepted for decision between the structures.

Experimental

M.p.'s were determined with a Büchi—Tottoli melting point measuring apparatus and are uncorrected. The IR spectra were recorded with a Perkin-Elmer 457 instrument, and the UV spectra with an Opton-DMR 21 spectrophotometer. The NMR spectra were obtained with a JEOL FX-100 instrument.

4-Benzyl-1-phenyl-6,7-dimethoxy-3(2*H*)-isoquinolinone (2)

1-Phenyl-6,7-dimethoxy-1,4-dihydro-3(2*H*)-isoquinolinone (**22**) [19] (5.66 g; 0.02 mol) was dissolved in anhydrous toluene (500 mL) and a dispersion in oil of NaH (1.06 g; 0.022 mol) was added in a stream of N_2 at 100 °C. After stirring for 15 min, benzaldehyde (2.12 g; 0.02 mol) was added by drops, the reaction mixture was stirred at 100 °C for 15 h, then poured into water (400 mL). The solid precipitate was filtered off, the two phases of the filtrate were separated, and the organic solution was washed with water. After concentration to about one-third volume and cooling, the product separated. It was filtered off and recrystallized from benzene to yield the pure product (3.6 g; 48.5%), m.p. 230 °C (from benzene).

$C_{24}H_{21}NO_3$. Calcd. C 77.61; H 5.70; N 3.77. Found C 77.61; H 6.04; N 3.95%.

IR: see Table IV.

UV: see Table IIa.

4-(3-Picolinyl)-1-(4-pyridyl)-3(2*H*)-isoquinolinone (9)

1-(4-Pyridyl)-1,4-hidydro-3(2*H*)-isoquinolinone (**24**) [14] (2.24 g; 0.01 mol) and 3-pyridinecarboxaldeyde (1.08 g; 0.01 mol) were stirred in freshly prepared PPA (20 g) at 140 °C for 16 h. The reaction mixture was poured into water, and made alkaline with conc. NH_4OH to obtain a precipitate, which was filtered off and dried (1.92 g; 58%), m.p. 221—222 °C.

$C_{20}H_{15}N_3O$. Calcd. C 76.65; H 4.82; N 13.40. Found C 76.42; H 5.14; N 13.15%.

IR: see Table IV.

UV: see Table IIa.

4-Methyl-1-(4-pyridyl)-3(2*H*)-isoquinolinone (10)

Compound **24** (2.24 g; 0.01 mol) was dissolved in anhydrous dimethylformamide (40 mL) and a dispersion in oil of NaH (1.44 g; 0.03 mol) was added, with stirring, in a stream of N_2. Stirring was continued at 140 °C for 1 h and the mixture was then poured into distilled water (400 mL) and neutralized with 2*N* HCl. The substance which separated was filtered off and dried to obtain the product (0.55 g; 23.3%), m.p. 265—267 °C (from ethanol).

$C_{15}H_{12}N_2O$. Calcd. C 76.25; H 5.12; N 11.86. Found C 76.28; H 5.15; N 11.96%.

IR: see Table IV.

UV: see Table IIa.

3-Allyloxy-1-phenyl-4-methylisoquinoline (17)

1-Phenyl-4-methyl-3(2*H*)-isoquinolinone (**4**) [15] (6.4 g; 0.0272 mol) was dissolved in anhydrous dimethylformamide (100 mL), and silver carbonate (7.45 g; 0.0272 mol) and allyl bromide (3.63 g; 0.03 mol) were added. The flask was stoppered and the mixture stirred with a magnetic stirrer for one day and then allowed to stand overnight. The precipitate was filtered off and the filtrate diluted with water (300 mL). The precipitate obtained thereupon was filtered off, washed with water and dried (4.6 g; 61.6%), m.p. 68—69 °C (from ethanol).

$C_{19}H_{17}NO$. Calcd. C 82.88; H 6.22; N 5.09. Found C 83.10; H 6.43; N 5.31%.

IR: see Table IV.

UV: see Table III.

NMR ($CDCl_3$): ArMe 2.47 s (3H), OCH_2 and $=CH_2$ 5.0—5.5 m (4H), $=CH$ 6.15 m (1H), ArH 7.1—7.75 m (7H), 7.88 d (1H), $J_0 = 8$ Hz, 8.00 d (1), $J_0 = 8$ Hz.

1-Phenyl-3-methanesulfonyloxy-4-methylisoquinoline (19)

Compound **4** (1.17 g; 0.005 mol) was dissolved in tetrahydrofuran (50 mL). Triethylamine (1.52 g; 0.015 mol) was added, with stirring, followed by a solution of methanesulfonyl chloride (0.572 g; 0.005 mol) in tetrahydrofuran (3 mL), and the solution containing a precipitate was stirred at room temperature for 2 h. The addition of triethylamine and methanesulfonyl chloride was repeated twice at 2-hour intervals. The triethylamine hydrochloride which separated was filtered off and the filtrate was evaporated to dryness. The residual oil was rubbed with ethanol, the solid was filtered off and dried to give 1.0 g (64%) of the product, m.p. 146—148 °C (from ethanol).

$C_{17}H_{15}O_3SN$. Calcd. C 65.16; H 4.82; N 4.62; S 10.23. Found C 65.21; H 4.95; N 4.47; S 10.30%.

IR: see Table IV.

UV: see Table III.

4-Benzylidene-6,7-dimethoxy-1-phenyl-1,4-dihydro-3(2*H*)-isoquinolinone (23)

Compound **22** (2.83 g; 0.01 mol) was dissolved in dry benzene (500 mL), and an oil dispersion of NaH (0.53 g; 0.011 mol) was added, under a stream of N_2. After stirring for 15 min, benzaldehyde (1.06 g; 0.01 mol) was added by drops, then the reaction mixture was stirred at 60 °C for 2 h. After cooling, it was washed with 2*N* HCl then with water, the benzene phase was separated, dried over Na_2SO_4 and evaporated to dryness. The residue was purified on a column packed with Al_2O_3 to give 0.7 g (18.9%) of the product, m.p. 196—198 °C.

$C_{24}H_{21}NO_3$ Calcd. C 77.61; H 5.70; N 3.77. Found C 77.31; H 5.87; N 3.75%.

IR (KBr): νC=O 1670, νC=C 1620 cm^{-1}.

UV (95% ethanol): λ_{max} (ε): 293 nm (1613), 334 nm (3684).

^{1}H-NMR ($CDCl_3$): MeO 3.42 s (3H), 3.81 s (3H), CHNH 5.57 d (1H, J_{CHNH} = 3 Hz), 7.13 d (1H), ArH 6.48 s (1H), 6.79 s (1H), 7.2—7.5 m (10H), =CH 7.77 s (1H).

*

The authors' thanks are due to Dr. G. Tóth for recording the NMR spectra, to Miss É. Draskóczy for technical assistance, and to the analytical group headed by Miss M. Fodor, for the elementary analyses.

REFERENCES

[1] Elguero, J., Martin, C., Katritzky, A. R., Linda, P.: Advances in Heterocyclic Chemistry, Suppl. 1; in: Tautomerism of Heterocycles, p. 99. (Eds. Katritzky, A. R. and Boulton, A. J.) New York, San Francisco, London 1976
[2] Katritzky, A. R., Lagowsky, J. M.: in: Advances in Heterocyclic Chemistry, Vol. **1**, p. 352. (Ed. Katritzky, A. R.) New York, London 1963
[3] Gensler, W. J.: in: Heterocyclic Chemistry, Vol. **4**, p. 441. (Ed. Elderfield, R. C.) Wiley, New York 1952
[4] Boyer, J. H., Wolford, R. T.: J. Org. Chem., **21,** 1297 (1956)
[5] Baumgarten, H. E., Murdock, W. F., Dirks, L. E.: J. Org. Chem., **26,** 803 (1961)
[6] Evans, D. A., Smith, G. F., Wahid, M. A.: J. Chem. Soc. (B), **1967,** 590
[7] McCorkindale, N. J., McCulloch, A. W.: Tetrahedron, **27,** 4653 (1971)
[8] Bodor, N., Dewar, M. J. S., Horget, A. J.: J. Am. Chem. Soc., **92,** 2929 (1970)
[9] Jones, D. W.: J. Chem. Soc. (C), **1969,** 1729
[10] Simchen, G.: Angew. Chem., **80,** 484 (1968)
[11] Ammon, H. L., Wheeler, G. L.: Acta Crystallogr., Sect. B., **30,** 1146 (1974)
[12] Deák, Gy., Hazai, L.: Acta Chim. (Budapest), **79,** 113 (1973)
[13] Deák, Gy., Hazai, L., Tóth, G.: J. Heterocycl. Chem., **14,** 583 (1977)
[14] Hazai, L., Deák, Gy., Szabó, G., Koltai, E.: Acta Chim. Acad. Sci. Hung., **102,** 305 (1979)
[15] Hazai, L., Deák, Gy., Tóth, G., Volford, J., Tamás, J.: J. Heterocycl. Chem., **19,** 49 (1982)
[16] Jones, D. W., Wife, R. L.: J. Chem. Soc., Perkin Trans. 1, **1972,** 2722
[17] Win, H., Tieckelmann, H.: J. Org. Chem., **32,** 59 (1967)
[18] Opitz, G., Schweinsberg, F.: Angew. Chem., **77,** 811 (1965)
[19] Csűrös, Z., Deák, Gy., Hoffmann, I., Török-Kalmár, A.: Acta Chim. Acad. Sci. Hung., **60,** 177 (1969)

BOOK REVIEWS

Host Guest Complex Chemistry, Vol. I. Editor: F. Vögtle, In: *Topics in Current Chemistry, Vol. 98.* 197 pp. with 80 Figures and 25 Tables. Springer Verlag, Berlin, Heidelberg, New York, 1981

Host Guest Complex Chemistry, Vol. II. Editor: F. Vögtle, In: *Topics in Current Chemistry, Vol. 101.* 203 pp. with 140 Figures and 40 Tables. Springer Verlag, Berlin, Heidelberg, New York, 1982

The practical and scientific interest in coronands, cryptands and podands as complexing agents for cations and neutral molecules is steadily increasing. Only in 1980 about 250 original papers dealing with crown chemistry appeared. There are numerous possibilities for the application of coronands in chemical syntheses, in analytical chemistry, in the use of the ion discriminating properties of crown compounds in ion-selective membrane electrodes, etc. Complex formation with crown compounds may transform a small alkali metal or alkaline earth metal ion into a voluminous organic cation, which, in principle, is highly soluble in organic media. The consequences of this transformation may be used for many different purposes. Some of these possibilities are the utilization of the ion-pairing and ion-aggregation effects. the change of the nucleophilicity-basicity balance, the modification of the reaction mechanism and the stereochemistry of the reactions, to mention just a few complexation with crown compounds can serve as a useful tool in stereoselective synthesis similarly.

Crown-type compounds are of general relevance as synthetic model substances for the study of physiological ion-transport processes in biological membranes. or for the investigation of receptor and enzyme interactions, and metabolic processes in the living organism. Pharmacological application in the form of pharmaceutical crown-type compounds is also very important. There are also some hints that the chemistry of macrocyclic ligands may solve some of the problems of energy storage.

Accordingly, the steadily rising research interest in this field is not surprising. Therefore, the edition of such a two-volume survey on the most important topics of this growing area is very appropriate.

The Editor of these volumes, F. Vögtle, gives an introductory review of this topic in order to push the reader into the field, and to soften the interfaces between the different chapters written by different specialists. In this introduction, entitled "Crown-Type Compounds—An Introductory Overview" (pp. 1—41), the Editor gives a general overview of the topic, e.g. he presents the classification, synthesis, porperties and applications of the crown-type ligands: crown ethers, other coronands, cryptands, podands (i.e. open-chain crown compounds and cryptands, octopus molecules), podandocoronands, macrocyclic oligoketones and spherands. The literature on this topic is so rich that, owing to lack of space, only reviews are quoted preferentially. These references are also further specified as: Comprehensive presentation; Fundamentals and general reviews; Reviews. In the lack of a review, several original papers are also quoted. Only in this chapter some 70 review articles are listed, and the additional literature might well involve twice this number.

The further chapters of Vol. I are as follows: "Concept, Structure, and Binding in Complexation" (pp. 43—106), by D. J. Cram and K. N. Truebold. This review is concerned with the applications of the different techniques of organic chemistry and crystallography to the study of the structure of complexes.

The chapter "Complexation of Uncharged Molecules and Anions by Crown-Type Host Molecules" (pp. 107—161), by F. Vögtle, H. Sieger, W. M. Müller, discusses the possibilities of the formation of neutral molecular complexes of coronands, cryptands, catapinands and pondands (open-chain crown-type compounds). This chapter has 130 main references, but ref. 1, for example, consists of references 1a—1m, and in ref. 5 over 30 papers and book chapters are included. Table 11 of this chapter contains data on the very interesting γ-cyclodextrin supercomplexes, in which the cation is enclosed by the crown ether and the latter is again encapsulated by γ-cyclodextrin — so that a "doll in a doll in a doll" system is obtained.

The last chapter of this volume is a review of the "Analytical Applications of Crown Compounds and Cryptands", by E. Blasins and K.-P. Janzen (pp. 163—190). This chapter contains 21 Tables and 99 references.

Volume II contains four reviews and a one-page "Closing Remarks" by the Editor. In the first review, "Structural Chemistry of Natural and Synthetic Ionophores and their Complexes with Cations", R. Hilgenfeld and W. Saenger (pp. 1—82) gives survey on the "prime" ionophores, the depsipeptides, on macrotetrolides and on polyether antibiotics. Then follows a subchapter dealing with synthetic macrocyclic multidentates. Subsequently, part the cryptands and the open-chain polyethers are discussed. 346 references, among them "unpublished results" and "private communications", are given. In this chapter the transport activity of ionophores is discussed, with emphasis on the effects of the membrane microenvironment on the transport mechanism. This part is extremely important from a biological point of view.

This can also be said about the following chapter, dealing with "Bioorganic Modelling, Stereoselective Reactions with Chiral Neutral Ligand Complexes as Model Systems for Enzyme Catalysis", by M. R. Kellog (pp. 111—145). Some of the headings are "Enantioselective Reactions", "Cyclodextrins" and "Peptides", which topics are only shortly treated. In the following part, having the title: "Catalytically Active Synthetic Macrocycles", among others, "Cyclic Hydrocarbon Systems that Imitate Proteases", "Macrocycles with Hydrogenase Activity" and "Macrocycles of Catalyzing Other Bond-Forming or Bond-Breaking Reactions" are topics discussed in detail and in a very comprehensive manner. The fine introduction begins with a 7-line citation from the inaugural address held by Leopold Rizicka as a newly appointed professor in 1926 — and later another reference dating from 1882 (Hantzsch, A.) is given. Numerous of the papers cited (93 references) are quite recent works: many of them were published in 1980.

The last review, "Phase-Transfer Catalyzed Reactions", by F. Montanari, D. Landini and F. Rolla (pp. 147—200), shows the most well-known applications of the crown compounds. This begins a detailed theoretical treatment with the title "General Principles and Mechanisms", and in the further parts "Ion Pair Extraction", "Solid-Liquid and Solid-Gas Phase-Transfer Catalysis", "Other PTC Catalysts" are reviewed. An interesting chapter deals with "Phase-Transfer in the Presence of Catalysts Bonded to a Polymeric Matrix" — a fairly new methodology with great future possibilities. Last, in the part "Appli cation of Phase-Transfer Catalysis" the different chemical reactions, such as displacement reactions, alkylations, eliminations, oxidations, reductions, etc. are reviewed. A fascinating application in "Asymmetric Syntheses" closes this review.

This is a very well-edited, comprehensive, up-to-date work. The Figures and formulae are as clear-cut as possible. The references given, in spite of the hints of the Editor in the Foreword, are very comprehensive, and the whole work must be regarded as that.

In conclusion, this excellent two-volume work, dealing with a new branch of current and future chemistry, reviewing a research field with so many recent and potential future possibilities ranging from new synthetic methods to enzyme model reactions, membrane research, theoretical and physical-organic chemistry, is a must for almost all researchers in different branches of chemistry, such as analytical, organic, bioorganic, pharmaceutical and others — just to mention several.

G. BERNÁTH

Institute of Pharmaceutical Chemistry,
University Medical School, Szeged

Elementary Organic Stereochemistry and Conformational Analysis

B. A. Marples. Monographs for Teachers. Number 34. The Royal Society of Chemistry. London, 1981. III and 82 pp.

This small book is an important contribution in the series of Monographs for Teachers, which was launched in 1959 by the Royal Institute of chemistry. The basic concepts of stereochemistry and conformational analysis are discussed in the following 4 Chapters: *1.* Introduction: Basic Stereochemical Concepts; *2.* Conformation; *3.* Physical Methods of Conformational Analysis; *4.* Conformation and Reactivity in Cyclic Systems; *5.* Conformation and Reactivity in Acyclic Systems.

The whole content is well balanced. The discussion is clear and concise, and the more modern concepts and new aspects of stereochemistry and conformational analysis are treated. The Figures (34) and the formulae (276) are clear-cut.

Several original literature data are given as foot notes. On p. 82, under the title "Suggestions for further Reading", the titles of 11 books on stereochemistry and conformational analysis (all in English), are given, though without any comments or explanation. Perhaps it would have been useful to mention which are elementary texts and which are designed for more advanced students, or to divide the listed books into groups accordings to their topics, but the present list does not appear to follow an alphabetical, a chronological, or any other system. Within the suggested literature, two volumes with no stereochemical or conformational analysis main topics are found with the title "Alicyclic Chemistry", dating from 1963 and 1972, while the two-volume work of Armarego, "Stereochemistry of Heterocyclic Compounds" (Wiley Interscience, 1977), and the most comprehensive many-volume series reviewing the recent stereochemical and conformational analysis research, "Topics in Stereochemistry", edited by N. L. Allinger and E. L. Eliel, are omitted.

Despite the moderate size of 82 pages, this small booklet contains the main up-to-date aspects of elementary organic stereochemistry and conformational analysis, and its purchase for chemistry major students can be warmly recommended. It is also useful for chemists not dealing with directly with stereochemistry and conformational analysis, to refresh and bring up-to-date their knowledge in these topics.

G. BERNÁTH

Institute of Pharmaceutical Chemistry,
University Medical School, Szeged

Heterocyclic Chemistry, Vol. 2
Specialist Periodical Reports. A review of the literature abstracted between July 1979 and June 1980

Senior Reporters: H. Suschitzky and O. Meth-Cohn. The Royal Society of Chemistry, Burlington House, London, 1981. XX and 441 pp.

Volume *2* of "Heterocyclic Chemistry" covers material abstracted from Volumes 91 and 92 of Chemical Abstracts, i.e. papers published in 1978–1979–1980. Mainly the material from 1979 dominates, though several papers which appeared in leading journal such as Tetrahedron and Tetrahedron Letters in 1978 (see: p. 39, 41, 152, 160, 291) are included, and the published material from 1980 is also considerable.

As mentioned in the Introduction, the source work of the compilation was Chemical Abstracts, so that books, conference abstracts and other, not always easily accessible materials are also included. In the latter cases the Chemical Abstracts references are also given, though in several cases exceptions can be found. e.g. in the citation of "Kokagaku Toronkai Koen Yoshishu" (p. 53). Schriftenr. Bundesapothekerkammer Wiss., Fortbild., Gelde Reiche (p. 283) or Sb. Vys. Sk. Chem.-Technol. Praze, Org., Chem. Technol. (p. 283) the Chemical Abstracts sources are missing. In several cases the citation of books or book chapters is not as usualy accepted. For instance, on p. 283 citation 7 is as follows: "G. Litkei: Recent Dev. Chem. Nat. Carbon Compd., 1979, *9*, 293" — from which it does not turn out that this review appeared in a volume of series of monographs, who the editors are, and what the publishing house is.

The arrangement of the chapters is the same as in Volume *1*. A very detailed "Contents" (pp. VII–XX) facilitates the searching. The main chapters are in the following logical arrangement.

Chapter *1*: "Three-membrered ring systems" (by T. J. Mason); In 9 subchapters the oxirans, oxirens, aziridines, azirines, thiirans, thiirens, diaziridines, diazirines and oxaziridines are discussed, on pp. 1–50.

Chapter *2* (pp. 51–72) deals with the "Four-membered ring systems" (by R. C. Storr). This includes the following topics: Systems containing one nitrogen atom; Systems containing two nitrogen atoms or one nitrogen and a second heteroatom; Systems containing one oxygen atom; Systems containing sulphur; Miscellaneous four-membered rings.

Chapters *3* deals with the "Five-membered ring systems" and is divided into three main parts. Part I: "Thiophens and their selenium and tellurium analogues (by S. Gronowitz)

on pp. 73—103 consists of 7 subchapters. Part II: "Systems containing nitrogen and sulphur, selenium or tellurium" (by P. A. Lowe) on pp. 104—144 is divided into 18 subchapters. Part III, dealing with "Other five-membered ring systems" (by G. C. Boyd), consists of 12 logically arranged subchapters.

Chapter *4* deals with the "Six-membered ring systems" and is divided into 2 parts. Part I (pp. 223—282) in 9 subchapters deals with "Systems containing nitrogen" (by S. D. Carter and G. W. H. Cheeseman). The topic of Part II is: "Other six-membered ring systems" (pp. 283—330). compiled by G. P. Ellis. This part is divided into 12 subchapters.

In Chapter *5* (pp. 331—358) the "Seven-membered ring systems" are reviewed by J. T. Sharp. This chapter consists of 7 subchapters, the main one of these being subchapter 3, dealing with "Azepines and diazepines" (pp. 331—345).

The topic of the relative short Chapter *6* is the "Eight-membered and larger ring systems" (by G. M. Brooke). This chapter contains altogether 21 pages (pp. 359—380), from which subchapter 1 discusses "Eight-membered rings" on one page, and subchapter 2 "Nine- and ten-membered heterocycles" (two pages), while the remaining part 3 "Macrocycles" also deals with a topic which is in the front line of recent chemical research: "Crown ethers and related compounds". This latter title on p. 367 has no numbering, and the considerable material on pp. 367—380 which deals with this topic, is also divided into several subchapters: "Effects of crown ethers on chemical reactions" (pp. 368—371). "Reactions of the macrocyclic ring of crown ethers and related compounds" (pp. 371—372), and "Formation of host-guest complexes" (pp. 372—379).

Chapter *7* reviews the "Bridged systems" (by J. M. Mellor) in 7 subchapters on pp. 381—410. This is to some extent form-breaking as compared with the earlier chapters, because after the usual title "Introduction" and "Reviews" — which are missing in Chapters 1 and 6 — the title of subchapter 3 is "Physical methods" and this (on pp. 382—386) deals with "X-Ray and neutron diffraction", "Photoelectron spectroscopy and related electrochemical studies", "Nuclear magnetic resonance spectroscopy" and "Miscellaneous methods". In the previous chapters these physical investigations are not discussed separately.

It is a good general practice in this volume that heterocycles which, due to their hetero-atom, origin or basic skeleton, are also included in other volumes of Specialist Periodical Reports, are also mentioned in the appropriate place here. For instance, "Five-membered ring systems containing nitrogen and sulphur, selenium or tellurium", which are discussed in detail in the volumes "Organic Compounds of Sulphur, Selenium and Tellurium" of the Specialist Periodical Reports series, are also mentioned here (see e.g. p. 105, and other places).

The formulae are clear-cut and almost without mistakes. A complete author index on not less than 30 pages, listing some 5500 author names, is very useful. Unfortunatelly, in the writing of the Hungarian names numerous mistakes are found; some letters are not always used: e.g. "Sumegi" is written instead of "Sümegi", though in other names, e.g. "Süss, or "Lüdersdorf", "ü" is used. Instead of "Szabó", in five authors' names "Szabo", is written. "Meszaros" and "Gal" are written instead of "Mészáros" and "Gál", "Nogradi" instead of "Nógrádi", "Lempert-Streter" instead of "Lempert-Stréter", "Neszmelyi" instead of "Neszmélyi" etc. This is to be mentioned, because other names with the same letters "á" or "é" are correctly written, e.g. "Poláková, Procházka, Perjéssy", etc., while in other names fairly rare letters such as "ł" in "Przyłcki", "š" and "ć" in "Šunjić" and "č" in "Vončina" are used. The well-known name "R. Bognár" is written twice as "R. Bognor" (pp. 105 and 143).

As the Senior Reporter mentions in the "Introduction": "For reasons of economy, our contributors had to keep their reviews within a strictly defined number of pages and were, therefore, obliged to select only the more significat advances in the field. We hope readers will agree that comprehensibility has in no way suffered."

To select the most important advances from such a vast material as that of heterocyclic chemistry is not an easy task. What is important, or perhaps more important, the choice of the real highlights depends to a considerable extent on the interests of the reviewer. This is why it is not easy to make comments in this respect. Let me mention only one topic. Under the title "Fused systems containing two six-membered rings (6,6)" follows barely two and half pages (pp. 270—273), and from this pyrido-pyrimidines are dealt with only in several lines with 3 references and 3 schemes — altogether on half a page. A comparison: a review by I. Hermecz and Z. Mészáros with the title "Chemistry of pyrido[1,2-*a*]-pyrimidines" appeared in "Advances in Heterocyclic Chemistry", Vol. *33*, in 1983. This 90-page review included 492 references, at least 10 per cent of which were published in the period reviewed in "Heterocyclic Chemistry, Vol. *2*."

G. BERNÁTH

Institute of Pharmaceutical Chemistry
University Medical School, Szeged

General and Synthetic Methods, Vol. 5
Specialist Periodical Reports. A review of the literature published during 1980

Senior Reporter: G. Pattenden. The Royal Society of Chemistry, Burlington House, London, 1982. XIII and 439 pp.

The main part of the volume, the first five chapters, cover the possible interconversions between the functional groups. The following four chapters are written from a different point of view than that in the earlier ones. An inportant part of this Report, Chapter 6, reviewing "Organometallics in Synthesis" (pp. 208—256), is divided into two parts. Part I treats the "Transition Elements" (by S. V. Ley and R. A. Porter), while Part II deals with the "Main Group Elements" (by P. F. Gordon and A. J. Nelson).

Chapter 7 deals with "Saturated Carbocyclic Ring Synthesis" (by A. J. Barker, K. Copper and G. Pattenden) (pp. 257—287). Three-membered rings; Four membered rings; Five-membered rings; Six-membered rings; Polyene cyclization and polycyclic synthesis; Seven-membered rings; Medium and large rings; and Spiro-ring annulation are the main headings. Under each title the general methods are discussed, but the main classes of the natural compounds are also separately treated. For instance, among the five-membered rings Prostaglandins and related natural compounds, and among the six-membered ring systems Anthracyclines are discussed separately in subchapters. A considerable part of the subchapter dealing with six-membered rings reviews the Diels-Alder reaction. This and the following two chapters of this Report are very interesting, instructive and useful for all organic chemists dealing with synthesis.

Chapter *8*, "Saturated Heterocyclic Ring Synthesis" (by R. C. Brown and A. H. Ingall) (pp. 288—386), is the longest chapter of this Report — covering nearly a quarter of the whole book. This is also very well compiled, and is instructive for the reader.

The title of Chapter *9* is "Strategy and Design in Synthesis" (by A. P. Johnson) (pp. 387—413). This reviews several types of "Syntheses dominated by a single strategy". A very fascinating subchapter discusses several selected syntheses, which can be considered the highlights of the 1980 literature, such as the synthesis of antibiotic monensin by Still and his collaborators. The synthesis of rifamycin S by the Kishi group is also treated. These appear under the heading: "The stereochemistry is the problem", while under the title "The skeleton is the problem", the syntheses of gibberellins, and (±)-quadrone are discussed, among others. A subchapter deals with computers in synthetic planning.

The last part of this Report, with the title "Reviews on General Synthetic Methods" has no chapter number. This part of this Report, compiled by K. Cooper and G. Pattenden, gives on pp. 414—418 a list of the reviews and books which appeared in 1980 on synthetic aspects of 1. Olefins; 2. Ethers; 3. Peptides; 4. Nitrogen-containing functional groups; 5. Organometallics (divided into parts: general; silicon, phosphorus and sulphur; transition elements); 6. Ring synthesis; 7. Heterocycles; 8. Photochemistry; 9. Stereochemistry; 10. General; 11. Miscellaneous. This compilation, listing some 90 titles, is very useful. However, the question arises of why such titles as Alcohols; Aldehydes and ketones; Carboxylic acid derivatives; Macrocyclic "Crown" polyethers and related compounds are missing. Especially on the latter topic, numerous reviews appeared in this period.

On pp. 419—439 an author index with some 3600 names can be found.

The literature cited in this volume was published almost exclusively in 1980. As regards t he literature sources, though some differences can be found in the chapters, one points must be mentioned. Some chapters are compiled mostly or even exclusively from primary literature sources, not using the seconday abstract services, and therefore several chapters show the language boundaries of the reviewers. For example, in Chapter *1* "Saturated Hydrocarbons" (by J. M. Clough) 255 references are given, mentioning altogether 258 papers. Merely 18 journals are cited, and only the top 10 with more than 3 papers. From the merely 8 remaining reviewed journals, altogether 19 papers are referred to. In the reviewed journals the English language predominates; very little German, and no French or Russian literature is given. The reviewed journals with the numbers of mentioned papers are as follows: Tetrahedron Letters 88; J. Org. Chem. 44; J. Chem. Soc. Chem. Commun. 29; J. Am. Chem. Soc. 20; Synthesis 20; Chem. Ber. 10; Synth. Commun. 9; Angew. Chem. Int. Ed. Engl. 8; Chem. Lett. 5; Tetrahedron 3; J. Chem. Soc. Perkin Trans. I 3; Can. J. Chem. 3; Bull. Chem. Soc. Japan 3; J. Organomet. Chem. 2; Recl. Trav. Chim. Pays-Bas 2; Liebigs Ann. Chem. 2; Org. Prep. Proces. Int. 1.

Another point of this list which must be mentioned is that over 50 per cent of the

papers cited (i.e. 130 papers) were published in 4 journals containing short, preliminary publications, usually without full experimental details.

As regards the reviewed journals in respect of Chapter *2*. "Aldehydes and Ketones" (by S. C. Eyley) (pp. 59—99), the situation is very similar. Here even Helv. Chim. Acta, Can. J. Chem., Recl. Trav. Chim. Pays-Bas and Org. Prep. Proced. Int. are missing from the former list, and only one further journal (Alrichimica Acta) with one reference is mentioned.

The sources of the cited literature are somewhat, but not considerably wider in Chapters 3 and 4. The remainder of this volume can be considered more comprehensive.

It is rather strange and hardly acceptable that in a book which has the task of reviewing the developments in a one-year period on such wide topics as general and synthetic methods of "Saturated and Unsaturated Hydrocarbons", "Aldehydes and Ketones" in two chapters on 99 pages with nearly 500 references, the source of the cited papers are restricted to 18 and 15 journals, respectively, and in these two reviews the citation of such established journals as Bull. Soc. Chim. France, Acta Chim. Scand., J. prakt. Chem., Monatshefte, Coll. Czechoslov. Chem. Commun., Acta Chim. Hung., Accounts Chem. Res., Austr. J. Chem., just a few to mention, the complete Russian language literature, and some more specialized journals are missing.

I am convinced that the comprehensiveness of a review using purely several top journals and compiled without the help of secondary sources must definitely be questionable.

Apart from the above, the volume is well edited. The vast material is arranged in an easy-to-treat manner. For the reviewer especially Chapters *7—9* were fascinating.

Not regarding the shortcomings in the literature coverage, the purchase of this volume can be recommended for synthetic chemists.

G. BERNÁTH

Institute of Pharmaceutical Chemistry,
University Medical School, Szeged

Organic Compounds of Sulphur, Selenium, and Tellurium, Vol. 6 Specialist Periodical Reports. A Review of the literature published between April 1978 and March 1980

Senior Reporter: D. R. Hogg. The Royal Society of Chemistry, Burlington House, London, 1981. XVIII and 313 pp.

This volume, 6th in the Series, has changed considerably as compared with Volume **5**. According to the Preface, the major changes in the format and contents of this volume were necessitated by economic considerations. Sulphur-containing heteroaromatic compounds, which in previous years were included in these Reports, are now covered in detail only in the new Reports "Heterocyclic Chemistry". However, the highlights of the literature on heteroaromatic compounds of sulphur, selenium, and tellurium are also discussed in Chapter *6* in this volume.

On pages VII—XVI a detailed "Contents" facilitates the search for the subject. Then follows a list of "Abbreviations". Chapters *1—5* are essentially organized as in the former volumes of this series.

Chapter *1*, "Aliphatic Organosulphur Compounds, Compounds with Exocyclic Sulphur Functional Groups, and their Selenium and Tellurium Analogues", by G. C. Barrett, consists of 20 subchapters. This 78-page review is in many respects, among them the amount of the cited literature, the richest chapter of the book. This chapter is very well divided according to the different topics and gives a very wide-ranging literature survey. 924 references are numbered, but under many numbers there are numerous citations, e.g. in ref. 1 (a)—(i), or in ref. 2 (a)—(w) citations can also be found. Furthermore, in almost all subchapters, a rich unnumbered "Additional bibliography" is given to the subject discussed — which is very instructive and useful. Thus, in Chapter *1* about 2000 references from the reviewed period are given. In this respect it is almost without example in comparison with other Reports of such size. The discussion in this part is also of a very high level. The mechanisms of several reactions are discussed in detail. The reading of this part is not only very useful for sulphur chemists: all synthetic chemists can obtain new ideas from it.

Chapter *2*. "Ylides of Sulphur, Selenium, and Tellurium, and Related Structures" (pp. 79—147), is divided into three parts. Part I deals with "Ylides and Carbanionic Compounds

of Sulphur", by E. Block. This (pp. 79—111) and the following Part II, "Ylides and Carbanionic Compounds of Selenium and Tellurium" (by D. L. J. Clive, pp. 112—125) are somewhat more detailed than those in the previous volume. In Part I 375 papers are reviewed, and a substantial majority of these deal with the anionic and ylidic sulphur reagents, which are extremely useful in modern organic synthetic practice. In subchapter II a Table is found giving a survey of the conditions under which the compounds ArSeCH(R)X have been deprotonated to produce carbanions. In this Table, 16 references are given. Part III of Chapter *2* deals with "Compounds with S=N Functional Groups", by S. Oae and N. Furukawa. These authors are the most frequently cited authors of the whole volume, e.g. the name of Oae is mentioned one or more times on 16 different pages of Chapter *1*, and many times too in the following parts of the book. Numerous papers of Furukawa are also cited. The topic of Chapter *3*, Part II, is "Compounds of S=N Functional Group". This subject is interesting from both Theoretical and practical (biological) points of view. S=N is not always a typical double bond. Sulphur nitrides $(SN)_x$ have recently been thoroughly investigated with regard to their physical properties, such as superconductivity.

Chapter *3*, "Thiocarbonyl and Selenocarbonyl Compounds", consists of two shorter and one longer Parts. Part I, "Thioaldehydes, Thioketones, and their Selenium Analogues", by A. Ohno (pp. 148—160), begins with the sentence: "No important review has been published in the past two years". Part II (pp. 160—165), by D. R. Hogg, reviews "Sulphines and Sulphenes". Part III of this chapter, "Thioureas, Thiosemicarbazides, Thioamides, Thiono- and Dithio-carboxylic Acids" (pp. 165—206), by J. K. Landquist, is a very comprehensive review, giving a good selection of the different synthetic applications of these widely-used types of compounds.

Chapter 4, "Small-ring Compounds of Sulphur and Selenium" (pp. 207—223), by C. G. Venier, in 14 subchapters shows the intensive work carried out in this field. Numerous interesting new ring systems are listed in subchapters 10—13, containing not only sulphur, but also nitrogen, phosphorus, silicon, germanium or boron. This part contains 262 references, one of them (p. 231) published in 1975, though the Chem. Abstr. reference appeared in 1978. Subchapter 14 is a list of further bibliography, with short explanations.

Chapter *5*, "Saturated Cyclic Compounds of Sulphur, Selenium, and Tellurium", by P. K. Claus (pp. 233—270), is a good survey of this field, often providing a valuable discussion, and not only mentioning, but also evaluating some of the more important results. Chapter 5 is therefore an important survey, though the synthesis of saturated heterocycles has also been summarised in "General and Synthetic Methods" Vol. *1* of "Specialist Periodical Reports". About 450 papers are reviewed (under 309 reference numbers) which were published in the period 1977—1980, numerous of them in 1977.

Chapter *6*, "Heteroaromatic Compounds of Sulphur, Selenium, and Tellurium" (pp. 271—301) by M. Davis. The organization of this chapter differs considerably from that followed in Volume *5*, because of the appearance of the new Report "Heterocyclic Chemistry" and therefore the Reporter has tried the review the topic from the standpoint of sulphur chemistry rather than of heterocyclic chemistry. This aim was followed with success. The highlights are discussed. The 11 subchapters are further divided with many titles, so that this chapter is very easy to handle. One such title: "The First S^{II}—N Bond in a Natural Product" 98 mg of dendrodoin, a 1,2,4-thiadiazole derivative, was isolated from 2.2 tonnes of a marine tunicate, *Dendrodoa grossularia* (Styelidae). As far as the Reporter is aware, this is the first natural product containing a sulphur(II)-nitrogen bond.

On pages 303—331 an author index can be found listing some 4000 names.

As mentioned in Chapter *5*, for instance the literature search has been assisted by computer, through the Lockheed search system. It therefore looks a litle strange that the Senior Reporter for this volume states in the Preface that "these Reports cover the period April 1978 to March 1980 inclusive, except in the case of Chapter *2* Part III, where the period ends in February 1980". Volumes treating other topics of the "Specialist Periodical Reports", e.g. "General and Synthetic Methods", give a survey of a one-year period, e.g. under the title of Volume 5 of this latter Report stands: "A Review of the Literature Published during 1980", The question arises of whether it would possibly have been better to review the literature published during one or two calendar years.

The chemistry of sulphur and selenium compounds is of growing importance. With the application of anionic and ylidic sulphur reagents, C—C bond formation in ring-closure, ring-contraction or ring-expansion can be achieved, and there are methods for C=C and C≡C bond formation under mild conditions.

On the whole, this volume follows the high standards of the previous ones. Though this Report is intended primarily for chemists dealing with organic compounds of sulphur selenium, and tellurium, it will be doubtless also be of value to a wider readership.

As sulphur compounds in organic syntheses have gained in importance in the recent period, permitting precise control over product stereochemistry and regioselectivity, the purchase of this very comprehensive volume may be warmly recommended to all synthetic chemists.

G. BERNÁTH

Institute of Pharmaceutical Chemistry,
University Medical School, Szeged

INTERNATIONAL CONFERENCE ON THERMAL ANALYSIS

The 8th International Conference on Thermal Analysis will take place in August 19—23, 1985, in *Bratislava, Czechoslovakia.*

After *Aberdeen* (Scotland), *Worcester* (U.S.A.), *Davos* (Switzerland), *Budapest* (Hungary), *Tokyo* (Japan), *Bayreuth* (F.R.G.) and *Kingston* (Canada) the Council of the International Confederation on thermal analysis accepted the invitation from Czechoslovakia to organize the 8th ICTA in Bratislava, Czechoslovakia.

The International Conference on Thermal Analysis, with its **twenty years tradition** offers the platform to report and learn about recent progress in the field of thermal analysis and its applications to material scientists and engineers, to solid-state physicists, physico-chemists, metallurgists, ceramists, mineralogists as well as chemists working in various field of organic, macromolecular chemistry and technology, biology and related sciences.

Papers in the following subject areas will be particularly welcomed:

— Improved instrumentation for thermal analysis and calorimetry
— Advances in theory of thermal analysis including kinetics and calorimetry
— Thermal analysis in inorganic chemistry, ceramics, metallurgy and earth sciences
— Thermal analysis in organic chemistry, biology, pharmacy and medicine
— Thermal analysis in polymer sciences, including investigations of glasses in general
— Thermophysical research, applied science, environmental and industrial applications

Workshops (round-table discussions) are planned on:

1. Thermal characterization of non-stoichiometric oxides and other compounds and their application for energy storage and conversion
2. Current problems of reliability of kinetic data evaluated by thermal analysis

3. The use of computers in everyday thermoanalytical practice and the databank in thermal analysis
4. Theory and practice of less-common thermoanalytical techniques (e.g. emanation thermal analysis, thermosonimetry etc.)

The **avard lectures** (DuPont-ICTA, Netzsch-GEFTA, etc.) and other **plenary lectures** are anticipated.

The conference language will be English. A prevailing majority of papers will be presented as *posters*, which will be of special advantage to those of participants who may have some difficulties in spoken English. All papers will be published in the shortened form in the Proceedings of the Conference. An abstract in English of 10—20 lines and the preliminary registration are expected by 30 JUNE 1984.

Further information and the registration form can be obtained from the Organizing Committee of the ICTA '85.

c/o Slovak Technical University
812 43 Bratislava, Czechoslovakia

V. Balek

vice-chairman of the Organizing Committee

ACTA BIOCHIMICA ET BIOPHYSICA

ACADEMIAE SCIENTIARUM HUNGARICAE

EDITED BY

F. B. STRAUB and J. TIGYI

VOLUME 17 NUMBERS 3–4

CONTENTS

Bot, Gy., Kovács E., Tóth, B., Dombrádi, V., Gergely, P.: Role of fructose-1-phosphate in the regulation of the dephosphorylation of glycogen phosphorylase *a*

Tóth B., Gergely, P.: Role of pyridoxal 5'-phosphate in the regulation of the interconversion of phosphorylase *a* into phosphorylase *a*

Vereb, Gy., Szűcs, K., Bot, Gy.: Immunological and allosteric identity of heart-specific glycogen phosphorylase isoenzymes from various mammals

Édes, I., Dózsa, E., Sohár, I., Guba, F.: Effect of plaster cast immobilization on the turnover rates of soluble proteins and lactate dehydrogenase isoenzymes of rabbit m. soleus

Csillag, A., Kálmán, M., Csató, Zs.: Adenosin-5'-diphosphate penetration into synaptosomes isolated from rat cerebral cortex

Misik, S., Masszi, G.: Microwave method for determining dielectric parameters of living biological objects II. Study of ionic water binding

Koszorus, L., Masszi, G.: Investigation of hydration of macromolecules II. Study of ethyleneglycol and 1—4-dioxane solutions by dielectric method

Vető, F.: Is the difference of vapour pressure the driving force of real osmotic water transport?

Papers in English. Published in one volume (4 issues) annually. Subscription rate per volume: $40.00

AKADÉMIAI KIADÓ

Publishing House of the Hungarian Academy of Sciences

Budapest

Distributed by KULTURA, Hungarian Foreign Trading Co., P.O.B. 149, H-1389 Budapest

ACTA GEODAETICA, GEOPHYSICA ET MONTANISTICA

ACADEMIAE SCIENTIARUM HUNGARICAE

EDITOR-IN-CHIEF

A. TÁRCZY-HORNOCH

EDITOR

J. VERŐ

VOLUME 17 NUMBER 2

CONTENTS

Ádám, J.—Halmos, F.—Varga, M.: On the concepts of combination of Doppler satellite and terrestrial geodetic networks

Ádám, J.—Tarcsai, Gy.: Doppler location equations for platform localization using satellites

Csernyák, L.—Steiner, F.: Amplifying residual filters

Csernyák, L.—Steiner, F.—Zilahi-Sebes, L.: A short note to prescribed w-properties

Abdelhamid Kamal Hassan: Comparison between results of the gyro-azimuths determined with old and new gyrotheodolites

Kardos, I.—Borza, T.—Vass, T.: Laser ranging observations at the Satellite Geodetic Observatory (SGO)

Krasnobaeva, A. G.—Diakonov, B. P.—Astafiev, P. F.—Batalova, O. V.—Vishnev, V. S.—Gavrilova, I. E.—Zhuravlyova, R. B.—Kirillov, S. K.: Magnetotelluric data on the geoelectric structure in the North-Eastern part of the Baltic Shield

Raspopov, O. M.—Afanasyeva, L. T.: Localization of the Pc5-source and of the auroral oval

Rösler, R.—Lindner, H.: Ableitung von Feldtransformationen für Profile von Potentialfeldanomalien

Немеши, Л.—Богнар, Е.—Лавдансурен—Хорван—Майкут, Т.—Том, Ч.: Комплексная геофизическая разведка в пустыне Гоби.

Gasco, J. C.—Febrer, J. M.—Demicheli, J.—Fournier, H. G.: Zarate MT sounding and upper mantle resistivity

Papers in English, German and Russian. Published in one volume (4 issues) annually.
Subscription rate per volume $40.00

AKADÉMIAI KIADÓ

Publishing House of the Hungarian Academy of Sciences

Budapest

Distributed by KULTURA, Hungarian Foreign Trading Co., P.O.B. 149, H-1389 Budapest

Text

The text of the paper should be concise. The description of new compounds (in the Experimental) must include the complete analytical data. Special attention must be paid to structural formulas given within the text. Complicated (non-linear) formulas should be drawn on separate sheets of paper and their position in the text should be clearly marked. The numbering of formulas and equations (in parentheses on the right-hand side) is only needed if they are referred to in the text. Units should conform to the International System of Units (SI). In nomenclature the rules of the I.U.P.A.C. are accepted as standard. Symbols for physical quantities are printed in italic type and should, therefore, be underlined in the manuscript.

References

References should be numbered in order of appearance in the text (where the reference number appears in brackets) and listed at the end of the paper. The reference list, too, should be typed double-spaced. Journal titles are to be abbreviated as defined by the Chemical Abstracts Service Source Index.

Examples:

[1] Brossi, A., Lindlar, H., Walter, M., Schneider, O.: Helv. Chim. Acta, **41**, 119 (1958)
[2] Parr, R. G.: Quantum Theory of Molecular Electronic Structure. Benjamin, New York 1964
[3] Warshel, A.: in Modern Theoretical Chemistry, Vol. 7, Part A (Ed. G. A. Segal), Plenum Press, New York 1977

Tables

Each table should be given a Roman number and a brief informative title. Structural formulas should not be used in column headings or in the body of tables.

Figures

Figures should be numbered consecutively with Arabic numerals. Their approximate place should be indicated in the text on the margin. All figures must be identified on the back by the author's name and the figure number in pencil. Standard symbols (such as circles, triangles, squares) are to be used on line-drawings to denote the points determined experimentally. Line-drawings must not contain structural formulas and comments. Spectra or relevant segments thereof, chromatograms, and X-ray diffraction patterns will be reproduced only if concise numerical summaries are inadequate to replace them. Drawings and graphs should be prepared in black ink on good-quality white or tracing paper. Photographs should be submitted on glossy paper as high-contrast copies. Xerox or similar copies are not suitable for reproduction, but may be used for duplicate copies.

Redrawn illustrations will be sent to the authors for checking. No corrections of figures will, therefore, be accepted in the proofs.

Submission of manuscript

After having completed the corrections suggested by the referees and editors, the final manuscript should be submitted in duplicate, in a form ready for publication. If the corrected manuscript is not returned to the editors *within six weeks*, the intended publication of the paper will be regarded as withdrawn by the authors.

Page charge will not be assessed for the publication, however, authors, from overseas countries must contribute to the postage of correspondence by sending, together with the manuscript, international postal coupons to the value of U.S. $ 10.—

Proofs and reprints

A set of proofs will be sent to the submitting author. The proofs must be returned within 48 hours of receipt. Late return may cause a delay in the publication of the paper. 100 reprints will be supplied to the authors free of charge.

Periodicals of the Hungarian Academy of Sciences are obtainable at the following addresses:

AUSTRALIA
C.B.D. LIBRARY AND SUBSCRIPTION SERVICE
Box 4886, G.P.O., *Sydney N.S.W. 2001*
COSMOS BOOKSHOP, 145 Ackland Street
St. Kilda (Melbourne), Victoria 3182

AUSTRIA
GLOBUS, Höchstädtplatz 3, *1206 Wien XX*

BELGIUM
OFFICE INTERNATIONAL DE LIBRAIRIE
30 Avenue Marnix, *1050 Bruxelles*
LIBRAIRIE DU MONDE ENTIER
162 rue du Midi, *1000 Bruxelles*

BULGARIA
HEMUS, Bulvar Ruszki 6, *Sofia*

CANADA
PANNONIA BOOKS, P.O. Box 1017
Postal Station "B", *Toronto, Ontario M5T 2T8*

CHINA
CNPICOR, Periodical Department, P.O. Box 50
Peking

CZECHOSLOVAKIA
MAD'ARSKÁ KULTURA, Národní třida 22
115 66 Praha
PNS DOVOZ TISKU, Vinohradská 46, *Praha 2*
PNS DOVOZ TLAČE, *Bratislava 2*

DENMARK
EJNAR MUNKSGAARD, Norregade 6
1165 Copenhagen K

FEDERAL REPUBLIC OF GERMANY
KUNST UND WISSEN ERICH BIEBER
Postfach 46, *7000 Stuttgart 1*

FINLAND
AKATEEMINEN KIRJAKAUPPA, P.O. Box 128
SF-00101 Helsinki 10

FRANCE
DAWSON-FRANCE S. A., B. P. 40, *91121 Palaiseau*
EUROPÉRIODIQUES S. A., 31 Avenue de Versailles, *78170 La Celle St. Cloud*
OFFICE INTERNATIONAL DE DOCUMENTATION ET LIBRAIRIE, 48 rue Gay-Lussac
75240 Paris Cedex 05

GERMAN DEMOCRATIC REPUBLIC
HAUS DER UNGARISCHEN KULTUR
Karl Liebknecht-Straße 9, *DDR-102 Berlin*
DEUTSCHE POST ZEITUNGSVERTRIEBSAMT
Sraße der Pariser Kommüne 3–4, *DDR-104 Berlin*

GREAT BRITAIN
BLACKWELL'S PERIODICALS DIVISION
Hythe Bridge Street, *Oxford OX1 2ET*
BUMPUS, HALDANE AND MAXWELL LTD.
Cowper Works, *Olney, Bucks MK46 4BN*
COLLET'S HOLDINGS LTD., Denington Estate
Wellingborough, Northants NN8 2QT
WM. DAWSON AND SONS LTD., Cannon House
Folkstone, Kent CT19 5EE
H. K. LEWIS AND CO., 136 Gower Street
London WC1E 6BS

GREECE
KOSTARAKIS BROTHERS INTERNATIONAL BOOKSELLERS, 2 Hippokratous Street, *Athens-143*

HOLLAND
MEULENHOFF-BRUNA B.V., Beulingstraat 2,
Amsterdam
MARTINUS NIJHOFF B.V.
Lange Voorhout 9–11, *Den Haag*
SWETS SUBSCRIPTION SERVICE
347b Heereweg, *Lisse*

INDIA
ALLIED PUBLISHING PRIVATE LTD., 13/14
Asaf Ali Road, *New Delhi 110001*
150 B-6 Mount Road, *Madras 600002*
INTERNATIONAL BOOK HOUSE PVT. LTD.
Madame Cama Road, *Bombay 400039*
THE STATE TRADING CORPORATION OF INDIA LTD., Books Import Division, Chandralok
36 Janpath, *New Delhi 110001*

ITALY
INTERSCIENTIA, Via Mazzé 28, *10149 Torino*
LIBRERIA COMMISSIONARIA SANSONI, Via Lamarmora 45, *50121 Firenze*
SANTO VANASIA, Via M. Macchi 58
20124 Milano
D. E. A., Via Lima 28, *00198 Roma*

JAPAN
KINOKUNIYA BOOK-STORE CO. LTD.
17-7 Shinjuku 3 chome, Shinjuku-ku, *Tokyo 160-91*
MARUZEN COMPANY LTD., Book Department,
P.O. Box 5050 Tokyo International, *Tokyo 100-31*
NAUKA LTD. IMPORT DEPARTMENT
2-30-19 Minami Ikebukuro, Toshima-ku, *Tokyo 171*

KOREA
CHULPANMUL, *Phenjan*

NORWAY
TANUM-TIDSKRIFT-SENTRALEN A.S., Karl Johansgatan 41–43, *1000 Oslo*

POLAND
WĘGIERSKI INSTYTUT KULTURY, Marszałkowska 80, *00-517 Warszawa*
CKP I W, ul. Towarowa 28, *00-958 Warszawa*

ROUMANIA
D. E. P., *Bucureşti*
ILEXIM, Calea Grivitei 64–66, *Bucureşti*

SOVIET UNION
SOJUZPECHAT — IMPORT, *Moscow*
and the post offices in each town
MEZHDUNARODNAYA KNIGA, *Moscow G-200*

SPAIN
DIAZ DE SANTOS, Lagasca 95, *Madrid 6*

SWEDEN
ALMQVIST AND WIKSELL, Gamla Brogatan 26
101 20 Stockholm
GUMPERTS UNIVERSITETSBOKHANDEL AB
Box 346, *401 25 Göteborg 1*

SWITZERLAND
KARGER LIBRI AG, Petersgraben 31, *4011 Basel*

USA
EBSCO SUBSCRIPTION SERVICES
P.O. Box 1943, *Birmingham, Alabama 35201*
F. W. FAXON COMPANY, INC.
15 Southwest Park, *Westwood Mass. 02090*
THE MOORE-COTTRELL SUBSCRIPTION AGENCIES, *North Cohocton, N. Y. 14868*
READ-MORE PUBLICATIONS, INC.
140 Cedar Street, *New York, N. Y. 10006*
STECHERT-MACMILLAN, INC.
7250 Westfield Avenue, *Pennsauken N. J. 08110*

YUGOSLAVIA
JUGOSLOVENSKA KNJIGA, Terazije 27, *Beograd*
FORUM, Vojvode Mišića 1, *21000 Novi Sad*

Index: 26.007

Acta Chimica Hungarica

VOLUME 116, NUMBER 4, AUGUST 1984

EDITOR-IN-CHIEF
F. MÁRTA

MANAGING EDITOR
GY. DEÁK

ASSISTANT EDITOR
L. HAZAI

EDITORIAL BOARD
M. T. BECK, R. BOGNÁR, GY. HARDY, K. LEMPERT,
B. LENGYEL, K. POLINSZKY, E. PUNGOR, G. SCHAY,
Z. G. SZABÓ, P. TÉTÉNYI

Akadémiai Kiadó, Budapest
ACTA CHIM. HUNG. ACASA2 116 (4) 323–417 (1984) HU ISSN 0231-3146

ACTA CHIMICA HUNGARICA

A JOURNAL OF THE HUNGARIAN ACADEMY OF SCIENCES

Acta Chimica publishes original reports on all aspects of chemistry in English.

Acta Chimica is published in three volumes per year, each volume consisting of four issues, by

AKADÉMIAI KIADÓ

Publishing House of the Hungarian Academy of Sciences
H-1054 Budapest, Alkotmány u. 21.

Manuscripts and editorial correspondence should be addressed to

Acta Chimica
H-1450 Budapest P.O. Box 67

Subscription information

Orders should be addressed to

KULTURA Foreign Trading Company
H-1389 Budapest P.O. Box 149

or to its representatives abroad

Acta Chimica is indexed in Current Contents

NOTICE TO AUTHORS

Acta Chimica publishes original papers on all aspects of chemistry in English. Before preparing a manuscript for submission to this journal authors are advised to consult recent issues.

Form of manuscript

Manuscripts, tables and illustrations should be submitted in triplicate. Manuscripts should be typewritten double spaced (25 lines, 50 characters per line including spaces). The *title page* should include (1) the title of the paper, (2) the full names of the author(s) in the sequence to be published; apply an asterisk to designate the name of the author to whom correspondence should be addressed, (3) name and address of the institution where the work was done. If the paper is part of a series, reference to the previous communication must be given as a footnote.

Abstract

A summary is printed at the head of each paper. This should not exceed 200 words and should state briefly the principal results and major conclusions of the work. It should be suitable for use by abstracting services.

CONTENTS

PHYSICAL AND INORGANIC CHEMISTRY

Dissociation constants of L-pyrrolidine-2-carboxylic acid at different temperatures, ionic strengths and in different aquoorganic solvents, **R. S. Saxena, A. Gupta** 327

Crystal and molecular structure determination and ESR-study of [*N*-(*n*-butyl)quinolinium]$^{+}$(7,7,8,8-tetracyanoquinodimethane)$_2^{-}$, **Gy. Menczel, J. Kürti, R. Lehőcz** 335

Immobilization of cells by radiation copolymerization of hydrophilic and hydrophobic monomers, **M. Kumakura, I. Kaetsu** 345

Synthesis of (π-fluorenyl) and (π-pyrrolyl)thallium(I) and their group transfer reactions with (π-C_5H_5)$TiCl_3$/(π-C_5H_5)$ZrCl_3$, **A. K. Sharma, N. K. Kaushik** 361

New ideas about the mechanism of action of detergent-dispersant (DD) oil additives, **O. L. Glavaty, A. I. Marchenko, G. G. Kravchook, E. V. Glavaty** 367

Vibrational analysis of the $(UO_2Cl_4)^{2-}$ and $(UO_2Br_4)^{2-}$ ions, **E. M. Nour, A. N. Abd El-Rahman** 377

Influence of the liquid junction potential on hydroxide activity measurements, **B. Lehoczky, L. Barcza** 383

ORGANIC CHEMISTRY

Synthesis of a novel diaza crown and a novel cryptand incorporating a methyl-4,6-*O*-benzylidene-α-D-glucopyranoside unit (Preliminary communication), **P. Bakó, L. Fenichel, L. Tőke** 323

ANALYTICAL CHEMISTRY

Direct determination of trace elements in polyacrylamide solutions by flame atomic absorption spectrophotometry, II. The effect of polymers on nebulization phenomena, **I. Lakatos, J. Lakatos** 389

CHEMICAL TECHNOLOGY

Selective production of *p*-dichlorobenzene from chlorobenzene, **I. Buzás, L. Szotyory, A. Ujhidy** 353

BOOK REVIEWS 407

Acta Chimica Hungarica 116 (4), pp. 323—325 (1984)

SYNTHESIS OF A NOVEL DIAZA CROWN AND A NOVEL CRYPTAND INCORPORATING A METHYL-4,6-*O*-BENZYLIDENE-α-D--GLUCOPYRANOSIDE UNIT

(PRELIMINARY COMMUNICATION)

P. BAKÓ, L. FENICHEL and L. TŐKE*

(Department of Organic Chemical Technology, Technical University, H-1521 Budapest, Műegyetem rkp. 3.)

Received February 20, 1984
Accepted for publication March 13, 1984

Numerous publications have appeared in the last few years reporting on the synthesis and chiral recognition abilities of chiral crown ethers incorporating sugar moieties [1]. In order to increase the complex stability constants and to study the relations between stability constants and the enantioface differentiating abilities in asymmetric reactions, we decided to build up chiral macrocyclic diaza crowns and chiral cryptands starting from (**1a**). A recent report [2] regarding the synthesis of macrocyclic compounds of similar type prompted us to disclose our early results in that area.

Reaction of (**1a**) with chloroacetic acid (Bu^tOK in Bu^tOH, reflux, 24 h) results in the formation of (**1b**) in 26% yield**, m.p. 135—136 °C, $[\alpha]_D^{22} = 88.1$ ($CHCl_3$, $c = 1.1$). Chlorination of (**1b**) with oxalyl chloride ($CHCl_3$, 20 °C, 20 h) gives (**1c**) in 90% yield, m.p. (d): 116—20 °C, $[\alpha]_D^{22} = 34.0$ ($CHCl_3$, $c = 1.1$). Using the high dilution technique, the acylation of (**2**) and (**5**) [3] by (**1c**) have been accomplished in a 5 : 1 mixture of toluene-$CHCl_3$ to give (**3**) (8 h, 22 °C) in 28% yield (by column chromatography on Kieselgel, $CHCl_3$—MeOH 10 : 1) m.p. 108—110 °C, $[\alpha]_D^{22} = 87.4$ ($CHCl_3$, $c = 1$), M^+ m/z 510, and (**6**), respectively, (22 °C, Et_3N) in 21% yield (column chromatography on alumina, benzene-$CHCl_3$ 2 : 1) m.p. 94—95 °C, $[\alpha]_D^{22} = 64.4$ ($CHCl_3$, $c = 1$), M^+ m/z 624. Reduction of bisamides (**3**) and (**6**) by $LiAH_4$ in refluxing THF affords diaza crown (**4**) (2 h, 92% yield) as a crystalline syrup $[\alpha]_D^{22} = 56.9$ ($CHCl_3$, $c = 1$), ^{1}H-NMR*** δ 7.45—7.22 (m, 5H, Ph) 5.49 (s, 1H, PhCH), 4.82 (d, 1H, $J = 4.5$ Hz, MeOCH), 4.36—3.37 (m, 18H $6\times OCH_2$ and 6H), 3.40 (s, 3H, OMe), 3.10—2.15 (m, 10H, $4\times NCH_2$ and $2\times NH$), M^+m/z 482,

* To whom correspondence should be addressed.
** All new compounds gave staisfactory analytical data.
*** ^{1}H NMR: 60 MHz, $CDCl_3$, Me_4Si.

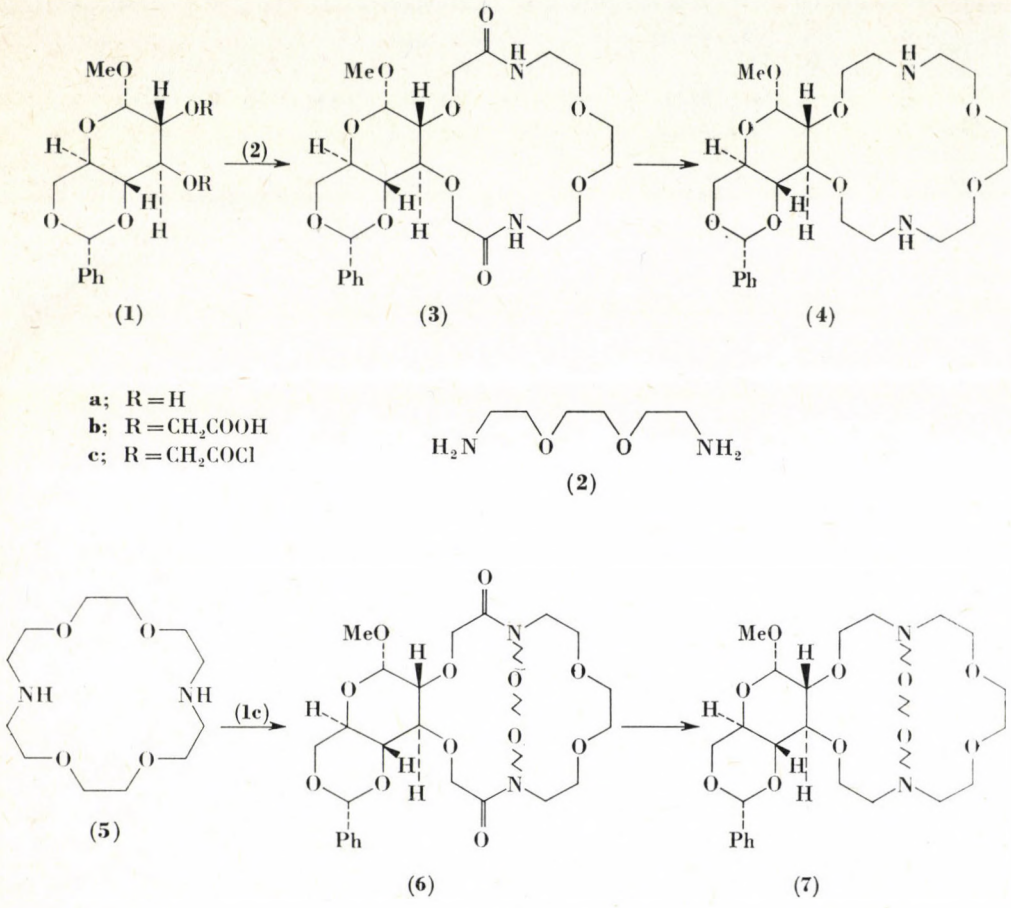


Fig. 1

and cryptand (**7**) (10 h, 84% yield), respectively, as a crystalline syrup, $[\alpha]_D^{22} = +12.3$ ($CHCl_3$, $c = 1$). ^{1}H-NMR δ 7.46—7.17 (m, 5H, Ph), 5.49 (s, 1H, CHPh), 4.77 (d, 1H, $J = 4$ Hz, MeOCH), 4.54 (s, 8H, OCH_2CH_2O), 4.02—3.30 (m,

Table I

Association constants (log K_a) *in* $CDCl_3$ *at* 22 °C

	log K_a		
	Na^+	K^+	NH_4^+
(3)	—	4.10	3.47
(4)	5.74	5.60	6.51
(6)	6.12	6.15	6.49
(7)	8.86	9.07	8.36

18H, $6\times OCH_2$ and 6H from the sugar unit), 3.35 (s, 3H, OMe), 2.75 (m, 12H, $6\times NCH_2$), M^+ m/z 596.

The complex stability constants of the new compounds (**3**), (**4**), (**7**) and (**5**) are measured and calculated using Cram's method [4]. The results are summarized in Table I.

Log K_a values are higher than those found for the bisglucosido crowns [1] by about one order of magnitude for diaza crown (**4**) and by four orders of magnitude for cryptand (**7**).

REFERENCES

[1] Laidler, D. A., Stoddart, J. F.: Carbohydrate Res., **55**, C1 (1977); Curtis, W. D., Laidler, D. A., Stoddart, J. F., Jones, G. H.: J. C. S. Perkin. I., **1977**, 1756; Hain, W., Lehnert, R., Röttele, H., Schröder, G.: Tetrahedron Lett., **1978**, 625; Tőke, L., Fenichel, L., Bakó, P., Szejtli, J.: Acta Chim. Acad. Sci. Hung., **98**, 357 (1978); Bakó, P., Fenichel, L., Tőke, L.: ibid., **111**, 297 (1982); Bakó, P., Fenichel, L., Tőke, L., Czugler, M.: Liebigs Ann. Chem., **1981**, 1163; Zhdanov, Yu. A., Alekseev, Yu. E., Sudareva, T. P., Tyumenev, V. A.: Dokl. Akad. Nauk SSSR, **265**, 1939 (1982)

[2] Pietraszkiewicz, M., Jurczak, J.: J. C. S. Chem. Commun., **1983**, 132; Pietraszkiewicz, M., Salanski, J., Jurczak, J.: ibid., **1983**, 1184

[3] Dietrich, B., Lehn, J. M., Sauvage, J. P., Blanzat, J.: Tetrahedron, **29**, 1629 (1973)

[4] Moore, S. S., Tarnowski, T. L., Newcomb, M., Cram, D. J.: J. Am. Chem. Soc., **99**, 6398 (1977)

Acta Chimica Hungarica 116 (4), pp. 327—333 (1984)

DISSOCIATION CONSTANTS OF L-PYRROLIDINE--2-CARBOXYLIC ACID AT DIFFERENT TEMPERATURES, IONIC STRENGTHS AND IN DIFFERENT AQUOORGANIC SOLVENTS

R. S. SAXENA* and A. GUPTA

(Department of Chemistry, Malaviya Regional Engineering College, Jaipur-302017, India)

Received August 2, 1983

Accepted for publication September 21, 1983

The dissociation constants of L-pyrrolidine-2-carboxylic acid have been determined in aqueous media at 25, 35 and 45 °C by employing the Henderson—Hasselbalch equation and the Albert—Serjeant method. The effects of ionic strength and various organic solvents (20% *v/v*), viz. dimethyl sulfoxide, *N*,*N*-dimethylformamide, acetonitrile, acetone, isopropanol, ethanol and methanol on the dissociation constants have been studied at 35 °C ($\mu = 0.1$ *M*). From the variation of pK_1 and pK_2 with temperature the values of ΔG, ΔH and ΔS were calculated for 35 °C.

Introduction

All amino acids contain ionizable groups that act as weak acids or bases, giving off or taking on protons when the pH is altered. Because of this bifunctional nature, their state of ionization depends strongly on the pH. This ionization follow the Henderson—Hasselbalch equation

$$pH = pK_a + \log_{10} \frac{[\text{unprotonated form (base)}]}{[\text{protonated form (acid)}]} .$$

The pK_a is the negative $\log_{10}$ of the acid dissociation constants of the ionizable group.

A knowledge of their dissociation constant is essential because their values reveal the proportions of different ionic species at any pH and this information is useful in ultraviolet spectrophotometry, preparative chemistry and in the study of complexation reactions of such compounds with metals.

L-pyrrolidine-2-carboxylic acid belongs to an important class of amino acids which has useful application in biological, pharmaceutical and chemical fields.

This communication reports the dissociation constants of L-pyrrolidine--2-carboxylic acid in aqueous media at 25, 35 and 45 °C. The effect of ionic

* To whom correspondence should be addressed.

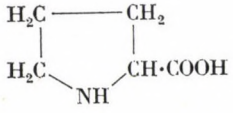
strength and organic solvents (20% *v/v*), viz. DMF, DMSO, acetonitrile, acetone, isopropanol, ethanol and methanol on the dissociation constants have also been studied at 35 °C ($\mu = 0.1$ *M*) by employing pH-metric titration technique. The thermodynamic parameters ΔG, ΔH and ΔS at 35 °C are obtained from the variation of pK_1 and pK_2 with temperature.

Experimental

L-pyrrolidine-2-carboxylic acid (PCA) was supplied by BDH Chemicals, Ltd., Poole, England, and all other chemicals were of AnalaR grade. Hydrochloric acid and sodium hydroxide were standardized in the usual way. All solutions were made in doubly distilled water. pH measurements were performed on a digital pH meter (accuracy ±0.01 pH) equipped with a combined glass-calomel electrode assembly. The electrodes were immersed in the appropriate solvent medium for equilibrium before the pH measurements.

Methods for determination of pK_1 and pK_2

L-pyrrolidine-2-carboxylic acid has two ionizable groups — carboxy group and a secondary amino group and exists as a dipolar or zwitter-ion at pH = 6.2 in water in which



the carboxy group is unprotonated ($-COO^-$) and the secondary amino group is protonated to give the substituted ions ($-NH_2^+$) having corresponding pK_1 and pK_2 values.

For the determination of the acid dissociation constant pK_1, a known concentration of PCA (0.200 mg in 20 mL of water) was neutralized to different extents with 1 *N* HCl and the hydrogen ion concentration was measured pH-metrically till the solution reached pH = 1.

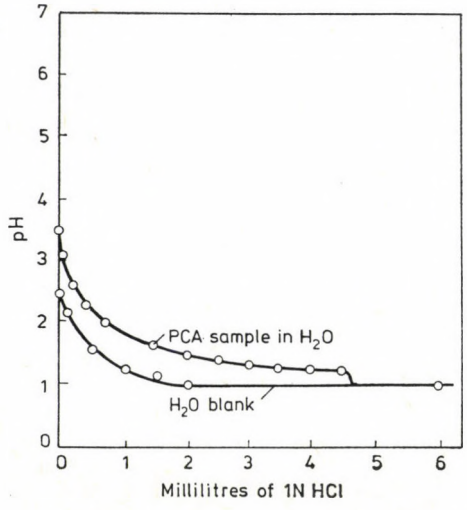


Fig. 1. Uncorrected titration curves of water blanks and PCA sample

Table I

Millilitres of 1 *N* HCl

pH	Water plus sample	Water blank	Difference
3.2	0.05	0	0.05
2.6	0.15	0	0.15
2.3	0.40	0.10	0.30
2.0	0.70	0.20	0.5
1.7	1.45	0.45	1.0
1.5	1.95	0.65	1.3

Again another titration of 20 mL of H_2O (water blank) with 1 *N* HCl was done in a similar way till the solution reached pH = 1.

For determining pK_2 a similar procedure was adopted by first titrating, the PCA sample with 1 *N* NaOH and then a water blank with 1 *N* NaOH as in the case of acid titration until the pH of the solution reached 12.0.

Now for determining the true titration curve of a substance, the quantity of HCl or NaOH consumed in titrating the solvent i.e. H_2O to each pH is measured and this amount is subtracted from the total amount of HCl or NaOH consumed in reaching that pH.

The acid side of the titration of the amino acid has been illustrated as under:

1. For both the PCA sample and the water blank, the volume of acid added versus pH reached has been plotted (Fig. 1).

2. From the above graph, Table I was prepared listing the amount of 1 *N* HCl required to reach each pH. The volume of 1 *N* HCl required to bring the water blank to any pH is then subtracted from the volume of 1 *N* HCl required to bring the PCA sample to the same pH. This difference represents the amount of 1 *N* HCl consumed in the titration of the amino acid only.

3. Using the data from Table I, the pH vs. the number of equivalents of 1 *N* HCl needed to titrate the amino acid (PCA) sample to any pH is plotted (Fig. 2).

A similar method of correction for dilution was applied to the base side of the curve [8]. Figure 3 represents the acid-base titration curve of L-pyrrolidine-2-carboxylic acid which shows that addition of 1 *N* HCl to the solution lowers the pH rapidly at first and then more slowly as the buffering action of the carboxy group is exerted. At pH 1.89, pK_1 is reached i.e. pK_a = pH, when one half of the acid has been consumed, and the carboxy group is half-

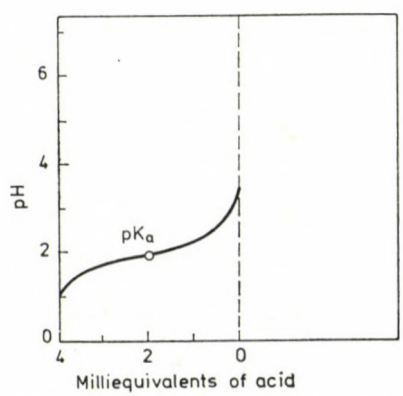


Fig. 2. Corrected titration curve at the PCA sample

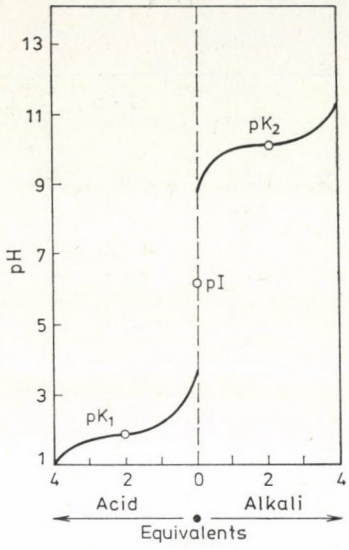


Fig. 3. Titration curves of L-pyrrolidine-2-carboxylic acid ($t = 35$ °C)

ionized and is most effective as a buffer. Titration of the secondary amino group with base follows a similar curve into the alkaline region with $pK_2 = 10.10$. The intersection between the titration of the carboxy group and the titration of the secondary amino group gives the isoelectric point (pI).

Dissociation constants were also determined by adopting the Albert—Serjeant method [1]. In this case pK_1 was determined by keeping the concentration of PCA at 0.01 *M* throughout. To this, an equivalent amount of $HClO_4$ was added and then this acidified PCA solution was further neutralized by adding the titrant, 0.1 *N* $HClO_4$ in ten equal portions, each a tenth of an equivalent and the pH was recorded as soon as equilibrium was reached after each addition. For the determination of pK_2, PCA solution was neutralized with 0.1 *N* NaOH in a similar manner.

Results and Discussion

L-Pyrrolidine-2-carboxylic acid has two replaceable hydrogen ions and the dissociation equilibria in acid and in alkali can be represented by Eqs (1) and (2)

$$RH_2^+ + H_2O \rightleftharpoons H_3O^+ + RH$$

$$K_1 = \frac{[H_3O^+]\,[RH]}{[RH_2^+]\,[H_2O]} \qquad (1)$$

and

$$RH + H_2O \rightleftharpoons H_3O^+ + R^-$$

$$K_2 = \frac{[H_3O^+]\,]R^-]}{[RH]\,[H_2O]}\,. \qquad (2)$$

Table II

Values of pK_1 *and* pK_2 *in aqueous media at various temperatures and ionic strengths*

	Temperature ($\mu = 0.1$ *M*)			Methods
	25 °C	35 °C	45 °C	
pK_1	1.91	1.88	1.85	Albert—Serjeant
	1.92	1.89	1.86	Graphical
pK_2	10.36	10.12	9.86	Albert—Serjeant
	10.35	10.10	9.85	Graphical

	Ionic strength (temp. = 35 °C)				Methods
	0.1 *M*	0.25 *M*	0.5 *M*	1.0 *M*	
pK_1	1.88	1.92	1.95	2.01	Albert—Serjeant
	1.89	1.91	1.94	2.0	Graphical
pK_2	10.12	10.17	10.26	10.46	Albert—Serjeant
	10.10	10.15	10.25	10.45	Graphical

Table III

pK_1 *and* pK_2 *values in several aquo-organic media* (20% *v/v*) *at* 35 °C ($\mu = 0.1$ *M* $NaClO_4$)

Solvents	Albert—Serjeant method		Graphical method	
	pK_1	pK_2	pK_1	pK_2
DMSO	2.34	10.81	2.35	10.80
DMF	2.31	10.76	2.30	10.75
Acetonitrile	2.24	10.71	2.25	10.70
Isopropanol	2.21	10.67	2.20	10.65
Ethanol	2.17	10.61	2.15	10.60
Methanol	2.11	10.56	2.10	10.55
Acetone	2.07	10.51	2.05	10.50

The values of pK_1 and pK_2 in aqueous and aqueous organic solvents, at different ionic strengths and temperatures employing a graphical, and the Albert—Serjeant method, are recorded in Tables II and III and are in close agreement with the literature values [2].

Effect of temperature and ionic strength

The dissociation constant values were determined at 25, 35 and 45 °C at a constant ionic strength of 0.1 *M* $NaClO_4$ (Table II). These values decrease with increasing temperature and also the plots of pK_1 and pK_2 against $1/T$

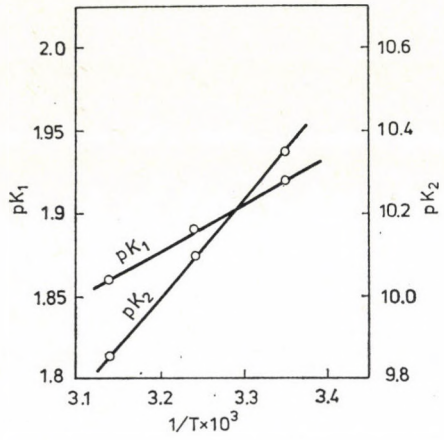


Fig. 4. Plots of pK_1 and pK_2 against $1/T$

(Fig. 4) were found to be linear agreeing with the relationship proposed by Pitzer [3]. It is also seen from Table II that the values of pK_1 and pK_2 increase with increasing ionic strength which is evidence for the dipolar structure of the ligand [4].

Effect of solvent

pK_1 and pK_2 values in several aquo-organic media, viz. 20% *v/v* DMSO, DMF, acetonitrile, acetone, isopropanol, ethanol and methanol (Table III) are found to follow the order

DMSO > DMF > acetonitrile > isopropanol > ethanol > methanol > acetone

Here acetone takes the last place. The order of the sequence is expected to be governed by the dielectric properties and proton solvation properties of the media [5]. Acetone has the least proton solvating capacity among the solvents. Braude [6] has also reported that the basicities of the pure solvent molecules decrease in the above order and hence the position of acetone in the sequence is explained.

Thermodynamic functions

From the variation of pK_1 and pK_2 with temperature, values of ΔG, ΔH and ΔS have been determined at 35 °C ($\mu = 0.1$ *M*) by applying the usual thermodynamic relations [7] and are found to be as follows:

pK	ΔG (kJ/mol)	ΔH (kJ/mol)	ΔS (J/mol K)
pK_1	−11.1	− 5.6	18.0
pK_2	−59.5	−45.9	44.2

REFERENCES

[1] Albert, A., Serjeant, E. P.: Ionization Constants of Acids and Bases, p. 16 Methuen Co. Ltd., London 1962
[2] Martell, A. E., Smith, R. M.: Critical stability constants, Vol. **I**, p. 69 (1916)
[3] Pitzer, K. S.: J. Am. Chem. Soc., **59**, 2365 (1937)
[4] Glasstone, S.: An Introduction to Electrochemistry, p. 433., Affiliated East-West Press, New Delhi 1974
[5] Day, M. C., Selbin, J.: Theoretical Inorganic Chemistry, Reinhold, New York 1966
[6] Braude, E. A.: J. Chem. Soc., **1948**, 1971
[7] Yatsimirskii, K. B., Vasilev, V. P.: Instability Constants of Complex Compounds Pergamon Press, Oxford 1960
[8] Clark, J. H., Switzer, R. L.: Experimental Biochemistry, N. H. Freeman and Co., San Francisco, 1977, p. 88

Acta Chimica Hungarica 116 (4), pp. 335—344 (1984)

CRYSTAL AND MOLECULAR STRUCTURE DETERMINATION AND ESR-STUDY OF [*N*-(*n*-BUTYL) QUINOLINIUM]$^+$ (7,7,8,8-TETRACYANOQUINODIMETHANE)$_2^-$

GY. MENCZEL*[1], J. KÜRTI[2] and R. LEHŐCZ[1]

([1]Department of Solid State Physics, L. Eötvös University, H-1445 Budapest, P.O.B. 327, [2]Department of Atomic Physics, L. Eötvös University, H-1455 Budapest)

Received August 10, 1983

Accepted for publication September 28, 1983

The crystal and molecular structure of the title compound (NBQ · $TCNQ_2$) has been determined by X-ray diffraction methods. The dimensions of the triclinic unit cell (S.P.PI): $a = 775$, $b = 1549$, $c = 1349$ pm; $\alpha = 72.9°$, $\beta = 99.8°$, $\gamma = 87.8°$. The structure was solved by Patterson-method with 2367 photographically observed reflexions with non-zero intensities. Final residual $R = 0.136$. The TCNQ moities are stacked along *c* and form tetramers with a large perpendicular gap of 357 pm between neighbouring tetramers. The similarity of the bond lengths in the two independent TCNQ molecules suggest an equivalency regarding the negative charge distribution between them.

The ESR fine structure can be explained assuming that two electrons in one tetramer form a triplet excited state. The fine splitting is due to magnetic dipole-dipole interaction between electron spins within a tetrade. The calculated D-tensor — using spin densities of the isolated $TCNQ^-$ ion — is in good agreement with the measured one. The unusually large distance between the tetramers accounts for the exchange interaction between electrons on different tetramers is very small; no exchange narrowing takes place even at high temperatures.

Introduction

A great number of paper deal with the molecular complexes of 7,7,8,8--tetracyanoquinodimethane (TCNQ). These materials have quasi one-dimensional electronic band systems and have unusual electrical and magnetic properties. Several summarizing papers appeared on this subject [e. g. 1—4], too. For the crystal structures of these substances is characteristic that the plane TCNQ moieties are stacked parallelly in columns along one crystallographic direction. Some of the complexes have a fine splitting in their ESR spectrum due to magnetic dipole-dipole interaction between electron spins, forming mobile triplets. NBQ · $TCNQ_2$ has an ESR fine splitting even at unusual high temperatures, therefore it is an ideal material for the ESR fine structure investigations on the basis of theoretical model for triplet excitons [5].

* To whom correspondence should be addressed.

Table I

Final atomic parameters
The fractional positional parameters are multiplied by 10^4;
$U_{eq} = (U_{11} \cdot U_{22} \cdot U_{33})^{1/3} \cdot 10^6$ (pm^2).
In parantheses: e.s.d. in the units of the last digit

	x/a	*y/b*	*z/c*	U_{eq}
C (1)	−2174 (13)	55 (6)	1003 (8)	1.62
C (2)	−1465 (13)	910 (7)	608 (8)	1.46
C (3)	382 (13)	908 (7)	818 (9)	1.77
C (4)	1432 (14)	163 (6)	1292 (9)	1.58
C (5)	810 (12)	− 710 (6)	1697 (8)	1.13
C (6)	−1110 (13)	− 705 (7)	1491 (8)	1.76
C (7)	1906 (12)	−1486 (7)	2180 (8)	1.00
C (8)	3772 (14)	−1449 (8)	2415 (9)	2.13
C (9)	1330 (15)	−2355 (8)	2517 (9)	2.54
C (10)	−2568 (13)	1696 (7)	133 (9)	1.80
C (11)	−1872 (14)	2553 (7)	−182 (9)	2.07
C (12)	−4475 (15)	1759 (7)	− 26 (10)	2.64
C (13)	− 790 (14)	− 769 (6)	3953 (8)	1.47
C (14)	− 165 (13)	113 (7)	3595 (9)	1.85
C (15)	1695 (13)	180 (7)	3762 (9)	1.65
C (16)	2827 (14)	− 573 (6)	4265 (9)	2.08
C (17)	2206 (12)	−1434 (7)	4672 (8)	1.20
C (18)	330 (13)	−1503 (7)	4468 (8)	1.86
C (19)	3393 (13)	−2165 (7)	5236 (9)	2.06
C (20)	5248 (16)	−2110 (8)	5390 (9)	2.58
C (21)	2831 (16)	−3049 (8)	5651 (10)	3.03
C (22)	−1329 (14)	866 (7)	3096 (8)	1.12
C (23)	− 751 (13)	1766 (7)	2732 (9)	2.08
C (24)	−3181 (14)	847 (7)	2948 (10)	2.23
C (25)	5156 (14)	4980 (7)	1821 (10)	1.80
C (26)	6033 (16)	4392 (7)	1416 (10)	2.60
C (27)	5186 (17)	3600 (8)	1268 (11)	3.71
C (28)	3700 (17)	3382 (9)	1659 (12)	4.38
C (29)	2846 (16)	3989 (8)	2060 (10)	3.66
C (30)	3576 (15)	4774 (8)	2152 (11)	3.33
C (31)	7652 (15)	4577 (8)	1061 (11)	3.30
C (32)	8332 (16)	5350 (9)	1185 (10)	3.45
C (33)	7484 (15)	5921 (7)	1620 (10)	2.58
C (34)	5220 (14)	6355 (7)	2462 (9)	2.42

(Table I continued)

	x/a	y/b	z/c	U_{eq}
C (35)	5682 (13)	6001 (7)	3630 (8)	2.14
C (36)	7595 (14)	6027 (7)	4165 (10)	2.77
C (37)	7965 (16)	5647 (10)	5341 (10)	4.11
N (1)	5259 (12)	−1448 (6)	2633 (8)	2.96
N (2)	823 (14)	−3055 (6)	2816 (9)	3.72
N (3)	−5979 (13)	1840 (7)	− 191 (9)	3.98
N (4)	−1294 (13)	3251 (6)	− 431 (8)	3.28
N (5)	6765 (13)	−2050 (7)	5538 (10)	3.60
N (6)	2439 (14)	−3763 (7)	6034 (10)	4.40
N (7)	−4698 (12)	843 (7)	2830 (10)	3.86
N (8)	− 364 (13)	2467 (6)	2423 (9)	3.29
N (9)	5992 (12)	5734 (5)	1949 (7)	1.88

Experimental

The crystals of the title compound were prepared by Mrs. Dr. M. Erő-Gécs [6].

(a) X-ray structure determination

Space group and cell parameters were determined by oscillation and Weissenberg X-ray photographs with Cu-Kα radiation. The intensities of the maxima were registered by multiple film Weissenberg photographs with unfiltered copper radiation and measured by calibrated spots. Two specimens were used, one for the $h = 0-4$ layers and another for the $l = 0-6$ layers. The first specimen had linear dimensions less than 0.4 mm, the other one was larger, its maximum length reached 0.6 mm. No absorption corrections of the intensities were made. 2392 of the 4323 independent reflexions were classed as observed; owing to the uncertainty of the intensity measurements 16 of them were excluded from the computations. Crystallographic data with standard deviations in the units of the last digit in parantheses: $C_{13}H_{16}N(C_{12}H_4N_4)_2$. Space group PI. $a = 775$ (4), $b = 1549$ (4), $c = 1349$ (6) pm, $\alpha = 72.9$ (5)°, $\beta = 99.8$ (5)°, $\gamma = 87.8$ (5)°. The density calculated with two formula units ($Z = 2$) in the unit cell $D_x = 1.309$ Mgm^{-3}, the density measured by flotation $D_m = 1.27$ Mgm^{-3}, $F(000) = 618$, R.M.M. = 594.7, $\mu_l = 564$ m^{-1}. The data show only slight deviations from those measured by Yashchurginskaya and coworkers [7].

Determination of the structure

Attempts with direct methods gave no results so the structure was solved by Patterson method. A sharpened three dimensional $P(u, v, w)$ -map was computed and (1): strong peaks in the vicinity of the origin allowed to fix the orientations of the TCNQ moieties in the unit cell (2): the similarly arranged peaks at the origin, around $w = 0.25$ and $w = 0.50$ revealed that four parallel and plane TCNQ-units were stacked along the c axis approximately at distances of $c/4$. Two of them denoted as units A and B are crystallographically independent, each being connected to its related pair, $\bar{A}$ and $\bar{B}$ respectively, by centres of inversion at 0, 0, 0 and 0, 0, 1/2. It is obvious that the four units must have been connected by three independent translational vectors. For two strong peaks (a): $u = 0.138$, $v = 0.074$, $w = 0.304$; (b): $u = -0.209$, $v = 0.145$, $w = 0.161$ it was supposed that their vectorial distances from the origin V_1 and V_2 represent translational vectors between adjacent TCNQ molecules. A third vector V_3, belonging to the medium strong peak (c): $u = -0.061$, $v = 0.027$, $w = 0.240$ was chosen by the reason that the vector equation $2V_1 + V_2 + V_3 = c$ holds approximately

Table II

Least squares planes thorugh the ring atoms of the TCNQ *moieties*

a) Equations of the planes. x', y', z' are absolute coordinates in pm. x' is along a, y' along $c \times a$ *and* z' along c.

$$\text{TCNQ}(A) - 0.0203x' + 0.1675y' + 0.9857z' = 165.15$$
$$\text{TCNQ}(B) - 0.0447x' + 0.1632y' + 0.9856z' = 486.38$$

b) Distances from the planes in pm. Asterisks denote atoms defining the planes

TCNQ(A)		TCNQ(B)	
C (1)	1.4*	C (13)	−1.4*
C (2)	−2.0*	C (14)	1.3*
C (3)	1.8*	C (15)	0.3*
C (4)	−0.9*	C (16)	−1.8*
C (5)	0.2*	C (17)	1.7*
C (6)	−0.5*	C (18)	−0.1*
C (7)	−4.8	C (19)	8.3
C (8)	5.1	C (20)	4.6
C (9)	−12.9	C (21)	10.5
C (10)	4.7	C (22)	4.9
C (11)	13.8	C (23)	10.7
C (12)	13.6	C (24)	11.6
N (1)	14.0	N (5)	6.5
N (2)	−14.5	N (6)	19.1
N (3)	16.5	N (7)	18.4
N (4)	21.9	N (8)	12.3

between the three vectors. A supposition was made that the translations between the neighbouring TCNQ-units $\bar{A}A$, AB and $B\bar{B}$ are in the same order of succession V_3, V_1 and V_2. This model gave the reliability index $R = 0.61$. The observation that for the reflexion I48 was $F_0 \approx 2/3\ (\Sigma f_j)$, allowed to improve the model to $R = 0.48$, by making the planes of the TCNQ-units coincide with this net plane. A Fourier-synthesis with the signs of the F_c's revealed the positions of the non-hydrogen atoms of the NBQ cation. Blocked full-matrix least squares refinement- first with isotropic then with anisotropic temperature coefficients was carried out and finished when the shift/e.s.d. ratio fell under 0.2 for the positional parameters. Before the last cycle of refinement the hydrogen atom positions were generated geometrically but they were not refined. 9 reflexions were excluded from the refinement being suspect of extinction effects. The final reliability index was R = 0.136 for 2367 observed reflexions. All calculations were performed on the R-40 computer of the Computing Centre of the L. Eötvös University with the program systems SHELX and XANADU [8, 9]. The atomic scattering factors of Cromer and Mann (for N and C) and of Cromer (for H) were involved in the SHELX program. Table I contains the positional parameters of the non-hydrogen atoms. The equations of the least squares planes through the ring atoms of the TCNQ molecules and the distances of the atoms from the planes are listed in Table II. List of the F_0, F_c, U_{ij} values and H-atom coordinates are available from the authors.

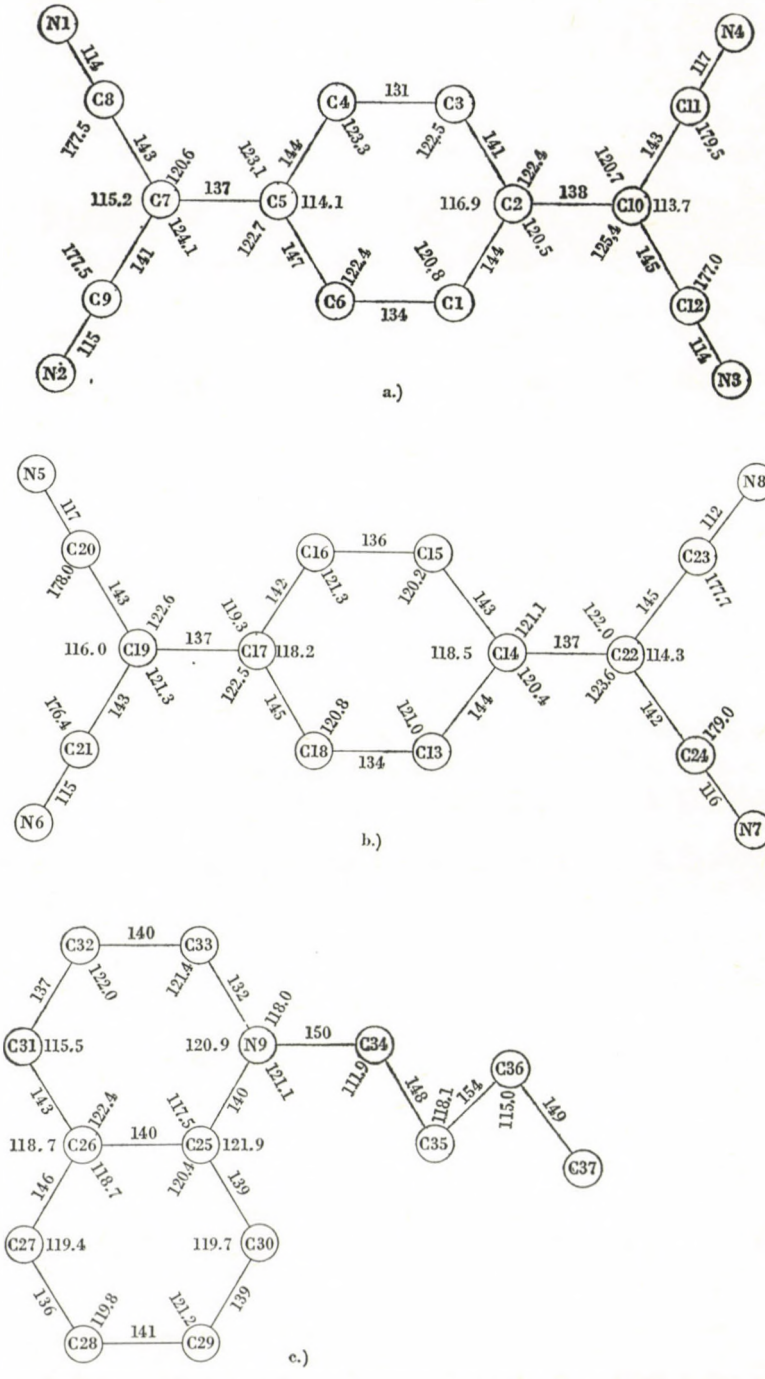


Fig. 1. Bond lengths in pm and angles in degrees; (a) TCNQ (*A*), (b) TCNQ (*B*), (c) NBQ-ion. The e.s.d. values for the bond lengths and bond angles, respectively are: TCNQ-moieties: 1.2—1.6 pm and 0.8—1.2°; NBQ-ion 1.5—2.0 pm and 1.0—1.4°

(b) ESR investigations

ESR investigations of this compound have been made earlier by Erő-Gécs [6] and Yashchurginskaya and co-workers [7]. For the interpretation of the ESR spectrum on the basis of the crystal structure two single crystal specimens have been measured, the same ones as for the crystal structure determination. The measurements were performed at room temperature on the standard ESR spectrometer ERS 220, in X-band. The rotation of the sample was performed with a device which provided rotations around two orthogonal axes. The uncertainty of the angle measurements around the vertical and horizontal axes was less than $\pm 1°$ and $\pm 3°$, respectively. The error of the crystal orientation was less than $\pm 5°$.

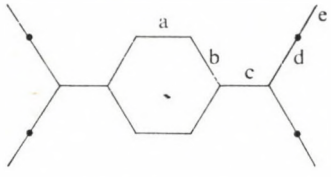
The crystals had well defined edges along *a* and a well developed surface parallel with (0I1). The ESR spectrum consists of two equal signals because of the so called fine structure splitting and of one "impurity" singlet in the middle. From the angular variation of the distance of the outer two lines the experimental fine splitting tensor (D-tensor) has been determined. The measured zero-field splitting parameters are: $D = 6.8 \pm 0.2$ mT, $E = 0.8 \pm \pm 0.2$ mT, in agreement with earlier data [6, 7]. The larger splitting was obtained when the magnetic field was oriented nearly parallel to the *c*-axis.

Discussion

Figs. 1a and 1b show the dimensions of TCNQ (A) and TCNQ (B). Averaged values of chemically equivalent bonds are summarized in Table III. Although the accuracy of the determination does not allow to set up quantitative relations — e.g. to apply the equations of Chasseau [3] — between the bond lengths and the charge distribution, the similarity of the dimensions of the TCNQ molecules suggests their equivalency regarding the negative charges on them.

Table III

Averaged values of the chemically equivalent bond lengths in the TCNQ's (pm)



	a	*b*	*c*	*d*	*e*
TCNQ (*A*)	1.325	1.439	1.372	1.429	1.150
TCNQ (*B*)	1.347	1.436	1.372	1.432	1.151

The planes of the TCNQ (*A*) and TCNQ (*B*) rings form an angle of 1.4° with each other. Both stand nearly at right angles to the (*yz*) plane, forming with it angles of 91.2° and 92.6° respectively. The normals of the planes of the TCNQ-rings make dihedral angle of 9.7° with the direction of *c*. The

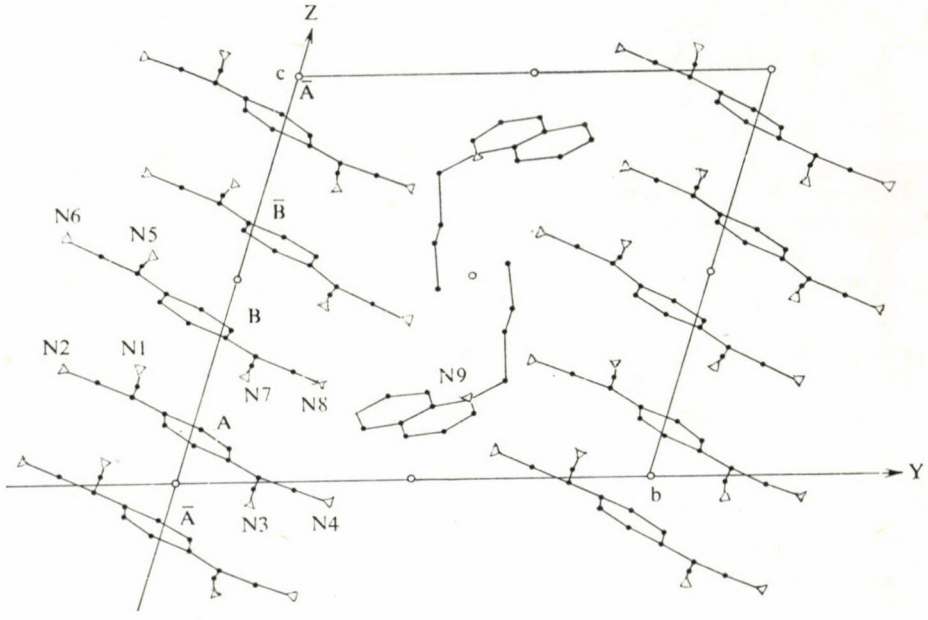


Fig. 2. Molecular arrangement viewed down *a*

C—CN groups are non-linear and bent so as to reduce the distance between the N-atoms of the C- $(CN)_2$ group. The latters are twisted around the bonds linking them with the rings and bowed so that their atoms are farther from the origin than the plane of the ring. Fig. 2 shows the unit cell viewed down *a*.

The TCNQ moieties form tetramers along *c*, having a large perpendicular gap of 357 pm between molecules *B* and $\bar{B}$. The spacing between *A* and *B* (so as between $\bar{A}$ and $\bar{B}$) is 321 pm, that between $\bar{A}$ and *A* is 330 pm, therefore the pairs *AB* and $\bar{A}\bar{B}$ can be regarded as dimers within the tetramers. Fig. 3 shows the overlaps between neighbouring TCNQ-molecules.

The dimensions of the NBQ ion are shown in Fig. 1c. The asymmetry of the bond lengths and angles are similar to that found by Sundarasan and Wallwork [10] in the *N*-propyl-quinolinium (NPQ) ion of the NPQ · $TCNQ_2$ complex. The equation of the least-squares plane through the atoms of the double-ring is:

$$0.4940x' - 0.4733y' + 0.7290z' = 123.47.$$

(Orthogonal coordinates are given in pm as in the equations of Table II). The atoms of the double-ring have not larger distances from this plane than ± 1.6 pm, except C(27), C(28) and N(9), whose distances are -6.3, 6.0 and 3.5 pm, respectively.

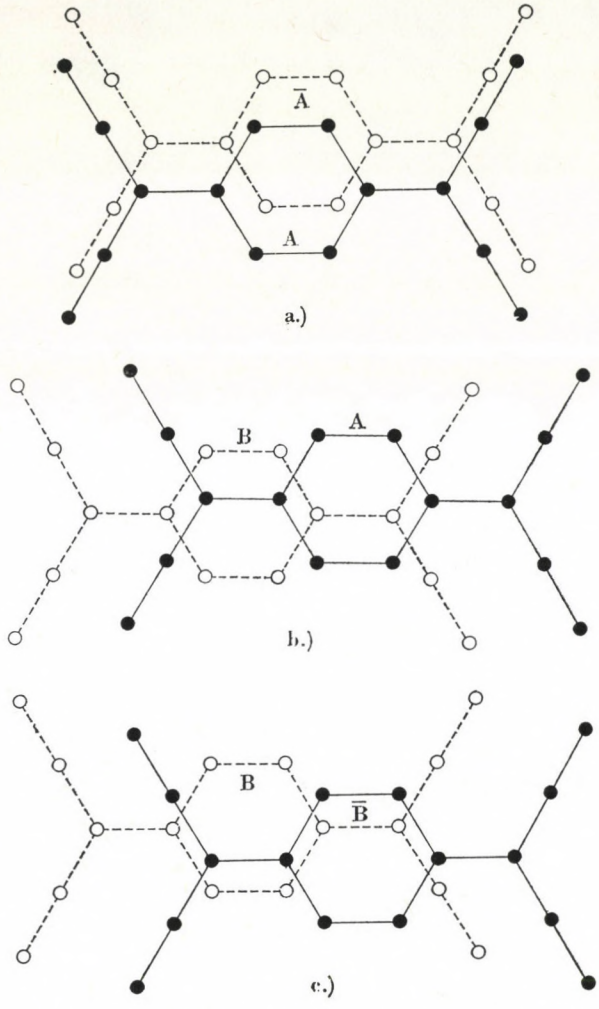


Fig. 3. Overlap of nearest neighbours. (a): projection of molecule $\bar{A}$ (...) on A (——), (b): projection of A (...) on B (——), (c): projection of B (...) on $\bar{B}$ (——)

Intermolecular distances less then 340 pm are listed in Table IV.

The temperature dependence of the ESR spectrum [6, 7] is characteristic of triplet excitons [5]. The fine structure splitting arises from the dipole-dipole magnetic interaction between two spins forming a triplet state within a tetramer. It is very unusual that the fine splitting takes place even at room temperature, but it can be understood knowing the crystal structure. The extremely large distance, 357 pm, between the tetramers means that the triplets are strongly isolated from each other. The collaps of the ESR signals due to exchange effects between triplets (exchange narrowing) could arise

Table IV

Short intermolecular contacts (pm)

Notation of the atomic positions: I x, y, z; II $-x, -y, -z$; IIIa $1 + x, y, z$; IIIb $-1 + x, y, z$; IV $1 - x, 1 - y, -z$; V $1 - x, -y, 1 - z$

From atom at x, y, z	To atom in the position	Distance
C (1)	C (22) I	339
C (1)	C (24) I	339
C (1)	C (4) II	335
C (2)	C (22) I	332
C (2)	C (5) II	333
C (3)	C (6) II	336
C (4)	C (15) I	331
C (5)	C (14) I	336
C (6)	C (13) I	326
C (7)	C (17) I	336
C (7)	C (10) II	335
C (8)	C (16) I	334
C (9)	C (11) II	335
N (4)	C (32) IV	330
N (5)	C (13) IIIa	336
N (5)	C (18) IIIa	335
N (6)	C (25) V	318
N (6)	C (26) V	328
N (7)	C (15) IIIb	333
N (7)	C (16) IIIb	337

only at very high temperatures. For NPQ · $TCNQ_2$ which has similar crystal structure as NBQ · $TCNQ_2$ [10], but the distance between the tetramers are smaller (343 pm), the fine splitting of the ESR spectrum can be seen only below 77 K. Above this temperature the exchange narrowing takes place and there exists only one very narrow ($\Delta H \approx 20$ μT) ESR signal.

The fine splitting due to magnetic dipole-dipole interaction can be descried by an *SDS* term in the effective spin Hamiltonian. As the TCNQ molecules form dimers within the tetramers, two electrons in a tetrade can be regarded as being delocalised on the AB and $\bar{A}\bar{B}$ dimers, respectively. Applying the well known formula [11] to our case:

$$D_{pq} = \frac{1}{2} g^2 \beta^2 \sum_{\substack{i \in A, B \\ j \in \bar{A}, \bar{B}}} \varrho_i \varrho_j (r_{ij}^2 \delta_{pq} - 3 p_{ij} q_{ij}) r_{ij}^{-5}.$$

Here p_{ij}, q_{ij} are differences of coordinates of atoms in different molecules B, A, $\bar{A}$, $\bar{B}$ within TCNQ tetramers, β = Bohr magneton. For the g-factor the free electron value $g = 2.0023$ can be used. For the spin density distributions $\{\varrho_i\}$ and $\{\varrho_j\}$ in molecules A, B and $\bar{A}$, $\bar{B}$, respectively, the results of quantumchemical computations for $TCNQ^-$ anion radicals [12] were used, assuming that the molecules preserve their spin distribution on going to TCNQ tetramers in solid state [5]. The donor-acceptor charge transfer was taken to be complete:

$$\sum_{i \in A, B} \varrho_i = \sum_{j \in \bar{A}, \bar{B}} \varrho_j = 1$$

similar to other closely related 1 : 2 TCNQ salts [13]. As in the values of the bond lengths and angles occurred no significant differences for the two TCNQ molecules, an equal electron distribution was assumed within the dimers. This is not so e.g. for the triethylammonium (TEA) complex, TEA · $TCNQ_2$ [5] or NPQ · $TCNQ_2$ [14], where unequal electron distributions were accounted for the fine splitting.

For the computed D-tensor, which has mean values and axes coinciding within the experimental errors with the measured ones, the largest splitting occurs when the magnetic field is nearly parallel with the c-axis. (The accurate value of the angle is 4.7°.) The computed zero-field splitting parameters are:

$$\mathbf{D} = -6.6\,\mathrm{mT}, E = 0.6\,\mathrm{mT}.$$

*

We thank Dr. D. Kotsis at the University Computing Centre for his help and advices in the use of R–40 facilities and their Operating System and Dr. K. Simon for the XANADU computations.

REFERENCES

[1] Shchegolev, I. F.: Phys. Stat. Sol. (a), **12,** 9 (1972)
[2] Shibaeva, R. P., Atovmyan, L. O.: J. Struct. Chem., **13,** 546 (1972)
[3] Chasseau, D.: Thèse, Université de Bordeaux (1979)
[4] Conference on the Physics and Chemistry of Low Dimensional Solids. Ed. L. Alcacer (1980)
[5] Silverstein, A. J., Soos, Z. G.: Chem. Phys. Letters, **39,** 525 (1976)
[6] Erő-Gécs, M.: KFKI-1979-38 (1979)
[7] Yashchurginskaya, O. A., Berkovsky, B. P., Vozgennikov, M. V., etc.: Proc. Congr. Ampère, 20-th. Magn. Reson. Relat. Phenom. (1978)
[8] Sheldrick, G. M.: SHELX76. Program for Crystal Structure Determination. Univ. of Cambridge, England (1976)
[9] Roberts, P., Sheldrick, G. M.: XANADU. Program for Crystallographic Calculations Univ. of Cambridge, England (1979)
[10] Sundarasan, T., Wallwork, S. C.: Acta Cryst. **B28,** 1163 (1972)
[11] Carrington, A., McLachlan, A. D.: Introduction to Magnetic Resonance. Harper and Row, New York (1966)
[12] Lowitz, A. D.: J. Chem. Phys., **46,** 4598 (1967)
[13] Kürti, J.: Menczel, Gy.: Phys. Stat. Sol. (b), **102,** 639 (1980)
[14] Erő-Gécs, M., Phan Tran Hung, Kürti, J.: KFKI-1981-45 (1981)

Acta Chimica Hungarica 116 (4), pp. 345—351 (1984)

IMMOBILIZATION OF CELLS BY RADIATION COPOLYMERIZATION OF HYDROPHILIC AND HYDROPHOBIC MONOMERS

M. KUMAKURA* and I. KAETSU

(Takasaki Radiation Chemistry Research Establishment, Japan Atomic Energy Research Institute, Takasaki, Gunma, Japan)

Received July 21, 1983

Accepted for publication October 3, 1983

The immobilization of cells *(Streptomyces phaeochromogenes)* by radiation copolymerization of hydrophilic and hydrophobic monomers at low temperatures was studied. The enzyme activity of the immobilized cells was affected by the nature of the polymer matrix having a porous structure. The structure of the polymer matrix varied with the monomer composition of the hydrophilic — hydrophobic monomer systems, and suitable structures have been found to obtain high enzyme activities. The relationship between the structure of the polymer matrix and the hydrophilicity of the monomer was clarified.

Introduction

Various methods are known for the immobilization of enzymes, cells, and organelles in a polymer matrix, and continuous efforts are being made to find new materials and techniques for gel formation [1—9]. Considerable interest has arisen in the use of immobilized biocatalysts in industrial processes of biotechnology. Hydrophilic gels such as natural and synthetic polymers have been employed for the immobilization of cells [4—9]. In immobilized cells resulting from the entrapping method, the diffusion of the substrate in the polymer matrix is a very important factor for the smooth proceeding of a desired enzymatic reaction. It is expected that such reactions with immobilized cells depend on the nature of the polymer matrix. The effect of the nature of the polymer matrix in the immobilization of cells has not been studied, though covalently linked cell fixing on the surface of the matrix has been tried to improve the contact of cells with the substrate [9].

In this work the immobilization of cells, in the present case *Streptomyces phaeochromogenes*, was affected by radiation copolymerization of hydrophilic and hydrophobic monomers at low temperatures, and the influence of the structure of the polymer matrix on the enzyme activity was studied. It has been shown that polymer matrices having various properties can be obtained by radiation copolymerization at low temperatures.

* To whom correspondence should be addressed.

Experimental

Materials

Streptomyces phaeochromogenes cells containing active glucose isomerase were obtained from Nagase Sangyo Co., Ltd. Hydroxyethyl methacrylate (HEMA), trimethylolpropane triacrylate (A-TMPT), hydroxybutyl methacrylate (HBMA), tetraethyleneglycol diacrylate (A-4G), and methyl methacrylate (MMA) were obtained from Shin Nakamura Chemical Industry Co., Ltd.

Preparation of immobilized cells

The dried cells (50 mg) were suspended in 0.05 *M* phosphate buffer solution, pH 7.2, containing 0.01 *M* $MgSO_4 7H_2O$ and the monomer. This solution (2.0 mL) was rapidly shaken in a glass tube of 20 cm in length and 0.8 cm in diameter. Immediately after shaking, the tube was cooled to −78 °C. The gamma ray irradiation (total irradiation dose: 10 kGy) was carried out using a ^{60}Co source of 18.5 PBq at a dose rate of 2.8 Wkg^{-1}. The irradiation temperature was maintained at −78 °C by immersing the tube in a Dewar flask filled with dry ice-methanol mixture. After irradiation, the immobilized cell composite piece was cut into pellets.

Measurement of water content

The hydrophilicity of the polymer matrix was evaluated by measuring the water content. The polymer samples were immersed into distilled water at room temperature for one week. The water content (%) of the polymer was determined as the ratio of weight of water to the weight of the polymer at swelling equilibrium.

Measurement of enzyme activity

The enzyme (glucose isomerase) activity (%) was determined by comparing the rate of D-fructose formation by non-immobilized and immobilized cells in a batch enzymatic reaction (1.0 h, 65 °C). The activity was evaluated from the initial reaction rate, which was inear during the reaction time of the assay.

D-Glucose solution (1.0% *w/v* in 0.05 *M* phosphate buffer containing 0.01 *M* $MgSO_4 7H_2O$, pH 7.2) was used as substrate, and the D-fructose formed was determined by the cystein-carbazole method [10].

Results and Discussion

Dependence of the enzyme activity on the number of repeated batch enzymatic reactions

The cells were immobilized by radiation copolymerization of hydrophilic HEMA and Hydrophobic A-TMPT at low temperatures, and the dependence of the enzyme activity of the immobilized cells on repeated batch enzymatic reactions was examined. This relationship is shown in Fig. 1. As the number of repetitions of the batch enzymatic reactions increased, the enzyme activity of the immobilized cells from HEMA first increased gradually to become then constant, while in case of the A-TMPT — HEMA system it was constant throughout the repeated batch enzymatic reactions, maintaining a high value. Thus it was found that the enzyme activity of the immobilized cells prepared by the radiation copolymerization of the A-TMPT — HEMA system was higher than the activity obtained with HEMA alone. The gradual increase of the enzyme activity in HEMA is due to the swelling of the matrix

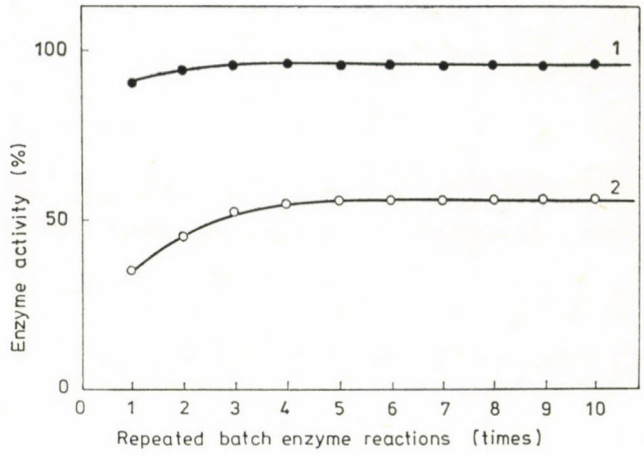


Fig. 1. Relationship between enzyme activity and repeated batch enzymatic reactions; (1) A-TMPT—HEMA 1 : 1 system, (2) HEMA. Monomer concentration: 30%

of the immobilized cells in the solution, because the polymer matrix from HEMA is of hydrophilic character so it can swell in water, affecting the diffusion conditions of the substrate in the matrix. When made by the present method, the polymer matrix from hydrophilic monomers, which are glass-forming monomers at low temperatures, had a soft, sponge-like consistency with a porous strcture, in which the cells are trapped on the surface of the matrix.

Swelling phenomena of polymer matrices in aqueous solution have usually been observed, increasing the enzyme activity owing to the increase of the ease of the enzymatic reaction of the trapped cells.

Effect of monomer concentration on the enzyme activity

The relationship between enzyme activity and monomer concentration for the A-TMPT — HEMA system is shown in Fig. 2. The enzyme activity decreased with increasing monomer concentration, indicating that the activity is intimately related to the structure of the polymer matrix.

The pore size in the porous polymer matrix obtained by the present method varies with the monomer concentration; the pore size usually increases with decreasing monomer concentration. In the present method, the formation of the pores in the polymer matrix results in the melting of the ice formed in the polymerized matrix after irradiation, so that the monomer concentration in the solution containing the monomer, cells and water affects the porosity or pore size in the resulting matrix. The polymer matrix from the A-TMPT — HEMA system was in a relatively rigid state having a porous structure

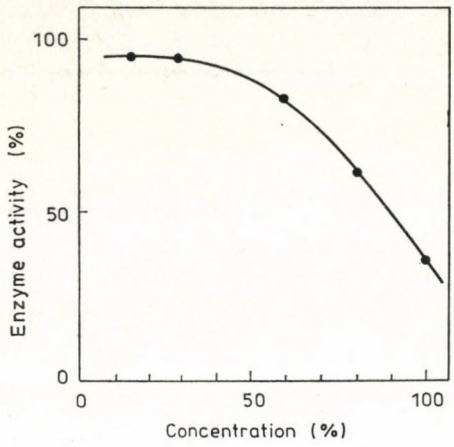


Fig. 2. Relationship between enzyme activity and monomer concentration in the immobilized cells for the A-TMPT—HEMA 1 : 1 system

owing to the presence of the crosslinking monomer, such as A-TMPT. Furthermore, the rigidity of the polymer matrix increased with increasing monomer concentration, thus the cells became firmly entrapped inside the polymer matrix. On the other hand, as the monomer concentration decreased, the porosity of the polymer matrix increased, and the cells became trapped near the surface of the polymer matrix, where the diffusion resistance is smaller, increasing the enzyme activity. As can be seen in Fig. 2, the enzyme activity of the cells immobilized at low monomer concentrations (below 30%) appeared to be very high, about 95%, indicating that the enzyme activity of the immobilized cells was comparable with that of intact cells.

Relationship between the monomer composition and the nature of the polymer matrix

Polymer matrices were prepared by radiation copolymerization of various A-TMPT — HEMA systems at 30% monomer concentration, and the relationship between the monomer composition and the nature of the polymer matrix was examined (Fig. 3). The form of the polymer matrix varied with the monomer composition; the polymer prepared from HEMA was in a bulk state having a porous structure and that from a composition rich in the A-TMPT component had a solid particle state of non-porous structure. With hydrophobic monomers, such as A-TMPT, the formation of the polymer matrix in particle form was due to the polymerization of the monomeric particle phase suspended in the aqueous solution, the irradiation of which was carried out in the frozen state (—78 °C). The size of the particle was affected by the hydrophilicity and concentration of the monomer, and the size range of the

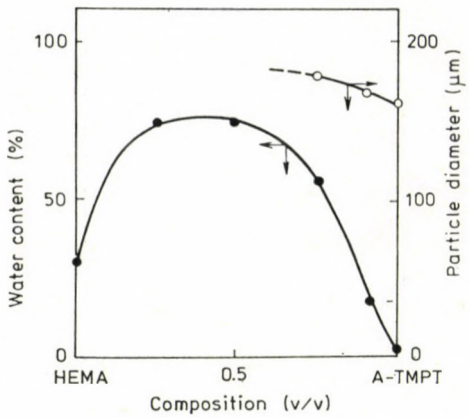


Fig. 3. **Relationship between monomer composition and water content or particle diameter in the immobilized cells for the A-TMPT—HEMA system. Monomer concentration: 30%**

particles was 10—1000 μm. The size of the polymer matrix particles from 30% A-TMPT suspension was about 100 μm in diameter. As the HEMA component was increased, the form of the particle apparently deformed, and the polymer matrix from the A-TMPT — HEMA 3 : 1 system was in a gragile flake state having slightly porous structure. The polymer matrix from the A-TMPT — HEMA 1 : 1 system was in a bulk porous state having flexible property.

The water content of the polymer matrix varied markedly with the monomer composition, as seen in Fig. 3. As the A-TMPT component increased, the water content of the polymer matrix also increased, reached a maximum at the monomer composition of A-TMPT — HEMA 1 : 1, and then decreased. From this result it is concluded that the polymer matrix from the A-TMPT — HEMA 1 : 1 system has a hydrophilic porous structure.

Effect of monomer composition on the enzyme activity

The effect of monomer composition on the enzyme activity in the HEMA — hydrophobic monomer system was also studied. The relationship between the activity and monomer composition is shown in Fig. 4. As the HEMA component decreased, the enzyme activity curves in the A-TMPT or HBMA — HEMA systems were similar to each other and had a maximum at the monomer composition of the 1 : 1 mixture, but in the MMA — HEMA system a marked decrease was found. Thus the enzyme activity of the immobilized cells obtained by the copolymerization of hydrophilic (HEMA) and hydrophobic monomers are affected by the kind of the hydrophobic monomer. A-TMPT, HBMA and HEMA are glass-forming monomers, which give a highly viscous liquid or an amorphous solid on supercooling at low temperatures,

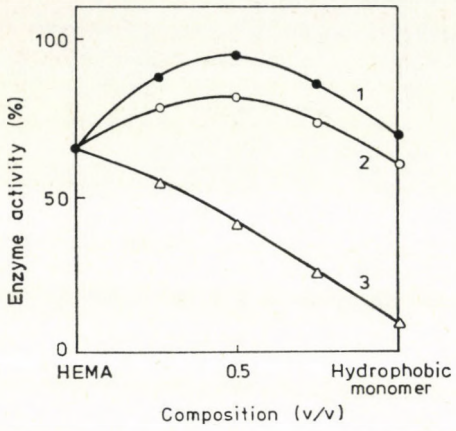


Fig. 4. **Relationship between enzyme activity and monomer composition in the immobilized cells for HEMA — various hydrophobic monomer systems. (1) A-TMPT—HEMA system, (2) HEMA—HEMA system, (3) MMA—HEMA system**

and have high polymerizability even at low temperatures. Therefore, the cells can mildly be trapped in the amorphous polymeric matric phase throughout the radiation copolymerization step at low temperatures (−78 °C). The polymer matrix of the immobilized cells from the A-TMPT — HEMA 1 : 1 system has a maximum porous structure, as can be seen in Fig. 3, and this can correspond to the maximum enzyme activity shown in Fig. 4. The enzyme activity in the HBMA — HEMA system was slightly lower than that in the A-TMPT — HEMA system, indicating that the diffusion depends on the molecular structure or on the nature of the monomer; A-TMPT and HBMA are triacrylate and dimethacrylate, respectively. MMA is a non glass-forming monomer so that the nature of the polymer matrix from the MMA — HEMA system was different from those from the A-TMPT or HBMA — HEMA systems, having non-porous structure. This difference in the polymer matrix appeared also in the data of enzyme activity, as seen in Fig. 4.

Thus it has been found that in the immobilization of cells by radiation copolymerization of hydrophilic and hydrophobic monomers, the enzyme activity of the immobilized cells varies with the monomer composition owing to the nature of the polymer matrix, and that an optimal porous polymer matrix can be found to attain maximum enzyme activity.

REFERENCES

[1] Abbot, B. T.: in "Annual Reports of Fermentation Process" (Ed. D. Perlman), Academic Press, New York 1977
[2] Ghose, T. K., Bandyopahyay, K. K.: Biotechnol. Bioeng., **22**, 1489 (1980)
[3] Sitton, O. C., Gaddy, J. L.: Biotechnol. Bioeng., **22**, 1735 (1980)
[4] Wada, M., Kato, J., Chibata, I.: Eur. J. Appl. Microbiol. Biotechnol., **8**, 241 (1979)

[5] Takata, I., Yamamoto, K., Tosa, T., Chibata, I.: Enzyme Microb. Technol., **2**, 30 (1980)
[6] Yamamoto, K., Tosa, T., Yamamoto, Y., Chibata, I.: Biotechnol. Bioeng., **14**, 1101 (1977)
[7] Hirano, K., Karube, I., Suzuki, S.: Biotechnol. Bioeng., **14**, 311 (1977)
[8] Kierstan, M., Bucke, C.: Biotechnol. Bioeng., **14**, 387 (1977)
[9] Jack, T. R., Zajic, J. F.: Biotechnol. Bioeng., **19**, 631 (1977)
[10] Discke, Z., Borenfrend, E.: J. Biol. Chem., **192**, 583 (1951)

Acta Chimica Hungarica 116 (4), pp. 353—360 (1984)

SELECTIVE PRODUCTION OF *p*-DICHLOROBENZENE FROM CHLOROBENZENE

I. BUZÁS, L. SZOTYORY and A. ÚJHIDY*

(Research Institute for Technical Chemistry of the Hungarian Academy of Sciences, H-8201 Veszprém, Schönherz Z. u. 2.)

Received July 29, 1982

In revised form September 15, 1983

Accepted for publication October 3, 1983

The possibility of selective production of *p*-dichlorobenzene was investigated via the process of decomposition of *p*-chlorobenzenesulfonyl chloride, obtained by selective chlorosulfonation of chlorobenzene, in sulfuryl chloride solution in the presence of 2,2'-azo-bis(isobutyronitrile) (AIBN) and hexamethylenetetramine (hexamine, methenamine). The optimal parameters of the chlorosulfonation and the decomposition were determined. It was found by kinetic measurements that the role of hexamethylenetetramine in the decomposition by sulfuryl chloride of *p*-chlorobenzenesulfonyl chloride is the acceleration of the thermal dissociation of AIBN. The order of the overall decomposition reaction and its apparent activation energy have been determined. This latter value is 87.51 kJ mol^{-1}. The activation energy of the dissociation of AIBN calculated from the experimental decomposition curves of *p*-chlorobenzenesulfonyl chloride is less than that given in the literature for the spontaneous thermal dissociation of AIBN. This fact also supports the accelerating effect of hexamethylenetetramine.

Introduction

Of chlorinated benzene derivatives *p*-dichlorobenzene is a valuable pesticide intermediate. It is traditionally produced by direct chlorination of benzene or chlorobenzene in the presence of catalysts. The reaction yields differently chlorinated derivatives, among these various isomers, the separation of which is difficult and costly. Especially the formation of the useless *o*-dichlorobenzene is undesirable, appearing in rather large quantities beside *p*-dichlorobenzene. In order to make the industrial production of the desired product more profitable, the possibility of its selective production from chlorobenzene was investigated.

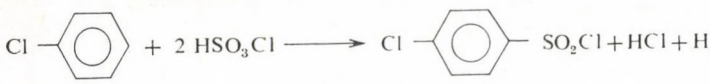
According to the literature, the SO_2Cl groups of aromatic sulfochlorides can be replaced by chlorine in the presence of Cl_2. Thus, the chlorinating decomposition of *p*-chlorobenzenesulfonyl chloride yields definitely *p*-$C_6H_4Cl_2$ [1, 2]. The reaction takes place according to radical mechanism, initiated by free radicals originating from the decomposition of organic compounds. A patent describes the production of *p*-$C_6H_4Cl_2$ in CCl_4 solution by means of chlorine

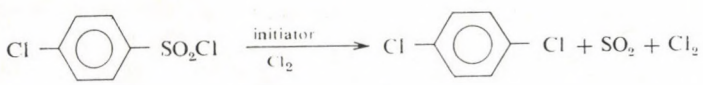
* To whom correspondence should be addressed.

gas in the presence of azo-bis(isobutyronitrile) (AIBN) and activated carbon at 350 K [1]; others suggest the decomposition in SO_2Cl_2 solution by the addition of 0.1% (*w*/*w*) of hexamethylenetetramine and 2% (*w*/*w*) of AIBN at a temperature close to the boiling point of SO_2Cl_2 [2].

p-Chlorobenzenesulfonyl chloride can be obtained from chlorobenzene by chlorosulfonation. In this case the $-SO_2Cl$ group enters exclusively in *para*-position to the chlorine atom. Beside *p*-chlorobenzenesulfonyl chloride, also the formation of *p*-chlorobenzenesulfonic acid and 4,4'-dichlorodiphenylsulfone takes place to a small extent. This, however, can be suppressed by the proper choice of the reaction parameters. It is advised to use an excess of the acid and to add chlorobenzene into the chlorosulfonic acid drop by drop [3, 4]. As to the role of temperature and the reaction time required, dissimilar data have been published.

Our main goal was to accomplish the selective production of p-$C_6H_4Cl_2$ by the combination of chlorosulfonation and the subsequent decomposition in SO_2Cl_2 according to the following reaction steps:





Although both reactions are known, in order to obtain p-$C_6H_4Cl_2$ in maximum yield we had to reveal the role and the order of importance of the parameters affecting the individual steps, and to determine their joint optimal values.

Since the mechanism and the kinetic evaluation of the decomposition reaction are not published, our further goal was a kinetic study of the decomposition with sulfuryl chloride and the elucidation of the role of hexamethylenetetramine. For this latter purpose reaction rate measurements were carried out. It was found in the experiments that hexamethylenetetramine accelerates the thermal dissociation of AIBN, which is also shown by the difference between the activation energy values calculated from the kinetic curves and those published in the literature.

Experimental

Chlorosulfonation of chlorobenzene

The chlorosulfonation was investigated with PhCl : HSO_3Cl molar ratios of 1 : 3 and 1 : 6 at 283, 298, 308, 318 and 353 K, with dropping times of 10, 30 and 90 min. The reaction was carried out in a batch reactor equipped with a reflux condenser and stirrer. At the given temperature chlorobenzene was added by drops into the appropriate amount of chlorosulfonic

acid, during the time periods given above. When the addition was complete, the stirring of the mixture and sampling were continued. After completing the reaction, the mixture was poured onto ice, and the precipitate was filtered off with suction, washed with water, and air-dried. In the subsequent decomposition reaction this crude product was used. The melting point of the vacuum-distilled p-$ClC_6H_4SO_2Cl$ was 326 K.

Decomposition of *p*-chlorobenzenesulfonyl chloride

During the preparative decomposition experiments of p-chlorobenzenesulfonyl chloride the effect of the amount of hexamethylenetetramine and AIBN on the yield of p-$C_6H_4Cl_2$ and the course of the reaction rate were investigated. The reactions were carried out at 338 K with hexamethylenetetramine — AIBN quantities of 0.1—2, 0.5—2, and 0.1—5% (w/w), with respect to the starting material. One mol of the crude p-$ClC_6H_4SO_2Cl$ and the above quantity of AIBN were dissolved in 2 mol of SO_2Cl_2. The mixture was heated up to 338 K and the reaction was started by the addition of hexamethylenetetramine. In order to avoid sampling inaccuracy and that caused by the volume change, the course of the reaction was followed periodically as a function of time for 6 hours.

The end-products of the preparative decomposition of the acid chloride were processed similarly to the samples, and pure (m.p. 326 K) p-dichlorobenzene was obtained by distillation in vacuum after the evaporation of benzene.

In order to determine the kinetic parameters of the overall decomposition, the reaction was carried out with a p-$ClC_6H_4SO_2Cl$: SO_2Cl_2 molar ratio of 1 : 20 (i.e. with a significant excess of SO_2Cl_2) at 338, 333 and 328 K, in the presence of 0.1% (w/w) of hexamethylenetetramine and 5% (w/w) of AIBN. In this way the volume change was negligible. The reaction was followed up to 45 min.

Analytical monitoring of the chlorosulfonation and decomposition reactions

The chlorosulfonation and decomposition samples of different reaction times were poured into ice, extracted with benzene, neutralized with $NaHCO_3$, and dried over Na_2SO_4. The p-$ClC_6H_4SO_2Cl$ and p-$C_6H_4Cl_2$ contents of the benzene-containing solutions were determined by means of a gas chromatograph using SE-54 stationary phase on 80/100 mesh Chromosorb-W. The column temperatures for sulfonyl chloride and p-dichlorobenzene were 453 K and 393 K, respectively.

Results and Discussion

The results of the chlorosulfonation experiments revealed that the optimal parameters of p-$ClC_6H_4SO_2Cl$ production are as follows:

— 308—318 K temperature

— addition of 50 mL of chlorobenzene drop by drop in the course of about 30 min into 196 mL of chlorosulfonic acid; under the given conditions, the isothermal chlorosulfonation of a 400 g reaction mixture could be effected.

— high excess of chlorosulfonic acid, with a $PhCl : HSO_3Cl$ molar ratio of 1 : 6.

Under these conditions the reaction was complete during the time of the dropwise addition and, according to the analysis, the yield of p-chlorobenzenesulfonyl chloride was 81% based on chlorobenzene.

The yield curves of the decompositions effected in the presence of different amounts of hexamethylenetetramine and AIBN, with a p-$ClC_6H_4SO_2Cl$: SO_2Cl_2 molar ratio of 1 : 2, are shown in Fig. 1. According to the procedure found in the literature, the p-dichlorobenzene yield was 85% with respect to the p-chlorobenzenesulfonyl chloride. Increasing the amount of hexamethy-

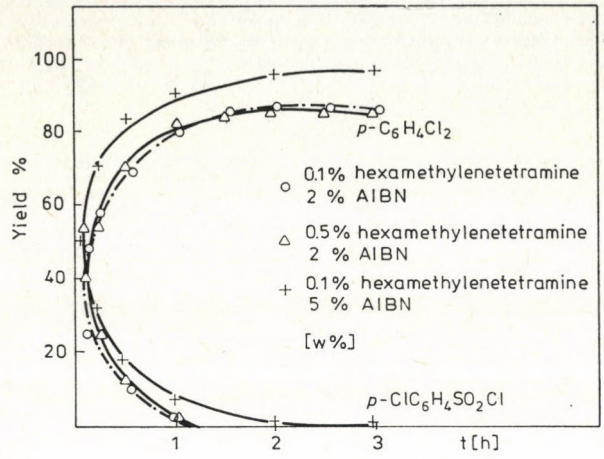


Fig. 1. **Change of the yields of p-$ClC_6H_4SO_2Cl$ and p-$C_6H_4Cl_2$ as a function of the reaction time during the decomposition at 338 K**

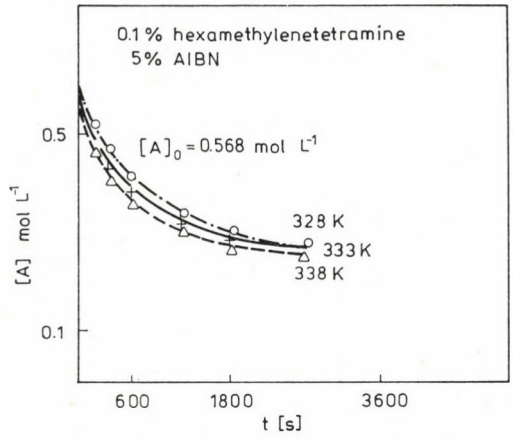


Fig. 2. **p-$ClC_6H_4SO_2Cl$ concentration vs. time curves at different temperatures with p-$ClC_6H_4SO_2Cl$: SO_2Cl_2 molar ratios of 1 : 20**

lenetetramine did not bring about any change in the yield. Using 5% (w/w) of AIBN instead of 2% (w/w), however, the acid chloride practically quantitatively decomposed to p-$C_6H_4Cl_2$ (95%) after a reaction time of 2 h.

Thus, considering the 81% yield of p-$ClC_6H_4SO_2Cl$, p-dichlorobenzene can be produced from chlorobenzene in a yield of 77%, according to analysis. The actual yield of the isolated pure product was 71%.

The p-$ClC_6H_4SO_2Cl$ concentration vs. time kinetic curves obtained in dilute SO_2Cl_2 solution at various temperatures are shown in Fig. 2.

When the decomposition reaction was tried in the absence of hexamethylenetetramine, the initial concentration of the acid chloride did not change at all. Boiling the SO_2Cl_2 separately with hexamine or with AIBN, no volume

change was observed, whereas using these agents together, SO_2Cl_2 decomposed rapidly. On the basis of all these it can be concluded that AIBN does not show initiation in the absence of hexamethylenetetramine, or the effect is very slow.

For the rate constant of the spontaneous thermal dissociation of AIBN the following expression is found in the literature [5]:

$$k_d = 3.68 \cdot 10^{15} \cdot e^{-131.047/RT}\ s^{-1}. \qquad (1)$$

At 338 K the value of k_d is very low. According to the results of the present investigations, the role of hexamethylenetetramine can be the acceleration of the thermal dissociation of AIBN. In the presence of hexamine AIBN quickly decomposes to organic radicals and N_2 at a temperature as low as 328 K. According to Davies, in the course of reactions with radical mechanism carried out in sulfuryl chloride, the R$^\bullet$ radical of the radical-forming agent attacks the SO_2Cl_2 molecule releasing Cl$^\bullet$ radicals [6]. We assume that this Cl$^\bullet$ radical reacts with the *p*-$ClC_6H_4SO_2Cl$ molecule, and the reaction probably takes place according to the mechanism shown in Fig. 3. The chain termination, as known [7], is the recombination of the radicals present.

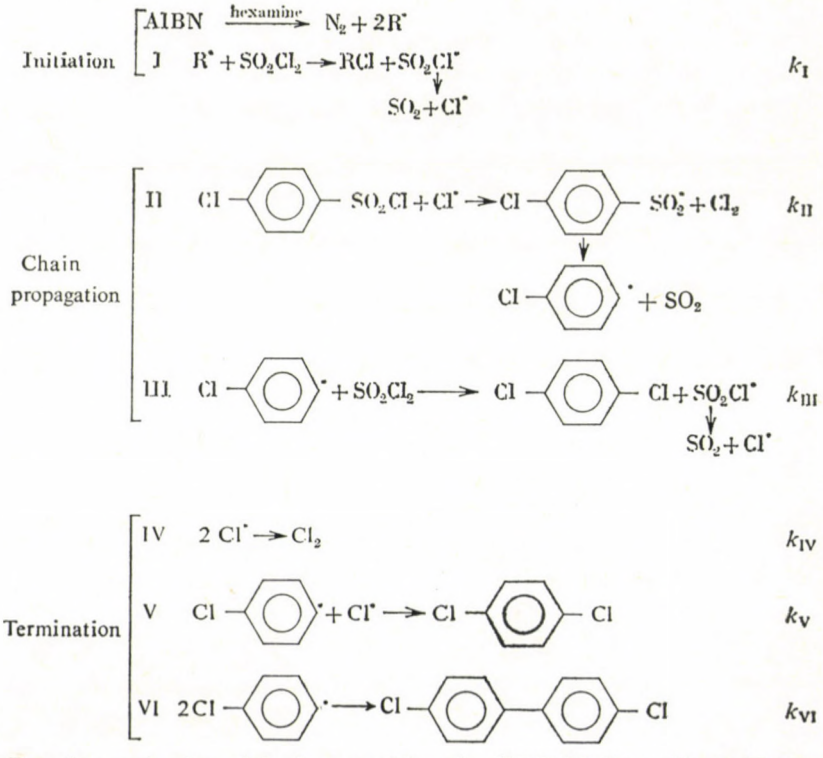


Fig. 3. **Reaction mechanism of the decomposition of *p*-$ClC_6H_4SO_2Cl$ in sulfuryl chloride solution**

Further on, the rate equation of the reaction was established on the basis of the assumed mechanism, and making use of this, the rate parameters were determined from the kinetic curves.

The rate of the overall reaction can be characterized with the decreases of p-$ClC_6H_4SO_2Cl$ (hereafter A):

$$-\frac{d[A]}{dt} = k_{II} \cdot [A][Cl^{\bullet}]. \tag{2}$$

As to the total reaction order and the part reaction orders, the chain starter and chain terminator reactions are of high importance [5, 7]. When sulfuryl chloride is present in great excess $[Cl^{\bullet}] \gg [ClC_6H_5^{\bullet}]$, and the chain termination takes place mainly by the recombination of the $Cl^{\bullet}$ radicals.

Applying the quasi-stationary assumption to $[Cl^{\bullet}]$ and expressing its value by the rate equation of the first order decomposition of the initiator, reducing and integrating the differential equation between $[A]_0 - [A]$, 0-t limits, the following equation is obtained, describing the change of the p-$ClC_6H_4SO_2Cl$ concentration as a function of time:

$$\ln \frac{[A]_0}{[A]} = 2 \cdot \frac{k'}{k_d} [AIBN]_0^{\frac{1}{2}} (1 - e^{-\frac{1}{2}k_d t}) \tag{3}$$

where

$$k' = \frac{k_I^{1/2} k_{II}}{k_{IV}^{1/2}} \text{ : the apparent rate constant of the overall reaction.}$$

k' can be calculated from the equation if k_d and the [A] vs. time curves are known.

When k' is determined from the concentration curves of Fig 2, using the value obtained for k_d by an expression found in the literature [1], the resulting values show a strongly decreasing tendency, that is AIBN decomposes with different k_d in the system. Therefore, both k' and k_d were considered unknown in Eq. (3), and the expression was fitted to the concentration curves of Fig. 2 with the proper choice of k_d, so that constant k' values as a function of time be obtained.

It can be seen from the data in Table I that the k' values obtained by $k_d = 3.2 \cdot 10^{-2}$ s^{-1} do not show any paricular trend, they scatter around an average value. In the same way, the overall rate constants show constant values as a function of time at 328 K and 338 K, with the respective k_d values of $1.72 \cdot 10^{-3}$ s^{-1} and $5.95 \cdot 10^{-3}$ s^{-1}.

Thus, when SO_2Cl_2 is present in a great excess, Eq. (3) can closely describe the kinetic curves, supporting our assumption that the reaction takes place

Table I

Apparent rate constants (k') of the decomposition of p-$ClC_6H_4SO_2Cl$ *obtained by* $k_d = 3.2 \cdot 10^{-3}\ s^{-1}$ at 333 K *with a* p-$ClC_6H_4SO_2Cl : SO_2Cl_2$ *molar ratio of* 1 : 20

t(s)	[A] (mol L^{-1})	$10^3 k'$ ($L^{1/2}$ $mol^{-1/2}$ s^{-1})
0	0.568	—
150	0.483	6.35
300	0.433	5.95
600	0.378	5.52
1200	0.318	5.69
1800	0.278	6.33
	Mean:	5.97

Table II

Apparent rate constants (k') of the decomposition of p-$ClC_6H_4SO_2Cl$ *and rate constants* (k_d) *of the decomposition of azo-bis (isobutyronitrile) at the temperatures investigated*

Temperature (K)	k' ($L^{1/2}$ $mol^{-1/2}$ s^{-1})	k_d (s^{-1})
328	$3.60 \cdot 10^{-3}$	$1.72 \cdot 10^{-3}$
333	$5.97 \cdot 10^{-3}$	$3.20 \cdot 10^{-3}$
338	$9.62 \cdot 10^{-3}$	$5.95 \cdot 10^{-3}$

according to the mechanism suggested above, and with these parameters the reaction order is 1.5.

At the temperatures investigated, the k' and k_d values obtained by the solution of the rate equation of the decomposition of p-$ClC_6H_4SO_2Cl$ are summarized in Table II.

From the Arrhenius representation of the apparent rate constants, the apparent activation energy and frequency factor values of the overall decomposition of p-$ClC_6H_4SO_2Cl$ in the 328—338 K temperature range are as follows:

$$E_{A1} = 87.51\ kJ\ mol^{-1}$$

and

$$k'_0 = 3.20 \cdot 10^{11}\ L^{1/2}\ mol^{-1/2}\ s^{-1}$$

Finally, from the Arrhenius representation of the calculated k_d values, the activation energy and the frequency factor of the dissociation of AIBN in the mixture are:

$$E_{Ad} = 114.88\ kJ\ mol^{-1}$$

$$k_{d0} = 3.34 \cdot 10^{15}\ s^{-1}.$$

This k_{d0} value hardly differs from the frequency factor given in [5]. The activation energy determined in this way, however, is by some 16 kJ mole^{-1} less than the published value for the spontaneous thermal dissociation. The decrease in activation energy can be due to the presence of hexamethylenetetramine proving its role in the acceleration.

Symbols

$[AIBN]_0$ = initial concentration of the initiator (mol L^{-1})
$[A]$ = concentration of *p*-$ClC_6H_4SO_2Cl$ (mol L^{-1})
$[A]_0$ = initial concentration of *p*-$ClC_6H_4SO_2Cl$ (mol L^{-1})
k_I = rate constant of the initiation (s^{-1})
$k_{II} \ldots k_{VI}$ = rate constants of the part reactions of the decomposition of *p*-$ClC_6H_4SO_2Cl$ (L mol^{-1} s^{-1})
k' = apparent rate constant of the overall decomposition of *p*-$ClC_6H_4SO_2Cl$ (L$^{1/2}$ mol$^{-1/2}$ s^{-1})
k_d = rate constant of the decomposition of the initiator (s^{-1})
k_0' = frequency factor in k' (L$^{1/2}$ mol$^{-1/2}$ s^{-1})
k_{d0} = frequency factor in k_d (s^{-1})
E_{A1} = apparent activation energy of the overall decomposition of *p*-$ClC_6H_4SO_2Cl$ (kJ mol^{-1})
E_{Ad} = activation energy of the decomposition of the initiator (kJ mol^{-1})
R = gas constant ($8.314 \cdot 10^{-3}$ kJ mol^{-1} K^{-1})

REFERENCES

[1] Mrva, B., Macko, J., Ruprik, M., Truchlik, S.: German Pat., 2,428,180 (1973)
[2] Semenü, V. Ya., Chernukho, N. P.: Otkrytiya Izobre. Prom. Obraztey Tavernye Znaki, **50,** 70 (1973); U.S.S.R. Pat., 391,122 (1973)
[3] Grigorovskij, A. M., Dykhanov, N. N.: Zh. Prikl. Khim., **28,** 616 (1955)
[4] Pummerer, R.: Ber. Dtsch. Chem. Ges., **42,** 1802 (1909)
[5] Jungers, J. C., Sajus, L.: L'Analyse Cinétique de la Transformation Chimique, **I,** pp. 291—310, Éditions Technip., Paris 1967
[6] Davies, D. J., Parrott, M. J.: Free Radicals in Organic Synthesis, **43,** Springer-Verlag, Berlin—Heidelberg—New York 1978
[7] Schwetlick, K.: Kinetische Methoden zur Untersuchung von Reaktionsmechanismen, pp. 75—85, Dtsch. Verl. d. Wissenschaften, Berlin 1971

Acta Chimica Hungarica 116 (4), pp. 361—365 (1984)

SYNTHESES OF (π-FLUORENYL) AND (π-PYRROLYL)THALLIUM(I) AND THEIR GROUP TRANSFER REACTIONS WITH (π-C_5H_5)$TiCl_3$/(π-C_5H_5)$ZrCl_3$

A. K. SHARMA and N. K. KAUSHIK*

(Department of Chemistry, University of Delhi, Delhi-110007, India)

Received July 16, 1982

In revised form July 18, 1983

Accepted for publication October 5, 1983

Thallous sulphate reacts with sodium-fluorinide and sodium pyrrolide in tetrahydrofuran to give dark yellow crystalline (π-fluorenyl)thallium(I) and (π-pyrrolyl)thallium(I), respectively. Reactions of (π-fluorenyl)thallium(I) and (π-pyrrolyl)-thallium(I) with (π-C_5H_5)$TiCl_3$ and (π-C_5H_5)$ZrCl_3$ in 1 : 1 stoichiometric ratio result in the formation, (π-C_5H_5)(π-$C_{13}H_9$)$TiCl_2$, (π-C_5H_5)(π-C_4H_4N)$TiCl_2$, (π-C_5H_5)(π-$C_{13}H_9$)$ZrCl_2$ and (π-C_5H_5)(π-C_4H_4N)$ZrCl_2$. The products have been characterised on the basis of elemental analyses, molecular weight determinations, conductance measurements, infrared and proton magnetic resonance studies.

Introduction

The study of organothallium(I) compounds have been a subject of keen interest over the last few years because of the fact that these compounds have been used for the preparation of other organometallic compounds by group transfer reactions [1, 2]. Organotitanium and organozirconium compounds on the other hand are known catalysts for the polymerization [3, 4] and hydrogenation [5, 6] of olefins and dienes. The present communication describes the syntheses of (π-fluorenyl)thallium(I) and (π-pyrrolyl)thallium(I). The reactions of these with (π-C_5H_5)$TiCl_3$ and (π-C_5H_5)$ZrCl_3$ were also studied.

Results and Discussion

The analytical data and physical characteristics of the complexes are listed in Table I. It is evident from analytical data that two mole of sodium fluorenide or sodium pyrrolide react with one mole of thallous sulphate in tetrahydrofuran according to the following equations:

$$2C_{13}H_9Na + Tl_2SO_4 \rightarrow 2(\pi\text{-}C_{13}H_9)Tl + Na_2SO_4$$
$$2C_4H_4Na + Tl_2SO_4 \rightarrow 2(\pi\text{-}C_4H_4N)Tl + Na_2SO_4$$

* To whom correspondence should be addressed.

Further the reactions of (π-fluorenyl)thallium(I) and (π-pyrrolyl)-thallium(I) with (π-C_5H_5)MCl_3 (M = Ti or Zr) may be expressed by following equations:

$$(\pi\text{-}C_{13}H_9)Tl + (\pi\text{-}C_5H_5)MCl_3 \rightarrow (\pi\text{-}C_5H_5)(\pi\text{-}C_{13}H_9)MCl_2 + TlCl$$
$$(\pi\text{-}C_4H_4N)Tl + (\pi\text{-}C_5H_5)MCl_3 \rightarrow (\pi\text{-}C_5H_5)(\pi\text{-}C_4H_4N)MCl_2 + TlCl$$

The elemental analyses and spectroscopic data indicates that the method used for the preparation of the compounds yield materials of good purity. Thallium(I) complexes are partially soluble in ethanol, benzene, nitrobenzene and tetrahydrofuran while titanium(IV) and zirconium(IV) complexes also have good solubility in acetone, chloroform and carbondisulphide. Conductance measurements and molecular weight determinations show that all the complexes are nonelectrolyte monomeric species.

The infrared spectra of all the compounds except (π-pyrrolyl)thallium(I) show usual peaks for C_5H_5 group [7]. Further the IR spectra of (π-$C_{13}H_9$)Tl and (π-C_5H_5)(π-$C_{13}H_9$)MCl_2 (M = Ti or Zr) also show some additional bands due to phenyl groups [8]. Besides theses (π-C_5H_5)(π-$C_{13}H_9$)MCl_2 and (π-C_5H_5)(π-C_4H_4N)MCl_2 (M = Ti or Zr) also absorb at 360 cm^{-1} which may be assigned to metal-chlorine stretching frequency. The band at 1140 cm^{-1} in case of (π-C_4H_4N)Tl and (π-C_5H_5)(π-C_4H_4N)MCl_2 may be assigned to ν(C—N—C) vibratons, characteristic of π-pyrrolyl ring.

The PMR spectra of the complexes have been recorded in deuterated chloroform. The resonance signal due to $C_{13}H_9$ group protons of (π-$C_{13}H_9$)Tl occurs as a multiplet in the region δ 6.60—7.10 ppm while in case of (π-C_4H_4N)Tl, the resonance due to C_4H_4N group observed at δ 4.65 and 5.70 which may be assigned to two pairs of equivalent protons bound to the α- and β-carbon atoms relative to the nitrogen atom of the pyrrolyl ring.

The ^1H NMR spectra of (π-C_5H_5)(π-$C_{13}H_9$)MCl_2 (M = Ti or Zr) show a singlet resonance at δ 6.10 which may be assigned to five equivalent protons of C_5H_5 ring and a multiplet resonance in the region δ 6.62—7.12 to $C_{13}H_9$ group.

In case of (π-C_5H_5)(π-C_4H_4N)MCl_2 (M = Ti or Zr) the resonance signal due to C_5H_5 group was observed as a singlet at δ 6.18, while the singlet resonance at δ 4.67 and 5.72 may be assigned to the two equivalent pairs of protons (bonded to the α- and β-carbon atoms relative to the nitrogen) of the pyrrolyl ring. The resonance signals due to the protons of the pyrrolyl group are very similar to the ^1H NMR spectra of (π-C_4H_4N)$Mn(CO)_3$ [9] and (π-C_5H_5)Fe(π-C_4H_4N) [10, 11].

A single resonance line for the protons of C_5H_5 ring in both the cases, (π-C_5H_5)(π-$C_{13}H_9$)MCl_2 and (π-C_5H_5)(π-C_4H_4N)MCl_2 (M = Ti, Zr) indicates the rapid rotation of the ring about metal ring axis. The intensities of all the resonance lines were determined by planimetric integration. The integrated proton ratios correspond to the formula assigned for these compounds.

Table I

Analytical data and physical characteristics of the complexes

Sl. No.	Compound	Dec. temp.* (°C)	Conductance data** molarity × 10^3	% Found (Calc.)					Mol. wt. Found (Calc.)
				C	H	N	Cl	M	
1.	(π-$C_{13}H_9$)Tl	158	0.22	42.32 (42.22)	2.46 (2.43)	—	—	55.20 (55.35)	66 (369.4)
2.	(π-C_4H_4N)Tl	216	0.20	18.78 (17.75)	1.54 (1.48)	5.12 (5.17)	—	75.48 (75.60)	264 (270.4)
3.	(π-C_5H_5)(π-$C_{13}H_9$)$TiCl_2$	190—192	0.28	62.98 (61.90)	4.02 (4.04)	—	20.40 (20.34)	13.64 (13.72)	352 (348.9)
4.	(π-C_5H_5)(π-C_4H_4N)$TiCl_2$	186—188	0.32	45.32 (43.23)	2.72 (2.61)	5.52 (5.60)	28.48 (28.40)	19.02 (19.16)	244 (249.9)
5.	(π-C_5H_5)(π-$C_{13}H_9$)$ZrCl_2$	200—202	0.30	56.12 (55.07)	3.64 (3.57)	—	19.18 (18.10)	23.10 (23.26)	388 (392.22)
6.	(π-C_5H_5)(π-C_4H_4N)$ZrCl_2$	162—164	0.34	36.92 (36.83)	3.18 (3.07)	4.64 (4.77)	—	31.12 (31.05)	287 (293.22)

* Uncorrected values.
** In $ohm^{-1}\ cm^2\ mol^{-1}$.

Experimental

All the reagents used were of analytical grade and all operation were carried out under strictly anhydrous conditions under nitrogen. The metal content was determined by the standard method [12, 13]. Nitrogen was estimated by Kjeldahl's method. Determinations of carbon and hydrogen contents were carried out in our Departmental Microanalytical laboratories. Nitrobenzene was purified for conductance measurements by the method described by Fay and Lowry [14].

Preparation of (π-fluorenyl)thallium(I) and (π-pyrrolyl)thallium(I)

A solution of 50 mmol of sodium fluorenide/sodium pyrrolide in 50 mL tetrahydrofuran was introduced dropwise with stirring to a suspension of thallous sulphate (2.52 g) in 50 mL of tetrahydrofuran. The reaction mixture was allowed to react for 2 hrs with rapid stirring at room temperature and then refluxed for 8 hrs. The colour of the solution turned dark yellow with the formation of some solid product. Excess of petroleum ether (60—80°) was added to the above solution. The crystals of the products were separated, and filtered, washed with water, then with petroleum ether and finally dried under vacuum over P_4O_{10} for 2 hrs.

Preparation of trichloro(π-cyclopentadienyl)titanium(IV) [15] and trichloro(π-monocyclopentadienyl)zirconium(IV) [16]

A solution of titanium(IV) tetrachloride or zirconium(IV) tetrachloride (0.01 mol) in 50 mL THF was cooled in ice bath and a solution of cyclipentadienylthallium (I) (0.01 mol) [17] in 50 mL THF added dropwise under constant stirring under nitrogen. After about 2 hrs, the thallous chloride was filtered off as a white salt. Assuming that the reaction proceeds to completion. The filtrate contains 0.01 mol (π-C_5H_5)$TiCl_3$ or (π-C_5H_5)$ZrCl_3$. The latter was not isolated and the THF solution was used as such for the reaction with (π-fluorenyl)thallium(I) and (π-pyrrolyl)thallium(I).

Reaction of (π-fluorenyl)thallium(I) and (π-pyrrolyl)thallium(I) with (π-C_5H_5)$TiCl_3$ and (π-C_5H_5)$ZrCl_3$

50 mL solution of (π-C_5H_5)$TiCl_3$ or $C_5H_5ZrCl_3$ (0.01 mol) in THF was gradually added to 50 mL solution of 0.01 mol (π-fluorenyl)thallium(I) or (π-pyrrolyl)thallium(I) in THF. The reaction was allowed to react for 8 hrs under rapid stirring at room temperature. The solution was then filtered and the filtrate was concentrated under vacuum to ca. 25 mL. Crystals of the products were obtained by adding excess of petroleum ether and allowing the mixture to stand overnight. The excess solvent was removed in vacuum and the brown products so obtained were dried over P_4O_{10} (2 hrs).

Conductance measurements were made in nitrobenzene solution with a Beckmann conductivity bridge model RC-18A. Solid state IR spectra in KBr pellets were run on a Parkin Elmer-621 Grating spectrophotometer in 4000—200 cm^{-1} region. ^1H NMR spectra were recorded at a sweep width of 900 Hz with a Perkin Elmer R-32 spectrophotometer using TMS as internal standard.

*

One of the authors (A.K.S.) is thankful to C.S.I.R., New Delhi for the award of Senior Research Fellowship.

REFERENCES

[1] Manzer, L. E.: J. Organometal. Chem., **110,** 291 (1976)
[2] Chandra, K., Sharma, R. K., Garg, B. S., Singh, R. P.: Inorg. Chem. Acta, **37,** 125 (1979)
[3] Ziegler, K., Martin, H.: Makromol. Chemie, **18,** 186 (1956)
[4] Pitzer, K. S., Gutowsky, H. S.: J. Am. Chem. Soc., **68,** 2204 (1946)
[5] Olive, G. H., Olive, S.: Angew. Chem., **79,** 764 (1967)
[6] Sonogashara, R., Hapihara, H.: Bull. Chem. Soc. Japan, **39,** 1178 (1966)
[7] Fritz, H. P.: "Advances in Organometallic Chemistry", **1,** 279 (1964)
[8] Scharf, G. W., Brown, P. K.: Can. J. Chem., **63,** 697 (1960)
[9] Joshi, K. K., Pauson, P. L.: Proc. Chem. Soc., **1962,** 326
[10] King, R. B., Bisnette, M. B.: Inorg. Chem., **3,** 796 (1969)

[11] Joshi, K. K., Pauson, P. L., Quazi, A. R., Stubbs, W. H.: J. Organometal. Chem., **1**, 471 (1964)
[12] Treadwell, F. P., Hall, T. W.: Analytical Chemistry, Vol. *II*, John Wiley, New York 1961
[13] Vogel, A. I.: "A Text book of Quantitative Inorganic Analysis, 3rd Edn., Logmans 1968
[14] Fay, R. C., Lowry, R. N.: Inorg. Chem., **6**, 1512 (1967)
[15] Chandra, K., Sharma, R. K., Kumar, N., Garg, B. S.: Chem. Ind., **1980**, 288
[16] Jain, V. K., Kumar, V., Garg, B. S.: Inorg. Chem. Acta, **15**, 197 (1978)
[17] Meister, H.: Angew. Chem., **69**, 533 (1957)

Acta Chimica Hungarica 116 (4), pp. 367—375 (1984)

NEW IDEAS ABOUT THE MECHANISM OF ACTION OF DETERGENT-DISPERSANT (DD) OIL ADDITIVES

O. L. GLAVATY*, A. I. MARCHENKO, G. G. KRAVCHOOK and E. V. GLAVATY

(Oil Chemistry Department of the Physical Organic Chemistry and Carbon Chemistry Research Institute, Academy of Sciences of the Ukrainian SSR, 252160 Kiev, Kharkovskoe chausse, 50.)

Received March 24, 1982

In revised form September 27, 1983

Accepted for publication October 7, 1983

The mechanism of action of additives is explained by stabilization of colloid dispersions in oil by means of:

a) solubilization of contaminant components soluble in polar media in the cores of micelles;

b) stabilization of insoluble components (carbon particles) by a solvated micellar layer.

Adsorbed — solvated layers are generated due to the heterocoagulation of unstable dispersion of carbon particles and stable micellar dispersion of DD additives. Stabilizing dispersions of the additives could be pure micellar solutions as well as solubilizates (microemulsions). Existence of the micellar layer on soot particles was proved by the small — angle x-ray diffraction method. Systems, which were generated in such a way, are local periodic colloid structures. Their stability is explained by the DLVO theory and the theory of steric stabilization of colloid dispersions due to diminishing of the depth of the secondary minimum of attraction and emergence of steric barrier caused by interaction of alkyls of the additives.

DD additives are the most important group of motor oil additives. That is why the investigation of its mechanism of action attracts general attention [1, 2]. It is known that the efficiency of DD additives is mainly explained by their ability to keep the insoluble contaminants in oil in a finely dispersed state [3]. Solubilization of the contaminants in the cores of micelles makes a considerable contribution to its dispersion [4]. However, it seems that the principal contribution to stabilization of contaminant dispersions and prevention of carbonization on hot metal surfaces is due to the dispersion (stabilization of dispersions) of carbon-like contaminants, prevailing among the insoluble impurities of used motor oils. Soot-like products are generated both during the burning of a fuel and oxidation of an oil [1]. So no wonder that the laboratory methods of evaluation of the detergent-dispersant properties, based on the use of soot, are correlating properly with the tests on diesel test engines [4, 5]. Thus, it is possible to model to a considerable extent the mechanism of action of the DD additives by the stabilization of soot in oil

* To whom correspondence should be addressed.

dispersions, taking into account the engine's working conditions. This means that the mechanism of action of the DD additives is related to the stability of colloid dispersions in hydrocarbon media at high temperatures.

The theory of stability of colloid dispersions in hydrocarbon media has been developing for the last 20 years [6]. It is based on the general principles of the DLVO (Derjagin, Landau, Verwey, Overbeek) theory, explaining the aggregative stability of electrostatically stabilized dispersions by the balance between attractive forces resulting from "long-range" Van der Waals — Hamaker forces [7], and electrostatic repulsive forces caused by the charge (double electrical layer) of particles. As a result of the fact that the small probability of the electrostatic repulsion in hydrocarbon media was proved experimentally [8] and theoretically [9], the forces of electrostatic repulsion are substituted in the theory of steric stabilization by the forces of steric repulsion [6].

Steric repulsion consists of two components: entropic — resulting from a decrease of the possible number of alkyl conformations during mutual approach of particles, and osmotic, which is the consequence of local rise in osmotic pressure, caused by the increase of alkyl concentration in the interpenetration zone of adsorbed — solvated layer [6]. The osmotic effect is considerably more important as a rule. In order to determine the possibilities of colloid stabilization, one should draw the so-called potential curves of interaction of the particles or in other words to plot the total interaction energy (V_i) against the distance between particles (H). $V_t = V_r + V_a$, where V_r — the repulsive energy, in that particular case the energy of steric repulsion, V_a — the attractive energy (long-range, of dispersion character); attraction posesses negative value and repulsion — positive. An equation has been derived for calculation of the attractive energy of identical spherical particles, covered with adsorbed — solvated layers [10].

$$\frac{V_a}{kT} = \frac{1}{12kT}\left(A_p^{1/2} - A_a^{1/2}\right)^2 H_a + \left(A_a^{1/2} - A_m^{1/2}\right)^2 H_m + \\ + 2\left[\left(A_p^{1/2} - A_a^{1/2}\right)\left(A_a^{1/2} - A_m^{1/2}\right)\right] H_{am} \tag{1}$$

where k — Boltzmann's constant, T — absolute temperature, kT — the energy of thermal (Brownian) motion, A_p — Hamaker constant of dispersion phase, A_m — the same for a dispersion medium, A_a — the same for adsorbed (and solvated) substance, H_a, H_m, and H_{am}-dimensionless geometrical functions. The full energy of steric repulsion, caused by the interaction of adsorbed — solvated layers can be calculated using the equation [12]:

$$V_r = RT\,\frac{4\pi c^2}{3V_p\varrho_a^2}\left(\psi_1 - \chi_1\right)\left(\delta - \frac{h}{2}\right)^2\left(3a + 2\delta + \frac{h}{2}\right) \tag{2}$$

where R — universal gas constant, T — absolute temperature, c — adsorbate concentration in the adsorbed — solvated layer (g/cm^3), ϱ_a — density of adsorbed — solvated layer, V_p — molar volume of solvent, δ — thickness of adsorbed — solvated layer, a — particle radius, ψ_1 — an entropy parameter (ideally it will be equal to 0.5) and χ_1 — parameter characterizing solvent — adsorbed substance interaction. ψ_1 and χ_1 parameters can be determined experimentally on the basis of viscosity measurements [13].

Basic osmotic contribution to steric repulsion can be calculated using a simpler equation [11]:

$$V_r = \frac{4\pi}{3} B' c^2 \left(\delta - \frac{h}{2}\right)\left(3a + 2\delta + \frac{h}{2}\right) \tag{3}$$

where B' — second virial coefficient from the equation of osmotic pressure of polymer (oligomers) solutions; other notations are the same as in Eq. (2).

To ensure the aggregative stability of the dispersions of soot, covered with layers of the additives, two conditions have to be met: (1) $V_i^{max} > 10\ kT$ and (2) $V_i^{min} < 1kT$ [6]. This means that during the Brownian collision of the particles an energy barrier, preventing mutual approach of the particles, equal to the tenfold energy of its thermal (Brownian) motion at a given temperature [1] should appear, and at the moment of contact of the adsorbed — solvated layers, Van der Waals attraction forces should be smaller than the energy of thermal motion [2] In case of violation of the first condition an irreversible coagulation will take place, and if the second condition is violated — reversible gelling will appear.

The χ_1 parameter is related to parameter ψ_1, which is expressed by the following equation [14]:

$$\chi_1 = \psi_1 \cdot \frac{\Theta}{T} \tag{4}$$

where Θ is the theta temperature of the solvent (temperature at which sedimentation of a stabilizer from solution occurs); other notations are the same.

Comparison of Eqs (2) and (4) demonstrates that both repulsion and attraction are possible, depending on the solvent power (related to the stabilizer) to effect coagulation below the Θ-temperature, owing to the sedimentation of stabilizer adsorbed on the particles. It follows from this that soot particles covered with a solvated layer of surfactants (DD additives) have to behave like polymers, containing these surfactants' alkyl groups, that is, they have to flocculate reversibly with the addition of a solvent which precipitates the hydrocarbons (surfactant alkyl groups). This assumption has been proved: colloid dispersions of soot, stabilized by DD additives, are reversibly precipitated from hydrocarbons by ketone and alcohols.

Table I

Data on adsorption of the additives on soot from 2% (active substance) solution in white oil

Type of additive	Quantity of adsorbed additive, % (of initial soot)	Dimensions of soot particles (specific surface, BET method), nm
Succinimide additive S — 5A		
Adsorption at 20 °C	18.7	0.052
Same with thermostating (250 °C) after adsorption (3 h)	8.0	0.051
Basic calcium alkylsalicylate (MASK)		
Adsorption at 20 °C	18.7	0.054
Same with thermostating (250 °C) after adsorption (3 h)	9.3	0.051
Neutral calcium sulfonate		
Adsorption at 20 °C	30.0	0.048
Same with thermostating (250 °C, 3 h)	18.0	0.050
Basic sulfonate (S-300)		
Adsorption at 20 °C	44.0	0.052
Same with thermostating (250 °C, 3 h)	36.0	0.054

Equation (3) shows that the efficiency of steric stabilization is influenced by the quantity of adsorbed surfactant, thickness of adsorbed and solvated layer and the interaction of solvent with the alkyl group (second virial coefficient). The thickness of the solvated layer depends on the length of the alkyl group and its solvation (which is accompanied by its straightening). The quantity of some additives, adsorbed on soot at 20 °C and after heating up to 250 °C, is given in Table I. Adsorption was carried out on soot PM-75 in white oil with ultrasound treatment (10 min) at 22 kHz, at soot and additive concentrations of 2 and 1.5% respectively (quantity of additive relative to the active substance). These proportions give maximum dispersion with the method of Ref. [5]. The particle dimensions were measured by: 1. electron microscopy; 2. small angle x-ray diffraction; and 3. measurement of specific surface.

The thickness of the solvated layer was evaluated on the basis of the viscosity of soot dispersions stabilized by additives. The calculation was carried out using the equation [15]:

$$\eta_s/\eta = 2.5f + K(2.5f)\varphi \tag{5}$$

where $\eta_s = \eta/\eta_r - 1$; η — viscosity of the dispersion; η_r — viscosity of the medium; φ — volume fraction of the dispersion phase; K — coefficient taking

into account particle interaction; f — an increasing ratio owing to the adsorbed — solvated layer. The thickness of the solvated layer determined by this method is approximately equal to 20—40 nm. Values of the order of 10—20 nm were obtained as a result of measurement of the micelles of various additives by small angle x-ray diffraction and evaluation of its solvation by viscosity measurements. The calculation of Van der Walls attraction (using Eq. 1) and steric repulsion (using Eq. 3) were performed on the basis of the acquired data, and potential curves of the soot particles interaction [16] were plotted. These curves show that the first criterion ($V_i = 10—15\ kT$) is satisfied for all soot particles (from 40 to 200 nm), which means that the soot, stabilized by additives, cannot coagulate irreversibly. As for the second criterion ($V_i^{2\min} < < 1\ kT$), it will not be satisfied if the thickness of the adsorbed — solvated layer is too small (smaller than 10 nm), or the soot particles are too large (larger than 200 nm), which leads to reversible gelling. Such gelling may be the cause of precipitation in different parts of the engine. It seems that carbonization occurs owing to the thermal transformation of this motionless phase on hot engine surfaces.

Steric stabilization by the adsorbed additives is possible only when there is no desorption at high temperatures in the engine (up to 300 °C) and during Brownian collisions of the particles. Experimentally determined values of the adsorption heats of DD additives are as follows [17]: 34—50 kJ/mol for succinimides, 130—170 kJ/mol for basic detergents and average values for neutral detergents. In order to asses the possibilities of desorption upon rising temperature, let us compare the adsorption energy (expressed in kT units) with the energy of thermal motion of particles (molecules). At 20, 100, 200 and 300 °C the kT value will be, respectively, 4.04, 5.14, 6.52, and 7.91×10^{-21} J/molecule. The above mentioned adsorption energies of additives (34—170 kJ/mol) are 5.64×10^{-20}—2.82×10^{-19} J/molecule. Therefore, the adsorption energy is approximately by an order of magnitude greater than the thermal energy, Nevertheless, desorption of additives happens in practice (see Table I). Comparing the values of energies, one can see that the desorption is not a result of the thermal motion of the particles themselves, but is caused by Brownian collisions of the particles. In that case the value 10—15 kT (which is of the order of 50—70 kJ/molecule) should also serve as a criterion for minimal adsorption energy of the dispersion stabilizing additives. In other words, this means that the energy of the barrier, preventing Brownian encounter of the particles, has to be equal to the bond energy of the barrier with the stabilized particle, otherwise Brownian collisions will cause desorption of the additive, which leads to flocculation.

The structure of the stabilizing adsorbed — solvated layer, formed by DD additives on particles, arouses considerable interest. Investigation of the structure [18] and the mechanism of action [19] of basic sulfonate additives

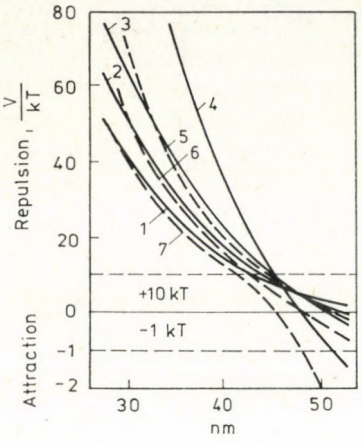


Fig. 1. Interaction energy of soot PM-75 particles (1—4) and graphitized soot (5—7), stabilized by the succinimide additive S — 5A, plotted against the interparticle distance. Diameters of the particles are: 1—40 nm; 2—60 nm; 3—100 nm; 4—200 nm; 5—20 nm; 6—30 nm; 7—50 nm

showed that calcium carbonate colloid particles measuring 5 nm, covered with the calcium sulfonate adsorbed layer of 1 nm thickness, are the active substance of highly basic sulfonate (with a total base number of 300 mg KOH/g). With maximum solvation, the thickness of the layer is 2—4 times larger. Then the dispersion phases were isolated from a number of highly basic detergents like sulfonates, salicylates and phenolates. Dimensions of unsolvated micelles in these additives, measured by small angle diffraction of x-ray, are: 1) $CaCO_3$ core, 3—7 nm; 2) unsolvated adsorbed layers, 0.5—1.5 nm. Dimensions of the solvated micelles are 10—20 nm. Surfactant is not desorbed from $CaCO_3$ particles even at 300—350 °C, which means that it is very strongly adsorbed. Nevertheless such particles, as shown in Table I, are more firmly adsorbed on soot, than neutral detergents and dispersants. The stabilization of soot dispersions by highly basic detergents due to their structure may happen only by means of formation of a micellar adsorbed—solvated layer (Fig. 2). In that case adsorption in fact is the process of heterocoagulation of the stable micellar additive dispersion with the particles of unstable soot dispersion. According

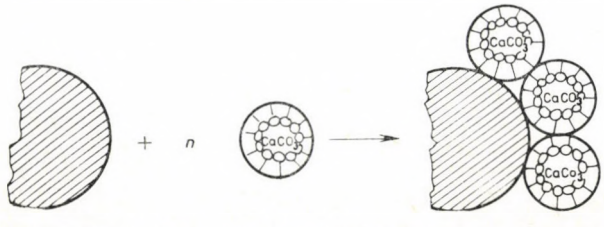


Fig. 2. Generation of the highly basic sulfonate stabilizing layer on the contaminant particles

to Ref. [20], this may lead to the stabilization of soot dispersion by means of formation of stable periodic colloid structures. Stabilization of such systems is explained as follows: the first layer of micelles is firmly fixed on the soot particles since the latter attract more strongly due to the larger size and far greater value of the Hamaker constant of soot (4 times greater than that of $CaCO_3$). Later on, during the Brownian collisions, it is not the particles which are interacting, but micelles fixed on their surface. The stability criteria for such systems are the sufficient dimensions of the micelles (depending on their diameter and solvation) and durability of their fixation on the soot particles. The second criterion is defined by the depth of the secondary minimum of the potential energy curve of soot particles (covered by micelles of the additive) and is related to the thickness of the adsorbed — solvated layer of micelles and the diameter of the carbonate core. In view of the fact that the neutral detergents exist in oils also in micellar form (the concentrations in common use are by far higher than the critical micelle concentration), we supposed that they are stabilizing the soot particles also by means of formation of micellar layers on their surface. With that purpose, the dependence of dispersive and adsorptive characteristics of highly basic and neutral sulfonates (obtained from identical raw materials) on the concentration was determined. Smooth rise of both adsorption and the soot dispersion stabilization with the increase of additive concentration was observed with the highly basic sulfonate. Sharp rise of the adsorption and stabilization above the critical micelle concentration was observed with the neutral sulfonate (Fig. 3).

Existence of a monomiceller layer of highly basic and neutral sulfonates on soot particles was proved by the method of small — angle x-ray diffraction of the initial additives and soot after adsorption of the additives on them. Small — angle x-ray diffraction pictures of dry concentrates of the neutral

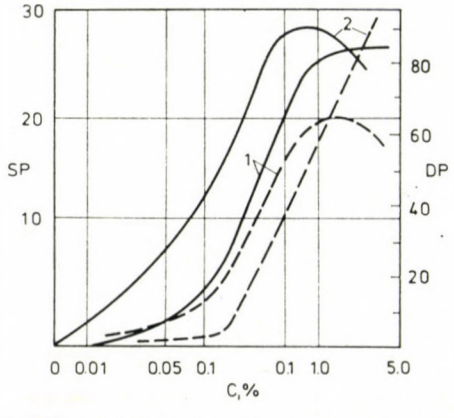


Fig. 3. Dependence of solubilizing (continuous lines) and dispersing (dashed lines) properties on the concentration of sulfonate additives. 1 — neutral sulfonate; 2 — highly basic sulfonate (SP — solubilizing and DP — dispersing properties)

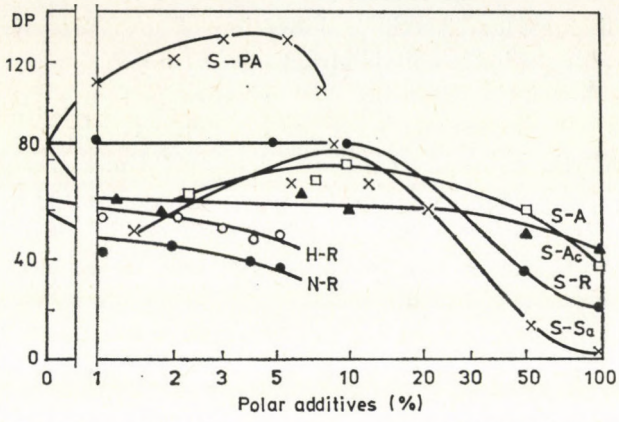


Fig. 4. Dispersion of the soot PM-75 by lubricant additives (S, H, N) in presence of various polar additives: S — succinimide; H — highly basic sulfonate; N — neutral sulfonate; R — Rodamin S; A — asphaltenes; PA — polyamines; A_c — acetic acid; S_a — sulfuric acid

and highly basic sulfonates show that they consist of closely packed micelles. Highly basic petroleum sulfonate S-300 consists of micelles with the dimensions of 7 nm, containing carbonate cores with 5 nm diameter. Neutral sulfonate, extracted from it, consists of 3 nm micelles with inorganic cores of 2 nm. When these additives are applied on soot, small — angle diffraction method registered that the interparticle distance increased by 14 and 16 nm, respectively. That confirms the existence of a monomicellar layer of these additives on the surface of the particles.

In the view of the fact that solubilization and stabilization phenomena are connected with the existence of micelles, their comparison is of considerable interest. The dispersion of soot in presence of different polar additives, generally used for the study of solubilizing power of DD additives, was investigated (Fig. 4). Some polar substances at a definite ratio can improve the dispersant ability of DD additives, but in high concentration all of them worsen it. Therefore, soot dispersions may be stabilized both by micelles and micellar solutions, that is solubilizates. The possibility of increasing the stabilizing power by means of solubilization of other agents in the micelle's core is also confirmed by the higher dispersant ability of highly basic sulfonates (in comparison with neutral ones). That happens because the highly basic sulfonates are carbonate solubilizates. The worsening of the soot dispersion at high concentration of the solubilizing agents may be considered as a competition of two phenomena, stabilization and solubilization. Ashless dispersants appeared to be the most sensitive to such an influence and the highly basic detergents were the least sensitive. This may be one of the reasons for the combination of these types of additives to give good results in the engines.

We are of the opinion that the mechanism of stabilization of impurities in engines includes mainly stabilization (dispersion) of the solid contaminants,

prevailing in the insoluble products of destruction and fuel. Dispersion in oil of agents with very limited solubility such as tars, asphaltenes and also water soluble agents such as acids and salts, occurs due to solubilization. Stabilization of solid contaminant (soot) dispersions may be carried out by means of adhesion of additive micelles or solubilizates, created by them on the surface of solid particles. Taking into account that all these processes take place in oil, that is in the dispersion medium with a small dielectric constant, micro- and macrodispersions, which are generated, are most probably stabilized due to the generation of steric repulsive forces.

Summarizing the suggested mechanism of action of DD additives, it is possible to draw the following conclusions:

1. The effectiveness of DD additives should depend more on the structure of alkyl, than on the nature of the polar groups, and should be determined to a greater extent by the alkyl chain length than its molecular mass (with the increase of linearity, its molecular mass may be lowered).

2. Efficiency of the neutral DD additives should be proportional to the ability to form sufficiently large micelles, stable at temperatures of 250—320 °C.

3. Micelles of the efficient additives should have a high energy of "adsorption" on the soot particles.

REFERENCES

[1] McLaughlin, E. G., Stuart, F. A.: VII World Petroleum Congress, Mexico City, PD 28.
[2] Wilderotter, M.: VDI-Berichte, **177,** 41 (1972)
[3] Schilling, A.: Motor Oils and Engine Lubrication. Scientific Publication Ltd, Broseley, Shropshire, England, 375 p., 1968
[4] Francois, F., Corvesier, A.: 8th World Petroleum Congress, Moscow, 1971, Khim. Tekhnol. Topl., Masel, **5,** 39 (1971)
[5] Glavaty, E. V., Rabinovich, I. L., Glavaty, O. L., et al.: Khim. Tekhnol. Topl. Masel, **3,** 60 (1976)
[6] Napper, D. H.: J. Coll. Interface Sci., **58,** 390 (1977)
[7] Hamaker, H. C.: Physica, **4,** 1058 (1937)
[8] Albers, W. A., Overbeek, J.: J. Coll. Sci., **14,** 501 (1959)
[9] Feat, G. R., Levine, S.: J. Coll. Interface Sci., **54,** 34 (1976)
[10] Vold, M. G.: J. Coll. Sci., **16,** 1 (1961)
[11] Fisher, G.: Koll.-Zeitschr., **160,** 120 (1958)
[12] Ottewill, R. H., Walker, T.: Koll.-Zeitschr. und Zeitschr. Polym., **227,** 108 (1968)
[13] Napper, D. H.: J. Coll. Interface Sci., **32,** 106 (1970)
[14] Flory, P. J.: Principles of Polymer Chemistry. Cornell University Press, Ithaca, New York, 672 p., 1953
[15] Fleer, G. I., Kopal, L. K.: Koll.-Z. und Z. Polym., **250,** 689 (1972)
[16] Glavaty O. L., Vipper, A. V., Glavaty, E. V., et al.: Khim. Tekhnol. Topl. Masel, **11,** 40 (1979)
[17] Groszek, A. J.: Proc. Int. Congress Surf. Act. Substances VII, Sect. *B*, Brussels, **1964,** 1015
[18] Glavaty, O. L., Fialkovskii, R. V., Marchenko, A. I., et al.: Kolloidn. Zh., **92,** 26 (1980)
[19] Glavaty, O. L., Marchenko, A. I., Premyslov, V. Kh., et al.: Neftepererab. Neftekhim., TSNIITEneftekhim., Moskva, **3,** 25 (1979)
[20] Efremov, I. F.: Surface and Colloid Science, Vol. **8,** Ed. E. Matijevic, p. 86—192, John Wiley and Sons, New York 1976

Acta Chimica Hungarica 116 (4), pp. 377—382 (1984)

VIBRATIONAL ANALYSIS OF THE $(UO_2Cl_4)^{2-}$ AND $(UO_2Br_4)^{2-}$ IONS

E. M. NOUR* and A. N. ABD EL-RAHMAN

(Department of Chemistry, Faculty of Science, Zagazig University, Zagazig, Egypt)

Received April 11, 1983

In revised form September 1, 1983

Accepted for publication October 7, 1983

Vibrational normal coordinate analysis based on a general quadratic force field has been made for the $(UO_2Cl_4)^{2-}$ and the $(UO_2Br_4)^{2-}$ ions. The good agreement between the calculated and the observed frequencies as well as the obtained values for the potential energy distributions in each mode made it possible to make a complete assignment for all the observed frequencies in both ions in terms of D_{4h} symmetry. The inactive B_{2u} mode in both ions is calculated at 113 and 73 cm^{-1} for $(UO_2Cl_4)^{2-}$ and $(UO_2Br_4)^{2-}$, respectively. Values of force constants are obtained. The U = O stretching force constant has value of 671 and 683 Nm^{-1} for the Cl^- and Br^- complexes, respectively. The U—Cl and U—Br stretching force constants have values of 112 and 145 Nm^{-1}. The values of force constants are used to calculate the U = O and U — Cl bond order in the $(UO_2Cl_4)^{2-}$ ion. This gives values of 1.08 and 0.365, respectively.

Introduction

Various infrared and Raman studies [1—6] in both the low and high frequency regions have been reported for both the $(UO_2Cl_4)^{2-}$ and $(UO_2Br_4)^{2-}$ ions of D_{4h} symmetry with different cations. However, the observed frequencies were tentatively assigned for both ions. There were a number of bands not observed in the case of the $(UO_4Br_4)^{2-}$ ion particularly those related to the E_u type of vibration. Several force constant calculations on the $(UO_2Cl_4)^{2-}$ ion have been reported [3, 5, 6, 7] with different assignments particularly for the A_{2u}, B_{1g}, B_{2g} and B_{2u} types of vibration. However, there are no such calculations reported on the $(UO_2Br_4)^{2-}$ ion. It was, therefore, considered worthwhile to reinvestigate these systems.

In the present work the normal coordinate treatment was carried out using a general quadratic force field utilizing no nonbonded interactions. The results obtained enabled us to determine the values of the force constants, to establish more concrete vibrational assignments and to give a full description of each vibration in both the $(UO_2Cl_4)^{2-}$ and $(UO_2Br_4)^{2-}$ ions. The effect of changing the coordinated halide ions from Cl^- to Br^- in terms of force constant values is of special interest regarding the nature of the chemical bonding in these ions.

* To whom correspondence should be addressed.

Normal coordinate calculations

Structural studies [8] on $(UO_2X_4)^{2-}$ ($X = Cl^-$ or Br^-) indicate that these ions belong to the D_{4h} symmetry where the two oxygens occupy the axial positions and the four halogens of the same type occupy the equatorial positions. Accordingly, each ion is expected to display fifteen modes of vibration four of them being doubly degenerate. The modes are distributed as follows:

$$\tau_{vib} = 2A_{1g}(R) + 2A_{2u}(IR) + B_{1g}(R) + B_{2g}(R) + \\ + B_{2u} + E_g(R) + 3E_u(IR).$$

Where (R) and (IR) refer to the Raman and infrared activities. The B_{2u} mode is inactive in both the Raman and infrared. From the above described fifteen vibrations, two, A_{1g} and A_{2u}, belong to the U = O bond stretch, while the U—X stretch shows four vibrations, belonging to the A_{1g}, B_{1g}, and E_u modes. The angle deformation motions are related to the remaining modes A_{2u}, B_{2g}, B_{2u}, $2E_u$ and E_g.

The normal coordinate analysis for both $(UO_2Cl_4)^{2-}$ and $(UO_2Br_4)^{2-}$ ions has been carried out using Wilson's FG matrix method [9]. A general quadratic potential energy function utilizing no non-bonded interactions was used with some simplifications in order to obtain meaningful values for force constants. A version of the Snyder—Schachtschneider programs [10] was used in the computation process.

The geometry, bond lengths and angles were taken from crystallographic data [8] for $(UO_2Cl_4)^{2-}$ and from related compounds in the case of $(UO_2Br_4)^{2-}$ ion. All the angles in both ions were taken as 90° and the U=O bond length

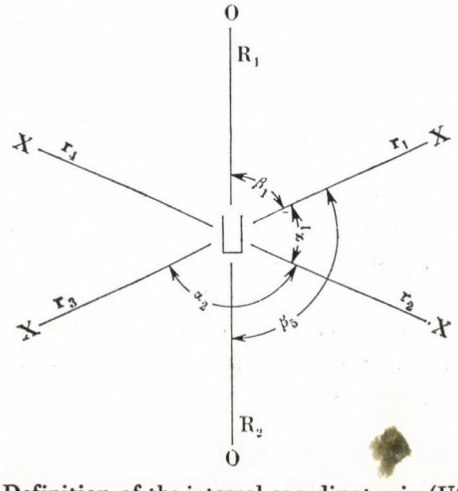


Fig. 1. Definition of the internal coordinates in $(UO_2X_4)^{2-}$

Table I

Symmetry coordinates for the $(UO_2X_4)^{2-}$; (D_{4h} symmetry)

	Description of coordinates
A_{1g}:	
$S_1 = \frac{1}{\sqrt{2}}(R_1 + R_2)$	ν(U=O)
$S_2 = \frac{1}{2}(r_1 + r_2 + r_3 + r_4)$	ν(U—X)
$S_3 = \frac{1}{2}(\alpha_1 + \alpha_2 + \alpha_3 + \alpha_4) = 0$	Redundant
$S_4 = \frac{1}{\sqrt{8}}(\beta_1 + \beta_2 + \beta_3 + \beta_4 + \beta_5 + \beta_6 + \beta_7 + \beta_8) = 0$	Redundant
A_{2u}:	
$S_5 = \frac{1}{\sqrt{2}}(R_1 - R_2)$	ν(U=O)
$S_6 = \frac{1}{\sqrt{8}}(\beta_1 + \beta_2 + \beta_3 + \beta_4 - \beta_5 - \beta_6 - \beta_7 - \beta_8)$	δ(OUX)
B_{1g}:	
$S_7 = \frac{1}{2}(r_1 - r_2 + r_3 - r_4)$	ν(U—X)
$S_8 = \frac{1}{\sqrt{8}}(\beta_1 - \beta_2 + \beta_3 - \beta_4 + \beta_5 - \beta_6 + \beta_7 - \beta_8) = 0$	Redundant
B_{2g}:	
$S_9 = \frac{1}{2}(\alpha_1 - \alpha_2 + \alpha_3 - \alpha_4)$	δ(U X_2)
B_{2u}:	
$S_{10} = \frac{1}{\sqrt{8}}(\beta_1 - \beta_2 + \beta_3 - \beta_4 - \beta_5 + \beta_6 - \beta_7 + \beta_8)$	δ(UOX)
E_g:	
$S_{11} = \frac{1}{2}(\beta_1 - \beta_3 + \beta_7 - \beta_5)$	δ(OUX)
$S_{12} = \frac{1}{2}(\beta_2 - \beta_4 + \beta_8 - \beta_6)$	
E_u:	
$S_{13} = \frac{1}{\sqrt{2}}(r_1 - r_3)$	ν(U—X)
$S_{14} = \frac{1}{\sqrt{2}}(r_2 - r_4)$	
$S_{15} = \frac{1}{2}(\alpha_1 + \alpha_4 - \alpha_3 - \alpha_2)$	δ(XUX)
$S_{16} = \frac{1}{2}(\alpha_1 - \alpha_4 - \alpha_3 + \alpha_2)$	
$S_{17} = \frac{1}{2}(\beta_1 - \beta_3 + \beta_5 - \beta_7)$	δ(OUO)
$S_{18} = \frac{1}{2}(\beta_2 - \beta_4 + \beta_6 - \beta_8)$	

ν, stretching mode; δ, bending mode

as of 181 pm. The internal coordinates for the $(UO_2X_4)^{2-}$ type of ions are given in Fig. 1.

The symmetry coordinates used in the calculations for both $(UO_2Cl_4)^{2-}$ and $(UO_2Br_4)^{2-}$ under D_{4h} symmetry were constructed as given in Table I. It should be noted that there are three redundant coordinates, belonging to $2A_{1g}$ and B_{1g}, involved in the construction of both the **F** and **G** matrices. However, the redundant coordinate gives zero frequency in the final results. Observed frequencies for both ions were taken from different sources [1—6] and in particular from the work of Newbery [1].

A series of force constants were introduced and altered until a series of frequencies were obtained which were as close as possible to those observed. The obtained set of force constants used in the computation as well as the observed and calculated frequences are given in Tables II and III. To make a reasonable assignment for each of the observed frequencies, the potential energy distribution in each normal vibration was calculated as given in Table III. The assignments for the $(UO_2Cl_4)^{2-}$ ion and the values of force constants for the U=O and U—Cl agree with those reported by Ohwada [6]. However, his values of the force constants for the angle deformation of Cl—U—Cl and OU—Cl are quite low compared with our values. This may be related to that the calculation of Ohwada [6] was based on the use of a Urey—Bradley force field which emphasizes non-bonded interactions. In the present work we have chosen a general quadratic force field utilizing no non-bonded interactions. The latter is generally the preferred force field although certain approximations or assumptions are often necessary. The force constant values

Table II

Quadratic force constants[a] *for* $(UO_2Cl_4)^{2-}$ *and* $(UO_2Br_4)^{2-}$ *ions*

Symbol	Description	Value	
		$(UO_2Cl_4)^{2-}$	$(UO_2Br_4)^{2-}$
F_R	U=O strech	671	683
F_r	U—X strech	112	145
F_α	X—U—X angle bend	48	39
F_β	O—U—X angle bend	92	81
F_{RR}	U=O, U=O	—28	—23
F_{rr}	U—X, U—X	14	11
$F_{\alpha\alpha}$	X—U—X, X—U—X	19	8
$F_{\beta\beta}$	OUX, OUX	21	19
$F_{R\beta}$	U=O, OUX	13.1	11
$F_{r\beta}$	U—X, OUX	14.5	6

[a] Stretching constants in Nm^{-1}; bending constants in $Nm^{-1}\,rad^2$

Table III

Observed and calculated frequencies, potential energy distributions and vibrational assignments for $(UO_2Cl_4)^{2-}$ *and* $(UO_2Br_4)^{2-}$ *ions*

	Frequency (cm^{-1})		Potential energy distribution[a]				Assignments
	Observed	Calculated	$F_{U=O}$	F_{U-X}	F_α	F_β	
$(UO_2Cl_4)^{2-}$	831	826	104	0	0	0	A_{1g}: ν_s (U=O)
	265	271	0	72	0	0	ν_s (U—Cl)
	907	909	96	0	0	0	A_{2u}: ν_{as} (U=O)
	—	139	0	0	0	101	δ (OUCl)
	203	212	0	115	0	0	B_{1g}: ν_{as} (U—Cl)
	131	142	0	0	124	0	B_{2g}: δ (Cl UCl)
	i.a.	113	0	0	0	100	B_{2u}: δ (OUCl)
	67	71	0	0	0	138	E_g: δ (OUCl)
	264	258	0	8	1	82	E_u^*: δ (OUO)
	240	241	0	109	3	21	ν_{as} (U—Cl)
	122	116	0	3	121	1	δ (ClUCl)
$(UO_2Br_4)^{2-}$	832	836	103	0	0	0	A_{1g}: ν_s (U=O)
	198	194	0	81	0	0	ν_s (U—Br)
	925	920	97	0	0	0	A_{2u}: ν_{as} (U=O)
	—	93	0	0	0	[0]	δ (OUBr)
	165	168	0	108	0	0	B_{1g}: ν_{as} (U—Br)
	89	86	0	0	101	0	B_{2g}: δ (BrUBr)
	i.a.	73	0	0	0	100	B_{2u}: δ (OUBr)
	53	51	0	0	0	217	E_g: δ (OUBr)
	253	251	0	25	1	82	E_u^*: δ (OUO)
	—	198	0	81	1	18	ν_{as} (U—Br)
	—	71	0	3	107	1	δ (BrUBr)

[a] Potential energy distribution totals 100 including contributions from interaction constants, which are not shown

* Coupled motions

given in Table II show that the U=O stretching force constants in both $(UO_2Cl_4)^{2-}$ and $(UO_2Br_4)^{2-}$ ions are very close, with value of 671 and 683 Nm^{-1}, respectively. This result indicates that the U=O bond character in both ions is very little effected by the change of the type of the coordinated halogen from Cl^- to Br^- in the equatorial positions. In other words, while the U=O modes share both the A_{1g} and A_{2u} symmetry with other vibrational modes, it appears that the U=O modes do not couple with any of the others. This result is also in good agreement with that based on the calculated force constants of the UO_2^{2+} species with various equatorial ligands using the equation

developed by Jones [11], $r = BF^{-1/3} + d$, where r is the U=O bond length (A°) and B and d are constants with values of 1.08 and 1.17, respectively. The above equation gives values of $\sim$680 Nm^{-1} for the U=O force constant in both the $(UO_2Cl_4)^{2-}$ and $(UO_2Br_4)^{2-}$ ions.

It is of interest to note that the force constant for the U—Br bond stretch is higher than that for the U—Cl. Using the bond stretch force constant as an approximate measure of equilibrium bond strength, it appears that the U—Br bond in $(UO_2Br_4)^{2-}$ is 1.21 times stronger than the corresponding U—Cl bond in $(UO_2Cl_4)^{2-}$ ion. This may suggest that the U—Br is more ionic than the U—Cl bond in these uranyl ions.

Poltizer and Kasten [12] have developed a method of calculating the bond order based on the stretching force constant. This method was tested [13] for both linear and non-linear polyatomic molecules and proved to give satisfactory results. The bond order is calculated according to the definition: bond order = $0.55747\sqrt{F/R}$ where, F and R are the force constant (Nm^{-1}) and the bond length (pm), respectively. Bond order values for U=O and U—Cl in the $(UO_2Cl_4)^{2-}$ ion are calculated as 1.08 and 0.365, respectively.

Finally, the B_{2u} mode in both ions, which is infrared and Raman inactive, is calculated at 113 and 73 cm^{-1} for the $(UO_2Cl_4)^{2-}$ and $(UO_2Br_4)^{2-}$ ions, respectively.

REFERENCES

[1] Newbery, J. E.: Spectrochim. Acta, **25A**, 1699 (1969)
[2] Bullock, J. I., Parrett, F. W.: Can. J. Chem., **48**, 3095 (1970)
[3] Ohwada, K.: Spectrochim. Acta, **31A**, 973 (1975)
[4] Day, J. P., Venanzi, L. M.: J. Chem. Soc. (A), **1966**, 1364
[5] Ohwada, K.: J. Inorg. Nucl. Chem., **40**, 1369 (1978)
[6] Ohwada, K.: Appl. Spect., **34**, 327 (1980)
[7] Risbud, A. C., Lele, A. B., Kale, A. J., Sathiananden, K.: Indian J. pure Appl. Phys., **13**, 94 (1975)
[8] Hall, D., Rae, A.,D., Waters, T. N.: Acta Cryst., **20**, 160 (1966)
[9] Wilson, E. B., Decius, J. C., Cross, P. C.: Molecular vibrations, McGraw-Hill, New York 1955
[10] Schachtschneider, J. H.: Vibrational Analysis of polyatomic Molecules, **V** and **VI**. Technical report, Shell Development Co., Emeryville California 1964
[11] Jones, L. H.: Spectrochim. Acta, **15**, 409 (1959)
[12] Poltizer, P., Kasten, S. D.: J. Phys. Chem., **80**, 283 (1976)
[13] Kumar, V., Verma, U. P., Pandey, A. N.: J. Mol. Struc., **49**, 411 (1978)

Acta Chimica Hungarica 116 (4), pp. 383—388 (1984)

INFLUENCE OF THE LIQUID JUNCTION POTENTIAL ON HYDROXIDE ACTIVITY MEASUREMENTS

B. LEHOCZKY and L. BARCZA*

(Institute of Inorganic and Analytical Chemistry, L. Eötvös University, H-1088 Budapest, Múzeum krt. 4/B)

Received July 28, 1983

Accepted for publication October 7, 1983

The change of hydroxide activity can be followed using mercury—mercury oxide electrodes even in more concentrated solutions, but the liquid junction potential formed on the interface between salt bridge and solution can be rather high. Studying this effect in solutions of constant ionic strength, the evaluation of the measured electrode potential (E_m, at 25.00 °C and in mV) has been found to obey the equation:

$$E_m = E_0 + 59.15 \lg \frac{[OH^-](1 + K[OH^-]_R)}{1 + K[OH^-]}$$

where $[OH^-]_R$ is the (constant) hydroxide ion concentration in the salt bridge, and K is a constant characteristic for the system. (Its values for 2, 4 and 6 mol dm^{-3} $NaNO_3$ supporting electrolytes are collected in Table I.)

The system under investigation

Several empirical, semi-empirical and theoretical methods are known for the interpretation, determination or/and elimination of the liquid junction potential disturbing hydrogen ion activity measurements, but none is available for hydroxide—anion systems, in spite of the fact that the mobility of hydroxide ion exceeds those of other anions by nearly a whole order of magnitude and, consequently, a rather high liquid junction potential could appear, falsifying the direct evaluation of the measured data.

Recently, an electrode pair constructed from mercury/mercury oxide has been developed [1], which is suitable for the potentiometric determination of hydroxide ion activity (or concentration) in the range of 10^{-2}—10^{1} mol dm^{-3} concentrations. The reproducibility is given as ± 0.3 mV. It can be supposed that the error caused by liquid junction potential is well above this value.

Our previous work [2] dealt with the consideration of the liquid junction potential in detail, which was caused by hydrogen ion/cation exchange in solutions of constant ionic strength; we have tried to solve the problem of hydroxide/anion exchange by a similar approach.

* To whom correspondence should be addressed.

The considerations are valid only for systems of constant ionic concentrations:

$$[M^+] = [A^-] + [OH^-] = \text{const.} \tag{1}$$

and at constant temperature. The assumption can be accepted that the ionic mobilities and activity coefficients are constant in such a solution, that is

$$f_M = \text{const.} \quad f_A = \text{const.} \quad f_{OH} = \text{const.} \tag{2}$$

and

$$u_M = \text{const.} \quad u_A = \text{const.} \quad u_{OH} = \text{const.} \tag{3}$$

(at least up to a given hydroxide—anion exchange), which permits to solve the general equation of liquid junction potential:

$$\mathrm{d}E_d = -\frac{R \cdot T}{F} \sum \frac{n_i}{z_i} \mathrm{d} \ln a_i \tag{4}$$

(where R, T and F are the usual symbols of constants; n_i, z_i and a_i are the transport number, charge and activity of the i-th ion passing through the interface), since concentrations can be used instead of activities. (Of course, the effect of assumptions will appear in the values of "molar conductivities" [Eq. 10].)

It follows that the reproducibility of the liquid junction potential depends not only on the constancy of concentrations but on the construction of the electrodes, too, first of all on the cylindrical symmetry of the interfaces [3], which is given by the shape of electrodes [1] used.

A further complication is that the mercury—mercury oxide electrode is stable only in alkaline media, the reference electrode must be connected by a salt bridge containing alkali hydroxide of constant concentration to the solution to be investigated. So the cell under investigation can be characterized as follows:

reference	$[OH^-]_R$ MOH	$[OH^-]$ MOH	meassuring
electrode	C—$[OH^-]_R$ MA	(C—$[OH^-]$) MA	electrode

where $[OH^-]$ is the hydroxide ion concentration to be measured, C the total concentration of the electrolyte, and $[OH^-]_R$ the constant hydroxide content in the salt bridge.

As the cation and its concentration is equal on both side of the interface between the salt bridge and the solution to be measured, the liquid junction potential is only influenced by the changes in the concentrations of anions.

Substituting the expression of transference number using ionic mobilities and concentrations:

$$n_i = \frac{u_i c_i}{\Sigma u_i c_i} \tag{5}$$

into Eq. (4), and knowing that the hydroxide ion concentration (x) can be changed passing through the interface from $[OH^-]$ to $[OH^-]_R$, the part of liquid junction potential caused by the hydroxide ions can be expressed as

$$E_{d,OH} = -\frac{R \cdot T}{F} \int_{[OH^-]_R}^{[OH^-]} \frac{x u_{OH}}{(C - x) u_A + x u_{OH} + C u_M} \, d \ln x \tag{6}$$

Integrating the last equation between the given limits, the following solution can be obtained:

$$E_{d,OH} = -\frac{R \cdot T}{F} \frac{u_{OH}}{u_{OH} - u_A} \ln \frac{C(u_M + u_A) + [OH^-](u_{OH} - u_A)}{C(u_M + u_A) + [OH^-]_R (u_{OH} - u_A)} . \tag{7}$$

The anion concentration changes between $(C - [OH^-])$ and $(C - [OH^-]_R)$ that is, on integrating an equation similar to Eq. (6), the liquid junction potential caused by the anion concentration change can be calculated as

$$E_{d,A} = -\frac{R \cdot T}{F} \frac{u_A}{u_A - u_{OH}} \ln \frac{C(u_M + u_A) + [OH^-](u_{OH} - u_A)}{C(u_M + u_A) + [OH^-]_R (u_{OH} - u_A)} . \tag{8}$$

Combining Eqs (7) and (8), we have the expression for liquid junction potential in the system under investigation:

$$E_d = E_{d,OH} + E_{d,A} = -\frac{R \cdot T}{F} \ln \frac{C(u_M + u_A) + [OH^-](u_{OH} - u_A)}{C(u_M + u_A) + [OH^-]_R (u_{OH} - u_A)} . \tag{9}$$

As the molar conductivities in the given solution of C total (constant) concentration are

$$u_M + u_A = \lambda_{MA} \quad u_M + u_{OH} = \lambda_{MOH} \tag{10}$$

(where λ_{MOH} is not strictily identical with the molar conductivity of C mol dm^{-3} MOH, but its constancy as a function of MOH concentration, that is, the validity of earlier assumptions can be experimentally controlled). Upon substitution of R, T and F for 25.00 °C and conversion to mV and lg, Eq. (9) changes to

$$E_d = -59.15 \ln \frac{C\lambda_{MA} + [OH^-](\lambda_{MOH} - \lambda_{MA})}{C\lambda_{MA} + [OH^-]_R (\lambda_{MOH} - \lambda_{MA})} . \tag{11}$$

As several values in last equation are constant, they can be reduced to

$$K = \frac{\lambda_{MOH} - \lambda_{MA}}{C\lambda_{MA}} \tag{12}$$

and the liquid junction potential can be represented as

$$E_d = -59.15 \lg \frac{1 + K[OH^-]}{1 + K[OH^-]_R} . \tag{13}$$

The molar conductivities λ_{MOH} and λ_{MA} can easily be measured in solutions of total concentration C by conductometry, that is, the liquid junction potential interesting for potentiometric measurements can be characterized in an independent way.

The electrode potential of the given cell is combined of three parts

$$E_m = E_0 + E_p + E_d \tag{14}$$

(where E_m is the measured, E_p the ideal electrode potential and E_0 is a cumulative constant characteristic of the cell) or in other form (at 25 °C and in mV):

$$E_m = E_0 + 59 \cdot 15 \lg [OH^-] - 59.15 \lg \frac{1 + K[OH^-]}{1 + K[OH^-]_R} . \tag{15}$$

The final expression is

$$E_m = E_0 + 59.15 \lg \frac{[OH^-](1 + K[OH^-]_R)}{1 + K[OH^-]} . \tag{16}$$

As E_0 can be measured separately, the unknown concentration of hydroxide ions can be calculated based on known constants

$$Y = \frac{E_m - E_0}{59.15}$$

and

$$[OH^-] = \frac{10^Y}{1 - K([OH^-]_R - 10^Y)} . \tag{17}$$

Experimental

The possibilities are demonstrated by data for NaOH — $NaNO_3$ systems.

The sodium ion concentration was kept constant at 2.000; 4.000 or 6.000 mol dm^{-3}; the temperature was kept at 25.00 ± 0.05 °C. During the measurements, the nitrate was

Table I

Constants measured in sodium nitrate solutions

C mol dm^{-3}	$NaNO_3$ mS	NaOH mS	K dm^3 mol^{-1}
2.000	63.7	142.4	0.617
4.000	44.2	96.2	0.293
6.000	31.9	62.6	0.160

replaced by hydroxide up to 60%. Carbonate-free sodium hydroxide and recrystallized sodium nitrate were used, their concentrations were checked very carefully. The conductivities were determined with a Radiometer CDM 2d instrument; a Radiometer pHM 4d potentiometer was used to check the validity of Eq. (16); the reference and measuring electrodes were as given in Ref. [1].

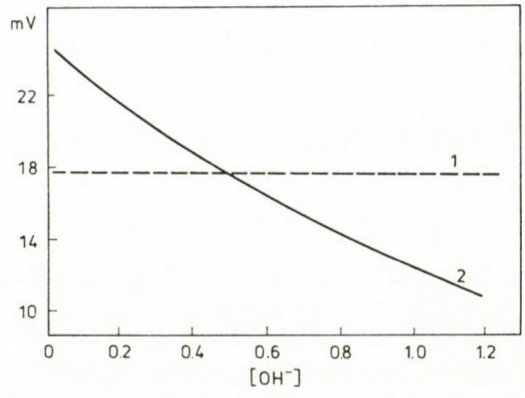


Fig. 1. Calculations of E_0 values with (1) and without (2) liquid junction potential. $C = 2.000$ mol dm^{-3}; $[OH^-]_R = 0.500$ mol dm^{-3}

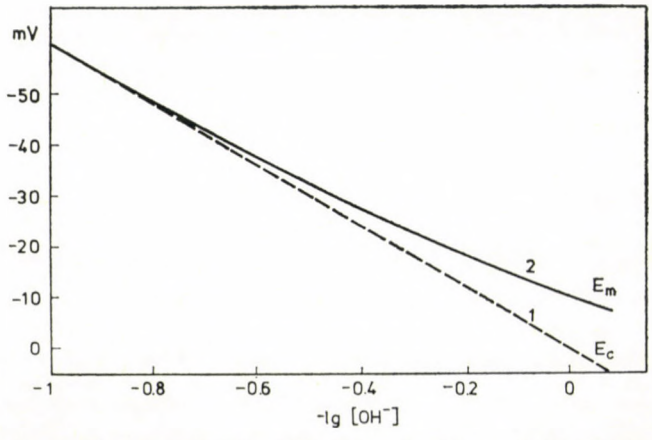


Fig. 2. Calculations of measured data with (1) and without (2) liquid junction potential. $C = 2.000$ mol dm^{-3}; $[OH^-]_R = 0.100$ mol dm^{-3}

The measured and calculated constants for three background electrolytes are summarized in Table I. It can be seen that with decreasing total concentrations, the influence of liquid junction potential increases.

One of the possibilities to check the validity of Eq. (16) is to calculate the E_0 values with and without liquid junction potential. In Fig. 1, these results are represented for 2.000 mol dm^{-3} $NaNO_3$, when the reference electrode was prepared with 0.500 mol dm^{-3} NaOH and 1.500 mol dm^{-3} $NaNO_3$. Of course, if the hydroxide concentrations are equal in the salt bridge and in the solution, the liquid junction potential is 0 and its sign changes. It follows that measurements with other hydroxide concentrations in the salt bridge show a similar picture, but the intersections appear at other concentrations.

The influence of liquid junction potential is rather high in solutions of 2.000 mol dm^{-3} total concentration, as shown by Fig. 2, where the measured data were calculated by two different ways: using Eq. (16) or neglecting the liquid junction potential. The results show that the difference (error) amounts to as high as 50%. Using Eq. (16), the effect of liquid junction potential can be reduced below the error of the reproducibility.

At higher total concentrations of background electrolyte, as the data in Table I show, the effect of liquid junction potential is smaller, but its neglect causes large errors in those cases, too.

REFERENCES

[1] Szabó, Z. G., Pálfalvi-Rózsahegyi, M., Orbán, M.: Acta Chim. Acad. Sci., **97**, 327, (1978)
[2] Barcza, L., Stróbl, L., Lehoczky, B.: Acta Chim. Acad. Sci. Hung. **63**, 319 (1970)
[3] Szabó, Z. G.: Z. Phys. Chem., **174A**, 33 (1935)

Acta Chimica Hungarica 116 (4), pp. 389–405 (1984)

DIRECT DETERMINATION OF TRACE ELEMENTS IN POLYACRYLAMIDE SOLUTIONS BY FLAME ATOMIC ABSORPTION SPECTROPHOTOMETRY, II*

THE EFFECT OF POLYMERS ON NEBULIZATION PHENOMENA

I. LAKATOS** and J. LAKATOS

(Chemical Research Laboratory for Mining, Hungarian Academy of Sciences, H-3515 Miskolc-Egyetemváros, POB 2.)

Received July 20, 1983

Accepted for publication October 11, 1983

The nebulization phenomena of polymer solutions were studied. It was concluded on the basis of experimental results that the unfavourable matrix effect of polymers can be attributed to a considerable diminishing of nebulization efficiency, and through this of the quantity of substance getting into the flame. Relationships proposed for the description of the partial processes of nebulization are not valid for polymer solutions, in view of the fact that these solutions have non-Newtonian flow characteristics, and are viscoelastic. Presumably the internal network formed by intermolecular interaction is responsible for the poor nebulization efficiency of polymer solutions. The authors consider the phenomena observed of general validity for all the atomic spectroscopial methods, if pneumatic nebulizers with mixing chamber are used for the feeding of the sample into the analytical light source.

Introduction

Few data are available in the literature on the qualitative and quantitative analysis of trace elements in macromolecular substances by atomic absorption methods. Slavin [1] and Drackman [2] analyzed solid polymers after acid decomposition, while Yanagisowa et al. [3] after ashing, in aqueous solution, and Henn [4] by electrothermal atomization. Olivier [5] used a direct atomic absorption method for the analysis of polymer solutions, while Caton and Bremner [6], further Bills et al. [7] applied a flame photometric analysis to determine trace elements in gelatin and sugar solutions, giving a matrix effect similar to that of polymers.

In agreement with the latter authors [6, 7], it has been established in our previous publication [8] that with increasing concentration, molecular mass and ionization state of the polymer present in the sample solution, absorbance measured at the resonance lines decreases, and as a consequence the detection power of the analytical method. Though rank-correlation analysis showed a close correlation between the analytical signal and the take-up rate

* Part I see Ref. [8].
** To whom correspondence should be addressed.

and the dynamic viscosity of the solution, it has been pointed out that decrease in take-up rate alone cannot be made responsible for the unfavourable matrix effect. In view of the fact that according to experimental data the role played by polymers in atomization processes is negligible, a further investigation of the nebulization phenomena of high-viscosity solutions seemed necessary. Thus, our present study deals with the partial processes of the introduction of the sample into the flame, and within this with the role of rheological properties, using flame emission and flame atomic absorption techniques.

Experimental

Experiments were performed on a single-beam spectrometer Zeiss Model AAS-1, in flame emission and atomic absorption mode of operation. In the latter case Zeiss hollow cathode lamps were used, uniformly with a heating current of 5 mA. Data were recorded on a Zeiss K-200 recorder and a digital printer made in the laboratory. Other experimental conditions are summarized in Table I.

A concentric nebulizer was used for studying of the nebulization phenomena. In measurements carried out at controlled take-up rate, the liquid was fed in with an automatic micropump (Radelkis OP-930).

The mass balance of the nebulization process

$$F_1 = F_a + F_v + F_w \tag{1}$$

was determined by the direct measurement of F_1, F_a, F_w, and from these F_v was calculated. Nebulization efficiency was calculated from the following relationship:

$$\varepsilon_n = \frac{F_a}{F_1} \cdot 100 \tag{2}$$

According to statistical tests, the relative error of the determination of ε_n is 5—10%. For the direct measurement of the liquid vapour getting into the flame the filter method described by Smith and Browner [9] was used. Fiberglass filter, type Whatman GF/F of 0.5 μm pore diameter was used as filter layer, the 100% aerosol retention of which was checked by feeding

Table I

Experimental conditions

Element	Li	K	Mg	Ca	Mn
Wavelength, nm	670.8	404.4	285.2	422.7	279.8
Mode of operation	FES	FES	AAS	AAS	AAS
Slit width, mm	0.05	0.05	0.05	0.05	0.05
Burner	Meker type		Three-slot		
Burner slot, cm			3×5	3×5	3×5
Type of flame	acetylene/air				
Rate of air flow, $dm^3\,h^{-1}$ (2.10^5 Pa)	500	500	500	500	500
Rate of acetylene flow, $dm^3\,h^{-1}$ (1.10^5 Pa)	80	80	100	120	100
Flame height of observation, mm	10	10	10	10	10

the aerosol-free gas into the flame. An Andersen's cascade impactor was used for the approximate determination of the size distribution of the aerosol particles getting into the flame. In the latter case the original arrangement of Novak and Browner [10] was modified, so that the aerosol leaving the nebulization chamber was fed without dilution into the impactor, and the aerosol fraction below 1 μm was introduced into the fibreglass filter instead of the aerosol spectrometer.

The following acrylamide—acrylic acid copolymers were used as model substances:

Marking of the polymer	Average molecular mass, 10^6	Degree of hydrolysis, %
NP-10	1.0	2—7
AP-30	3.5	30
AN-34	9.5	40

The rheological properties of the polymer solutions of different concentration were determined with Contraves Low Shear 30 viscometer in rotational and in oscillo-rheometer mode of operation.

Results and Discussion

Experiments show that relative intensities measured at the lithium and potassium lines, and relative absorbances measured at the calcium and magnesium lines decrease according to the curves shown in Figure 1 to a near identical degree with increasing polymer concentration in the sample solution.

As concerns absorption technique, element independence is true only in the case when decrease in absorbance caused by the matrix effect of the polymer is connected with nebulization and sample feeding. The absorbance of an arbitrarily chosen element is namely according to Lambert—Beer's law:

$$A = klN \tag{3}$$

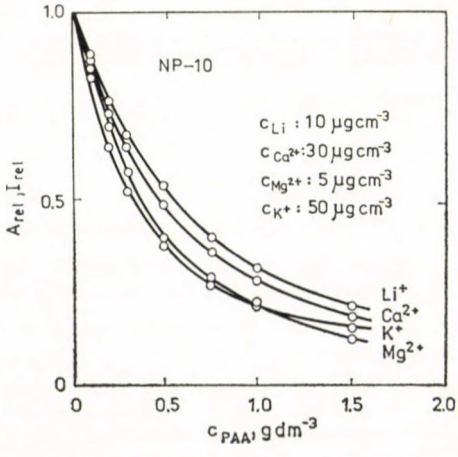


Fig. 1. Effect of polymer concentration on relative intensities and absorbances

and the number of free atoms in unit volume of the flame

$$N = \frac{F_a c \beta_s \beta_v \beta_a}{v} . \tag{4}$$

Thus

$$A = \frac{k\, l\, F_a c \beta}{v} \tag{5}$$

if

$$\beta = \beta_s \beta_v \beta_a . \tag{6}$$

Assuming that k, l, c and v are constant, the relative absorbance at different polymer concentrations is:

$$\frac{A_{c,i}}{A_{c,0}} = \frac{F_{a,i}}{F_{a,0}} \frac{\beta_1}{\beta_0} . \tag{7}$$

The indentity of relative absorbances

$$\left[\frac{A_{c,i}}{A_{c,0}}\right]_{Me_1} = \left[\frac{A_{c,i}}{A_{c,0}}\right]_{Me_2} = \ldots . \left[\frac{A_{c,i}}{A_{c,0}}\right]_{Me_n} \tag{8}$$

is satisfied according to Takado and Nakano [11] if

$$\frac{\beta_i}{\beta_0} = 1 \tag{9}$$

that is, the analytical signal reduction, observed as a function of polymer concentration, can be exclusively brought into connection with nebulization or feeding problems. Though deviation between the curves shown in Figure 1 exceeds measuring accuracy, so that condition (9) is only approximately satisfied, it can be concluded that the matrix effect can be attributed to a decisive degree (>90%) to its effect on the partial processes of polymer solution feeding. On this basis the conclusion can be ventured already at this point that phenomena and experimental experiences discussed are of general validity for all those atomic spectroscopic methods, where pneumatic nebulizers with external mixing chamber are used for the introduction of the sample into the analytical light source.

Relationships are known for the description of the liquid flow rate of nebulization, which include the viscosity of the solutions as independent variable. In simple flow models only this is taken into consideration of the physical and chemical characteristics of liquids, while in other cases surface tension, boiling point, etc. are also incorporated in the relationships. In view

of the fact that polymers result on the one hand extreme increase in viscosity, and on the other hand, their effect on surface tension is in most of the cases negligible, the rheological concept dominates also in this part of our study.

Aerosol flow rate getting into the atomization system is a function of take-up rate, initial aerosol drop size distribution and of the processes proceeding in the mixing chamber [12]. Dependence of take-up rate on polymer concentration has been discussed in our previous study [8]. In our present work we restrict to investigate only, whether Hagen—Poisseuille's equation is suitable for the description of take-up rate. The application of the relationship to concentric nebulizers is accepted [13], though its general validity was questioned by several authors because of capillary end effect, slip effect, the formation of resting layers, etc. [14—16]. In our case the applicability of the Hagen—Poisseuille equation is questioned also in principle by the fact that this equation can describe only in the case of solutions with Newtonian flow properties, so called particulate solutions, the flow of liquids in a capillary. However, disperse systems (molecular colloids, suspensions, emulsions, etc.) are characterized by non-Newtonian properties, which can be traced back to molecular effects or interaction between the particles. In polymer solutions the non-Newtonian property is manifested in first approximation by structural viscosity as shown in Figure 2, that is, the viscosity of the solution strongly depends on the shear rate.

Moreover, according to another approach, the take-up rate of polymer solutions cannot be described by the known simple relations, because these are valid only for perfectly viscous liquids. As contrary to this, the aqueous

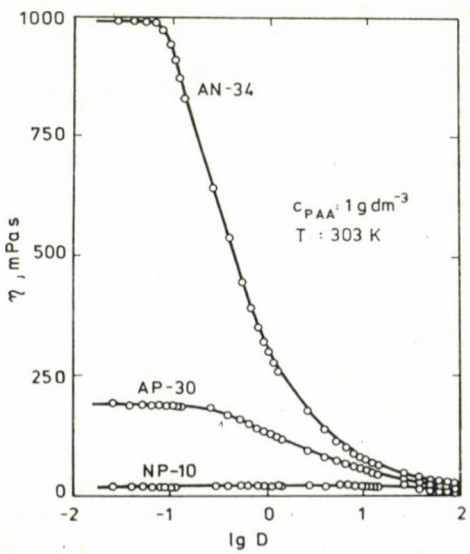


Fig. 2. Dependence of the apparent viscosity of polymer solutions on the shear rate

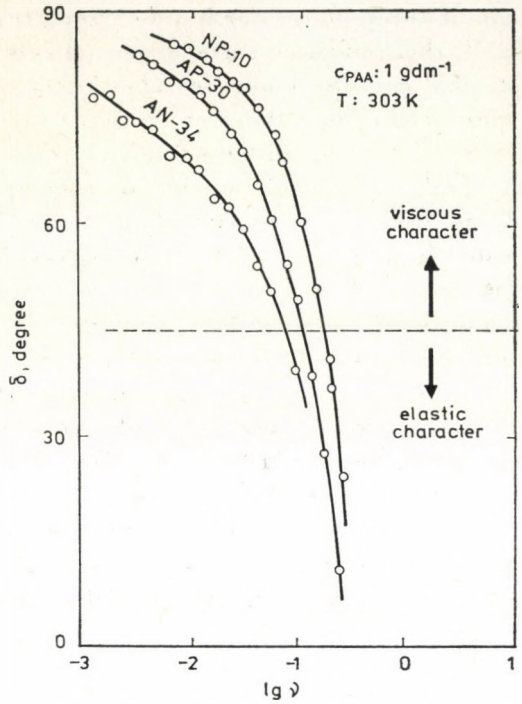


Fig. 3. Viscoelastic character of polymer solutions. Loss angle as a function of deformation frequency

solutions of chain like polymers can be considered because of intermolecular interaction as solutions of so called network type, so that they are qualified from the rheological aspect as viscoelastic systems. If the viscous and elastic character of the polymer solutions studied is characterized by the loss angle, than it becomes evident on the basis of Figure 3, that the solutions of 1 gdm^{-3} of the polymers used as model substances can be considered only in a very narrow range of shear rate (frequency) as approximately (but not perfectly) viscous, while outside this range, e.g. in the region of regular take-up rate, fundamentally the elastic character is dominant.

However, under consideration of the foresaid it is remarkable that the reciprocal of take-up rate changes linearly with the length of the capillary, and the take-up rate with the pressure difference established between the two ends of the capillary. This seems to indicate an apparent validity of the Hagen—Poisseuille relationship. (Fig. 4—6). This can be explained by the circumstance that at the actual take-up rates used the change in shear rate produced by changing the length of the capillary and the pressure difference does not result in a considerable change in viscosity, because in the metal capillary determining flow resistance the characteristic shear rate falls into

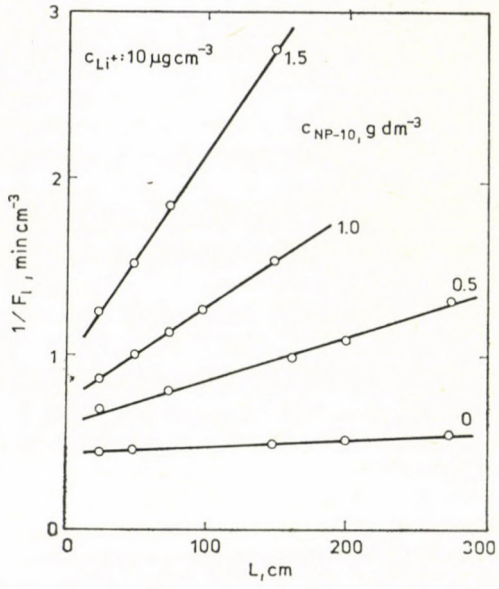


Fig. 4. Dependence of the reciprocal of take-up rate on the length of the polyethylene capillary at different polymer concentrations

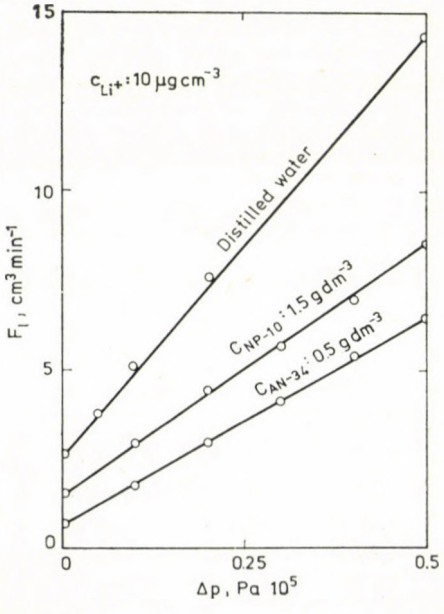


Fig. 5. Dependence of take-up rate on nebulizing pressure in the feeding of distilled water and various polymer solutions

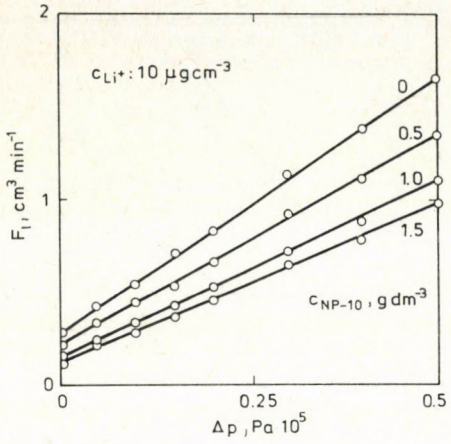


Fig. 6. Dependence of take-up rate on nebulizing pressure in the feeding of polymer solutions of different concentration

the lower, i.e. essentially Newtonian section of the yield curve. For example, in the metal capillary used by us the shear rate was 3100 s^{-1}, while in the polyethylene capillary 85 s^{-1} at an take-up rate of 2.26 cm^3 min^{-1}. Under these conditions an investigation of the dependence of take-up rate on viscosity causes difficulties, since on the one hand the apparent viscosity of the polymer solution is higher in the polyethylene capillary than in the metal capillary, and on the other hand the flow of the polymer solution in the former is still of non-Newtonian character. A further problem is raised by the fact that deviation from Newtonian flow character strongly depends on the structure and concentration of the polymer. In conjunction with this the well known fact should be taken into consideration that in the flow of liquids in pipes frictional pressure loss is substantially decreased, and the upper limit of

Table II

Dependence of take-up rate, measured and calculated viscosity, and of the product $F_1\eta$ on the concentration of Polymer NP-10

c_{PAA} gdm^{-3}	F_1 cm^3 min^{-1}	$\eta_{meas.}$ mPas	$F_1\eta_{meas.}$	$\eta_{calc.}$ mPas
0	2.27	0.987	2.24	0.987
0.25	2.27	1.136	2.59	0.986
0.50	2.14	1.390	2.97	1.046
0.75	1.89	1.730	3.26	1.185
1.00	1.67	2.145	3.58	1.340
1.25	1.49	2.550	3.79	1.500
1.50	1.34	2.980	3.99	1.671

Table III

Dependence of take-up rate, measured and calculated viscosity, and of the product $F_1\eta$ on the concentration of polymer AN-34

c_{PAA} gdm^{-3}	F_1 cm^3 min^{-1}	η meas. mPas	$F_1\eta_{meas.}$	$\eta_{calc.}$ mPas
0	2.27	0.987	2.24	0.987
0.1	1.90	2.350	4.46	1.173
0.3	1.23	8.000	9.84	1.810
0.4	0.88	11.500	10.12	2.530
0.5	0.71	17.000	12.07	3.140

laminar flow is shifted towards higher Reynolds numbers in the presence of chain like polymers [17—19]. This results finally that take-up rate calculated with Hagen—Poisseuille's equation is different from the value measured, if the apparent viscosity, characteristic only at high or low shear rates and measured with an experimentally independent method, is substituted into the formula. The difference between calculated and measured values is the larger, the higher the molecular mass, the degree of hydrolysis and the concentration of the polymer (Table II and III).

On the basis of the data in the two tables it can be unequivocally established that in the pneumatic nebulization of network polymer solutions with non-Newtonian flow characteristics the product of take-up rate and viscosity is not constant, but increases with increasing molecular mass, degree of hydrolysis and concentration of the polymer. From the point of view of take-up rate the liquid behaves as if its viscosity were lower than the value measured. The so called effective apparent viscosity, calculated with Hagen—Poiseuille's equation, given in the last columns of Tables II and III, may be a fraction of the measured value, depending on the structure and the concentration of the polymer.

It is evident on the basis of results discussed so far that the apparent validity of the Hagen—Poisseuille relationship holds true at the most for a solution of given concentration of a distinct polymer, and this only in the case, when the modification of take-up rate occurs via changing L or ΔP. We wish to stress, however, that in the nebulization of solutions of different types and concentrations it is erroneous also in principle to use relationships valid for perfectly viscous systems of Newtonian flow properties for the description of the flow of liquids having structural viscosity or viscoelastic properties.

It was shown earlier that the take-up rate of the polymer solution rapidly decreases with increasing polymer concentration. Therefore, from

the practical point of view the compensation of increased flow resistance, that is, the maintenance of constant take-up rate seems logical. Aerosol concentration in the nebulizing chamber increases with increasing take-up rate, but the coarsening of droplet size increases also the losses. Thus, as a resultant of the two effects, the amount of aerosol getting into the flame changes as a function of take-up rate according to a curve passing through a maximum or revealing saturation value, depending on the construction of the system [20]. Though the analytical signal plotted versus take-up rate is also a function of other factors, the relationship reflects in our case the change in quantity of the metal ions got into the flame. Figure 7 shows the intensity of a lithium line as a function of take-up rate at different polymer concentrations. It can be seen already from this figure, but still more evidently from Figure 8, that the effect of the polymer on take-up rate does not play a decisive role in the unfavourable matric effect, as was assumed earlier [8]. According to experimental data, the signal decrease arising within the matrix effect decisively from a decrease in take-up rate can be put at the most at 10%.

Even if the maintenance of controlled take-up rate does not mean a great advantage from the analytical aspect, a further investigation of the mass transport makes its application unavoidable. As a next step we are going to investigate the dependence of the quantity of material getting into the flame on the physical and chemical properties of the sample solution.

The quantity of material getting into the flame is determined besides take-up rate by the nebulization efficiency. On the basis of the rheological properties of the polymer solution it is to be expected that the higher is the polymer concentration and the greater the entanglement, the lower is the nebulization efficiency. This experimental finding was unequivocally proved.

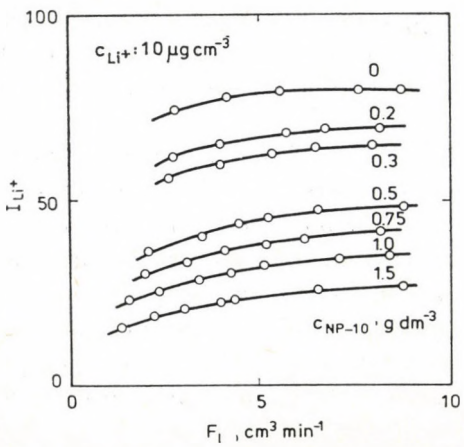


Fig. 7. Increase in intensity obtained by controlled take-up rate (increase of take-up rate) in the feeding of polymer solutions of different concentration

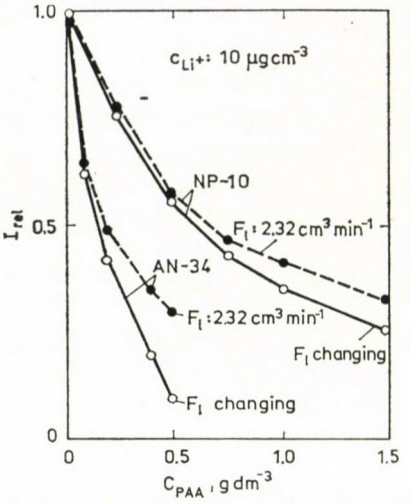


Fig. 8. Dependence of relative intensity on polymer concentration in spontaneous and controlled take-up rate

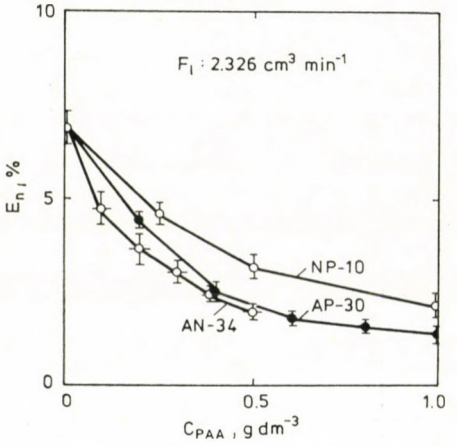


Fig. 9. Dependence of nebulization efficiency on polymer concentration at controlled take-up rate

Nebulization efficiency was determined at controlled take-up rate. Results are shown in Figure 9.

As proved by the figure, nebulization efficiency gradually worsens with increasing polymer concentration, molecular mass and degree of hydrolysis. There are no data in literature for the correlation between nebulization efficiency and rheological properties. The presumable reason of this is that a description on rheological basis of primary and secondary aerosol formation is not possible either with theoretical or with empirical relationships.

The relationship suggested by Nukiyama and Tanasawa [21], containing the viscosity of the sample solutions as independent variable, is more or less suitable for the description of the drop size distribution of the so called primary aerosol getting into the mixing chamber. However, owing to the rheological properties of polymer solutions, the application of the formula raises similar problems as the Hagen—Poisseuille equation. In view of the fact that the mathematical description of processes proceeding in the mixing chamber (secondary aerosol formation, loss processes, etc.) is inconvenient [9], we must be satisfied with a qualitative statement that on the one hand average drop size increases with in creasing viscosity, and on the other hand, the amount of aerosol getting into the flame at constant take-up rate changes then considerably, when the drop size distribution of the primary aerosol is modified.

According to the generally accepted theory of the mechanism of aerosol formation [22] (formation of liquid bridges, filaments and bags, then their disintegration), in the pneumatic nebulization of liquids the nebulization efficiency can be brought into connection with cohesive forces needed for the rupture of the liquid bridges, and in the case of polymer solutions with the elastic properties of liquids (e.g. with the complex dynamic shear modulus). Of these characteristics we could determine only the latter. Its dependence on concentration is shown in Figure 10.

Complex dynamic shear modulus is proportional to that energy, which is lost in the shear deformation (depending on the measuring method) of a

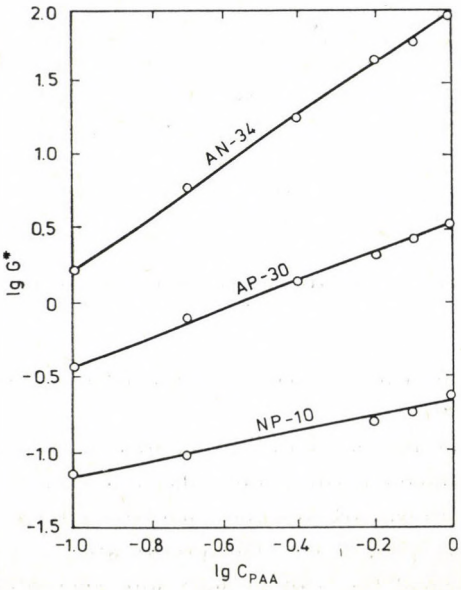


Fig. 10. Dependence of the absolute value of complex dynamic shear modulus on polymer concentration

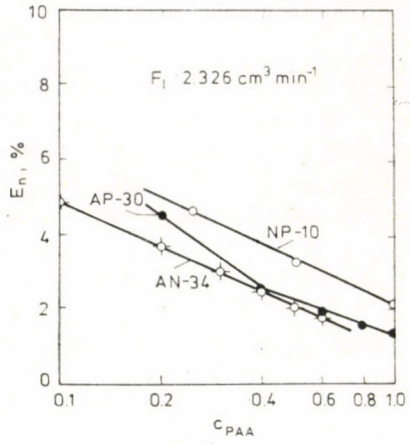


Fig. 11. Dependence of nebulization efficiency on the logarithm of polymer concentration at controlled take-up rate

liquid layer in the form of frictional heat dissipation and in the stretching of the network formed by the macromolecules. For the tearing off of a single liquid drop by shear deformation the higher energy is needed, the higher is the absolute value of the complex dynamic shear modulus. From this it follows that at identical nebulization (deformation) energy and liquid flow rate the number of torn off liquid drops decreases with increasing elasticity of the solution. A natural consequence of this is the increase in drop size and the decrease in nebulization efficiency, expected also qualitatively on the basis of Nukiyama and Tanasawa's relationship [21]. Presumably the decisive factor in the formation of an aerosol having corser drop size from polymer solutions is that in the case of particulate solutions also the thick ring forming the neck of the liquid bag disintegrates after bag formation into small droplets by the action of shear force exerted by the air stream, while in the case of solutions containing macromolecules this is partly or totally prevented by intermolecular interaction (internal network). A direct consequence of this is the relative strengthening of the loss process, and the decreasing of the quantity of aerosol getting into the flame. According to our experimental results nebulization efficiency and the logarithm of polymer concentration are inversely proportional. Figure 11 proves this finding unequivocally for two polymers, while the break in the line of polymer AP-30 requires further investigations. A comparison of Figures 10 and 11 makes it probable that there is a similar relationship between the nebulization efficiency and the complex dynamic shear modulus. This indirectly supports our starting hypothesis, according to which the cause of the matrix effect is to be primarily attributed to the non-Newtonian, viscoelastic character of polymer solutions and to the decrease in nebulization efficiency following from it.

Though the quantity of substance getting into the flame is influenced also by interfacial and electrokinetic phenomena besides those already mentioned, several authors [23—25] deduced relatively simple relationships for the determination of F_a, involving e.g. the boiling point, viscosity and surface tension. Of these neither relationship $F_a - \eta$ [23], nor relationship $F_a - 1/\eta$ [24—25] result straight lines (for latter see Fig. 12), which makes the general validity of the relationships doubtful.

Finally, a summary will be given on how the components of the mass balance of nebulization depend on polymer concentration at spontaneous take-up. Figure 13 shows curves characteristic of liquid currents obtained for the polymer of low molecular mass and degree of hydrolysis. It can be stated from the course of the curves that liquid currents show with exception of F_v a decreasing tendency. The flow of solvent vapour becomes stabilized at about 5.5%, however, its magnitude is comparable to that of the aerosol getting into the flame, so that it cannot be neglected in the determination of nebulization efficiency. It should be mentioned moreover that often neglections are made also in cases, when the character of the flame is basically influenced by the solvent, and this naturally gives misleading results e.g. in the calculation of the reductivity factor. The error is the larger, the higher the vapour pressure of the solvent and its oxygen consumption in the flame. If, however, the change in quantity of the sample getting into the flame is not accompanied by an essential change in flame character, and in general in atomization processes, as has been originally assumed, then the intensity or the absorbance measured is directly proportional to the concentration of atoms, present in excited or ground state in the flame, and consequently is

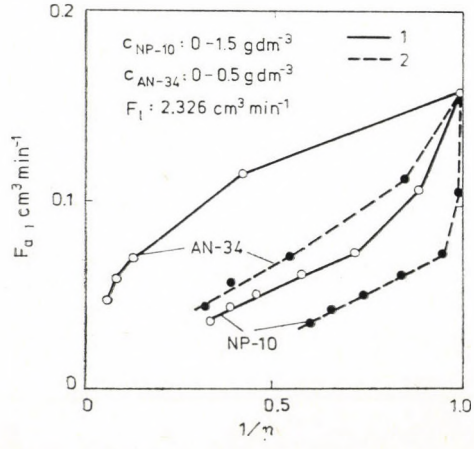


Fig. 12. Dependence of the quantity of sample getting into the flame on the reciprocal of the viscosity of the sample solution at controlled take-up rate and different polymer concentrations (1) measured; (2) calculated viscosity

directly proportional to the amount of aerosol calculated with the correction mentioned. In this case a direct proportionality must exist between the analytical signal and F_a, and the data obtained in the analysis of polymer-free and polymer-containing solutions should lie on a straight line. Figure 14, in which data obtained at controlled take-up rate are marked for aqueous solutions with filled-in circles and for polymer solutions with empty circles, proves the correctness of the initial assumption, namely that the matrix effect

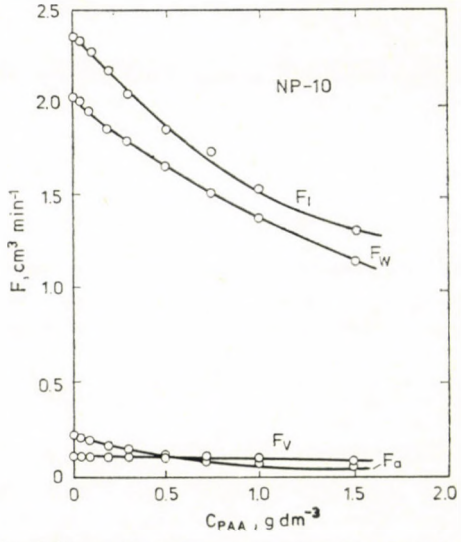


Fig. 13. Dependence of the different liquid currents on polymer concentration at spontaneous take-up rate

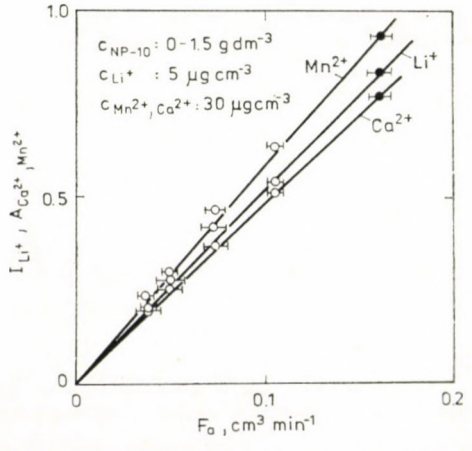


Fig. 14. Dependence of intensity and absorbance on the quantity of sample getting into the flame at spontaneous take-up

caused by the polymer is of feeding character, and that the phenomenon is of general validity for all those atomic spectroscopic methods, where the solution is introduced into the light source with a pneumatic nebulizer.

To avoid any misunderstanding, it should be finally mentioned that the linear relationship between analytical signal and the quantity of the sample getting into the flame is true only if the chemical interaction between the polymers and the cations present in the solution is negligible, or if at constant concentration of the cations F_a depends only on polymer concentration. This condition is often not fulfilled in practice. Moreover, a precondition is that the drop size distribution of the aerosol getting into the flame shall not be essentially changed by the polymer. Our experiments with the cascade impactor show that while the polymer evidently coarsens the primary aerosol, there is no substantial difference in the drop size distribution of the secondary aerosol (getting into the flame) on feeding water or polymer solution.

Conclusions

The results of laboratory investigations, dealing with the flame emission and flame atomic absorption analyses of aqueous solutions containing polyacrylamides, can be summarized as follows:

1) The matrix effect produced by polymers is unequivocally caused by feeding phenomena.

2) Decrease in take-up rate plays an insignificant part in the decrease of intensities and absorbances, while nebulization efficiency, and through it decrease in amount of aerosol getting into the flame, and in general the poor nebulization properties of polymers solutions must be considered as decisive factors.

3) The analytical signal is directly proportional to the quantity of substance getting into the flame in those cases, where chemical interaction between the polymers and the cations present in the sample solution is negligible.

Moreover, it was unequivocally stated that relationships known from the literature and often considered as generally valid, which among others take into consideration of the rheological properties of the sample solution only viscous properties, are unsuitable for the description of the nebulization phenomena of polymer solutions. Structural viscosity of polymer solutions, further their viscoelastic properties preclude also in principle the application of formulas based on the apparent or dynamic viscosity of the solution. On the other hand, there is an interpretable close correlation between nebulization efficiency, decisive from the point of view of the feeding of the sample into the flame, and complex dynamic shear modulus.

Symbols

c	concentration, gdm^{-3}, $\mu g\ cm^{-3}$
k	constant, —
Δp	nebulizing pressure, Pa
t	time, s
v	flame volume, cm^3
A_x	absorbance, —
A_{rel}	relative absorbance, —
D	shear rate, s^{-1}
F_a	liquid current getting into the flame, $cm^3\ min^{-1}$
F_t	take-up rate, $cm^3\ min^{-1}$
F_v	solvent vapour current getting into the flame, $cm^3\ min^{-1}$
F_w	effluent liquid current, $cm^3\ cmin^{-1}$
G^*	complex dynamic shear modulus, mPa
I_x	intensity, —
I_{rel}	relative intensity, —
L	length of capillary, cm
N	number of atoms in the flame, —
β_v	evaporation efficiency, %
β_s	concentration efficiency, %
β_a	atomization efficiency, %
δ	loss angle, degree
ε_n	nebulization efficiency, %
η	viscosity, mPas
ν	frequency, s^{-1}

REFERENCES

[1] Slavin, W.: At. Abs. Newaletter, **4,** 192 (1965)
[2] Drackman, O.: At. Abs. Newsletter, **6,** 113 (1967)
[3] Yanagisowa, M., Suzuki, H., Talenechi, T.: Talanta, **14,** 933 (1967)
[4] Henn, E. L.: Anal. Chim. Acta, **73,** 273 (1974)
[5] Olivier, M.: Z. Anal. Chem., **248,** 145 (1969)
[6] Caton, R. D., Bremner, R. W.: Anal. Chem., **26,** 805 (1954)
[7] Bills, C. E., McDonald, F. G., Medermeyer, W., Schwartz, M. C.: Anal. Chem., **21,** 1076 (1949)
[8] Lakatos, I.: Acta Chim. Acad. Sci. Hung., **109,** 313 (1982)
[9] Smith, D. D., Browner, R. F.: Anal. Chem., **54,** 533 (1982)
[10] Novak, J. W., Browner, R. F.: Anal. Chem., **52,** 287 (1980)
[11] Takado, T., Nakano, K.: Spectrochim. Acta, **36B,** 735 (1981)
[12] Browner, R. F., Boorn, A. W., Smith, D. D.: Anal. Chem., **54,** 1411 (1982)
[13] Kirkbright, G. F., Sargent, M.: Atom Absorption and Fluorescence Spectroscopy. Acad. Press. New York 1974
[14] Winefordner, J. D., Latz, H. W.: Anal. Chem., **33,** 1727 (1971)
[15] Culp, J. H., Windham, R. L., Whealy, R. D.: Anal. Chem., **43,** 1321 (1971)
[16] Cresser, M. S.: Prog. Analyt. Atom. Spectroscop., **5,** 35 (1982)
[17] Hershey, H. C., Zakin, J. L.: Chem. Eng. Sci., **22,** 1847 (1967)
[18] Patterson, G. K., Zakin, J. L., Rodriguez, J. M.: Ind. Eng. Chem., **61,** 22 (1969)
[19] Savins, J. G.: Soc. Pet. Engr. J., **4,** 203 (1964)
[20] Willis, J. B.: Spectrochim, A, **23A**cta, 811 (1967)
[21] Nukiyama, S., Tanasawa, T.: Trans. Soc. Mech. Engrs. Japan, **5,** 68 (1939)
[22] Turba, J.: Porlasztók (Atomizers) Műszaki Kiadó. Budapest 1976
[23] Lemond, A. J., McClellan, B. E.: Anal. Chem., **45,** 1455 (1973)
[24] Szivós, K., Pólos, L., Pungor, E.: Spectrochim. Acta, **31B,** 289 (1976)
[25] Trischler-Szivós, K.: Ph. D. Thesis, Budapest 1981

Acta Chimica Hungarica 116 (4), pp. 407—417 (1984)

BOOK REVIEWS

New Polymerization Reactions
Advances in Polymer Science, Vol. 42

Springer Verlag, Berlin—Heidelberg—New York, 1982, 172 pages

The book contains four surveys about new polymerization reactions.

Masaki Hasegawa: *Four-Center Photopolymerization in the Crystalline State.* This new type of solid-state polymerization reaction was first described by the author in 1967. On the basis of a large number of conjugated diolefin monomeric crystals and the structure investigation of the obtained polymers, it has been demonstrated that this reaction is a typical topochemical process, involving a direct rearrangement of the monomer crystal to the polymer crystal having an extended rigid rod-like structure. In 1978, Lahav and co-workers (Weizmann Institute, Israel) succeeded in achieving an absolute asymmetric synthesis of chiral dimers and oligomers through the crystallization of an achiral monomer in a chiral crystal, followed by the four-center type photopolymerization in the crystalline state. This review covers all the important fields: preparation, chemical structures of polymers, mechanism of polymerization, crystallography of the monomers and polymers, changes of morphology in the course of polymerization, polymer properties and characteristic features of four-center polymerization.

David Samuel Johnston: *Macrozwitterion Polymerization.* When the counterion is covalenty bound to the chain, the polymerization is termed macrozwitterionic. This relatively unexplored area of polymer chemistry is reviewed. The literature review shows addition polymerizations of vinyl, carbonyl and strained-ring monomers, the charge cancellation polymerization of aryl-substituted cyclic sulfonium zwitterions, acetonitrile oxide, diazoalkanes and spontaneous alternating copolymerizations.

In the part discussing the mechanism of macrozwitterion polymerization, various factors are treated, such as covalent initiators, reactivity of covalent base-monomer adducts, the influence of chemically inert salts on the polymerization rate, the role of solvent in charge separation and, finally, the zwitterion propagation. The last part contains the conclusions of the author concerning interesting areas for further research in this field.

Y. Yokoyama and K. H. Hall, Jr.: *Ring-Opening Polymerization of Atom-Bridged and Bond-Bridged Bicyclic Ethers, Acetals and Orthoesters.* During the last two decades many polymerizations of bicyclic compounds have been studied to obtain basic knowledge on ring-opening polymerization and practical information for industrial and biomedical applications. In 1961 Korshak et al. reported the stereospecific polymerization of 1,6-anhydro-2,3,4-tri-*O*-methyl-D-glucopyranose. After this, scientists all over the world investigated this type of compounds to obtain polymers mainly of biomedical interest. This review provides a good survey of literature concerning the polymerization of bicyclic compounds containing oxygen atoms, their polymerizability, the thermodynamics of polymer formation, monomer conformation, the discussion of gauche and anomeric effects, polymer conformation, kinetics of polymerization reactions and comparison of bicyclic monomer reactivities with the monocyclic compounds, polymerization mechanism and stereoregularity. The last chapter of the review shows the medical application of these polymers, mainly their high drug release behavior.

B. P. Morin, I. P. Breusova and Z. A. Rogovin: *Structural and Chemical Modifications of Cellulose by Graft Copolymerization.* This review is one of the last works of the late professor Zakhar Aleksandrovich Rogovin, a world-wide famous, excellent scientist in the field of the chemistry and technology of cellulose. With decreasing oil resources and rising prices of oil and its products, increasing interest in cellulose and polymers made from it can be prognosed (renewable natural products). From this point of view cellulose modification by grafting is exceptionally promising. The first part of this review deals with the factors influencing the graft copolymerization with cellulose, the structures and properties of the products. The second part shows the kinetics of chemically initiated graft copolymerization and its features

arising from the heterogeneous nature of the process. The third part discusses the basic trends in grafting to cellulose fibers in industry, and many technological aspects of this questions. The last part gives a description of polymer analogous conversions of functional groups in polymer chains grafted to cellulose.

This book can be warmly recomended to all specialists, scientists and students who are interested in new polymerization reactions, and who wish to extend their knowledge in these exciting new fields of polymer science.

GY. HARDY

Research Institute for Plastics Industry,
Budapest

Interactions Between Macromolecules in Solution and Intermolecular Complexes Advances in Polymer Science, Vol. 45

Springer Verlag, Berlin—Heidelberg—New York, 1982, 130 pages

In this book a review by Eishun Tsuchida and Koji Abe is published on Interactions Between Macromolecules in Solution and Intermacromolecular Complexes. The topic is very exciting from both the theoretical and practical point of view. The products of interaction of macromolecules in solution can be classified as polyelectrolyte complexes, complexes formed by hydrogen bonding, stereocomplexes and charge-transfer complexes. The polymeric nature of the reacting species results in cooperative phenomena in complexation processes. The survey discusses the selective intermacromolecular complexation phenomena and the supermolecular structure of intermacromolecular complexes. Intermacromolecular interactions are very important for a better understanding of biological systems, such as the self-assembling of proteins, molecular recognition, biomembranes, etc. The last part of the review visualizes the future development of intermacromolecular complexes tailored to special uses: intermacromolecular interactions applied to ecological protection, ultrafiltration membranes, coacervate complexes as artifical cells, mechanochemistry, matrix polymerization, application of macromolecular complexes and molecular assemblies in the biomedical field. A great merit of this book is the very well collected up-to-date literature, the quantitative description of phenomena where it is possible, the clear and logical discussion of problems. The book can be warmly recommended to macromolecular chemists, physicists and also to biophysicists.

GY. HARDY

Research Institute for Plastics Industry,
Budapest

H. Biltz, W. Klemm, W. Fischer: *Experimentelle Einführung in die Anorganische Chemie* (Experimental Introduction to Inorganic Chemistry), 72nd revised edition

Walter de Gruyter. Berlin, New York 1982. 285 pages

It is a strange feeling for the reviewer, to hold in his hands the 72nd edition of a textbook on introduction into inorganic chemistry. This is namely the case for the book bearing the above title, as the first edition written by H. Biltz was published in 1898, with the aim to intensify exercises carried out at that time in the chemical laboratories of the University of Kiel. Following this, 20 editions of the book served for acquiring fundamental chemical knowledge, and not only at the University of Kiel. Thus it is understandable that in 1937, W. Klemm and W. Fischer, former pupils of H. Biltz and W. Biltz, respectively, undertook with the full consent of author and publisher a thorough revision of the book. Since then 50 new editions were published, and characteristic of each new edition was the endeavour of the authors to fit knowledge contained in the book to recent results of development. All along, the actuality of the work was maintained by the inductive approach characteristic of the mode of discussion, that is, by the method to that great recognitions of chemical sciences are due. Indeed, if we

wish to acquaint undergraduates with the pleasure of observation, and to develop their aptitude for experimental work, it is unimaginable to achieve it solely by a deductive way. Moreover, it can be avoided by an inductive approach that in the lack of sufficient factual knowledge, the student should have to "work" in a void space during the imparting of theoretically exacting knowledge.

However, this does not mean by far that the book is a haphazard collection of prescriptions, as the authors attempt to emphasize essentials in the choosing of the experiments, and lay stress upon the recognition of general relationships.

In the introductory part, the book summarizes among others necessary devices, most important knowledge needed for their handling, the most important operations during laboratory work, and general laboratory rules.

Both the non-metal and the metal compounds are divided into two chapters, and in the first chapters the authors describe for the given elements general laws and relationships needed for the performance of the work, the SI system included.

In the appendix the solubility of some compounds in water and the list of reagents are given.

An important advantage of the book is that it introduces first-year students, by experiments to be carried out by themselves to the most important problems of inorganic chemistry, and generally these experiments can be performed on small quantities, in a test tube. During this, all along, the unequivocal interpretation of concepts is stressed. Better understanding and successful experimental work are promoted also by typography, as setting and make-up contribute to a complete separation of theoretical and practical relations, and to the unequivocal distinguishing of initial substances and reaction products.

Evidently, the book does not comprise all the knowledge needed in the study of inorganic chemistry, but this "gap" can be filled by the students in lecture courses and from other textbooks. Owing to the structuring of the book, certain parts can be omitted without impairment of the essence, thus, "Experimental Introduction . . ." is an introductory textbook of inorganic chemistry, which can be equally well used in educational institutions of various levels and aims.

S. PAPP

Department of General and Inorganic Chemistry,
University of Chemical Industry,
Veszprém

Euroanalysis, IV. Reviews on Analytical Chemistry

Edited by L. Niinistö, Association of Finnish Chemical Societies, Helsinki; Akadémiai Kiadó, Budapest, 1982. 258 pages

Euroanalysis Conferences, organized triannually are sponsored by the Analytical Chemical Working Party of the Frederation of European Chemical Societies (FECS). The organization of the Fourth Euroanalysis Conference was undertaken by the Association of Finnish Chemical Societies. The Conference was held in Helsinki between August 25—28, 1981. The president was L. Niinistö, Professor of the Analytical Department of the Helsinki University, who accepted not only the role of the host and the job of directing the organization of the meeting but also worked as the editor of the volume containing the plenary lectures presented by the invited speakers. Thus the book entitled Euroanalysis IV is the fourth volume of the proceedings of the Euroanalysis Conferences.

Euroanalysis Conferences cover the entire field of analytical chemistry. Yet, in this very broad field, the most up-to-date problems and topics always receive special attention. In the plenary lectures, the role of analytical chemistry and that of the analytical chemist in modern society was the subject of important discussions. Up-to-date and highly efficient analytical methods were also treated, which play an important part in microanalysis, in the examination of high-purity materials, and in the analysis of the surfaces of solids (Spark Source Mass Spectrometry, Secondary Ion Mass Spectrometry, etc.).

The author of the first lecture Prof. H. Laitinen (USA), gives a survey of the development of analytical chemistry. The second lectures, by Prof. Mäkitie (Finland) is a commemoration of the work of the first great analytical chemist in Finland, J. Gadolin (1760—1852). The author of the third lecture, H. Egan (UK), deals with the position of the analytical chemist in the society of today. The lecture presented by W. Pfannhauser (Austria) is also concerned with the situation of analytical chemists, and their responsibilities.

The authors of lectures No. 5, 6, 7, 10, 12, 13, 14, 15 report on modern analytical methods and the new results achieved by their use G. L. Ramendik (USSR) spoke about Spark Source Mass Spectrometry, A. Lodding (Sweden) about Secondary Ion Mass Spectrometry, I. Cornides (Hungary) about the mass spectrometry of inorganic substances, K. Ballschmiter (FRG) discussed high-resolution gas chromatography, J. Slanina (the Netherlands) treated ion chromatography, Z. Kowalski (Poland) reported on recent results in voltammetry, D. Hadzi (Yugoslavia) on IR spectrometers coupled with computers, while the topic of the lecture by Pham V. Huong (France) was recent developments in Raman spectroscopy.

V. Simeonov (Bulgaria) and H. Malissa (Austria) reviewed the informatical role of picture representation. Prof. D. Dyrssen (Sweden) described the chemical analytical equipment and analytical work of a Swedish expedition (YMER-80) under the title Arctic Automatic Analysis.

Tasks and problems of microanalysis aiming at the determination of contaminants in the environment were treated in the lecture of E. Wänninen (Finland), while the deterimnation of asbestos powder, important in environmental protection was described by P. G. Byrne (Ireland).

As shown by the above list of the contents of chapters, the book presents a survey and gives competent information about the most actual topics in the development and application of analytical chemistry. The book is recommended to all those, who wish to keep abreast with the developments in chemical science and want to obtain information on the present trends in chemical analysis.

The pleasent appearance of the book does credit to the careful work of the Akadémiai Kiadó, Budapest.

J. Inczédy

Dept. of Analytical Chemistry,
University of Veszprém,
Veszprém

Unusual Properties of New Polymers
Advances in Polymer Science, Vol. 50

Springer Verlag, Berlin—Heidelberg—New York, 1983, 149 pages

Unusual properties of new-polymers hold out the promise of great chances in macromolecular chemistry and physics, leading to important new developments in both theory and practice. In this volume there are three surveys about various very exciting fields.

Josef Pitha: *Physiological Activities of Synthetic Analogs of Polynucleotides.* The main idea of this study is: to penetrate through an organism, a synthetic compound must be not only water soluble but also lipid-soluble. The lipid solubility is necessary for penetration through lipid membranes. After giving the chemical and biophysical background, the author discusses the effects of synthetic polynucleotide analogs on enzymatic systems and at cell and organism levels. A special chapter deals with the fate of synthetic polynucleotide analogs in the organism, and it is concluded that the use of oligomers rather than polymers would result in the solution of application problems of these polymers.

Georg Smets: *Photochromic Phenomena in the Solid Phase.* This review summarizes many years of experience of Prof. Smets in this field. The way how the polymer background influences photochromism and photomechanical processes is relatively well known on the low molecular mass level in the solid phase. The photochemical reactions involved in these processes are mainly the *trans-cis* isomerization of aromatic azo compounds and stilbene derivatives, as well as the ring-opening and ring-closure reactions of spirobenzopyran derivatives in a solid polymer matrix. Photomechanical phenomena discussed are those occuring on cross-linked polymers and swollen gels, in the case of non-cross-linked bulk polymers, and photoresponsive polymer monolayers. All these are very closely connected with the non-silver color photography, with the dinamic photoresponse of polymer films, and can be considered as model photoreceptors for photoregulated biological processes; they could play an important role in many fields such as photoprinting and photocontrolled drug relase from vesicles.

Dieter Wöhrle: *Polymer Square Planar Metal Chelates for Sciences and Industry, Synthesis, Properties and Applications.* The topic is divided into two main parts according to the type of the polymer: one is the group of polymers with coordinative polymer bond in metal chelates (porphyrins, phthalocyanines, Schiff-base chelates, bis-1,2-dioximes); the second is the group

of polymers with covalent polymer bond in metal chelates (the same types of compounds with vinyl groups, or polycondensation products). The synthesis and properties of these polymers is described in detail. Binding of small molecules such as oxygen, and the catalytic activity of these polymers are the main promising properties. Further, they can be used as photoconductors, in arrangements for photovoltaic and photogalvanic elements.

This book was written by excellent scientists, and it is a great pleasure to read it. The volume can be recommended to all who are interested in new research and development in the field of polymer science.

GY. HARDY

Research Institute for Plastics Industry, Budapest

Boris Alexeevics Lopatin, Ottó Klug: *Conductometric and oscillometric analyses*

László Kékedy: *Gas sensors*

Advances in Chemistry (Ed. B. Csákvári) Vol. *56*. Akadémiai Kiadó, Budapest 1983, 465 pages

The first part of the volume deals with one of the most widely used branches of the electroanalytical techniques, with methods of the measurement of electric conductivity, and with its special field, oscillometry, the high frequency methods.

During its history of about a hundred years, conductometry made advances parallel to the development of electrochemical and electrotechnical measuring techniques.

The field of application of conductometry can be divided into three parts:

1. Study of physicochemical processes

2. Conductometric titration

3. Industrial analytical conductometry

Conductometry as an analytical method makes possible determination in both concentrated and dilute solutions, in coloured, turbid and impure solutions, in the presence of oxidizing and reducing agents.

The method has the disadvantage of not being selective in the analysis of multicomponent solutions. This disadvantage can be eliminated by indirect measurement, or by combination with other methods.

After the elucidation of basic concepts, the properties of low-frequency conductivity cells and oscillometric cells, and the appropriate measuring methods are discussed. In the part dealing with conductometric and oscillometric titration, the possibilities of titrations of different types are shown, illustrated by many practical examples.

A separate chapter covers the application of conductometry in industrial process control methods, then gives a detailed survey on commercial measuring instruments of various types.

The second part of the volume discusses gas sensors and their fields of application. Gas sensors are signal transducers, in which the input signal is provided by some, gaseous substance which, upon interaction with the sensor generates an output signal proportional to the concentration of the gas. The output signal is in most of the cases of electric character (current, electrode potential), so that most of the gas sensors are electrochemical sensors. The author discusses and classes gas sensors on the basis of the principles of classification of electrochemical processes, according to the nature of the output signals. In compliance with it, amperometric gas sensors, primarily the most widely used oxygen sensor, are discussed. Of the potentiometric liquid electrolyte gas sensors, hydrogen, carbon dioxide, ammonia and sulfur dioxide sensors are discussed. With potentiometric solid electrolyte gas sensors, certain gases can be determined continuously, even at high temperatures.

In addition to amperometric and potentiometric gas sensors, less widely used are gas sensors operating on conductometric, piezoelectric, radiometric, chemiluminescent, thermocatalytic and other principles.

Advantages of gas sensors: simple construction, simple response signal, easy handling, no need for special training.

Ample bibliography is contained in the volume in conjunction with both subjects, which will give useful help also to theoretical experts, studying the methods. The fields of application of the methods are illustrated by several examples, of value to chemists applying the methods.

E. GRÁF-HARSÁNYI

Institute for General and Analytical Chemistry, Technical University, Budapest

László Mázor: *Methods of Organic Analysis*

Akadémiai Kiadó, Elsevier Scientific Publishing Co., Budapest, Amsterdam, 1983.

The English version of the book appeared as volume *15* of Wilson and Wilson: *Comprehensive Analytical Chemistry*. so that the author took into consideration chapters discussing this subject in the volumes already published of the comprehensive monograph series, to avoid needless repetitions.

The book falls into two main parts. The first part of 272 pages covers qualitative elemental and functional group analysis, the second part of 257 pages the quantitative elemental and functional group analysis of organic compounds.

Chapter headings of the first part are:

1. Introduction, methods of identification of organic compounds
2. Preliminary analysis
3. Qualitative elemental analysis
4. Determination of physical constants
5. Qualitative group analysis
6. Microreactions for the detection of some important organic compounds
*7.*Application of methods of instrumental analysis in the analysis of organic compounds

Chapters of the second part:

8. Quantitative elemental analysis
9. Quantitative functional group analysis
10. Automated analysis

Each chapter closes with an extensive bibliography, facilitating the finding of the original publication. The first part contains 300 references, the second part cites more than 1200 sources.

With a work of several decades the author himself is an active contributor to the development of methods, his particular field being the analysis of organic compounds containing halogens.

As concerns the weighing of the single chapters, it seems that his aim was to mention only briefly widely used modern instrumental analytical methods, in view of the volumes published so far of the comprehensive monograph series.

The volume is addressed to research and analytical chemists and university students alike.

Institute for General and Analytical Chemistry, Technical University, Budapest

L. Pólos

S. Görög: *Quantitative Analysis of Steroids*

Akadémiai Kiadó. Budapest 1983. 440 pages.

The new book of Prof. Sándor Görög is published as the fifth volume of the series "Studies in Analytical Chemistry". His earlier work, S. Görög and Gy. Szász: "Analysis of Steroid Hormone Drugs", has been published in 1978 by Akadémiai Kiadó and Elsevier, Amsterdam. This work focused on the analysis of steroid hormones used as drugs.

The present book covers a wider field, also dealing with other important groups of steroids. As indicated by the title, the subject of the book is the description and application of quantitative methods. Within this context not only pharmaceutical drugs and preparations are treated, but biological and clinical analytical methods are also discussed. These are of major importance, because the analysis of body fluids is a considerable part of the work in clinical laboratories. In addition, special themes are also treated, such as the determination of steroids in food, cardiac glycosides in plants, etc. At a same time, connections are established between various theoretical and practical relations.

The subject discussed is organized in the following chapters:
Sex hormones and related materials
Corticosteroids
Cholesterol and related sterols

Vitamin D and related materials
Bile acids
Cardiac glycosides
Diosgenin and related sapogenins
Miscellaneous steroids

An intraductory general part is given to each chapter, which is of great help in the elucidiation of the individual themes. Next, the methods applied are described. These involve, besides classical titrimetry and gravimetry, optical, electrometric, and chromatographic methods, further those radio-immunoassay ad enzyme-immunoassay methods, which are used in clinical analysis. Procedures of the quantitative analysis of individual steroids are discussed, and on several occasions the problems of purity tests are mentioned.

Throughout the book we find all the chemical properties and formulas of individual steroids: the analytical results and their evaluation are illustrated by numerous figures. A bibliography of about 2500 references helps the reader in his further research.

The book of S. Görög fills a gap, no monograph on this subject has been published even in other countries. The book of the excellent Hungarian expert in steroid analysis is a valuable addition to the literature of analytical chemistry.

K. Nikolics

Pharm. Centre,
Sopron

Gordon A. Parker: *Analytical Chemistry of Molybdenum*

Springer Verlag, Berlin—Heidelberg—New York, 1983

The book provides comprehensive informations on classical and modern analytical methods for testing and determining molybdenum in a variety of materials important both in laboratory and in industrial practices.

As an introduction the traditional qualitative identification of molybdenum in the presence of different ions, the spot test reaction, and the separation methods of molybdenum by precipitation, extraction, ion exchange, and chromatography procedures are summarized, and also the regions of the practical applications of the different methods are given (Chapter *1*, *2* and *3*). In Chapter *4* the author describes the classical gravimetric procedures, in Chapter *5* the titrimetric methods together with the procedures carried out by precipitation, complexometric, and oxidation-reduction titration are discussed. In Chapter *6*, *7*, *8* and *9* colorimetric, emission, and atomic absorption spectrometric and x-ray fluorescence methods are described; these methods are applied also in determining low concentrations of molybdenum in different matrices. In Chapter *10* the voltammetric (polarographic and anodic-stripping voltammetric) procedures are dealt with in detail.

It is remarkable that the author devotes a separate part to the catalytic reactions (in Chapter *11*) although, according to the character of the methods, these could have been mentioned among the colorimetic or potentiometric methods too. In the book we find an interesting discussion on the determination of molybdenum by isotope dilution and activation analysis. The applicability of these methods is often restricted by the rather expensive devices and safety aspects (Chapter *12*).

Numerous useful instructions are given by the author for the main analytical working processes concerning rock and mineral samples, molybdenum and molybdenum-base alloys, ferrous and non-ferrous alloys, biological materials and environmental samples.

On editing the book, the author emphasized the practical aspects of molybdenum determination disregarding the theoretical bases of the analytical procedures. For the sake of the practice, to each analytical section detailed and correct working procedures are given with the help of which the different analytical problems can be solved. The book will be a very useful means for analytical chemists, first of all, to those active industrial and research laboratories.

The book has only one single insufficiency: it does not discuss the analysis of the non-stoichiometric molybdenum compounds e.g. the M_xMoO_3 bronzes and MoO_{3-y} oxides, although the scientific and industrial importance of these compounds is increasing.

A. B. Kiss

Tungsram Ltd.,
Budapest

Michael Thor Pope: *Heteropoly and Isopoly Oxometalates*
Inorganic Chemistry Concepts 8

Springer Verlag, Berlin, Heidelberg, New York, Tokyo, 1983 180 pp with 71 Figures and 40 Tables

The isopoly- and heteropolyoxoanions may be represented by the general formulas:

$$[M_mO_y]^{p-} \text{ and } [X_xM_mO_y]^{q-} \quad (x \leq m)$$

where M is the addenda atom: molybdenum or tungsten (less frequently: vanadium, niobium or tantalum) or mixtures of these elements and X is the heteroatom. Heteropolyanions may incorporate primary ("central") and/or secondary ("peripheral") heteroatoms. The number of primary heteroatoms (elements) known currently is above fifty and that of secondary ones is more than fifteen, that is the majority of Periodic Table (except the rare gases) is represented in polyoxometalate formations. It follows, that the group of polyoxometalates consists of several thousands of different complexes. Considering the field, it seems reasonable that the less known and — it seems currently — less important but more complicated insoluble polyoxometalates are only mentioned in the book.

The study of well defined recrystallized (both from aqueous or organic solvents) polyoxometalates, which is mainly the topic of the book reviewed, gives one of the very few points of contact between solution and solid state chemistry. In addition to this, the chemistry, structures and applications of these species deserves a new modern survey.

Pope's book excels in its References (altogether 771 ones, not an exhausted bibliography but all important or representative papers published through early 1982 can be found) and in its economical structure: the volume is only 180 pages, but every sentence has its new and substantial information. It means that the book is an extremely concentrated monograph.

Chapter *1* is an introduction with the problems of definition and historical backgrounds but first of all about the methods of investigation of polyanions in solution. It is not by chance that nearly the half of the whole Chapter deals with the possibilities of NMR techniques.

Chapter *2* is rather heterogeneous but very interesting: it consists of the methods of synthesis in both aqueous and nonaqueous solutions, of the problems of common structures (like the hexametalates and heteropolymetalates having octahedral, tetrahedral or icosahedral central heteroatoms). The third part of this Chapter on the properties and applications of polyoxometalates has only two and a half pages, but so many informations can be found about analytical, biochemical, catalytical, etc. applications that the whole text would be worth of copying in a recension, too.

The next two Chapters are comprehensive reviews of isopolyanions (vanadates, niobates, tantalates, molybdates, tungstates and their mixed species) and heteropolyanions (having tetrahedral, octahedral and eight or twelve coordinated heteroatoms, or heteroatoms with unshared electron pairs), resp.

Chapter *6* deals with the redox chemistry of polyoxometalates and with the heteropoly blues, and contains one of the author's most important establishment on reducibility of polyanions: type I polyoxometalates, where all addenda atoms have only one terminal oxygen can be reduced but not the type II polyoxometalates having addenda atoms with two (*cis*) terminal oxygens.

The next (7) Chapter summarizes the newest (and less known) results on organic and organometallic polyoxometalate derivatives with four, five, six, eight or twelve (addenda) metal atoms and those on the very promising field of organometallic complexes derived from lacunary Keggin and Dawson structures.

In the final (*8*) Chapter, the current limits and remaining challenges are estimated. It can be hardly assumed that great series like the iso- and heteropolymolybdates and -tungstates are existent but the similarity of some Te^{VI}, I^{VII} or Xe^{VIII} complexes to those is very probable. The polyoxocations are less investigated, although the structure of $[Al_{13}O_4(OH)_{24}(OH_2)_{12}]^{7+}$ is known to correspond to one type of Keggin structures. Further possibilities are that some of the oxygen atoms of polyoxometalates can be replaced by peroxide, fluoride, sulfide or nitride groups, but the chemistry of peroxo-, fluoro-, thio- and nitridopolyoxoanions is very poor. A lot of questions can be found with respect to bonding in polyoxometalates and, especially, to the mechanism of their formation (the rate of formation is generally surprisingly fast).

The book is ended with a short appendix (5 pages) on nomenclature of polyanions written by Y. Jeannin and M. Fournier. The referee does not find the co-publication of this very important but totally different topic a fortunate solution, an independent article in one special journal would be more favourable.

M. T. Pope's book is one of the best new monograph — it would be impossible to comprise more information with style in a such a minor volume. This book may be recommended not only to readers interested in inorganic, coordination and analytical chemistry, but for organic chemists, especially those concerning with homogeneous and heterogeneous catalysis, and for biochemists, solid state- and materials scientists.

L. Barcza

Institute of Inorganic and
Analytical Chemistry,
Eötvös L. Univ. of Budapest

J. Stepek, H. Daoust: *Additives for Plastics*

Springer Verlag, New York, Heidelberg, Berlin 1983. 243 pages

Similarly to metal materials of construction, which are used only in the rarest cases without alloying additives, plastics systems for practical purposes always contain additives. One group of these additives improves the properties of plastics in the desired direction: they plasticize or elastify, increase impact strength or rigidity, render color or improve transparency, etc. The other group of additives stabilizes: it protects plastics from an early deterioration of their useful properties, e.g. from thermal degradation, from the harmful effect of ultraviolet radiation, from oxidation, or e.g. it reduces the inflammability of plastics.

Though technical literature even on the single subjects amounts to almost a library, it is justified to survey from time to time in a concise summary this important field. The greatest advantage of this book of 243 pages by the Czechoslovakian — Canadian pair of authors is besides conciseness a uniform didactic concept. The book of Stepek and Daoust is an excellent textbook addressed to students, research and industrial engineers of plastics industry. It presumes basic knowledge in macromolecular chemistry, and resting on it, it concisely summarizes the theoretical aspects of the effect of additives on plastics, and presents solutions proved best in the present practice of plastics technology.

The book is organized in two parts with a total of 14 chapters.

Part I. Additives which modify physical properties
1. Plasticizers
2. Lubricants and mold-release agents
3. Macromolecular modifiers
4. Reinforcing fillers, reinforcing agents, coupling agents
5. Colorants and brightening agents
6. Chemical and physical blowing agents
7. Antistatic agents

Part II. Antiaging additives (antidegradants)
8. Diffifultly stabilizable and nonstabilizable factors provoking plastic degradation
9. Heat-stabilizers
10. Antioxidants and metal ion deactivating agents
11. Ultraviolet protecting agents
12. Flame retardants
13. Biocides against biological degradation of plastics
14. Brief survey of methods used to incorporate additives into polymer matrices.

The book does not discuss additives of polymer technology producing changes in the chemical structures (initiators, catalysts, cross-linking agents, etc.).

The first chapter of the well organized work written in proportional chapters, briefly summarizes thermodynamic fundamentals of macromolecular mixtures. The effect of plasticizers is discussed on the basis of the solubility of polymers, giving several actual data. In addition to the concise description of the known free volume theory, the most important plasticizers are discussed, mentioning also the anomalous effects of plasticizers (antiplasticization).

The other chapters are of similar compactness, and the theoretical discussion of the given sections is closed similarly by useful practical information. The chapter on lubricants

gives in concrete examples several dozens of waxes, metal soaps, fatty acid esters, etc., of practical importance, avoiding at the same time any advertisment-style propaganda. Similarly to other subjects it is difficult to give on about twenty pages a brief, concise summary on macromolecular additives improving impact properties or facilitating processing, or — as in the next chapter —, on plastics systems with fiber-reinforcement. It seems, however, that the authors present the subject clearly, in an easily understandable form, catch the attention of the reader, without enlarging on topics to be considered as known, calling the attention to those fields, which are most profitable for polymer technologists, and which can be further developed. Thus, for example, in Chapter 4 the description of the coupling agents of reinforced substances is excellent. Silanes, organotitatium compounds and other additives used for the "sizing" of glass fibers, for improving adherence, their mode of action, and their forms of industrial realization yield useful information.

Naturally, this compactness involves the danger of simplification, and often even of oversimplification. This danger could be scarcely avoided in the chapters on the stabilization of plastics in the second part of the book. The description on 16 pages of the mechanism of thermo-oxidative decomposition of plastics, and of the additives preventing it, is indeed possible only by simplifications on a large scale.

In spite of this, the brief summarizing work can be recommended as a useful handbook for all future and presently active engineers and research workers of macromolecular chemistry and technology. The 54 figures and numerous structural formulas, the final chapter describing the machines and methods of admixing, the subject index are all very useful. The total of 650 references, grouped according to chapters, presents a good basis for further studies.

Research Institute for Plastics Industry, Budapest

T. CZVIKOVSZKY

Ion Exchangers in Chemical Technology
(Ionity v Khimicheskoy Technologii) (in Russian)

Edited by B. P. Nikolskii and P. G. Romankov. Authors: L. K. Archangelskii, F. A. Belinskaya, A. I. Volzhinskii, I. B. Vysokoostrovskaya, G. E. Yelkin, N. M. Korolkov, V. V. Palchevskii, V. I. Paramonov, V. O. Reuhsfeld, N. N. Smirnov, V. V. Sokolov, Khimia, Leningrad 1982; 416 pages; Subject index, Price 1 Rbl.

The book is a well balanced excellent monograph of ion exchangers and their applications, written by eleven competent authors who contributed to the chemistry and applications of ion exchangers.

In spite of its limited volume the book contains many new and important informations in a readable form to all readers who are interested in the work with ion exchangers.

Usually, books written by more than two authors look heterogeneous, but this is not the case with this book. The contents of the chapters are well balanced and there are no superfluous overlappings at all.

The reader has to agree with the editors, who give their opinion in the preface of the book, that many textbooks and monographs deal with the usual chemical processes like liquid-liquid extraction, absorption, adsorption but relatively few are concerned with ion-exchange processes, although they are today of growing importance.

In the book nicely are amalgamated the known classical fundamentals, with the own results of the authors. The treatment and introduction of the different topics is well understandable to those all who can read the Russian text easily.

The deductions are prepared correctly, carefully and very clearly.

The brief content of the book is as follows:

Part *1.* Theoretical

In the first part of the book all important relations and formulas for description equilibria, the dependence of equilibria from temperature and pressure, the fundamental theories and formulas of ion-exchange kinetics and mass transfer are summarized with instructions for calculations of ion-exchange processes.

I. Thermodynamics of ion-exchange equilibria and the selectivity of ion exchangers (Archangelskii)

II. Kinetics of ion exchangers (Volzhinskii, Smirnov)

III. Mass transfer in the ion-exchange processes (Volzhinskii, Smirnov)

IV. Methods and models for calculation of ion-exchange processes (Volzhinskii, Smirnov)

Part *2.* Ion-exchange materials

In the second part of the book not the synthesis and classification of ion-exchange materials but rather their properties, are introduced. The thermodynamics of the processes, the relation between selectivity, solvent uptake and structure of ion exchanger. Calculation methods for estimation of selectivity etc. A special chapter is devoted to oxidation reduction resins and liquids. The theories of their functioning, their properties are dealt with in a comprehensive form.

V. Organic ion exchangers (Archangelskii)

VI. Inorganic ion exchangers (Belinskaya)

VII. Oxidation-reduction resins (Palchevskii)

Part *3.* Application of ion exchangers. In this part not only a review is given on the different application fields, but rigorous descriptions of the topics introduced.

VIII. General problems of the applications (Volzhinskii, Smirnov). Apparatus, equipments, selection of them using economic calculations.

IX. Inorganic technology (Smirnov, Sokolov). Production of fertilizers, purification of phosphoric acid, removal of iodine from natural substances, deionisation of water.

X. Organic technology (Smirnov, Korolkov, Yelkin). Purification of organic acids, organic solvents, production of pharmaceutical products.

XI. Catalytic processes using ion exchangers (Reuhsfeld). Ion exchangers as catalysts and catalyst carriers. Theoretical background, the influencing factors, stability, fields of applications.

XII. Radiochemical applications (Vysokoostrovskaya, Paramonov). Special problems at the applications, examination of solutions, adsorption of isotopes. Preparative and analytica applications, the nuclear industry.

XIII. Applications in medicine and biology (Belinskaya). Using ion exchangers for balancing the electrolyte equilibrium in internal medicine. First aid materials at radiation damages, etc.

As it was mentioned in the introduction, the book has many interesting, well constructed chapters, modern views and fills a gap in the literature. Therefore it is suggested to translate it into English (and also in to Hungarian) to make it available also to those who can not read the Russian text.

J. INCZÉDY

Dept. of Analytical Chemistry,
Veszprém University of Chemical
Engineering, Veszprém

PRINTED IN HUNGARY

Akadémiai Kiadó és Nyomda, Budapest

Text

The text of the paper should be concise. The description of new compounds (in the Experimental) must include the complete analytical data. Special attention must be paid to structural formulas given within the text. Complicated (non-linear) formulas should be drawn on separate sheets of paper and their position in the text should be clearly marked. The numbering of formulas and equations (in parentheses on the right-hand side) is only needed if they are referred to in the text. Units should conform to the International System of Units (SI). In nomenclature the rules of the I.U.P.A.C. are accepted as standard. Symbols for physical quantities are printed in italic type and should, therefore, be underlined in the manuscript.

References

References should be numbered in order of appearance in the text (where the reference number appears in brackets) and listed at the end of the paper. The reference list, too, should be typed double-spaced. Journal titles are to be abbreviated as defined by the Chemical Abstracts Service Source Index.

Examples:

[1] Brossi, A., Lindlar, H., Walter, M., Schneider, O.: Helv. Chim. Acta, **41**, 119 (1958)
[2] Parr, R. G.: Quantum Theory of Molecular Electronic Structure. Benjamin, New York 1964
[3] Warshel, A.: in Modern Theoretical Chemistry, Vol. 7, Part A (Ed. G. A. Segal), Plenum Press, New York 1977

Tables

Each table should be given a Roman number and a brief informative title. Structural formulas should not be used in column headings or in the body of tables.

Figures

Figures should be numbered consecutively with Arabic numerals. Their approximate place should be indicated in the text on the margin. All figures must be identified on the back by the author's name and the figure number in pencil. Standard symbols (such as circles, triangles, squares) are to be used on line-drawings to denote the points determined experimentally. Line-drawings must not contain structural formulas and comments. Spectra or relevant segments thereof, chromatograms, and X-ray diffraction patterns will be reproduced only if concise numerical summaries are inadequate to replace them. Drawings and graphs should be prepared in black ink on good-quality white or tracing paper. Photographs should be submitted on glossy paper as high-contrast copies. Xerox or similar copies are not suitable for reproduction, but may be used for duplicate copies.

Redrawn illustrations will be sent to the authors for checking. No corrections of figures will, therefore, be accepted in the proofs.

Submission of manuscript

After having completed the corrections suggested by the referees and editors, the final manuscript should be submitted in duplicate, in a form ready for publication. If the corrected manuscript is not returned to the editors *within six weeks*, the intended publication of the paper will be regarded as withdrawn by the authors.

Page charge will not be assessed for the publication, however, authors, from overseas countries must contribute to the postage of correspondence by sending, together with the manuscript, international postal coupons to the value of U.S. $ 10.—

Proofs and reprints

A set of proofs will be sent to the submitting author. The proofs must be returned within 48 hours of receipt. Late return may cause a delay in the publication of the paper. 100 reprints will be supplied to the authors free of charge.

Periodicals of the Hungarian Academy of Sciences are obtainable at the following addresses:

AUSTRALIA
C.B.D. LIBRARY AND SUBSCRIPTION SERVICE
Box 4886, G.P.O., *Sydney N.S.W. 2001*
COSMOS BOOKSHOP, 145 Ackland Street
St. Kilda (Melbourne), Victoria 3182

AUSTRIA
GLOBUS, Höchstädtplatz 3, *1206 Wien XX*

BELGIUM
OFFICE INTERNATIONAL DE LIBRAIRIE
30 Avenue Marnix, *1050 Bruxelles*
LIBRAIRIE DU MONDE ENTIER
162 rue du Midi, *1000 Bruxelles*

BULGARIA
HEMUS, Bulvar Ruszki 6, *Sofia*

CANADA
PANNONIA BOOKS, P.O. Box 1017
Postal Station "B", *Toronto, Ontario M5T 2T8*

CHINA
CNPICOR, Periodical Department, P.O. Box 50
Peking

CZECHOSLOVAKIA
MAĎARSKÁ KULTURA, Národní třida 22
115 66 Praha
PNS DOVOZ TISKU, Vinohradská 46, *Praha 2*
PNS DOVOZ TLAČE, *Bratislava 2*

DENMARK
EJNAR MUNKSGAARD, Norregade 6
1165 Copenhagen K

FEDERAL REPUBLIC OF GERMANY
KUNST UND WISSEN ERICH BIEBER
Postfach 46, *7000 Stuttgart 1*

FINLAND
AKATEEMINEN KIRJAKAUPPA, P.O. Box 128
SF-00101 Helsinki 10

FRANCE
DAWSON-FRANCE S. A., B. P. 40, *91121 Palaiseau*
EUROPÉRIODIQUES S. A., 31 Avenue de Versailles, *78170 La Celle St. Cloud*
OFFICE INTERNATIONAL DE DOCUMENTATION ET LIBRAIRIE, 48 rue Gay-Lussac
75240 Paris Cedex 05

GERMAN DEMOCRATIC REPUBLIC
HAUS DER UNGARISCHEN KULTUR
Karl Liebknecht-Straße 9, *DDR-102 Berlin*
DEUTSCHE POST ZEITUNGSVERTRIEBSAMT
Sraße der Pariser Kommüne 3–4, *DDR-104 Berlin*

GREAT BRITAIN
BLACKWELL'S PERIODICALS DIVISION
Hythe Bridge Street, *Oxford OX1 2ET*
BUMPUS, HALDANE AND MAXWELL LTD.
Cowper Works, *Olney, Bucks MK46 4BN*
COLLET'S HOLDINGS LTD., Denington Estate
Wellingborough, Northants NN8 2QT
WM. DAWSON AND SONS LTD., Cannon House
Folkstone, Kent CT19 5EE
H. K. LEWIS AND CO., 136 Gower Street
London WC1E 6BS

GREECE
KOSTARAKIS BROTHERS INTERNATIONAL BOOKSELLERS, 2 Hippokratous Street, *Athens-143*

HOLLAND
MEULENHOFF-BRUNA B.V., Beulingstraat 2,
Amsterdam
MARTINUS NIJHOFF B.V.
Lange Voorhout 9–11, *Den Haag*

SWETS SUBSCRIPTION SERVICE
347b Heereweg, *Lisse*

INDIA
ALLIED PUBLISHING PRIVATE LTD., 13/14
Asaf Ali Road, *New Delhi 110001*
150 B-6 Mount Road, *Madras 600002*
INTERNATIONAL BOOK HOUSE PVT. LTD.
Madame Cama Road, *Bombay 400039*
THE STATE TRADING CORPORATION OF INDIA LTD., Books Import Division, Chandralok
36 Janpath, *New Delhi 110001*

ITALY
INTERSCIENTIA, Via Mazzé 28, *10149 Torino*
LIBRERIA COMMISSIONARIA SANSONI, Via Lamarmora 45, *50121 Firenze*
SANTO VANASIA, Via M. Macchi 58
20124 Milano
D. E. A., Via Lima 28, *00198 Roma*

JAPAN
KINOKUNIYA BOOK-STORE CO. LTD.
17-7 Shinjuku 3 chome, Shinjuku-ku, *Tokyo 160-91*
MARUZEN COMPANY LTD., Book Department, P.O. Box 5050 Tokyo International, *Tokyo 100-31*
NAUKA LTD. IMPORT DEPARTMENT
2-30-19 Minami Ikebukuro, Toshima-ku, *Tokyo 171*

KOREA
CHULPANMUL, *Phenjan*

NORWAY
TANUM-TIDSKRIFT-SENTRALEN A.S., Karl Johansgatan 41–43, *1000 Oslo*

POLAND
WĘGIERSKI INSTYTUT KULTURY, Marszałkowska 80, *00-517 Warszawa*
CKP I W, ul. Towarowa 28, *00-958 Warszawa*

ROUMANIA
D. E. P., *Bucureşti*
ILEXIM, Calea Grivitei 64–66, *Bucureşti*

SOVIET UNION
SOJUZPECHAT — IMPORT, *Moscow*
and the post offices in each town
MEZHDUNARODNAYA KNIGA, *Moscow G-200*

SPAIN
DIAZ DE SANTOS, Lagasca 95, *Madrid 6*

SWEDEN
ALMQVIST AND WIKSELL, Gamla Brogatan 26
101 20 Stockholm
GUMPERTS UNIVERSITETSBOKHANDEL AB
Box 346, *401 25 Göteborg 1*

SWITZERLAND
KARGER LIBRI AG, Petersgraben 31, *4011 Basel*

USA
EBSCO SUBSCRIPTION SERVICES
P.O. Box 1943, *Birmingham, Alabama 35201*
F. W. FAXON COMPANY, INC.
15 Southwest Park, *Westwood Mass. 02090*
THE MOORE-COTTRELL SUBSCRIPTION AGENCIES, *North Cohocton, N. Y. 14868*
READ-MORE PUBLICATIONS, INC.
140 Cedar Street, *New York, N. Y. 10006*
STECHERT-MACMILLAN, INC.
7250 Westfield Avenue, *Pennsauken N. J. 08110*

YUGOSLAVIA
JUGOSLOVENSKA KNJIGA, Terazije 27, *Beograd*
FORUM, Vojvode Mišića 1, *21000 Novi Sad*

Index: 26.007